United States
Environmental Protection
Agency

Industrial Environmental Research
Laboratory
Research Triangle Park NC 27711

EPA-600/7-79-105b
April 1979

EPA

Comparative Assessment of Residential Energy Supply Systems That Use Fuel Cells
(Technical Report)

Interagency Energy/Environment R&D Program Report

RESEARCH REPORTING SERIES

Research reports of the Office of Research and Development, U.S. Environmental Protection Agency, have been grouped into nine series. These nine broad categories were established to facilitate further development and application of environmental technology. Elimination of traditional grouping was consciously planned to foster technology transfer and a maximum interface in related fields. The nine series are:

1. Environmental Health Effects Research
2. Environmental Protection Technology
3. Ecological Research
4. Environmental Monitoring
5. Socioeconomic Environmental Studies
6. Scientific and Technical Assessment Reports (STAR)
7. Interagency Energy-Environment Research and Development
8. "Special" Reports
9. Miscellaneous Reports

This report has been assigned to the INTERAGENCY ENERGY-ENVIRONMENT RESEARCH AND DEVELOPMENT series. Reports in this series result from the effort funded under the 17-agency Federal Energy/Environment Research and Development Program. These studies relate to EPA's mission to protect the public health and welfare from adverse effects of pollutants associated with energy systems. The goal of the Program is to assure the rapid development of domestic energy supplies in an environmentally-compatible manner by providing the necessary environmental data and control technology. Investigations include analyses of the transport of energy-related pollutants and their health and ecological effects; assessments of, and development of, control technologies for energy systems; and integrated assessments of a wide range of energy-related environmental issues.

EPA REVIEW NOTICE

This report has been reviewed by the participating Federal Agencies, and approved for publication. Approval does not signify that the contents necessarily reflect the views and policies of the Government, nor does mention of trade names or commercial products constitute endorsement or recommendation for use.

This document is available to the public through the National Technical Information Service, Springfield, Virginia 22161.

EPA-600/7-79-105b

April 1979

Comparative Assessment of Residential Energy Supply Systems That Use Fuel Cells (Technical Report)

by

R.V. Steele, D.C. Bomberger, K.M. Clark, R.F. Goldstein, R.L. Hays, M.E. Gray
and
G. Ciprios, R.J. Bellows, H.H. Horowitz, C.W. Snyder (Exxon)

SRI International
333 Ravenswood Avenue
Menlo Park, California 94025

Contract No. 68-02-2180
Program Element No. EHB534

EPA Project Officer: Gary L. Johnson

Industrial Environmental Research Laboratory
Office of Energy, Minerals, and Industry
Research Triangle Park, NC 27711

Prepared for

U.S. ENVIRONMENTAL PROTECTION AGENCY
Office of Research and Development
Washington, DC 20460

SRI INTERNATIONAL

COMPARATIVE ASSESSMENT OF RESIDENTIAL ENERGY SUPPLY SYSTEMS THAT USE FUEL CELLS

EXECUTIVE SUMMARY

What Are Fuel Cells?

Fuel cells are devices capable of converting the chemical energy stored in a fuel directly into electrical energy without a step involving combustion. Hydrogen contained in the fuel is chemically combined with oxygen from the air to produce water and an electric current that can be regulated and used. Fundamentally, the process is just the inverse of the electrolysis of water into its component parts, a process often demonstrated in high school chemistry classes. Practically, a fuel cell consists of two electrodes, a catalyst used to promote the chemical reaction, and an electrolyte (a chemical substance that conducts electricity) separating the electrodes. As might be suspected, a device of such fundamental simplicity was first conceived long ago--in 1839 by Sir William Grove, a British jurist.

Are Fuel Cells Commercially Available Today?

Although old in concept, as practical devices for producing electricity in significant amounts, fuel cells are in their infancy. For space missions, fuel cells have been shown to be ideal power sources, partly because they convert on-board stores of hydrogen and oxygen to electrical power without producing excessive heat or vibration-producing mechanical motion. In fact, they provided electrical power in Gemini and Apollo spacecraft, but were still considered novel and exotic devices.

Made in limited quantities, and to extreme reliability standards, fuel cells for space craft are understandably expensive. Nevertheless, much has been learned from the space program about fuel cells and that knowledge is beginning to find earthbound applications in much-improved and less costly devices.

More than 60 small (12.5 kW) fuel-cell power plants were field tested in 1972 and 1973. A 40-kW device was demonstrated in 1975, and now work is underway to demonstrate a 4.5-MW fuel cell in the Consolidated Edison (New York) utility system by 1980. Fuel-cell technology has come a long way and is nearing commercial readiness.

Do Fuel Cells Possess Attractive Attributes?

Much of the present interest in fuel cells derives from their unusually low environmental impact and their high efficiency. Because no combustion is involved, even fuel cells that use common fuels produce very low emissions of nitrogen or sulfur oxides; the emissions are many times below federal standards. Moreover, fuel cells generally consume no water and operate very quietly.

As a result of its environmental good- neighborliness, a fuel-cell power plant can easily be located very near the power demands it serves, thereby lessening the need for high voltage electric transmission lines.

The ability to site fuel-cell power plants locally is much enhanced by their modular design (which allows off-site manufacturing) and their rapid installation. Accordingly, electric power utilities may soon have commercially available a device that enables system expansion in small increments.

How Might Fuel Cells Fit into Electric Power Systems?

Besides being suitable for small, dispersed, locally sited power stations, fuel cells can easily operate in applications that require output to follow demand closely. In fact, electric utility interest in fuel cells often centers on mid-1980s deployment for load-following. Again, because of their cleanliness, fuel cells may be installed in buildings or residential complexes where the combined production of electric power and heat could be used to satisfy heating and cooling demands in an integrated (or "cogeneration") fashion. The fuel-cell-derived electricity would be used to operate heat pumps to provide cooling and supplemental heating.

Can Fuel Cells Use Coal or Coal-Derived Fuels?

Fuel cells, like most fuel-consuming devices are indifferent to the origin of the fuel—as long as in final form it conforms to the chemical requirements of the device. Accordingly, natural gas, petroleum products, or similar fuels are perfectly acceptable in fuel cells provided that the fuels are first reformed to hydrogen and carbon dioxide and that harmful sulfur contamination is removed before the fuels enter the fuel cell proper.

Fuel cells, therefore, can have a place in a largely coal-based U.S. energy future.

What Are Leading Coal-Based Alternatives to Fuel Cells?

Already, U.S. electrical power is largely generated in coal-fired plants and the federal government is pushing for even more in an effort to save relatively scarce and expensive oil and natural gas for other uses. Larger, conventional coal-fired power plants, often located in remote areas and connected to urban load centers by high voltage transmission lines, certainly provide a well-proven alternative to electric power generated from fuel cells.

So-called "combined-cycle" electrical power generation--a conventional boiler and steam turbine generator supplemented by a high-temperature gas turbine—is an improving technology gaining considerable attention among utilities. Certainly, by the time fuel-cell systems are perfected sufficiently to allow commercial deployment, combined-cycle systems will already be in use and fuel-cell systems will have to compete with them.

Much of the U.S. space heating demand is met by the combustion of natural gas. Because so many consumer-owned heaters are already in place, gas utilities have strong incentive to supplement natural gas supplies with coal-derived substitutes that would not require alteration of either consumer appliances or habits.

Synthetic natural gas, (SNG) derived from coal, then, offers strong competition for the electric heating role a fuel-cell/heat pump combination could play in the market place.

Can Fuel Cells be Compared with the Alternative Technologies?

Because fuel cells must compete with so many electric power and heat-producing fuel and technology combinations, the relative advantages and disadvantages of fuel cells have proven difficult to discern clearly. Consequently, as a part of its mission to preserve and enchance environmental quality, the U.S. Environmental Protection Agency commissioned this study precisely to learn more about what might be expected from fuel cells when actually deployed in utility systems.

To address this question, SRI International conceptually designed twelve energy systems able to provide residential heating and cooling using technologies projected to be available toward the end of this century. Only a few systems used fuel cells. As in most comparisons, some constraints were imposed to eliminate unnecessarily confusing complexities while providing a uniform framework for comparison. Accordingly, all systems use western coal as the primary energy resource, and all residences are assumed to have identical heating and cooling demands typical of the mid-continent United States. After winnowing out the clearly least attractive combinations, we selected five systems and compared them in great detail.

For all the comparisons, we examined the entire chain of the system, starting with the coal mine and ending with the heating and cooling of residences, to be sure that the claimed environmental advantages of the fuel cells at the point of electric power generation did not distract us from some important environmental impacts elsewhere in the system. Our five surviving systems, four of which use heat pumps for heating and cooling are:

- System 1—A coal-fired power plant supplies electricity and a coal gasification plant supplies SNG to residences; electricity powers air conditioners and SNG is burned in gas furnaces.
- System 2—A 26-MW fuel-cell power plant fueled by coal-derived SNG supplies electricity to residences with heat pumps.
- System 3—A 26-MW fuel-cell power plant fueled by coal-derived naphtha supplies electricity to residences with heat pumps.
- System 4—A combined-cycle power plant fueled by coal-derived fuel oil supplies electricity to residences with heat pumps.
- System 5—A 100-kW fuel-cell power plant fueled by coal-derived SNG, sited in a housing complex, supplies electricity to townhouses with heat pumps; heat recovered from the fuel cell supplies supplemental space heating and hot water.

Of these five, the first one most resembles the existing order in the utility industry, and the fourth constitutes an already evident evolutionary change of the industry.

What do the Comparisons Show?

The scorecard for the various systems is mixed—no single system stands out as superior in all the attributes that will ultimately decide which systems will be deployed. Nevertheless, some very interesting facts emerge about energy systems that use fuel cells.

Which System Costs the Consumer More?

The three fuel-cell systems provide heating and cooling to our standard residences at considerably higher cost that the two more conventional systems. In fact, the annual energy bill to a consumer using System 5 is over 63% higher than for one using System 1, the most conventional and lowest cost option. The order of cost, from the least expensive system to the most expensive, is 1,4,2,3,5.

Are There Differences in the Capital Investment Required?

The scorecard for the capital intensiveness of the five systems largely follows the pattern of the annual cost to consumers. In order, from least to most capital intensive, are Systems 1, 4, 3, 2, 5. Because capital is itself a scarce resource, utilities most likely will show most interest in Systems 1 and 4.

Which Has the Best System Performance?

Because all five systems contain at least one element not yet proven in commercial service, such things as reliability, the degree of redundancy needed in a system, and the ability to integrate smoothly the new devices into a system are difficult to assess, more so than for most other comparison attributes. We judge, however that, overall, the most conventional system is most likely to give the best performance. System performance, from best to worst comes in this order: Systems 1, 2, 4, 3, 5.

Which System is Most Efficient?

When making a comparison of system efficiency, we were careful to account for energy losses at every step in proceeding from the coal mine to the heated and cooled residence. All fuel-cell systems are considerably more efficient than the most conventional system, System 1. Indeed, System 5 is 75% efficient, while System 1 is only 41% efficient. Systems 2, 3, and 4 possess nearly equal efficiencies in the 64% to 67% range. This attribute is particularly important because it shows that the systems using fuel cells required less coal to accomplish the same end—a virtue that, besides conserving resources, carries over into lessened environmental impact.

What About Air Quality?

Because maintenance of air quality around electric power generation plants is a vexing and costly problem, the relative scores for this indicator could prove especially important to utilities in the years ahead. We weighted equally pollutants emitted at the fuel production site and the fuel consumption site (both overwhelm the emissions from fuel transportation). Again, all three systems using fuel cells are superior to the two more conventional systems, with System 5 being the cleanest and System 1 emitting the most pollutants. In order, from least to most polluting are Systems 5, 2, 3, 4, 1.

Are There Differences in Water Quality?

For this indicator we weighted equally effluents and water consumption at the fuel production and the fuel consumption locations.

All three fuel-cell systems are cleaner than the two more conventional systems. Again, System 5 is the cleanest, but this time System 4 degrades water quality the most. In order of cleanliness are Systems 5, 2, 3, 1, 4.

How Do They Compare on Solid Waste?

Most solid waste for this set of five systems is produced as ash in converting the coal to a more useful energy form. Consequently, scores in this category essentially mirror the overall system energy efficiency ratings—the most efficient System 5 also produces the least solid waste and the least efficient System 1 produces the most solid waste. Systems 2, 3, 4 are nearly tied, and produce about the same intermediate quantities.

What About Land Use, Noise and Aesthetics?

The three parameters are closely linked because aesthetics and human exposure to noise produced are greatly affected by location and the amount of land occupied or disturbed. Overall, least obtrusive is System 5 and the most obtrusive is System 1.

Is There a Pattern in the Comparison?

A striking pattern emerges when we assemble the scores for all categories of comparison. The fuel-cell systems are the most costly—to build and install as well as in end-use cost to consumers—but are the most environmentally benign and consume the least coal to get the heating and cooling job done.

We expected from the outset of this study that the fuel cells themselves would be clean compared to alternatives, but our finding that entire fuel-cell systems from resource extraction to final demand offer overall environmental benefits is new.

Will Fuel Cell Systems Actually Be Used?

How the trade-off between environmental cleanliness and economic cost will be valued in the next several decades will prove crucial to the question of whether fuel-cell systems resembling those we have examined will actually be deployed in meaningful numbers. One thing is certain: Fuel-cell systems possess a mixture of attributes much different from the more conventional electric power systems. As a result, U.S. utilities will have available an important new electric power option in the years ahead.

Full analysis is available in the 500-page report: "Comparative Assessment of Residential Energy Supply Systems That use Fuel Cells," Environmental Protection Agency, Report No. 600/7-79-105b, 1979.

ACKNOWLEDGMENTS

The work reported here was sponsored by the U.S. Environmental Protection Agency under Contract 68-02-2180. The EPA Project officer was Gary L. Johnson of the Special Studies Staff, Industrial Environmental Research Laboratory, Research Triangle Park, North Carolina.

The bulk of the project work was carried out at SRI International, Menlo Park, California, under the leadership of Dr. Robert V. Steele in the Center for Resource and Environmental Systems Studies. Overall project supervision was provided by Dr. Edward M. Dickson who also wrote the executive summary and aided in compiling and editing the final report.

Most of the systems analysis, and the analysis of residential heating and cooling requirements, was carried out by Dr. Steele. Roger Goldstein, assisted by other members of SRI's Energy Center, carried out the engineering and economic analysis of energy system components (excluding fuel cells and residential heating and cooling equipment). Specification of environmental control requirements for coal conversion facilities was done by Dr. David Bomberger of the Environmental Control Department while environmental analysis of other energy system components was performed by Roy Hays, Mary Gray and Kristin Clark.

Under subcontract to SRI International, Exxon Research and Engineering Co., Lindon, New Jersey, carried out all the conceptual design work, cost and efficiency calculations, and environmental analysis for the phosphoric acid and molten carbonate fuel-cell power plants. Exxon also provided the overview of fuel-cell technology

presented in Chapter II. George Ciprios of Exxon supervised the subcontracting effort.

Others who assisted in the report but not cited as authors include Dr. Buford R. Holt who assisted in the compilation of environmental impact data and in the development of criteria for assessing the relative impacts of air pollutants. The procedure for calculating residential heating and cooling loads was programmed by Dr. Barry Scott-Walton. The editor for the final report was Barbara J. Stevens, and the illustrations were done by Grace Tsai and L. H. Wu.

CONTENTS

LIST OF ILLUSTRATIONS xix

LIST OF TABLES. xxv

GLOSSARY OF ABBREVIATED TERMS xxxiii

GLOSSARY OF UNITS xxxiii

I INTRODUCTION. I-1

II OVERVIEW OF FUEL-CELL TECHNOLOGY. II-1

A. The Fuel-Cell Concept II-1

B. Fuel Cell Applications II-4

C. Potential Fuel Cell Advantages and Disadvantages . . II-7

D. The Complete Fuel-Cell System II-11
1. Fuel-Cell Reactants II-12
2. Fuel-Cell Operating Characteristics II-16
3. Fuel-Cell Economics II-20
4. Fuel-Cell Technologies and Trade-Offs II-24

E. Specific Fuel-Cell Technologies II-26
1. Phosphoric Acid Fuel Cells II-26
2. Molten Carbonate Fuel Cells II-29
3. Solid Oxide Fuel Cells II-34
4. Alkaline Fuel Cells II-36
5. Ion Exchange Membrane Cells II-38

III SELECTION OF ENERGY SUPPLY SYSTEMS FOR DETAILED ANALYSIS. . . III-1

A. Criteria for Proposed Systems III-1

B. Proposed Systems III-3
1. Type 1: Conventional Power Plant/SNG III-3
2. Type 2: 26-MW Fuel-Cell Power Plant III-8
3. Type 3: Combined-Cycle Power Plant III-10
4. Type 4: 100-kW Fuel-Cell Power Plant with Heat Recovery III-10

C. Evaluation of System Components III-13
1. Cost and Efficiency III-13
2. Sulfur Dioxide Emissions III-14
3. Ranking of Proposed Systems III-16

D. Selection of Systems III-16

E. References--Chapter III III-22

IV CONCEPTUAL SYSTEMS DESIGNS IV-1

A. System 1 . . . . . IV-2
1. Coal Mine IV-2
2. Unit Train IV-7
3. Coal-Fired Power Plant IV-10
4. Electricity Transmission and Distribution . . . IV-13
5. Coal Gasification Facility IV-16
6. Gas Pipeline IV-24
7. Gas Distribution IV-25
8. Gas Furnace and Air Conditioner IV-26

B. System 2 . . . . . IV-29
1. Coal Mine IV-29
2. Coal Gasification Facility IV-29
3. Gas Pipeline IV-29
4. Gas Distribution IV-29
5. 26-MW Fuel-Cell Power Plant IV-31
6. Distribution of Electricity IV-47
7. Heat Pump IV-48

C. System 3 . . . . . IV-53
1. Coal Mine IV-53
2. Coal Liquefaction Plant IV-53
3. Liquids Pipeline IV-61
4. Distribution of Naphtha IV-62
5. 26-MW Fuel-Cell Power Plant IV-63
6. Distribution of Electricity IV-72
7. Heat Pump IV-72

D. System 4 . . . . . IV-74
1. Coal Mine IV-74
2. Coal Liquefaction Plant IV-74
3. Liquids Pipeline IV-78
4. Fuel Distribution IV-78
5. Combined-Cycle Power Plant IV-79
6. Transmission and Distribution of Electricity IV-82
7. Heat Pump IV-82

E. System 5 . . . . . IV-84
1. Coal Mine IV-84

2. Coal Gasification Facility IV-84
3. Gas Pipeline IV-84
4. Gas Distribution IV-84
5. 100-kW Fuel-Cell Power Plant IV-84
6. Heating and Cooling System IV-104

F. References--Chapter IV IV-112

V THERMAL EFFICIENCY OF THE SYSTEM COMPONENTS V-1

A. Coal Mine V-2

B. Unit Train V-3

C. Coal-Fired Power Plant V-4

D. Coal Gasification Plant V-5

E. Coal Liquefaction Plant V-7

F. Gas Pipeline V-10

G. Liquids Pipeline V-10

H. Liquid Fuel Distribution V-11

I. Gas Distribution V-12

J. Combined-Cycle Power Plant V-12

K. 26-MW Fuel-Cell Power Plant (SNG) V-14

L. 26-MW Fuel-Cell Power Plant (Naphtha) V-15

M. Electricity Transmission and Distribution V-15

N. 100-kW Fuel-Cell Power Plant
with Heat Recovery V-17

O. Gas Furnace and Air Conditioner V-21

P. Heat Pumps V-23

Q. Heat Delivery System V-26

R. References--Chapter V V-30

VI ENVIRONMENTAL IMPACTS OF SYSTEM COMPONENTS VI-1

A. Coal Mine VI-1

1. Environmental Setting VI-2
2. Surface Mining Operation Requirements VI-3
3. Environmental Impacts of Surface Mining VI-5

B. Unit Train (Coal). VI-10
1. Loading/Unloading VI-10
2. Line Haul VI-10

C. Coal-Fired Power Plant VI-15
1. Flue Gas Treatment System VI-18
2. Solids Handling System VI-20
3. Pollutant Emissions VI-21

D. Coal Gasification Plant VI-28
1. Sulfur Recovery Plant VI-32
2. Process Condensate Treatment System VI-34
3. Solids Processing system VI-37
4. Pollutant Emissions VI-37

E. Coal Liquefaction Plant VI-42
1. Pollution Control System VI-42
2. Pollutant Emissions VI-47

F. Pipelines VI-50
1. Physiography VI-50
2. Hydrology VI-52
3. Vegetation VI-53
4. Wildlife VI-54
5. Air Quality VI-55

G. Fuels Distribution VI-56

H. Combined-Cycle Power Plant VI-61

I. 26-MW Fuel-Cell Power Plant (SNG) VI-64
1. Spent Fuel-Cell Stack Disposal VI-66
2. Spent Catalyst Guard Bed Disposal VI-66
3. Noise VI-67

J. 26-MW Fuel-Cell Power Plant (Naphtha) VI-67

K. Electricity Transmission and Distribution VI-69
1. Transmission Line Characteristics VI-70
2. Transmission Line Impacts VI-71

L. Gas Furnace VI-77

M. 100-kW Fuel-Cell Power Plant VI-77
1. Spent Fuel-Cell Stack Disposal VI-81
2. Spent Catalyst Bed Disposal VI-81
3. Normal Power Plant Operation VI-82

O. References--Chapter VI VI-83

VII CAPITAL AND OPERATING COSTS OF SYSTEM COMPONENTS. VII-1

A. Coal Mine. VII-3

B. Unit Train VII-7

C. Coal-Fired Power Plant VII-7

D. Coal Gasification Plant. VII-13

E. Coal Liquefaction Plant. VII-13

F. Gas Pipeline VII-20

G. Liquids Pipeline VII-27

H. Liquid Fuel Distribution VII-32

I. Gas Distribution VII-35

J. Combined-Cycle Power Plants. VII-38

K. 26-MW Fuel-Cell Power Plant (SNG). VII-38
1. Fuel-Cell Trailer Cost. VII-42
2. Reformer Module Cost. VII-46
3. Equipment Module Cost VII-46
4. Condenser Cost. VII-47
5. Power Conditioning Costs. VII-47
6. Total Power Plant VII-48

L. 26-MW Fuel-Cell Power Plant (Naphtha). VII-53

M. Electricity Transmission and Distribution. VII-62

N. 100-kW Fuel-Cell Power Plant VII-66

O. Hot Water Distribution System. VII-72

P. Gas Furnace and Air Conditioner. VII-76

Q. Heat Pumps VII-78

R. References--Chapter VII. VII-79

VIII THERMAL AND ELECTRICAL LOAD FACTORS VIII-1

A. Light and Appliance Loads. VIII-2

B. Daily Temperature Variations VIII-5

C. Thermal Response of the Residences VIII-7

D. Energy Consumption for Heating and Cooling VIII-12

E. References--Chapter VIII VIII-24

IX COMPARATIVE ANALYSIS. IX-1

A. Energy Efficiency. IX-1

B. Economics. IX-10
1. Cost of Heating and Cooling IX-10
2. Capital Intensiveness IX-19

C. Environmental Impact IX-24
1. Pollutant Emissions IX-24
2. Land Use, Noise, and Aesthetics IX-37

D. System Performance IX-42

E. References--Chapter IX IX-48

X SUMMARY AND CONCLUSIONS X-1

A. Summary of Advantages and Disadvantages. X-1
1. System 1. . . . . X-1
2. System 2. . . . . X-3
3. System 3. . . . . X-3
4. System 4. . . . . X-3
5. System 5. . . . . X-3

B. Conclusions. X-4

APPENDICES

A ENTHALPIES BASED ON THE GIRDLER CATALYSTS DATA HANDBOOK. A-1

B MOLTEN CARBONATE FUEL CELL PERFORMANCE B-1

C ENERGY SUPPLY/DEMAND PROGRAM FOR RESIDENCES SUPPLIED BY THE 100-kW FUEL-CELL POWER PLANT C-1

LIST OF ILLUSTRATIONS

II-1	The Fuel-Cell Concept.	II-2
II-2	Conventional Energy Generation	II-2
II-3	Efficiency Characteristics of Total Energy System. . . .	II-5
II-4	Efficiency of Various Energy Conversion Devices.	II-8
II-5	Part-Load Efficiency	II-8
II-6	The Fuel-Cell System	II-12
II-7	The EMF Series	II-14
II-8	Fuel-Cell Losses	II-18
II-9	Characteristic Fuel-Cell Performance Curve	II-18
II-10	Fuel-Cell Power Plant.	II-19
II-11	Effect of Current Load on Voltage Efficiency	II-19
II-12	Capital Charges.	II-21
II-13	Fuel Charges	II-21
II-14	Stack Replacement Charges.	II-23
II-15	Design Point Selection	II-23
II-16	Progress in Molten Carbonate Fuel-Cell Performance . . .	II-32
III-1	Type 1a: Coal-Fired Power Plant/SNG	III-5
III-2	Type 1b: Oil-Fired Power Plant/SNG.	III-7
III-3	Type 2: 26-MW Fuel-Cell	III-9
III-4	Type 3: Combined-Cycle Power Plant.	III-11
III-5	Type 4: 100-kW Fuel Cell with Heat Recovery	III-12
IV-1	Block Flow Diagram of System 1	IV-3
IV-2	Dragline Method of Overburden Removal.	IV-5
IV-3	Block Flow Diagram for an 800-MW Coal-Fired Power Plant.	IV-12

IV-4	High-Voltage Transmission Economy for Long Distance. . .	IV-14
IV-5	Block Flow Diagram of Hygas SNG Plant.	IV-19
IV-6	Cooling Capacity of the Westinghouse SL030C/EC030 Air Conditioner	IV-28
IV-7	Block Flow Diagram of System 2	IV-30
IV-8	Block Flow Diagram for 26-MW Fuel-Cell Power Plant (SNG Fuel).	IV-33
IV-9	Fuel Cell Trailer Layout	IV-40
IV-10	Reformer/Heat Exchanger Package.	IV-43
IV-11	Equipment Module Layout.	IV-45
IV-12	Power Plant Layout	IV-46
IV-13	Recommended Heat Pump Configuration for Split System Air-to-Air Units.	IV-50
IV-14	Heating and Cooling Capacity of 26.0 MJ/hr (24,600 Btu/hr) Heat Pump	IV-52
IV-15	Block Flow Diagram of System 3	IV-54
IV-16	H-Coal Process Flow Diagram.	IV-56
IV-17	Block Flow Diagram for 26-MW Fuel-Cell Power Plant (Naphtha Fuel)	IV-64
IV-18	Block Flow Diagram of System 4	IV-75
IV-19	H-Coal Process Flow Diagram.	IV-76
IV-20	Combined-Cycle Power Plant Block Flow Diagram.	IV-81
IV-21	Block Flow Diagram of System 5	IV-85
IV-22	100-kW Power Plant Components.	IV-87
IV-23	Heat Integration for 100-kW Fuel-Cell Power Plant. . . .	IV-88
IV-24	Phosphoric Acid Fuel Cell Performance Data	IV-93
IV-25	Phosphoric Acid Fuel Cell Performance Curve.	IV-97
IV-26	Reformer Package for 100-kW Power Plant.	IV-102
IV-27	System Layout for 100-kW Power Plant	IV-105

IV-28 Site Plan for 100-kW Fuel-Cell Power Plant and Townhouses IV-107

IV-29 Schematic of Hot Water and Space Heat System Using Recovered Fuel-Cell Heat. IV-108

IV-29 Heating and Cooling Capacities of 19.3 MJ/hr (18,300 Btu/hr) Heat Pump IV-110

V-1 Effect on Thermal Efficiency of Operating the 100-kW Total Energy System at Part Load. V-19

V-2 Heat Availability for 100-kW Fuel-Cell Power Plant . . . V-20

V-3 Effect of Water Return Temperature on Overall Thermal Efficiency. V-22

V-4 Coefficient of Performance of Westinghouse SL030 Air Conditioner V-24

V-5 Coefficients of Performance of Advanced Heat Pumps . . . V-27

V-6 Heat Transfer Rates From Hot Water Delivery System to Space Heating. V-29

VI-1 Integrated Pollution Control System for an 800-MW Coal-Fired Power Plant. VI-17

VI-2 Solids Handling System for an 800-MW Coal-Fired Power Plant. VI-22

VI-3 Integrated Air, Water, and Solids Pollution Control System for a Hygas Coal Gasification Plant That Produces 7.8 Million nm^3 of SNG per Day . . . VI-31

VI-4 Wastewater Treatment Plant for Coal Gasification VI-36

VI-5 Integrated Pollution Control System for an H-Coal Liquefaction Plant That Produces 7,950 nm^3 per Day of Fuel VI-46

VII-1 Sensitivity of Unit Train Costs to Volume of Traffic on New Portion (80 km) of Track VII-10

VII-2 Sensitivity of the Cost of Electricity to Plant Capital Cost and Delivered Coal Cost. VII-14

VII-3 Sensitivity of the Cost of SNG to Plant Capital Cost and Coal Cost VII-17

VII-4 Sensitivity of the Cost of Distillate Fuel Oil to Plant Capital Cost and Coal Cost. VII-23

VII-5 Sensitivity of the Cost of Hydrotreated Naphtha to Plant Capital Cost and By-Product Fuel Oil Credit . VII-24

VII-6 Sensitivity of SNG Transmission Cost to Pipeline Capital Cost and SNG Cost VII-28

VII-7 Effect of Pipe Diameter on SNG Transmission Costs. . . . VII-29

VII-8 Sensitivity of Liquid Fuel Transmission Cost to Pipeline Capital Cost VII-33

VII-9 Railroad Tank Car Transport Costs (Fuel Oil) VII-34

VII-10 Tank Truck Transportation Costs (Naphtha). VII-36

VII-11 Sensitivity of Cost of Electricity to Power Plant Capital Cost and Distillate Fuel Cost VII-41

VII-12 Sensitivity of the Cost of Electricity to Power Plant Capital Cost and SNG Cost VII-54

VII-13 Sensitivity of the Cost of Electricity to Power Plant Cost and Naphtha Cost VII-61

VII-14 Sensitivity of the Cost of Electricity to Load Factor and Hot Water Credit. VII-74

VIII-1 Variation in Hourly Average Light and Appliance Loads and DHW Demand with Time of Day - Residence 3 . . . VIII-4

VIII-2 DHW Demand Relative to Fuel Cell Heat Available from Operations of Lights and Appliances VIII-16

VIII-3 Hourly Average Temperature, Heating Load, and Supply of Recovered Fuel Cell Heat for Residence 3 on the Coldest Day of the Year VIII-17

VIII-4 Hourly Average Electrical Loads for Residence 3 on the Coldest Day of the Year VIII-18

VIII-5 Variations in Average Space Heating Electrical Load and Delivered Fuel Heat with External Temperature . VIII-20

VIII-6 Hourly Average Temperature and Electrical Load for Residence 3 on the Hottest Day of the Year. VIII-22

IX-1 Annual Energy Flows and Energy Efficiency for System 1. . . . . IX-4

IX-2 Annual Energy Flows and Energy Efficiency for System 2. . . . . IX-5

IX-3 Annual Energy Flows and Energy Efficiency for System 3. . . . . IX-6

IX-4 Annual Energy Flows and Energy Efficiency for System 4. . . . . IX-7

IX-5 Annual Energy Flows and Energy Efficiency for System 5. . . . . IX-8

IX-6 Total Annual Energy Flows (per Residence) for Fuel-Cell Power Plant Supplying Townhouses. . . IX-9

IX-7 Variation in the Cost of Heating and Cooling with Heating Load - System 5. . . . . IX-16

C-1 Program for Energy Supply/Demand Calculations. C-1

LIST OF TABLES

II-1	Efficiency Limits of Conventional Thermal Energy Conversion Systems	II-3
II-2	Full Selection Trade-Off	II-15
II-3	Estimated Installed Investment Costs for Fuel-Cell Power Plants	II-24
II-4	Fuel-Cell Technology Classifications	II-25
III-1	Categorization of Proposed Residential Energy Supply Systems	III-4
III-2	Ranking of Cost, Efficiency, and SO_2 Emissions for Energy Supply Systems	III-17
IV-1	Main Process Flows for an 800-MW Coal-Fired Power Plant	IV-14
IV-2	Economic Power Loading of Transmission Lines	IV-15
IV-3	Main Process Flows for SNG from Coal via the Hygas Process	IV-22
IV-4	Process Flow Streams for 26-MW Fuel-Cell Power Plant (Naphtha)	IV-37
IV-5	Equipment List for 26-MW Fuel-Cell Power Plant (SNG)	IV-38
IV-6	Piping Specifications	IV-47
IV-7	Composition of Major Streams in H-Coal Process	IV-57
IV-8	Properties of H-Coal Distillate Fuel Oils	IV-58
IV-9	Process Flow Steams for 26-MW Fuel-Cell Power Plant (Naphtha)	IV-69
IV-10	Equipment List for 26-MW Fuel-Cell Power Plant (Naphtha)	IV-73
IV-11	Composition of Major Streams in H-Coal Process	IV-77
IV-12	Mass Flow Rates for 270-MW Combined-Cycle Power Plant	IV-83
IV-13	Additional Details for Figure IV-23	IV-94

IV-14 Process Conditions and Flow Rates for 100-kW Fuel-Cell Power Plant. IV-98

IV-15 100-kW Fuel-Cell Power Plant IV-101

V-1 Energy Balance for an 800-MW Coal-Fired Power Plant That Uses Subbituminous Coal. V-5

V-2 Energy Balance for a 7.8 x 10^6 nm^3 (275 x 10^6scf) per Day Coal Gasification Plant Based on the Hygas Process. V-6

V-3 Energy Balance for a 7950 m^3 (50,000 bbl) per Day Coal Liquefaction Plant That Produces Distillate Fuel Oil. V-8

V-4 Energy Balance for a 7630 m^3 (48,000 bbl) per Day Coal Liquefaction Plant That Produces Naphtha and Fuel Oil V-9

V-5 Energy Balance for a 270-MW Combined-Cycle Power Plant. V-12

V-6 Estimated Heat Rates at Part Load for Combined-Cycle Power Plant V-13

V-7 Energy Balance for a 24.0-MW Fuel-Cell Power Plant that Uses SNG V-14

V-8 UTC Projection of Part-Load Heat Rate for Molten Carbonate Fuel Cells Using Reformable Fuels. V-16

V-9 Energy Balance for a 25.6-MW Fuel-Cell Power Plant That Uses Naphtha V-16

V-10 Energy Balance for a 100-kW Fuel-Cell Power Plant That Uses SNG. V-18

V-11 Operating Characteristics of 100-kW Total Energy Power Plant at Part Load. V-18

VI-1 Projected Particulate Emissions from Surface Mines--Gillette Area. VI-6

VI-2 Air Pollutant Emissions for a 4.5 Million Tonne (5 Million Ton) per Year Surface Mine VI-8

VI-3 Air Pollutant Emissions from Diesel Locomotives-- 100-Car Unit Coal Train VI-14

VI-4 Emissions from a Coal-Fired Power Plant. VI-16

VI-5 Summary of Major Emissions from an 800-MW Coal-Fired Power Plant. VI-23

VI-6 Concentrations of several Toxic Trace Elements in Powder River Basin Coal. VI-26

VI-7 Emission of Toxic Trace Elements from an 800-MW Coal-Fired Power Plant. VI-27

VI-8 Emissions of Polycyclic Aromatic Hydrocarbons from an 800-MW Coal-Fired Power Plant VI-28

VI-9 Major Sources of Pollution for a Coal Gasification Plant VI-30

VI-10 Major Emissions from Hygas Coal Gasification (7.8 Million nm^3 of SNG per Day) VI-39

VI-11 Combustion-Related Emissions of Fine Particulates, Trace Elements, and PAH from the Hygas Coal Gasification Plant VI-40

VI-12 Major Sources of Pollution for a Coal Liquefaction Plant VI-43

VI-13 Major Emissions from H-Coal Liquefaction (7,950 m^3 of Distillate Fuel Oil per Day) VI-48

VI-14 Combustion-Related Emissions of Fine Particulates, Trace Elements, and PAH from an H-Coal Liquefaction Plant VI-49

VI-15 Air Pollutant Emissions from a Compressor Station on an 81 cm (32 in.) Natural Gas Pipeline VI-57

VI-16 Air Pollutant Emissions from a Pumping Station on a 51 cm (20 in.) Liquid Fuels Pipeline. VI-57

VI-17 Diesel Truck Noise Sources VI-59

VI-18 Urban and Suburban Detached Housing Residential Areas and Approximate Daytime Residual Noise Level (L_{90}) VI-60

VI-19 Air Pollutant Emissions from a Diesel-Powered Tank Truck VI-61

VI-20 Emissions from a 270-MW Combined-Cycle Power Plant . . . VI-62

VI-21 Emissions of Toxic Trace Elements from a 270-MW Combined-Cycle Power Plant. VI-63

VI-22 Emission of PAH from a 270-MW Combined-Cycle Power Plant. VI-64

VI-23 Composition of Effluent Process Stream for a 24.0-MW Fuel-Cell Power Plant VI-65

VI-24 Predicted Reformer Furnace NO_x Production VI-65

VI-25 Composition of Effluent Process Stream for a 25.6-MW Fuel-Cell Power Plant VI-68

VI-26 Predicted Reformer Furnace NO_x Production VI-68

VI-27 Average Requirements for Rights-of-Way VI-71

VI-28 60-Hz Electric and Magnetic Fields VI-75

VI-29 Emission of Air Pollutants from a 70-MJ/hr Residential Gas Furnace. VI-78

VI-30 Composition of Effluent Stream from a 100-kW Fuel-Cell Power Plant. VI-78

VI-31 Predicted Reformer Furnace NO_x Production VI-79

VI-32 Published Pollution Characteristics of Experimental Phosphoric Acid Fuel Cells. VI-80

VII-1 Capital Investment Required for a 4.5 Million Tonne (5 Million Ton) per Year Surface Coal Mine in the Powder River Basin. VII-5

VII-2 Capital Investment Required for a 4.5 Million Tonne (5 Million Ton) per Year Surface Coal Mine in the Powder River Basin. VII-6

VII-3 Estimated Investment for 80 km (50 mi) of New Track and Two 100-Car Unit Trains VII-8

VII-4 Operating Cost and Revenue Required for New Unit Train, 80 km (50 mi) New Track, and 1,200 km (750 mi) Existing Track. VII-9

VII-5 Capital Investment for 800-MW Coal-Fired Power Plant with FGD VII-11

VII-6 Operating Costs and Revenue Requirements for 800-MW Coal-Fired Power Plant with FGD (35% Load Factor) VII-12

VII-7 Investment Required for a 7.8×10^6 nm^3 (275×10^6scf) per Day SNG Plant Based on the Hygas Process. VII-15

VII-8 Operating Costs and Revenue Requirements for a 7.8×10^6 nm^3 (275×10^6 scf) per Day SNG Plant Based on the Hygas Process. . . . VII-16

VII-9 Capital Investment for a 7,950 nm^3 (50,000 bbl) per Day Plant Producing Distillate Fuel Oil from Coal by the H-Coal Process VII-18

VII-10 Capital Investment for 7,630 nm^3 (48,000 bbl) per Day Plant Producing Naphtha and Fuel Oil from Coal by the H-Coal Process VII-19

VII-11 Operating Costs and Revenue Requirements for a 7,950 nm^3 (50,000 bbl) per Day Plant Producing Distillate Fuel Oil from Coal by the H-Coal Process VII-21

VII-12 Operating Costs and Revenue Requirements for a 7,630 nm^3 (48,000 bbl) per Day Plant Producing Naphtha and Fuel Oil from Coal by the H-Coal Hygas Process VII-22

VII-13 Capital Investment for a 81-cm (32-in.) Diameter Gas Transmission Pipeline--1,300 km (800 mi). . . . VII-25

VII-14 Operating Costs and Revenue Requirements for an 81-cm (32 in.) Diameter Gas Pipeline --1,300 km (800 mi) VI-26

VII-15 Capital Investment for a 51-cm (20-in.) Diameter Coal Liquids Pipeline -- 1,300 km (800 mi) VII-30

VII-16 Operating Costs and Revenue Requirements for a 51-cm (20-in.) Diameter Liquids Pipeline -- 1,300 km (800 mi). VII-31

VII-17 Capital Investment for a 270 MW Combined-Cycle Power Plant Using Distillate Fuel from the H-Coal Process. VII-39

VII-18 Operating Costs and Revenue Requirements for a 270-MW Combined-Cycle Power Plant Using Distillate Fuel from Coal (35% Load Factor) VII-40

VII-19 Fuel-Cell Stack Characteristics. VII-43

VII-20 Fuel-Cell Trailer Cost Summary VII-44

VII-21 Equipment Module Cost Breakdown. VII-47

VII-22 24.0-MW Fuel-Cell Power Plant Cost Estimate. VII-49

VII-23 Optimistic Cost Projection for 24-MW Fuel-Cell Power Plant VII-52

VII-24 Operating Costs and Revenue Requirements for a 24.0-MW Fuel-Cell Power Plant VII-53

VII-25 Cost Breakdown of Naphtha Reformer Package VII-55

VII-26 Equipment Module Cost Breakdown. VII-56

VII-27 25.6-MW Fuel-Cell Power Plant Cost Estimate. VII-57

VII-28 Optimistic Cost Projection for 25.6-MW Fuel-Cell Power Plant VII-59

VII-29 Operating Costs and Revenue Requirements for a 25.6-MW Fuel-Cell Power Plant VII-60

VII-30 Fuel-Cell Stack Costs. VII-67

VII-31 Cost Summary for 100-kW Power Plant. VII-70

VII-32 Optimistic Projection of Advanced 100-kW Power Plant. VII-71

VII-33 Operating Costs and Revenue Requirements for a 100-kW Fuel-Cell Power Plant with Heat Recovery. VII-73

VII-34 Capital Investment Required for a System That Delivers 82°C (180°F) Hot Water to Twenty Townhouses VII-75

VII-35 Capital Cost for Residential Heating and Cooling System--Gas Furnace and Air Conditioner VII-77

VII-36 Capital Costs for Residential Heating and Cooling Systems -- Heat Pumps VII-78

VIII-1 Monthly Light and Appliance Electrical Loads for Three Types of Residences VIII-3

VIII-2 Normal Monthly Average Temperatures, °C (°F) VIII-5

VIII-3 Comparison of Normal Monthly Conditions With Actual Monthly Conditions of Months Chosen as "Best Match". VIII-6

VIII-4 Components of the Cooling Load -- Omaha Summer Afternoon Conditions VIII-10

VIII-5 Summary of Heating and Cooling Loads by Month. VIII-11

VIII-6 Electricity Consumption for Heating and Cooling. VIII-13

VIII-7 Residence 3 Electricity Consumption and Fuel-Cell Heat Utilization VIII-23

IX-1 Cost of Heating and Cooling for System 1 . . . . . IX-12

IX-2 Cost of Heating and Cooling for System 2 . . . . . IX-12

IX-3 Cost of Heating and Cooling for System 3 . . . . . IX-13

IX-4 Cost of Heating and Cooling for System 4 . . . . . IX-13

IX-5 Cost of Heating and Cooling for System 5 . . . . . IX-14

IX-6 Capital Intensiveness of the System Components IX-20

IX-7 Capital Intensiveness for System 1 . . . . . IX-21

IX-8 Capital Intensiveness for System 2 . . . . . IX-22

IX-9 Capital Intensiveness for System 3 . . . . . IX-22

IX-10 Capital Intensiveness for System 4 . . . . . IX-23

IX-11 Capital Intensiveness for System 5 . . . . . IX-23

IX-12 Pollutant Emissions Associated with System 1 . . . . . IX-25

IX-13 Pollutant Emissions Associated with System 2 . . . . . IX-26

IX-14 Pollutant Emissions Associated with System 3 . . . . . IX-27

IX-15 Pollutant Emissions Associated with System 4 . . . . . IX-28

IX-16 Pollutant Emissions Associated with System 5 . . . . . IX-29

IX-17 Geographically Weighted Pollutant Emissions for the Five Systems. IX-32

IX-18 Occupational Exposure Standards for Toxic Pollutants Time-Weighted Averages. IX-33

IX-19 Weighting Factors for the Relative Hazards of Air Pollutants IX-35

IX-20 Hazard-Weighted Air Pollutant Emission Factors for the Five Systems IX-35

IX-21 Land Use Factors for System Components IX-38

IX-22 Total Land Use for the Five Systems. IX-39

IX-23 Sources of Involuntary Exposure to High Noise Levels IX-40

X-1 System Rankings in Various Categories. X-2

GLOSSARY OF ABBREVIATED TERMS

AN	audible noise
BaP	benzo(a)pyrene
COP	coefficient of performance
DCF	discounted cash flow
DHW	domestic hot water
ESP	electrostatic precipitator
FGD	flue gas desulfurization
HDS	hydrodesulfurization
HHV	higher heating value
L&A	light and appliances
NSPS	new source performance standards
PAH	polycyclic aromatic hydrocarbons
PFI	plant facilities investment
SNG	synthetic natural gas

GLOSSARY OF UNITS

bbl	barrel
Btu	British thermal unit
cm	centimeter
dB	decibel
dBA	decibel measured on the "A" scale
E	cell potential
E^o	theoretical cell potential
EMF	electromotive force (half-cell potential

ft	foot
g	gram
gal	gallon
gal/min	gallon per minute
GJ	gigajoule
hr	hour
in.	inch
kg	kilogram
kJ	kilojoule
km	kilometer
kPa	kilopascal
kV	kilovolt
kW	kilowatt
kWh	kilowatt-hour
lb	pound
m	meter
m^3	cubic meter
mA	*milliampere*
mi	mile
MJ	megajoule
mph	miles per hour
MW	megawatt
nm^3	normal cubic meter
ppm	parts per million
psi	pounds per square inch
psia	pounds per square inch atmospheric
psig	pounds per square inch gauge
scf	standard cubic foot
tonne	metric ton
V	volt
yd^3	cubic yard

I. INTRODUCTION

Within the past few years, fuel cells have received substantial research and development attention. This R&D effort sponsored by the Environmental Protection Agency, the Department of Energy, the Electric Power Research Institute, the Gas Research Institute and individual companies, this R&D effort is endeavoring to commercialize first-generation fuel-cell power plants in the early 1980s, and to develop advanced fuel-cell technology for applications in the late 1980s and early 1990s.

Although fuel cells have been in existence since the early 1800s and were used successfully in the U.S. space program as spacecraft power plants, they have not yet become cost-competitive for terrestrial applications. Successful completion of current R&D programs would yield clean, cost-effective, energy-efficient power plants for use in utilities, industry, and buildings.

The deployment of fuel cells in dispersed electrical power plants promises considerable operational and environmental advantage over current methods of power generation. However, as the nation relies more on coal and coal-based fuels for its energy sources, the effects of the entire fuel cycle associated with new energy technologies will become more significant. Because of its continuing interest in fuel cells as potentially clean power sources, and its responsibility to understand the impacts of advanced energy systems, the Environmental Protection Agency (EPA) contracted with SRI International and its subcontractor, Exxon Research and Engineering, to perform an assessment of fuel cells and their associated fuel cycles.

The work reported here represents the first wide-ranging assessment of energy supply systems based on fuel cells. It addresses the environmental impacts, costs, energy efficiencies, and performance characteristics of several complete energy supply systems, including extraction of energy resources and the end use of the delivered energy. In particular, this work analyzes the advantages and disadvantages of energy supply systems based on fuel cells. The objective of this report is to determine whether fuel cells and the fuel cycles that support them will provide advantages over other systems in comparable applications. Because of the considerable potential for fuel cells to provide clean, efficient power generation, it is important to determine whether that potential can be realized when broader systems considerations are taken into account relative to alternatives in similar applications.

Both fuel-cell and nonfuel-cell systems are analyzed, but only systems comparable in terms of their primary energy resource, end use, and time frame for deployment are compared. The specific criteria used to select the systems (as determined by EPA in the Statement of Work) are discussed in Chapter III.

Our method of approach in the analysis was to specify the structure of the systems in a general way, then to describe the operating characteristics of the system components in detail. Next, we analyzed the economic, efficiency, environmental, and performance characteristics of the components. Finally, we combined the component parameters to determine the overall attributes of the systems.

The structure of this report closely follows the method of approach and is designed to present a logical, step-by-step approach to the description, analysis, and conclusions regarding the implementation of energy systems based on fuel cells.

Chapter II presents an overview of fuel-cell technology, economics, and applications. Designed to familiarize the reader with the fuel-cell

concept, it provides a basis for understanding the technical discussions of fuel cells in subsequent chapters. Electrochemical reactions, operational characteristics, and innovative fuel-cell technologies are described.

Chapter III outlines the procedures by which five energy systems were selected for detailed analysis. Complete energy systems included coal extraction and transportation, coal conversion, product transportation, electricity generation and transmission, and residential energy use. The selection procedure first limited the number of systems to 12 energy supply possibilities, which included several power plants using a variety of coal-derived fuel types. Utilizing a careful ranking procedure, we chose five systems representative of viable, economical, efficient energy supply systems likely to be available after 1985 but before 2000.

Chapter IV presents detailed descriptions of the five systems, including the particular technology chosen for each system component, the operation of each component, and, where appropriate, flow charts, material balances and equipment layouts. In the case of fuel-cell power plants, detailed information is presented on design criteria, fuel-cell performance, and power plant components.

Chapter V presents an analysis of the energy efficiency of each system component, based on thermal balances and estimated conversion efficiencies. Chapter VI describes the environmental aspects of the systems components, including the specification of environmental control equipment, rates of pollutant emissions to the air, water, and land, and discussion of such factors as land use, aesthetics, and noise. Chapter VII describes the economic aspects of the systems, including the capital costs of the systems components, the cost of operating each component, and cost sensitivity curves. In addition, detailed discussions of the cost components of fuel-cell power plants are included.

In Chapter VIII, the energy use characteristics of the residences supplied by the systems are determined. The monthly electricity consumption by lights and appliances is estimated, and a procedure for calculating monthly heating and cooling energy use is shown.

In Chapter IX, the areas of economics, energy efficiencies, environmental impact, and overall system performance of the five systems are analyzed and compared. Overall system performance parameters are derived based on system information described in previous chapters.

Finally, in Chapter X, the advantages and disadvantages of each system are summarized and conclusions are drawn regarding the relative merits of each, particularly those that use fuel cells.

II. OVERVIEW OF FUEL-CELL TECHNOLOGY

A. The Fuel-Cell Concept

A fuel cell is a device for converting the chemical energy of a fuel directly into electrical energy, using electrochemical reactions. Fuel-cell reactions are carried out selectively in two distinct, decoupled zones within a device that contains an ionically conductive (electrolytic) medium. Such a device is shown schematically in Figure II-1, using hydrogen as fuel, oxygen or air as oxidant, and an aqueous acid electrolyte. The reactions (in this example) take place within a porous electrode structure containing hydrophobic regions to permit access of gaseous reactants and hydrophilic regions accessible to the liquid electrolyte. Suitable catalysts may also be incorporated to increase reaction rates.

The specific fuel-cell reactions taking place at each electrode are as follows:

Anode reaction	$H_2 \longrightarrow 2H^+ + 2e^-$
Cathode reaction:	$\frac{1}{2}O_2$ (air) $+ 2H^+ + 2e^- \longrightarrow H_2O$
Overall reaction:	$H_2 + \frac{1}{2}O_2 \longrightarrow H_2O$ + direct electrical energy

The result is the direct generation of electrical energy (electrons) that can be used to produce useful work in external circuits.

Conventional energy conversion devices, on the other hand, operate in an indirect manner, shown schematically in Figure II-2. Chemical energy is first converted to heat in high-temperature combustion reactions. This heat, usually the form of steam, is converted to mechanical work in a steam turbine and then to electrical energy using a rotating electrical generator.

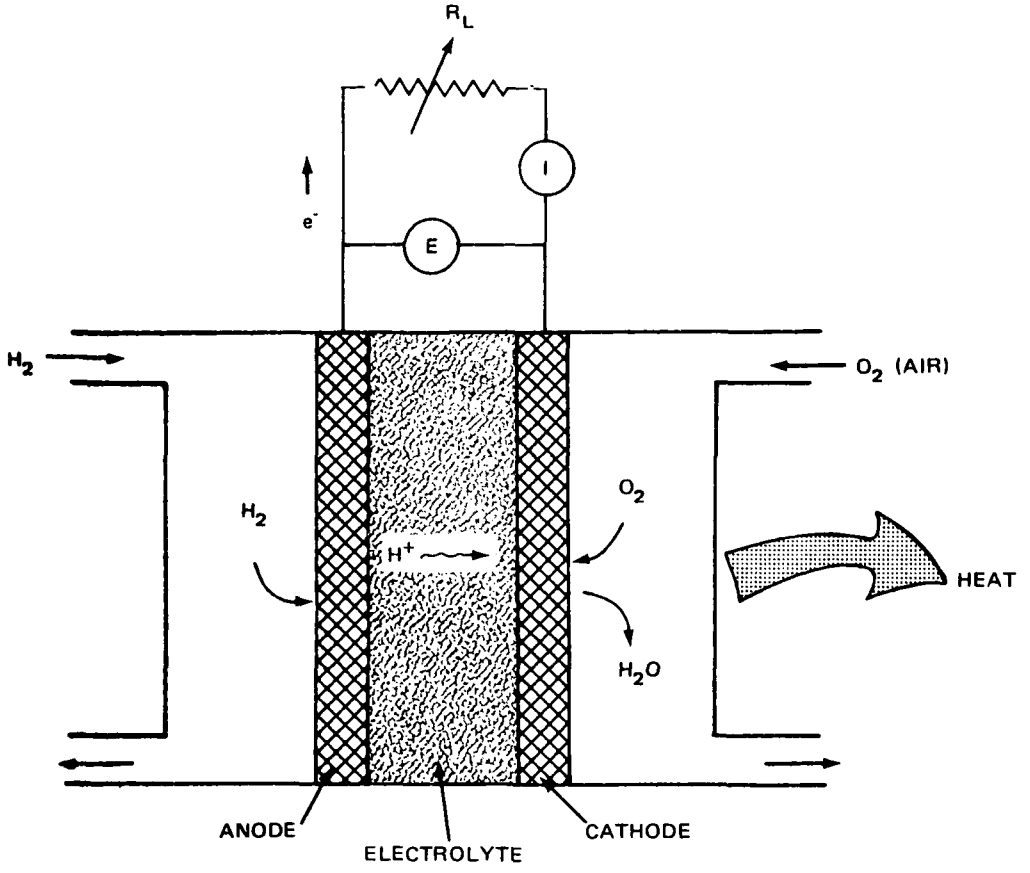

FIGURE II-1. THE FUEL-CELL CONCEPT

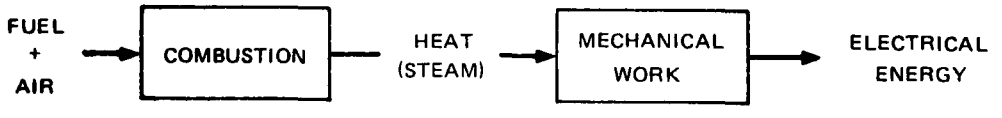

FIGURE II-2. CONVENTIONAL ENERGY GENERATION

The maximum conversion efficiency of a thermal cycle is given by the Carnot efficiency equation:

$$\text{Carnot efficiency} = \frac{\text{Net work done}}{\text{Total heat absorbed}} = \frac{T_H - T_c}{T_H}$$

where T_H and T_c are the absolute temperatures at which heat is absorbed and rejected to the environment, respectively. The effect of varying T_H on Carnot efficiency when the rejection temperature is fixed at 30°C (86°F) is shown in Table II-1.

Typically, modern conventional steam power plants operate with a T_H of about 500°C (930°F), yielding a maximum theoretical conversion efficiency of 61%. Mechanical and other losses further reduce the efficiency to a practical limit of about 40%. Attempts to improve this efficiency level by increasing T_H have been hindered by severe materials problems associated with high-temperature operation. Furthermore, production of NO_x pollutants increases substantially as higher combustion temperatures are employed in these thermal systems.

Table II-1
EFFICIENCY LIMITS OF CONVENTIONAL
THERMAL ENERGY CONVERSION SYSTEMS

Heat Absorption Temperature, T_H °C (°F)	Carnot Efficiency* (percent)
500 (930)	61
700 (1,300)	69
1,000 (1,800)	76
1,200 (2,200)	79

*Heat rejected at T_c = 30°C (86°F).

The direct energy generation approach used in the fuel cell is intrinsically more efficient. Here, an equivalent "thermal" efficiency can be defined, using a thermodynamic characterization of the fuel-cell reaction:

$$\Delta G = \Delta H - T \Delta S$$

where ΔG is the reaction free energy, ΔH is the enthalpy of reaction (equivalent to the higher heat of combustion), and ΔS is the entropy change, with all values calculated at an absolute reaction temperature, T. Thus, the following relationship exists for the fuel cell:

$$\text{Equivalent thermal efficiency} = \Delta G / \Delta H = 1 - T \Delta S / \Delta H$$

Examination of a wide range of potential fuel-oxidant electrochemical reactions show that efficiencies approaching 100% are theoretically possible.

This intrinsic efficiency advantage of direct energy conversion, involving reduced fuel consumption, is the principal reason for the ongoing interest in fuel-cell technology. In addition, fuel-cell reactions are generally carried out at relatively low temperatures with minimal NO_x production, in "static" configurations having few rotating components. Thus, the fuel cell shows considerable promise for energy generation with minimum adverse environmental effects such as air pollutant emissions, and thermal or noise pollution.

B. Fuel-Cell Applications

A number of power generation applications have been proposed to capitalize on the advantages of fuel-cell technology. The applications that are currently under consideration for commercial development include on-site total energy systems; dispersed-site electric utility systems; and central-site, base-load electric utility systems.

Because of low emissions, fuel cells can be installed on-site very close to a load center. In turn, this close geographic coupling of power plant and electric demand makes recovery of the waste heat generated during fuel-cell operation attractive.[1*] Such total energy or cogeneration systems are being studied actively. Typical sites under consideration include residential apartment complexes, commercial shopping centers, and industrial facilities.[2,3]

First generation phosphoric acid fuel-cell power plants have been proposed for this application. Typical electrical power levels range from 40 kW to several megawatts. Waste heat recovery in the form of steam or hot water could raise the effective utilization of fuel energy to levels approaching 90%, as shown in Figure II-3.

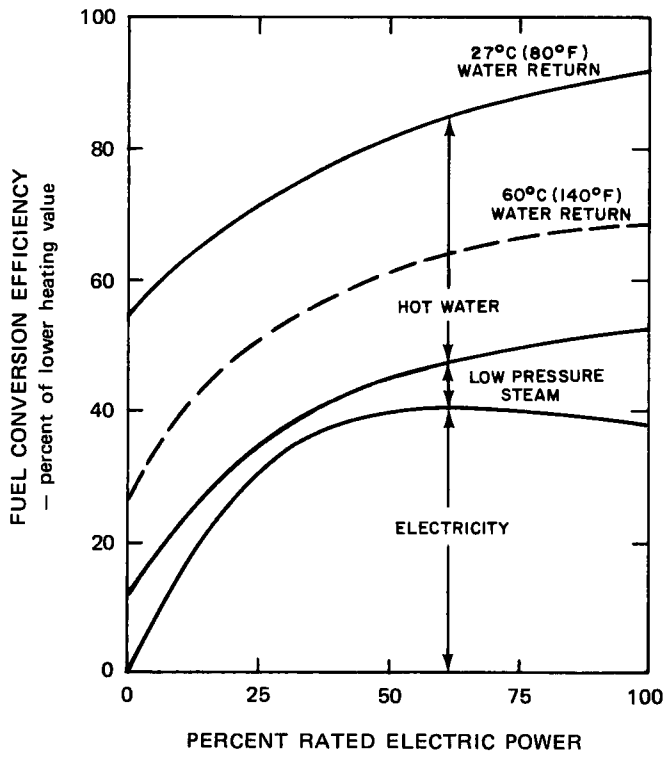

Source: Reference 2

FIGURE II-3. EFFICIENCY CHARACTERISTICS OF FUEL-CELL POWER PLANT WITH HEAT RECOVERY

*Numbered references are listed at the end of each chapter.

Fuel-cell siting flexibility also permits the installation of larger power plants at substation locations close to load centers within electric utility grids.[4-6] Such installations, rated at about 25 MW, operating in efficient cycling or load-following modes, are expected to have a number of beneficial effects on utility operation and economics, including:

- Production cost credits associated with load management of utility cyclic intermediate and peaking generation capacity.
- Efficient provision of required spinning reserve capacity; also, many small redundant generators installed on the system will reduce reserve requirements.
- Transmission and distribution (T&D) credits resulting from capital cost savings due to deferred T&D expansion and reduced line losses, as the distance between generation site and load demand center is shortened.

Translating these benefits for installing fuel-cell power plants yields anticipated investment credits in the range of $50-150/kW.[5] However, such credits are very site-dependent and will vary considerably from utility to utility. Initially, utilities serving constrained urban markets are expected to benefit most from the use of fuel cells.

Similar benefits have also been projected for 5 to 10-MW fuel cells installed in small municipal and rural utilities.[7] Here again, high efficiency under varying load output or even base-load conditions provides the incentive for introducing fuel cells.

Finally, advanced technology fuel cells, such as the molten carbonate or solid oxide electrolyte systems, have been proposed for 600-MW+ base-load power plants using abundant coal resources as primary fuel.[8,9] Coal would be gasified to form hydrogen and carbon monoxide rich mixtures, prior to entering the fuel cell. Initial projections indicate high energy conversion efficiency. The installed cost of such systems, based on conceptual power plant designs, appears competitive with alternative conversion technologies, but further study is required to firm up these cost estimates.

C. Potential Fuel-Cell Advantages and Disadvantages

The attractive characteristics of fuel cells can be classified broadly as follows: thermodynamic, environmental, structural, operational, and economic. Some characteristics are intrinsic to the concept of "fuel cell;" others are derivative, based on practical operating devices. Naturally, considerable overlap occurs and some attributes show up in several categories.

The major reason for initial and continued interest in fuel cells is their intrinsic thermodynamic advantage. The high efficiency of fuel cells, which conserves natural fuel resources, is not a functon of fuel-cell plant size or power output level, and can be obtained in a variety of potential applications, from small dispersed apartment complex units to large central utility units (see Figure II-4, which compares the efficiency of fuel cells with other competing technologies).

High efficiency can be maintained at rated or part load, so that fuel cells have attractive load-following characteristics (see Figure II-5). Furthermore, the efficiency can be enhanced by the use of the heat generated during fuel-cell operation, particularly in total energy concepts with a thermal load demand in addition to the usual electrical load demand.

Fuel cells are projected to be low-pollution energy conversion devices. Low levels of air pollution are attained through the selectivity and completeness of the clean fuel oxidation reaction, compared with the uncontrollable high temperature combustion reactions involved in conventional devices. Thus, low temperature fuel-cell reactions do not produce the CO and NO_x by-products characteristic of normal combustion. The waste products of fuel-cell operation are generally harmless and nonpolluting water and carbon dioxide.

High efficiency operation results in less waste heat, so that the thermal pollution burden is low. Also, many fuel-cell systems reject

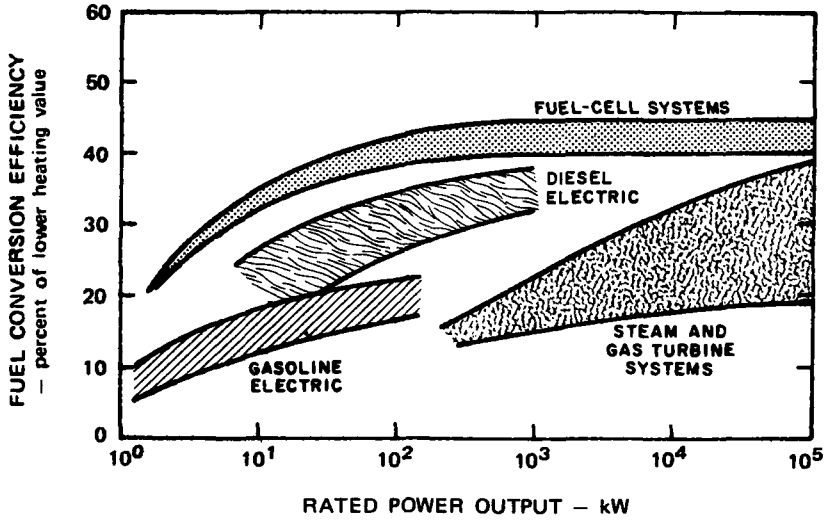

Source: Reference 4

FIGURE II-4. EFFICIENCY OF VARIOUS ENERGY CONVERSION DEVICES

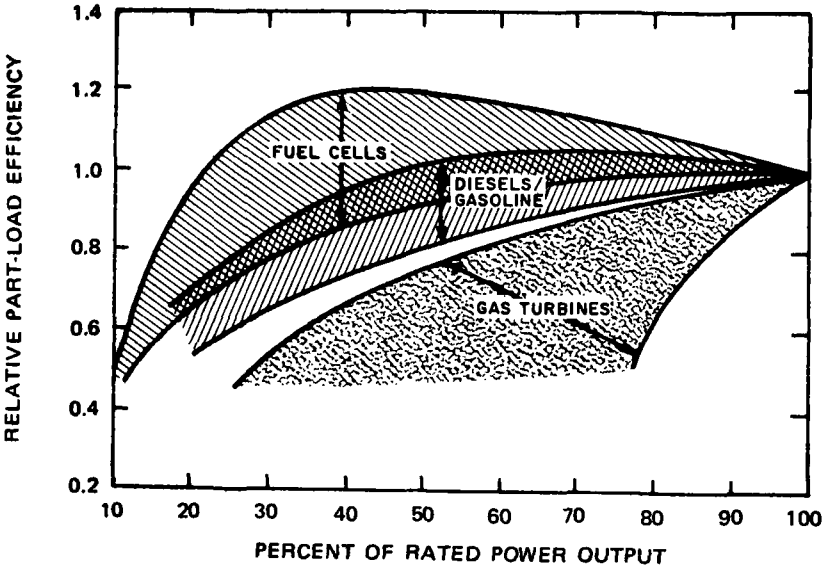

Source: Reference 4

FIGURE II-5. PART-LOAD EFFICIENCY

waste heat to the atmosphere, not to surface water systems. Thus, thermal pollution to adjacent water bodies is eliminated.

In addition to having low pollutant releases, fuel-cell design and assembly is flexible, and unobtrusive power plants can be designed having wide siting capability that makes effective use of available land while maintaining an aesthetically acceptable appearance.

The structural advantages of fuel cells result from modular, filter-press construction, which is the current technology approach to solving the complex reactant segregation and electrochemical constraints of most fuel cells. Modular building blocks allow the same technology to be packaged for widely different market needs, over a wide range of voltage and power levels, watts to kW to MW, for portable to transportable to stationary applications. Small modular units imply high unit sales volume, which can result in high production rates, low-cost factory assembly, and improved quality control. Moreover, modular assembly will bring about reduced lead time for ordering parts and installing total generating plants, reduced installation and check-out times, and increased ease of installation. Therefore, field construction costs can be minimized.

Rapid installation of basic modules in prefabricated increments is responsive to demand growth. Self-contained modules can be placed in rapidly gowing demand areas, including existing communities with underground constraints or site inflexibility. Modular elements can be assembled and used in various forms and spatial geometries, according to application needs and volume constraints. Compact, lightweight power plants are possible, depending on reaction kinetic factors and reactants used, leading to high power density and high energy density.

The expected operational advantages of fuel cells can be divided into those applying to the fuel cells themselves, and those applying to the technology that will be based on them. Fuel cells generally contain multiple units that are easily operated in parallel, and are built in

modular units, allowing power availability even though a portion of the plant is off-line; remaining modules can temporarily increase output without major efficiency or operating cost penalty. A modular subsystem gives redundancy and thus increases overall reliability.

Fuel cells are expected to provide ease of maintenance with resulting low cost. Balanced rotation and unstressed moving parts in auxiliary equipment give low maintenance, good reliability, and long life. They operate at a constant temperature, so that lower thermal stresses are exerted. They also contain simple elements that are easily operated or stored, and that offer automatic operation capability, ease of startup, and remote site operation capability.

Fuel-cell technology in its various applications can offer distributed, efficient power generation close to load centers, provide power generation capability involving minimum interactions with other utility functions, and provide transportable power generation in such emergencies as flood, earthquake, and hurricane. It is also adaptable to energy storage schemes coupled with periodic generation (e.g., solar) via a hydrogen electrolysis/conversion operation.

The future trend in alternative power generation technologies is toward higher cost due to rising fuel prices, labor rates, and cost of debt capital, and the imposition of new, higher cost, environmental regulations. This trend will improve the competitive stance of fuel cells because fuel-cell technology is still developing and prospects exist for improved life-cycle costs with the potential for reasonable investment costs, lower installation, operation, and maintenance costs over a period of years.

A particular economic advantage of fuel cells is that they could add utility service capability incrementally, in phase with actual demand. This feature should minimize financial risks and costs, and provide cash flow advantages by eliminating the delay time during which demand must increase to meet increased installed capacity. Fuel cells

also have a short lead time and high availability of plants versus existing alternatives. In addition, their flexibility permits installation closer to consumer, reducing transmission/distribution costs and utility service distribution infrastructure costs.

At present, the principal disadvantage of fuel-cell technology is its relative newness. Few, if any, complete power plants have been constructed, installed, and tested for prospective users to assess the expected operating advantages of fuel cells. This situaton will change as ongoing programs provide demonstration systems. However, considerable uncertainty still exists concerning the eventual installed cost, durability, and lifetime of mature fuel-cell technologies. Fuel cells will have to compete with other, more established, forms of energy conversion. These alternative systems are also being improved so that fuel-cell technology has to match moving performance and cost targets.

Earlier fears about the availability of liquid hydrocarbon supplies used by first-generation (phosphoric acid) fuel-cell systems have eased recently.[10] In any event, the high conversion efficiency of fuel cells should represent the most effective use of potentially scarce fuel resources.

D. The Complete Fuel-Cell System

The complete fuel-cell system consists of an integrated modular assembly of subsystems including the fuel conditioner for converting primary fuels to hydrogen; the fuel-cell stacks containing planar electrodes and an electrolyte-holding matrix as sandwiched sheets, housed in plate-and-frame filter-press assemblies; and a power conditioner for converting the primary fuel-cell electric output (direct current) to alternating current at a suitable voltage. The interrelationship of these components is shown in Figure II-6.

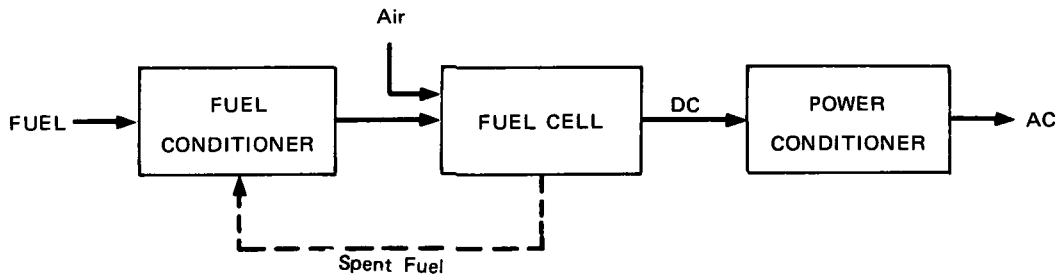

FIGURE II-6. THE FUEL-CELL SYSTEM

These modular assemblies can be scaled in size for any power level (kW to MW) application. In general, a high level of factory assembly of individual components into shippable arrays is projected, which will facilitate power plant installation in the field. The key factors in the design and operation of a complete fuel-cell power plant are fuels (or reactants) to be used, the fuel-cell operating characteristics, the overall economics of power plant operation, and the technology trade-offs among types of fuel-cell stacks, operating conditions, lifetime, and so on. These factors are discussed in the following sections.

1. Fuel-Cell Reactants

A wide range of reactants, particularly fuels, can be considered for use in fuel-cell power plants. In principle, many fuels will undergo direct electrochemical oxidation at the fuel-cell anode. Possible fuels include hydrogen, methanol, and hydrocarbons such as methane. The anode (fuel) reactions are:

$$H_2 \longrightarrow 2H^+ + 2e^-$$

$$CH_3OH + H_2O \longrightarrow 6H^+ + CO_2 + 6e^-$$

$$CH_4 + 2H_2O \longrightarrow 8H^+ + CO_2 + 8e^-$$

In general, only oxygen (from ambient air) is considered a practical oxidant. The cathode (air) reaction is:

$$\tfrac{1}{2}O_2 + 2H^+ + 2e^- \longrightarrow H_2O$$

A characteristic half-cell potential (EMF) is associated with each of these reactions, as shown in Figure II-7. The difference between the anodic (fuel) and the cathodic (O_2) half-cell potentials is the theoretical cell potential, E^o. For example, E^o for the H_2/O_2 fuel-cell couple is +1.23 - 0.0 = +1.23V (at 25°C). E^o may also be computed from the overall change in free energy of reaction, G:

$$E^o = - \Delta G/nF$$

where n is the number of electrons involved in the reaction and F is the Faraday constant, all expressed in consistent units.

However, the kinetics of electrochemical reactions must also be considered in selecting appropriate fuels for fuel cells. Once again, a number of trade-offs are involved, including:

- Fuel availability or cost
- Electrochemical activity
- Fuel storage and logistic factors.

As indicated in Table II-2, the least expensive, most easily stored fuels are not very reactive. Hydrogen, on the other hand, is very reactive, but costly to store and transport.

This fuel convenience, cost, and reactivity mismatch has been resolved by incorporating a fuel conditioning device in the fuel-cell system that converts unreactive fuels into reactive hydrogen. In the steam reforming reactor, the most widely used of such devices, primary hydrocarbon fuels are reacted with water (steam) to produce hydrogen for the fuel cell via the following endothermic steam-reforming reaction:

$$CH_4 + 2H_2O \xrightarrow[\text{Heat}]{\text{Catalyst}} 4H_2 + CO_2$$

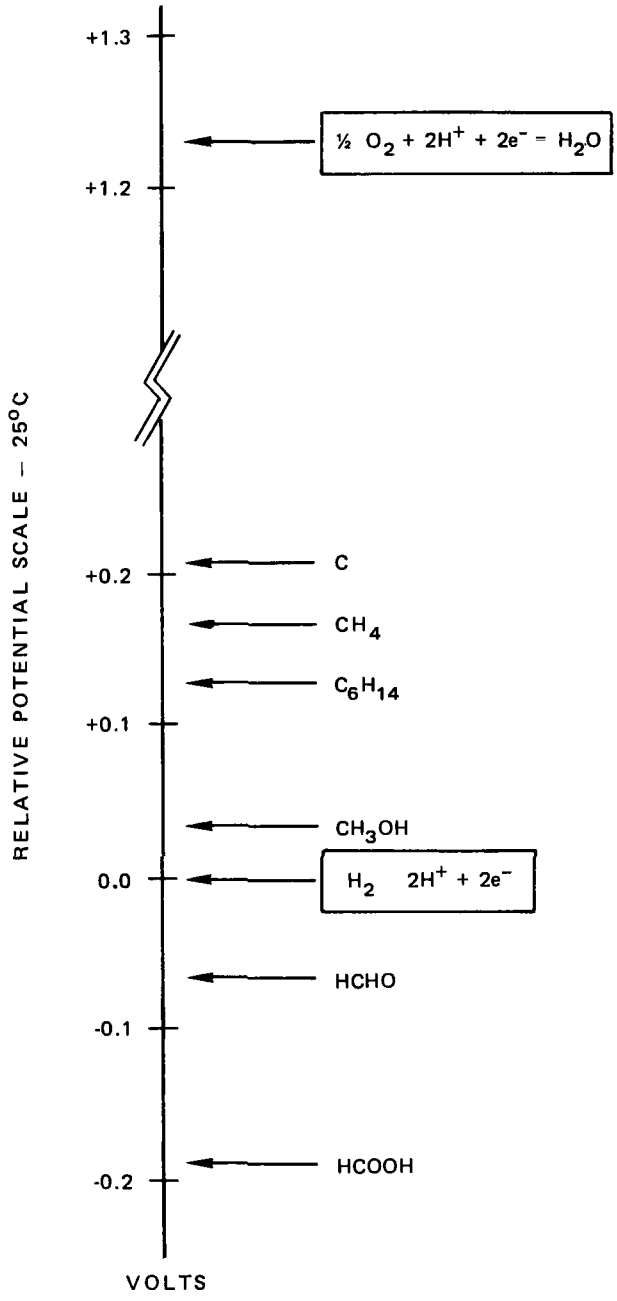

FIGURE II-7. THE EMF SERIES

Table II-2

FUEL SELECTION TRADE-OFF

Fuel	Relative Delivered Cost	Relative Electrochemical Activity
Hydrogen	High	Very high
Methane	Low	Low
Methanol	Moderate	Moderate
Ethanol	Moderate	Low
Hydrocarbons	Low	Low
Coal	Very Low	Very Low

The reaction is carried out at an elevated temperature (700°C or 1,290°F) in a fired tubular reactor packed with nickel-based reforming catalyst. Heat for the reaction is generally provided by burning spent anode fuel gas containing unreacted hydrogen. Because nickel-based catalysts are susceptible to sulfur poisoning, sulfur levels in the feed to the reactor must be kept below 1 ppm. If organic sulfur compounds are present in the primary feed, they must be converted to H_2S in a hydrodesulfurizer using, say, colbalt-molybdenum catalyst. The H_2S is then adsorbed in a replaceable zinc oxide guard bed. Also, excess steam is added to the reformer feed to limit the amount of by-product carbon deposited on the catalyst bed. Typical steam/carbon molar ratios are 3 and 4 to 1.

Lastly, for fuel-cell systems using noble metal (e.g., platinum) anode catalysts, the level of carbon monoxide in the reformer effluent must be kept low (below 1%) to prevent excessive performance loss caused by carbon monoxide adsorption. Carbon monoxide content can be controlled using additional catalytic reactors to establish a favorable water-gas shift reaction equilibrium:

$$CO + H_2O \longleftrightarrow CO_2 + H_2$$

This sequence of conversion steps can be used with hydrocarbon feeds through the naphtha boiling point range. Heavier liquid feedstocks have excessive carbon-forming tendencies. For these fuels,

alternative conversion reactions such as partial oxidation can be used to produce hydrogen. However, the use of air as a reactant results in excessive nitrogen diluent in the hydrogen product gas. Similarly, coal can be gasified using oxygen or air and steam to form hydrogen-rich mixtures suitable for use in certain fuel-cell systems.

The interaction between the fuel and fuel cell is further complicated by the availability of intermediate fuels that could be produced from primary fuel resources, such as coal. For example, storable methanol fuel could be produced from coal for certain applications where the logistical advantages of liquid fuels are required. Further discussion of fuel interchangeability is beyond the scope of this brief overview, however.

2. Fuel-Cell Operating Characteristics

Although the theoretical or open-circuit potentials of a fuel cell, E^o, are high, certain irreversible voltage losses are encountered when practical levels of current are produced during fuel-cell operation. These polarization or overvoltage losses can be characterized as follows:

- Activation Polarization. Electrochemical reactions proceed at finite rates in a number of elementary steps such as activated adsorption/desorption and electron transfer. A potential loss, termed activation polarization, is associated with the slow step in the reaction sequence. This loss is small with reactive fuels such as hydrogen, but can be quite large for the oxygen reduction (consumption) reaction, particularly for low-temperature fuel cells. Activation polarization losses can be reduced by using appropriate electrocatalysts. In general, these losses are small at the temperatures (600°C+ or 1,100°F+) employed in high-temperature fuel-cell systems.

- Concentration Polarization. Fuel cells generally use porous electrode structures to maximize the surface area available for electrochemical reaction. Furthermore, maximum utilization of reactants is sought. As a result, reactant concentration gradients are established throughout the electrode structure and flow-path through the cell. These gradients, and the resulting reactant and product diffusion or

mass transfer requirements, cause a polarization loss associated with the effect of local concentrations on potential. This concentration polarization loss can be estimated using the Nernst equation:

$$E = E^{o} - (RT/nF)\ln\left[(\text{Products})/(\text{Reactants})\right]$$

where E is the cell voltage corrected for concentration differences between standard state and actual cell conditions, R is the gas constant, and the terms in the logarithm are suitable concentration (activity) terms. The Nernst equation can also be used to estimate the effect of high-pressure fuel-cell operation. Such operation is usually beneficial. Concentration polarization losses occur in all fuel-cell systems, including the high-temperature molten carbonate and solid oxide electrolyte systems.

- Ohmic Polarization. The movement of ions and electrons requires a potential gradient. In turn, an ohmic polarization loss is incurred that is directly proportional to the current flow (ionic or electronic) and pathway resistance. Proper selection of electrolyte composition and design and assembly of fuel-cell structural components can minimize, but not eliminate, ohmic polarization losses.

The impact of these polarization losses is to reduce the fuel-cell terminal voltage. Because these losses increase as load current is increased (see Figure II-8), fuel cells exhibit a characteristic performance curve (voltage vs. current load) shown in Figure II-9. In turn, the power (P=EI) delivered by a fuel cell varies with current load (see Figure II-10). Although high power operation is desirable, such operation results in reduced energy conversion efficiency. A modified efficiency parameter, the voltage efficiency, can be used to characterize this effect:

$$\text{Voltage efficiency} = \frac{\text{Actual cell voltage}}{\text{Theoretical cell voltage}} = E/E^{o}$$

Voltage efficiency decreases somewhat as current load is increased (see Figure II-11). For a given power plant, cell and system efficiency increase as load output is reduced.

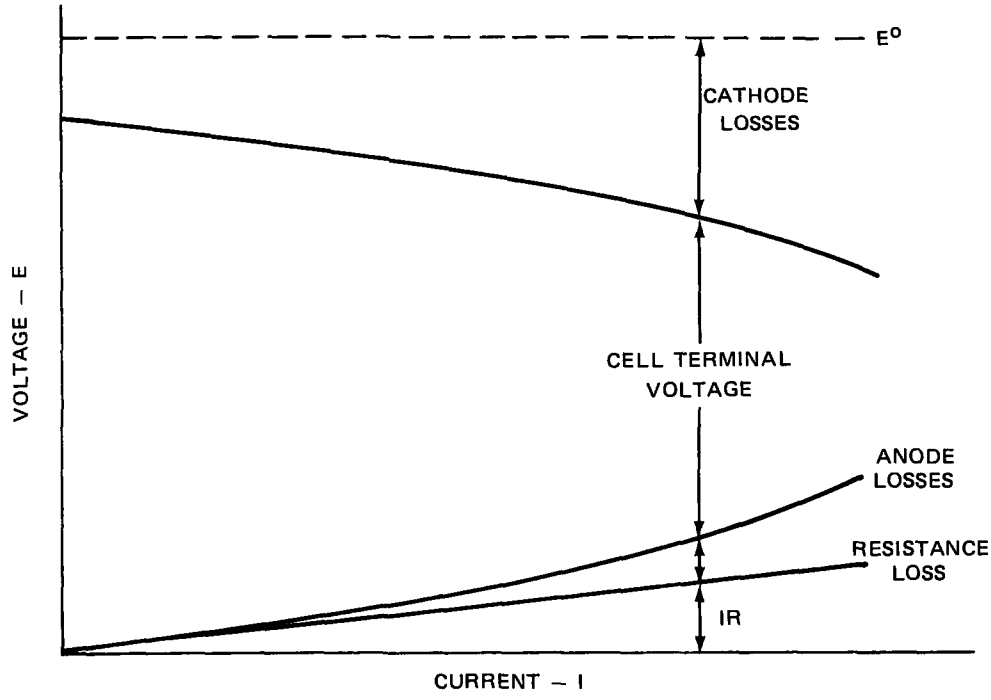

FIGURE II-8. FUEL-CELL LOSSES

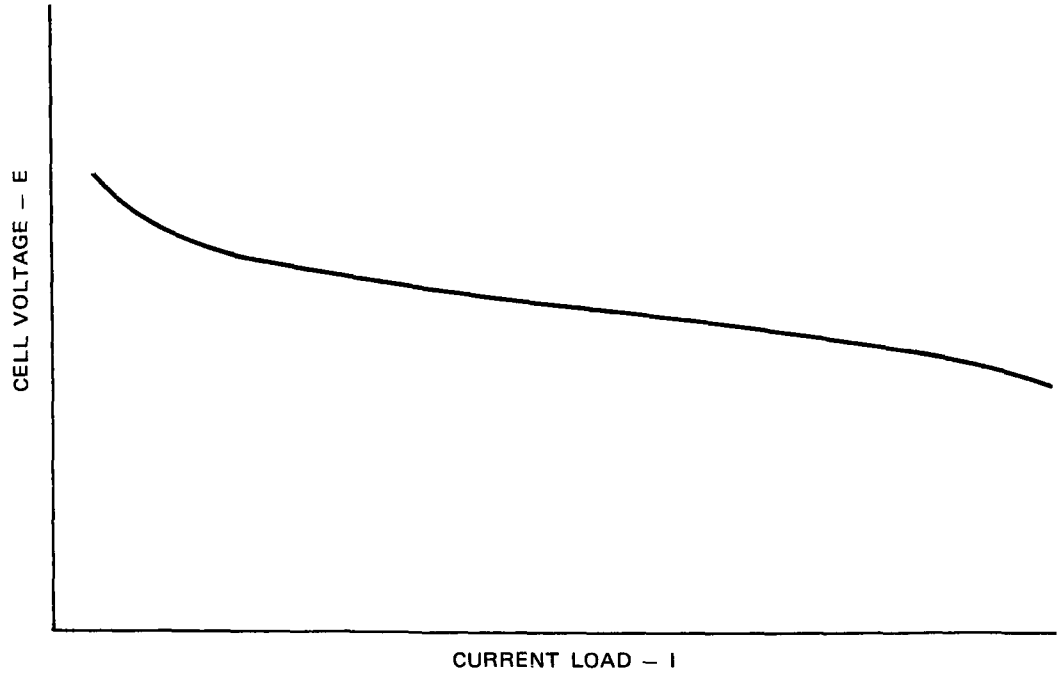

FIGURE II-9. CHARACTERISTIC FUEL-CELL PERFORMANCE CURVE

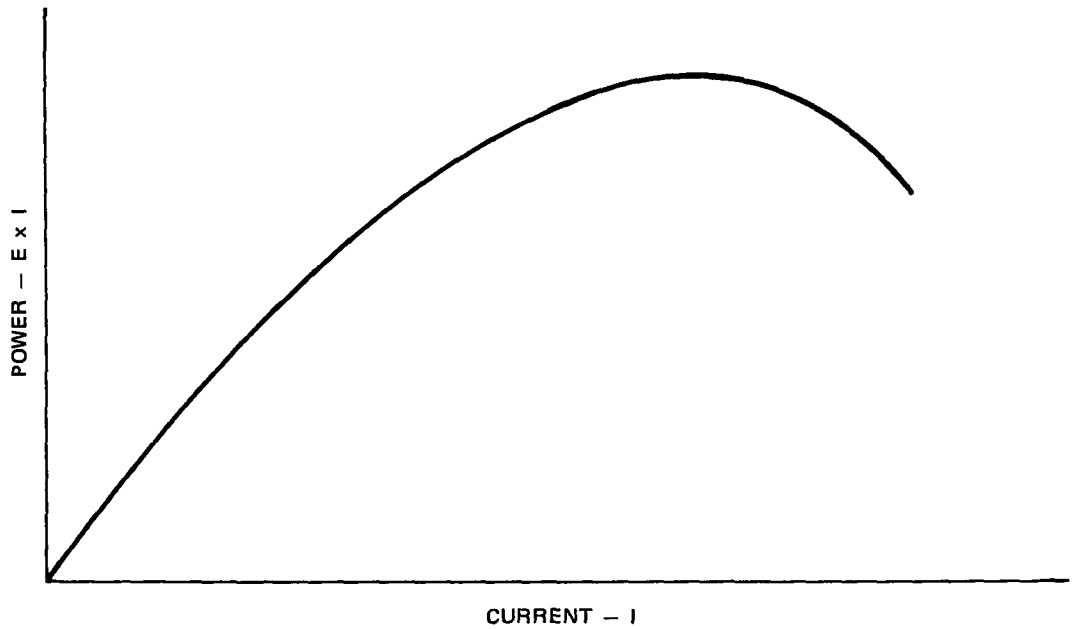

FIGURE II-10. FUEL-CELL POWER OUTPUT

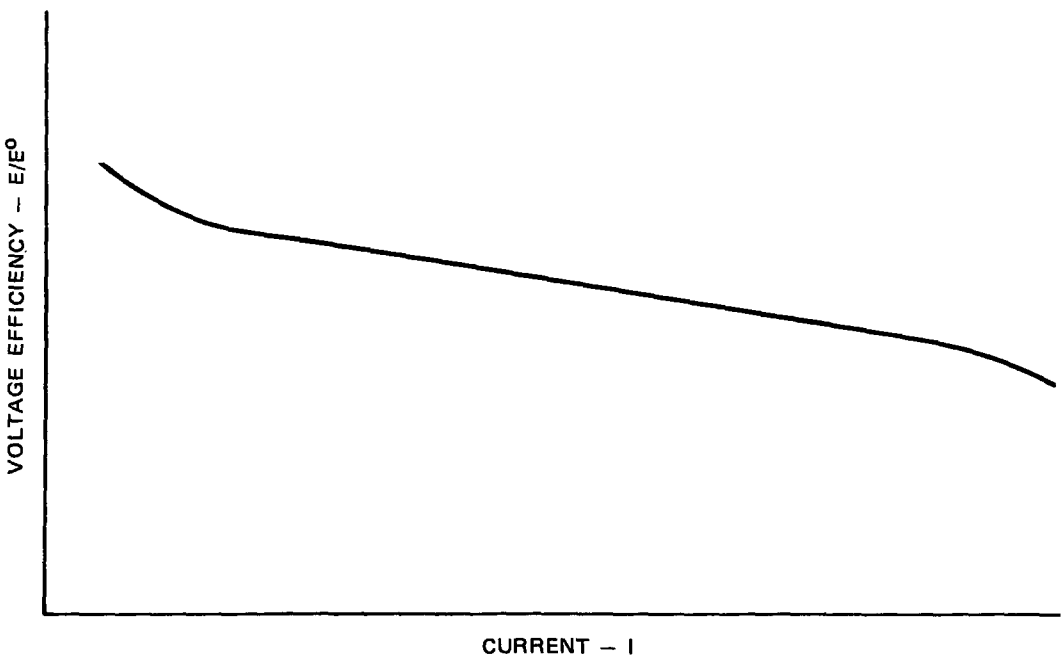

FIGURE II-11. EFFECT OF CURRENT LOAD ON VOLTAGE EFFICIENCY

3. Fuel-Cell Economics

The cost of energy delivered by a power plant is the sum of three factors: capital charges, fuel charges, and operating and maintenance (O&M) charges. Estimations of the cost of energy and selection of strategies to reduce it are ongoing concerns of fuel-cell R&D programs. Associated with each power plant is a total installed cost that must be invested by the user. This investment cost must be amortized over the operating life of the power plant. Capital charges for this investment can be estimated from:

$$\text{Capital charges } (¢/\text{kWh}) = \frac{\text{Investment cost } (\$/\text{kW})}{\text{Annual operating hours}} \times f_{CR} \times 100$$

where f_{CR} is a capital recovery factor that includes depreciation, taxes, overhead, profit, and other costs associated with owning the power plant. A typical value for electric utility operation is $f_{CR} = 0.18$. Clearly, as shown in Figure II-12, capital charges can be minimized by reducing the installed cost and by increasing the annual operating time (load factor).

Fuel charges include the cost of fuel consumed by the fuel cell to deliver a specified amount of electrical energy. It is directly related to the delivered cost of fuel based on the higher heating value (HHV) of the fuel. Fuel charges also are a function of the power plant conversion efficiency. Here, system overall efficiency is expressed as the heat rate (i.e., the amount of fuel consumed per kWh of electrical energy delivered to the busbar). In addition to the efficiency of the fuel cell itself, some losses are associated with standby fuel requirements and power plant auxiliaries such as pumps, fans, blowers, and power conditioning equipment. A power plant operating at 100% efficiency would have a heat rate of 3,600 kJ/kWh (3,413 Btu/kWh). Thus, the fuel charge is the product of fuel cost and heat rate. This relationship is shown in Figure II-13 for typical values of fuel cost.

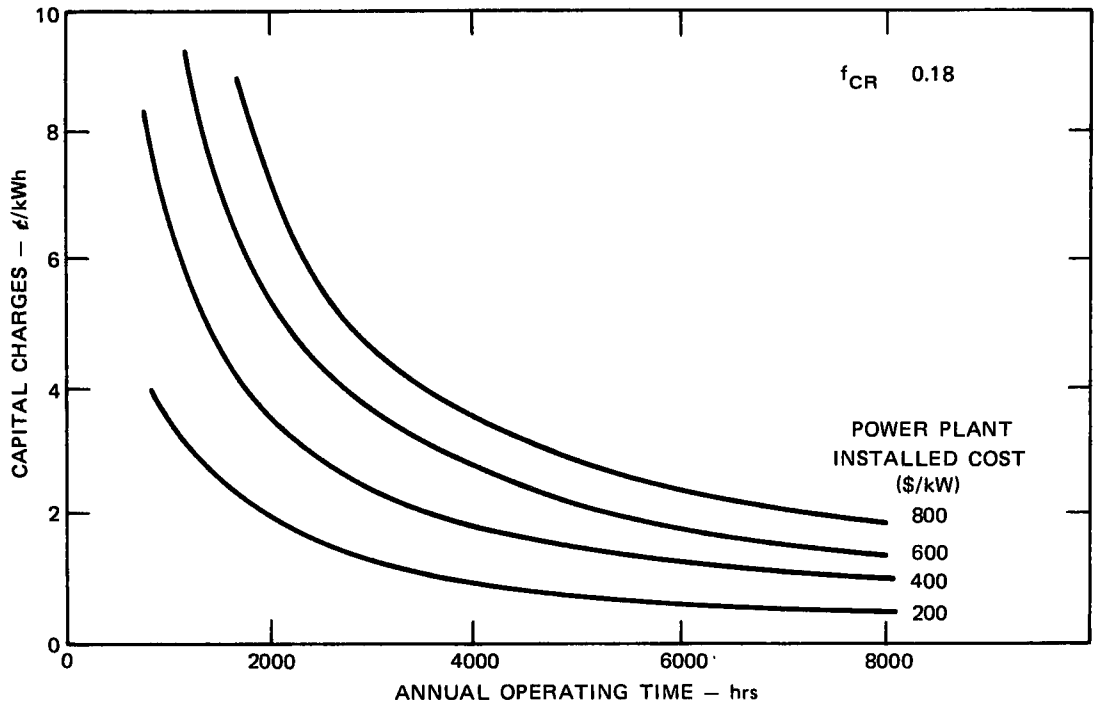

FIGURE II-12. CAPITAL CHARGES

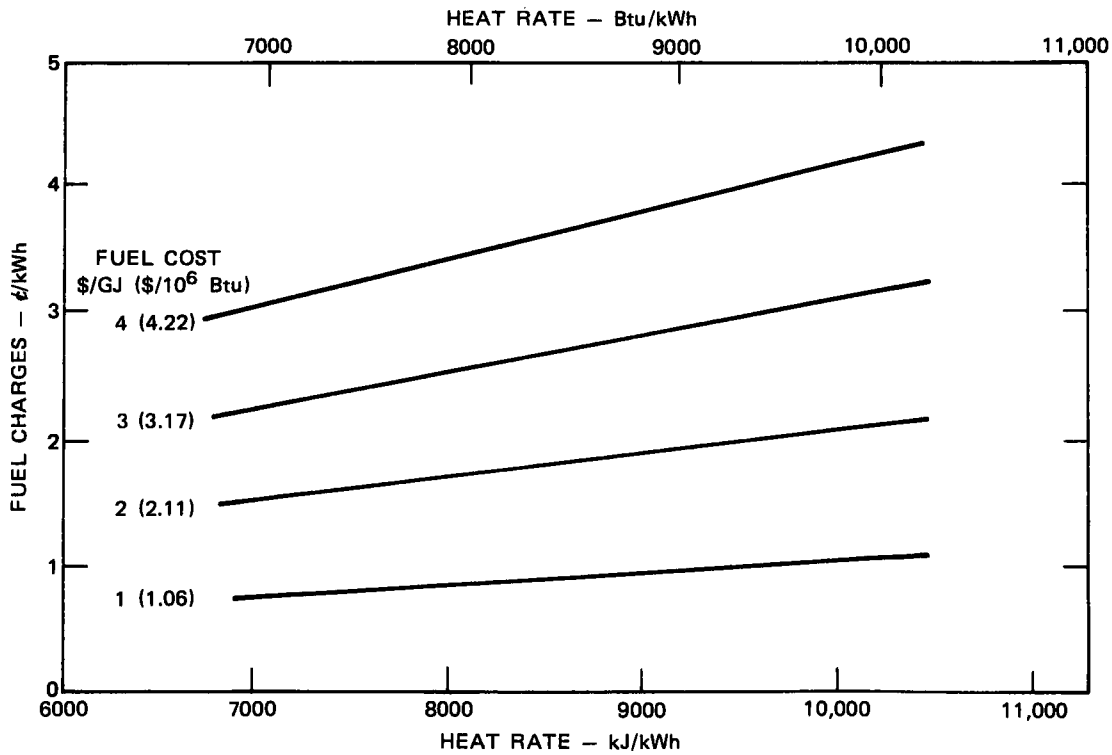

FIGURE II-13. FUEL CHARGES

O&M charges are associated with the routine operating and maintenance functions normally required to run a reliable power plant. They are usually directly proportional to the operating time at a given power output. In addition, fuel-cell power plants are expected to incur cost related to the periodic replacement of spent fuel-cell stacks, which can conveniently be treated as an operating expense directly proportional to the net stack replacement cost and inversely proportional to the stack life. In this study, net stack replacement costs include the stack cost itself, together with required installation labor costs, minus the salvage value of the replaced stacks. Experience with spent stack recovery is insufficient to project this salvage value, but most of the noble metal catalyst content of low-temperature fuel-cell stacks is expected to be effectively recovered.

The effect of stack life and net replacement cost on the O&M charges is shown in Figure II-14. Clearly, stack durability or life has a negligible impact on costs for lifetimes exceeding 40,000 hours. Accordingly, this value is usually selected as a goal for R&D demonstration programs.

Selection of an optimum design point for the fuel-cell power plant involves analysis of each cost factor discussed above. The effect of load current on the cost of energy is shown schematically in Figure II-15. Capital charges decrease as current (therefore, power output) increases. At the same time, fuel charges will increase as cell voltage efficiency decreases at high load. O&M charges should be relatively constant, assuming that stack life is independent of design current load. Generally, the total cost of energy shows only a moderate effect of operating load.

Determining the expected installed cost of fuel-cell power plants, together with demonstration of target stack durability, is currently very difficult because very few detailed descriptions of fuel-cell system capital costs have been published. Expected or cost goals for

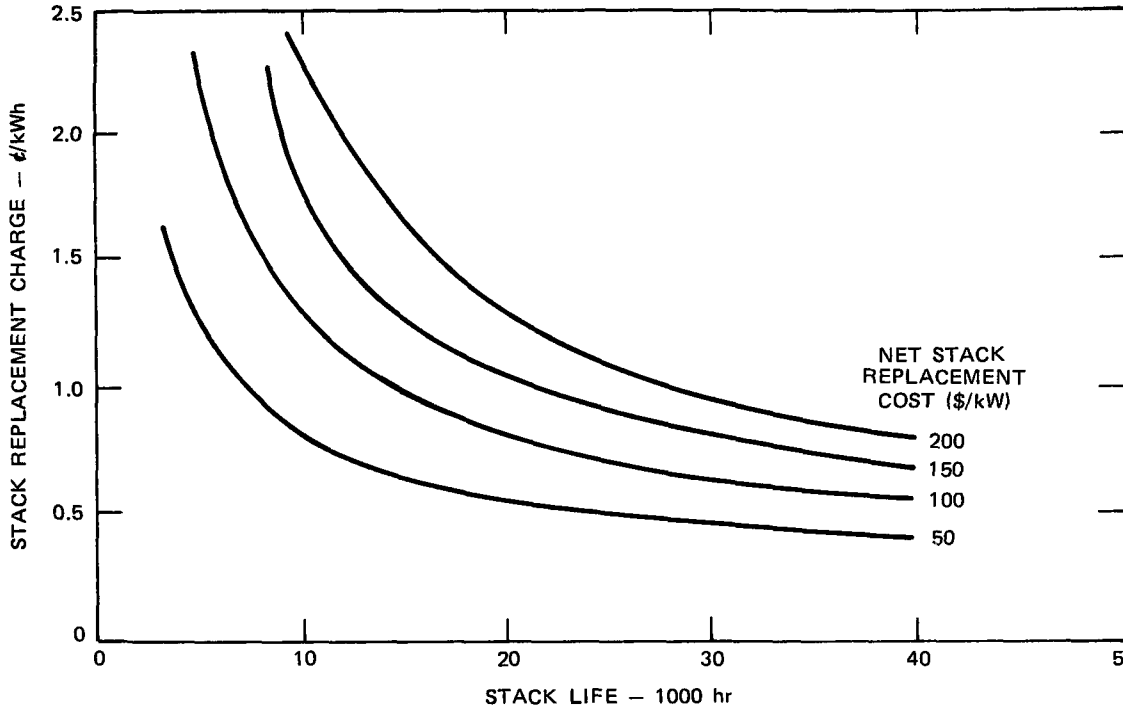

FIGURE II-14. STACK REPLACEMENT CHARGES

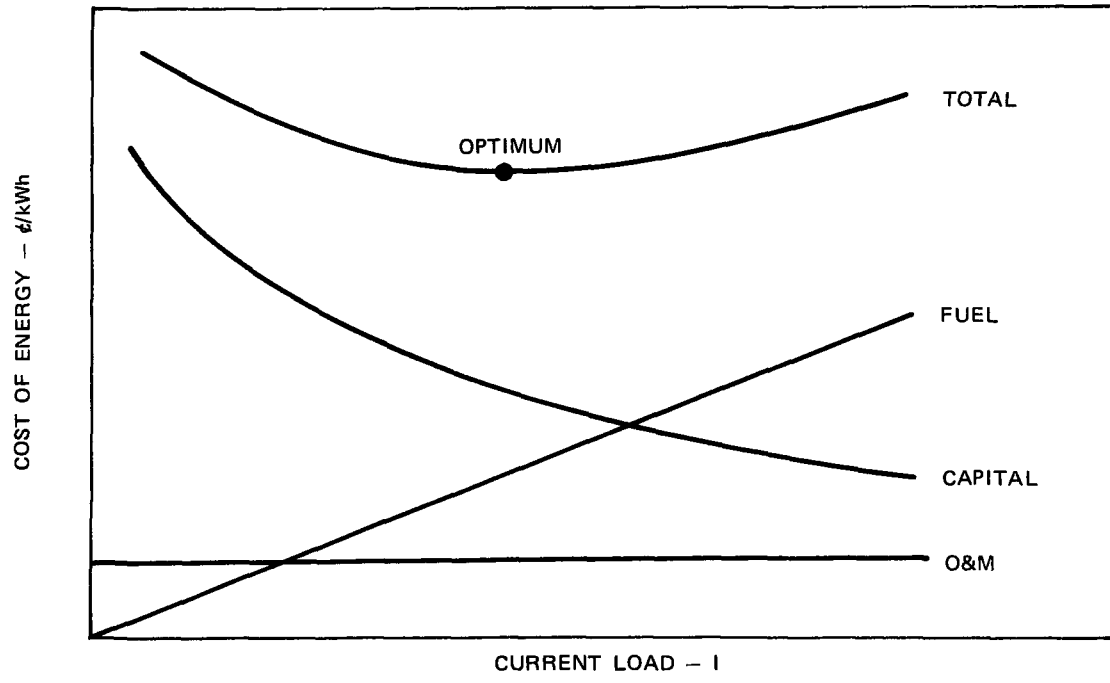

FIGURE II-15. DESIGN POINT SELECTION

mature technology are listed in Table II-3. Recent estimates of the cost of dispersed site phosphoric acid fuel-cell systems, at initial production levels, range between $500-700/kW.[10]

In summary, the greatest hurdle facing fuel-cell technology is the simultaneous achievement of interrelated goals for performance (power output and efficiency), durability (life and reliability), and cost.

Table II-3

ESTIMATED INSTALLED INVESTMENT COSTS
FOR FUEL-CELL POWER PLANTS

Fuel-Cell System	Application	Estimated or Target Installed Cost, $/kW (1980$)*
First-generation phosphoric acid (40 kW+)	On-site total energy	400-500[1]
First-genertion phosphoric acid (5-26 MW+)	Dispersed site Utility	350[11]
Second-generation molten carbonate (5-26 MW+)	Dispersed site Utility	280[11]
Second-generation molten carbonate with coal gasifier (600 MW+)	Central site Utility	834[8]

*Escalated at 7%/year from original estimate year.

4. Fuel-Cell Technologies and Trade-offs

Many technological approaches have been studied to reduce the fuel-cell concept to a practical device. These approaches can be classified according to the electrolyte composition and a corresponding operating temperature level, as shown in Table II-4. Definition of an optimal choice is difficult because the following practical trade-off factors must be considered:

- Reactant Activity. In general, electrochemical reactions proceed more rapidly at elevated temperature. Thus, higher power outputs are possible at high temperatures, reducing the need for catalysts to promote the reactions. In fact, high-temperature (600°C+, 1,100°F+) fuel cells do not require the expensive platinum catalysts required by low-temperature technologies.

- Materials Life and Cost. On the other hand, high-temperature operation also increases the rate of corrosion reactions, imposing problems of materials stability and cost. For maximum cost-effectiveness, fuel-cell power plants have to function for several years. Thus, the question of component durability is important.

- System Application. Fuel-cell power plants have been proposed for many divergent power generation applications, including small-scale total energy systems; large-scale, intermittent power dispersed-site systems; and even larger, central-site base-load systems, as well as specialty aerospace and terrestrial applications. Each application poses unique requirements for which certain fuel-cell technologies may be more suitable than others.

- Electrolyte Properties. Fuel-cell electrolytes must have reasonably high ionic conductivity. This requirement is met by the composition-temperature combinations listed in Table II-4. In addition, the electrolytes must be stable and invariant with the reactants and trace contaminants encountered in fuel-cell operation.

Table II-4

FUEL-CELL TECHNOLOGY CLASSIFICATIONS

Electrolyte		Operating Temperature
Type	Example	Range, °C (°F)
Solid Polymer	Ion exchange membrane	70-100 (160-210)
Aqueous	Acid: H_3PO_4*	170-200 (340-390)
	Base: KOH	70-120 (160-250)
Molten	Carbonates: Li_2CO_3/K_2CO_3*	600-700 (1,100-1,300)
Solid	Oxides: ZrO_2/Y_2O_3	1,000-2,000 (1,800-3,600)

*Technologies undergoing major development effort at this time.

E. Specific Fuel-Cell Technologies

A number of fuel-cell technologies are available for development into power plant systems. This section describes the status of specific fuel-cell technologies currently under study in major development programs, including:

- First-generation technology: phosphoric acid fuel cells
- Second-generation technology: molten carbonate fuel cells
- Third-generation technology: solid oxide fuel cells.

The status of other technologies such as alkaline and ion-exchange membrane fuel cells is also reviewed briefly.

1. Phosphoric Acid Fuel Cells

Phosphoric acid fuel cells are under intensive development by United Technologies Corporation (UTC), Energy Research Corporation/ Westinghouse, and Engelhard Industries for both on-site or dispersed-site power generation applications. This technology uses a concentrated phosphoric acid electrolyte, operating at temperatures up to 190°C (374°F) at pressures ranging from atmospheric to about 345 kPa (50 psia). The electrolyte is contained within a silicon carbide matrix sandwiched between the electrodes. Platinum electrocatalysts are employed, in the form of highly dispersed crystallites supported on a carbon substrate. Total cell catalyst loading is less than 1 mg Pt/cm^2 of electrode geometric area. Cell cooling is accomplished by water evaporation in isolated tubes or by flowing excess air through some of the cathode compartments. Graphite is the principal material of construction.

Natural gas and liquid hydrocarbons through the naphtha boiling range are the usual primary feeds to the fuel-conditioning section of the power plant. These fuels are converted to a hydrogen-rich feed gas

using the steam reforming reaction. In some cases, by-product hydrogen from other sources has also been considered.

A number of trade-offs are involved in selecting the operating conditions of the phosphoric acid fuel cell. Performance (voltage and current, hence power) improve as temperature and pressure are increased. UTC is exploring the effects of increased temperature (200°C or 392°F) and pressure (640 kPa or 93 psia). The impact of trace carbon monoxide content in the reformed gas feed is reduced at high temperature. Operation at high pressure, hence reduced gas flow volumes, reduces the extent of phosphoric acid vaporization that occurs at high temperature. However, efficient system operation at elevated pressure requires the use of a close-coupled compressor/expander set for the air stream. Cost-effective devices are available for the MW-sized fuel-cell systems, but not for the smaller on-site power plant systems. Excessive electrolyte loss limits fuel-cell durability (life), but UTC has recently developed electrode structures that contain an electrolytic reservoir to compensate for vaporization losses.

Air electrode (cathode) operation appears to be the major source of concern regarding phosphoric acid fuel-cell life. The following cathode performance degradation mechanisms have been identified and are currently under intensive study:

- Platinum catalyst sintering or surface area loss resulting in reduced catalytic sites for the oxygen reduction reaction.[12] Recent UTC studies suggest that the larger platinum crystallites may be more accessible to reactants, compensating for the loss in the catalyst area.

- Platinum dissolution at high cathode potentials, such as open-circuit or low-current load operation.[13] The dissolved platinum species migrate towards the anode (H_2 electrode), thus reducing the number of active sites in the cathode. In effect, this places a limit on the maximum cell voltage and efficiency achievable by phosphoric acid fuel-cell technology. The heat rate goal for this technology is 9,800 kJ/kWh (9,300 Btu/kWh) at end of life, corresponding to a cell terminal voltage somewhat below 0.7 volts.

- "Corrosion" or oxidation of the carbon support on which platinum catalyst is dispersed[14], which results in subtle changes in electrode structure, thickening the electrolyte film through which dissolved oxygen must diffuse to reach a catalytically active site. A search is under way for more stable carbon supports.

There are no reports in the literature indicating that target life (40,000 hours) at design performance levels has been achieved in phosphoric acid fuel-cell stacks. Demonstration of this goal will be a key milestone.

The use of platinum electrocatalysts in this technology appears cost-effective. Suitable procedures for recovering catalyst from spent stacks must be developed. The search for alternative catalyst composition, less susceptible to sintering, poisoning, or dissolution has been attempted in the past without notable success. The extremely corrosive nature of the electrolyte and cell-operating conditions severely limits the range of potential substitutes for platinum.

Studies are also under way to develop acidic electrolyte substitutes for phosphoric acid. Fluoro-sulfonic acid derivatives appear to give improved cathode performance at lower temperature, but problems with stability and/or excessive vapor pressure have been encountered.

Phosphoric acid fuel cells are prime candidates for near-term commercialization. A number of technology demonstration programs are nearing the critical phase. These include construction, installation, and testing of several 40-kW power plants for on-site total energy systems throughout the United States and a 4.8-MW demonstrator system to be installed in New York City on the Consolidated Edison grid. If these demonstration programs are completed successfully, the anticipated benefits of fuel-cell technology will be confirmed.

2. Molten Carbonate Fuel Cells

The molten carbonate cell has been selected for development as the second-generation fuel-cell system. Substantially improved electrochemical performance is projected for this high-temperature cell (650°C or 1,200°F). Target heat rate for hydrocarbon-fueled intermediate-load power plants is about 7,900 kJ/kWh (7,500 Btu/kWh) compared with 9,800 kJ/kWh (9,300 Btu/kWh) for first-generation phosphoric acid fuel-cell systems. In addition, recent studies by UTC[8] showed that a base-load, integrated coal gasifier/molten carbonate fuel-cell system might operate at energy-conversion efficiencies approaching 50% (7,400 kJ/kWh or 7,000 Btu/kWh). Significant progress has been made in recent years to overcome the problems encountered in earlier molten carbonate fuel-cell studies. The molten carbonate fuel cell is under active development by UTC, Energy Research Corporation, the Institute of Gas Technology, General Electric, and several National Laboratories.

The molten carbonate fuel cell contains a lithium aluminate matrix or tile impregnated with a mixed potassium/lithium carbonate electrolyte, sandwiched between two porous sintered-nickel electrodes. The carbonate ion participates actively in the electrode reactions:

Anode reaction: $H_2 + CO_3^{=} \longrightarrow H_2O + CO_2 + 2e^-$

Cathode reaction: $\frac{1}{2}O_2 + CO_2 + 2e^- \longrightarrow CO_3^{=}$

Overall reaction: $H_2 + \frac{1}{2}O_2 \longrightarrow H_2O$ + direct electrical energy

Typical fuel gases include steam-reformed hydrocarbons (containing mostly H_2 with some CO_2) and gasified coal (containing roughly equimolal mixtures of H_2 and CO, with N_2 diluent if air is used as gasifier feed). At the elevated cell temperatures, about 650°C (1,200°F), hydrogen electro-oxidation proceeds rapidly on the nickel electrode surface. Direct electrochemical reaction of CO probably plays a minor role, but substantial quantities of additional H_2 are

generated via the water gas shift reaction that also takes place on the nickel electrode:

$$CO + H_2O \longleftrightarrow CO_2 + H_2$$

On the other hand, kinetics of the oyxgen reduction reaction on the nickel (oxide) electrode are not very rapid, so that some activation polarization loss is encountered.[15] Ionic-resistive losses in the molten carbonate electrolyte are another major source of performance loss. These losses can be reduced by operating with thinner electrolyte tiles or by increasing the temperature. However, the former approach increases the risk of reactant gas leakage or crossover and the latter aggravates the materials problems encountered with corrosive carbonate melts.

Large-scale, coal-fueled molten carbonate fuel-cell power plants are projected to operate at elevated pressure, 1,034 kPa (150 psia), with 85% utilization of fuel (H_2 + CO) and 50% oxygen utilization per pass through the cell. To preserve electrolyte invariance, carbon dioxide must be supplied to the air electrode. At present, burning the spent anode gas conveniently accomplishes this through use of cathode air fuel. The response of molten carbonate fuel-cell performance to variations in composition can be estimated from the Nernst equation:[16]

$$E = -\frac{RF}{nF} \ln \left[\frac{(CO_2)_a \, (H_2O)_a}{(H_2)_a} \cdot \frac{1}{(CO_2)_c \, (O_c)^{1/2}} \right]$$

where the terms in parentheses are reactant partial pressures and the subscripts refer to anode (a) and cathode (c) conditions. Increased pressure operation improves cathode performance, but slightly decreases anode performance. Recent evidence suggests there may be a beneficial effect of pressure on reaction kinetics as well. However, high-pressure operation may also lead to formation of inert methane, resulting in a loss of fuel utilization:

$$3H_2 + CO \longleftrightarrow CH_4 + H_2O$$

or:

$$4H_2 + CO_2 \longleftrightarrow CH_4 + 2\,H_2O$$

Molten carbonate fuel cells are usually cooled by recirculating the cathode air stream to a separate heat exchanger. Waste heat from the cell is thus available at a very attractive temperature (600°C or 1,100°F) for further use. For example, heat can be recovered as steam for use in cogeneration facilities or for use in a steam-bottoming cycle for additional power production. In this manner, substantial quantities of energy can be generated, greatly improving the overall fuel-to-electricity conversion efficiency. In a UTC design for a 635-MW integrated coal-fueled power plant, the steam-bottoming cycle provided one-third of the delivered power output.[8]

The performance of molten carbonate fuel cells has improved impressively in recent years, as shown in Figure II-16. Nevertheless, considerable progress is still required to achieve acceptable durability or life in multicell stack operation. Individual cells have operated stably, at reduced performance levels, in excess of 12,000 hours. The corresponding value for a 19-cell stack of 0.093 m^2 (1 ft^2) cells is about 1,500 hours.[15] The following life-limiting phenomena were recently reviewed in an EPRI-sponsored workshop:[18]

- Electrolyte Tile Stability. The crystal structure of the lithium aluminate matrix changes with time. Density differences among the different crystal types can produce reactant gas crossover paths, particularly if the tile is thermally cycled. Such cycling is expected in typical molten carbonate fuel-cell system applications. The result is reduced reactant utilization and lower cell performance. In extreme cases, explosive gas mixtures may be formed. This problem might be aggravated by projected operation at elevated pressure and by the desire to reduce tile thickness to achieve lower internal ohmic losses.

- Wet Seal Corrosion. At present, the edges of the cell are sealed by pressing the nickel electrode against the tile containing the mixed carbonate electrolyte. The resulting seal develops a surface with air on one side and fuel gas on the other, leading to local corrosion reactions. Alloys and surface coatings containing chromium or aluminum are under study to solve this problem.

- Electrode Sintering. Long-term operation of earlier porous nickel electrode structures showed that loss of surface area occurred via a sintering mechanism. This problem appears to have been solved by the addition of stabilizing components to the nickel.

- Materials Stability. Recent cost estimates for large-scale molten carbonate fuel-cell systems have assumed that stainless steels can be used as current collectors and spacers in the cell. Long-term stability of these steels has not yet been demonstrated. Nickel can be used as an alternative construction material at somewhat greater cost.

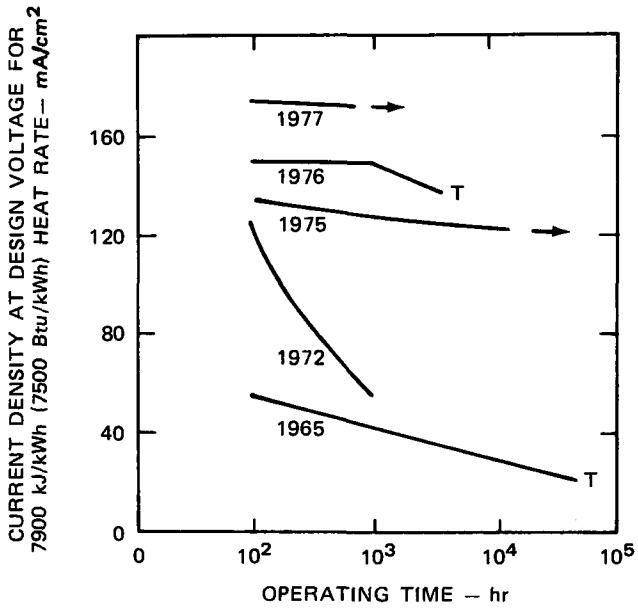

Source: Reference 17

FIGURE II-16. PROGRESS IN MOLTEN CARBONATE FUEL CELL PERFORMANCE

- The Carbon Problem. Initial designs for the integrated coal gasifier/molten carbonate fuel-cell power plant resulted in a projected fuel gas feed that is thermodynamically unstable with respect to carbon deposition:

$$2\ CO \longleftrightarrow CO_2 + C\downarrow$$

  Subsequent cell tests have verified that the nickel electrode surface is an effective catalyst for this reaction, resulting in carbon deposition and cell blockage. Proposed solutions to this problem involve reducing the CO partial pressure at the cell inlet by means of steam injection or anode gas recycle. Fortunately, the feed gases produced by hydrocarbon steam reforming are thermodynamically stable.

- The Sulfur Problem. Recent experiments have confirmed a suspected deleterious effect of sulfur on molten carbonate fuel-cell operation. Sulfur compounds (H_2S, COS, mercaptans) are present in feed gases derived from high-sulfur primary fuels such as coal or heavy liquid hydrocarbons. These sulfur compounds can react with the nickel anode to form nickel sulfides, some of which are molten at cell-operating temperatures. The result is a substantial loss in performance. In addition, if spent fuel is burned with cathode air feed to provide the required CO_2 recycle, the resulting SO_2 will be absorbed by the carbonate electrolyte. Again, performance losses are expected.

  At present, it appears that the maximum inlet sulfur content will be limited to a few ppm. These low concentration levels can be achieved by existing gas purification processes, but at extra cost and, perhaps, loss of efficiency. On the other hand, coupling the molten carbonate fuel cell with current steam-reforming processes should not be a problem because extensive feed desulfurization is already required to protect the nickel-based steam-reforming catalyst.

This discussion of molten carbonate fuel-cell technology has focused on current mainline programs. Another approach is being studied. SRI International is conducting an exploratory effort to define the feasibility of converting carbon (coal) directly to electrical energy in a form of molten carbonate fuel cell.[19] Here carbon anodes are consumed electrochemically. Preliminary cost studies are under way to define the economic feasibility of this approach.

The molten carbonate fuel cell holds considerable promise as an advanced energy conversion system. Improved energy conversion

efficiencies are obtained at the higher cell temperatures. Coupling the molten carbonate fuel cell with primary fuel provides a good match for the CO_2 balance required for the fuel-cell operation. Thus, the molten carbonate fuel cell could become dominant in large-scale, coal-fueled, base-load power generation. Applications involving substantial thermal cycling may not be attractive, if current problems with tile stability remain unresolved.

3. Solid Oxide Fuel Cells

A further improvement in the efficiency of large-scale fuel cells is projected through the use of solid oxide electrolyte fuel cells. Here, advantage is taken of the ionic conductivity shown by certain oxides, such as yttria-stabilized zirconia, at very high temperatures -- about 1,000°C (1,800°F). Reaction rates at these temperatures are rapid, so that ohmic and concentration polarization are the principal sources of performance loss. Apparently, carbon monoxide can also react electrochemically at 1,000°C, an advantage when the solid oxide cell is fed with gasified coal (H_2 + CO).

Solid oxide cell electrochemical reactions can be written as:

Anode reactions:	$H_2 + O^{=} \longrightarrow H_2O + 2e^-$
and/or :	$CO + O^{=} \longrightarrow CO_2 + 2e^-$
Cathode reaction:	$\frac{1}{2}O_2 + 2e^- \longrightarrow O^{=}$
Overall reactions:	$H_2 + \frac{1}{2}O_2 \longrightarrow H_2O$ + direct electrical energy
and/or :	$CO + \frac{1}{2}O_2 \longrightarrow CO_2$ + direct electrical energy

Oxide ion is the ionic current carrier, presumably moving through vacancies in the anionic lattice of the mixed zirconia oxide crystals. As written, the electrolyte appears invariant.

Structurally, the solid oxide cell differs considerably from other fuel-cell technologies. To form a total cell, thin layers of active material are deposited on the outer surface of a porous ceramic support tube. Fuel gas is fed to the tube interior and air to the exterior. Currently, active cell components include a nickel-zirconia cermet anode, yttria-stabilized zirconia electrolyte, a doped indium oxide cathode, and a lanthanum-chromite interconnect containing aluminum ions for improved thermal expansion characteristics and magnesium ions for improved electronic conductivity. The mechanical, thermal, and chemical stability of this interconnect material are critical factors controlling the ability to fabricate high voltage series-connected cells along the length of the support tube. Accurate matching of component coefficients of thermal expansion is necessary to prevent cracking and reactive mixing during initial startup heating and subsequent thermal cycling. Apparently, cell fabrication procedures also influence stability through their effect on final component morphology and microstructure. Additional constraints on the critical interconnect section include:[20]

- Moderate material cost.
- Invariant composition in both air and fuel atmospheres.
- No deleterious reaction with other cell components at 1,000°C (1,800°F).
- Resistivity less than 20-50 ohm cm and nearly 100% electronic conduction at 1,000°C (1,800°F).
- Negligible metal ion conduction.

Westinghouse, the principal investigator of solid oxide technology in the United States, has made substantial progress in this area in recent years, although considerable effort remains to demonstrate viable large-scale structures.[21] As usual, materials problems dominate at high temperature. Problems involving the migration of dopant ions at elevated temperature under the influence of the inter-electrode potential, and electrolyte "aging" or ionic conductivity degradation due to a reordering of atomic defects, have been discussed.[22] Possible electronic (in addition to ionic) conductivity of the solid oxide

electrolyte may further complicate the progress of solid oxide technology.

Systems studies on large, coal-fueled, central-station power plants provide the incentive for further development of solid oxide technology. Initial studies by Westinghouse in 1970[9] and recently, as part of the NASA-sponsored Energy Conversion Alternatives Study,[22] suggest that coal-to-busbar efficiencies exceeding 50% might be achieved. Similar studies by General Electric indicate lower efficiencies, and much remains to be clarified concerning system installed cost.

As with the molten carbonate system, the high-temperature waste heat from the solid oxide cell can be recovered effectively as steam for use in a bottoming cycle. On the other hand, little is known of the effect of impurities (H_2S, COS, particulates) in the gasified coal feed on solid oxide cell performance and life. As stated earlier, this technology appears limited to use in large-scale continuously operated power plants rather than smaller cycling plants.

4. Alkaline Fuel Cells

Alkaline electrolytes (e.g., KOH) may also be used to provide the ionic pathway between fuel and air electrodes. In particular, the oxygen reduction reaction appears to proceed more rapidly at high pH, compared with acid (low pH) electrolytes. Further, the somewhat less corrosive properties of aqueous alkaline electrolytes opens up the possibility of finding less expensive, stable, nonnoble metal catalysts. The characteristic electrochemical reactions in alkaline fuel calls are:

Anode reaction: $H_2 + 2OH^- \longrightarrow 2H_2O + 2e^-$

Cathode reaction: $1/2\ O_2 + H_2O + 2e^- \longrightarrow 2OH^-$

Overall reaction: $H_2 + 1/2\ O_2 \longrightarrow H_2O$ + direct electrical energy

Alkaline fuel cells have reached an advanced state of development for aerospace applications where high efficiency (hence, low reactant payload requirements) is a premium.[23] Such systems use ultrapure hydrogen and oxygen reactants. Attempts to develop a terrestrial fuel-cell system based on alkaline electrolyte technology were recently carried out by Exxon,[24] using thin, inexpensive plastic fuel-cell components developed jointly with the Alsthom Company in France.

The principal difficulty facing alkaline fuel cells in terrestrial applications involving carbonaceous fuels (hydrocarbons, coal, methanol) is lack of electrolyte invariance in the presence of carbon oxides:

$$2OH^- + CO_2 \longrightarrow CO_3^= + H_2O$$

Effective procedures for removing carbonate ion, regenerating the spent caustic electrolyte, or preventing carbon oxides from entering the fuel cell must be developed. Novel electrochemical techniques were explored for the former, but considerable effort is required for development to commercial status. On the other hand, adequate existing technology is available for precleaning fuel gases containing CO_2 (and H_2S) and for removing trace amounts of CO_2 from incoming ambient air (350 ppm CO_2). These processes include absorption in promoted carbonate or caustic solution, and pressure-swing adsorption cycles using molecular-sieve adsorbents. Further, the efficiency and cost of these pretreatment steps appear reasonable.[24] Large, 400-MW, intermediate-load power plants were designed, using reformed naphtha or methanol fuel, with heat rates between 7,100 and 7,900 kJ/kWh (6,700 and 7,500 Btu/kWh). These values compare favorably with those of other second-generation technologies. These low heat rates were projected, although the assumed temperatures for the alkaline system were between 70 and 120°C (158 and 148°F), too low for effective conversion of waste heat to electricity via a bottoming cycle. Rather optimistic levels of cell performance were used, assuming a successful but costly R&D program to overcome problems with internal component contact resistance and to develop improved cathode electrocatalysts. Prospects exist for

substituting spinel and perovskite oxide cathode catalysts for platinum, but these remain to be explored fully.

Although alkaline fuel-cell technology is not being developed for utility power generation at present, it remains the most promising approach for electricity production from relatively pure hydrogen fuels that may be available from future thermochemical or electrolytic hydrogen production. Indeed, the operating characteristics of the current second-generation molten carbonate technology are such that CO_2 would actually have to be manufactured independently to maintain electrolyte invariance in such applications.

5. Ion Exchange Membrane Cells

The ion exchange membrane fuel cell uses a hydrogen ion-conducting solid polymer as electrolyte. Initial ion exchange membranes were formed using the strong acid, polystyrene divinyl benzene sulfonic acid, although recently membranes have been formed from more stable and costly fluorinated polymer resins. Electrochemical reactions in the ion exchange membrane cell are similar to those noted earlier for the phosphoric acid system.

Ion exchange membrane calls have been under continuous development by General Electric since the early 1960s, primarily for aerospace applications such as the Gemini missions.[25] From time to time, attempts have been made to exploit this technology in terrestrial power plants.[26] Initial problems with dimensional and thermal stability have been overcome, resulting in an extension of cell operating temperatures to somewhat more than 100°C (212°F). Care must be exercised to prevent membrane drying, particularly when dilute reactants (reformed fuels, air) are used.

The lower operating temperature of the ion exchange membrane, coupled with its acidic nature, appear to be the principal technology

issues limiting its widespread application. Noble metal catalysts are required and the prospects for raising catalyst utilization by operating at much higher temperature (200°C or 390°F) are restricted. Further, catalyst sensitivity to the trace CO content of reformed fuel feeds may require the use of alloy anode catalysts. Lastly, opportunities for effective waste heat recovery are also limited by the low operating temperature, as with current alkaline fuel-cell technology.

REFERENCES

1. Bolan, P., "Heat Pumps and Fuel Cells," Paper 23d, 69th Annual AIChE Meeting (November 30, 1976)

2. United Technologies Corporation, Power Systems Division, "Venture Analysis Case Study for On-Site Fuel Cell Energy Systems," Report No. FCR-0787, final report in three volumes (July 31, 1978).

3. Stickles, R. P., et al., "Assessment of Industrial Applications for On-Site Fuel-Cell Cogeneration Systems," NASA CR-135429 (September 1978).

4. United Technologies Corporation, Power Systems Division, "National Benefits Associated with Commercial Application of Fuel-Cell Power Plants," ERDA 76-54, UC-93 (February 17, 1976).

5. Public Service Electric and Gas Company, "Economic Assessment of the Utilization of Fuel Cells in Electric Utility Systems," Final Report, EPRI EM-336 (November 1976).

6. Gillis, E. A., "Fuel Cells for Dispersed Generation of Electric Power," International Conference on Energy Use Management, Tucson, Arizona (October 24, 1977).

7. Burns and McDonnell Engineering Company, "An Assessment of the Fuel Cell's Role in Small Utilities," EPRI Report EM-696, Vol. 1 (February, 1978).

8. King, J. M., "Integrated Coal Gasifier/Molten Carbonate Fuel-Cell Power Plant Conceptual Design and Implementation Assessment," NASA CR-134955, FCR-0157 (October 19, 1976).

9. Sverdrup, E. G., et al., "Project Fuel Cell," Final R&D Report No. 57, Westinghouse (1970).

10. Inside D.O.E., p. 2 (November 27, 1978).

11. Fickett, A., Fuel Cell R&D Status Reports, EPRI Journal, p. 14 (April 1976), p. 46 (June/July 1977), p. 34 (June 1978).

12. Pan, Y. C., et al., "Fuel Cell Catalyst Sintering Studies," Final Report, EPRI EM-833 (July 1978).

13. Communications from Dr. P. Stonehart, Stonehart Associates.

14. Communications from Professor E. Yeager, Case Western Reserve University, Cleveland, Ohio.

15. Blurton, K. F., et al., "The Performance of Molten Carbonate Fuel Cells," presented at the 11th INternational Power Sources Symposium, Brighton, England (1978).

16. Kunz, M. R., "Molten Carbonate Fuel-Cell Performance," National Fuel Cell Seminar, San Francisco, California, July 11-13, 1978, Abstracts, p. 96.

17. King, J. M., "Advanced Technology Fuel-Cell Program," Interim Report, EPRI EM-576 (November 1977).

18. Molten Carbonate Fuel-Cell Workshop, held at Oak Ridge National Laboratories, October 31-November 2, 1978.

19. Weaver, R. D., et al., "Direct/Coal Air Fuel Cell," National Fuel-Cell Seminar, Boston, Massachusetts, June 21-23, 1977, Abstracts, p. 77.

20. Ruka, R. J., et al., "Electrical Interconnection of High Temperature, Solid Oxide Fuel Cells," National Fuel-Cell Seminar, Boston, Massachusetts, June 21-23, 1977, Abstracts, p. 79.

21. Ruka, R. J., "Development of a Practical Interconnection for Solid State High Temperature Fuel Cells," National Fuel-Cell Seminar, San Francisco, California, July 11-13, 1978, Abstracts, p. 159.

22. Dragoo, A. L., et al., "Solid Oxide Fuel Cells," National Fuel-Cell Seminar, Boston, Massachusetts, June 21-23, 1977, Abstracts, p. 91.

23. Bolan, P., et al., "Hydrogen-Oxygen Alkaline Fuel Cells," National Fuel-Cell Seminar, Boston, Massachusetts, June 21-23, 1977, Abstracts, p. 115.

24. Elzinga, E. R., et al., "Application of the Alsthom/Exxon Alkaline Fuel Cell System to Utility Power Generation," Final Report, EPRI EM-384 (January 1977).

25. McElroy, J. F., "Status of H_2/O_2 Solid Polymer Electrolyte Fuel-Cell Technology," National Fuel-Cell Seminar, Boston, Massachusetts, June 21-23, 1977, Abstracts, p. 95.

26. MacLeod, E. N., et al., "Evaluation and Optimization of Solid Polymer Electrolyte (SPE) Fuel Cells," Final Report, MPR-022 (May 15, 1978).

III. SELECTION OF ENERGY SUPPLY SYSTEMS FOR DETAILED ANALYSIS

A. Criteria for Proposed Systems

To analyze five energy supply systems in detail, we were initially to propose 10-15 energy systems, of which several were to utilize fuel cells. To put all proposed systems on a common basis, EPA specified the following constraints:

- All systems will utilize western coal.
- All systems will provide residential heating and cooling.
- All systems will be based on advanced technology capable of being commercialized in the period 1980-2000.
- The residences to be provided heating and cooling will be located 800-1,600 km (500-1,000 mi) from the coal mine.

In addition to the constraints listed above, some other limiting factors had to be applied to the selection of systems to ensure that they were representative of the array of technologies that would actually be available to utilities in the coming decades, and to which they would give serious consideration. We only examined systems that could readily supply the type of load specified. For example, heating and cooling tend to constitute a large part of a utility's intermediate- and peak-load demand. Thus, intermediate and peaking electricity generation technologies are more appropriate than base-load technologies for inclusion in the proposed systems.

Market penetration studies have indicated that the primary application of fuel cells in future utility generation mixes will be as intermediate-load devices.[1] This result is supported by two simple economic facts: (1) the high cost of fuels, especially coal-based fuels,

that fuel cells must use makes them too expensive for base-load use; and (2) gas turbines will almost always be cheaper to use as peak-load devices because of their lower capital cost.

Thus, to make all proposed systems under consideration consistent with likely fuel-cell systems, we limited the electricity generation components of the systems to intermediate-load devices. This choice eliminated those technologies which, because of high capital cost or lack of cycling capability, are primarily restricted to base-load application. For example, fluidized bed combustion, coal gasification coupled with either a combined-cycle system or a molten carbonate fuel cell, and conventional coal-fired steam technology were not included. The exclusion of the latter technology is limited only to new plants, however, because older base-load plants are commonly reassigned to intermediate-load service. Naturally, technologies such as gas turbines that are primarily used in peak-load applications were also excluded.

Finally, those technologies that, although very promising and with some likelihood of achieving commercialization by the year 2000, but that are not at a stage of development sufficiently advanced to enable a thorough analysis, were not considered. An example of such a technology is the direct coal-fueled fuel cell.

To further aid in defining the systems choices, we chose a geographical setting for the end use. To be generally applicable, this location should have climate characteristics typical of regions of the United States where a significant fraction of the population lives. The most populated area of the country is in the northeastern corridor. That climatic zone has a winter heating season of 2,800 - 3,900 Centrigrade degree-days (5,000-7,000 Farenheit degree-days) and a summer cooling season of 280-830 Centigrade degree-days (500-1,500 Farenheit degree days)*.

---

*A degree-day is the difference between the average temperature and 18°C (65°F) over one 24-hour period.

Because that region is too far from the western coal fields for economical use of western coal or its conversion products, a more westerly location was considered desirable for analytical purposes. The region bounded by Kansas City, Des Moines, and Omaha appeared to be suitable. Its climatic conditions of 3,300 heating and 560 cooling Centigrade degree-days (6,000 heating and 1,000 Farenheit cooling degree-days) are similar to those of the heavily populated Northeast, and its distance from the coal fields of Wyoming and Montana is about 1,300 railroad kilometers (800 miles). Thus, this region was chosen as the location for the end-use components of all the systems considered.

B. Proposed Systems

Twelve energy supply systems that met all the criteria previously set forth were proposed for evaluation. Because of similarities in fuel type, energy conversion technology, and end-use, these systems were classified into four broad system types for supplying residential energy, each having one or more fuel supply options (see Table III-1). A brief discussion of each type, including a system diagram, follows.

1. Type 1: Conventional Power Plant/SNG

Type 1a is a dual system in which residential cooling is provided by an air conditioner, and heating is supplied by a gas furnace (see Figure III-1). The electricity that powers the air conditioner is generated by an older coal-fired power plant that has been reassigned to intermediate-load service. It is equipped with a stack gas scrubber to remove SO_2. The gas furnace burns synthetic natural gas (SNG) derived from coal. The power plant is assumed to be located near the point of electricity use, requiring the coal to be shipped by unit train from the mine. The SNG facility is assumed to be located near the mine, requiring the transport of gas via interstate pipelines.

This system type was chosen to represent, as closely as possible, the conventional energy supply system in the West North

Table III-1

CATEGORIZATION OF PROPOSED RESIDENTIAL ENERGY SUPPLY SYSTEMS

Off-site Generation of Electricity

Electric/Gas Residence

Type 1a: Coal-fired power plant; SNG

Type 1b: Coal-derived oil-fired power plant; SNG

All Electric Residence

Type 2a: 26-MW fuel cell; methanol

Type 2b: 26-MW fuel cell; SNG

Type 2c: 26-MW fuel cell; coal-derived naphtha

Type 2d: 26-MW fuel cell; hydrogen

Type 3a: Combined-cycle power plant; methanol

Type 3b: Combined-cycle power plant; SNG

Type 3c: Combined-cycle power plant; coal-derived distillate fuel

On-Site Cogeneration of Electricity and Heat

All-Electric Residence

Type 4a: 100-kW fuel cell; methanol

Type 4b: 100-kW fuel cell; SNG

Type 4c: 100-kW fuel cell; coal-derived naphtha

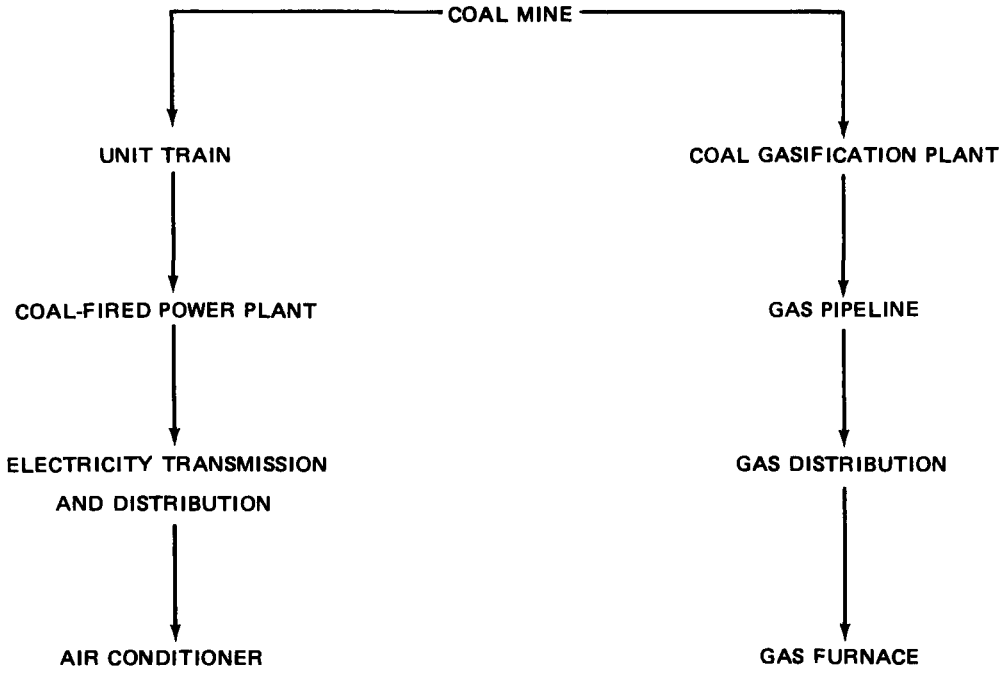

FIGURE III-1. TYPE 1a: COAL-FIRED POWER PLANT/SNG

Central region of the United States, which includes Kansas City, Des Moines, and Omaha. Of course, no SNG is being used at this time, but it would be a likely candidate as a supplemental source of pipeline gas in the future when natural gas is expected to be in short supply. Electricity generation in that part of the country is largely carried out in direct coal-fired steam plants. Older plants are commonly reassigned from base-load to intermediate-load service, with peak-load service typically provided by gas turbines. The use of stack gas scrubbers on plants burning low-sulfur western coal is likely to be required to meet revised federal new source performance standards (NSPS).

Type 1b was proposed as an alternative to Type 1a in which a coal-derived liquid fuel would be burned in an oil-fired power plant to provide electricity for air conditioners (see Figure III-2). This system type would require the construction of new oil-fired power plants because very few are now in operation in the West North Central states.

The main advantage of this system type, compared to Type 1a, is environmental, because clean fuels would be burned in place of coal. The resulting cost of electricity would be very high, however, because of high fuel costs and high capital recovery costs resulting from the construction of new plants that would operate with a load factor of only 30-40%.

The option of producing solvent-refined coal (SRC) for Type 1b was initially considered. However, for low-sulfur western coal, very little benefit is achieved relative to the high processing costs. Upgrading the product to a liquid fuel that can be sent through pipelines makes more sense, because transporting fuel by pipeline saves enormously on shipping costs and a liquid fuel would have wider market potential.

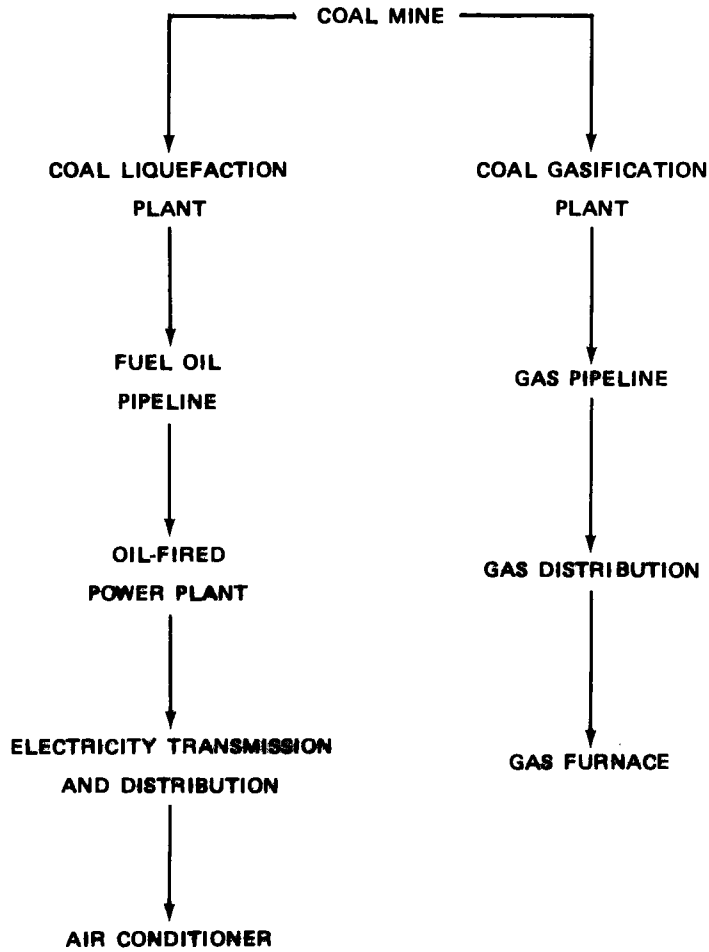

FIGURE III-2. TYPE 1b: OIL-FIRED POWER PLANT/SNG

2. Type 2: 26-MW Fuel-Cell Power Plant

The 26-MW fuel cell was chosen for Type 2 as representative of the size envisioned for near-term application of first generation fuel cells. A 26-MW device (which actually consists of six modules of about 4.5 MW each) is small enough to be located at dispersed sites throughout a utility grid (see Figure III-3). Furthermore, units can be added incrementally to meet increasing loads, thus deferring large commitments of capital required for larger units. Because fuel cells are environmentally unobtrusive at the point of operation they are easily sited, even in urban areas.

Coal-based fuels can be supplied to fuel cells in several ways. Because the small size and dispersed location of the fuel cells precludes on-site coal conversion activities, location of coal conversion facilities at the mine was assumed. Four fuels -- methanol (Type 2a), SNG consisting primarily of methane (Type 2b), coal-derived naphtha (Type 2c), and hydrogen (Type 2d) -- are compatible with fuel-cell operation, and can be transported over long distances by pipeline. All the fuels except hydrogen must be reformed at the fuel-cell site. SNG and hydrogen could be distributed to the fuel cells by pipeline, while liquid fuels would be distributed by trucks. On-site storage capability would be required for the liquid fuels.

The electricity produced by the fuel cells is assumed to power heat pumps located in individual residences. The heat pumps supply heating in the winter, and are operated as air conditioners in the summer.

The use of heat pumps implies that the residences are all-electric. Although this does not typically occur in the region under consideration, it is an option when natural gas may be in short supply. Already in many areas of the country obtaining natural gas connections for new homes is not possible. In such cases, all-electric homes equipped with heat pumps provide a viable, reasonably economical alternative.

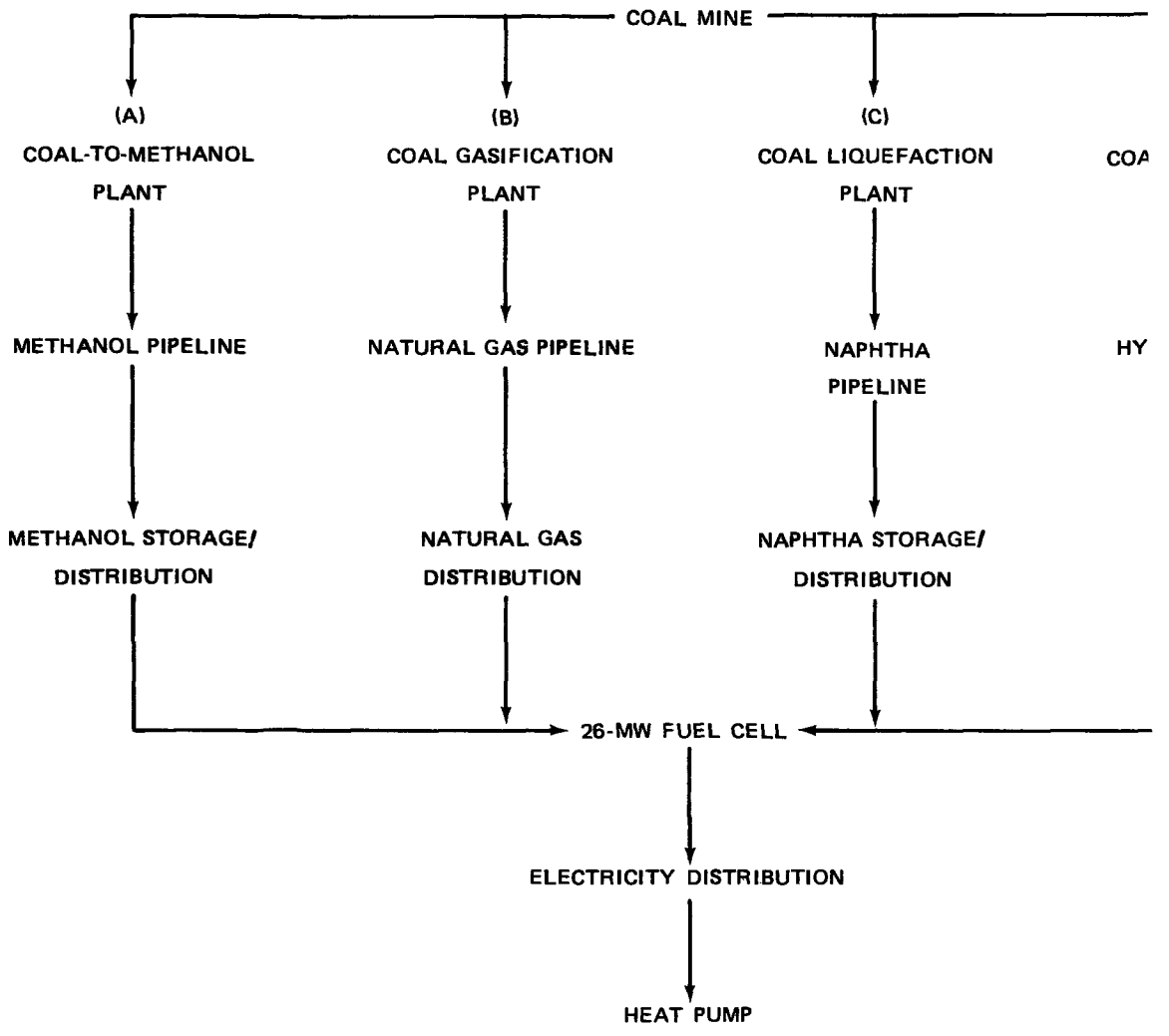

FIGURE III-3. TYPE 2: 26-MW FUEL CELL

In addition, the high electrical demand implied by the construction of new all-electric homes necessitates new electrical generation capacity of all kinds. Not enough older fossil steam plants are likely to be available to reassign to the intermediate use for which fuel cells are well suited; thus, the construction of new facilities is required.

3. Type 3: Combined-Cycle Power Plant

Type 3 is proposed as an alternative to fuel cells that can economically provide intermediate electrical loads (see Figure III-4). The low capital costs and low heat rate of combined-cycle systems make them competitive with fuel cells. The end use for electricity is identical to that in Type 2. The system type envisioned here would consist of a gas turbine coupled with a steam bottoming cycle. Suitable coal-derived fuels for the combined-cycle plant include SNG (Type 3a), distillate fuel (Type 3b), and methanol (Type 3c). (A hydrogen system was not proposed because without the advantage of avoiding reforming there are no benefits to balance the additional costs and problems of hydrogen transport and handling.) Combined-cycle power plants would be sized in the 200-300 MW range so that dispersed siting would not be practical. However, the fuel distribution costs would be reduced compared to the fuel-cell case.

4. Type 4: 100-kW Fuel-Cell Power Plant with Heat Recovery

Type 4 takes advantage of the ability to construct small fuel-cell power plants so they can be located at the site of electricity demand (see Figure III-5). If this site is an apartment building or cluster housing complex, the fuel-cell waste heat that is normally rejected to the atmosphere may be recovered and used to supply domestic hot water and supplemental heat for heat pumps.

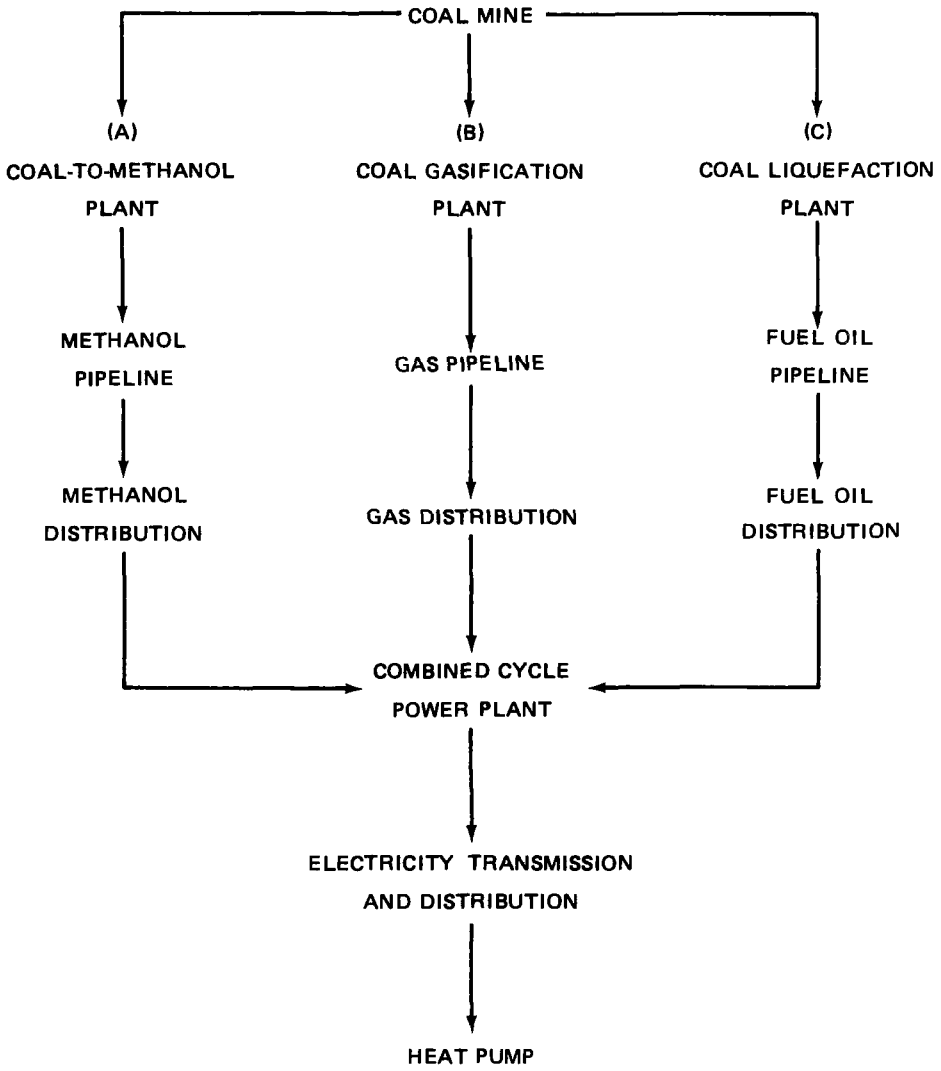

FIGURE III-4. TYPE 3: COMBINED-CYCLE POWER PLANT

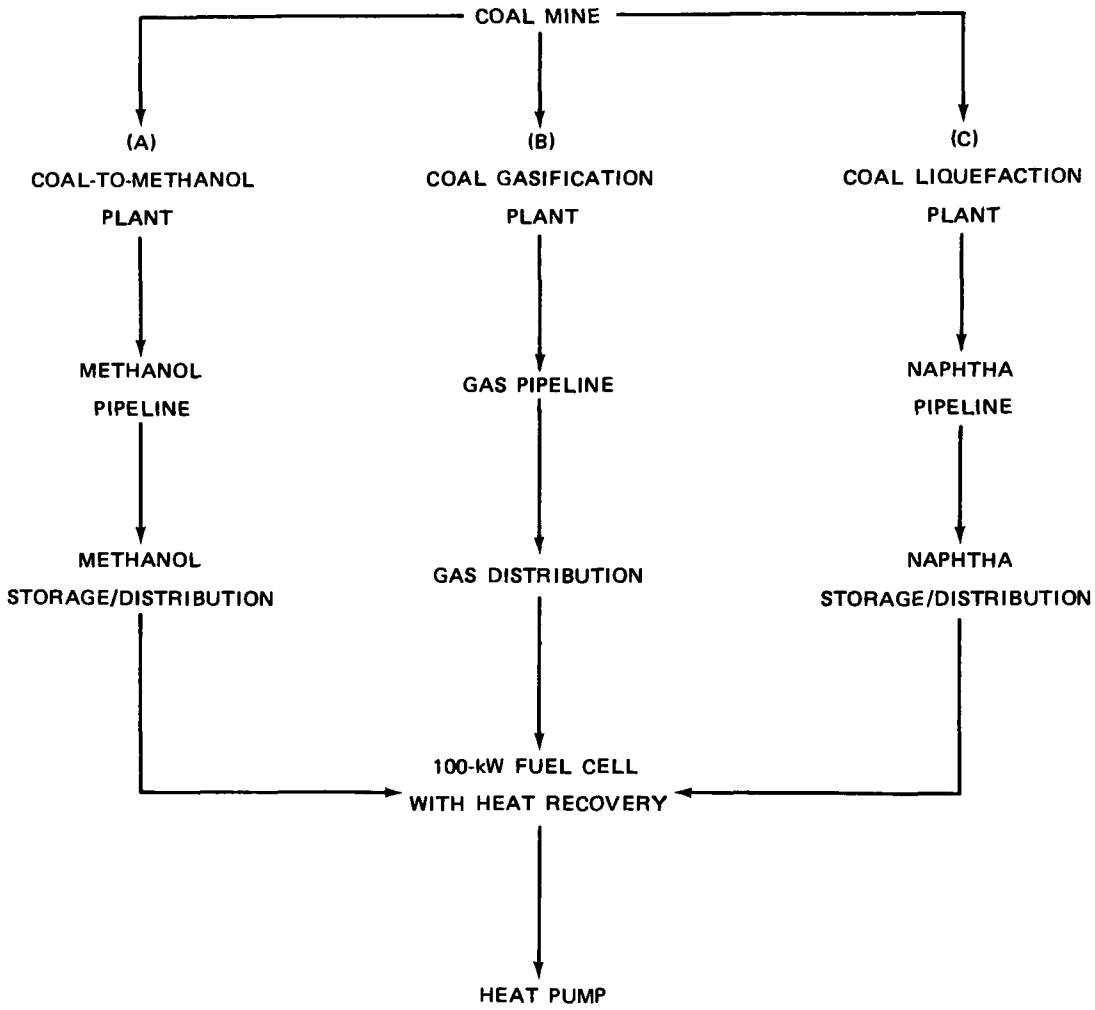

FIGURE III-5. TYPE 4: 100-kW FUEL CELL WITH HEAT RECOVERY

The fuel supply options for this system are the same as for Type 2, except that hydrogen is omitted, because of anticipated difficulty of installing a dense hydrogen distribution network in the time frame considered by the study. Thus, suitable coal-derived fuels are methanol (Type 4a), SNG (Type 4b), and naphtha (Type 4c).

C. Evaluation of System Components

The next step in this study was to select five energy-supply systems for detailed analysis from the 12 systems initially proposed. The selection was based on preliminary estimates of cost, energy efficiency, and environmental impact. The analyses of the systems that supported the selection procedure are described below.

1. Cost and Efficiency

The individual system components or process steps for each of the 12 candidate energy systems were analyzed. Component cost and energy efficiency were estimated, with data taken from SRI studies or from the published literature.

The cost and thermal efficiency estimates were prepared from specific cost studies and were for new equipment. The costs were normalized on the basis of the higher heating value (HHV) of the principal product. Normalizing costs in this manner avoided analytical anomalies caused by mismatches in the various plant sizes. All plants were assumed to be sufficiently large so that maximum reasonable advantage could be claimed for economies of scale. For ease of handling, cost estimates were compiled from the three major cost components: plant investment, plant operating costs (exclusive of plant amortization), and cost of feedstock consumed in the conversion process. A capital recovery factor of 18.2% per year was assumed (equivalent to a regulated utility cost basis of 65% debt at 10% interest, and 35% equity at 15% return on equity).

2. Sulfur Dioxide Emissions

To provide some guidance to the environmental impact of each energy supply system, we chose a single parameter for analysis. This parameter was the total amount of SO_2 emitted by the components of each system. Because SO_2 is a major pollutant of concern and is subject to a wide range of regulatory activity, it provided a convenient focus for a preliminary environmental analysis. Because the primary sources of SO_2 emissions are the coal conversion technologies, the sulfur balances for those technologies were examined in detail.

Coal conversion has two principal sources of sulfur emission--the coal-burning utility part of the plant, which burns coal to provide steam, electricity, and process heat, and the gasification or liquefaction part of the plant. The utility sulfur emissions are in the stack gases and consist almost entirely of SO_2 from oxidation of the sulfur in the coal. The liquefaction or gasification of coal produces principally H_2S in product or by-product gas streams. Small amounts of carbonyl sulfide and other volatile sulfur compounds may also be formed. These gas streams are purified by scrubbing systems that use amines (MEA, DEA) or organic solvents such as methanol. This scrubbing generates a waste stream of concentrated sulfur compounds which can then be treated in a sulfur recovery process such as the Claus process.

Minor amounts of sulfur are contained in ash and unreacted char streams, as well as in water effluents, but this sulfur is not included in the present discussion because it has little effect on the system analysis.

There are three possible strategies for controlling sulfur emissions:

- Each installation would be controlled to achieve some standard emission rate per GJ (0.948 million Btu) of coal input (e.g., NSPS). The major impact on particular technologies would be cost differences, because for some processes the capital required to meet the standard will be higher than for others.

- Each installation would have the same total expenditure for air pollution control. The major impact on particular technologies would be differences in sulfur emission rates. For some conversion technologies this fixed expenditure would be sufficient to achieve very low sulfur emission rates whereas for others it would not.

- Each installation would have the best available technology installed. Different coal conversion technologies would have different control costs and different sulfur emission rates with this strategy.

The third option was chosen for this study; the best available technology was defined to be:

- Electrostatic precipitators and lime/limestone scrubbers for stacks of coal-fired boilers. Scrubbing removes 85% of the stack gas sulfur.

- Claus or Stretford units followed by incinerators and lime/limestone scrubbers used on sulfur-rich gases leaving the conversion process. The Claus or Stretford unit removes 90-95% of the feed sulfur, and the incinerator and scrubber removes 85% of the sulfur remaining in the tail gas.

Those particular choices of technology resulted in sulfur emissions that are somewhat lower than the proposed federal NSPS for coal gasification and also yielded boiler stack gases that are cleaner than required by current federal and state standards for new sources. The technology chosen will also be suitable for controlling carbonyl sulfide, hydrocarbons, particulates, as well as other pollutants that will be considered later in this study.

The control technology is fixed so that each coal conversion technology will have different sulfur emissions, primarily because of differences in process efficiency. Low efficiency technologies such as methanol production have larger utility requirements, resulting in a larger percentage of the coal delivered to the plant going to the utility plant rather than to the gasification or liquefaction reactor. With the choices of best available technology made for this study, coal burned in the utility plant releases 15% of its sulfur to the environ-

ment whereas coal processed in the converter releases less than 1% of its sulfur to the environment.

3. Ranking of Proposed Systems

Using the parameters estimated for each system component, the overall costs, efficiency, and release of SO_2 associated with providing residential heating and cooling were estimated. All quantities were calculated on the basis of providing one year's heating and cooling to a single residence. Those figures were then used to rank the twelve energy systems and aid in the selection of five systems for further analysis.

Because the estimates of cost, efficiency, and SO_2 emissions for both the system components and the total systems were preliminary in nature, and to avoid confusion with more precise estimates given later in this report, results of those estimates will not be presented here. However, the relative rankings of the systems, based on those preliminary estimates, are given in Table III-2.

D. Selection of Systems

Selecting five systems from the twelve proposed was complicated because multiple parameters in addition to nonquantifiable considerations had to be used in evaluating the systems. In general, a unique set of systems could not be chosen without attaching precise weighting factors to each parameter of interest (cost, efficiency, SO_2 emissions) to obtain an overall impact parameter for each system. Such impact parameters, tempered by nonquantitative considerations, could then be used to guide the systems selection. The task was made easier, however, by recalling that the purpose of the systems selection was to select systems to evaluate that would be competitive in similar applications and would represent realistic choices for utilities in the

Table III-2

RANKING OF COST, EFFICIENCY, AND
SO_2 EMISSIONS FOR ENERGY SUPPLY SYSTEMS

System	Cost Ranking (lowest cost = 1)	Efficiency Ranking (most efficient = 1)	SO_2 Emissions Ranking (lowest emissions = 1)
1a	1	3	9
1b	2	6	7 (tie)
2a	12	12	11
2b	7	9	5 (tie)
2c	11	10	5 (tie)
2d	8 (tie)	5	3
3a	10	11	10
3b	4	7 (tie)	4
3c	5	7 (tie)	12
4a	8 (tie)	4	7 (tie)
4b	3	1	1
4c	6	2	2

1980-2000 time frame. Each system had to pass judgments as to its likelihood of implementation in that time frame before other parameters were weighed. Once that criterion had been satisfied, the cost, efficiency, and SO_2 emission comparisons could then be applied to the remaining systems.

Because four broad types of systems with different fuel options were proposed, we selected at least one system within each type to make the study representative. Table III-2, which shows the relative ranking of costs, efficiency and SO_2 emissions for all the systems was used to assist in the selection process.

Type 1a (Figure III-1) was found to have the lowest cost of heating and cooling of any system, moderately high efficiency, and SO_2 emissions that are high relative to most other systems. This system type is closest to current practice in the West North Central region, and thus represents a case with high likelihood for future use.

The total cost of heating and cooling from Type 1b (Figure III-2) was only slightly higher than that of Type 1a, even though the cost of electricity is more than twice as high, because of the relatively small amount of electricity used compared to SNG. SO_2 emissions were lower and the efficiency was about the same.

At present, there are essentially no large oil-fired steam electric plants in the West North Central region, and it is questionable whether any will be built in the future, especially for intermediate load applications.

In Type 2 (Figure III-3), which included four fuel supply options, the methanol option appeared to be the least favorable in terms of cost, efficiency and SO_2 emissions (primarily because of the high cost and low efficiency of the coal-to-methanol conversion step), whereas hydrogen was the most favorable. The SNG and naphtha options were intermediate. Although hydrogen appeared most attractive in terms of

these quantitative parameters, several aspects of this system make it unlikely that it would be used before 2000. The main problem is the necessity of constructing hydrogen pipelines and distribution systems in the absence of other significant demands for hydrogen. Because nearly any use that can be foreseen for hydrogen over the next 25 years could be filled equally well by methane, there seems little incentive for constructing hydrogen systems where natural gas systems already exist. Furthermore, some serious technical problems, such as embrittlement of pipeline steel, would have to be overcome before hydrogen systems could be constructed. In addition, no one is likely to construct a hydrogen system solely dedicated to supplying fuel cells, whereas the presence of existing natural gas and petroleum distribution systems favors the use of SNG, naphtha, or methanol.

In Type 3 (Figure III-4), methanol again ranked unfavorably, having the highest cost, lowest efficiency, and high SO_2 emissions relative to the other fuels. SNG and fuel oil rank approximately equally in cost and efficiency. The higher SO_2 emissions from the fuel oil option result from the small amount of sulfur in the fuel oil that is released during combustion. In the future, utilities may be restricted in their use of natural gas for electricity generation. Certainly, natural gas will be phased out as a boiler fuel, but whether it will continue to be allowed as turbine fuel is not clear. SNG will probably be subject to the same restrictions as natural gas because it will serve the same needs, and the tendency will be to preserve it for higher priority users (e.g., residential and commercial customers).

In Type 4 (Figure III-5) cost, efficiency, and SO_2 emissions are improved compared to Type 2 because of the recovery of waste heat from the fuel cell. Among the three fuel options, methanol appeared the least attractive overall for the reasons mentioned previously. SNG is superior in cost and efficiency to naphtha, but comparable in SO_2 emissions. Assuming that gas or electric utilities were to own and maintain small fuel cells located in housing complexes, there does not seem to be an overwhelming advantage to using SNG rather than naphtha,

except that supplying SNG through the gas distribution grid would be a more convenient, and perhaps a more secure, source of supply than delivering naphtha by truck.

The final selection of five systems resulted from several judgments about their relative attractiveness. First, compared to other fuels, methanol always appeared less attractive in terms of cost, efficiency, and SO_2 emissions. Therefore, Types 2a, 3a, and 4a were eliminated.

Second, large-scale systems for transporting and distributing hydrogen are unlikely to be constructed before the end of the century. Thus, Type 2d was removed as an option.

Third, future restrictions on natural gas use are likely to limit its availability (SNG included) for large new electricity generation facilities. Therefore, coal-derived fuel oil would be a likelier prospect as a fuel for combined-cycle power stations. This judgment favored option 3c over 3b.

Consideration of the merits of Type 1b led to a fourth judgment: that there will be relatively little incentive to build new oil-fired steam plants to meet intermediate loads in the West North Central region. Compared to combined-cycle plants, oil-fired steam plants are more capital intensive and less efficient, resulting in a 13% higher cost of electricity when coal-derived fuel oil is used. Thus, Type 1b was eliminated.

Of the remaining six systems there was no clear-cut single choice for elimination. We retained Types 1a and 3c to compare with the fuel-cell options, however. This left two fuel supply options for the 26-MW fuel cell (Types 2b and 2c), and two for the 100-kW fuel cell (Types 4b and 4c). We judged that because the thrust of research to date on fuel cells for on-site residential applications has been directed toward the use of natural gas as a fuel, the SNG supply option

should be retained for the 100-kW system; thus, Type 4c was eliminated. For the 26-MW system, SNG and coal-derived naphtha appeared to be equally likely. Therefore, both fuel options were retained.

In summary, the five systems selected for detailed analysis are:

- System 1: A coal-fired power plant that supplies electricity to residences and a coal gasification plant that supplies SNG; electricity is used to power air conditioners and SNG is burned in gas furnaces (Type 1a).
- System 2: A 26-MW fuel-cell power plant fueled by SNG derived from coal; electricity is provided to residences that are heated and cooled by heat pumps (Type 2b).
- System 3: 26-MW fuel-cell power plant fueled by coal-derived naphtha; electricity is provided to residences that are heated and cooled by heat pumps (Type 2c).
- System 4: A combined-cycle power plant fueled by coal-derived fuel oil; electricity is provided to residences that are heated and cooled by heat pumps (Type 3c).
- System 5: A 100-kW fuel-cell power plant fueled by SNG, sited in a housing complex; electricity is provided to residences that are heated and cooled by heat pumps. In addition, heat is recovered from the fuel cell to supply supplemental space heating and hot water (Type 4b).

E. References -- Chapter III

1. W. Wood, M. P. Bhavaraju, and P. Yatcko, "Economic Assessment of the Utilization of Fuel Cells in Electric Utility Systems," Electric Power Research Institute Report EM-336 (November 1976).

IV CONCEPTUAL SYSTEMS DESIGNS

After the five energy supply systems were selected for analysis, the next task was to provide conceptual designs of the systems so that further economic, environmental, and energy efficiency analysis could be carried out. The conceptual designs were to specify technology types, sizes, flow rates, and other characteristics. Those specifications were subject to limitations on knowledge of the actual process designs that will characterize commercial-scale facilities built around advanced energy technologies. All our conceptual designs of advanced energy conversion processes can be considered representative but not definitive; other designs may be equally credible.

Generally speaking, the conceptual designs of advanced processes were based on optimistic extrapolations of current pilot plant data. Only time will tell whether these results will be borne out in large-scale commercial facilities and whether major process changes from the ones now envisioned will be required. Nevertheless, the conceptual designs represent the process features that must be attained if advanced energy conversion concepts are to achieve a significant market within the next 20 years.

The conceptual designs presented in the chapter are described in terms of the functional units or "building blocks" of which each system is composed. Each building block defines a system component that is logically sized to achieve economies of scale and that represents current or anticipated future industrial practices. Thus, the components are not sized to represent equal flow of energy; the output of energy from one component in a system does not equal the energy input to the following component. One may envision, for example, that the output from several coal gasification plants would be required to fill a major interstate pipeline, or that the output of such a pipeline would supply

many 26-MW fuel-cell power plants in addition to homes, businesses, and industries. Thus, the mismatches in size inherent in the systems represent the situation that would likely prevail if such systems were actually constructed. Whenever possible in the following descriptions, the energy output of one component will be related to the energy input requirements of the following component in the system.

The conceptual design of each component consists of a general description, followed by a more specific description of equipment size, flow rates, and so on. When the system component is an energy conversion facility (e.g., coal gasification plant, fuel-cell power plant), a block flow diagram showing major process elements is presented, along with material balances. The level of detail is sufficient to allow an accurate determination of costs, energy efficiencies, and pollutant emissions in subsequent analyses. Excessive detail has been avoided.

In the following descriptions some components will be common to more than one system. In such cases, the description of the component will be presented only once, in the discussion of the first system in which it appears. In subsequent discussions, the reader will be referred to the initial description of the component.

A. System 1

A block flow diagram of System 1 is shown in Figure IV-1. The components of the system are described below.

1. Coal Mine

The mine that supplies coal for electricity generation, gasification, and liquefaction is a large surface mine typical of those operating and planned in the Powder River Basin of northeastern Wyoming and southeastern Montana. Such mines extract low-sulfur subbituminous coal

Figure IV-1

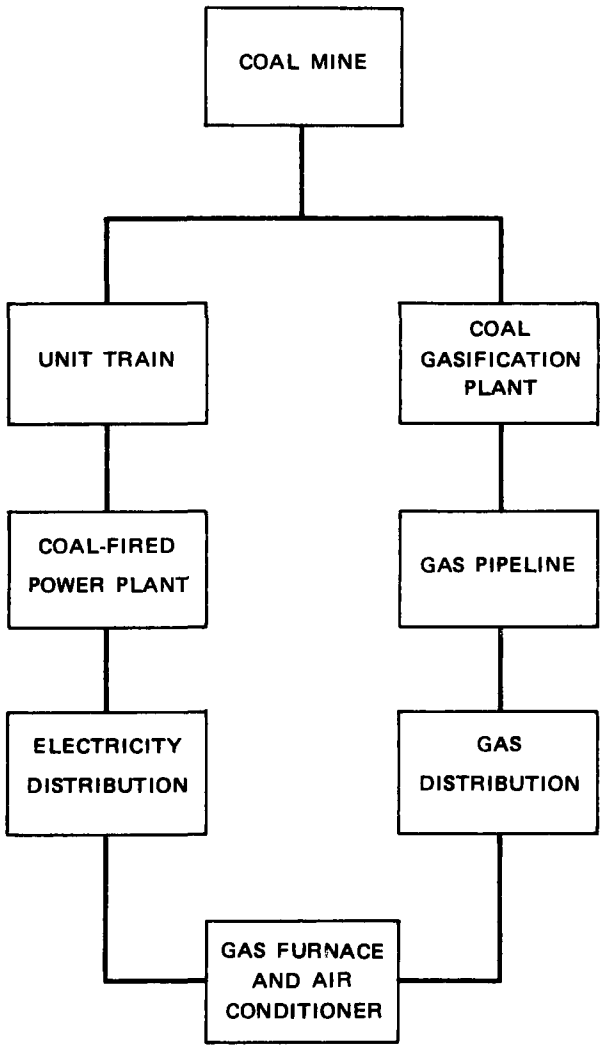

FIGURE IV-1. BLOCK FLOW DIAGRAM OF SYSTEM 1

from very thick, relatively shallow seams. Because mining operations vary according to the geological conditions associated with particular mining sites, we have selected a hypothetical mining operation that represents more or less typical conditions.

The hypothetical mine produces 4.5 million tonnes (5 million tons) of coal per year from a seam 15 m (50 ft) thick. The average overburden thickness is 21 m (70 ft). The characteristics of the coal produced from the mine, based on Rosebud Seam coal mined in Rosebud County, Montana, are as follows:

Proximate Analysis:	
Moisture	22.0%
Volatile matter	29.4
Fixed carbon	42.6
Ash	6.0
Ultimate Analysis (Dry):	
Carbon	67.7%
Hydrogen	4.6
Nitrogen	0.85
Oxygen	18.5
Sulfur	0.66
Ash	7.7
Heating Value:	20.4 MJ/kg (8800 Btu/lb)

Surface mining of 4.5 million tonnes of coal per year requires large amounts of accessible coal, large equipment to remove the earth above the coal, and large trucks to haul the coal away. Surface mining can be accomplished in several ways -- using large power shovels, draglines, or bucketwheel excavators. We assume that the dragline method is used, as illustrated in Figure IV-2.

The procedures involved in operating a large surface mine are extensive. After permits have been acquired and the coal seam has been mapped, the base camp office and equipment maintenance building and yard

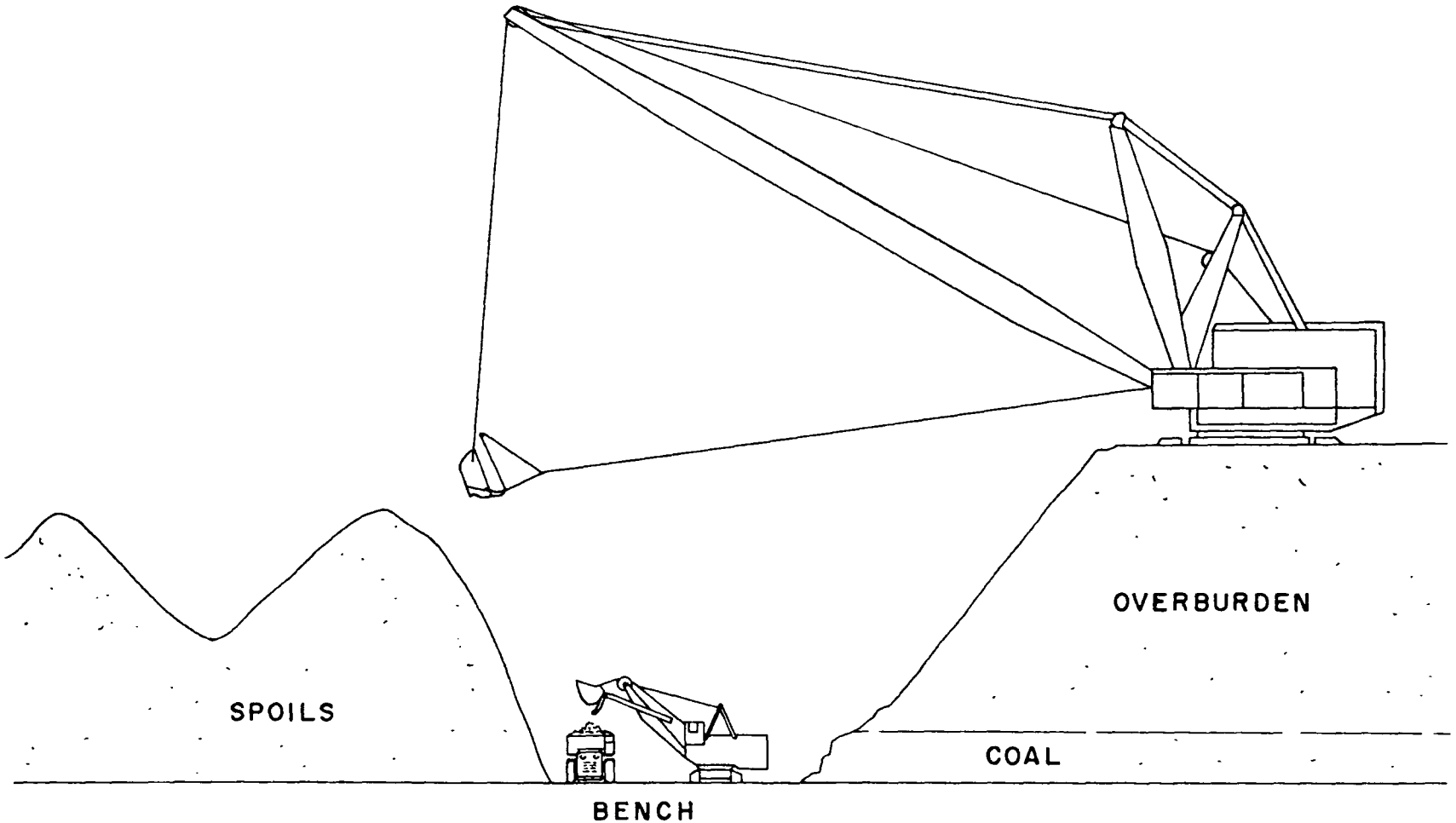

Source: Reference 1

FIGURE IV-2. DRAGLINE METHOD OF OVERBURDEN REMOVAL

are set up. Storage areas for spare parts and explosives are located, access roads to the mining area are established, and electric power for the office and for the dragline operation are provided. The first excavation removes the ground cover and topsoil. The soil is stockpiled and later replaced on the mined-over areas to help reestablish ground cover. If overburden under the topsoil and above the coal cannot support plant life, it has to be segregated. The earth moving equipment (such as bulldozers and scrapers) used for removing the soil is also used in the construction and maintenance of the access roads.

Next, a rotary-type rig drills blasting holes from 14 cm (5.5 in.) to 39 cm (15.5 in.) in diameter in a grid pattern with 15 x 18 m (50 x 60 ft) spacing down to the top of the coal seam. The explosives set off in the holes loosen the overburden and make it less difficult to remove. Draglines then remove the overburden.

The largest draglines today have bucket capacities between 137 and 158 m^3 (180 and 220 yd^3). The boom is as long as a football field (97 m or 300 ft) and the cab is as tall as a five-story building and a third as long as the boom. Draglines offer the most versatile way to remove the overburden, as they are able to remove large amounts with each pass of the bucket. They can also be used for coal seams with a variety of depths.

After the dragline removes the overburden, it swings to one side and drops the overburden in the swath previously cut. Overburden from the first cut is dropped on the surface. Subsequent cuts fill the previous hole after the coal is removed. At the end of the stripping operation the last cut is left open for lack of overburden to put into the hole. To date, it has not been cost-effective to haul the first cut overburden pile left on the surface to the remaining hole, but the 1977 Surface Mining Control and Reclamation Act and state laws now require that the remaining highwall be removed and the area returned to its original contour as closely as possible. That will require grading the first pile that was left on the surface and filling in the last cut so that no highwall remains.

The coal is removed first by blasting the seam to loosen the coal. Rear or bottom dumping trucks are then loaded by a large front-end loader or power shovel. The coal is hauled from the mine, dumped, crushed to the proper size, and delivered to a nearby conversion facility or stored ready for loading on a unit train.

Reclamation must then follow the mining. The overburden is to be graded as closely as possible to its original contour and the topsoil replaced. A vegetative cover is established with the goal of achieving long-term rehabilitation of the mined area.

The following major items of equipment are required to carry out the mining and reclamation operations:

Quantity	Item
1	Dragline, 53 m^3 (70 yd^3) capacity
1	Power shovel, 12 m^3 (16 yd^3) capacity
9	Dump trucks, 50-53 m^3 (65-70 yd^3) capacity
1	Scraper
1	Overburden drill
1	Coal drill

2. Unit Train

In System 1, we assume that unit trains are used to transport coal from the Powder River Basin coal mine via Gillette, Wyoming, to coal-fired power plants in the Omaha-Des Moines-Kansas City area, a distance of approximately 1,300 km (800 mi). We assume for the purposes of subsequent analysis that 80 km (50 mi) of this distance is newly constructed spur line from the coal mine to Gillette, Wyoming. The remaining 1,220 km (750 mi) is previously existing track connecting Gillette to the tricity area mentioned above.

Unit trains are a relatively new concept in railroading.[2] Their principal advantages compared with other railroad services are lower cost and faster delivery. A large percentage of unit trains in use today transport coal. They achieve their economies by dedicating an entire train to continual mass shipments from a single location (the coal mine) to a single destination (the power plant). Because the entire train has one destinaton, time-consuming stops at train switching yards can be avoided. The use of the equipment is uniform, so that repairs are more predictable and more easily scheduled.*

The train considered in this discussion is new and runs on a roadbed and rails, parts of which have recently been constructed. The proportion of newly constructed track is an important characteristic because it heavily influences the cost of service.

Each train is powered by four 2.24-MW (3,000 horsepower) diesel-electric locomotives.[4] The coal cars are aluminum-sided light weight cars with a net carrying capacity of 91 tonnes (100 tons). The equipment is usually leased by the coal recipient (steam electric power plant), from the railroad. There is some concern that one hundred 91-tonne (100-ton) cars are too heavy for optimum track and car maintenance cost. However, arguments are advanced that even heavier trains would be optimal with proper track and car maintenance.[4]

To minimize transportation cost, a railroad seeks to maximize the amount of coal moved each year. That provides an incentive to minimize train-loading time. Short loading times can be accomplished by "flood loading," which basically involves building a surge container over the tracks. The container may be a trackside concrete silo similar

---

*An effective alternative to the unit train is a coal slurry pipeline. Generally, the slurry pipeline is more capital-intensive but less labor-intensive and therefore less vulnerable to inflation than railroads. Long distances, large quantities, and rugged terrain tend to favor pipelines over railroads. Current discussions on the relative merits of coal slurry pipelines and unit trains are lively and frequently influenced by political and institutional considerations.[3]

to a grain silo, or a pile of coal on top of a train tunnel. Coal is dumped into the cars while the train is pulled at 3-6.5 km per hour (2-4 mph) past the coal discharge spout on the surge hopper. Loading rates of 3,600 tonnes (4,000 tons) per hour have been claimed.[5] Such a loading rate would allow a train with 9,100 tonne (10,000 ton) capacity to be filled in 2.5 hours. To be conservative, a full 8-hour shift has been assumed for loading.

Once a train is loaded, it can proceed directly to its unloading point (the coal-fired power plant). We have assumed an average train speed (mine-to-mine) of 32 km per hour (20 mph), not including loading and unloading.[6]

Unloading should be expedited for the same reasons as loading. The fastest unloading method is to pull the train at 6.5 to 10 km per hour (4 to 6 mph) over an unloading trestle. The trestle has a release mechanism that opens the bottom of the rapid discharge hopper cars and dumps their coal between the tracks onto the storage pile beneath the trestle. Individual cars can be dumped in about 20 seconds. An entire train can be unloaded in less than 1 hour. As a conservative estimate for this study, we allowed one 8-hour shift for receiving a loaded train, unloading it, and sending it back to the mine for refill.

A thawing shed is sometimes necessary at the unloading station. The thawing shed is used to warm coal in cars that have frozen during cold weather. Intense radiant heat is used to warm the bottom and sides of the cars enough that the coal will flow out of the car during the normal unloading process. Both gas-fired and electric radiant heaters are available. Some electric thawing sheds can thaw five cars per hour, consuming 5.5 kWh of energy for each tonne of coal thawed.[7] For the unit train in our example, thawing would take 20 hours and would require 60,000 kWh of electricity.

For the 800-MW coal-fired power plant discussed in the following section, approximately 1.3 million tonnes (1.4 million tons) of coal

would be required yearly to maintain a load factor of 35%. That requirement could be met by dispatching a 100-car train every 48 hours. Thus, two unit trains would be dedicated entirely to the operation of such a power plant.

3. Coal-Fired Power Plant

a. Background

The coal-fired power plant is an older unit that has been reassigned to intermediate-load service. The nominal unit size is 800 MW. Typically, such units are constructed to provide base-load service (60-80% load factor). However, after a number of years of base-load operation, they may be reassigned to intermediate or cycling duty. That practice is economical for facilities whose capital costs have been partially written off. To employ a new plant in such an application is too costly because the capital charge rate per kWh would be effectively doubled with a load factor of only 30-40%.

Because the time frame under consideration in this study extends to the year 2000, we have assumed that the power plant is built in the 1970s. Such a plant could be reassigned to intermediate-load service in the 1990s, or possibly sooner. Consistent with national and local environmental protection policies, we have assumed that a coal-fired power plant constructed in the 1970s requires a flue gas desulfurization system as well as a fly ash removal system.

Although flue gas desulfurization (FGD) has been the subject of intense controversy in the past, its use in conjunction with conventional combustion of coal has become the standard against which alternatives are judged.[8] The principal alternatives now available for meeting current new source performance standards (NSPS) and state implementation plans (SIP) are low-sulfur coal and physical coal cleaning; the choice depends on site-specific factors. If performance stan-

dards are made more stringent or "best available technology" becomes required, neither low-sulfur coal nor physical coal cleaning alone is likely to be acceptable. For purposes of this study, lime scrubbing is chosen as a well-proven technology suitable for treating flue gas from western subbituminous coal.

b. Process Description

Figure IV-3 is a block flow diagram for a conventional coal-fired power plant with FGD. The principal stream flows are shown in Table IV-1 for an 800-MW net capacity, adjusted from those in a recent report according to the coal properties and requirements of the current study.[9]

In the plant, coal is transported from the coal storage pile to the raw coal bunkers via conveyor belt. From the bunker it is fed to the pulverizer where it is ground to about 50 mesh and mixed with air equal to 10-15% of the total combustion air. The coal/air mixture is blown to the burners where it is combined with the remaining combustion air (which has been preheated) and combusted. About 20% of the ash in the coal drops to the bottom of the furnace in solid form, while the remaining 80% stays with the combustion gases as fly ash.

After combustion, the hot combustion gases pass through several stages of heat exchange to provide heat to the steam cycle. These stages consist of: (1) the boiler in which feedwater is evaporated to saturated steam; (2) the superheater, in which steam is heated beyond the saturation point; (3) the reheater, in which steam exiting the first stage of the steam turbine is reheated for use in subsequent stages; and (4) the economizer in which boiler feedwater is preheated. Modern steam-electric plants typically operate at a superheated steam pressure and temperature of 24,200 kPa (3,500 psig) and 540°C (1,000°F), with a 540°C reheat.

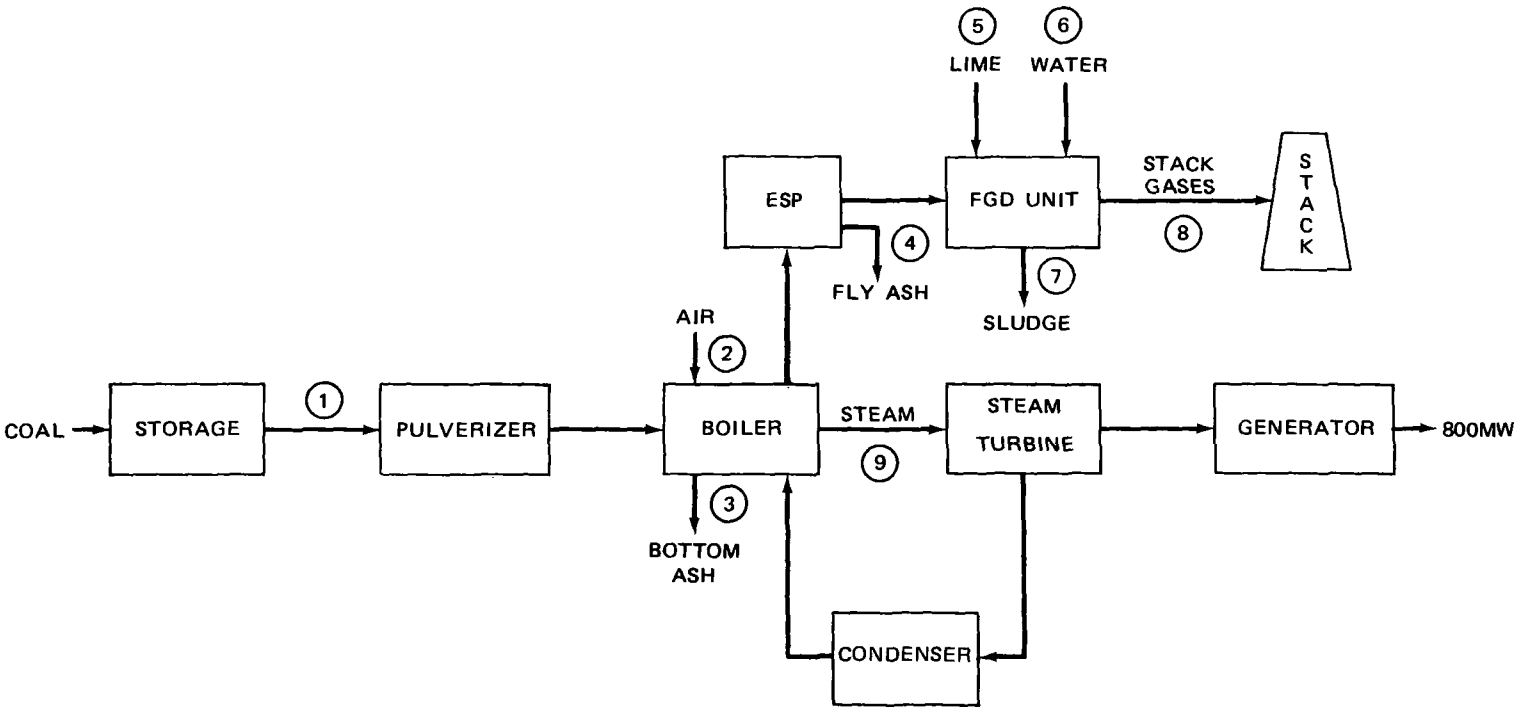

FIGURE IV-3. BLOCK FLOW DIAGRAM FOR AN 800MW COAL-FIRED POWER PLANT

The superheated steam passes through the steam turbines that power the generator, is cooled in the condenser, and returned to the boiler. The stack gases, containing fly ash, SO_2, and other pollutants, are directed first to the electrostatic precipitators (ESPs) for fly ash removal, and then to the FGD plant for SO_2 removal, before being exhausted to the stack. (Operation of the ESP and FGD plant is described further in Chapter VI.)

The most economical power plant configuration is for a single furnace/boiler unit to supply steam to a single steam turbine-generator set. Units of the size required to produce 800-MW net power output, and larger, are readily available. The steam requirement for such a plant is about 2.6×10^6 kg/hr (5.7×10^6 lb/hr).

4. Electricity Transmission and Distribution

Electricity transmission is the high voltage (more than 69 kV), long-distance movement of bulk electrical power.[10] Distribution is the subdivision of the bulk power from the transmission lines and its dispersal to the ultimate consumer. Conceptually, transmission and distribution (T&D) are simple processes; power from a generating station is sent along a wire to an end user. However, in reality, T&D is very complicated and expensive. Approximately two-thirds of the current cost of residential electricity is related to T&D expense[11].

Transmission usually includes transforming power at the generation station up to the voltage of the tranmission line. If a large amount of power is being moved, very high voltages will allow the most efficient and least expensive transport (see Figure IV-4). Table IV-2 shows that the highest voltage lines in commercial service in the United States are 765 kV. However, 1,100- and 1,500-kV systems are under consideration.[13] Transmission lines are frequently interconnected to form large power pools. The redundancy provided by pooling provides a very reliable power supply to the consumer. However, reliability requirements also contribute to the complexity of planning for new transmission systems.

TABLE IV-1

MAIN PROCESS FLOWS FOR 800-MW COAL-FIRED POWER PLANT

	Stream Name and Number	Mass Flow Rate (10^3 kg/hr)	Temperature °C	(°F)
1	Run-of-Mine Coal	410	16	(60)
2	Air	3,500	16	(60)
3	Bottom Ash	5.0	--	--
4	Fly Ash	20	150	(300)
5	Lime	4.5	16	(60)
6	Water	140	16	(60)
7	Sludge	26	49	(120)
8	Stack Gas	4,000	79	(175)
9	Superheated Steam	2,600	540	(1,000)

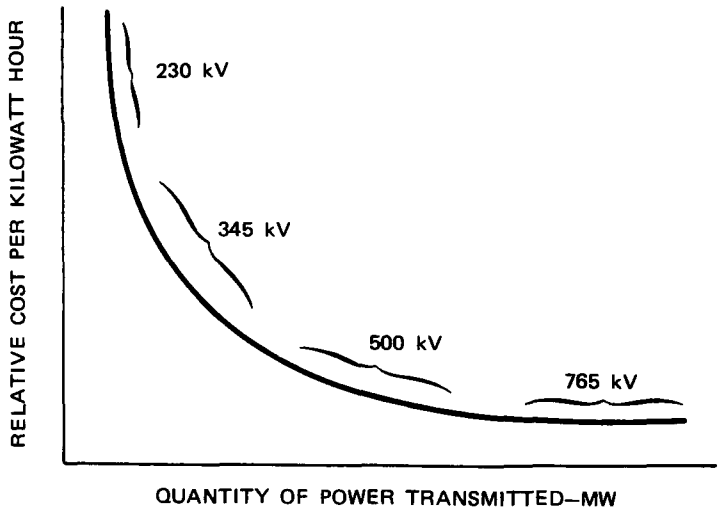

Source: Reference 14

FIGURE IV-4. HIGH-VOLTAGE TRANSMISSION ECONOMY FOR LONG DISTANCE

Table IV-2

ECONOMIC POWER LOADING OF TRANSMISSION LINES

Voltage (kV)	Loading (MW)
69	15
138	60
230	170
345	430
500	1,000
765	2,000
1,000	5,000

Source: Reference 13

For the power plant described in the previous section, a single 765-kV line would be sufficient to transmit the 800 MW of power generated. However, such an arrangement would hardly ever be encountered. More likely, two or more 345-kV transmission lines would transmit varying portions of the power to several load centers, or provide interties to other utility networks.

An example of such an arrangement is the 801-MW Cooper nuclear plant owned by the Nebraska Public Power System (NEPP). The plant is connected to utilities serving Omaha, Des Moines, and Kansas City via three 345-kV lines as well as to other parts of the NEPP grid via a fourth 345-kV line. The total length of 345-kV lines associated with the plant is on the order of 480 km (300 mi). A similar arrangement

might be expected for a new coal-fired power plant located in the tri-city region.

Transmission substations, primary distribution lines, distribution substations, and line transformers are included in the increasingly small subdivisions of lower voltage power between the high-voltage transmission lines and the final customer.

Transmission substations are provided in the grid to interconnect different parts of the system. Such a substation may include high-voltage switching equipment, circuit breakers, and transformers for reducing voltages from high-voltage lines to those of lower voltage (e.g., from 345 kV to 138 kV).

The electricity distribution system begins at the level of the distribution substations. Here the high transmission voltages (69 kV and above) are reduced to voltages used in the primary distribution feeders (2.4 kV to 34.5 kV). Those substations may also contain circuit breakers and switching equipment.

From the substation, the primary feeders are constructed in a radial fashion, typically via overhead power poles and lines, and are connected to major and minor primary lateral lines that supply the customers. Near each customer is a transformer that reduces the distribution voltage to 120/240 V for use in homes and business.

5. Coal Gasification Facility

a. Background

Because System 1 is a dual energy mode system, a parallel system for supplying residences with pipeline gas is required in addition to the electricity production and distribution system. This system is based on the production of synthetic natural gas (SNG) from coal.

The facility for producing SNG is assumed to be located near the coal mine. Thus, coal is transported directly from the mine to the coal storage facility for the SNG plant.

The facility we have chosen to analyze produces 7.8 million nm^3 (275 million scf) of SNG per day. Such a plant would consume 5.6 million tonnes (6.2 million tons) of subbituminous coal per year, equivalent to about 1.25 times the output of the hypothetical 4.5 million tonne per year (5 million ton per year) mine.

Coal can be converted to SNG by a gasification process followed by clean-up and methanation processes. Coal gasification has been practiced on a commercial scale since the early part of the last century. However, early coal gasification did not produce a high heating value SNG for long distance transmission in high-pressure pipelines. To be transmitted economically, gas must have a high heating value. The processes necessary to convert the product of the gasifier to gas with a high heating value (shift conversion, acid gas removal, and methanation) are currently being adapted from other industrial processes.

There are two generations of coal gasification technology. The first-generation processes are being operated on a commercial scale. Perhaps the best current examples are the fixed-bed Lurgi coal gasifiers at the South African Gas and Oil Co. (SASOL) plants and the entrained-flow Koppers-Totzek gasifiers associated with the manufacture of fertilizer (ammonia). Those processes have proved to be more expensive and less efficient than desired. The developing second-generation processes promise to improve upon the shortcomings of the first generation.

The Hygas process for the manufacture of SNG is an example of a second generation coal gasification process followed by the necessary upgrading processes to produce SNG. The Hygas process has a potential economic advantage over the current, first-generation

gasification processes (Lurgi, Winkler, Koppers-Totzek). Hygas was not selected for this study as necessarily the best technology, but as an example of a second-generation process likely to become practical in the next 10 to 20 years. Investment estimates and process flows have been adapted from a study by C. F. Braun.[14]

A block flow diagram of the SNG production plant is shown in Figure IV-5. The principal processes are coal storage and preparation, coal gasification, shift conversion, acid gas removal, methanation, and product drying. Other processes and facilities providing support are the cryogenic oxygen plant, steam and power production, the plant water system, sulfur recovery, solids disposal, and water reclamation (sour water stripping, ammonia recovery, and biological oxidation).

b. Process Description

The process flow is illustrated by the Hygas process flow diagram, Figure IV-5, and the accompanying list (Table IV-3) of major stream flow rates and compositions.

Coal is delivered from the mine on belt conveyors. After sampling and magnetic removal of tramp iron, the coal is sent to a 30-day storage pile. The pile serves as a surge damper to mitigate upsets in the mine or delivery systems and as a method of averaging the feed compositions. The coal is usually stacked and reclaimed in patterns that mix or average the composition of coal. The mixing reduces process operating problems that result from the rapidly changing characteristics of feedstock.

Coal from the storage pile is sent to both the steam boiler and the grinding mill for preparation of the process feed. Two parallel coal preparation trains are used; each processes 50% of the feed. Ground coal is moved in a water slurry from the mill to the high-pressure slurry pump. Surge tanks and mixers minimize fluctuations in the flow rate and allow adjustment of the content of the slurry water.

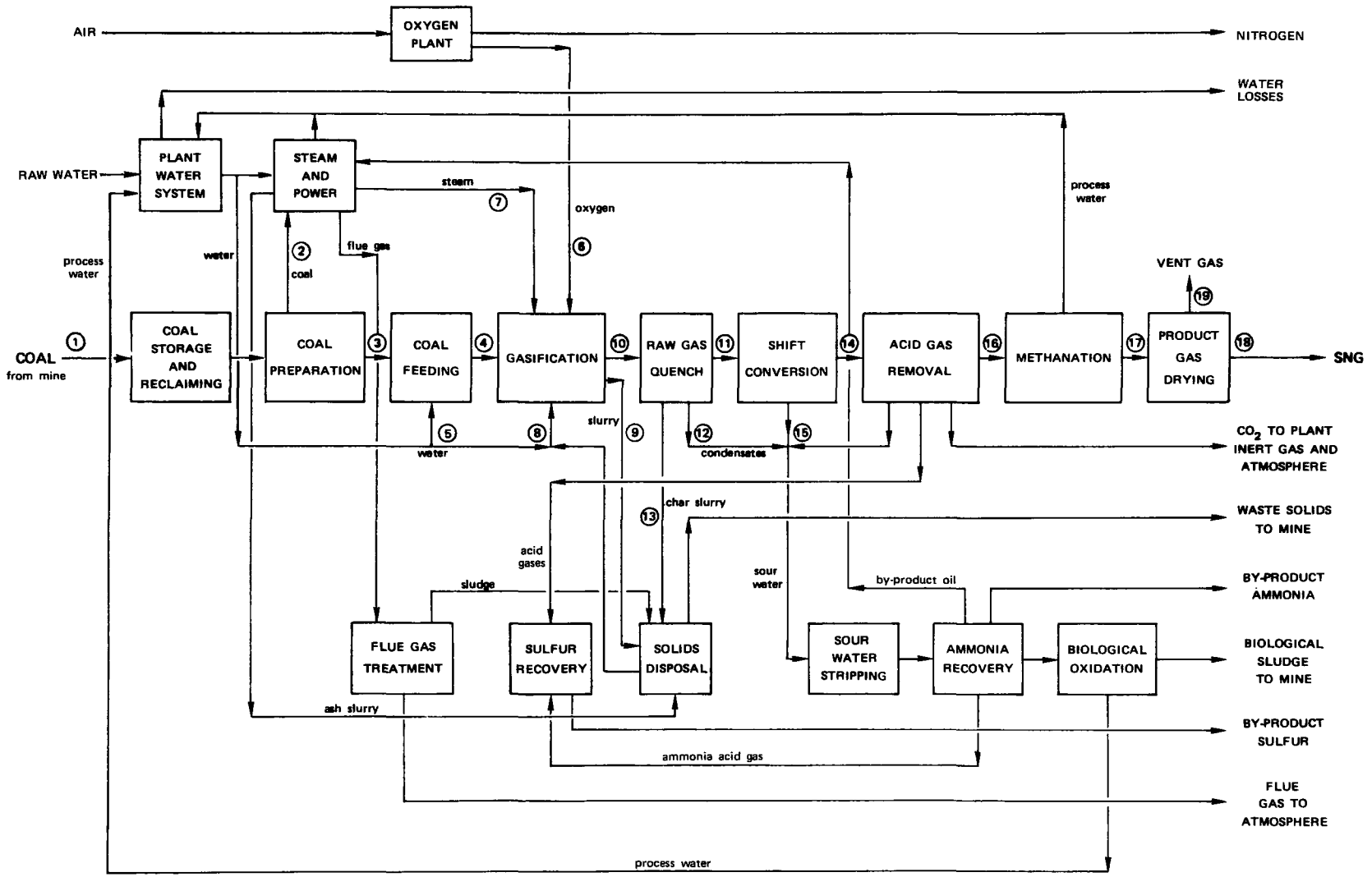

FIGURE IV-5. BLOCK FLOW DIAGRAM OF A HYGAS SNG PLANT

Table IV-3

MAIN PROCESS FLOWS FOR SNG FROM COAL VIA THE HYGAS PROCESS

		Stream Name and Number								
Component	Quantity	1 Coal From Mine	2 Boiler Feed Coal	3 Process Feed	4 Gasi-fier Feed	5 Water to Slurry Tank	6 Oxygen to Gas-ifier	7 Steam to Gas-ifier	8 Water to Char Ash Slurry	9 Char Ash Slurry
Dry coal	10^3 kg/hr	560	47	515	515	--	--	--	--	--
Water with coal	10^3 kg/hr	160	13	145	570	425	--	--	--	--
Char & ash	10^3 kg/hr	--	--	--	--	--	--	--	--	50
H_2O	10^3 g-mole/hr	--	--	--	--	--	--	28,000	8,200	8,200
H_2	10^3 g-mole/hr	--	--	--	--	--	--	--	--	--
CO	10^3 g-mole/hr	--	--	--	--	--	--	--	--	--
CO_2	10^3 g-mole/hr	--	--	--	--	--	--	--	--	--
CH_4	10^3 g-mole/hr	--	--	--	--	--	--	--	--	--
C_2H_6	10^3 g-mole/hr	--	--	--	--	--	--	--	--	--
NH_3	10^3 g-mole/hr	--	--	--	--	--	--	--	--	--
H_2S/COS	10^3 g-mole/hr	--	--	--	--	--	--	--	--	--
Oxygen	10^3 g-mole/hr	--	--	--	--	--	3,500	--	--	--
Benzene	10^3 g-mole/hr	--	--	--	--	--	--	--	--	--
C_7+	10^3 g-mole/hr	--	--	--	--	--	--	--	--	--
Solids	10^3 kg/hr	--	--	--	--	--	--	--	--	--
Temperature	°C	--	--	--	290	--	--	300	--	--
	(°F)	--	--	--	(550)	--	--	(580)	--	--
Pressure	kPa	--	--	--	8,820	--	--	8,820	--	--
	(psig)	--	--	--	(1,265)	--	--	(1,265)	--	--

(Continued)

Table IV-3 (Concluded)

Component	Quantity	Stream Name and Number 10 Raw Gas	11 Quenched Raw Gas	12 Conden-sate Slurry	13 Slurry	14 Cooled Shifted Gas	15 Conden-sate	16 Scrubbed Gas	17 Methanated Gas	18 SNG	18 Vent Gas
Dry coal	10^3 kg/hr	--	--	--	--	--	--	--	--	--	--
Water with coal	10^3 kg/hr	--	--	--	--	--	--	--	--	--	--
Char & Ash	10^3 kg/hr	--	--	--	--	--	--	--	--	--	--
H_2O	10^3 g-mole/hr	44,000	25,000	19,000	590	35	20,000	2	13	1	--
H_2	10^3 g-mole/hr	11,000	11,000	5		16,000	--	16,000	1,600	1,600	--
CO	10^3 g-mole/hr	9,400	9,400	3		4,700	--	4,700	14	14	--
CO_2	10^3 g-mole/hr	9,500	9,500	8	2	14,000	--	220	220	220	--
CH_4	10^3 g-mole/hr	6,500	6,500	4	--	6,500	--	6,500	12,000	12,000	1
C_2H_6	10^3 g-mole/hr	500	500	--	--	500	--	410	--	--	--
NH_3	10^3 g-mole/hr	210	170	39	1	--	170	--	--	--	--
H_2S/COS	10^3 g-mole/hr	110/4.4	110/4.4	1/-	--	100/2.2	10	--	--	--	--
Oxygen	10^3 g-mole/hr	--	--	--	--	--	--	--	--	--	--
Benzene	10^3 g-mole/hr	76	76	--	--	--	--	--	--	--	--
C_7+	10^3 g-mole/hr	150	150	--	--	(C_6+)64	160	--	--	--	--
Solids	10^3 kg/hr	1.9	--	--	1.9		--	--	--	--	--
Temperature	°C	315	238	238	260	38	332	343	38	41	--
	(°F)	(600)	(460)	(460)	(500)	(100)	(630)	(650)	(100)	(105)	--
Pressure	kPa	8,290	8,160	8,160	827	7,580	8,100	7,440	6,990	6,960	--
	(psig)	(1,200)	(1,185)	(1,185)	(120)	(1,110)	(1,175)	(1,080)	(1,015)	(1,010)	--

Two 50% capacity coal feeding trains are used. Each train uses three reciprocating pumps with one spare pump. The high-pressure (9,470 kPa or 1,360 psig) coal slurry is preheated to 290°C (550°F) by heat exchange with quenched raw gas and shift gas effluent.

The coal slurry is then injected into the fluidized top bed of the gasifier (reactor), where the slurry water is flashed off at 315°C (600°F). The average residence time in the bed is 15 minutes (all residence times were estimated by the Institute of Gas Technology). Dried coal then falls to the entrained bed low-temperature (740°C or 1,360°F) reactor, where the residence time is about 10 seconds. This low-temperature gasification-devolatilization-pyrolysis is partly responsible for the high efficiency of the Hygas process. The less reactive coal is gasified in the fluidized high-temperature (940°C or 1,720°F) reactor with an average residence time of 44 minutes. Ash and char not reacting in the parts of the reactor described so far fall into the very high temperature (1,000°C or 1,850°F) fluidized bed steam-oxygen gasifier. Most of the remaining carbon is either gasified by the steam carbon reaction ($H_2O + C \rightarrow H_2 + CO$) or burned with oxygen ($C + O_2 \rightarrow CO_2$) to provide heat for the endothermic steam-carbon reaction. Ash from the gasifier is quenched with water in a spent char slurry tank. The char ash slurry is depressurized, cooled, and sent to the solids disposal unit.

Two reactors would be needed in an SNG installation, each handling 50% of the process flow. The reactor vessels would be huge, even compared with large modern oil refinery equipment. Overall height would be 67 m (220 ft) with a maximum diameter of 7.3 m (24 ft).[15]

The vessel walls would be from 13 to 18 cm (5 to 7 in.) thick, and the gasifier would weigh about 1,800 tonnes (2,000 tons). Such a large size and heavy weight precludes any significant construction in the shop and requires that it be built in the field, which is more time-consuming.[16]

The vessel would have dry-wall construction (no external water jacket for cooling). The "low-alloy" (1% Cr and 0.5% Mo) shell will be clad with a stainless steel (18% Cr, 8% Ni) liner and have refractory lining for high-temperature zones.[17]

Product gas from the gasifier goes through a cyclone to remove carry-over coal dust, which is injected into the high-temperature zone of the gasifier. Product gas at 315°C (600°F) is then directly quenched with water to remove more entrained solids. Indirect heat exchange with the reactor feed slurry and boiler feed water reduces the gas temperature to 240°C (460°F). At that temperature, the water vapor concentration is 39 mole percent--at the proper level for shift conversion. In the shift process, about one-half of the gas is bypassed around the reactors. The shift is accomplished with two 50% capacity shift trains. Each train has two reactors of equal size. The shifted gas is combined with the bypassed stream and cooled in a series of steam generators and boiler feed water heaters. Condensate formed by cooling the shifted gas is rich in ammonia and is sent to the effluent treating section. The shifted gas then goes to the acid gas removal plant.

The acid gas (H_2S and CO_2) removal process (such as Allied Chemical's Selexol process or Lurgi's Rectisol process) separates two streams from the methanation feed. One stream is rich in H_2S, and the other is principally CO_2. Separating the bulk of the CO_2 from the H_2S stream simplifies the sulfur recovery unit design. Because details of the processes are proprietary, no process flow diagrams are included; however, a brief description of typical applications[18] follows. The process is dependent on physical absorption, with the dimethyl ether of polyethylene glycol or cold methanol as a solvent. H_2S and CO_2 are absorbed into the solvent at high pressure. By lowering the pressure of the "rich" solvent in successive stages, it is possible to release fuel gas, CO_2, and H_2S from the solvent. Final stripping of the solvent can be done in a column with a heated feed.

After acid gas removal, the feed goes to the methanation section and is heated to 340°C (650°F) before passing through a zinc

oxide sulfur-scavenger bed. This guard bed is designed to protect the sulfur-sensitive methanation catalyst from minor amounts of feed sulfur. Because of the large exothermic heat of reaction of methanation, the gas is reacted in three serial reaction stages. The product from each stage is cooled in waste heat boilers. Four parallel sets of methanation reactors (12 reactors in all) are required. To reduce the temperature rise in the methanation reactors, a large product gas recycle stream (about twice the flow rate of the net methanation product) is used to dilute the methanation feed. The recycle compressor for this diluent stream has a 340°C temperature at the inlet and requires careful engineering design. Methanation product gas is dried in a triethylene glycol dehydration unit and sent into the product SNG pipeline.

Some significant process variations are currently under development. One variation is a combined shift and methanation process, which would be performed after the acid gas is removed. Chem Systems and Ralph M. Parsons Co. (RMP) are both developing combination processes. The RMP process offers the potential of more efficient heat recovery from the methanation reaction. For this study, those combined shift-methanation processes should be considered process variations unlikely to significantly change the cost or efficiency of SNG production.

6. Gas Pipeline

To transport the SNG produced in the Powder River Basin to markets in the Midwest requires a pipeline approximately 1,300 km (800 mi) long. New long-distance interstate pipelines are generally 81 or 91 cm (32 or 36 in.) in diameter, with corresponding capacities of 23 and 28 million nm^3 (800 and 1,000 million scf) per day, respectively. Those capacities represent the output of three or four 7.8 million nm^3 (275 million scf) per day SNG plants. To supply a single large interstate pipeline, the SNG plants would deliver gas to smaller capacity branch lines, which would feed the larger line. A branch line of 50 cm (20 in.) in diameter could handle the output from a 7.8 million nm^3 per day facility.

Because no major interstate pipelines currently connect the Powder River Basin with the Midwest, new pipelines have to be built if an SNG industry with the intent of supplying midwestern and eastern markets is to develop in the region. Likewise, a branch line connecting each SNG facility to a larger interstate line is required.

We assume that the 1,300-km interstate pipeline is 81 cm in diameter, has an approximate capacity of 23 million nm^3 per day, and crosses one river and three roads per 160 km (100 mi) of length. Input pressure at the coal gasification plant is 6,900 kPa (1000 psi). Pressure is maintained along the pipeline by 11 compressor stations. Each station has a 66.6 GJ/hr (24,800 horsepower) average centrifugal compressor driven by a gas turbine. Fuel for the gas turbines is taken from the SNG in the pipeline. A standby turbine-compressor is in each station. In the past, reciprocating compressors have been used in place of centrifugal compressors. Even though less efficient, the centrifugal machines have become more popular because of greater simplicity and greater reliability. Compressor stations are carefully instrumented, highly automated, and frequently unmanned.

Typical pressure in the pipeline varies from 7,600 kPa (1100 psi) at the compressor discharge to 3,450 kPa (500 psi) at the compressor suction. If the pipeline has sufficient strength, it can be used for gas storage. Called line packing, this storage technique is employed by raising the average pressure of the pipeline. The normal capacity of the 1,300-km pipeline is about 5 days' production of a 7.8 million nm^3 per day SNG plant. By line packing, the line storage capacity can be increased 50 to 100%.

7. Gas Distribution

At the point where the pipeline passes nearest the city where the gas is to be delivered, a city gate station transfers gas into the local distribution system at 790 to 1,140 kPa (100 to 150 psig). Beyond

this point is a system of gas mains, valves, regulators, and meters that controls and transmits the flow of gas to the ultimate users. As the distribution network becomes more dense, the gas pressure is reduced, finally reaching a delivery pressure of 103 to 104 kPa (0.25 to 0.35 psig) for residential customers.

8. Gas Furnace and Air Conditioner

The heating and cooling equipment employed in residences must be sized to meet the peak heating and cooling loads expected throughout the year. Those loads are dependent on both the temperature extremes encountered in the geographic area under consideration and the thermal properties of the residences. We assume, for the purpose of analysis, that all residences supplied by the energy supply systems have the same thermal characteristics. The characteristics are based on a study by Westinghouse for the Electric Power Research Institute.[19]

The residences are split-level, wood frame houses with 136 m^2 (1,460 ft^2) of interior floor area excluding the garage area of 36 m^2 (390 ft^2). The houses are insulated to FHA minimum standards; that is, insulation values of R-11 in the walls, R-19 in the ceiling, and R-7 over the garage. Air infiltration rate is one complete air change per hour. Based on those parameters, and other features of the houses such as window area, the heat loss parameter is 360 kJ/hr-^{o}C (610 Btu/hr-^{o}F).[19] That means that 360 kJ/hr is lost from the house for each ^{o}C difference between the interior and exterior temperatures. If we assume that the interior temperature is maintained at 21°C (70°F) and calculate an average internal heat load (people, lights, and appliances) of 4,870 kJ/hr (4,620 Btu/hr), then the heat load, Q, as a function of exterior temperature T (^{o}C or ^{o}F), is found to be

$$Q = 39{,}900 - 360T \text{ kJ/hr}$$
$$(Q = 37{,}800 - 610T \text{ Btu/hr}).$$

Thus, the heat load for an extremely low temperature encountered during the winter heating season in the Omaha-Des Moines-Kansas City region -- say, -29°C (-20°F) -- would be 53 MJ/hr (50,000 Btu/hr). The gas furnace chosen in the Westinghouse study for use in the residences described above delivers 69.6 MJ/hr (66,000 Btu/hr) with a fuel input of 87.0 MJ/hr (82,500 Btu/hr), and thus has ample capacity to meet the heat load.

The procedure for choosing the appropriate air conditioner is somewhat more complicated because the cooling load depends on factors such as solar heat input and relative humidity, as well as external temperature. Air conditioner size is based on a design point of temperature and humidity not likely to be exceeded more than 2.5% of the time during the summer months (June through September). The design conditions for the region under consideration (using Omaha data as average for the three cities) are a dry bulb temperature of about 34°C (94°F) and a wet bulb temperature of about 26°C (78°F). The wet bulb temperature is a measure of the relative humidity, which, for the two temperatures just mentioned, is 49%. The cooling load calculated for those conditions is 25.0 MJ/hr (23,700 Btu/hr), assuming the interior temperature is to be maintained at 26°C (78°F). (See Chapter VIII.)

An air conditioner that can meet that cooling load is the Westinghouse SL030C/EC030, with a cooling capacity of 29.9 MJ/hr (28,300 Btu/hr), rated at 35°C (95°F) exterior dry bulb temperature and 26°C (78°F) dry bulb, 19°C (67°F) wet bulb interior return air temperature. Because cooling capacity increases with decreasing exterior temperature, capacity is clearly ample at the design condition for this choice of air conditioner.

The cooling capacity of the Westinghouse SL030C/EC030 air conditioner is shown in Figure IV-6 as a function of temperature, along with the cooling load calculated for average summer afternoon humidity and solar heat input. (The calculation of the cooling load is discussed in Chapter VIII.)

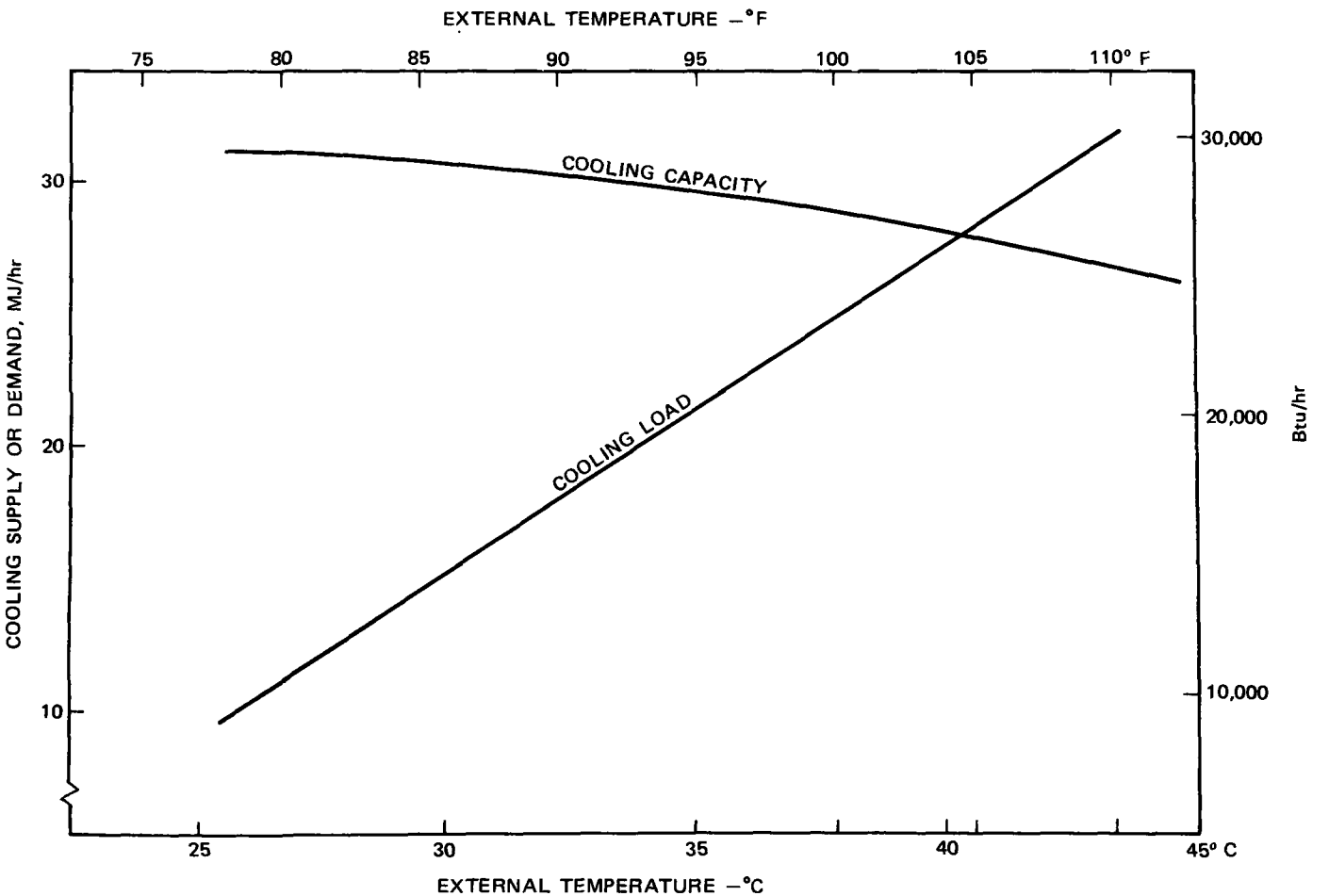

FIGURE IV-6. COOLING CAPACITY OF THE WESTINGHOUSE SL030C/EC030 AIR CONDITIONER

B. System 2

A block flow diagram of System 2 is shown in Figure IV-7. The components of the system are described below.

1. Coal Mine

See Section IV-A for the complete description of a surface coal mine located in the Powder River Basin.

2. Coal Gasification Facility

See Section IV-A for the complete description of the Hygas coal gasification process.

3. Gas Pipeline

See Section IV-A for the complete description of the interstate natural gas pipeline.

4. Gas Distribution

The distribution of SNG or natural gas to a 26-MW fuel-cell power plant (described in the following section) is considerably different from the distribution to individual residences described in Section IV-A6. Whereas a residence may consume 140 to 280 nm^3 (500 to 1,000 scf) of gas per day during the winter season (with a gas-fired furnace), a 26-MW power plant consumes on the average 53,800 nm^3 (1.9 x 10^6 scf) per day. That amount represents one-quarter of 1% of the capacity of the 81 cm (32 in.) interstate pipeline.

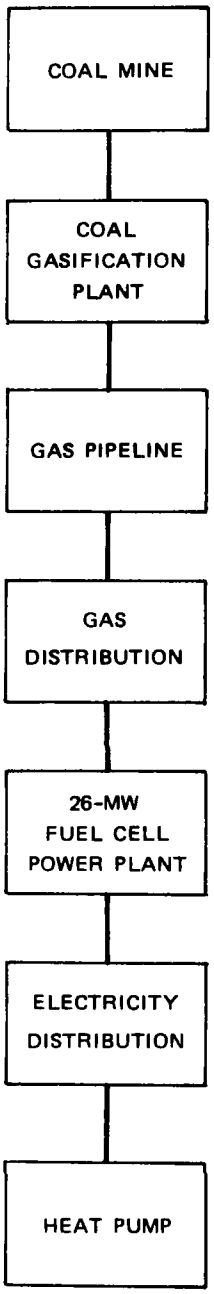

FIGURE IV-7. BLOCK FLOW DIAGRAM OF SYSTEM 2

Fuel-cell power plants located within a city would be served by individual lines originating at the city gate. Such a system would be similar to that used for supplying large (greater than 71 nm^3 or 2,500 scf per hour) commercial and industrial customers.

5. 26-MW Fuel-Cell Power Plant

a. Background

In this system, we assume that dispersed fuel-cell power plants provide intermediate-load electric power to residential customers. To represent the most advanced technology likely to be available for this application in the late 1980s or early 1990s, we assume that such power plants use molten carbonate fuel cells. This technology was chosen because it represents advancement in both cost and efficiency over first-generation (phosphoric acid) fuel-cell technology, and because it more effectively illustrates the advantages of the concept of fuel cells.

The choice of this technology is justified by the following considerations. First, although phosphoric acid technology will be used to prove the effectiveness of fuel cells in utility applications, and to achieve initial market penetration, because of inherent limitations in the technology, further advances in costs and performance will probably not be dramatic. Second, achieving widespread utilization of fuel-cell power plants will require technology considerably more advanced than that represented by phosphoric acid. Because present molten carbonate technology is more susceptible to dramatic improvements than phosphoric acid technology it is the only realistic candidate for this study.

The fuel-cell power plants described in this section are designed to achieve the DOE-EPRI-UTC heat rate goal of 7,910 kJ/kWh (7,500 Btu/kWh). They are also designed to be water-conservative--that is, no liquid water is delivered to the site of the power plant, nor

discharged from it. The only outside material supplied is the SNG fuel, other than occasional maintenance materials, periodic replacement of the zinc oxide guard bed, and, after 40,000 hours of operation, refurbishment of the fuel-cell stack.

The description of the fuel-cell power plant in this section is much more detailed than the description of other system components, because other system components represent either well-known, accepted technology (e.g., pipelines) or more advanced technology (e.g., coal gasification), which have been analyzed in great detail in other studies. Fuel-cell power plants of the kind considered here represent truly new technology for which little detailed analysis has been carried out. Thus, we have specifically analyzed fuel cell design and power plant configuration to effectively assess the environmental and economic feasibility of using fuel cells in the applications specified in Chapter III.

b. System Description

A flow plan for the 26-MW molten carbonate fuel cell power plant was developed, and is shown in Figure IV-8. This integrated system was designed to achieve the target heat rate and to be water conservative. Molten carbonate fuel-cell technology and systems concepts are at a relatively early stage of development, however, and alternative approaches could be used to satisfy the imposed target goals[20]. The nonoptimized design used in this analysis can be considered as representative. Full optimization was beyond the scope of this study.

The system is best understood by following the SNG stream. The SNG supply (Stream 0) contains small amounts of mercaptans, most of which can be removed by a zinc oxide adsorption bed. The desulfurized SNG (Stream 1) and recycled water (Stream 5) are preheated in a series of heat exchangers E-1, E-2, and E-3. They enter the reformer superheated relative to the reformer outlet temperature.

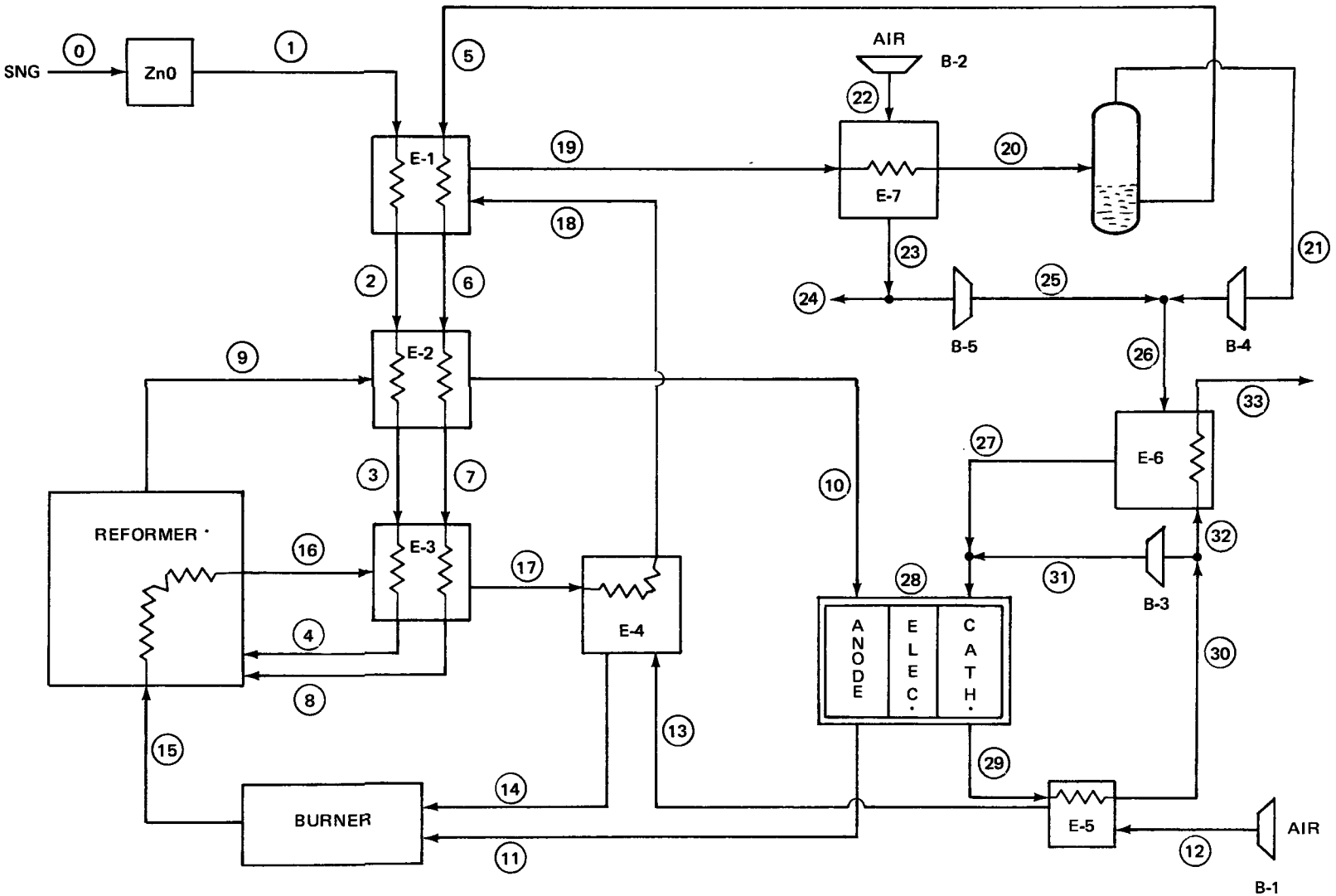

FIGURE IV-8. BLOCK FLOW DIAGRAM FOR 26MW FUEL CELL POWER PLANT (SNG FUEL)

Reformed SNG (Stream 9) must be cooled before entering the fuel cell anode compartment (Stream 10). The heat is used to preheat the reformer feeds in E-2. In the fuel cell, H_2 and CO are oxidized to H_2O and CO_2, and a stoichiometric amount of CO_2 is added from the electrolyte. The unused anode fuel (Stream 11) is burned with preheated air (Streams 12, 13, and 14) to supply heat for the reformer (Stream 15). The hot burner gas leaves the reformer (Stream 16) and is cooled down to condense enough product H_2O to maintain a net water balance in the system (Stream 5). Heat from Streams 16, 17, and 18 preheats the reformer feeds in E-3, the burner air feed in E-4, and again the reformer feeds in E-1. The final cooldown and condensation of Stream 19 is accomplished by air in exchanger E-7. A knockout drum separates Stream 20 into the water recycle (Stream 5) and saturated gas (Stream 21).

Part of the cooling air (Stream 25) combines with Stream 21 to become make-up feed for the cathode (Stream 26). Stream 26 is preheated in E-6 and Stream 27 is then blended with a cathode recycle (Stream 31) to make the cathode feed (Stream 28). In the cathode, 1/2 O_2 and CO_2 are stoichimetrically reacted into the electrolyte. The cathode exhaust (Stream 29) is used to preheat burner air (Stream 12) in E-5, and is then partially recycled via Stream 31 to the cathode. The remaining cathode exhaust (Stream 32) is used to preheat the cathode make-up feed (Stream 26) in E-6.

Many modifications of this design, both major and minor, could also meet the design goals. These designs, however, would also require a fairly elaborate system of thermal integration.

c. System Design Basis

Several points in the design of this power plant deserve further discussion to clarify the assumptions and constraints of the design:

- Sulfur in the SNG fuel, in the form of odorant mercaptans, can gradually poison both the reformer catalyst and the fuel cell electrodes. The zinc oxide bed must lower the sulfur content below 1 ppm.

- SNG reforming is highly endothermic, so the reactor is limited by heat transfer rather than catalyst activity. The reformer requires high temperature heat. The reformed SNG composition can be estimated, based on the equilibrium between CH_4 and the shift reactants, CO, CO_2, H_2, and H_2O.

- Low methane slip (unconverted CH_4) in the reformer is desirable. CH_4 is not active in the anode reaction and sequesters potential anode fuel (H_2 and CO).

- Heat for the reformer is best supplied by burning unused anode fuel. Anode waste is preheated and the most active components have already contributed to electrochemical energy generation. Direct burning of SNG would need additional preheat heat exchangers and would not contribute to the DC output. Preheating both the reformer feed (Streams 4 and 8) and the burner air (Stream 14) reduces the fuel requirement for the reformer.

- CO_2 is a major reactant at the cathode and dramatically affects cell voltage. CO_2 is conveniently supplied to the cathode by the burned anode exhaust.

- The cathode inlet must be preheated. The air for exchanger E-7 (Streams 23 and 24) has been partially preheated.

- The cathode recycle (Streams 29, 30, 31, and 32) recycles heat and keeps the average concentration of CO_2 and O_2 in the cathode compartment at higher levels than a single pass cathode.

- The fuel-cell power density is increased by lowering the output voltage and by reducing the consumption of reactants at both the anode and the cathode.

- Water conservation is somewhat easier to achieve by condensation from the burned anode effluent rather than from the cathode effluent. H_2O is more concentrated in Stream 19 so that less final cooling is necessary. Also, H_2O acts as a diluent at the cathode. Removing H_2O from the cathode feed improves cathode activity.

SNG reformate composition was estimated using procedures developed by Imperial Chemicals Industries (see Section IV-E). System heat balances were computed using component enthalpy data published by

the Girdler Corportion[21]. The calculation procedure is outlined in Appendix A.

The effect of reactant composition and utilization, operating pressure, and cell design parameters on molten carbonate fuel cell performance were estimated using an approximate analytical procedure developed at Exxon Research and Engineering by H.H. Horowitz. This procedure is detailed in Appendix B.

d. System Operating Characteristics

Several iterative calculation cycles were carried out to define a set of system operating parameters that would meet the performance targets. The final system material and heat balance is summarized in Table IV-4. Corresponding fuel-cell performance was estimated as 0.8 V/cell at an average current density of 120 mA/cm^2. Combined H_2 and CO fuel utilization at the anode was 77%. Near atmospheric pressure operation was selected, based on predictions showing small effects on cell performance for elevated pressure operation. High-pressure operation is feasible for this system, using a coupled turbocompressor/expander set in the air loop. However, cost savings resulting from smaller line sizes at higher pressure were assumed to be negligible.

e. Conceptual System Design

A conceptual design was prepared for the System 2 power plant components and assembled layout. The equipment list, showing capacity, size, and materials of each component, is given in Table IV-5. Modular configurations are envisioned, with components sized to permit factory assembly and subsequent shipment in individual trailers. That requirement determines the capacities of the fuel-cell trailer and the reformer/heat exchange package, which are the largest and heaviest components in the system. The modular sizes are shown in columns 4 and 5 of Table IV-5.

Table IV-4

PROCESS FLOW STREAMS FOR 26-MW FUEL-CELL POWER PLANT (SNG)

Stream	Temperature °C	Temperature (°F)	Enthalpy (GJ/hr)	Flow Rate, 10^3 g-moles/hr H_2	$H_2O(g)$	CH_4	CO	CO_2	O_2	N_2	$H_2O(l)$	Total	Stream
0	15.6	(60)	-12.92	27.74	0.3	204.0	0.24	3.74	--	--	--	236.1	0
1	15.6	(60)	-12.92	27.74	0.3	204.0	0.24	3.74	--	--	--	236.1	1
2	471	(879)	-8.05	27.74	0.3	204.0	0.24	3.74	--	--	--	236.1	2
3	593	(1,100)	-6.34	27.74	0.3	204.0	0.24	3.74	--	--	--	236.1	3
4	760	(1,400)	-3.78	27.74	0.3	204.0	0.24	3.74	--	--	--	236.1	4
5	74.4	(166)	-219.9	--	--	--	--	--	--	--	817	817	5
6	471	(879)	-174.2	--	817	--	--	--	--	--	--	817	6
7	593	(1,100)	-170.3	--	817	--	--	--	--	--	--	817	7
8	760	(1,400)	-164.8	--	817	--	--	--	--	--	--	817	8
9	702	(1,295)	-131.0	714.1	521.2	9.18	94.4	104.7	--	--	--	1,443.5	9
10	593	(1,100	-136.6	714.1	521.2	9.18	94.4	104.7	--	--	--	1,443.5	10
11	704	(1.300)	-496.9	164.2	1,071	9.18	21.7	799.9	--	--	--	2,066.0	11
12	15.6	(60)	3.68	--	6.30	--	--	--	121.5	489.8	--	617.7	12
13	593	(1,100)	14.6	--	6.30	--	--	--	121.5	489.8	--	617.7	13
14	704	(1,300)	16.8	--	6.30	--	--	--	121.5	489.8	--	617.7	14
15	1,160	(2,120)	-480.1	--	1,259.9	--	--	830.8	11.05	489.8	--	2,591.6	15
16	849	(1,560)	-517.6	--	1,259.9	--	--	830.8	11.05	489.8	--	2,591.6	16
17	774	(1,425)	-525.7	--	1,259.9	--	--	830.8	11.05	489.8	--	2,591.6	17
18	759	(1,399)	-527.9	--	1,259.9	--	--	830.8	11.05	489.8	--	2,591.6	18
19	287	(548)	-578.6	--	1,259.9	--	--	830.8	11.05	489.8	--	2,591.6	19
20	74.4	(166)	-632.6	--	442.7	--	--	830.8	11.05	489.8	817	2,591.6	20
21	74.4	(166)	-412.8	--	442.7	--	--	830.8	11.05	489.8	--	1,774.4	21
22	15.6	(60)	-220.8	--	377.1	--	--	--	7,323.2	29,293	--	37,148	22
23	65.6	(150)	274.8	--	377.1	--	--	--	7,323.2	29,293	--	37,148	23
24	65.6	(150)	260.0	--	356.9	--	--	--	6,917.3	27,718	--	35,004	24
25	65.6	(150)	14.8	--	20.27	--	--	--	393.6	1,574.4	--	1,988.3	25
26	70.2	(159)	-397.9	--	463.0	--	--	830.8	404.7	2,064.2	--	3,762.5	26
27	322	(690)	-360.6	--	463.0	--	--	830.8	404.7	2,064.2	--	3,762.5	27
28	557	(1,035)	-611.0	--	1,543.2	--	--	1,316.8	622.5	6,880.7	--	10,363	28
29	704	(1,300)	-346.9	--	1,543.2	--	--	694.3	311.3	6,880.7	--	9,429.4	29
30	672	(1,241)	-357.8	--	1,543.2	--	--	694.3	311.3	6,880.7	--	9,429.4	30
31	672	(1,241)	-250.5	--	1,080.2	--	--	486.0	217.9	4,816.5	--	6,600.6	31
32	672	(1,241)	-107.3	--	463.0	--	--	208.3	93.4	2,064.2	--	2,828.8	32
33	279	(534)	-144.7	--	463.0	--	--	208.3	93.4	2,064.2	--	2,828.8	33

Table IV-5

EQUIPMENT LIST FOR 26-MW FUEL-CELL POWER PLANT (SNG)

Unit	Capacity	Size	Modular Size	Dimensions	Materials
Fuel Cell Trailer	26.7 MW D C	27.8 (x 10^3 m^2)	3.48 (x 10^3 m^2)	3.1 x 7.3 x 3.7 m	UTC Advanced Design
E-1	50.5 GJ/hr	0.99 (x 10^3 m^2)	0.22 (x 10^3 m^2)		304 SS
E-2	5.6 GJ/hr	0.19 (x 10^3 m^2)	0.046 (x 10^3 m^2)		309 SS
E-3	8.1 GJ/hr	0.38 (x 10^3 m^2)	0.096 (x 10^3 m^2)	See Figure IV-10	304 SS
E-4	2.2 GJ/hr	0.12 (x 10^3 m^2)	0.031 (x 10^3 m^2)		304 SS
E-5	10.9 GJ/hr	0.18 (x 10^3 m^2)	0.045 (x 10^3 m^2)	102 cm dia x 3.7 m long	304 SS
E-6	37.2 GJ/hr	1.44 (x 10^3 m^2)	0.36 (x 10^3 m^2)	122 cm dia x 7.9 m long	304 SS
E-7	54.0 GJ/hr	1.93 (x 10^3 m^2)	0.48 (x 10^3 m^2)	6.7 x 9.1 x 4.6 m high	C.S.
Reformer Section	37.6 GJ/hr	0.86 (x 10^3 m^2)	0.21 (x 10^3 m^2)	See Figure IV-10	HK 40
Reformer Catalyst	714,140 g-mole/hr H_2	20.2 m^3	504 m^3	--	Girdler G-56A
Burner	2,005,700 g-mole/hr	169 GJ/hr	42.2 GJ/hr	See Figure IV-10	C.S. & Refractory
ZnO Bed	1.22 kg/day S	1.8 m^3/hr	0.46 m^3	0.61 m dia x 2.1 m high	Girdler G-72
Knockout Drum	817,200 g-mole/hr H_2O	7.25 m^3	1.18 m^3	1.3 m dia x 2.1 m long	Galvanized
Condensate Pump	4.1 liter/sec.	--	1.0 liter/sec	0.61 x 0.61 x 1.3 m long	C.S.
B-1	229 m^3/min	--	57.3 m^3/min	0.91 x 0.91 x 0.91 m	C.S.
B-2	13,800 m^3/min	--	3,450 m^3/min	Part of E-7	C.S.
B-3	2,460 m^3/min	--	616 m^3/min	1.5 x 1.5 x 1.8 m	304 SS
B-4	662 m^3/min	--	166 m^3/min	1.3 x 1.3 x 1.3 m	C.S.
B-5	741 m^3/min	--	185 m^3/min	1.3 x 1.3 x 1.3 m	C.S.

The limiting size for normal transport by truck is 3.8 x 3.8 x 12 m (12.5 x 12.5 x 40 ft), with a maximum weight of 31,800 kg (35 tons). Railroad flat cars can carry units up to 3.8 x 3.8 x 15 m (12.5 x 12.5 x 50 ft) in size and 63,600 kg (70 tons) in weight. Based on weight estimates, the proposed modular packages are shippable by rail, but smaller modules could be designed if shipping by truck were considered necessary. The overall size and cost of the plant would be somewhat greater if smaller modules were used.

Fuel-Cell Trailer Design -- The molten carbonate fuel-cell stacks are mounted in shippable trailer modules. The design of the fuel-cell section was based on the following parameters:

- Gross DC power output - 26.7 MW
- Cell current density - 120 mA/cm^2
- Cell voltage - 0.800 V
- Total active area - 27,800 m^2 (299 x 10^3 ft^2)
- Cell active area - 0.85 m^2 (9.16 ft^2)
- Number of cells per stack - 510
- Total number of stacks - 64
- Stack voltage - 408 V (DC)
- Number of stacks per trailer - 8
- Trailer voltage - 816 V (DC).

The configuration of the fuel-cell trailer is shown in Figure IV-9. Eight stacks, 1.2 x 2.4 x 1.2 m (4 x 8 x 4 ft) in size, are mounted on a steel base structure with a steel framework to support the upper row of four stacks. A possible gas manifolding arrangement is indicated. Each row of stacks is connected electrically in parallel. The two rows are connected in series, to give a trailer voltage of 816 volts DC. Higher voltages are possible by connecting more stacks in series. The stacks are thermally insulated and the trailer, which

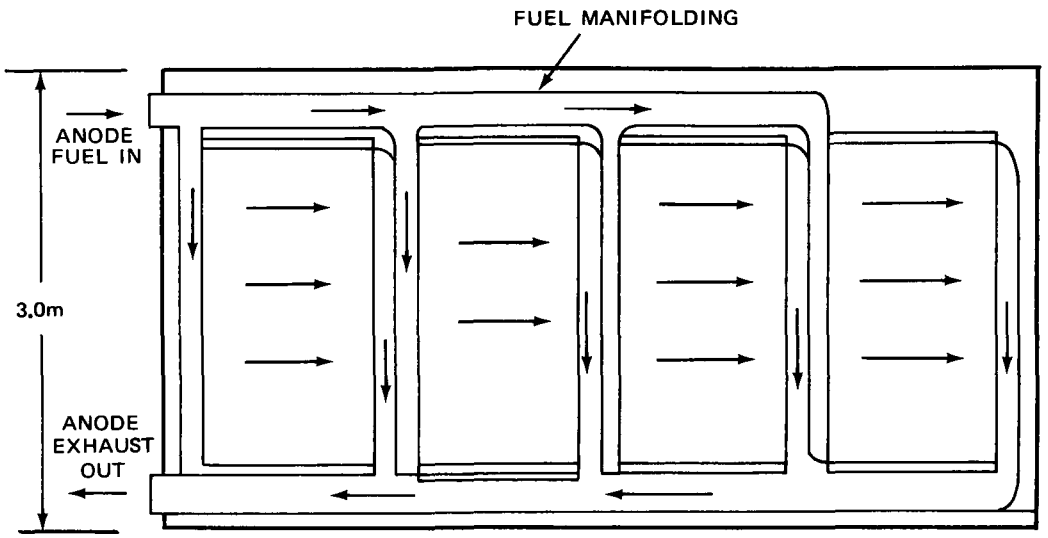

SIDE VIEW

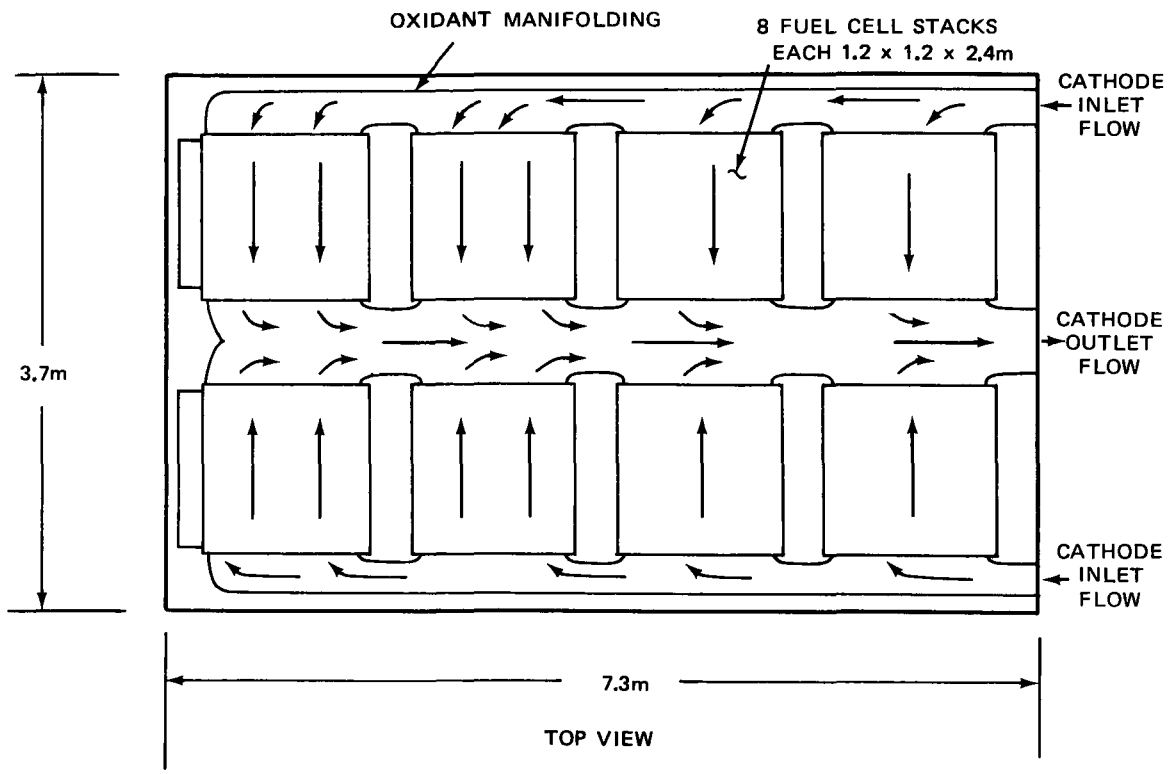

TOP VIEW

FIGURE IV-9. FUEL CELL TRAILER LAYOUT

weighs about 44,500 kg (49 tons), is enclosed with corrugated panels. The power plant requires eight fuel-cell trailers. Fuel to each pair of trailers is supplied by one reformer package.

Reformer/Heat Exchanger Module Design -- The reformer and heat exchangers for the power plant were sized, based on discussion with Exxon design engineers and information supplied by Girdler[22]. The reformer was sized for 9.4 cm (3.7 in.) i.d. tubes at about 152 kPa (1.5 atm) total pressure, using a space velocity of 1,600 m^3 gas/hr-m^3 catalyst, based on the total feed rate of SNG and steam. Small diameter tubes were chosen to minimize both the volume of catalyst and total area of the tube. The reformer tubes are made of HK-40, a high-alloy steel required by the temperatures and H_2 partial pressure. The reformer catalyst is Girdler G-56a, a standard methane reforming catalyst (nickel supported on alumina).

Heat exchanger area estimates were based on overall heat transfer coefficients, which ranged between 100 and 200 kJ/m^2-^oC-hr (5 and 10 Btu/ft^2-^oF-hr). The lower coefficient applies to heat transfer by convective mechanisms between two air streams. That coefficient is increased somewhat by the presence of H_2 in one or both streams, or by other heat transfer processes, such as radiation at high temperatures, liquid convection, boiling or condensation. The heat transfer coefficients were applied to 5 cm (2 in.) i.d. tubes. The material specified for exchangers E-1, E-3, E-5, and E-6 is 304 stainless steel (SS) and 309-SS for exchanger E-2. The other heat exchange tubes can be fabricated from normal carbon steel.

Pressure drops in the various units are extremely small -- less than 6.9 kPa (1 psi) in the reformer and a few kPa (less than 1 psi) in the heat exchangers. Thus, the entire system operates at near atmospheric pressure. Pumps and blowers were specified by their flow rates and pressure drops.

The zinc oxide sulfur trap was sized using data on Girdler G-72, which can reduce gaseous sulfur to 0.2 ppm S and has a maximum sulfur loading of 250 kg/m^3 (15 lb/ft^3). The ZnO is non-regenerable and must be periodically discarded. However, because the input level of mercaptans in SNG is expected to be low--10 kg/million m^3 (0.6 lb/million ft^3) of gas--the yearly replacement of the zinc oxide bed is a minor consideration.

This study's conceptual design of the reformer/heat exchanger package is a unit that contains a burner, reformer section, and several heat exchangers. The configuration is shown in Figure IV-10. The burner is located at the base of a cylindrical furnace. The shell is assumed to be fabricated from 0.64 cm (0.25 in.) thick carbon steel with 15.2 cm (6 in.) thick castable refractory inner lining. The reforming section is positioned directly above the burner and consists of a series of 10 cm (4 in.) o.d. tubes cast in HK 40 alloy steel (25 Cr-20 Ni). The reformer tubes will most likely be positioned vertically to avoid set- tling of the catalyst pellets, which would result in bypassing of steam and SNG and incomplete conversion to H_2.

Heat exchangers are of canal-type recuperator design. They are located in the flue gas flow path above the reforming section. Heat exchanger E-2 is mounted vertically on the side of the cylinder. Exhaust gas flows from the top of the unit and is ducted to the air fin condenser (E-7).

This configuration is proposed as a compact package that can be factory assembled and that would have relatively short sections of ducting between components. This particular design was used as a basis for estimating power plant size and investment costs. The package may prove impractical, however, if experience shows that the reformer section requires periodic maintenance. In that case, it would be better to build the reformer as a separate unit, and have the heat exchangers mounted on a separate platform. The optimized configuration can only be determined after detailed designs and cost information are known.

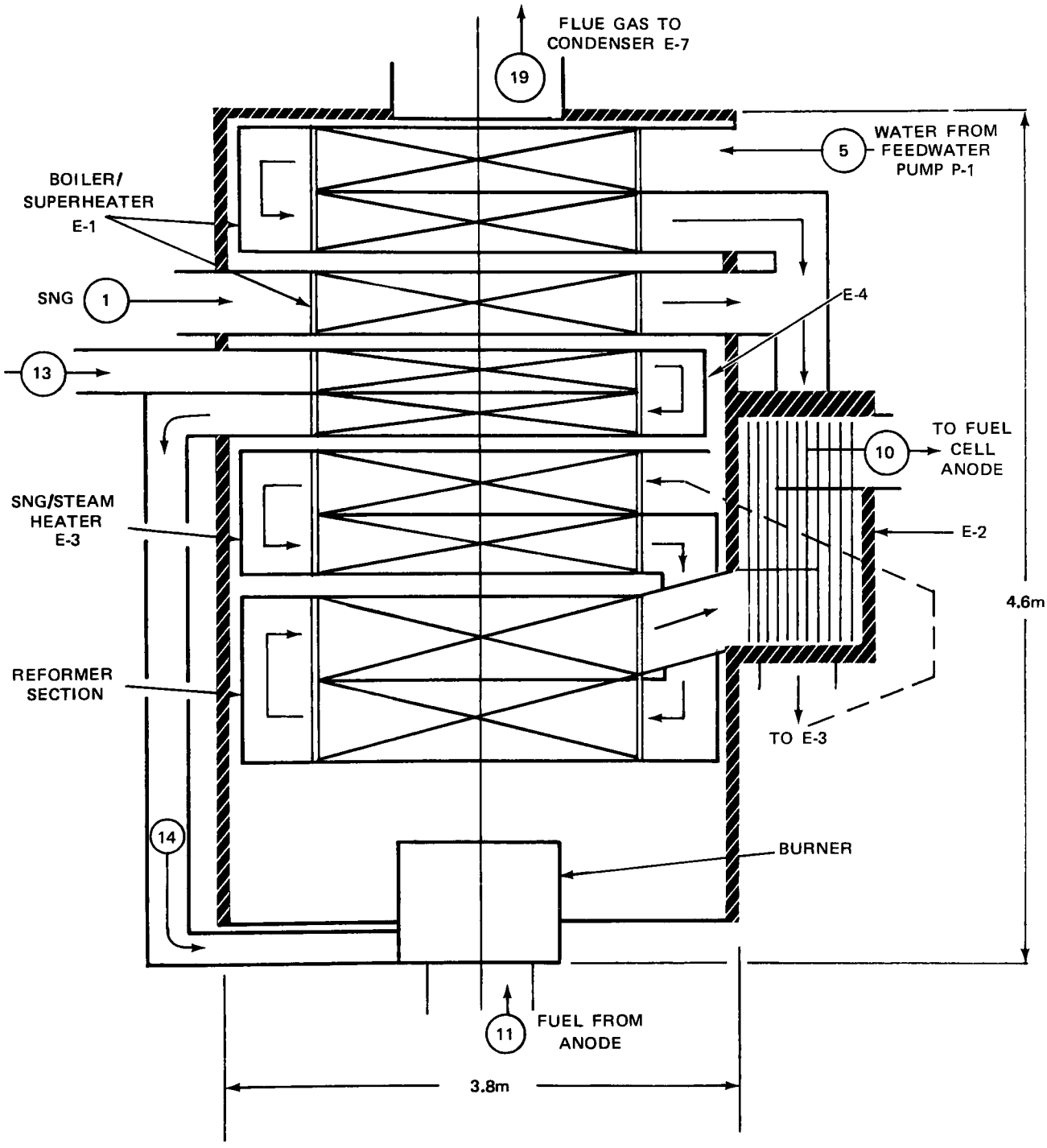

FIGURE IV-10. REFORMER/HEAT EXCHANGER PACKAGE

Table IV-5 lists the capacity, size, and materials of construction for the various components in the package. The weight of the package is approximately 45,500 kg (50 tons). Four reformer package units are required for the complete power plant.

Equipment Module -- The equipment module shown in Figure IV-11 contains the smaller components in the system. All components in an individual equipment module were sized to service one reformer and two fuel-cell trailers. The components are mounted on a steel-welded I-beam base with space above used for fluid piping and ducting. The components in the equipment module include: heat exchangers E-5 and E-6; the ZnO tower; the knockout drum; blowers B-1, B-3, B-4, and B-5; and condensate pump P-1. The overall dimensions of the equipment module are approximate.

Other configurations are certainly possible. This design uses shell and tube heat exchangers for E-5 and E-6. However, because the system pressures are very low, other types of heat exchangers could be used. For example, either canal type or plate fin recuperator exchangers may be selected. That would result in somewhat different module dimensions.

The power plant is designed to be water-conservative. However, make-up water may be required during periods of operation at excessive ambient temperature. In this case, a small ion exchange bed system could be provided in the equipment module to provide the clean water necessary for reformer operation. This deionized water production facility was omitted from the conceptual power plant design.

Power Plant Layout--A possible layout of one subsystem of modules is shown in Figure IV-12. Four subsystems make up the total plant. The overall plant size is estimated to be 39 by 55 m (128 by 180 ft). Considerable space is required for the air fin condenser E-7, which transfers waste heat to the atmosphere. These units contain fans (B-2) that pull atmospheric air (Stream 23) pressurized by B-5 and fed back into the cathode inlet mixture (Stream 26).

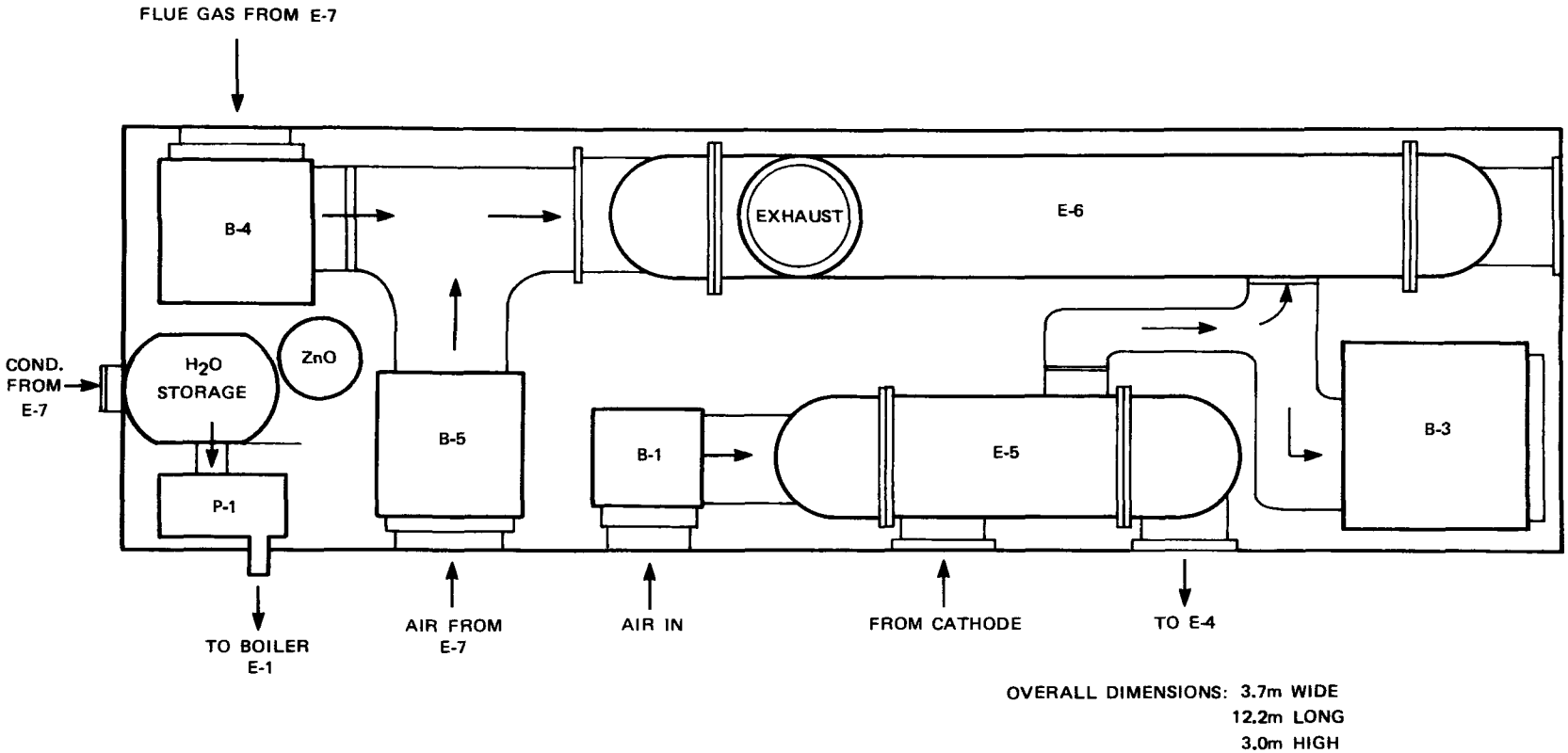

FIGURE IV-11. EQUIPMENT MODULE LAYOUT

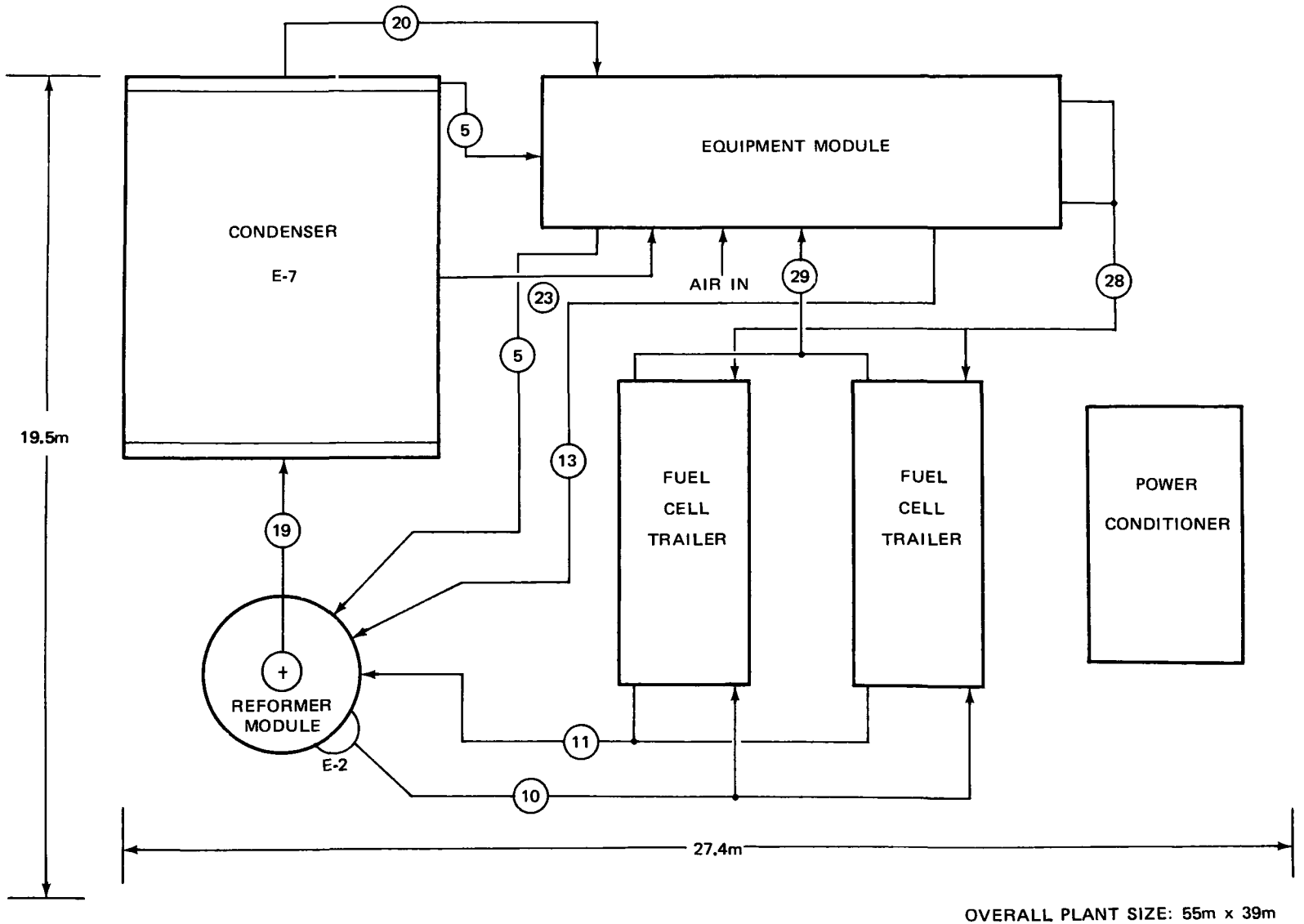

FIGURE IV-12. POWER PLANT LAYOUT

System piping was sized assuming an average gas velocity of 20.3 m/sec (4,000 ft/min). Piping specifications are listed in Table IV-6. Insulation is required on air piping to prevent heat loss.

Table IV-6

PIPING SPECIFICATIONS

Stream No.	Diameter, cm (in.)	Length, m (ft)	Material
5	5.1 (2)	22.3 (73)	302 SS[a]
10	66.0 (26)	18.3 (60)	304 SS
11	86.4 (34)	18.3 (60)	304 SS
13	43.2 (17)	38.4 (126)	304 SS
19	71.1 (28)	10.4 (34)	Galvanized
20	45.7 (18)	18.3 (60)	Galvanized
28	173. (68)	19.8 (65)	304 SS
29	198. (78)	9.2 (30)	304 SS

[a]SS = Stainless Steel.

6. Distribution of Electricity

Because fuel-cell power plants are intended for use as dispersed power sources, the arrangement for transmitting electricity to the ultimate users is different than that described in Section IV-A for remotely sited plants.

Most likely, electricity generated by dispersed fuel-cell power plants will enter the utility grid at the substation level. Therefore, no high voltage transmission will be associated with the facilities. In essence, the fuel-cell power plant will serve as its own substation, and will include transformers to step up the fuel-cell operating voltage to that used in the local distribution system (13.8 kV). Additionally, the appropriate switching apparatus and circuit breakers will be provided for integration with the utility grid and isolation of the fuel-cell equipment in case of an emergency.

7. Heat Pump

The residences supplied with electricity by the 26-MW fuel-cell plant are heated and cooled by heat pumps. We assume that the heat pumps are of advanced design, displaying performance characteristics discussed below.

A heat pump is a machine that transfers heat from a lower temperature reservoir to a higher temperature reservoir. Because it is a heat transfer rather than a heat generating device, its "efficiency," measured as the heat supplied to the higher temperature reservoir divided by the work required of the device, can be greater than unity. Therefore, heat pumps can provide more space heating per unit of consumed energy than combustion devices or electric resistance heating. The effectiveness of heat pumps is measured by a parameter called the coefficient of performance (COP), which is equal to the ratio of the heat supplied to the electricity consumed. Modern heat pumps have COPs ranging from 1.5 to 3 (depending on the exterior temperature, size of the unit, and so on). The equivalent parameter for electric resistance heat is 1.0, while for combustion furnaces it would be 0.5 to 0.7. A particular advantage of heat pumps is that the same device that provides space heating in the winter can provide air conditioning in the summer by simply reversing the refrigerant cycle.

In the 1950s and 60s, when heat pumps first began to have a sizable market, their reputation suffered because many early models had low reliability and high maintenance costs. By and large, however, the defects that caused problems in the early models have been corrected, and models currently available are reliable and economical. As a result of aggressive advertising by electric utilities to improve the heat pump's image, their sales have grown at a dramatic rate in the past several years. They are especially popular in areas where natural gas is not available or has been curtailed, and in which electric resistance heating and home heating oil are expensive alternatives.

Problems remain, however. Typically, the heat pumps are designed to function in moderate climates where the air conditioning load is larger than the space heating load. They are optimized for air conditioning, and do not perform nearly as well in cold northern climates where heating loads far exceed cooling loads. To achieve significant market penetration in the North, they will have to be optimized for northern seasonal conditions.

Under contract to the Electric Power Research Institute, Westinghouse Electric Corportion carried out a set of optimization studies to determine the changes in the design of present-day heat pumps that would make them suitable for northern climates[19]. A computer program was constructed that modeled the performance and costs of major heat pump components, including the compressor, evaporator coil, condenser coil, and air blower, with the sizes of these components variable. A set of ten hypothetical heat pump designs were examined. These heat pump designs resulted from a program that minimized the annual ownership costs (amortization, electricity cost, maintenance, taxes, and insurance) for a particular set of conditions that included external temperature, price of electricity, and changes in heat pump configurations and use of advanced components (such as the compressor). The ten designs were then subjected to a seasonal performance simulation for an actual northern location (Albany, New York) using current electric rates, to determine actual ownership costs, seasonal COP, and so on.

Of the ten designs proposed, several were comparable in terms of performance and cost. However, one in particular appeared to be most favorable for purposes of this study. That design (referred to as Heat Pump No. 2 in the Westinghouse report) is changed with respect to current models mainly in that the compressor is located indoors rather than outdoors (and, of course, its components are sized for optimum heating performance). That change greatly reduces the heat loss from the compressor and allows heat that is lost to be recovered as part of the heat supply. The layout of the components of that advanced heat pump system is shown in Figure IV-13.

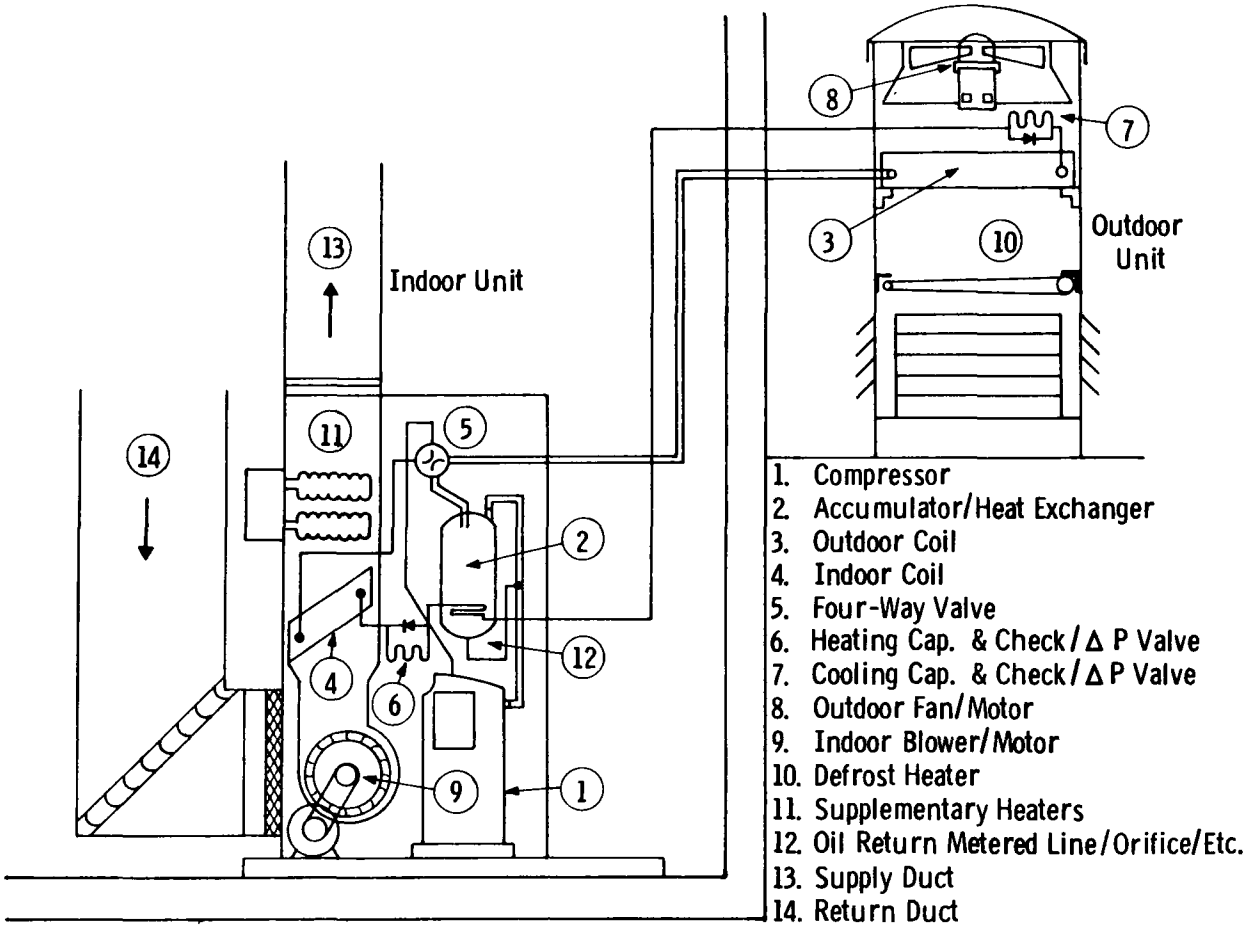

Source: Reference 19

FIGURE IV-13. RECOMMENDED HEAT PUMP CONFIGURATION FOR SPLIT SYSTEM AIR-TO-AIR UNITS

Because heat pumps provide both winter heating and summer cooling, sizing of the unit to meet a particular residence's heating and cooling loads most economically is more complicated than for the gas furnace/air conditioner case. The situation is simplified somewhat because the heat pump need not be designed to meet the maximum heat load; supplementary electric resistance heating can be used when required.

The customary practice in sizing heat pumps is to choose a unit that can meet the maximum summer cooling load. In northern climates, this size is generally too small to meet the maximum winter heating load; enough capacity for electric resistance heating must be provided to meet the load on the coldest winter day. In a region with a very small cooling load, the unit should be somewhat oversized to minimize the amount of expensive resistance heat required in the winter.

In Section IV-A, the design summer cooling load was given as 25.0 MJ/hr (23,700 Btu/hr) for 34°C (94°F) dry bulb, 26°C (78°F) wet bulb temperatures. The cooling capacity of the optimized heat pump (Heat Pump No. 2) analyzed in the Westinghouse study nearly matches that load. It has a rated cooling capacity of 26.0 MJ/hr (24,600 Btu/hr) at 35°C (95°F) exterior temperature, and 26°C (78°F) dry bulb and 19°C (67°F) wet bulb interior temperatures. The heating and cooling capacities of the heat pump as a function of temperature are shown in Figure IV-14. The heating and cooling capacities reflect an assumed 21°C (70°F) indoor temperature for heating, and 26°C dry bulb and 19°C wet bulb indoor temperatures for cooling. Superimposed on those curves are the heating and cooling loads for the residences described in Section IV-A. The cooling load curve assumes average summer afternoon conditions of humidity and insolation (see Chapter VIII).

As can be seen from Figure IV-14, the heating balance point (the point at which heating capacity equals the heat load) is -1°C (30°F). Below that temperature, supplementary electric resistance heating must be used. Resistance heating would be provided in units of

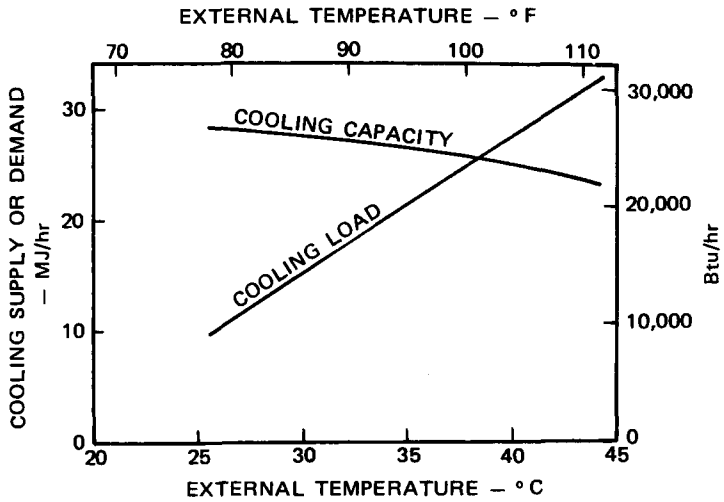

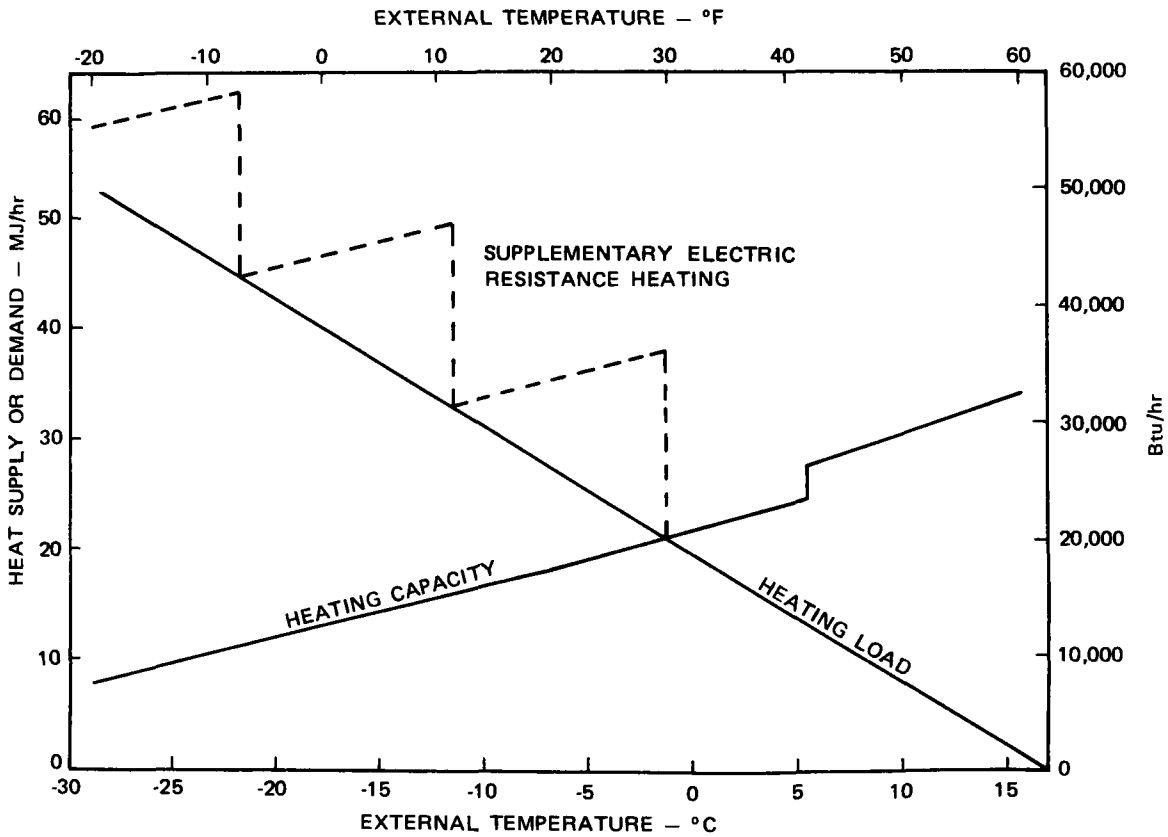

FIGURE IV-14. HEATING AND COOLING CAPACITY OF 26.0 MJ/hr (24,600 Btu/hr) HEAT PUMP

4.7 kW (16,000 Btu/hr) each. When the temperature falls below -1°C, the units are cycled on and off as required to maintain the interior temperature at 21°C. Three units of 4.7-kW capacity are sufficient to maintain that temperature down to an exterior temperature of -29°C (-20°F). The additional capacity added by the resistance heaters is shown by dashed lines in Figure IV-14.

C. System 3

A block flow diagram of System 3 is shown in Figure IV-15. The components of this system are described below.

1. Coal Mine

See Section IV-A for the complete description of a surface coal mine located in the Powder River Basin.

2. Coal Liquefaction Plant

a. Background

Coal may be converted to liquid fuels by several processes currently under development. H-Coal is the liquefaction process selected for review in this study because it can be modified to produce only distillate fuels and it is one of the processes most likely to be commercialized by 1990. The naphtha (C_5-200°C boiling range) from the H-Coal process can be severely hydrotreated to produce a feedstock that should be capable of being steam reformed to provide synthesis gas fuel for a fuel cell.[23,24,25] For the purposes of this study, the heavier distillate products (200°C+) of the H-Coal process are considered uneconomical to hydrocrack into naphtha and are sold as a low-sulfur fuel oil.

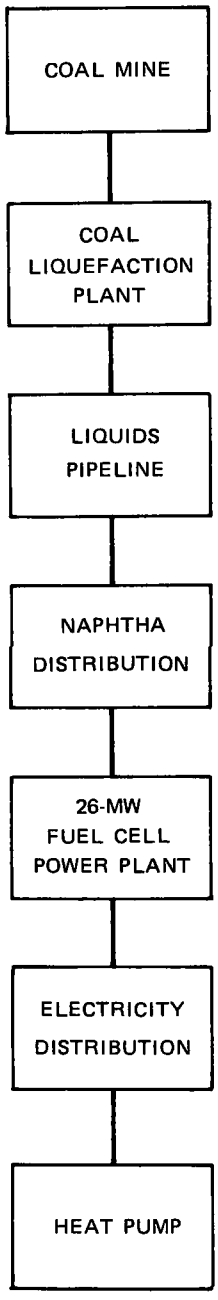

FIGURE IV-15. BLOCK FLOW DIAGRAM OF SYSTEM 3

The H-Coal process has been developed by Hydrocarbon Research Inc. (HRI) as an analog of their H-Oil hydrocracking process. The Department of Energy, the State of Kentucky, and a consortium of the Electric Power Research Institute, Ashland Oil, and Standard Oil of Indiana are cooperating to build a 550 tonne per day (600 ton per day) H-Coal pilot plant in Cattletsburg, Kentucky.

The size of the plant chosen for analysis is one that produces 7,630 m^3 (48,000 barrels) per day of mixed distillate products and consumes 22,300 tonnes (24,600 tons) per day or 7.3 million tonnes (8.1 million tons) per year of subbituminous coal. The plant conceptual design is a modification of one that would produce 7,950 m^3 (50,000 barrels) per day of distillate fuel oil. That plant is described in Section IV-D.

b. Process Description

The H-Coal process is illustrated in Figure IV-16. Major stream compositions and flow rates are shown in Table IV-7 for a plant that produces 7,630 m^3 (48,000 bbl) per day of naphtha and fuel oil. Sized coal from the mine is dried, crushed, and ground to less than 60 mesh. The ground coal is mixed with an equal weight of a recycled oil (distillation range: 345-525°C) to form a slurry which is then pumped to 20,260 kPa (200 atm) pressure, mixed with a recycled hydrogen stream, and then heated to 455°C (850°F). The slurry then enters the bottom of the ebullating bed reactors, where the coal is hydrogenated and partially liquefied. The reactors contain a bed of fluidized cylindrical catalyst. Catalyst fluidization is maintained by the upward flow of oil, coal, and hydrogen. Small fractions of catalyst may be withdrawn for regeneration. Generally, the longer the coal-oil slurry is held in the reactor, the lighter and more nearly hydrogen-saturated the products become, and the greater the consumption of hydrogen. Significant fractions of the sulfur and nitrogen in the coal are converted to H_2S and ammonia. Reactor products, gases, oils, ash, and unconverted coal are cooled and separated in a series of flash drums and distillation

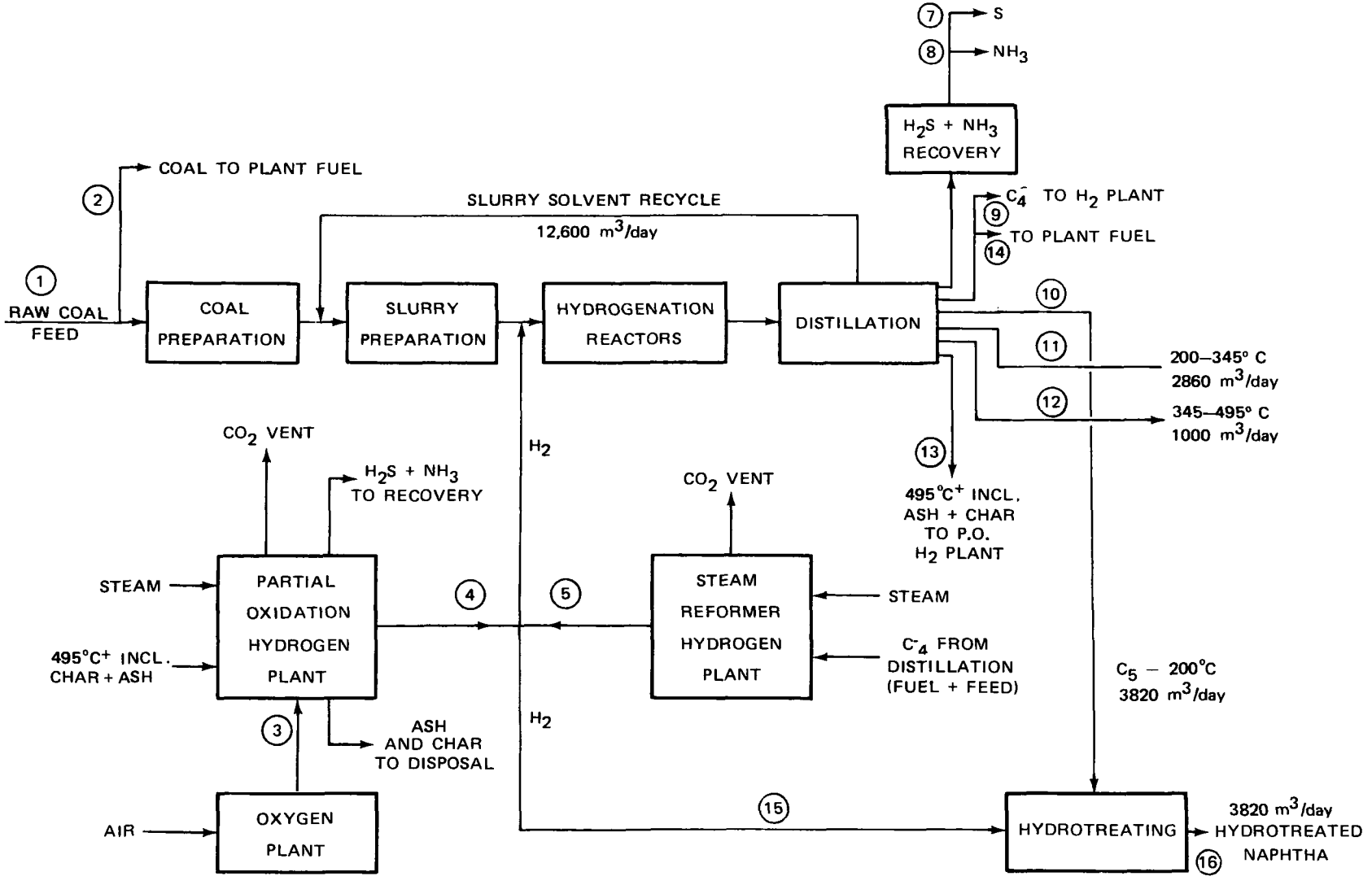

FIGURE IV-16. H-COAL PROCESS FLOW DIAGRAM

Table IV-7

COMPOSITION OF MAJOR STREAMS IN H-COAL PROCESS

Component	Quantity	Stream Number 1	2	3	4	5	6	7	8	9	10	11	12	13	14	15	16
Raw coal	10^3 kg/hr	930	165	--	--	--	--	--	--	--	--	--	--	--	--	--	--
MAF* coal	10^3 kg/hr	670	120	--	--	--	--	--	--	--	--	--	--	--	--	--	--
H_2 (10^3 nm^3/hr)	10^3 kg/hr	--	--	--	(280)	(195)	--	--	--	--	5.8	--	--	0.58	(19)	--	--
C_1	10^3 kg/hr	--	--	--	--	--	--	--	--	29	--	--	--	--	2.9	--	--
C_2	10^3 kg/hr	--	--	--	--	--	--	--	--	35	--	--	--	--	3.5	--	--
C_3	10^3 kg/hr	--	--	--	--	--	--	--	--	32	--	--	--	--	3.2	--	--
C_4	10^3 kg/hr	--	--	--	--	--	--	--	--	31	--	--	--	--	3.1	--	--
C_5-200 °C	10^3 kg/hr	--	--	--	--	--	--	--	--	--	240	--	--	--	--	--	240
200-345 °C	10^3 kg/hr	--	--	--	--	--	--	--	--	--	--	220	--	--	--	--	--
345-495 °C	10^3 kg/hr	--	--	--	--	--	--	--	--	--	--	--	85	--	--	--	--
495 °C +	10^3 kg/hr	--	--	--	--	--	--	--	--	--	--	--	--	140	--	--	--
Char	tonnes/day	--	--	--	--	--	--	--	--	--	--	--	--	1,300	--	--	--
Ash	tonnes/day	--	--	--	--	--	--	--	--	--	--	--	--	1,100	--	--	--
Oxygen	tonnes/day	--	--	3,100	--	--	--	--	--	--	--	--	--	--	--	--	--
Sulfur	tonnes/day	--	--	--	--	--	--	100	--	--	--	--	--	--	--	--	--
Ammonia	tonnes/day	--	--	--	--	--	--	--	120	--	--	--	--	--	--	--	--

*MAF = Moisture and Ash Free

columns. The principal liquid products (boiling between 27 and 495°C) are produced as sidecuts in the distillation columns. A list of the components of those liquid products is presented in Table IV-8.

The separation of solids from viscous liquid residues has proved to be very difficult. Many separation methods are under investigation, including pyrolysis, filtration, distillation, and solvent separation. None has yet been proven clearly superior. In the flow scheme shown in Figure IV-16, separation of solids from liquids is accomplished by distillation and the entire 495°C+ (925°F+) vacuum bottoms stream is sent to the partial oxidation hydrogen plant where most of the carbon is gasified and the ash is melted to a slag.

Table IV-8

PROPERTIES OF H-COAL DISTILLATE FUEL OILS

	Distillation Range			
	C_5-200°C (C_5-400 °F)	200-345 °C (400-650 °F)	345-495 °C (650-925 °F)	C_5-200°C After Hydrotreating
Elemental analysis (wt%)				
Carbon	84.7	86.4	88.1	85.4
Hydrogen	13.5	11.0	8.0	14.6
Oxygen	1.6	2.2	3.2	0.04
Sulfur	0.08	0.11	0.2	10 ppm
Nitrogen	0.15	0.23	0.5	30 ppm
Hydrocarbon type analysis (vol%)				
Paraffins	20	20	10	20
Naphthenes	64	47	30	77
Aromatics	16	33	60	3

Source: Reference 23 (except hydrotreating data).

A large amount of hydrogen (623 nm^3 per tonne or 20,000 scf per ton of coal) must be produced to satisfy the requirements of the H-Coal process. For the process envisioned in Figure IV-16, the product gases lighter than pentane (C_5) are desulfurized and steam-reformed to produce hydrogen in addition to that supplied by the partial oxidation plant. The cut point on the distillation column (495°C) is adjusted to vary the partial oxidation plant feed and thus balance the total hydrogen requirement.

A large air separation plant is needed to supply oxygen to the partial oxidation hydrogen plant. The partial oxidation plant also provides a convenient disposal of difficult-to-separate tars and phenolic compounds produced in the H-Coal process. Some early tests have indicated that H-Coal process residues will provide a satisfactory feed to the partial oxidation plant.

In this system, coal is liquefied in a mine-mouth H-Coal plant. A portion of the coal liquid (the naphtha) is sent by pipeline to 26-MW fuel-cell stations at dispersed locations. At the fuel-cell stations, the naphtha must be steam-reformed to provide a synthesis gas (CO and H_2) fuel for the anode of the fuel cell. If the naphtha is to be steam-reformable, it must have a low sulfur content (10 ppm maximum)[26] to avoid poisoning the nickel reformer catalyst. The H-Coal naphtha product (C_5 - 200°C) will not satisfy the maximum sulfur specification without further processing to reduce its sulfur content.

One effective method of reducing the naphtha sulfur content is to hydrotreat catalytically only the naphtha portion of the H-Coal product. Hydrotreating has been developed for use in the petroleum refining industry and is simple conceptually. Liquid feed (naphtha) containing sulfur compounds is combined with hydrogen and passed over a hot (370 - 425°C), pressurized (10,300 kPa or 1500 psig) catalyst. Most of the sulfur is converted to H_2S, which is separated from the clean product naphtha by distillation and acid gas absorption. Properties of the H-Coal naphtha after hydrotreating are shown in Table IV-8. The equipment required for naphtha desulfurization constitutes a

major processing facility. It is most reasonable to locate the naphtha desulfurizer at the mine-mouth H-Coal plant where the required hydrogen supply could be produced incrementally in the partial oxidation hydrogen plant. In this case, the extra feed for the partial oxidation plant is supplied by lowering the end point of the H-Coal distillate product from 525°C to 495°C (975°F to 925°F), which reduces the distillate output from the H-Coal plant by 3 weight percent. The changes required to desulfurize the naphtha will reduce the overall efficiency by 2% down to 64%.

An alternative to hydrotreating the naphtha before steam-reforming would be to employ a reforming process that could tolerate a sour (sulfur-bearing) feedstock. Such a process, called autothermal reforming[27], is under development for use in fuel-cell power plants. The principal conceptual difference between normal (thermal) reforming and autothermal reforming is the manner in which the heat for the endothermic reaction is supplied. In thermal reforming, the catalyst is packed in specially manufactured tubes built into a furnace. The furnace supplies the heat of reaction for the steam-reforming. As the sulfur content of the feed increases, it must be reformed at higher temperatures. Furnace tube metallurgy limits the use of higher temperatures and therefore limits feed sulfur content.

Autothermal reforming generates the endothermic heat of reaction by injecting oxygen into the catalyst bed and combusting some of the hydrocarbon feed. Because the heat is generated inside the catalyst bed, the walls can be insulated. Thus, a given metallurgy can support higher reaction temperatures and more feed sulfur.

The product from the two types of reformers will differ in one important component -- sulfur. The thermal steam-reformer has no product sulfur and may be sent to the fuel cell anode without clean-up. The autothermal reforming product contains too much H_2S to be processed directly in a molten carbonate or possibly phosphoric acid anode. Some form of H_2S removal (for example, amine scrubbing) would

be necessary. This requirement for a sulfur removal system eliminates autothermal reforming from this study. The fuel-cell systems studied here assume a dispersed location, and H_2S scrubbing systems that accompany autothermal reforming would not be compatible with dispersed locations.

3. Liquids Pipeline

Unlike the case for SNG, petroleum pipelines currently connect the Powder River Basin with the Midwest. Two crude oil pipelines originate in southeastern Wyoming and pass near Kansas City. One of them might be used for shipments of synthetic petroleum products at some later time if the production of crude oil declines in eastern Wyoming. However, such an assumption would be speculative. To place the analysis of System 3 on an equal footing with that of System 2, we assume that a new pipeline must be constructed to transport coal liquefaction products from plants located in the Powder River Basin.

A pipeline 51 cm (20 in.) in diameter is sufficient to transport about 32,000 m^3 (200,000 bbl) per day of mixed petroleum products. A length of 1,300 km (800 mi) is required to serve the Omaha-Des Moines-Kansas City region. Ten pumping stations employing multistage centrifugal pumps powered by diesel engines are required over the length of the pipeline. Unlike the situation with the natural gas pipeline, we assume here that diesel fuel would be purchased externally. The pumping stations maintain pipeline pressures at 5,600 to 7,900 kPa (800 to 1,100 psig) at their outlets, declining to 450 to 790 kPa (50 to 100 psig) at the entrance to the next pumping station.

Two separate liquids (e.g., naphtha and fuel oil) can be sent through the same pipeline. At the flow velocities used in most liquid pipelines, the liquids act as though they are in plug flow, that is, with very little backmixing. The fuel oil is pumped through the pipeline for some time, and then naphtha is pumped after the fuel oil.

The two liquids would flow as nearly separate "plugs" of unmixed liquid. Some mixing, called the "cuff," occurs. Depending on the properties of the cuff, it is usually blended with one product (in this example, the cuff would probably be blended with the fuel oil). In some cases, greater product separation can be achieved by inserting a liquid-filled sphere (called a "pig") into the pipeline between the fuel oil and the naphtha. The pig moves down the pipe helping to maintain the separation between the naphtha and the fuel oil.

4. Distribution of Naphtha

Naphtha will be moved by tank truck from a bulk terminal to local 26-MW fuel-cell power plants. The method of distribution and the equipment used would be similar to that now used for distributing petroleum products such as gasoline and light fuel oils.

The design of tank trucks is influenced by market demands and government regulations covering the weight, size, and operating speed of the vehicle, and type of delivery it will make. Large, full trailer tank trucks with up to 34,000-liter (9,000-gallon) capacities are used on long runs and for bulk deliveries.

Tank trucks are now being designed with either submerged or bottom loading to permit greater safety, faster loading time, and vapor recovery in the bulk terminal. Unloading rates of up to 32 liters/sec (500 gal/min) are possible with gravity discharge systems, and on-board pumps permit unloading rates up to 64 liters/sec (1,000 gal/min). Vapor recovery is now required when either the storage tank or the truck tank is being filled. Equally stringent operating procedures are expected to be required for naphtha fuel-cell fuel.

With a load factor of 35%, a 26-MW fuel-cell power plant will consume 49,200 liters (13,000 gallons) of naphtha per day. An on-site storage capacity of several days' supply, or about 150,000 liters

(54,000 gallons), would probably be required. To maintain the power plant's fuel supply, a 34,000-liter tank truck would deliver fuel about ten times per week.

The storage of naphtha would most likely be in underground tanks, in much the same way that gasoline is stored at service stations. Volumes of fuel as high as 150,000 liters are routinely stored in such facilities.

5. 26-MW Fuel-Cell Power Plant

System 3 also uses dispersed fuel-cell power plants with 26-MW nominal output to provide electric power to residences. Here, coal-derived naphtha is the fuel, rather than SNG as in System 2. As a result, a modified fuel conditioning section is required to generate H_2 and CO feed for the fuel cell. Once again, advanced molten carbonate fuel-cell technology was selected for the power plant, based on higher projected efficiency levels.

a. System Description

A flow plan for the System 3 power plant is shown in Figure IV-17. The plan includes provision for desulfurizing the coal-naphtha fuel to prevent poisoning of the steam-reforming catalyst. Target heat rate for the system was 7,910 kJ/kWh (7,500 Btu/kWh) coupled with water-conservative operation. Again, moderately complex heat integration is required.

Naphtha feed (Stream 1) and recycled water (Stream 5) are fed through a series of preheaters (E-1, E-2, and E-3) so that they enter the reformer at 815°C (1,500°F). Although these streams are shown as segregated, in practice they would be mixed after naphtha vaporization to suppress carbon deposition.

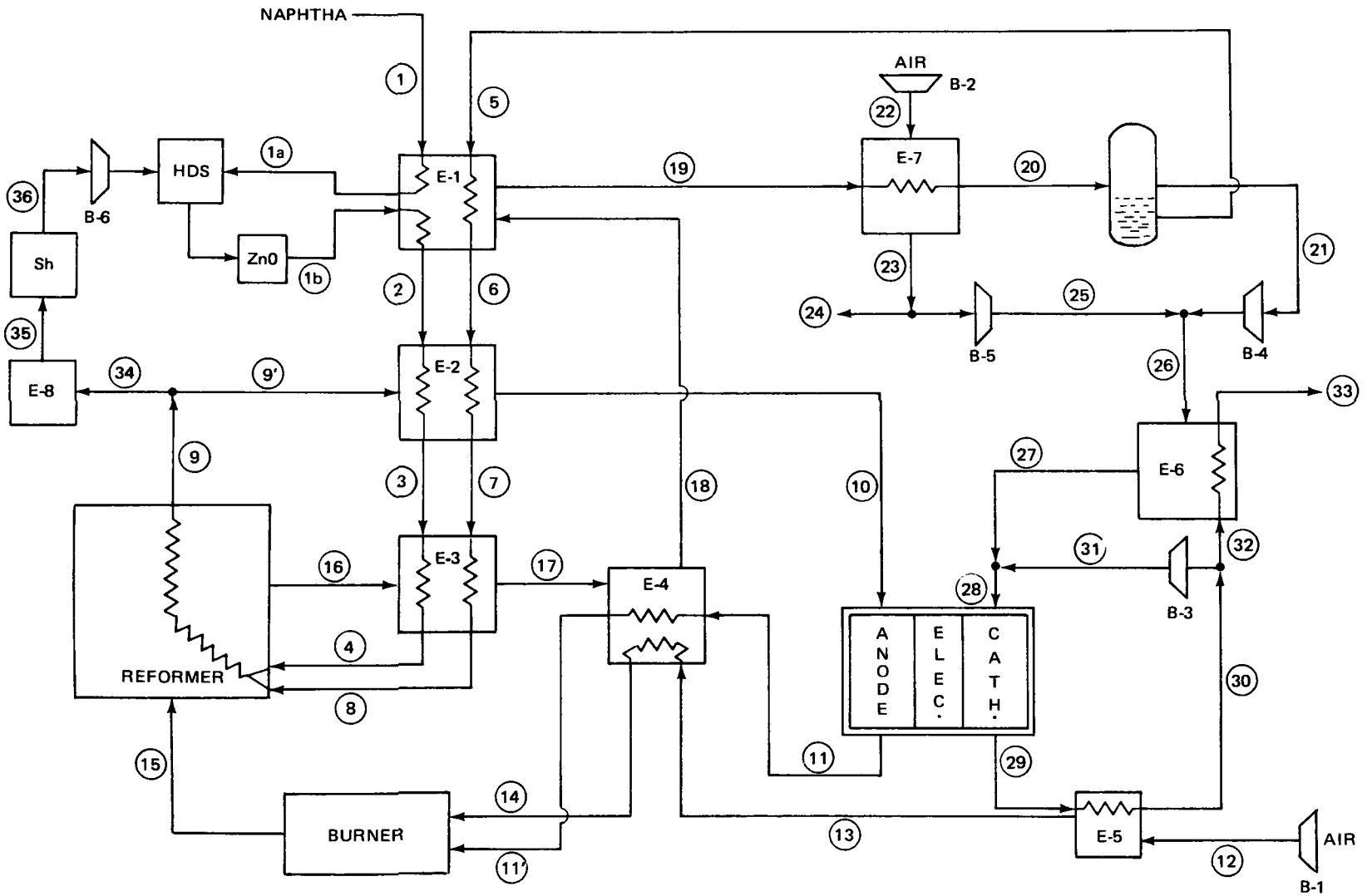

FIGURE IV-17. BLOCK FLOW DIAGRAM FOR 26MW FUEL CELL POWER PLANT (NAPHTHA FUEL)

The reformer operates at a 3:1 ratio of steam to carbon. At these temperatures and H_2O/C conditions given above, the methane slip equals 0.7% of the reformer carbon feed. Most of the reformer effluent (Stream 9) is fed to the anode (Stream 10) after being cooled in E-2, where it preheats the reformer feeds.

Naphtha must first be hydrodesulfurized to transform the sulfur compounds to H_2S, which are then removed with the use of a ZnO adsorbent. The desulfurization procedure is shown in Figure IV-17. Stream 1a is withdrawn from E-1 and sent to the hydrodesulfurization (HDS) reactor. There, it reacts with hydrogen (Stream 36), producing H_2S, which is removed by the ZnO. Stream 1b is then returned to E-1 with 0.2 ppm S, which is low enough to protect the reformer catalyst from sulfur poisoning. The hydrogen stream (Stream 36) is obtained by diverting about 1.5% of Stream 9 (Stream 34) into a series of coolers (E-3 $\longrightarrow$ Stream 36)and a shift converter (Sh $\longrightarrow$ Stream 36) to shift CO to H_2 and CO_2. The final hydrogen stream (Stream 36) is mostly H_2 and H_2O. The small amounts of CH_4, CO, and CO_2 in Stream 36 were neglected in further analyses. In the molten carbonate fuel cell, 75% of the combined H_2 and CO in Stream 10 are reacted. (CH_4 remains inert at this temperature.) The utilized H_2 and CO are oxidized to H_2O and CO_2, and a stoichiometric amount of CO_2 is transferred to the anode via the electrolyte. Unused anode fuel, consisting of CH_4, CO and H_2 (Stream 11), is preheated in E-4 and combined (Stream 11') in the burner with 10% excess air (Stream 14), which has been preheated in E-4 and E-5. The burner gases are catalytically ignited, producing an adiabatic flame temperature of 1,224°C (2,236°F). The burner gases (Stream 15) supply heat to the catalytic reformer, preheat (Stream 16) the reformer feeds in E-3, preheat (Stream 17) the burner feeds in E-4, and again preheat (Stream 18) the cold reformer feeds in E-1. Finally, the cooled burner gases (Stream 19) are further cooled in E-7 by air (Stream 22) until enough water is condensed to maintain a net H_2O balance for the system. Cooler gas and condensate (Stream 20) are separated in the knockout drum into a recycled H_2O stream (Stream 5) and a saturated gas (Stream 21).

Part of the cooling air (Stream 25) from E-7 is mixed with the CO_2-rich burner exhaust (Stream 21) for use as cathode make-up feed. That mixture (Stream 26) is preheated in E-6 and blended with a recycled cathode exhaust stream (Stream 31) to provide cathode feed (Stream 28). In the cathode, 1/2 O_2 and CO_2 react stoichiometrically into the electrolyte. Half of the O_2 fed to the cathode is reacted per pass. The cathode exhaust (Stream 29) is used to preheat the burner air (Stream 12) in E-5. Seventy percent of the cathode exhaust is recycled (Stream 31) and mixed with Stream 27 to provide cathode feed (Stream 28). The remaining cathode exhaust (Stream 32) preheats the cathode make-up feed (Stream 26) and is released to the atmosphere (Stream 33).

This design meets the goals of heat rate and H_2O conservation, but various modifications of the sytem could also meet the same design goals. All such designs still require fairly elaborate thermal integration.

b. System Design Basis

The general design bases for integrated molten carbonate fuel-cell systems were discussed earlier in Section IV-B.

The properties of the hydrotreated H-Coal naphtha product to be used in the fuel-cell power plant were presented in Table IV-8. The thermal properties of the naphtha were estimated as:

- Heat of Combustion (HHV): 46.7 MJ/kg (20,100 Btu/lb).
- Heat of Vaporization: 325 kJ/kg (140 Btu/lb).
- Vapor Heat Capacity at 16°C (60°F): 1.65 kJ/kg-°C (0.395 Btu/lb-°F).

The values reflect a weighted average of similar naphthenes and paraffins. Those estimates were used to calculate naphtha enthalpies, consistent with the Girdler data book bases.[21]

The use of coal-derived naphtha fuel imposes an additional system design constraint. Sulfur compounds in the naphtha can gradually poison both the reformer catalyst and the fuel cell electrodes. Hydrodesulfurization (HDS) and ZnO treatment of the feed naphtha is necessary to reduce the sulfur content below 0.2 ppm. The hydrogen recycle stream used in the HDS reactor is passed through a small shift conversion section to lower the CO content to levels that will not poison the HDS catalyst (Ni-Mo on alumina).

Naphtha fuel delivered to the power plant site has already undergone extensive desulfurization processing. We assume that the remaining refractory organic sulfur compounds can be hydrotreated successfully on-site, but laboratory verification of this assumption is required, using specific coal-naphtha feed stocks.

As indicated, different steam reforming conditions were selected for the naphtha feed (815°C, $H_2O/C = 3$), compared with the SNG feed (760°C, $H_2O/C = 4$). This change does not reflect the relative ease of steam reforming; rather, it reflects an evolution in process design during this study. Flow plan optimization requires the iterative assessment of varying fuel-cell design voltages, reformer operating conditions, and system thermal integration. These analyses must be carried through to the cost estimation stage. Such optimization was beyond the scope of this study.

Acceptable methane slip values can be achieved by increasing the reformer temperature and/or increasing the steam/carbon ratio. Lower steam diluent concentration increases anode performance in the fuel cell. However, this effect is counterbalanced by the favorable effect of high partial pressure of the water on the

equilibrium conversion of CO to H_2 within the anode compartment. The size and cost of the water recovery condenser is also affected. Further, optimal designs for SNG and naphtha fuels differ somewhat, based on differing carbon/hydrogen ratios in the feed, and the impact of resulting CO_2 partial pressures on cathode performance for typical process flow integration. Again, considerable opportunity exists for future optimization.

Lastly, some comments are in order to justify the selection of steam reforming as the fuel conditioning process. Autothermal reforming was considered briefly as a possible alternative. This process can be used with relatively heavy feedstocks, beyond the naphtha boiling range. However, its use in the naphtha-fueled power plant did not appear promising, based on the following considerations:

- Lower anode performance is expected, due to the presence of air-derived nitrogen diluent in the anode feed. Also, the fuel conversion efficiency of the autothermal process will be lower than for steam reforming.
- The combustion value of the spent anode fuel, containing unused H_2 and CO reactants, cannot be used effectively because the autothermal reformer has low fuel firing requirements. Furthermore, the 26-MW power plant is probably too small for cost-effective addition of a gas turbine or steam bottoming cycle for generating additional electrical energy from the spent anode fuel.

c. System Operating Characteristics

The final system material and heat balance at full load operation is summarized in Table IV-9. Net power output is estimated to be 25.6 MW, with a system heat rate of 7,720 kJ/kWh (7,315 Btu/kWh) (HHV basis).

Corresponding fuel-cell performance was estimated at 0.78 V/cell at an average current density of 165 mA/cm^2. Again, near

Table IV-9

PROCESS FLOW STREAMS FOR 26-MW FUEL-CELL POWER PLANT (NAPHTHA)

Stream	Temperature °C	Temperature (°F)	Enthalpy (GJ/hr)	Flow Rate (10^3 g-moles/hr) H_2	$H_2O(g)$	CH_4	CO	CO_2	O_2	N_2	$H_2O(l)$	Flow Rate Naphtha (kg/hr)	Total*	Stream
1	15.6	(60)	-7.52	--	--	--	--	--	--	--	--	4,256 kg/hr	4,256	1
1a	349	(660)	-2.70	--	--	--	--	--	--	--	--	4,256 kg/hr	4,256	1a
1b	341	(645)	-2.88	17.91	1.36	--	--	--	--	--	--	4,256 kg/hr	4,256 + 14.74	1b
2	462	(863)	-1.07	17.91	1.36	--	--	--	--	--	--	4,256 kg/hr	4,256 + 14.74	2
3	689	(1,273)	2.77	17.91	1.36	--	--	--	--	--	--	4,256 kg/hr	4,256 + 14.74	3
4	816	(1,500)	5.15	17.91	1.36	--	--	--	--	--	--	4,256 kg/hr	4,256 + 14.74	4
5	66	(150)	-244.4	--	--	--	--	--	--	--	906.1	--	542.9	5
6	462	(863)	-193.4	--	906.1	--	--	--	--	--	--	--	542.9	6
7	689	(1,273)	-185.3	--	906.1	--	--	--	--	--	--	--	906.1	7
8	816	(1,500)	-189.6	--	906.1	--	--	--	--	--	--	--	906.1	8
9	816	(1,500)	-129.5	739.3	485.2	2.14	179.8	121.3	--	--	--	--	1,527.8	9
9'	816	(1,500)	-127.6	728.4	478.5	2.11	177.2	119.5	--	--	--	--	1,505.3	9'
10	593	(1,100)	-139.6	728.4	478.5	2.11	177.2	119.5	--	--	--	--	1,505.3	10
11	704	(1,300)	-534.9	182.1	1,024.4	2.11	44.30	931.6	--	--	--	--	2,184.5	11
11'	760	(1,400)	-528.6	182.1	1,024.4	2.11	44.30	931.6	--	--	--	--	2,184.5	11'
12	15.6	(60)	3.89	--	6.65	--	--	--	129.2	516.6	--	--	652.4	12
13	649	(1,200)	16.6	--	6.65	--	--	--	129.2	516.6	--	--	652.4	13
14	760	(1,400)	-19.0	--	6.65	--	--	--	129.2	516.6	--	--	652.4	14
15	1,224	(2,236)	-510.4	--	1,217.3	--	--	978.0	11.74	516.6	--	--	2,723.7	15
16	870	(1,598)	-556.2	--	1,217.3	--	--	978.0	11.74	516.6	--	--	2,723.7	16
17	816	(1,500)	-563.3	--	1,217.3	--	--	978.0	11.74	516.6	--	--	2,723.7	17
18	747	(1,376)	-571.3	--	1,217.3	--	--	978.0	11.74	516.6	--	--	2,723.7	18
19	234	(454)	-628.9	--	1,217.3	--	--	978.0	11.74	516.6	--	--	2,723.7	19
20	66	(150)	-683.8	--	311.2	--	--	978.0	11.74	516.6	906.1	--	2,723.7	20

(Continued)

*The unit for total flow rate for Streams 1 and 1a is kg/hr; the unit for Streams 1b, 2, 3, and 4 is kg/hr + 10^3 g-moles/hr; the unit for Streams 5 - 36 is 10^3 g-moles/hr.

Continued

TABLE IV-9

PROCESS FLOW STREAMS FOR 26-MW FUEL-CELL POWER PLANT (NAPHTHA)

Stream	Temperature °C	Temperature (°F)	Enthalpy (GJ/hr)	Flow Rate (10^3 g-moles/hr) H_2	$H_2O(g)$	CH_4	CO	CO_2	O_2	N_2	$H_2O(l)$	Flow Rate Naphtha (kg/hr)	Total*	Stream
21	66	(150)	439.4	--	311.2	--	--	978.0	11.74	516.6	--	--	1,817.6	21
22	15.6	(60)	199.9	--	382.8	--	--	--	7,432.0	29,728	--	--	37,543	22
23	66	(150)	254.7	--	382.8	--	--	--	7,432.0	29,728	--	--	37,543	23
24	66	(150)	238.6	--	360.6	--	--	--	7,002.3	28,008	--	--	35,372	24
25	66	(150)	16.1	--	22.13	--	--	--	429.8	1,719.0	--	--	2,170.9	25
26	66	(150)	-423.2	--	333.3	--	--	978.0	441.5	2,235.6	--	--	3,988.5	26
27	327	(620)	-388.3	--	333.3	--	--	978.0	441.5	2,235.6	--	--	3,988.5	27
28	541	(1,006)	-640.2	--	1,111.1	--	--	1,675.2	679.2	7,452.1	--	--	10,918	28
29	704	(1,300)	-347.2	--	1,111.1	--	--	996.0	339.6	7,452.1	--	--	9,898.8	29
30	668	(1,235)	-359.9	--	1,111.1	--	--	996.0	339.6	7,452.1	--	--	9,898.8	30
31	668	(1,235)	-251.9	--	777.8	--	--	697.2	237.7	5,216.4	--	--	6,929.1	31
32	668	(1,235)	-108.0	--	333.3	--	--	298.8	101.9	2,235.6	--	--	2,969.6	32
33	323	(613)	-142.9	--	333.3	--	--	298.8	101.9	2,235.6	--	--	2,969.6	33
34	816	(1,500)	-1.91	10.89	7.15	0.03	2.65	1.79	--	--	--	--	22.51	34
35	349	(660)	-2.28	10.89	7.15	0.03	2.65	1.79	--	--	--	--	22.51	35
36	232	(450)	-2.46	13.37	4.67	0.03	0.17	4.27	--	--	--	--	22.51	36

*The unit for total flow rate for Streams 1 and 1a is kg/hr; the unit for Streams 1b, 2, 3, and 4 is kg/hr + 10^3 g-moles/hr; the unit for Streams 5 - 36 is 10^3 g-moles/hr.

atmospheric pressure operation was assumed. The base case performance (power density) of the System 3 fuel cell was projected to be higher than that obtained for the System 2 power plant. Selection of a somewhat lower design voltage is partly responsible for this increase, as noted in the discussion below. Another reason is the slightly more favorable fuel cell inlet reactant concentrations calculated for System 3:

	Inlet Reactant Composition, mole fraction		
	Anode (H_2+CO)	(O_2)	Cathode (CO_2)
System 2 (SNG)	0.560	0.060	0.127
System 3 (Naphtha)	0.602	0.062	0.153

These differences reflect the impact of the higher carbon/hydrogen ratio of the primary fuels (naphtha versus SNG) as well as evolving selection of optimal reformer operating conditions and flow stream integration.

As discussed earlier, alternative combinations of process variables would also achieve the efficiency and water-balance goals. In this case, even lower design voltages could probably have been assumed. The impact of lower voltage operation on cell current density is large, resulting in substantially increased power density and lower fuel cell costs. A major reason for this sensitive current density response is the optimistic value used for cell resistance. Thin electrolyte tiles with low ionic resistance were assumed, based on expected improvements in cell technology. The impact of these factors on projected system cost is discussed in Section VII-K.

d. Conceptual System Design

The conceptual design of the System 3 power plant is similar to that developed for System 2. Power plant equipment, listed

in Table IV-10, would be assembled into modular, shippable units. Major differences between the two conceptual designs are as follows:

- The steam reforming reactor contains a different catalyst, Girdler G-91C. This potassium-activated nickel on alumina catalyst was developed by Girdler for naphtha reforming. The vendor claims improved activity and lower cost compared with previous available catalysts.

- The reformer package again contains the burner, reformer section, and heat exchangers E-1 through E-4. The surface areas of the heat exchangers, however, are larger than those in the System 2 module. Thus, the overall size, weight, and cost of the package are greater. It may be necessary to use a larger number of reformer units (perhaps one for each fuel-cell trailer or a total of eight) to avoid exceeding the size and weight limit for a shippable unit. For this study, however, we assume that four reformer units are used.

- The fuel cell operates at a higher power density, resulting in a smaller active area requirement per cell and lower fuel cell cost.

- The components of the HDS loop can be fitted into the equipment module envelope. Additional space was available, based on a reduction in the length of exchanger E-6. The HDS reactor bed was sized assuming a design space velocity of 1,000 m^3 output/hr-m^3 catalyst.

- The arrangement of modules is nearly identical to that shown in Figure IV-12 for the SNG-fueled power plant. The overall plant size is 58.5 x 29 m (192 x 128 ft), somewhat larger than the SNG-fueled plant, because of the larger air fin condenser E-7.

6. Distribution of Electricity

See Section IV-B for the complete description of the distribution of electricity from a 26-MW fuel-cell power plant.

7. Heat Pump

See Section IV-B for the complete description of the use of heat pumps for residential heating and cooling.

Table IV-10

EQUIPMENT LIST FOR 26-MW FUEL-CELL POWER PLANT (NAPHTHA)

Unit	Capacity	Size	Modular Size	Dimensions	Materials
Molten Carbonate Fuel Cell	28.4 MW D C	22.1 x 10^3 m^2	2.77 x 10^3 m^2	Fuel-Cell Trailer 3.1 x 7.3 x 3.7m	UTC Advanced Design
Heat Exchangers					
E-1	57.6 GJ/hr	1.40 (x 10^3 m^2)	0.35 (x 10^3 m^2)	Included in	304 SS
E-2	12.0 GJ/hr	0.35 (x 10^3 m^2)	0.088 (x 10^3 m^2)	Reformer Package	309 SS
E-3	7.1 GJ/hr	0.45 (x 10^3 m^2)	0.11 (x 10^3 m^2)	3.8 m dia x 7.3 m high	304 SS
E-4	8.0 GJ/hr	1.01 (x 10^3 m^2)	0.25 (x 10^3 m^2)		304 SS
E-5	12.7 GJ/hr	0.26 (x 10^3 m^2)	0.065 (x 10^3 m^2)	122 cm dia x 3.7 m long	304 SS
E-6	34.9 GJ/hr	1.15 (x 10^3 m^2)	0.29 (x 10^3 m^2)	122 cm dia x 7.0 m long	304 SS
E-7	54.9 GJ/hr	2.40 (x 10^3 m^2)	0.60 (x 10^3 m^2)	8.5 x 9.1 x 4.6 m high	C.S. Finned
E-8	0.37 GJ/hr	0.009 (x 10^3 m^2)	0.003 (x 10^3 m^2)	0.30 x 0.30 x 0.61 m	309 SS Finned
Reformer Section	45.9 GJ/hr	0.91 (x 10^3 m^2)	0.23 (x 10^3 m^2)	Included in Reformer Package	HK40 Cr-Ni Tubes
Reformer Catalyst	740,020 g-mole H_2/hr	21.3 m^3	5.33 m^3	--	Girdler G-91C
Burner	2,183,700 g-mole/hr	179 GJ/hr	44.6 GJ/hr	Included in Reformer Package	C.S. and Refractory
Shift High-Temp. Catalyst	22,510 g-mole H_2/hr	0.77 m^3	0.19 m^3	0.45 m dia x 1.7 m high	Girdler G-3A
Shift Low-Temp. Catalyst		0.35 m^3	0.087 m^3	0.30 m dia x 1.1 m high	Girdler G-66
Shift Intercooler	0.19 GJ/hr	0.68 m^3	0.17 m^3	0.15 m dia x 0.30 m long	C.S.
Hydrodesulfurization Catalyst	4,256 kg naphtha/hr	1.20 m^3	0.30 m^3	--	Girdler G-51C
ZnO Bed	1.02 kg S/day	1.567 m^3	0.40 m^3	0.61 m dia x 2.1 m long	Girdler G-72
Knockout Drum	906,200 g-mole H_2O/hr	8.05 m^3	2.01 m^3	1.3 m dia x 2.1 m long	Galvanized
Condensate Pump	4.5 liter/sec.	--	1.1 liter/sec	0.61 x 0.61 x 1.2 m long	C.S.
Blowers					
B-1	249 m^3/min	--	62.3 m^3/min	0.91 x 0.91 x 0.91 m	C.S.
B-2	14,000 m^3/min	--	3,510 m^3/min	Part of E-7	C.S.
B-3	2,580 m^3/min	--	651 m^3/min	1.5 x 1.5 x 1.8 m	304 SS
B-4	679 m^3/min	--	170 m^3/min	1.2 x 1.2 x 1.2 m	C.S.
B-5	821 m^3/min	--	205 m^3/min	1.2 x 1.2 x 1.2 m	C.S.
B-6	5.5 m^3/min	--	1.4 m^3/min	0.30 x 0.30 x 0.30 m	C.S.

D. System 4

A block flow diagram of System 4 is shown in Figure IV-18. The components of the system are described below.

1. Coal Mine

See Section IV-A for the complete description of a surface coal mine located in the Powder River Basin.

2. Coal Liquefaction Plant

The H-Coal liquefaction process was described in Section IV-C. The product of interest in that discussion was hydrotreated naphtha, which was to be used as fuel for the 26-MW fuel cell. In System 4, the required product is a low-sulfur distillate fuel for a combined-cycle power plant. The flow diagram for a facility that produces 7,950 m^3 (50,000 bbl) per day of such a product is shown in Figure IV-19; the stream compositions are shown in Table IV-11. The principal difference between the facility shown in Figure IV-19 and that shown in Figure IV-16 is that the C_5-200°C naphtha stream is not further hydrotreated. Rather, the entire H-Coal distillate product is sold as-is, for use as turbine fuel in a combined-cycle power plant. The quality inspection for the fuel was shown in Table IV-8.

The major process difference between the two facilities is that when fuel oil is the required product, the end point of the distillate product is raised from 495°C (925°F) to 525°C (975°F), raising the distillate product output by 3%. The increase in the end point reduces the feed to the partial oxidation plant, in conformance with the reduced hydrogen requirement of the process.

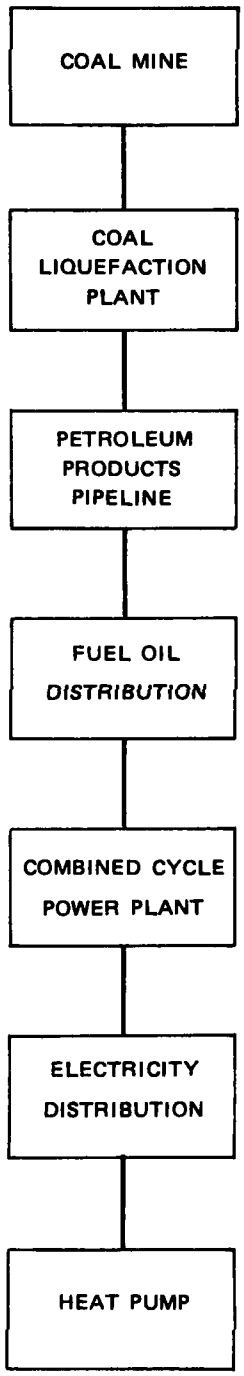

FIGURE IV-18. BLOCK FLOW DIAGRAM OF SYSTEM 4

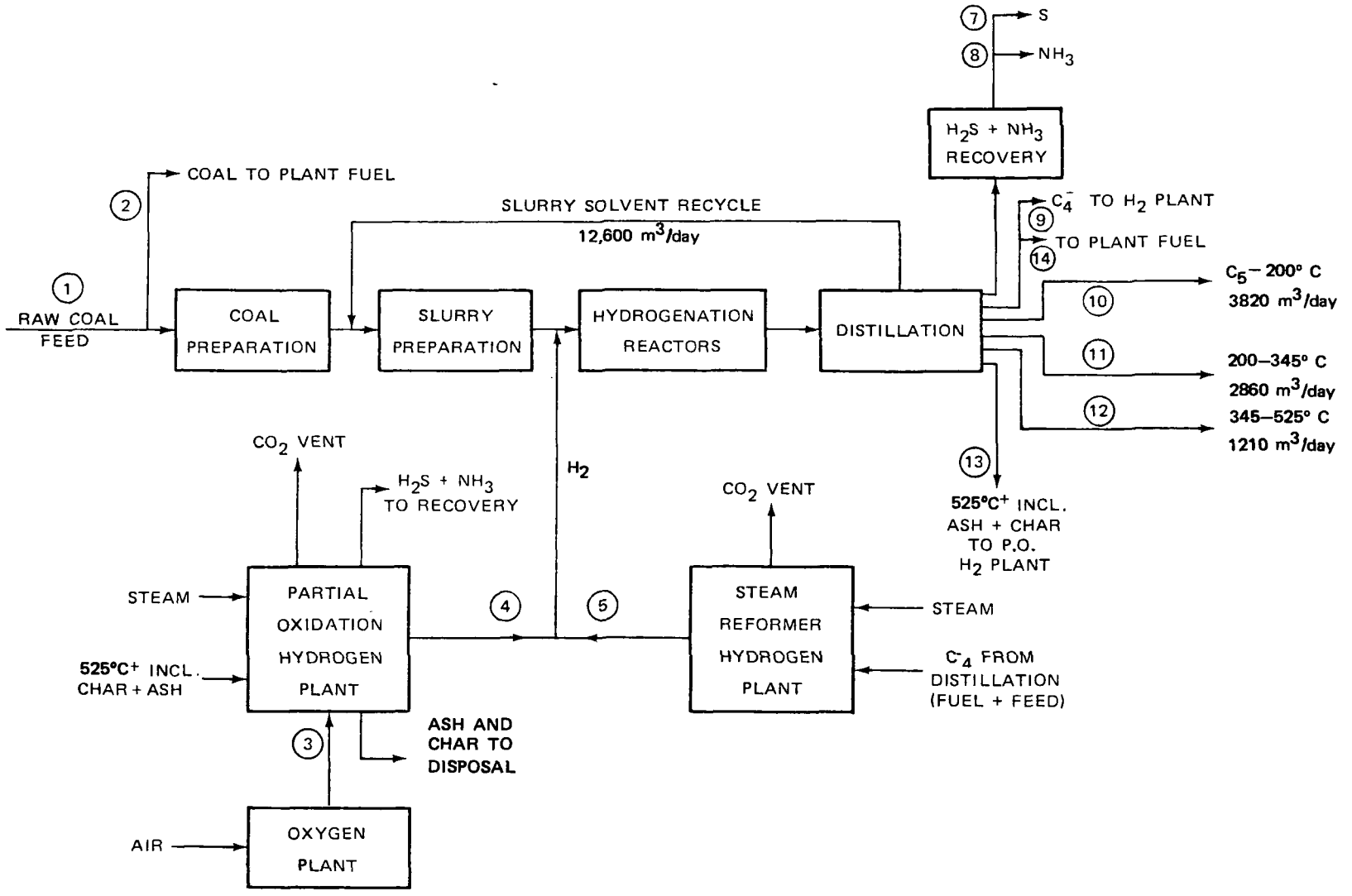

FIGURE IV-19. H-COAL PROCESS FLOW DIAGRAM

Table IV-11

COMPOSITION OF MAJOR STREAMS IN H-COAL PROCESS

Component	Quantity	Stream Number 1	2	3	4	5	6	7	8	9	10	11	12	13	14
Raw Coal	10^3 kg/hr	925	160	--	--	--	--	--	--	--	--	--	--	--	--
MAF* Coal	10^3 kg/hr	670	115	--	--	--	--	--	--	--	--	--	--	--	--
H_2 (10^3 nm^3/hr)	10^3 kg/hr	--	--	--	(260)	(195)	--	--	--	5.8	--	--	--	--	0.58
C_1	10^3 kg/hr	--	--	--	--	--	--	--	--	29	--	--	--	--	2.9
C_2	10^3 kg/hr	--	--	--	--	--	--	--	--	35	--	--	--	--	3.5
C_3	10^3 kg/hr	--	--	--	--	--	--	--	--	32	--	--	--	--	3.2
C_4	10^3 kg/hr	--	--	--	--	--	--	--	--	31	--	--	--	--	3.1
C_5-200 °C	10^3 kg/hr	--	--	--	--	--	--	--	--	--	240	--	--	--	--
200-345 °C	10^3 kg/hr	--	--	--	--	--	--	--	--	--	--	220	--	--	--
345-525 °C	10^3 kg/hr	--	--	--	--	--	--	--	--	--	--	--	100	--	--
525 °C +	10^3 kg/hr	--	--	--	--	--	--	--	--	--	--	--	--	120	--
Char	tonnes/day	--	--	--	--	--	--	--	--	--	--	--	--	1,300	--
Ash	tonnes/day	--	--	--	--	--	--	--	--	--	--	--	--	1,100	--
Oxygen	tonnes/day	--	--	2,900	--	--	--	--	--	--	--	--	--	--	--
Sulfur	tonnes/day	--	--	--	--	--	--	100	--	--	--	--	--	--	--
Ammonia	tonnes/day	--	--	--	--	--	--	--	120	--	--	--	--	--	--

*MAF = Moisture and Ash Free

Although the suitability of coal-derived fuels for use in gas turbines has not yet been demonstrated, an H-Coal distillate fuel with the properties shown in Table IV-8 is expected to meet most specifications for turbine fuels,[28] partly because the fuel contains no 525°C+ (975°F+) fraction, and thus has a relatively high H/C ratio.

3. Liquids Pipeline

See Section IV-C for a complete description of an interstate pipeline suitable for transporting a combination of liquid petroleum products.

4. Fuel Distribution

Because of the large volume of fuel required for the combined-cycle power plant, the most effective method of supply would probably be railroad tank cars. For the 270-MW power plant described in the following section, 430 m^3 (2,700 bbl) of distillate fuel oil would be consumed daily, assuming a load factor of 35%. If the power plant is located a significant distance from the pipeline terminus, shipments of fuel oil by unit train from the bulk terminal to the power plant are an effective means of supply.

A unit train consisting of 80 tank cars, each with 37,850 liter (10,000 gallon) capacity, could supply the power plant requirements with one weekly delivery. To ensure against disruptions in the supply, a significant on-site storage capacity is required. For large, centralized power plants, that requirement is typically met by above-ground steel storage tanks. To maintain a 30-day fuel supply would require a storage capacity of 13,000 m^3 (3.5 million gal).

5. Combined-Cycle Power Plant

a. Background

Conceptually, a combined-cycle power plant is similar to a fossil-fired steam electric plant, with the addition of a device for improving the process efficiency. The device is a gas turbine-generator set that extracts work (electricity) from the combustion gases before they go to the steam boiler-steam turbine-generator system. The gas turbine enables the system of combined cycles to take advantage of higher combustion temperatures than would be practical with a steam turbine alone. That advantage results in a higher system efficiency. Even higher efficiencies could be obtained if gas turbines can be developed to withstand still higher inlet temperatures. The system used as an example for this study was modeled on a system designed by Westinghouse for the Energy Conversion Alternatives Study (ECAS).[29] The gas turbine analyzed in that study can tolerate an inlet temperature 1,380°C (2,500°F). The high inlet temperature would be made possible by using air-cooled ceramic gas turbine blades and nozzles. Currently, typical operating conditions for utility turbines are:

- Turbine inlet temperature between 980 and 1,090°C (1,800 and 2,000°F).
- Compression discharge pressure ratio (compressor discharge/ambient pressure) 8:1 to 15:1.

Because there is such a wide gap between the current clean-oil-fed turbine technology and that advocated in the Westinghouse study, some people have recommended developing an intermediate technology that would use residual petroleum feeds for turbines.[30]

High combustion temperatures are not always beneficial. More nitrogen oxides (NO_x) are formed with high-temperature combustion. Additional water can be injected to reduce the NO_x effluents, but that also reduces the turbine inlet temperature and, therefore, also reduces the process efficiency.[31] Various NO_x reduction methods for gas turbines are being studied, but none are currently able to provide passable performance with coal-derived liquids for an NO_x limit of 0.14 kg per GJ (0.3 lb per million Btu) (HHV). Two sources of nitrogen form NO_x:

- Chemically bound nitrogen in the gas turbine fuel
- Molecular nitrogen from combustion air.

Natural-gas-fueled combined-cycle plants have no chemically bound nitrogen in the fuel and thus must cope only with "thermally fixed" nitrogen from combustion air. However, just as the NO_x emission regulations are being tightened, changes in turbine fuels toward those with considerable chemically bound nitrogen content are being mandated . H-Coal distillate is an example of such a high nitrogen feed. Nitrogen can be removed from the H-Coal distillate by hydrotreating, but it is not economical. Just developing the hardware that can burn the hydrogen-deficient fuel is a problem.[32] Lowering the NO_x emission is a second-order objective,[33] but one that must be met if combined-cycle systems are to achieve widespread application.

b. Process Description

Figure IV-20 shows a block flow diagram of a coal-liquid-fired combined-cycle plant. The fuel (H-Coal distillate) is first prepared by filtering, washing with water, and centrifuging to remove soluble salts of sodium and potassium. Magnesium fuel additives (e.g., $MgSO_4$-$7H_2O$ or MgO emulsion) can also be used to inhibit vanadium attack in the turbine.[34,35]

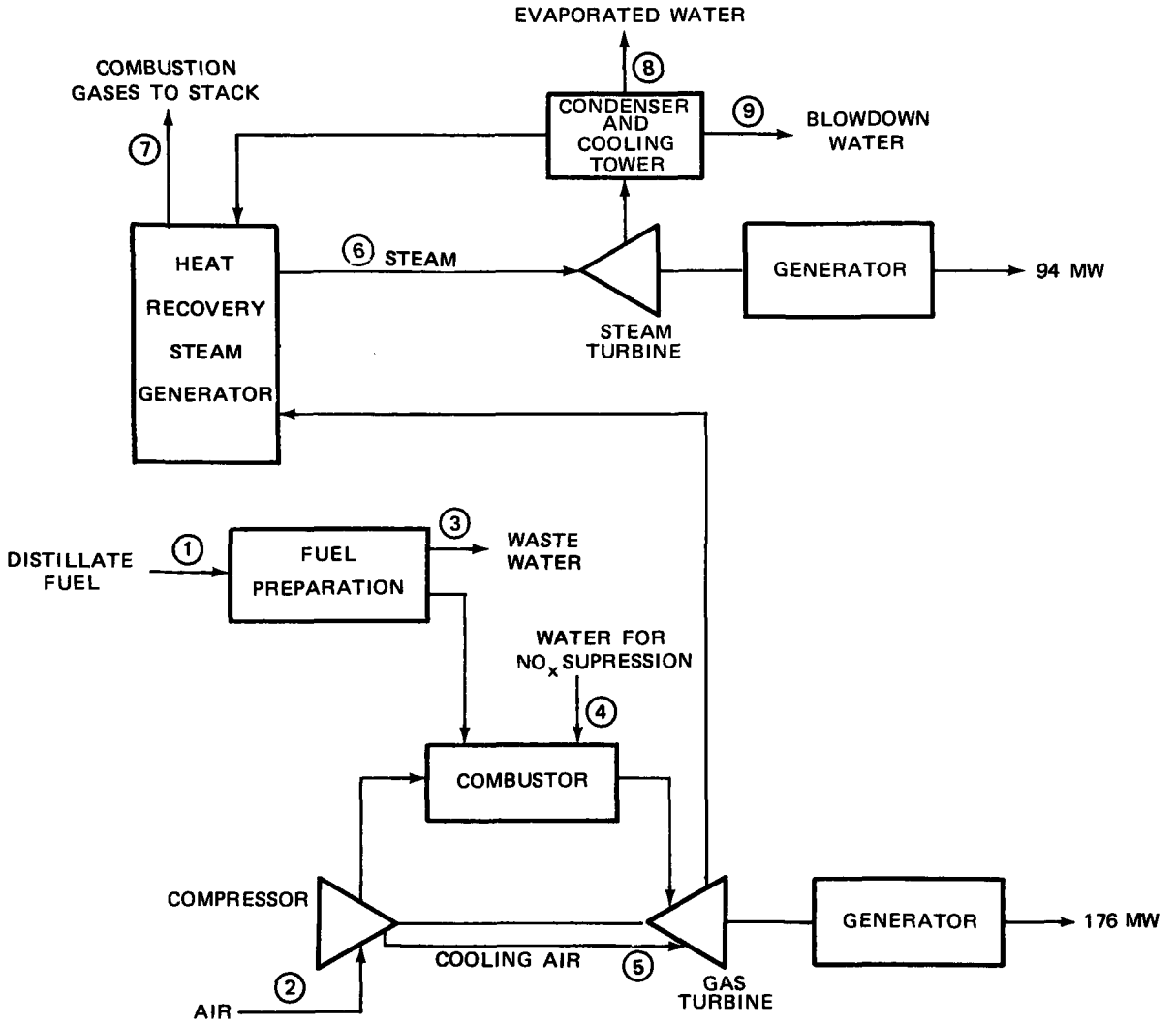

FIGURE IV-20. COMBINED CYCLE POWER PLANT BLOCK FLOW DIAGRAM

Air for combustion is compressed to a pressure ratio of 16:1 in the gas turbine driven compressor. Fuel and compressed air are burned in the combustor. The 1,370°C (2,500°F) combustion gases drive the gas turbine-generator set.

Exhaust gases from the gas turbine then enter the non-fired heat recovery steam generators (HRSG) at 670°C (1,240°F). High-pressure steam (16,500 kPa or 2,400 psia) is raised in the HRSGs to drive a conventional steam turbine-generator set. Condensed exhaust from the steam turbine is returned to the HRSGs.

Table IV-12 shows the mass flow rates for the 270-MW combined-cycle power generating plant. Several streams are combined in Table IV-12 to show overall flow rates. Two gas turbine-generator sets have 91-MW capacity each. There is one HRSG for each gas turbine, and these send combined steam flows to the single 97-MW steam turbine-generator set.

Not shown in Table IV-12 or Figure IV-18 is a single reheat cycle in which 350°C (660°F) steam exhausted from the first stage of the steam turbine is routed to the HRSG for reheating to 540°C (1,000°F). The reheated steam powers the second and third (intermediate and low pressure) stages of the steam turbine.

6. Transmission and Distribution of Electricity

See Section IV-A for the complete description of the electricity transmission and distribution system.

7. Heat Pump

See Section IV-B for the complete description of the use of heat pumps for residential heating and cooling.

Table IV-12

MASS FLOW RATES FOR 270-MW COMBINED-CYCLE POWER PLANT

	Stream Name and Number	Mass Flow Rate (10^3 kg/hr)	Temperature °C	(°F)	Pressure kPa	(psia)
1	Distillate Fuel	42	150	(300)	101	(14.7)
2	Air	1,500	60	(16)	101	(14.7)
3	Waste-water	6	--	--	--	--
4	Water for NO_x Suppression	22	--	--	--	--
5	Cooling Air	58	--	--	--	--
6	Steam	250	540	(1,000)	16,500	(2,400)
7	Combustion Gases	1,550	670	(1,240)	107	(15.6)
8	Evaporated Water	190	100	(212)	101	(14.7)
9	Blowdown Water	180	--	--	--	--

E. System 5

A block flow diagram of System 5 is shown in Figure IV-20. The components of the system are described below.

1. Coal Mine

See Section IV-A for the complete description of a surface coal mine located in the Powder River Basin.

2. Coal Gasification Facility

See Section IV-A for the complete description of the Hygas coal gasification process.

3. Gas Pipeline

See Section IV-A for the complete description of an interstate natural gas pipeline.

4. Gas Distribution

See Section IV-A for the complete description of the natural gas distribution system.

5. 100-kW Fuel-Cell Power Plant

This power plant uses a first-generation phosphoric acid fuel cell as an energy converter in a total energy package. Heat recovered

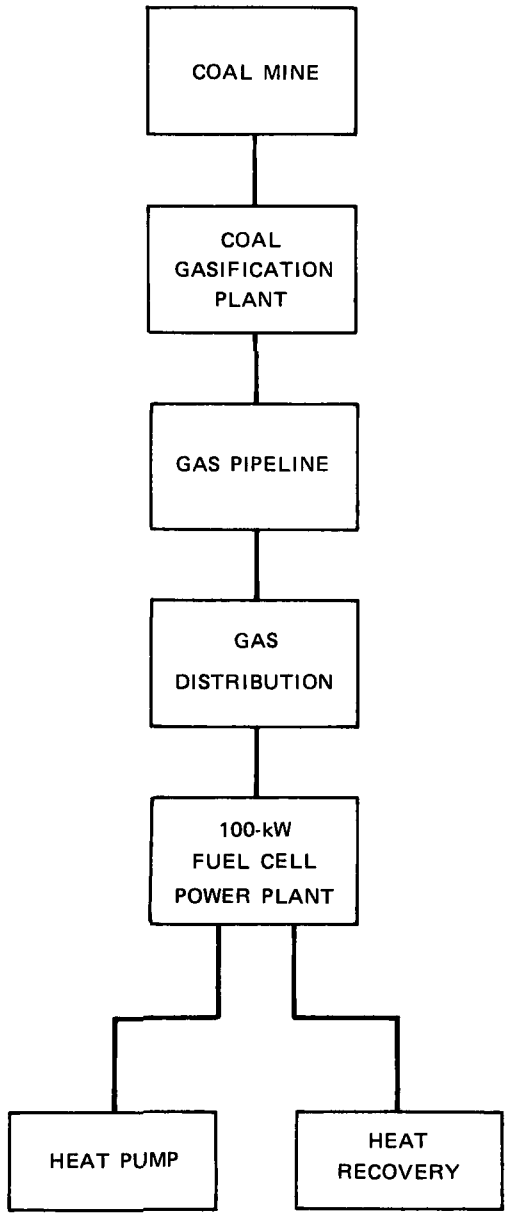

FIGURE IV-21. BLOCK FLOW DIAGRAM OF SYSTEM 5

from the fuel cell is used to provide hot water to satisfy part of the thermal load demand in a housing complex. The system concept is based on published United Technologies Corporation reports, supplemented by cell design and performance data from current phosphoric-acid fuel-cell technology programs at Energy Research Corporation and Universal Oil Products. Target electrical generation efficiency is in the 30 to 35% range for expected operation at partially rated to full-rated electrical load (100 kW).

a. System Description

The 100-kW power plant contains fuel-cell power stacks and associated auxiliary process equipment, including a fuel conditioner that converts SNG feed into hydrogen fuel, air supply system, waste heat recovery system, and an inverter to convert power plant DC output to AC. Figure IV-22 is a block diagram showing the functional arrangement of these components.

Details of the process flow stream integration are shown in Figure IV-23. Odorant sulfur compounds are removed from the incoming SNG feed in a small zinc oxide guard bed. Steam is added to the SNG feed prior to entering the reformer section, where the methane-steam reforming reaction is carried out to produce hydrogen for the fuel cell. The hot reformed gases are then cooled and passed through a series of shift conversion reactors to reduce carbon monoxide content prior to entering the fuel cell. Spent fuel from the fuel cell is used to fire the reformer furnace. A heat exchanger network is provided to accomplish the required reactant preheat and product cool-down.

The fuel-cell stacks are cooled with a circulating silicone oil coolant. The hot oil is first used to generate steam for the reformer. Major waste heat recovery is then accomplished by cooling the oil exchanger E-7, using a hot water stream. This stream is heated to 82°C (180°F), the design return temperature for the housing

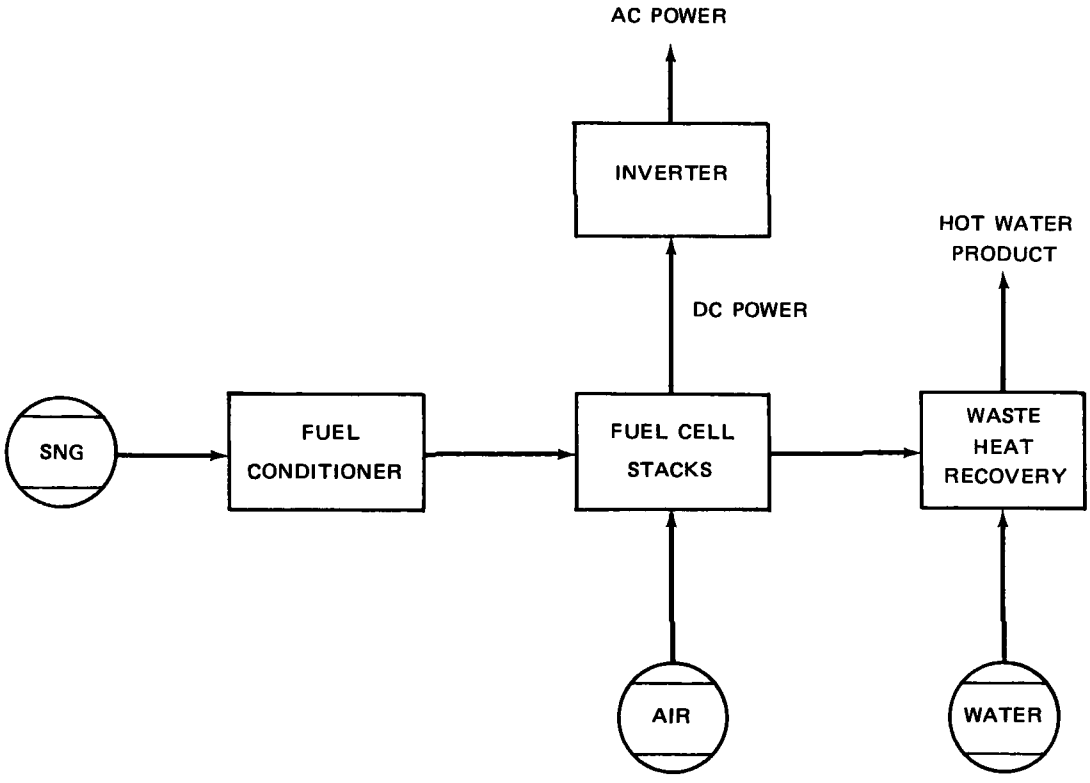

FIGURE IV-22. 100-kW POWER PLANT COMPONENTS

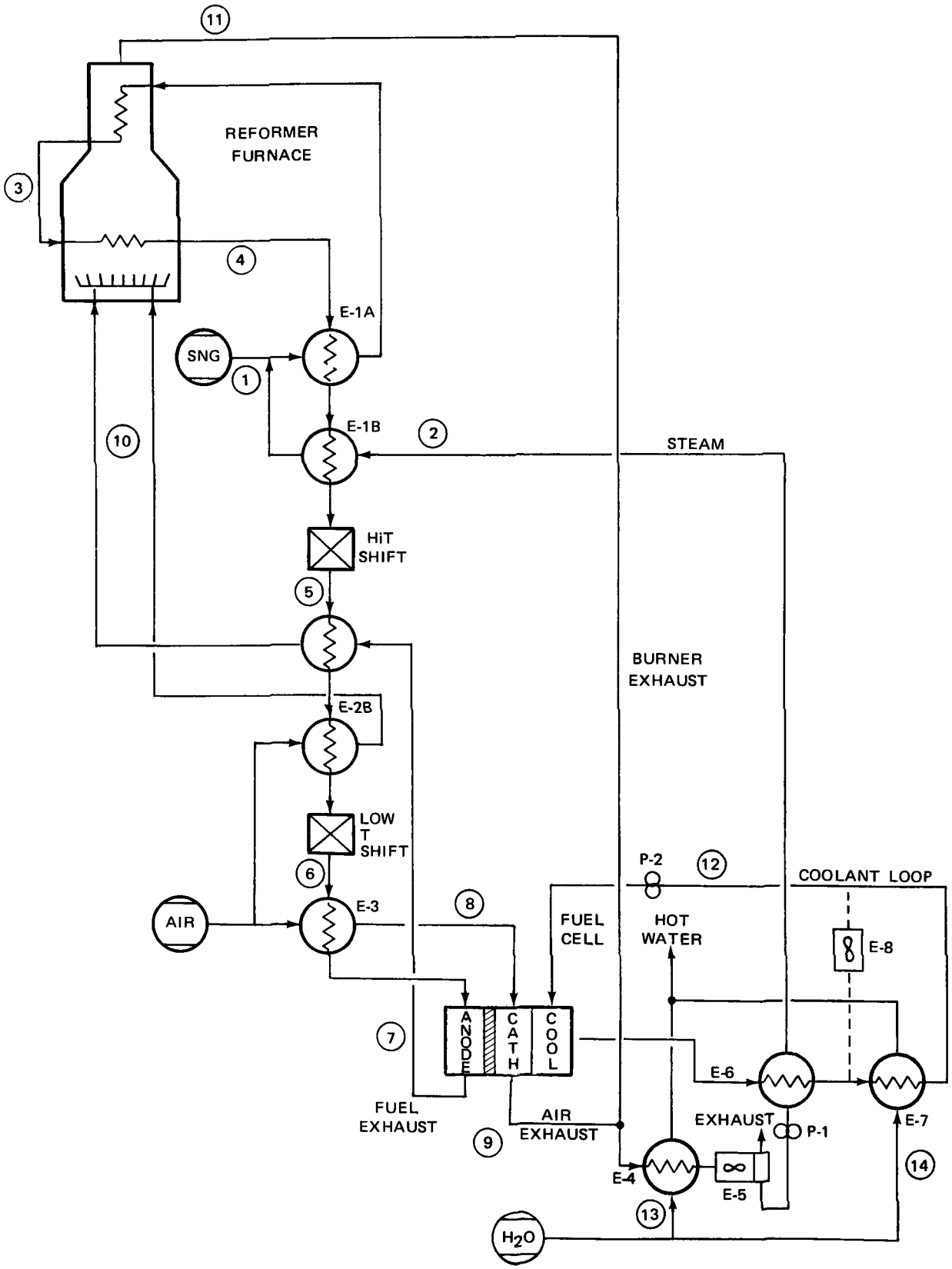

FIGURE IV-23. HEAT INTEGRATION FOR 100-kW FUEL-CELL POWER PLANT

complex hot water system. Additional quantities of 82°C water are produced by cooling the combined exhaust air and reformer furnace flue gas streams in exchanger E-6. Final combined gas cooling is carried out in air-cooled exchanger E-5. Here, condensed water is recovered and used to generate process steam for the reformer.

Depending on the demand, situations may arise where electrical power is required, but thermal energy (hot water) is not. Steady-state operation of the fuel-cell system will still require removal of waste heat from the circulating oil coolant and water recovery from the exhaust gas streams. To accomplish this, an air-cooled bypass exchanger E-8 is provided in the oil coolant loop. In addition, trim cooler E-5 in the air loop is oversized to permit total cool-down of the exhaust gas streams to the design dew point.

b. System Design Basis

This section discusses the rationale for the specific design parameters selected for the 100-kW power plant study. Phosphoric acid fuel-cell technology was used because extensive programs are currently underway to develop this technology for total energy power plants. Participants in these programs include United Technology Corporation (UTC), Energy Research Corporation (ERC), Westinghouse, and Engelhard Industries. The designs developed in this study represent a synthesis of various features of the UTC and ERC systems.

Fuel-Cell Design -- The static electrolyte fuel cell contains multiple assemblies of cells formed by stacking electrodes sandwiched around a silicon carbide matrix and formed bipolar plates containing grooves for reactant distribution. Cost studies were based on cells designed by ERC for the U.S. Army, which have been described in considerable detail[36].

Platinum electrocatalysts were assumed, with a total (anode plus cathode) loading of 1 mg/cm^2. This is somewhat higher than the

0.75 mg/cm^2 loading in UTC cells, but appears consistent with current ERC values. Data for Engelhard cells are not available.

Cell cooling is accomplished using cooling plates within the stack. These plates contain embedded cooling tubes for circulating an inert silicone oil coolant, based on an early UTC design concept. Further study of this configuration revealed that the oil was not truly inert, and if leakage occurred, subsequent corrosion products had an adverse effect on fuel-cell performance. Current UTC designs employ a two phase pressurized boiling water coolant, used in cells operating at a nominal temperature of 190°C (395°F). ERC and probably Engelhard designs, on the other hand, use circulating air as coolant. These differences may have an impact on the heat transfer surface area required to recover waste heat from the fuel cell. The silicone oil design is assumed to be adequate for purposes of this study.

Fuel-Cell Operating Conditions and Performance -- Fuel-cell operating temperature and pressure were set at 170°C (338°F) and 1 atm, respectively. These conditions appear to offer a workable compromise among several competing factors including stack performance, life, and cost.

Fuel-cell performance improves as temperature and pressure are raised. Current UTC designs call for large, multi-megawatt power plants that operate at 190°C (375°F) and 640 kPa (93 psia). Improved performance can result in improved power plant efficiency (if operating voltage is increased) or in reduced power plant cost (if operating current density, hence power density, is increased). On the other hand, prospects for achieving target stack life, assumed to be 40,000 hours, are reduced at these more severe conditons. Life-limiting factors include gradual loss of cathode catalyst surface area via sintering and dissolution, and degradation of electrode structure caused by corrosion of the carbon supports on which the platinum catalyst is dispersed. The latter adversely affects the reactant gas-electrolyte-catalyst interface within the electrode structure.

Previous ERC stacks, developed for the U.S Army, operate at 176°C (350°F) and recent cell evaluations using catalysts supplied by Universal Oil Products Corporation have been conducted at 180°C.

To date, there have been no published reports of phosphoric acid fuel-cell stack operation extending to 40,000 hours. For this study, we selected a low operating temperature of 170°C (338°F) as most likely to achieve that target lifetime.

Waste heat utilization applications can also influence the choice of operating temperature. Cogeneration schemes requiring substantial amounts of heat as low-pressure steam appear more attractive if higher fuel-cell operating temperatures are selected. In System 5, we assume that all waste heat is used to produce relatively low grade hot water at 82°C. Fuel-cell operation at 170°C appears adequate for this application.

Loss of phosphoric acid electrolyte via vaporization from the cell matrix and electrolyte structures is another life-limiting factor controlling the choice of operating temperature. Those vaporization losses (into the flowing air stream) increase as temperature increases. Operation at high pressure can reduce electrolyte loss, but cost-effective means to do this are not available (see below). Again, operation at 170°C appears to offer a suitable compromise.

High-pressure operation improves performance. However, to operate efficiently at elevated pressure, a coupled turbocompressor/expander set must be used to compress ambient air and to recover energy from the hot compressed fuel-cell exhaust air stream. Efficient devices that accomplish those tasks at the flow rates used in the 100-kW power plant are too costly.

Increased operating temperature reduces the extent of reversible adsorption or "poisoning" of the platinum anode catalyst by carbon monoxide. The latter is present in the reformed gas feed.

Operation at 170°C would tend to aggravate this poisoning effect.

Published phosphoric acid fuel-cell performance characteristics were reviewed. Those data are shown in Figure IV-24 and Table IV-13. As indicated, the data base is sparse. Few total cell performance data have been published, particularly for advanced cell designs such as those of UTC, which are usually considered proprietary.

Figure IV-24 shows initial performance data for relatively small single cells at a variety of temperatures. Life-limiting phenomena will cause performance degradation with time. In addition, performance losses can be expected as cells are scaled-up to commercial size, stacked into multicell assemblies, and used in the field. It is not possible to predict such losses at this time.

Figure IV-24 also shows the base-case performance curve and design point used in this study. This estimate of average cell performance in the 100-kW power plant at end-of-life conditions (40,000 hr) is assumed to be conservative. Clearly, performance will improve as cell designs evolve. Figure IV-24 also includes a projected design point, used to assess the impact of advanced phosphoric fuel cell performance.

The base case design curve was established in mid-1977. Subsequently, published cell performance data show that improvements have indeed occurred, particularly for cells operating at elevated temperature (190°C) and pressure (345 kPa or 50 psia). Additional advances are required to achieve target lifetimes.

<u>Fuel Conditioning System</u> -- The fuel conditioning system is used to convert the SNG feed to hydrogen fuel via the endothermic steam reforming reaction:

$$CH_4 + 2H_2O \longrightarrow 4H_2 + CO_2$$

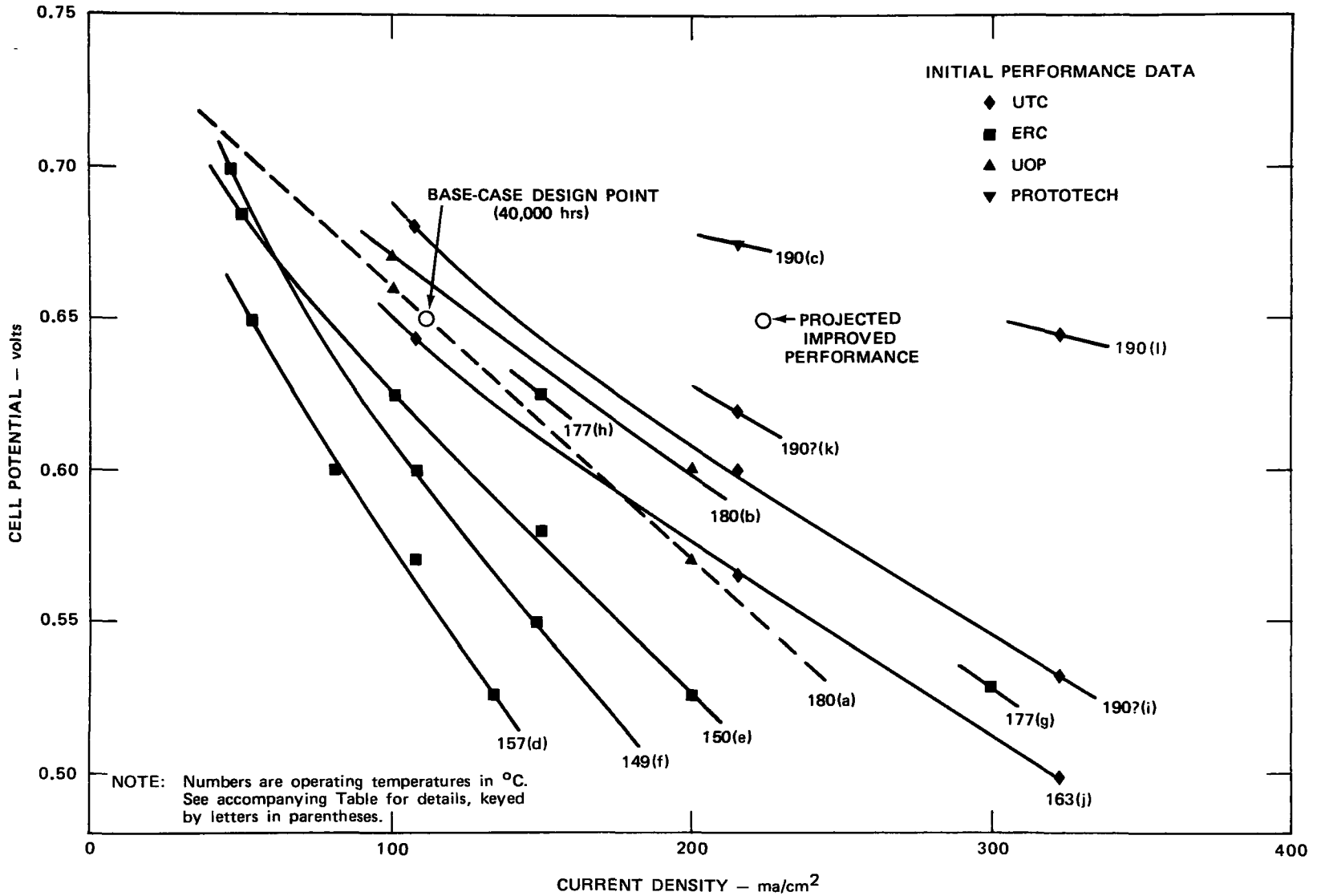

FIGURE IV-24. PHOSPHORIC ACID FUEL CELL PERFORMANCE DATA

Table IV - 13

ADDITIONAL DETAILS FOR FIGURE IV - 24

Data Source	Data Set Indicated in Fig. IV-23	Operating Conditions Temp. (°C)	Operating Conditions Pressure (kPa)[a]	Total Catalyst Loading ($mgPt/cm^2$)[b]	Remarks	Reference
UOP	a	180	101	2.5	Pure H_2	37
UOP	b	180	101	1.2	Pure H_2	38
Prototech	c	190	101	0.5	Pure H_2	39
ERC	d	157	101	4.0	H_2 + 2% CO	40
ERC	e	150	101	4.0	Pure H_2	41
ERC	f	149	101	4.0	Pure H_2	42
ERC	g	177	101	0.5[d]	n.a.	43
ERC	h	177	101	n.a.	n.a.	44
ERC	i	190[d]	n.a.	1.0	Simulated reformate	45
ERC	j	163	101[d]	0.5	Reformed natural gas	46
ERC	k	190[d]	101[d]	1.0	Simulated reformate	47
ERC	l	190	345	0.75	Simulated reformate[c]	48

[a] 101 kPa = 14.7 psia = 1 atmosphere.

[b] Anode + cathode.

[c] Realistic reactant utilizations.

[d] Assumed, not reported.

At steam reforming conditions, the water gas shift equilibrium affects the product gas composition:

$$CO + H_2O \longrightarrow H_2 + CO_2$$

Reformed gas composition was estimated using a thermodynamic calculation procedure developed by Imperial Chemicals Industries (ICI). The computation was modified to reflect the actual Hygas SNG composition assumed for this study:

Component	Moles/Mole CH_4
CH_4	1.0000
CO	0.00115
CO_2	0.01830
H_2	0.13580
H_2O	0.00015

Preliminary studies were carried out to establish reasonable reforming conditions, temperature, and steam/carbon ratio, subject to the following constraints:

- Minimum methane slip (unconverted CH_4 in product gas). Methane is an inert gas that passes intact through the fuel cell. The anode exhaust, containing CH_4 and unreacted H_2 is used as burner feed for the reformer furnace. On the other hand, excessive methane slip reduces fuel conversion efficiency.

- Minimum CO in the product gas. Carbon monoxide is a fuel-cell poison, as noted earlier. Iterative procedures are required to establish CO content of the reformer effluent, because subsequent downstream processing in the shift reactors will reduce CO content down to target levels. A target level of about 1 volume percent CO in the fuel cell feed (dry gas basis) was assumed, based on cell operation at 170°C and discussions at the 1977 National Fuel Cell Seminar held in Boston. Recent UTC reports indicate that higher temperature cells (190°C) are designed to operate with about 1.7 volume percent CO[48].

Trade-off studies were carried out to develop an internally consistent, but not necessarily optimal, balance between those

constraints. Methane slip decreases rapidly as the reforming temperature is increased, but CO content also increases. Methane slip and CO content both decrease as the steam/carbon ratio increases, but excessive H_2O/C ratios involve costly water recovery heat exchangers and increased energy consumption for steam generation.

The final integrated system heat balance resulted in a somewhat excessive temperature for the reformer furnace flue gas effluent. Additional optimization studies are required to lower this temperature. Nevertheless, the system as designed provides adequate flame temperature and temperature differences within the furnace to carry out the required heat transfer.

Heat Recovery System -- The heat recovery system was designed to provide maximum hot water product at 82°C (180°F). We assumed design hot water return temperature of 60°C (140°F). Design revisions are required for alternative applications involving simultaneous heat recovery at several different temperatures.

c. System Operating Characteristics

The electrical and thermal operating characteristics of the 100-kW fuel-cell power plant were evaluated at rated load and at part load. A complete material and energy balance was carried out for operation of the power plant at full rated electrical load. A fuel-cell design point of 0.65 V was selected as an effective compromise between high efficiency for electrical generation and production of waste heat. The voltage-current performance characteristics of the fuel cell are shown in Figure IV-25. As indicated, the operating current density is 112 mA/cm^2 (104 A/ft^2). The system material balance is summarized in Table IV-14.

Potential problems with operational stability and system control strategy were uncovered during the analysis. The thermal

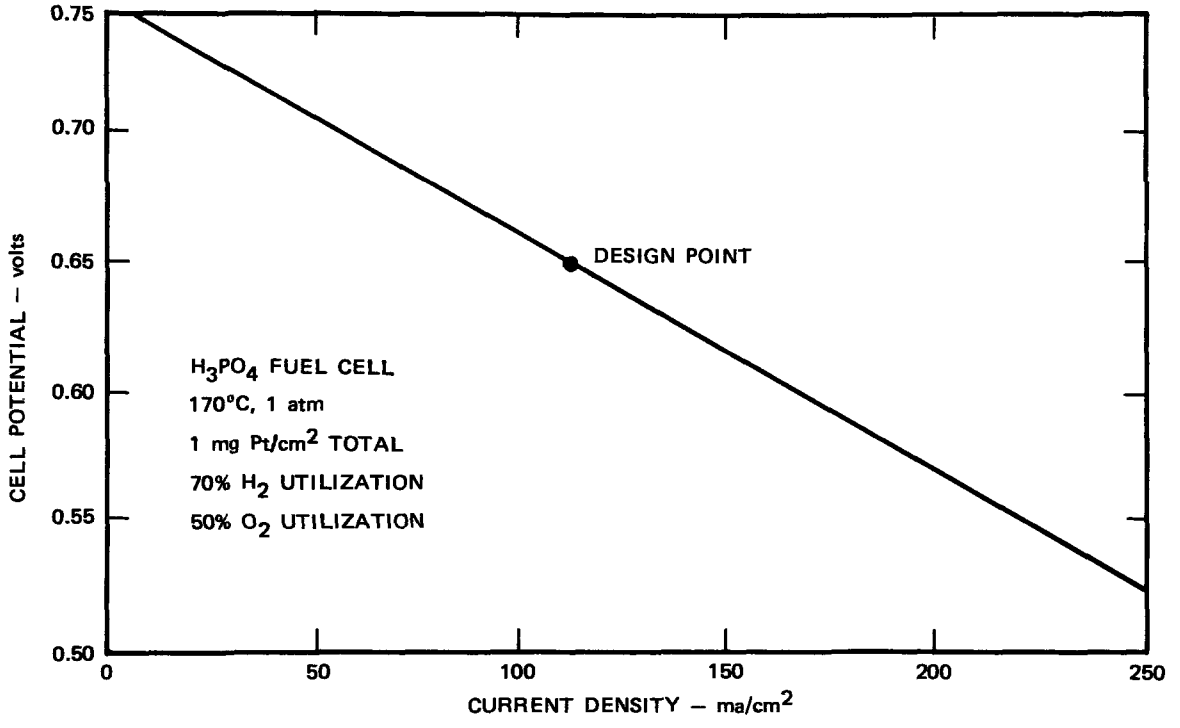

FIGURE IV-25. PHOSPHORIC ACID FUEL CELL PERFORMANCE CURVE

TABLE IV-14

PROCESS CONDITIONS AND FLOW RATES FOR 100-kW FUEL-CELL POWER PLANT
(Design Basis: 100 kW-Net AC Power Output)

	SNG Feed	Steam	Reformer Feed	Reformer Product[a]	High T Shift Product[b]	Low T Shift Product[b,c]	Fuel-Cell Anode Exhaust[d]
Temperature							
°C	24	112	700	700	375	235	170
°F	75	233	1,292	1,292	707	455	338
Pressure[e]							
kPa	152	152	152	145	138	131	103
psia	22	22	22	21	20	19	15
Flow Rate (g-moles/hr)							
CH_4	1,216	--	1,216	106	106	106	106
CO	1.36	--	1.36	634	275	60.8[f]	60.8
CO_2	21.8	--	21.8	500	857	1,073	1,073
H_2	166	--	166	3,972	4,331	4,546	1,363
H_2O		3,648	3,648	2,061	1,702	1,487	810
O_2	--	--	--	--	--	--	--
N_2	--	--	--	--	--	--	--
Total	1,405	3,648	5,053	7,273	7,271	7,273	3,413

[a]Reformer outlet temperature = 700 °C (1,292 °F) @ 1.5 atm. Methane approach to equilibrium = 15 °C (27 °F); T_{eq} = 685 °C (1,265 °F).

b Shift Reactor	Girdler Catalyst	Temperature, °C (°F) Inlet	Outlet	Average	Equilibration	Space Velocity (vol/vol/hr)
High-Temperature	G-3A	316(600)	375(707)	346(654)	400(752)	562
Low-Temperature	G-66B	204(400)	235(455)	220(428)	260(500)	761

[c]Composition equivalent to fuel-cell anode feed.

[d]70% H_2 conversion.

[e]Pressures approximate only.

[f]Equivalent to 0.83 vol. percent (wet basis), 1.05 vol. percent (dry basis).

Table IV-14 (Concluded)

	Fuel Cell Cathode Feed[g]	Fuel Cell Cathode Exhaust	Furnace Feed	Furnace Exhaust	Coolant	Hot Water Feed	Hot Water Feed
Temperature							
°C	69	170	249	833	170	60	60
°F	157	338	480	1,532	338	140	140
Pressure[e]							
kPa	103	103	103	103	--	--	--
psia	15	15	15	15	--	--	--
Flow Rate (g-moles/hr)							
CH_4	--	--	106	--	--	--	--
CO	--	--	60.8	--	--	--	--
CO_2	--	--	1,073	1,239	--	--	--
H_2	--	--	1,363	--	--	--	--
H_2O	364	4,223	926	2,500	--	3,122[h]	1,788[h]
O_2	3,182	1,592	1,016	91.1	--	--	--
N_2	11,972	11,972	3,820	3,820			
TOTAL	15,518	17,787	8,365	7,650	17,668[i]	3,122[h]	1,788[h]

[e]Pressures approximate only.

[g]50% O_2 conversion, ambient air @ 32 °C (90 °F), 50% relative humidity.

[h]Oil Coolant flow rate = 85,902 kg/hr (38,958 lb/hr).

[i]Hot water feed flow rate in kg/hr.

recovery system requires bypass loops for effective operation and maintenance of desired stream operating temperatures. The impact of variable load operation on the highly integrated fuel processing section was not ana- lyzed. However, considerable changes in steady state stream tempera- tures could be encountered by operating a system designed for 100-kW output at reduced load. Additional studies are required to ensure that the fuel-cell operating temperature remains close to the 170°C design value and that sufficient water is recovered to satisfy steam reformer requirements.

d. Conceptual System Design

A conceptual design was prepared for the 100-kW power plant components and assembled layout. The equipment list, showing capacity, size, and materials of each component, is given in Table IV-15.

Fuel-Cell Stack -- The design of the phosphoric and fuel-cell stacks is based on published ERC reports.[49,50] The following design parameters were used:

- Fuel-cell design performance - 112mA/cm^2(104 A/ft^2) @ 0.65 V/cell
- Total DC power - 111 kW (gross)
- Number of stacks - 4
- Active area per cell - 0.19 m^2 (2 ft^2)
- Stack voltage - 133 V (DC)

The size of each fuel-cell stack, including fuel and air manifolding, is approximately 94 x 43 x 107 cm (37 x 17 x 42 in.).

Reformer Package Design -- The conceptual design of the reformer is shown in Figure IV-26. It includes a burner at the base, which mixes and feeds the anode exhaust gas and preheated air into a

Table IV-15

100 kW FUEL-CELL POWER PLANT

Unit	Type	Capacity	Size	Dimensions	Weight (kg)	Materials
Phosphoric Acid Fuel Cell	E.R.C.	111 kW DC	Total Cell Area 153 m^2	4 stacks each 94x43x119 cm	1,590	--
Reformer Package	Vertical Tube	233 MJ/hr	Reformer Section 2.85 m^2 Convection Section 0.73m^2	84x84x173 cm	1,550	RK 40
Reformer Catalyst	Pellets	3980 $\frac{\text{g-mole } H_2}{\text{hr}}$	0.036 m^3	--	--	G-56A
Burner	Low Pressure	6130 $\frac{\text{g-moles}}{\text{hr}}$	428 MJ/hr	Included in reformer package	--	C.S. & Refractory
Heat Exchangers						
E-1A	Canal	89.6 MJ/hr	2.59 m^2	38 x 38 x 15 cm	18	304 SS
E-1B	Canal	7.0 MJ/hr	0.20 m^2	10 x 15 x 28 cm	2.7	304 SS
E-2A	Canal	9.8 MJ/hr	0.37 m^2	14 x 15 x 36 cm	4.6	304 SS
E-2B	Canal	31.7 MJ/hr	1.38 m^2	13 x 23 x 28 cm	14	C.S.
E-3	Canal	16.9 MJ/hr	0.48 m^2	14 x 20 x 36 cm	5.5	C.S.
E-4	Canal	290 MJ/hr	9.30 m^2	25 x 38 x 56 cm	82	C.S.
E-5	Air Fin	290 MJ/hr	8.73 m^2	1.2 x 1.5 x 1.2 m	230	C.S.
E-6	S&T	158 MJ/hr	2.15 m^2	25cm dia x 194 cm long	45	C.S.
E-7	S&T	167 MJ/hr	2.00 m^2	16.5cm dia x 104 cm long	38	C.S.
E-8	Air Fin	167 MJ/hr	0.93 m^2	53 x 53 x 50 cm	39	Copper & Aluminum Finish
Blower B-1	Centrifugal	8.1 nm^3/min @ 102 cm H_2O	7.5 H.P. Motor Drive	81 x 76 x 86 cm	91	C.S.
Pumps P-1	Centrifugal		0.25 H.P. Motor		18	C.S.
P-2	Centrifugal		1.0 H.P. Motor		45	C.S.
Inverter		111 KW	--	0.91 x 0.46 x 0.30 m	91	--
Shift Reactor						
High Temperature	Packed Column	4310 $\frac{\text{g-mole } H_2}{\text{hr}}$	0.31 m^3	0.46 m dia x 1.8 m high	105	Girdler G-3A
Low Temperature	Packed Column	4540 $\frac{\text{g-mole } H_2}{\text{hr}}$	0.23 m^3	0.43 m dia x 1.7 m high	77	Girdler G-66
Instrumentation	--	--	--	--	45	
Base and Enclosure	--	--	--	--	320	
Piping, Wiring, Misc.	--	--	--	--	45	
				Total Weight	4,450	

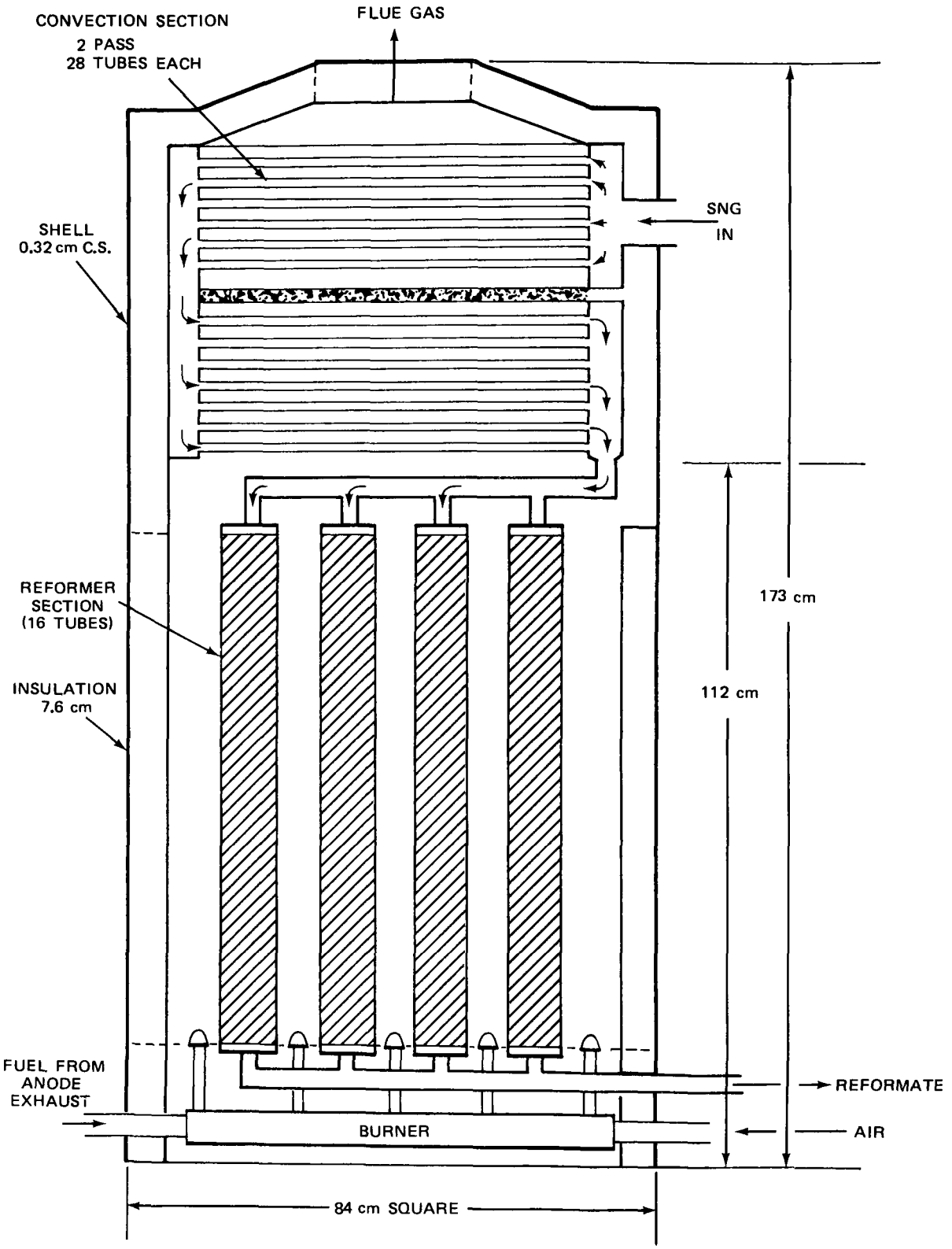

FIGURE IV-26. REFORMER PACKAGE FOR 100-kW POWER PLANT

combustion chamber. Vertical reformer tubes (7.6 cm o.d.) are uniformly distributed within the combustion chamber at a center distance of 15.2 cm (6 in.). The chamber is lined with castable refractory. Reformer catalyst (Girdler G-56-A) is the same as proposed for System 2 and its volume is based on a design space velocity of 1,600 m^3H_2 product/hr-m^3 catalyst. The heat flux is 105 MJ/hr-m^2 (9,250 Btu/hr-ft^2), based on the tube i.d. of 5.9 cm (2.34 in.).

A preheater for SNG and steam is located above the reformer section. It is a two-pass cross counterflow design with the cooler SNG mixture flowing through the 2.5 cm (1 in.) tubes and the hot flue gas passing over the tubes.

That assembly is based on the following details of construction, from which materials costs are later estimated:

- Reformer tubes - 7.6 cm (3 in.) o.d., cast in HK 40
- Convection section - 2.5 cm (1 in.) tubes in 309 SS
- Insulation - 7.6 cm (3 in.) thick castable refractory
- Shell - 0.32 cm (0.125 in.) thick carbon steel
- Catalyst - Girdler 56A

The small zinc oxide guard bed was omitted from the conceptual design and cost estimate.

Shift Reactors -- The sizing of the high- and low-temperature shift reactors is based on space velocities of 562 and 761 m^3 inlet gas/hr-m^3 catalyst, respectively. These values were obtained from the Girdler handbook using Type G-3A and G-66B catalysts. A length/diameter ratio of four was used and the configuration is assumed to be a welded carbon steel vessel with an internal insulating lining and baffle plates to support the catalyst and distribute the gas.

Heat Exchangers -- The heat exchanger dimensions were given in Table IV-15. Heat Exchangers E-1A through E-4 are canal type designs, which would be lighter and less costly than the shell and tube type. Canal heat exchangers are roughly one-third as expensive as shell and tube exchangers assuming the same surface area. They have lower pressure capability and are generally used for heat recovery applications. Materials shown in Table IV-15 assume a maximum temperature capability of 343°C (650°F) for carbon steel. Heat transfer areas were based on overall heat transfer coefficients of 200 kJ/hr-m^2-°C (10 Btu/hr-ft^2-°C) for gas/gas duty and 1,000 to 1,400 kJ/hr-m^2-°C (50 to 70 Btu/hr-ft^2-°F) for liquid/liquid and air fin units.

System Packaging -- A layout of the system was prepared assuming that all components are assembled into a single unit. The estimated package size, shown in Figure IV-27, is 2.6 x 3.7 x 3.0 m (8.5 x 12 x 10 ft). The package is assumed to have a welded steel base using channel sections and a frame of steel angles forming a superstructure to support heat exchangers, ducting, and enclosure. The package is designed for outdoor installation. The size and weight of the package falls well within the limits for transport by truck.

6. Heating and Cooling System

The 100-kW fuel-cell power plant described in the previous section is designed to provide electricity and heat to an apartment, condominium, or cluster housing complex. In our analysis, the residences are townhouses arranged in a cluster that minimizes the cost of distributing heat recovered from the fuel cell.

The townhouses are similar in floor space and construction to the detached houses described in Section IV-A, with the exception that they share common walls. The effect of that arrangement on heating and cooling requirements is to reduce the heat loss or gain as a function of temperature relative to the detached houses. The heat loss parameter

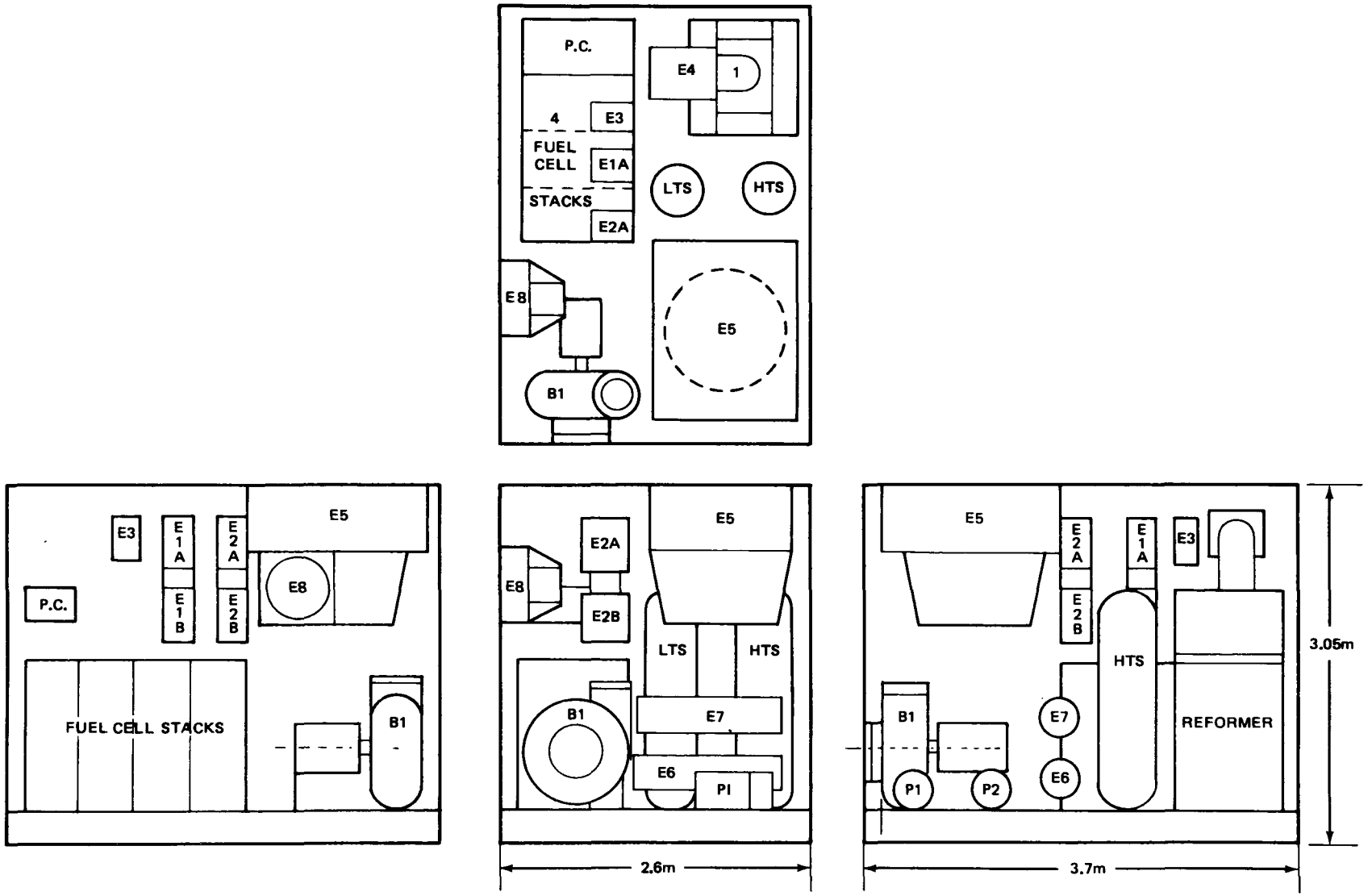

FIGURE IV-27. SYSTEM LAYOUT FOR 100-kW POWER PLANT

for the townhouses is 230 kJ/^{o}C-hr (390 Btu/^{o}F-hr), compared to 360 kJ/^{o}C-hr (610 Btu/^{o}F-hr) for the detached houses. The corresponding heat loss equation, which includes internal heat sources, is

$$Q = 23{,}900 - 230\ T\ \text{kJ/hr}$$
$$(Q = 22{,}600 - 390\ T\ \text{Btu/hr}),$$

where Q is the heat input required to maintain the house at 21°C (70°F), and T is the external temperature in ^{o}C (^{o}F).

Because the fuel-cell power plant is designed to allow heat to be recovered, the most economical method of meeting the heating load is to use recovered fuel-cell heat whenever it is available. When fuel-cell heat is not sufficient, heat pumps are used to make up the difference. The heat pumps are also used to provide air conditioning in the summer.

The arrangement chosen for this analysis is for 20 residences to be served by a 100-kW fuel-cell power plant. The recovered heat is distributed from a central location through a stream of 82°C (180°F) water. In addition to space heating in the winter, the hot water stream provides domestic hot water (DHW) throughout the year. The residences are equipped with individual heat pumps. The site plan for the power plant and townhouses is shown in Figure IV-28. The details of the hot water distribution system are shown in Figure IV-29. As the hot water is piped into a residence, it is distributed either to the heat exchanger in the DHW tank or to the heat exchanger in the central heating duct. The flow is controlled by thermostats in the DHW tank and on one of the interior walls of the residence. The availability of recovered heat from the fuel cell is a function of the electrical load, which is determined by the use of lights, appliances, and heat pumps in the residences.

Because of the lower heat gain or loss from the townhouses, the heat pumps can be of smaller capacity than those described in

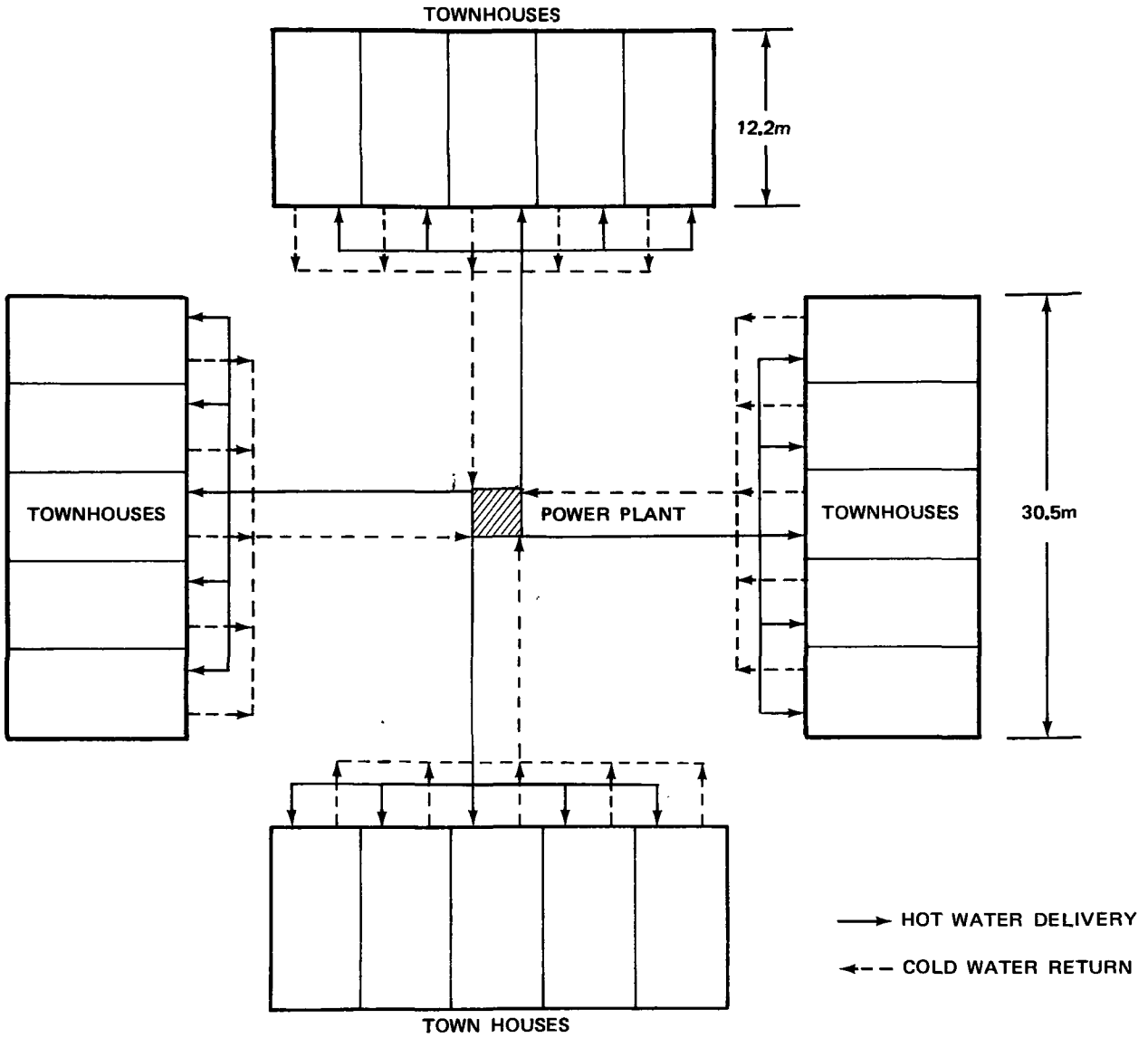

FIGURE IV-28. SITE PLAN FOR 100-kW FUEL-CELL POWER PLANT AND TOWNHOUSES

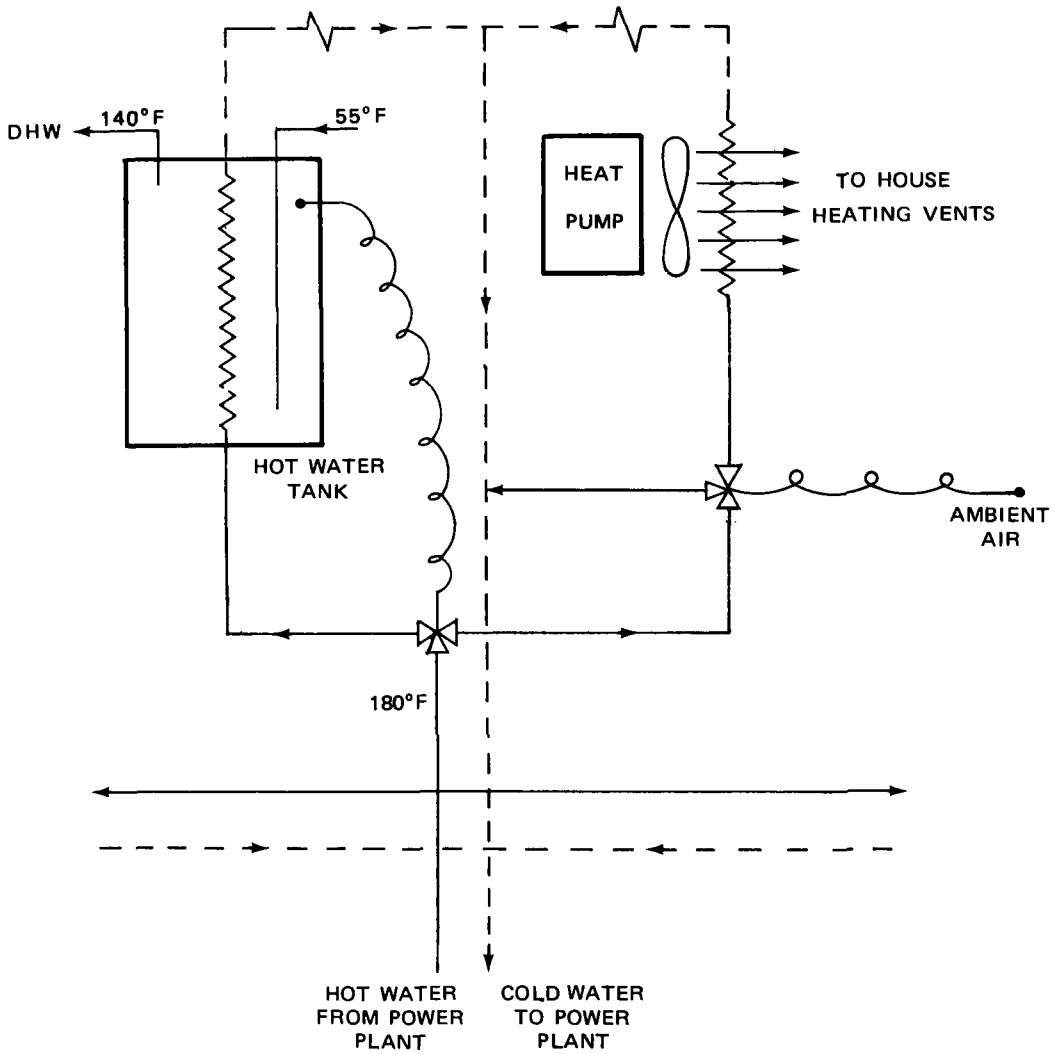

FIGURE IV-29. SCHEMATIC OF HOT WATER AND SPACE HEAT SYSTEM USING RECOVERED FUEL-CELL HEAT

Section IV-B. A heat pump that meets the design cooling load of 15.6 MJ/hr (14,800 Btu/hr) is one scaled to 3/4 capacity of the advanced model described in Section IV-B. It has a rated cooling capacity of 19.3 MJ/hr (18,300 Btu/hr) at 35°C (95°F). Its heating and cooling performance are shown in Figure IV-30, along with the heating and cooling loads of the residences. The cooling load is based on average summer afternoon conditions of humidity and insolation (see Chapter VIII). Two banks of 4.7 kW electric resistance heaters provide additional heating capacity below the balance point at -5°C (23°F). Their effect is shown as dashed lines in Figure IV-30.

Other important components of the heat delivery system are the heat exchangers that transfer heat from the 82°C fuel-cell hot water stream to the DHW tank and the space heating system. The water-to-water heat exchanger in the DHW tank was assumed to be a simple coiled copper tube, which effectively transfers heat at the approach temperatures and flow rates that characterize this system. The choice of a water-to-air heat exchanger is more complicated, reflecting the many variables in the system, including duct size, air flow rates, water flow rates, and approach temperatures.

The water-to-air heat exchanger (or heating coil) was chosen using available manufacturer's literature.[51] It can effectively transfer heat from hot water (82°C) with flow rates ranging from 0.0057 liter/sec (0.090 gal/min) to 0.070 liter/sec (1.11 gal/min), heat pump exit air temperatures ranging from 21°C (70°F) to 43°C (110°F), and a fixed air flow rate of 0.26 m^3/sec (550 scf/min). Furthermore, it was required to fit in a heating duct that was about 0.30 m (1 ft) square. The heating coil chosen for this application was the Trane type WC, Series 18 (with turbulators), with 30 cm x 30 cm (12 in. x 12 in.) active area. The heat transfer characteristics of this device are discussed in Chapters V and VIII.

Physically, the heating coil is located in the hot air duct between the heat pump condenser coil and the supplementary resistance

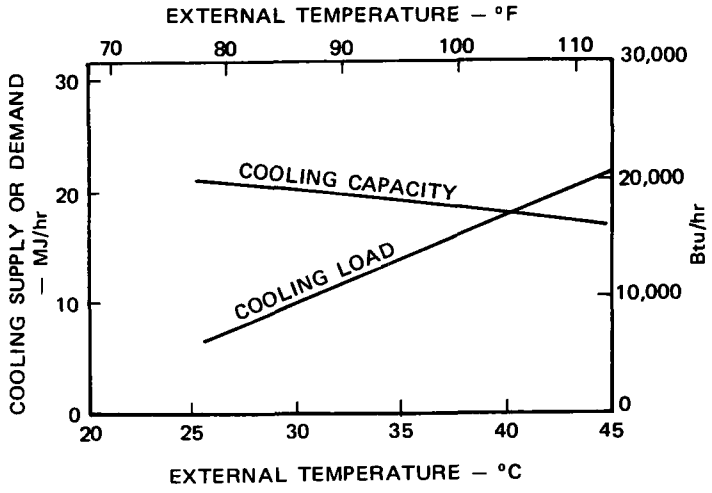

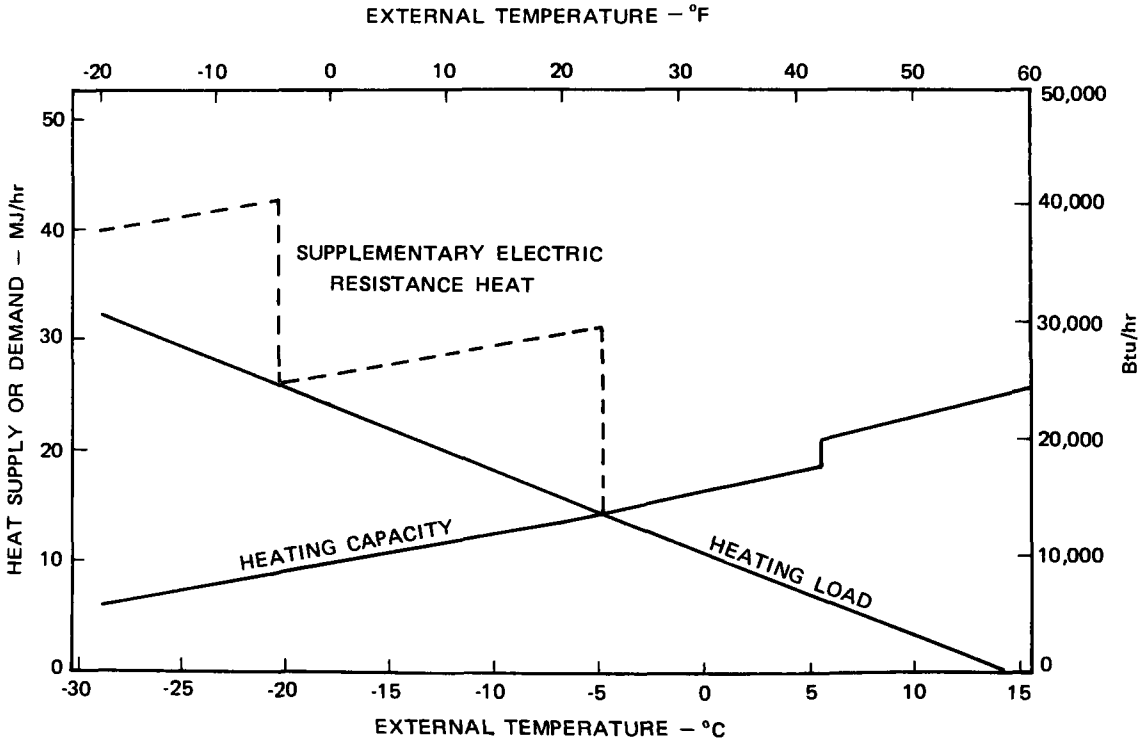

FIGURE IV-30. HEATING AND COOLING CAPACITIES OF 19.3 MJ/hr (18,300 Btu/hr) HEAT PUMP

heaters. Heating loads are met by either the heating coil alone, heating coil plus heat pump, or, on very cold days, heating coil, heat pump, and resistance heaters combined.

F. References--Chapter IV

1. "Energy Alternatives: A Comparative Analysis," Science and Public Policy Program, University of Oklahoma (1975).

2. G. R. Rowe, "Overall Economics of the Unit Train for Western Coal," Burlington Northern, Inc. (1975).

3. Proceedings of the 2nd International Technical Conference on Slurry Transportation, Las Vegas, Nevada, March 2-4, 1977.

4. "Critique and Response to Coal Transportation," Peabody and Associates, Inc., National Technical Information Service Number PB-251-521 (April 1976).

5. "From Mine to Market by Rail...The Indispensible Transport Mode," Coal Age, p. 106 (July 1974).

6. A. J. Frabetti, "A Study to Develop Energy Estimates of Merit for Selected Fuel Technologies," Development Sciences, Inc. (September 1975).

7. "Rail Transportation...Equipment," 1976 Keystone Coal Industry Manual, p. 196.

8. W. H. Ponder, et al., "SO_2 Control Technologies -- Commercial Availabilities and Economics," Third Annual Conference of Coal Gasification and Liquefaction, Pittsburgh, Pennsylvania, August 1976.

9. "Coal-Fired Power Plant Capital Cost Estimates," Bechtel Corporation, EPRI Report AF-342 (January 1977).

10. R. S. Jens, "System Planning: Transmission," Perspectives on the Electric Utility Industry: A Handbook by Electric Power Research Institute, p. 10-7 (May 1977).

11. M. L. Baughman, and D. J. Bottaro, "Electric Power Transmission and Distribution Systems Costs and Their Allocation," IEEE Transactions on Power Apparatus and Systems, p. 782 (May/June 1976).

12. Federal Power Commission, The 1970 National Power Survey, Part 1, p. 1-13-9.

13. "Transmission Lines," from Encyclopedia of Energy, D. N. Lapedes, ed., p. 698.

14. R. Detman, et al., "Factored Estimates for Western Coal Commercial Concepts," Interim Report, Energy Research and Development Administration (October 1976).

15. R. D. Howell, "Mechanical Design Consideration in Commercial Scale Coal Gasification Plants," Sixth Synthetic Pipeline Gas Symposium.

16. W. L. Hecklen, "The Construction of Conversion Vessels," Energy Communications, p. 133 (1976).

17. A. J. McNab, "Design and Material Requirements for Coal Conversion" (November 1975).

18. R. N. Maddox, Gas and Liquid Sweetening (1974).

19. H. S. Kirschbaum, and S. E. Veyo, "An Investigation of Methods to Improve Heat Pump Performance and Reliability in a Northern Climate," Westinghouse Electric Corporation, EPRI Report EM-319 (January 1977).

20. J. M. King, Jr., "Advanced Technology Fuel Cell Program," EPRI EM-335, Final Report (October 1976).

21. Girdler Catalysts, Chemtron Corporation, "Physical and Thermodynamic Properties of Elements and Compounds," GC 245-10-869, Rev. 3.

22. Girdler Catalysts, Girdler Chemical, Inc., "Hydrogen and Synthesis Gas Production."

23. Stanford Research Institute, "Synthetic Petroleum for Department of Defense Use," Defense Advanced Research Projects Agency Report AFAPL TR-74-115 (November 1974).

24. Exxon Research and Engineering Company, "Evaluation of Methods to Produce Aviation Turbine Fuels from Synthetic Crude Oils, Phases 1 and 2," Air Force Aero-Propulsion Laboratory/SSF WRight Patterson Air Force Base, Ohio: Reports AFAPL-TR-75-10, Volumes 1 and II (March 1975 and May 1976).

25. A. C. Antoine and J. P. Gallagher, "Synthesis and Analysis of Jet Fuels from Shale Oil and Coal Syncrudes," U.S. Department of Commerce, Report N76-21341 (August 1976).

26. E. R. Elzinga, et al., "Application of the Alsthon/Exxon Alkaline Fuel Cell System to Utility Power Generation," Electric Power Research Institute, Report EM-384 (January 1977).

27. United Technologies Corporation, "Advanced Technology Fuel Cell Program," Electric Power Research Institute (October 1976).

28. J. G. Bendoraitis, et al., "Upgrading of Coal Liquids for Use as Power Generation Fuels," Electric Power Research Institute Report 361-1 (January 1976).

29. D. T. Beecher, et al., "Energy Conversion Alternatives Study -- Combined Gas/Steam Turbine Plant Using Coal-Derived Liquid Fuel," NASA CR-134942 (November 1976).

30. J. Neal, "New Gas Turbines Could Provide Fuel Benefits," Public Power, p. 28 (November-December 1976).

31. "Mixing NO_x," Chemical Engineering, p. 70 (April 25, 1977).

32. EPRI Journal, p. 49 (August 1977).

33. Private communication, Pratt and Whitney Aircraft Division of United Technology Corp.

34. Massachusetts Institute of Technology, "Economic and Technical Aspects of Gas Turbine Power Stations in Total Energy Applications," U.S. Army Facilities Engineering Support Agency, FESA-RT-2013, p. 56 (January 30, 1976).

35. W. B. Wilson and W. J. Hefner, "Economic Selection of Plant Cycles and Fuels for Gas Turbines," Combustion, p. 7 (April 1974).

36. S. Abens, et al., "Fuel Cell Stacks," Final Technical Report, Contract No. DAAK02-74-C-0367, Project No. 7763580, Energy Research Corp.

37. L. B. Welsh, et al., "Optimization of Pt-Doped Kocite^R Electrodes in H_3PO_4 Fuel Cells," Interim Technical Report, Contract No. DAAG53-76-C-0014, p. 25 (January 1978).

38. Ibid., p. 2.

39. H. G. Petrow, et al., U.S. Patent No. 4082-699, April 4, 1978.

40. S. G. Abens, et al., "Fuel Cell Stacks," Semi-Annual Report, December 1974-August 1975, ERC-7396-S, p. 22 (March 1976).

41. Ibid., Third Interim Report, ERC-7396-III, p. 5 (May 1976).

42. Ibid., Fourth Interim Report, ERC-7396-IV, p. 11 (February 1977).

43. H. C. Maru, et al., "Phosphoric Acid Fuel Cell Cathode," National Fuel Cell Seminar Abstracts, San Francisco, California, July 11-13, 1978, p. 76.

44. B. S. Baker, Paper presented at Hybrid Vehicle Workshop, Los Alamos, New Mexico, August 15, 1977.

45. J. C. Trocciola, et al., U.S. Patent 4000-006, December 28, 1976.

46. R. D. Breault, U.S. Patent 4017-663, April 12, 1977.

47. Ibid., U.S. Patent 4017-664, April 12, 1977.

48. United Technologies Corp., "Improvement of Fuel Cell Technology Base," Technical Progress Report No. 2, FCR-0809, April 1, 1977 - April 1, 1978.

49. S. Abens, et al., "High Temperature Molten Carbonate Fuel Cells": Fourth Quarter Technical Progress Report-E-3-4 (March 1977); Fifth Quarter Technical Progress Report-E-3-5 (July 1977).

50. H. C. Maru and B. S. Baker, "Status of ERC's Phosphoric Acid Fuel Cell Technology," presented at Fuel Cell Workshop, Sarasota, Florida, November 14-17. 1977.

51. Trane Corporation, "Application and Selection Data for Trane Cooling and Heating Coils."

V. THERMAL EFFICIENCY OF THE SYSTEM COMPONENTS

Within each component of the five systems described in the previous chapter, the energy-containing product is either moved from one place to another or its physical and/or chemical form is altered. At each stage of each system, some energy must be expended in carrying out these processes. Ultimately, all energy entering the system as stored chemical energy in the coal will be degraded to heat (random thermal motion) in the environment. However, during this process of thermodynamic degradation (or loss in the capacity to do work), a certain amount of useful work is obtained. In the systems under consideration in this study, the desired end result is to provide heated or cooled air to the interiors of residences. The effectiveness with which this goal is carried out can be measured by the overall thermal efficiency of each system.

For purposes of this chapter, the thermal efficiency of an energy transport or transformation process is simply the energy content of the product of the process divided by the energy content of the product entering the process, plus any additional energy contributed by another source. This latter term would apply to diesel fuel consumed by a coal-carrying unit train, for example. The five systems will be compared in terms of their overall efficiency in providing residential heating and cooling, starting with coal in the ground.

In subsequent calculations, the energy content of any energy-containing product (solid, liquid or gaseous fuel) will be expressed in terms of its higher heating valve (HHV), which is the amount of thermal energy released upon combustion, including the heat of condensation of water vapor produced during combustion.

The energy required to carry out any process that must be supplied by an external source will be assessed only in terms of the direct fuel,

heat, or electricity consumed. No calculations will be made of indirect energy requirements. Those are generally expressed as the energy embodied in materials, chemicals, or human activities necessary for carrying out the process.

Purchased fuel will be evaluated in terms of its higher heating value, as previously discussed. Purchased electricity will be evaluated in terms of the thermal energy required to produce it at the generating plant, or approximately 10,550 kJ/kWh (10,000 Btu/kWh).

A. Coal Mine

The energy consumed in surface coal mining is in two principal forms: (1) electricity for powering draglines, drills, and coal-loading shovels, and (2) diesel fuel used in mobile equipment -- coal-hauling trucks, bulldozers, and scrapers. Minor amounts of energy are used in heating and lighting shops and offices, powering small vehicles such as foremen's trucks, and so on.

The use of electric power for the 4.5 million tonne (5 million ton) per year mine described in Section IV-A is estimated to be 14 million kWh per year.[1] This represents an equivalent energy input of 1.5×10^5 GJ (140×10^9 Btu) per year.

Data from proposed western surface mining operations on consumption of fuel by mobile equipment indicate that a 4.5 million tonne per year surface mine would use about 3.8 million liters (1 million gallons) of diesel fuel per year.[2] Part of this fuel (5-10%) is used for preparation of ammonium nitrate-fuel oil mixtures which are used as explosive charges to loosen coal and overburden. Smaller equipment consumes considerably less gasoline than diesel fuel -- approximately 340,000 liters (90,000 gallons).[2] The total energy content of these two fuels is about 1.5×10^5GJ.

A 4.5 million tonne per year mine producing coal with a heating value of 20.4 MJ/kg (8800 Btu/lb) produces the energy equivalent of 9.3×10^6 GJ (8.8×10^{12} Btu) per year. The "process" thermal efficiency is assumed to be 100%, because none of the coal is thermally degraded during extraction.

The total consumption of liquid fuels and electricity during the mining process is 3×10^5 GJ per year, or about 3.2% of the energy output of the mine. The overall thermal efficiency, then, as defined at the beginning of this chapter, is 97%.

B. Unit Train

The principal use of energy in shipping coal by unit train is the diesel fuel consumed by the locomotives. To obtain a figure for the quantity of fuel consumed it is customary to apply a factor of fuel consumption per gross tonne-km (or ton-mi). The gross weight distance factor includes the weight of the locomotives and cars for both the delivery and return legs of the trip. Locomotives weigh approximately 140,000 kg (310,000 lb) each and there are four per train. Coal cars weigh about 28,000 kg (61,000 lb) each. Thus, the gross weight of a loaded 100-car unit train is 12,400 tonnes (13,700 tons), while the weight of an empty train is 3,340 tonnes (3,670 tons). The total gross weight distance for a 1,300-km (800-mi) shipment is thus 20.3 million gross tonne-km (13.9 million gross ton-mi).

The appropriate figure for diesel fuel consumption for unit train operation, assuming fuel-efficient throttling practices, is 3.6 liters per 1000 gross tonne-km (1.4 gallons per 1,000 gross ton-miles).[3] Therefore, the round-trip fuel consumption for a 9,070-tonne (10,000-ton) unit train carrying coal 1,300 km (800 mi) from the Powder River Basin to the Kansas City-Omaha-Des Moines region is approximately 72,000 liters (19,000 gallons). This figure represents an energy consumption of 230 kJ per tonne-km (320 Btu per ton-mi) of coal shipped, or a total energy consumption equal to 1.5% of the heating value of the coal.

Another use of energy in shipping coal is in the thawing sheds used to warm coal in cars that have frozen during cold weather. Electrically powered thawing sheds consume about 6.6 kWh per tonne (6 kWh per ton) of coal and are typically capable of thawing five cars per hour. As a conservative assumption, thawing sheds are required on days when the average temperature is less than $0^{o}C$ ($32^{o}F$). Daily temperature data for Omaha (see Chapter VIII) indicate that the average temperature is less than $0^{o}C$ ($32^{o}F$) on about 85 days in an average year. Thus, a total of (85/365) x 1.27 million = 0.30 million tonnes (0.33 million tons) of coal per year will require thawing. The electricity consumption is 1.98 million kWh, or 20,900 GJ (20×10^{9} Btu) thermal equivalent. This figure represents 0.08% of the heating value of the coal shipped in a year. This quantity is insignificant compared to the fuel consumed in transporting the coal.

C. Coal-Fired Power Plant

New, uncontrolled fossil fuel power plants can have thermal efficiencies approaching 40%. However, environmental control requirements and the effects of age and cycling duty will reduce the actual thermal efficiency well below this figure.

The net electrical output of the 800-MW coal-fired power plant described in Section IV-C is estimated to be 34% of the energy represented by the higher heating value of the coal input to the plant. The energy balance for this facility is shown in Table V-1. The largest source of thermal energy loss is in the steam cycle. Forty-five percent of the energy input to the plant is lost from this source, mostly in the form of heat ejected from the cooling towers. The next biggest loss, at 12%, is boiler loss consisting of radiation losses and sensible and latent heat in the flue gases. This figure is higher for subbituminous coal than for bituminous coal because of the higher moisture content of subbituminous coal, resulting in a greater latent heat content of the stack gases.

Table V-1

ENERGY BALANCE FOR AN 800-MW COAL-FIRED POWER PLANT THAT USES SUBBITUMINOUS COAL

Energy Input	GJ/hr	Percent of Input
Coal	8,470	100
Energy Output		
Product		
Electric Power	2,880	34
Losses		
Steam cycle losses	3,810	45
Boiler losses	1,020	12
Auxiliary power	420	5
FGD system	250	3
Electrostatic precipitator	85	1

The use of electrical power in auxiliary equipment, such as boiler feed pumps and coal pulverizers, results in a net loss of 5% of input energy. The FGD system uses electrical energy equivalent to about 3% of the total energy input. Finally, the electrostatic precipitator for this facility, which must be large to handle the high-resistivity fly ash associated with low-sulfur western coal, consumes power equivalent to about 1% (maximum) of the energy input.

D. Coal Gasification Plant

The Hygas coal gasification facility described in Chapter IV is designed to be self-sufficient in its energy needs, so no electricity is purchased from an external source and fuel requirements are met by burning part of the coal brought into the plant or by-product oil. The combustion of by-product oil derived from the gasification process as boiler fuel reduces the amount of coal required for this purpose by

about one-half. Thus, the overall plant efficiency based on the ratio of SNG heating value to total coal heating value is increased. However, plant economics are affected because the revenue that could be derived from the sale of by-product oil is not realized. Environmentally, burning by-product oil is preferable to burning coal.

The overall energy balance for a 7.8×10^6 nm^3 (275×10^6 scf) per day plant is shown in Table V-2. The thermal efficiency for the production of SNG from the coal entering the gasifier is 81%, reflecting the high methane yield of the Hygas process.[4] Because of the high process efficiency, and the reduced requirement for coal as boiler fuel due to the combustion of by-product oil, the overall plant thermal efficiency is high -- 74%.

Table V-2

ENERGY BALANCE FOR A 7.8×10^6 nm^3 (275×10^6 scf)
PER DAY COAL GASIFICATION PLANT
BASED ON THE HYGAS PROCESS

Energy Input	GJ/hr	Percent of Input
Coal	14,900	100.
Energy Output		
SNG	11,000	74.
Char	310	2.
By-products (sulfur & ammonia)	80	0.5
Thermal Losses	3,510	23.5
Steam & Power Requirements	2,320	15.5
Coal	1,340	9.0
By-product oil	980	6.5

Accounting for the plant's thermal losses is considerably more difficult than accounting for those in the coal-fired power plant. Heat is released from numerous sources within the coal gasification plant; furthermore, it is thermally integrated so that heat generated in one portion of the plant is recovered and used elsewhere. For example, the coal/water slurry feed to the gasifier is preheated using heat recovered from the hot gases exiting the gasifier, and process steam is generated using excess heat recovered from the methanation reactors.

An analysis of the various sources of heat release in the Hygas plant[5] indicates that, overall, about 20% of the thermal losses in the plant are direct losses from boiler stacks, electric motors, sensible heat of condensates and ash, and so on. The remaining 80% are indirect losses in the form of wet or dry cooling, with the relative amounts of these dependent on the location of the plant and the resulting cost and availability of water. Using the integrated pollution control system described in Chapter VI, in which a large fraction of the cooling tower make-up water is derived from recycled process water, about two-thirds of the plant's indirect heat loss is in the form of evaporative (wet) cooling, and the remaining one-third is in the form of dry cooling. The balance of wet and dry cooling will vary considerably, however, from one plant design to the next.

The sources of heat within the plant that must be dissipated by wet or dry cooling are many. Some of the main contributors are acid gas removal, turbine condensers, and compressor interstage cooling.

E. Coal Liquefaction Plant

The conversion of coal to fuel oil via the H-Coal process is less thermally efficient overall than the production of SNG via the Hygas process. Although the conversion of coal entering the process stream to end products has about the same thermal efficiency in both cases (around 80%), the steam, heat, and power requirements are about twice as high for H-Coal as they are for Hygas for several reasons, including fuel

needed for coal drying, higher compression energy requirements to attain a coal slurry pressure of 18,600 kPa (2,700 psi) compared to 8,680 kPa (1,260 psi) in the Hygas case, and the energy requirements for separate gasification and steam reforming plants to supply hydrogen for the liquefaction process.

The overall energy balance for a coal liquefaction plant that produces distillate fuel oil is shown in Table V-3. The overall thermal efficiency of the plant is 66%. Of the 32.5% of the coal input energy that is represented by thermal losses, 50-60% is accounted for by direct heat losses (boiler stacks, coal drying, steam reformer stacks, electric equipment, etc.) Of the remaining indirect heat loss, about one-half is dissipated by wet cooling as shown in the integrated pollution control system described in Chapter VI, and the other half is dissipated by dry cooling.

Table V-3

ENERGY BALANCE FOR A 7950 m^3 (50,000 bbl) PER DAY COAL LIQUEFACTION PLANT THAT PRODUCES DISTILLATE FUEL OIL

Energy Input	GJ/hr	Percent of Input
Coal	18,900	100
Energy Output		
Fuel oil	12,400	66
Char	180	1
By-products (sulfur and ammonia)	120	0.5
Thermal losses	6,140	32.5
Steam, Heat, & Power Requirements	5,750	30
Coal	3,270	17
By-product gases	2,480	13
Hydrogen Requirements		
Partial oxidation plant feed (char and heavy bottoms)	4,200	22
Reformer feed (by-product gases)	1,690	9

Table V-3 also shows the energy requirements for steam, heat, and power and for hydrogen production. A large part of the energy requirement (2,100 GJ/hr of by-product gases) is for fuel for the reformer that drives the highly endothermic steam/hydrocarbon reforming reactions.

The energy balance for an H-Coal plant that produces hydrotreated naphtha plus fuel oil is shown in Table V-4, whose data are similar to Table V-3. The major differences are in the slightly higher steam, heat and power requirements resulting from the addition of the naphtha hydrotreater, and the larger feed of char and heavy bottoms to the partial oxidation plant to provide additional hydrogen for hydrotreating. These additional requirements reduce the overall thermal efficiency of coal liquefaction to 64%.

Table V-4

ENERGY BALANCE FOR A 7630 m^3 (48,000 bbl) PER DAY COAL LIQUEFACTION PLANT THAT PRODUCES NAPHTHA AND FUEL OIL

Energy Input	GJ/hr	Percent of Input
Coal	19,000	100
Energy Output		
Naphtha	5,590	29
Fuel oil	6,540	34
Char	180	1
By-products (sulfur and ammonia)	120	0.5
Thermal losses	6,540	34
Steam, Heat, & Power Requirements	5,860	31
Coal	3,380	18
By-product gases	2,480	13
Hydrogen Requirements		
Partial oxidation plant feed (char and heavy bottoms)	4,540	24
Reformer feed (by-product gases)	1,690	9

F. Gas Pipeline

The 1300-km (800 mi) long, 81-cm (32-in.) diameter pipeline that carries SNG from the Powder River Basin to the Omaha-Des Moines-Kansas City region has 11 pumping stations. Between pumping stations the gas pressure falls from 7,580 kPa (1,100 psia) to 4,100 kPa (600 psia). Each pumping station requires a compressor capacity of 18.5 MW (24,800 horsepower) to recompress 943,000 nm^3 (3.33×10^6 scf) per hour of gas to 7,580 kPa (1,100 psia). Typically, the pumping stations are powered by feeding part of the pipeline gas to the turbines that drive the compressors.

The turbine-compressor units have a thermal efficiency of about 29%. Thus, 229 GJ (218×10^6 Btu) per hour of SNG must be consumed as turbine fuel. For all 11 compressor stations, the total fuel requirement is 2,520 GJ ($2,400 \times 10^6$ Btu) per hour, or 7.9% of the SNG that flows through the pipeline. Therefore, the thermal efficiency of the pipeline is 92%.

G. Liquids Pipeline

The operation of the 51-cm (20-in.) diameter fuel oil or naphtha/fuel oil pipeline is similar to that of a gas pipeline, except that pressure drops between pumping stations are greater -- from 5,500 kPa (800 psi) to 35 kPa (50 psi). However, the compression energy requirements for liquids are much less than for gases. The pumping station capacity is only 2.4 MW (3,200 horsepower) for a mass flow rate 75% higher than for the gas pipeline. Ten pumping stations are required for the 1,300 km (800 mi) pipeline to transport 31,800 m^3 (200,000 barrels) per day of liquid fuels.

Typically, diesel fuel is purchased and supplied to the pumping stations to run the diesel engines that power the centrifugal pumps. As in the case of the gas pipeline, a diesel engine/centrifugal pump

thermal efficiency of about 29% can be expected. The resulting diesel fuel requirement is 788 liters (208 gal) or 29.6 GJ (28.1 x 10^6 Btu) per hour. For the entire pipeline the fuel requirement is 296 GJ (281 x 10^6 Btu) per hour. This figure represents 0.59% of the heating value of the fuel passing through the pipeline. The thermal efficiency of the liquids pipeline is therefore 99.4%.

H. Liquid Fuel Distribution

The major source of energy use for the delivery of naphtha by truck is the consumption of diesel fuel. Data on fuel consumption by gasoline delivery trucks indicate that a 34,000-liter (9,000-gal) truck will achieve an average fuel economy of 1.9-2.1 km/liter (4.4-4.9 mi/gal) in a metropolitan area.[6] Assuming an average round-trip distance of 80 km (50 mi) for the delivery of naphtha from a bulk storage terminal to dispersed fuel-cell power plants (see Section VII-H), the diesel fuel consumption per trip would be approximately 40 liters (11 gal) or 1.6 GJ (1.5 x 10^6 Btu). A 34,000-liter (9,000-gal) truckload of naphtha has a heating value of 1,200 GJ (1,130 x 10^6 Btu). Therefore, diesel fuel consumption is 0.13% of the heating value of the delivered fuel.

Other sources of energy consumption and loss include pumping energy and evaporation during loading and unloading. However, these quantities are very small.

The delivery of distillate fuel oil from a bulk terminal to a combined cycle power plant by unit train also requires consumption of diesel fuel. Fuel consumption would be comparable to that of the coal unit train discussed earlier, or 230 kJ per net tonne-km (320 Btu per net ton-mi). Assuming a one-way distance of 160 km (100 mi) (see Section V - H) and using a distillate fuel density of 0.85 kg/liter (7.1 lb/gal), the diesel fuel consumption is 31 MJ/m^3 (4,800 Btu/bbl) of fuel delivered. This figure represents 0.10% of the heating value of the distillate fuel.

I. Gas Distribution

No energy is consumed in the distribution of natural gas because the gas enters the distribution system at pipeline pressure, which is gradually reduced as the gas proceeds through the distribution system to individual customers. No additional compression is required.

Some gas may be lost through leaks, but this amount is likely to be small, and in any case would be very difficult to quantify. The efficiency of gas distribution is assumed to be 100%.

J. Combined-Cycle Power Plant

The combined-cycle power plant achieves a high thermal efficiency by using advanced, high-temperature gas turbines and by recovering a substantial amount of the turbine exhaust heat in the form of high pressure steam, which drives a steam turbine. The overall thermal efficiency of the plant described in Chapter IV is 52% (heat rate = 6,920 kJ/kWh) at its rated load of 270 MW.[7] The energy balance for the plant is shown in Table V-5.

Table V-5

ENERGY BALANCE FOR A 270-MW COMBINED-CYCLE POWER PLANT

Energy Input	GJ/hr	Percent of Input
Distillate fuel	1,870	100
Energy Output		
Electric Power	970	52
Gas turbine generator	640	34
Steam turbine generator	330	18
Losses		
Steam cycle losses	540	29
Stack gas losses	330	17.5
Auxiliary power	30	1.5

The efficiency of the combined-cycle plant will vary with load. Estimates of the heat rate at part-load operation have been made for a similar combined-cycle plant that uses an advanced high temperature gas turbine.[8] Those estimates have been used to derive values of the heat rate at part loads (see Table V-6).

The main source of thermal loss in the plant is in the steam cycle, which accounts for nearly a third of the energy input to the plant. Most of this heat loss is dissipated in the cooling towers. The turbine exhaust heat that is not recovered in the heat recovery steam generators (17.5% of the energy input to the plant) is released with the stack gases. The recovery of turbine exhaust heat is fairly high -- 73%. However, the subsequent steam cycle is relatively inefficient (39%), so more than 60% of this heat is ultimately lost.

Even with several substantial sources of thermal loss, the combined-cycle system is one of the most efficient electricity generating technologies. Although further improvements in turbine technology are possible, efficiencies will probably not exceed 55%, due to temperature limitations in the turbines and the inherent limitations of the steam cycle.

Table V-6

ESTIMATED HEAT RATES AT PART LOAD FOR COMBINED-CYCLE POWER PLANT

Percent of Rated Load	Heat Rate (kJ/kWh)
100	6,920
75	7,020
50	7,040
25	7,650

K. 26-MW Fuel-Cell Power Plant (SNG)

A final energy balance for this power plant is given in Table V-7. Net power ouput is estimated to be 24.0-MW after allowances are made for DC/AC inversion and transformation losses to 13.8 kV (AC) and auxiliary power requirements. The system heat rate at full-load operation is estimated to be 7,920 kJ/kWh (7,509 Btu/kWh) using 930.6 kJ/g-mole CH_4 (400,500 Btu/lb-mole CH_4) as the higher heating value of the SNG feed.

Other process flow combinations might achieve the heat rate target, but a substantial optimization effort would be required to define the most cost-effective scheme. For example, lowering the cell voltage from 0.800 V to 0.787 V increases the current density to 150 mA/cm^2. That would reduce the total area of the fuel cell by 19%, thereby reducing investment costs. However, the system heat rate would increase to about 8,010 kJ/kWh (7,595 Btu/kWh), exceeding the 7,910 kJ/kWh (7,500 Btu/kWh) goal.

Table V-7

ENERGY BALANCE FOR A NOMINAL 26-MW FUEL-CELL POWER PLANT THAT USES SNG

Energy Input	GJ/hr	Percent of Input
SNG	190	100
Energy Output		
Electricity	86	45
Cathode exhaust	43	23
Air cooling	51	27
Inverter losses[a]	4.0	2
Auxiliary power[b]	5.8	3

[a]Taken as 4% of DC power output, assuming inverter improvements.

[b]Primarily system blowers.

The effect of part-load operation on the system heat rate was not calculated. However, this variation has been estimated by United Technologies Corporation (UTC) for a similar molten carbonate fuel-cell system.[9] A minimum heat rate of 7,490 kJ/kWh (7,100 Btu/kWh) at 60% of rated load was projected, as shown in Table V-8.

Lastly, the estimated values quoted above do not include efficiency penalties reflecting possible fuel consumption required to maintain system operating temperature during periods of stand-by operation. The power plant load profile and a transient thermal balance are required to evaluate this penalty.

L. 26-MW Fuel-Cell Power Plant (Naphtha)

The energy balance for this power plant is given in Table V-9. Net power output is estimated to be 25.6 MW, with a system heat rate of 7,720 kJ/kWh (7,315 Btu/kWh). The effect of part load operation on the power plant heat rate is similar to that shown in Table V-8.

The somewhat higher thermal efficiency of this power plant relative to the SNG-fueled power plant is a result of the more favorable anode reactant concentrations, as discussed in Chapter IV.

M. Electricity Transmission and Distribution

The main sources of energy loss between the generating plant and the ultimate consumer are resistive and inductive losses in the high voltage transmission lines and transformer losses in the distribution system. The actual losses in a given utility system are a function of many variables, including the transmission line voltages, distance from generating plants to load centers, and average loads on transformers. Rather than attempt to estimate such losses quantitatively, a more reasonable approach is to use national statistics. On a nationwide

Table V-8

UTC* PROJECTION OF PART LOAD HEAT RATE
FOR MOLTEN CARBONATE FUEL CELLS USING REFORMABLE FUELS

Percent of Rated Load	Approximate Heat Rate, kJ/kWh (Btu/kWh)
100	7,910 (7,500)
75	7,540 (7,150)
60	7,490 (7,100)
50	7,560 (7,170)
25	8,280 (7,850)

[a]United Technologies Corporation.

Table V-9

ENERGY BALANCE FOR A NOMINAL 26-MW
FUEL-CELL POWER PLANT THAT USES NAPHTHA

Energy Input	GJ/hr	Percent of Input
Naphtha	198.0	100
Energy Output		
Electricity	92.0	46
Cathode exhaust	44.0	22
Air cooling	52.0	26
Inverter losses[a]	4.1	2
Auxiliary power[b]	6.1	3

[a]Taken as 4% of DC output, assuming inverter improvements.

[b]Primarily system blowers.

basis, the ratio of electricity metered to customers to that generatedby utilities is about 0.91.[10] This figure is commonly cited as the average efficiency of electricity transmission and distribution, and will be used in this study because more accurate methods of estimation are not readily available.

The efficiency of distribution alone, appropriate where dispersed fuel-cell power plants are used, is estimated to be 97%. Losses are due mainly to energy dissipation in transformers.

N. 100-kW Fuel-Cell Power Plant with Heat Recovery

Energy balance calculations show that the 100-kW fuel-cell power plant would generate 111 kW (DC) gross power to deliver 100 kW (AC) net electrical power output at 120-220 V (AC). Corresponding electrical energy conversion efficiency is 31.8%, based on the HHV of the SNG feed consumed. At this rated load operating point, the waste heat recovery system has a thermal output of 45.7 MJ/hr (443,000 Btu/hr), equivalent to 4,915 kg/hr (10,827 lb/hr) of hot water product at 82°C. The corresponding thermal energy conversion efficiency is 40.3%. Thus, the total input fuel energy utilization is 72.1% (HHV basis). The overall energy balance for the power plant at rated load is shown in Table V-10.

The characteristics of the 100-kW power plant operating at part load were assessed. Parasitic electrical energy losses were estimated for the DC/AC inverter and power plant auxiliary equipment. Recovery of waste heat thermal energy was also estimated. The results are given in Table V-11 and Figure V-1. As shown, overall system energy utilization exceeds 65% for power plant operation at 25-100% of rated electrical load. Thermal output of the waste heat recovery system at part load operation is shown in Figure V-2.

Table V-10

ENERGY BALANCE FOR A 100-kW FUEL-CELL POWER PLANT THAT USES SNG

	GJ/hr	Percent of Input
Energy Input		
SNG	1.13	100
Energy Output		
Electricity	0.36	32
Recovered heat	0.46	40
Cathode/reformer exhaust	0.27	24
Inverter losses	0.02	2
Auxiliary power	0.02	2

Table V-11

OPERATING CHARACTERISTICS OF 100-kW TOTAL ENERGY POWER PLANT AT PART LOAD

Fuel Cell Output, kW (DC) Gross	Electrical Losses (kW)		Power Plant Output kW (AC) Net	Input Fuel Energy Utilization (%)		
	Inverter	Auxiliaries		Electrical	Thermal	Total
111	5.50	5.50	100	31.8	40.3	72.1
83	5.23	4.8	73	32.5	38.7	71.2
56	4.93	4.0	47.1	32.4	37.1	69.5
28	4.20	4.0	19.8	28.4	35.5	63.9
11	2.44	4.0	4.6	17.3	35.3	52.6

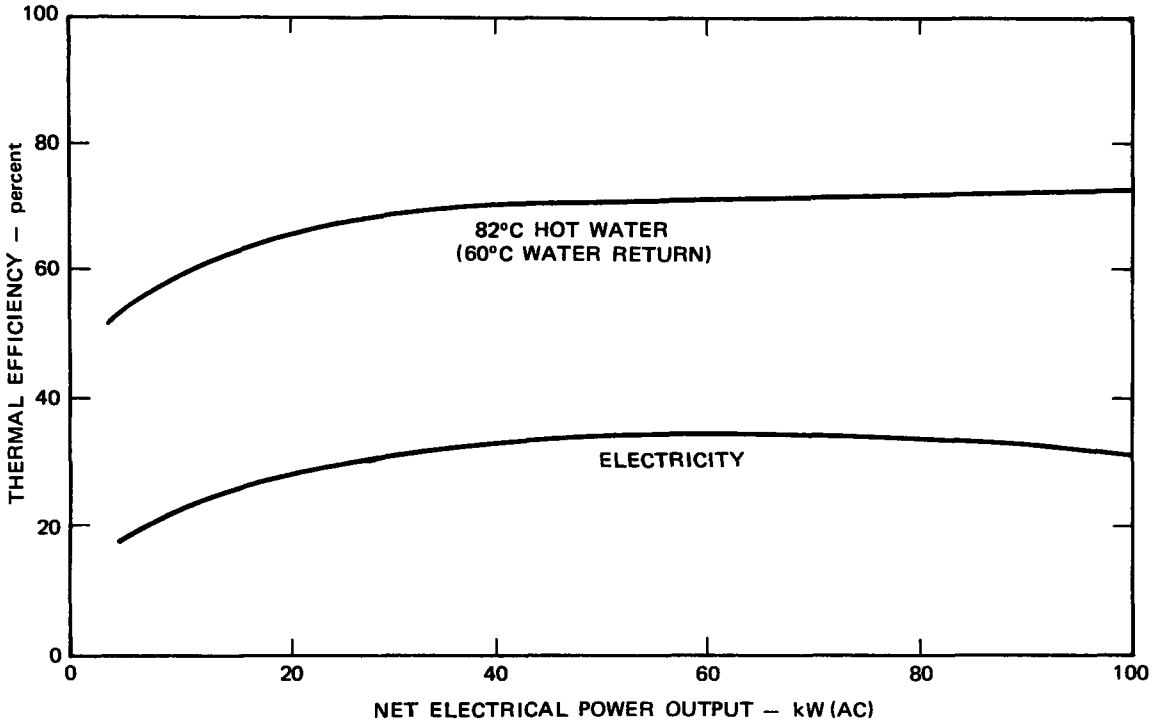

FIGURE V-1. EFFECT ON THERMAL EFFICIENCY OF OPERATING THE 100-kW TOTAL ENERGY SYSTEM AT PART LOAD

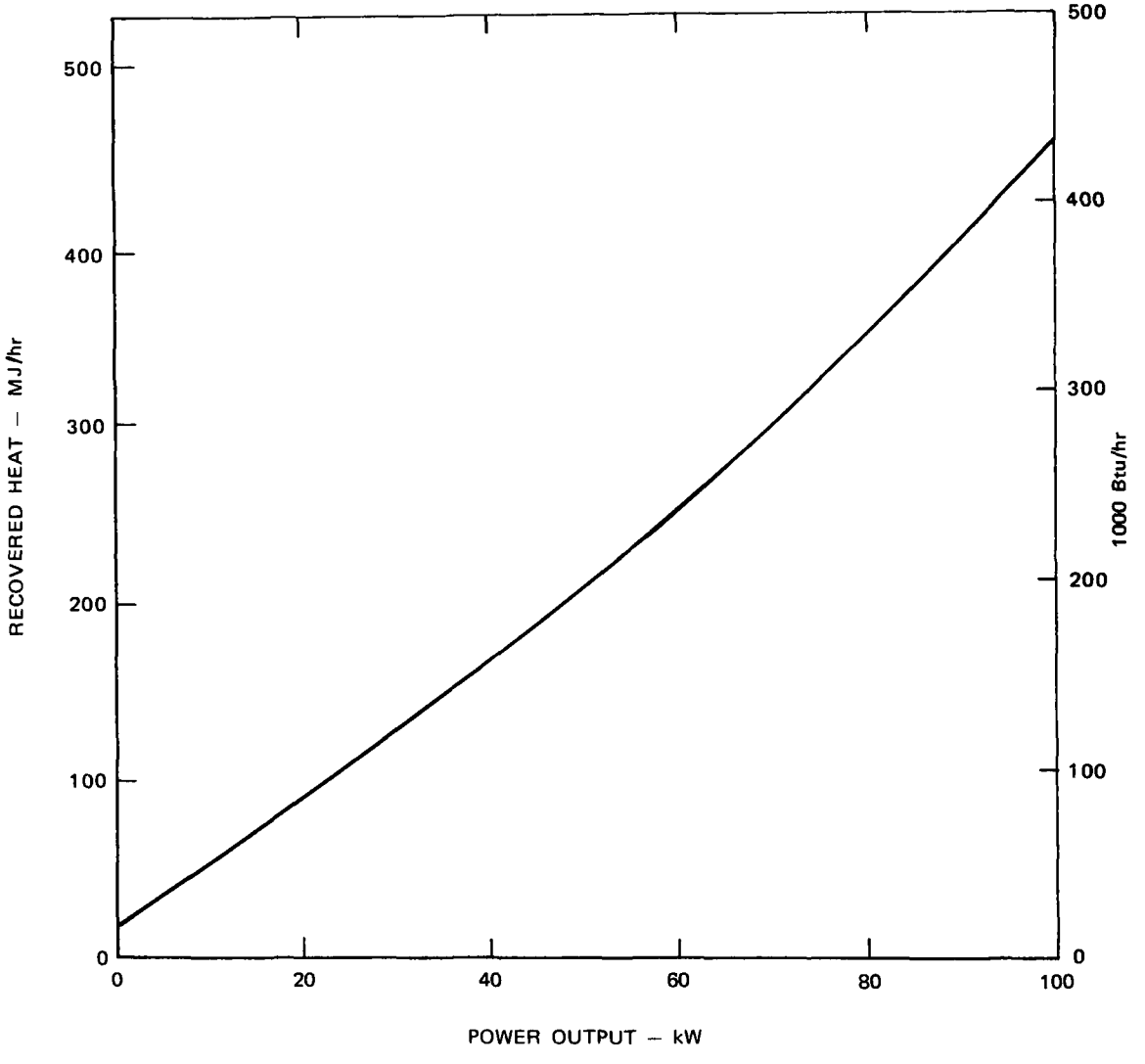

FIGURE V-2. HEAT AVAILABILITY FOR 100-kW FUEL-CELL POWER PLANT

Projected response of the 100-kW power plant to part-load operation is similar to that reported by UTC for a 40-kW system.[11] The UTC system efficiency drops off more rapidly at very low load operation, so that the estimated electrical losses given in Table V-11 may be optimistic. A major difference exists in the estimated electrical conversion efficiency. UTC reported a value of about 38%, but that was based on the fuel's lower heating value. Conversion to an HHV basis would reduce that figure to 34.2%. The remaining difference may be due to selection of a higher cell voltage design point and/or extensive optimization of the intergrated system components by UTC.

The impact of variable water return temperature was also assessed, assuming that the thermal energy recovery heat exchanger design was based on a 60°C (140°F) water return temperature. Increasing the water return temperature (and keeping the exchanger area constant) had a slight adverse effect on the overall system efficiency, as shown in Figure V-3.

O. Gas Furnace and Air Conditioner

The rated efficiency of the gas furnace described in Section IV-A is 80% -- 87 MJ/hr (82,500 Btu/hr) of gas is burned to yield 69.6 MJ/hr (66,000 Btu/hr) of heated air. However, this is an instantaneous efficiency achieved when the furnace has attained its appropriate operating temperature. Because a furnace typically cycles on and off to meet its heating load, it must start cold at the beginning of each cycle. During start-up, while the plenum is being heated to its desired operating temperature, no air is circulated, and most of the furnace heat is lost through the flue. Over an entire heating season, these cold starts will consume considerable additional energy. In addition, residential furnaces are not often maintained in optimum condition so that the rated efficiency of the furnace is not usually attained over the life of the furnace. Because of those and other smaller sources of energy losses, the seasonal average energy efficiency for gas furnaces is estimated to be 60%.

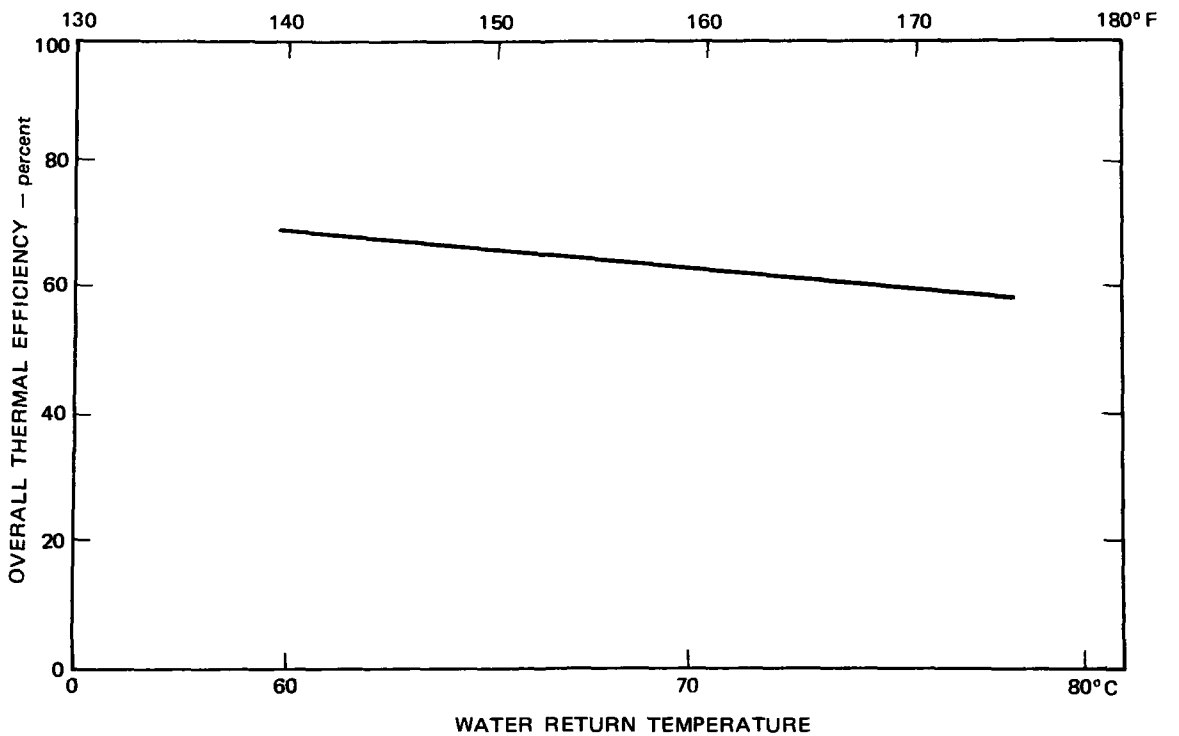

FIGURE V-3. EFFECT OF WATER RETURN TEMPERATURE ON OVERALL THERMAL EFFICIENCY

Another source of energy consumption in a gas furnace is the blower that is used to force air through the plenum and into the heating ducts. The blower motor for the Westinghouse FGUE-082Q furnace is rated at 895 kW (1/3 horsepower). Over the entire heating season, the electricity consumption by the blower motor is about 7.8 kWh per GJ (8.2 kWh per 10^6 Btu) of heat delivered by the furnace.

The energy efficiency of the combined Westinghouse SL030C condenser and EC030 evaporator unit is taken directly from the manufacturer's literature. The measure of this efficiency is the coefficient of performance or COP. The COP is simply the ratio of heat removed from the conditioned space to the heat equivalent of the electricity consumed by the air conditioner. The COP provided by the manufacturer must be adjusted, however, by including the electrical energy required to power the fan that forces air through the EC030 evaporator unit, and by reducing the cooling ouput by the heat generated by the fan motor. The net effect is to decrease the rated capacity of the air conditioner from 30.9 MJ/hr (29,250 Btu/hr) at 35°C (95°F) exterior temperature to 29.8 MJ/hr (28,200 Btu/hr) and to increase the electrical load from 4.0 to 4.3 kW. The resulting COP for the SL030C/EC030 air conditioning system as a function of exterior temperature is shown in Figure V-4. Interior air temperatures are presumed constant at 26°C (78°F) dry bulb and 19°C (67°F) wet bulb over the range of exterior temperatures. The COP ranges from 2.25 at 27°C (80°F) to 1.58 at 43°C (110°F). The COP decreases with increasing temperature because the compressor must perform more work per unit of cooling as the temperature difference between the higher temperature reservoir, to which heat is exhausted, and the lower temperature reservoir, from which heat is extracted, increases.

P. Heat Pumps

The advanced heat pumps described in Sections IV-B and IV-E have excellent COPs, ranging from 1.7 to 3.6 as a function of external

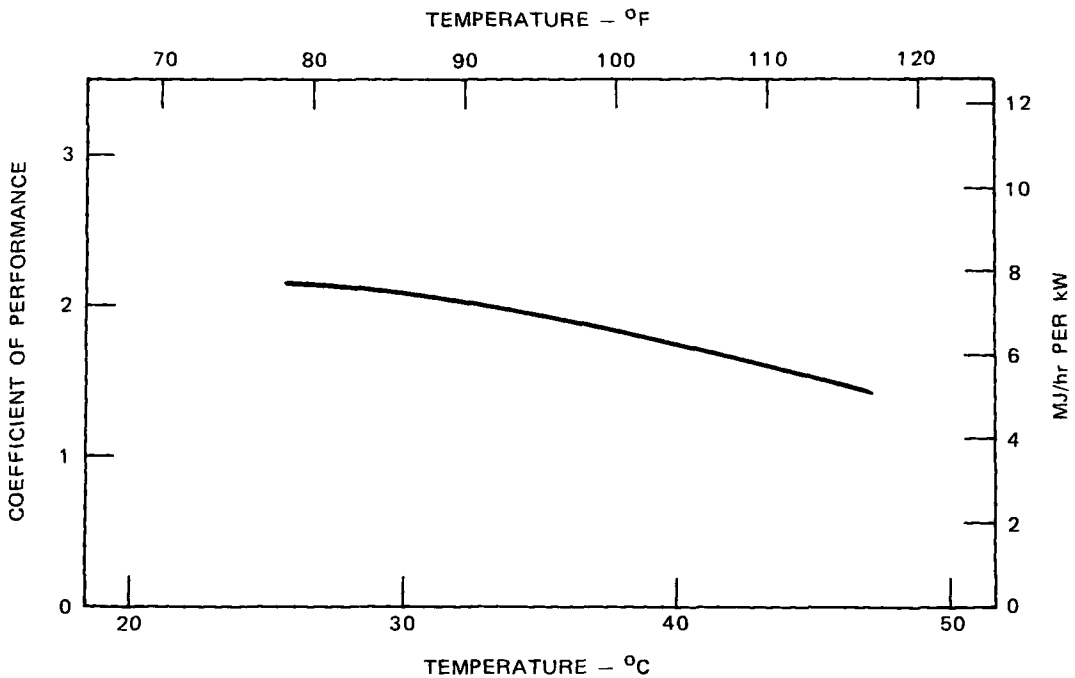

FIGURE V-4. COEFFICIENT OF PERFORMANCE OF WESTINGHOUSE SL030 AIR CONDITIONER

temperature.[12] Current state-of-the-art heat pumps typically have COPs in the range of 1.0 to 2.8. The COPs for the 26.0 MJ (24,600 Btu) per hour and the 19.3 MJ (18,300 Btu) per hour heat pumps are shown in Figure V-5 for both the heating and cooling modes. Because these heat pumps have been been optimized for operation in a northern climate, their performance in the heating mode is superior to that in the cooling mode. The sudden drop-off in heating performance below 5.6°C (42°F) is due to the effect of the defrost cycle, which must be engaged to prevent frost build-up on the exterior evaporator coil.

As indicated in Section IV-B, it is not economical to size the heat pumps large enough to meet all anticipated heating needs. Therefore, supplemental heating must be provided to meet the heating load when it exceeds the capacity of the heat pump. For the 26.0 MJ (24,600 Btu) per hour heat pump that is used in the detached, single family homes described in Section IV-B, that condition (called the "balance point") occurs at about - 1°C (30°F). Below this temperature, resistance heaters must be employed to balance the heat load. A bank of 3-4.7 kW (16.9 GJ/hr or 16,000 Btu/hr) heaters would be capable of maintaining the house at 21°C (70°F) at temperatures below -29°C (-20°F).

Because resistance heaters have a COP of 1.0, their use will lower the effective COP of the heating system. This effect is shown in Figure V-5 in which the dashed line shows the effective COP of the system below the -1°F (20°F) balance point. The effective COP is an average over time because resistance heaters are either on or off at any given instant, cycling as required to maintain the interior temperature.

The balance point of the 19.3 MJ (18,300 Btu) per hour heat pump that heats and cools the townhouses described in Section IV-E depends on the amount of space heating supplied by recovered heat from the 100-kW fuel-cell power plant. With no recovered heat, the balance point would be at -5°C (23°F). For average light and appliance loads (1.01 kW) and domestic hot water (DHW) demand (1.87 MJ/hr), as determined in Chapter VIII, the balance point is shifted downward to -12°C (10°F).

Below this temperature the supplemental resistance heater must be used. The overall system COP is shown in Figure V-5, assuming no fuel-cell heat is recovered, with the dashed line showing the effective COP below the balance point of -5°C.

Naturally, the balance point of the system will vary with the actual light, appliance, and DHW load. This variation is not great, however, ranging from about - 13°C (9°F) to -11.5°C (11°F).

Q. Heat Delivery System

The key components of the system that delivers 82°C (180°F) hot water from the fuel-cell power plant to the space heating and DHW systems of the townhouses are the heat exchangers. The properties of these heat exchangers determine the effectiveness with which the hot water can be utilized.

The efficiency of the simple water-to-water heat exchanger used in the DHW tank is assumed to be essentially 100%. This is a reasonable assumption, because those heat exchangers are very efficient at the flow rates and approach temperatures used in the system. As will be seen in Chapter VIII, sufficient heat is available from the fuel-cell power plant to meet all DHW demands during both the heating and cooling season.

The heat transfer efficiency of the water-to-air heat exchanger described in Section IV-E is a function of the flow rate of the hot water entering the exchanger and the temperature of the air flowing across it. (It is also a function of the air flow rate and the water temperature, but these quantities are constant in this system). The air temperature is the same as the hot air stream delivered by the heat pump and is a function of the external temperature. The hot water flow rate is a function of the heat recovered from the fuel-cell power plant, which in turn is determined by the electical load. The heat pump exit air temperature varies from 26°C (79°F) at -29°C (-20°F) external temperature to 43°C (110°F) at 16°C (60°F). The hot water flow rate varies from 5.6×10^{-3} liter/sec (0.089 gal/min) at

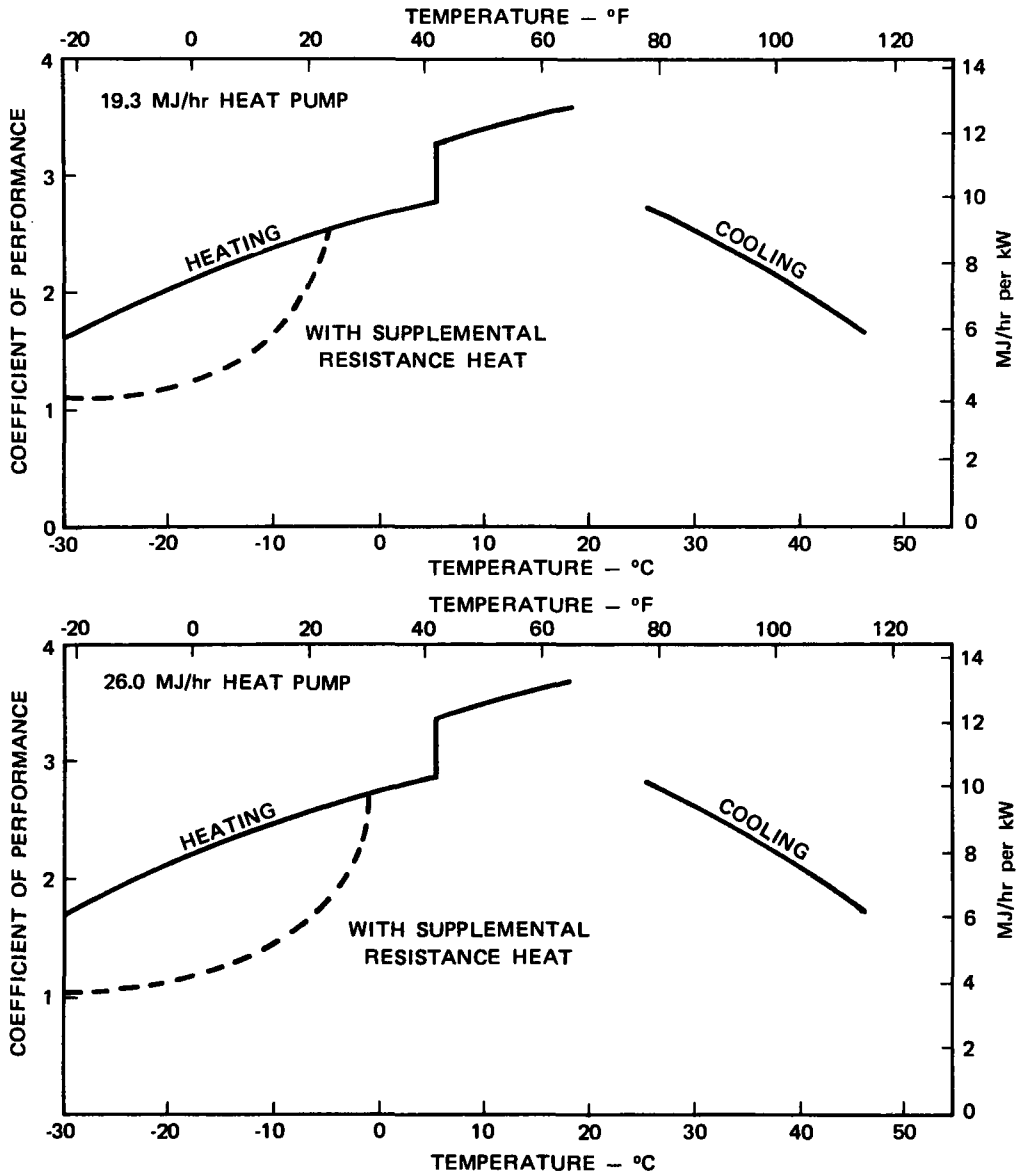

FIGURE V-5. COEFFICIENTS OF PERFORMANCE OF ADVANCED HEAT PUMPS

the minimum electrical load of 5.4 kW to 0.070 liter/sec (1.11 gal/min) at 100 kW.

Using the heat transfer parameters supplied in the manufacturer's literature for the Trane 30 x 30 cm (12 x 12 in.), WC Series 18 heating coil (with turbulators), the water-to-air heat transfer rates were calculated as a function of external temperature and electrical load. The entering hot water temperature and air flow rates were held constant at 83°C (180°F) and 0.26 nm^3/sec (550 scf/min), respectively. The results of the calculations are displayed in Figure V-6. The uppermost curve in the figure is the heat available (per residence) from the fuel-cell power plant and represents the upper limit on the heat that can be transferred to space heating.

Figure V-6 displays several interesting features. The first is that at a given electrical load (above 2 kW per residence) the efficiency of heat transfer increases with decreasing external temperature. That occurs because the temperature of air exiting the heat pump decreases with decreasing external temperature, and the heat transfer efficiency increases as the difference between air and water streams. (The maximum heat transfer occurs when the heat pump is off, since the air stream is near room temperature). This effect is beneficial, allowing the most heat to be transferred precisely where it is required most -- at lower external temperatures, where the heating load is greatest.

The heat transfer efficiency decreases with increasing heat availability from the fuel-cell power plant because of the decline in heat transfer effectiveness with increasing water flow rate. This represents a disadvantage because the highest electrical loads occur at low external temperatures where the heat demand is greatest.

Overall, the heat transfer efficiency ranges from a maximum of 100% for various combinations of electrical loads and external temperatures, to 49% at maximum electrical load and an external temperature of 16°C (60°F).

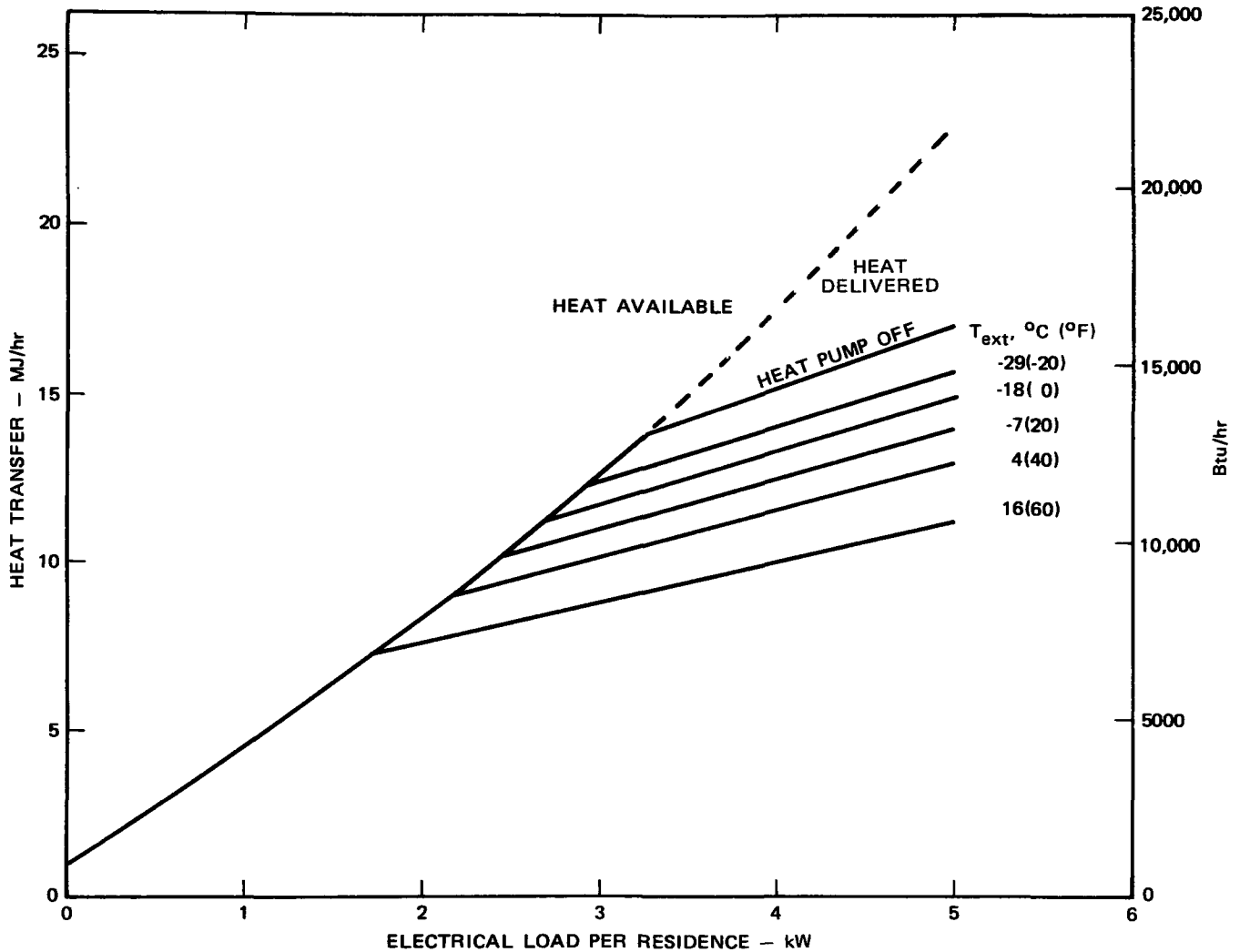

FIGURE V-6. HEAT TRANSFER RATES FROM HOT WATER DELIVERY SYSTEM TO SPACE HEATING

R. References--Chapter V

1. Estimate of SRI International staff.

2. State of Montana, Department of State Lands, "Final EIS, Proposed Plan of Mining and Reclamation, East Decker and North Extension Mines, Decker Coal Co., Big Horn County, Montana," U.S. Department of the Interior (June 1977).

3. M. E. Jacobs, "Fuel Efficiency Improvement in Rail Freight Transportation: Multiple Unit Throttle Control to Conserve Fuel," NTIS PB 262-470.

4. R. Detman, et al., "Factored Estimates for Western Coal Commercial Concepts," Interim Report, U.S. Energy Research and Development Administration (October 1976).

5. R. F. Probstein and H. Gold, "Water in Synthetic Fuel Production -- The Technology and Alternatives" (The MIT Press, Cambridge, MA, 1978).

6. A. Melcher, et al., "Net Energy Analysis: An Energy Balance Study of Fossil Fuel Resources," Colorado Energy Research Institute (April 1976).

7. D. T. Beecher, et al., "Energy Conversion Alternatives Study -- Combined Gas/Steam Turbine Plant Using Coal-Derived Liquid Fuel," NASA-CR-134942 (November 1976).

8. Curtiss-Wright Corporation, "High Temperature Turbine Technology Program -- Phase I Topical Report," U.S. Energy Research and Development Administration (January 1977).

9. J. M. King, "Advanced Technology Fuel-Cell Program," Electric Power Research Institute Report EM-335 (October 1976).

10. Hittman Associates, Inc., "Environmental Impacts, Efficiency and Costs of Energy Supply and End Use," Report No. HIT-561 (January 1975).

11. P. Bolan, "Heat Pumps and Fuel Cells," Paper No. 23d, AIChE 69th National Meeting, November 30, 1976.

12. H. S. Kirschbaum and S. E. Veyo, "An Investigation of Methods to Improve Heat Pump Performance and Reliability in a Northern Climate," Electric Power Research Institute Report EM-319 (January 1977).

VI ENVIRONMENTAL IMPACTS OF SYSTEM COMPONENTS

In this chapter, the environmental impacts of all the components described in Chapter IV are analyzed. Wherever possible, the physical factors (e.g., pollutant emissions) that are the source of environmental problems are quantified. However, many of the problems addressed are qualitatively discussed because quantification is difficult or impossible. For systems components for which engineering controls are required to reduce environmental impact, those controls are described, and their effect on the relevant environmental factors are quantified. All control systems have been conceptually designed to meet or exceed current and projected performance standards established by EPA.

The results of this chapter will be used in the comparison of the five systems in Chapter IX. As discussed in Chapter I, EPA requested that only physical environmental factors be used in the comparison of the systems; therefore, we made no attempt to establish absolute levels of impacts (e.g., human health effects).

A. Coal Mine

Several important environmental impacts result from strip mining coal in the Powder River Basin, including:

- Air quality impacts
- Water resources impacts
- Land use impacts
- Topographic and geologic impacts.

These impacts are discussed in the following sections.

1. Environmental Setting

The headwaters of the Powder River, the major drainage for the basin, begin in the Big Horn Mountains in north central Wyoming. The river flows in a northerly direction, crossing into the state of Montana and continuing until it drains into the Yellowstone River.

Bordered by the Big Horn Mountains to the west, the Black Hills to the east, the Laramie Mountain Range to the south, and the Cedar Creek anticline in Montana to the north, the Powder River Basin covers an area of 36,066 km^2 (13,914 mi^2)in Montana and Wyoming.

The Powder River Basin lies in the Missouri Plateau physiographic region. The terrain includes mountains, rough lands and badlands, hilly areas, and moderately sloping lands. The average annual rainfall 25-41 cm (12-16 in.), comes mainly from thunderstorms that drop large amounts of rain in short periods of time. The general climate of the area, according to the Koppen climate classification system is middle latitude steppes climate. Cut off by mountains from the invasion of maritime air masses, the area is semiarid, with great annual temperature variations between summer and winter. Its growing season is from 120 to 140 days long.

Water resources in the basin consist mainly of the Powder River. The average discharge for the Powder River at Locate, Montana, from 1938 to 1979 was 17 m^3/sec (600 ft^3/sec) or 535 million m^3 (434,700 acre-ft) per year. Ground water availability is greater than 31.5 liter/sec (500 gal/min) in the areas immediately adjacent to the Powder River and falls off to less than 3.2 liter/sec (50 gal/min) for most of the basin area.

The major land use is cattle and sheep ranching. The average ranch size for this area is 2,950 hectares (7,280 acres). Small amounts of hay are raised as winter feed for the local livestock.

Population distribution in the area is sparse with a density of 1.3 persons per square kilometer (3.4 per square mile). Major towns of the basin include Gillette, Wyoming, population 7,194; Buffalo, Wyoming, population 3,394; Midwest, Wyoming, population 825; and Broadus, Montana, population 799.

2. Surface Mining Operation Requirements

The majority of the coal in the Powder River Basin lies close enough to the surface that strip mining techniques are the most effective means of extracting the resources. Montana, Wyoming, and recently the federal government have developed strict laws to regulate surface mining. To narrow the scope of this analysis, it is assumed that the coal resource will be mined in Campbell County, Wyoming, by an area mining technology, and that the mine will supply 4.5 million tonnes (5 million tons) of coal per year to markets in the Midwest or to minemouth conversion plants.

Mining companies are required to have a federal permit prior to mining under the Surface Mining Control and Reclamation Act of 1977. Companies applying for permits must meet the following conditions:

- Incorporation (e.g., partnership, corporation, individual)
- Established financial capabilities
- Mining rights
- A boundary map prepared
- Buyers for the coal
- Available equipment and personnel
- Coal transportation arranged.

The first step in the application process for a federal permit is to design a field program for a baseline study to collect the data

necessary to meet federal requirements. The baseline studies should examine the following areas:

- Hydraulic areas (surface and underground water)
- Subsurface geology
- Air quality
- Topography
- Archaeological and historical sites
- Socioeconomic impacts
- Land use impacts
- Noise
- Terrestrial biomes
- Aquatic biomes.

These areas can be addressed with the following procedures:

- Make literature searches
- Collect field data
- Write preliminary reports
- Devise a mining plan
- Prepare and submit a reclamation plan
- Assess the environmental impacts.

After these procedures have been completed, the following remains to be done:

- Prepare and submit permit applications
- Advertise the applications
- Receive comments on the environmental impacts and the reclamation plan.

The permitting agent then decides whether a hearing is necessary or whether to grant the permit without a hearing. If a hearing is neces-

sary, it is advertised and held. The decision is then made on granting of a permit. If the permit is denied, a hearing on the denial is advertised and held. The permit process may take up to 2 years, or even longer if litigation is involved.

3. Environmental Impacts of Surface Mining

Surface coal mining greatly affects the surrounding environment. Air-borne dust and particulates cause air pollution when large-scale earth moving operations and wind erode the exposed and loosened soil. Soil stripped of ground cover increases water runoff. Ground water aquifers are disturbed by the excavation of overburden and removal of the coal seams which often are aquifers. Land use is at least temporarily converted from range and farmland to coal mining. Topographic and geologic impacts occur after the removal of the coal itself. These primary physical impacts are discussed below.

a. Air Resource Impacts

Several surface mining operations contribute to air pollution, including emissions from coal-haul trucks and grading and drilling equipment, as well as the dust created by excavation, grading, and construction. Dust from the coal-haul roads and wind erosion of exposed soil further increase air pollution. In addition, the electrically powered shovels and draglines contribute considerable dust during earth moving.

Table VI-1 shows the particulate emissions for existing mines and projects emissions from mines that are planned to be in operation in Campbell County, Wyoming in 1980 and in 1985.

The Wyodak Resources expansion for 1985 is projected to be mining 4.5 million tonnes (5 million tons) of coal per year. This concides

with the conceptual unit mining operation described in Chapter IV-A. The particulate emissions are projected to be 375 x 10^3 kg/yr (825 ton/yr).

The air quality is now considered to be good. The projected expansion of current mining activity as indicated in Table VI-1 will tend to considerably degrade air quality in the basin. Table VI-2 lists air pollutant emission factors for major mining activities, assuming uncontrolled emissions.

Table VI-1

PROJECTED PARTICULATE EMISSIONS FROM SURFACE MINES - GILLETTE, WYOMING AREA

Source	Comment	Annual Tonnes Mined	Particulate Emissions (10^3kg/yr)
Year: 1975			
Amax Coal, South	Existing	2,730,000	225
Wyodak Resources	Existing	636,000	52
Year: 1980			
Amax Coal, South	Expansion	9,270,000	760
Wyodak Resources	Expansion	2,270,000	190
Amax Coal, North	New	13,600,000	1,130
Carter Oil	New	7,270,000	600
Sun Oil	New	9,090,000	750
Kerr-McGee North	New	3,820,000	315
Year: 1985			
Amax Coal, South	Expansion	13,600,000	1,130
Wyodak Resources	Expansion	4,550,000	375
Amax Coal, North	Expansion	18,200,000	1,500
Carter Oil	Expansion	10,900.000	900
Sun Oil	Expansion	10,900,000	900
Kerr-McGee North	-	3,820,000	315

Source: Reference 1

Wyoming's reclamation laws require that regrading and containing of exposed soils and establishing of new ground cover begin as soon as possible. This plus the required treating of haul roads with chemicals and watering will help control dust, although the dust created by the dragline remains a major contributor to air pollution (see Table VI-2).

b. Water Resources Impacts

Surface mining can cause major problems in surface and ground water resources. The surface water runoff from a surface mining area is very turbid. This problem is exacerbated by the pattern of rainfall in this area, which typically occurs in the form of short, intense thunderstorms. As much as 2 to 3 inches of rain can fall during a 24-hour period, inundating the unprotected and exposed soils and carrying away large amounts to local streams and then into the Powder River.

Ground water is affected more drastically in areas of shallow aquifers, which are removed completely when they lie between the coal and the surface. After the overburden is removed, the materials making up the aquifers are mixed with the rest of the overburden. The ground water recharge capacity is thus temporarily and possibly permanently affected by this rearrangement of overburden material. Moreover, the water quality may be affected by leaching of toxic substances that have been disturbed in the mining processes.

Dewatering the mine can also result in the discharge of contaminated water, typically on the order of 30 liters/sec (500 gal/min). Regulations proposed under the Surface Coal Mining and Reclamation Act (30 CFR 715), limit the average concentrations of suspended solids, iron, and manganese in such discharges to 30, 3.5 and 2.0 mg/liter respectively. Because of the alkalinity of the water, however, the concentrations of iron and manganese are not likely to reach those limits. Concentrations of 0.5 and 0.1 mg/liter have been estimated for iron and manganese, respectively.[3]

Table VI-2

AIR POLLUTANT EMISSIONS FOR A 4.5 MILLION TONNE (5 MILLION TON) PER YEAR SURFACE MINE

Activity	Emissions (10^3kg/yr				
	SO_2	NO_x	Particulates	Hydrocarbons	CO
Dragline operation (annually disturbing 100 acres at an overburden depth of 70 ft)	-	-	385	-	-
Scrapers (3 in operation)	-	-	58	-	-
Haul road traffic (haul trucks=1.0 kg/VMT) (pickup trucks=0.4 kg/VMT)	-	-	380	-	-
Shovels and front-end loader	-	-	84	-	-
Trucks dumping at hopper	-	-	84	-	-
Vehicle exhaust					
Haul trucks (assuming 6 45-ton trucks)	14	230	7.6	13	39
Pickup trucks			Negligible		
Scrapers, graders, and loaders	1	12	0.79	.3	1
Total vehicle exhaust emissions	15	242	8.4	16	40
Wind erosion of exposed soil (0.24 tons/year-acre, assuming 800 acres exposed before reclamation begins)	-	-	180	-	-

Note: VMT = vehicle miles traveled.

Source: References 1 and 2.

c. Land Use Impacts

Land in this area is primarily used for ranching and farming. Native wildlife species including deer, antelope, and upland game birds such as the sage hen make it their home range. The area is also a stopover for migratory waterfowl. The reclamation process may take as long as 4 years from the time the area is disturbed until it is regraded and reclaimed.

The total area disturbed at any given time is about 270 hectares (680 acres). Approximately 120 hectares (300 acres) of this area will be semipermanent coal haul road, stage areas, and equipment maintenance areas. Approximately 40 hectares (100 acres) will be newly mined each year, and the other 110 hectares (280 acres) will be undergoing reclamation.

Areas used for farming of particular crops such as wheat or hay may not be restored to their original use. These areas may be restored to grazing lands, but bringing them back to original crop production capacity may be beyond the goals of the reclamation plan. The land may be out of use during the mining process and also permanently decrease productive crop acreage. In compensation, however, this action increases range land for livestock and native wildlife.

When ponds are permanently eliminated by regrading the area, water for livestock and wildlife is decreased. Waterfowl are displaced and forced to seek a new habitat.

Oil and water wells are also in this region and may be temporarily or permanently out of service if the land they occupy is mined.

d. Topographic and Geologic Impacts

Topographic and geologic impacts are related because the topography of the land surface is changed in areas where thick coal seams are

extracted close to the land surface. The average overburden thickness is 21 m (70 ft.). However, in some places it is only 6.1 m (20 ft.) thick with an 18 m (60 ft.) coal seam under it. When the 18 meters of coal are removed, a 24 m (80 ft.) hole with only 6.1 m of overburden takes its place. Grading the adjacent areas to avoid the highwall compensates for the remaining steep drop, but the resulting land surface is lower. Disturbing an average of 40 hectares (100 acres) per year for 30 years means that an area of 1200 hectares (3,000 acres) of land is altered. The handling of overburden during the mining process can involve as much as 310 million m^3 (339 million $yd.^3$) of material (assuming 40 hectares (100 acres) per year at an average overburden thickness of 21m (70 ft.) for 30 years.

B. Unit Train (Coal)

Loading, line haul (transit), and unloading are activities associated with movement of coal from the mine to the powerplant. The severity of the environmental impacts of these activities is dependent on the equipment involved as well as the location of the activity.

1. Loading/Unloading

The primary impact of loading and unloading is on air quality because of the coal dust released. The dust generally affects only the area immediately adjacent to the facility. This impact is not considered to be significant since the coal dust rapidly settles out of the air.

2. Line Haul

Operating the unit train causes the most extensive environmental impacts. Several different population groups as well as

the vegetation and wildlife along the route are affected. The groups impacted include property owners along the right-of-way, residents in nearby communities, and highway users. The new traffic intensifies existing railroad-related impacts including noise and vibration, visual intrusion, air pollution, and danger of accidents. The degree of impact varies with the:

- Distance of affected persons from the railroad.
- Volume, scheduling, and type of railroad operations.
- Topography of the surrounding area.
- General condition of the right-of-way.
- Design and maintenance of the railroad's rolling stock.
- Level of maintenance of roadbed, track, and structures.
- Type of grade crossings.
- Land use of the surrounding area.
- Quality of construction and condition of buildings in adjacent communities.

Railroad noise, together with the attendant vibration, often annoys persons occupying nearby properties. Train horns and crossing warning bells, the squeal of the train's brakes and of steel wheels negotiating a curve, and switching operations all contribute to the obtrusiveness of trains.

The noise profile around the railroad corridor varies with the topography of the surrounding area, the weather, the degree of track maintenance, the location of grade crossings equipped with warning bells, the design of the railroad cars, and the roadbed. For example, depressing the right-of-way relative to the surrounding land dampens noise considerably, whereas elevating the track on a steel trestle distributes the sound more widely. Deep setback of buildings from the tracks, together with screening shrubs, lessens the perceived effect of the train operations, although tests have shown that shrubs have little

actual effect on sound transmission. Also, a relatively high background noise level tends to mask the train noises, so that railroad noises have less effect in industrial and commercial districts.

Measurements of sound level made in Canada at a distance of 30m (100 ft.) from a freight train traveling at roughly the same grade as the surrounding land are given in the following tabulation:

Source	Sound Level (dBA at 30 meters)
Train horn	98-100
Freight train--50 mph	90
Freight train engine--30 mph	87-92
Freight cars--30 mph	75-85

A noise level of about 90 dBA (the sound of train travel at 50 mph) can cause workers to make significantly more errors than they would otherwise. Noises above about 80 to 84 dBA are considered noticeable or obtrusive. Outdoor noise levels of 70 dBA are considered to be a reasonable maximum in residential neighborhoods by the U.S. Department of Housing and Urban Development. These levels would obviously be surpassed when coal trains pass.

Danger involved with railroad operation almost exclusively involves persons who cross the tracks, whether highway users, bicyclists, or pedestrians. This danger is of special concern to nearby residents, employees, and customers because they are the people who are most frequently exposed. Most pedestrian accidents happen to children playing on the tracks or taking short cuts across them.

Other kinds of danger are associated with railroads, but are usually not so important or as common as the hazard to pedestrians, unless the community has experienced particular kinds of accidents such as derailment. The effects are often more serious in rural areas where speeds are higher than in urban areas.

A railroad line is quite visible and usually unattractive unless depressed below ground level or buffered by buildings or landscaping. The equipment is designed for functionality, not appearance. Even when painted, rail cars seem like rolling billboards to many. Dirt, rust, and lubricants frequently mar the right-of-way. The motion of the train and its attendant noise attract attention.

Railroad rights-of-way are maintained for functional rather than visual reasons. Poor weed control and wind-borne paper often add to the usual litter of spilled lading and discarded railroad equipment. This unsightliness often prompts local citizens to discard even more waste in the right-of-way.

The smoke from the diesel locomotives visually intrudes in local areas, both as it is emitted and as it blackens buildings and structures. A well tuned and maintained diesel engine does not normally emit smoke except under periods of heavy load, such as acceleration. Thus, areas where the locomotives accelerate or where switching operations are conducted will be especially subjected to smoke. Switch engines emit approximately 0.006 kg of particulate per km (0.02 lb per mi), and a fully loaded train emits about 0.14 kg per km (0.5 lb per mi). In comparison, a heavy diesel truck emits 0.0009 kg of particulates per km (0.003 lb per mi).

Another source of air pollution from diesel engines is the emission of unburned or partially burned hydrocarbon fuel. The average emissions are 0.034 kg per km (0.12 lb per mi) for switching service and up to about 0.5 kg per km (1.8 lb per mi) for fully loaded trains. Comparable diesel truck emissions, 0.002 kg per km (0.007 lb per mi), are substantially greater per unit of load but are not so concentrated. Again, the hydrocarbon emissions increase under acceleration or hillclimbing, thus concentrating pollutants around these locations. Other air pollutant emissions from diesel locomotives are shown in Table VI-3.

As motor vehicles slow down or stop for grade crossings, then accelerate back to speed, they emit more pollutants than they would were they to continue along the same distance at a steady speed. These effects of the emission at grade crossings are felt in some measure all over the air basin, but the effects are most pronounced near the sources of the emissions. Therefore, this emission problem is both a neighborhood and a community impact.

In addition to the pollutants discussed above, the unit coal trains also add coal particles to air as they travel along the track. Various estimates have been made of the amount of coal dust that is lost, but there is little agreement on specific quantities because of the number of variables involved. A figure of 1% of the coal load is sometimes mentioned.

Table VI-3

AIR POLLUTANT EMISSIONS FROM
DIESEL LOCOMOTIVES--100-CAR UNIT COAL TRAIN

Pollutant	Emissions, kg/km (lb/mi) Fully loaded	Emissions, kg/km (lb/mi) Round trip average
Particulates	0.13 (0.47)	0.085 (0.30)
SO_2 *	0.30 (1.1)	0.19 (0.68)
CO	0.68 (2.4)	0.43 (1.5)
Hydrocarbons	0.50 (1.8)	0.32 (1.1)
NO_x	2.0 (6.9)	1.2 (4.4)
Aldehydes	0.029 (0.10)	0.018 (0.065)

*Assumes fuel sulfur content of 0.4%.
Source: Reference 2

C. Coal-Fired Power Plant

A coal-fired power plant can be a major source of air and water pollution, and generates large amounts of solids that require disposal. Table VI-4 lists the major emission sources for a coal-fired plant that uses an FGD system to control sulfur emissions and a cooling tower for steam condensation. The FGD system has been included even though the plant is burning low-sulfur coal, because recent amendments to the Clean Air Act indicate that, in the future, burning low-sulfur coal will not be considered sufficient for sulfur emission control.

Figure VI-1 shows an integrated air and water pollution control system that would be suitable for controlling most emissions. The system does not include all of the possible technology; rather, it reflects what could be readily installed in a new power plant. The major feature of the treatment system is the use of the cooling tower, boiler, and demineralizer blowdowns as make-up streams for the FGD system and the boiler ash sluicing system. A chromium removal system (reduction with SO_2 and neutralzation to precipitate $Cr(OH)_3$) is included to treat cooling tower blowdown to limit plant discharge or to protect the scrubber chemistry. That system minimizes fresh water intake and final effluent discharge and also minimizes the release of dissolved solids, because the FGD and boiler ash solids carry some blowdown water to the solid disposal facilities as interstitial water.

Acidic runoff from the coal pile and the yard that contains dissolved iron, heavy metals, and sulfuric acid in addition to coal dust is sent to ponds prior to neutralization and clarification. The treated runoff is routed to the final effluent pond for recycling and discharge. Miscellaneous chemical wastes from laboratory operations and condenser tube cleanup are neutralized and released to the final effluent pond.

Two air emission sources -- coal pile fugitive dust emissions and dust from coal handling (which includes crushing for boiler injection) -- listed in Table VI-4 are not shown in Figure VI-1. Coal pile

Table VI-4

MAJOR SOURCES OF POLLUTION FOR A COAL-FIRED POWER PLANT

Medium	Source	Emissions
Air	Boiler Stack	SO_x NO_x CO Hydrocarbons Particulates Trace elements
	Coal pile	Coal dust
	Coal crushing and handling	Coal dust
Solid	Boiler	Bottom ash
	Coal storage	Coal fines Heavy metal hydroxides
	Coal crushing and handling	Coal fines
	Flue gas treatment	Fly ash Desulfurization solids
	Water treatment	Suspended solids
Water	Coal pile and yard runoff	Dissolved solids, heavy metals Suspended solids, organic carbon compounds
	Cooling tower blowdown	Dissolved solids, suspended solids, heavy metals
	Boiler blowdown	Dissolved solids
	Boiler feedwater treatment	Dissolved solids
	Condenser tube cleaning	Dissolved solids Suspended solids
	Flue gas treatment cleanup	Dissolved solids

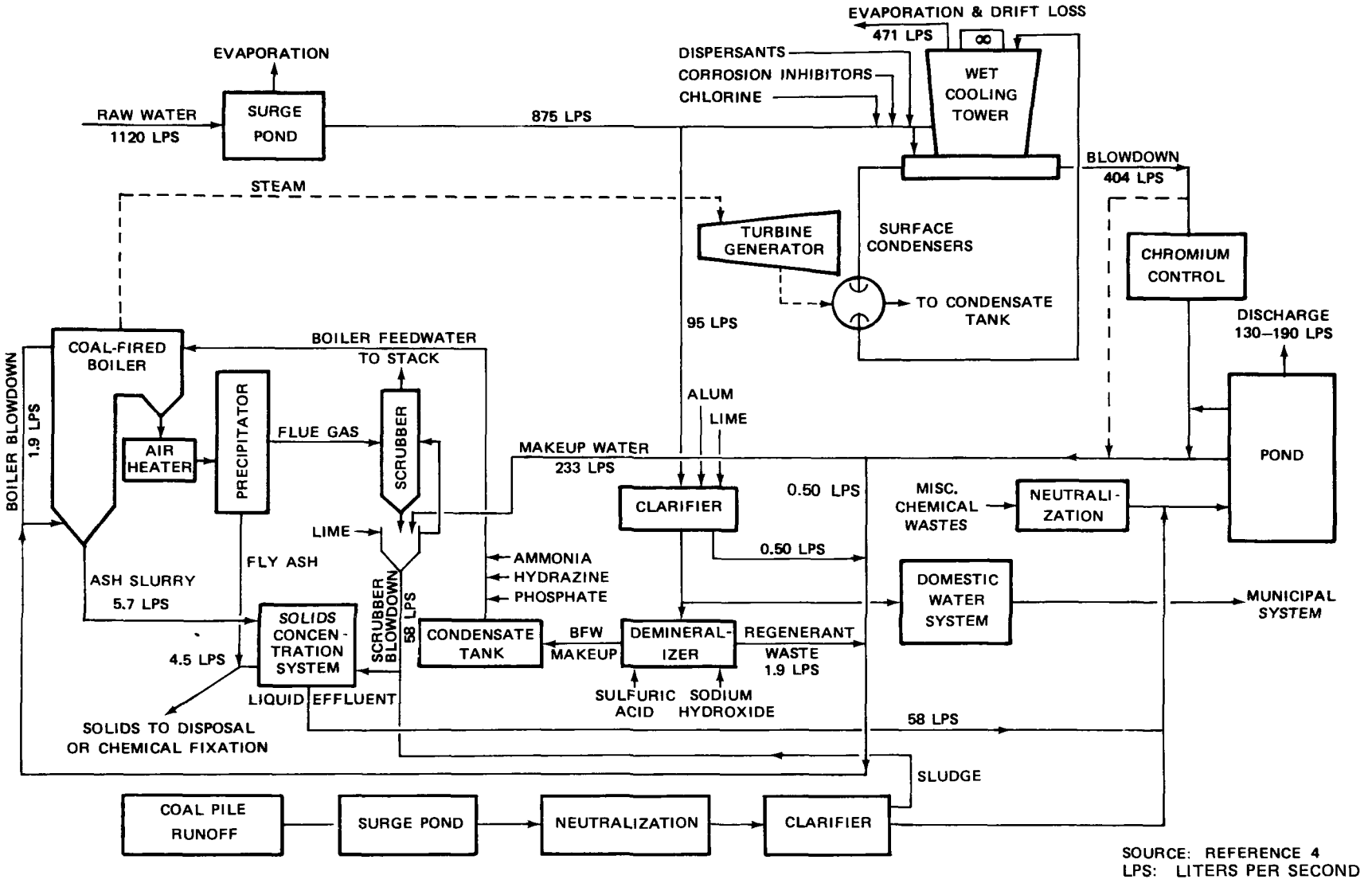

SOURCE: REFERENCE 4
LPS: LITERS PER SECOND

FIGURE VI-1. INTEGRATED POLLUTION CONTROL SYSTEM FOR AN 800-MW COAL-FIRED POWER PLANT

emissions are uncontrolled, but emissions from handling are controlled by using covered conveyers and processing facilities. Air in those facilities is treated in a baghouse before release to the atmosphere.

The water requirements (and discharge) of the power plant shown in Figure VI-1 are primarily related to the cooling tower. The cooling tower shown has a concentrated factor of between 2 and 3 and therefore has a significant blowdown. Depending on the chemistry of the actual water supply, the concentration factor could be increased by 5 or 10 with either a simple lime-softening step on the makeup stream or by withdrawing some recirculating cooling water for lime softening. Proper choice of the concentration factor would allow the plant to discharge no effluent to surface waters. All blowdown streams would be incorporated as interstitial water in the solid waste stream.

The flue gas treatment system and the solids handling system, which are the major pollution control systems on a power plant, are discussed in detail below.

1. Flue Gas Treatment System

The flue gas contains approximately 80% of the ash content of the coal in the form of a fine, particulate fly ash. Between 95 and 100% of the sulfur contained in the coal is in the flue gas in the form of SO_2 and SO_3. Other major components in the flue gas are NO_x, which is created by high temperature reactions between atmospheric oxygen and nitrogen in the fire box, CO_2, and water vapor. Some unburned hydrocarbons and some CO are also present.

Emissions of CO and unburned hydrocarbons are controlled by proper boiler design. No other control measures are practical at this time. In new boilers, some control of NO_x emissions is possible by appropriate design. Flue gas recirculation to lower combustion temperatures, two-stage combustion that limits the oxygen concentration in the hottest part of the flame, and careful control of excess air can reduce

NO_x emissions by 40-60%. These control techniques have been successfully put into practice on some oil and gas-fired boilers by retrofitting, and have been designed into coal-fired boilers built after 1971 when NO_x limitations were promulgated by the federal government. Additional control of NO_x with those techniques, along with careful burner design, may yield new coal-fired boilers with NO_x emissions 50-70-% lower than the current best practice. The additional NO_x reduction probably will not be available to power plants now in existence, however. Further control of NO_x emissions is possible with flue gas treatment -- catalyzed and uncatalyzed reduction using ammonia, and oxidation with ozone or hypochlorite processes have been partially developed -- but those systems are not likely to be installed on power plants in the near future, because they are generally more expensive than sulfur dioxide control systems. The power plant in Figure VI-1 is assumed to meet currently mandated new source performance standards (NSPS) of 0.30 kg NO_x/GJ (0.7 lb $NO_x/10^6$ Btu) by a combination of good burner design, two-stage combustion and control of excess air.

The fly ash in the flue gas must be removed. For this purpose, wet scrubbers, electrostatic precipitators, and baghouses are the most suitable technologies. Wet scrubbers are not considered further because collecting the fly ash in a dry form has several advantages, an important one being that controlled addition of dry fly ash and certain chemical additives to the sludge, which results from lime or limestone scrubbing of flue gases (for removal of sulfur oxides), solidifies the sludge and significantly aids in its disposal.

Baghouses have not been widely used in power plants because of reliability and maintenance problems. The large space requirements of baghouses have also limited their use. However, western coal, because of its low sulfur content and the composition of its ash, produces a high resistivity fly ash that is difficult to collect using standard electrostatic precipitators. Accordingly, there is increased interest in baghouses. Some plants designed to burn western coal are expected to use precipitators (designed for the high-resistivity fly ash) and some

will use baghouses. The performance of the two is expected to be equivalent, and will readily surpass meet the current Federal NSPS for particulates of 0.043 kg/GJ (0.1 lb/10^6 Btu) by removing 99% of the fly ash from the flue gas.

There are many options for flue gas desulfurization. Lime or limestone scrubbing to produce a solid calcium sulfite and sulfate phase is the most developed technology, and the most likely to be installed in the next 10 years. Double alkali systems and regenerative systems are attractive alternatives and may eventually displace lime or limestone-based systems. The double alkali system uses a soluble base to adsorb SO_2, which has at least two benefits: it avoids much of the pumping and spraying of slurries, as well as scaling, that are associated with lime/limestone systems, and the soluble base is more reactive than lime or limestone, so lower recirculation rates and smaller scrubbers can be used. The regenerative process produces a salable product such as sulfur or sulfuric acid rather than a solid waste (e.g., calcium sulfite or gypsum) that has a limited market potential.

The lime/limestone scrubbing system can easily remove 85% of the sulfur from the flue gases. The system in Figure VI-1 is based on lime, which is more reactive than limestone. The scrubber removes primarily SO_3 and SO_2, but also takes out some flue gas particulates that were not removed by the electrostatic precipitator or baghouse. We have assumed that it removes 50% of the remaining fly ash, which means that the scrubbing slurry is approximately 1% fly ash.

2. Solids Handling System

The recirculating slurry used in the FGD unit is 5-10% solids. A slurry blowdown is required to remove the $CaSO_3$ and $CaSO_4$ resulting from reaction of SO_2 with the added lime. Calcium sulfite is the primary reaction product, but some oxidation of the sulfite to sulfate occurs. Oxidation rates are increased by high O_2/SO_2 ratios, so

western coal, with its low sulfur content, produces a slurry with higher $CaSO_4/CaSO_3$ ratios than the slurry from the desulfurization of high-sulfur coals. The higher calcium sulfate content aids in dewatering the slurry, which facilitates its disposal.

For the system shown in Figure VI-2, we have assumed that 40% of the $CaSO_3$ is oxidized to $CaSO_4$. The slurry can be thickened and dewatered to a 50% solids cake on a rotating vacuum filter, after which it can be mixed with the dewatered bottom ash slurry and the dry fly ash to produce a waste stream containing only 31% water. This solid waste can be handled with front-end loaders and trucks for disposal in the landfill or transported back to the mine in coal cars for disposal in the mine. Care must be exercised in the disposal, because the calcium salts, the heavy metals from the fly ash, and the soluble salts in the cooling tower blowdown can be leached from the material if it contacts groundwaters or surface waters.

Other disposal options include placing the bottom ash and scrubber blowdown slurries in ponds. Settling occurs in the ponds and the clear supernatants can be recycled. The material in the pond bottom is about 50% water. When the ponds are full they can be abandoned as active disposal sites or dredged (the dredged solids are either disposed by landfill or returned to the coal mine). However, abandonment results in land that probably can never be returned to productive use.

Either ponding option is environmentally more risky than the dry handling option because of the potential for pond water to overflow during severe rainstorms or leach through the pond bottom into the groundwater. Currently, no regulations prohibit ponding, but the EPA considers it to be only a temporary solution.

3. Pollutant Emissions

a. Major Pollutants

The major emissions from a coal-fired power plant using the pollution control methods discussed in the preceding sections are shown

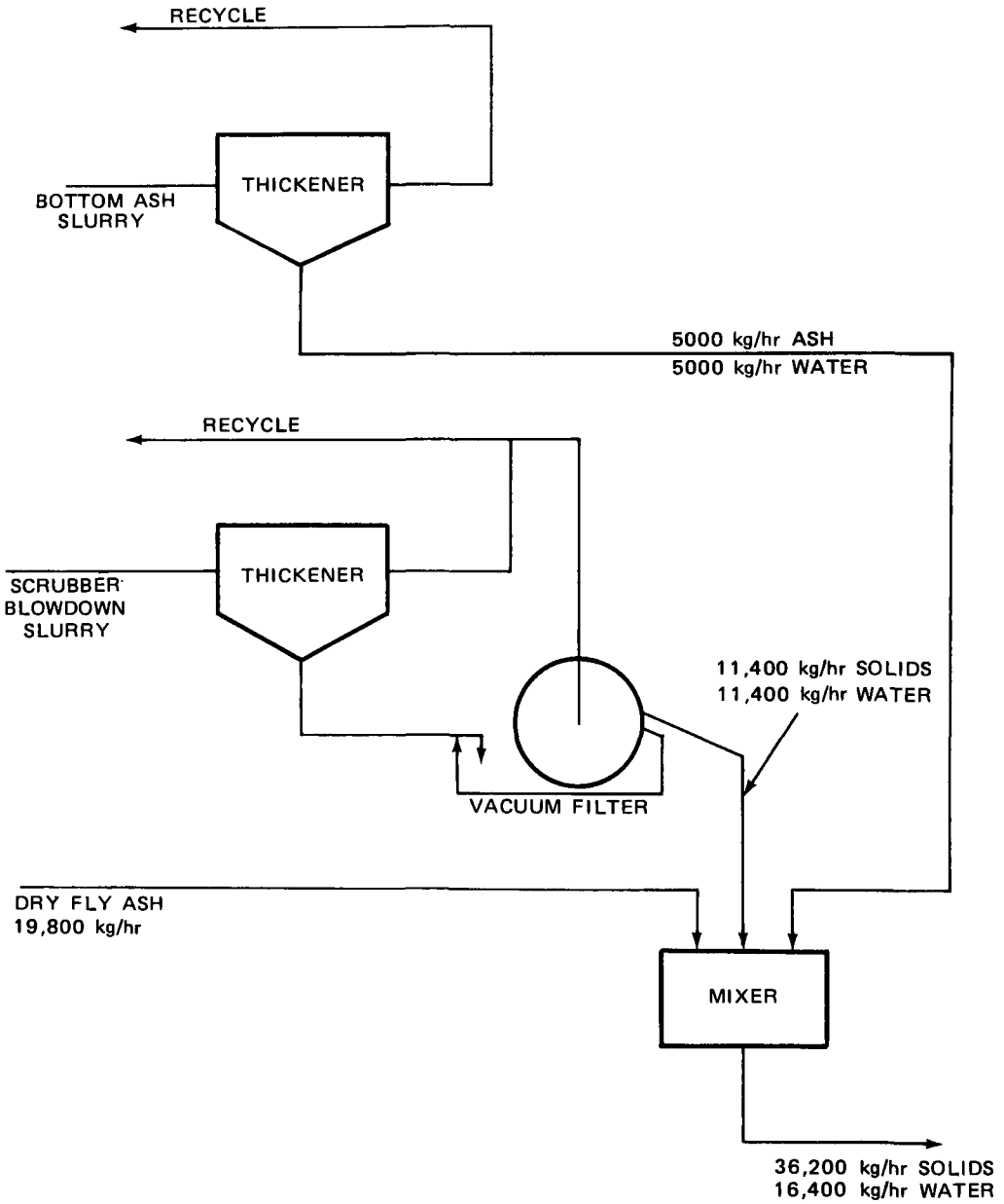

FIGURE VI-2. SOLIDS HANDLING SYSTEM FOR 800 MW COAL-FIRED POWER PLANT

TABLE VI-5

SUMMARY OF MAJOR EMISSIONS FROM AN 800-MW COAL-FIRED POWER PLANT

Source	Uncontrolled Emissions (kg/hr)	Control Method	Control Efficiency (%)	Controlled Emissions (kg/hr)
Steam Boiler				
SO_2 - SO_3	5,200	FGD unit	85	780
NO_x	--	burner design	--	2,560
CO	--	"	--	207
hydrocarbons	--	"	--	62
fly ash	19,900	precipitator plus FGD	99.5	100
Coal Handling				
coal dust	160	bag house	99	1.6
Coal Storage				
coal dust	70	none	--	70
Solids Disposal				
dry FGD solids	11,400	burial in		11,400
dry fly ash	19,800	controlled		19,800
dry boiler ash	4,980	landfill or		4,980
interstitial water	16,400	mine		16,400
Total	52,580			52,580
Water Discharge[a,b]				
suspended solids	--			20
oil and grease	--	neutralization		10
iron	--	and		0.7
copper	--	settling		0.7
chlorine[c]	--			0.3[d]

[a]Recycle pond overflow when cooling tower is operated at low cycles of concentration Concentrations are based on BPCT standards in Reference 5.

[b]Based on 190 liter per second (300 gal/minute).

[c].2 ppm for a maximum of 2 hr/day.

[d]kg/day.

in Table VI-5. We calculated the emissions of SO_2 and fly ash from the known concentrations of sulfur and ash in the coal. The emission of NO_x assumes a burner that meets the Federal NSPS for NO_x of 0.30 kg per GJ (0.7 lb per 10^6 Btu) of fuel combusted. Emissions of CO and hydrocarbons are based on standard emission factors for coal-fired boilers.[2] Fly ash and SO_2 emissions are significantly lower than the current Federal NSPS 0.043 kg/GJ (0.10 lb/10^6 Btu) and 0.52 kg/GJ (1.2 lb/10^6 Btu), respectively. The control methods for those pollutants are designed to meet not only current but also anticipated future emissions standards for coal-fired boilers*.

In addition to the emission pollutants listed in Table VI-5, there are emissions of several types of pollutants not currently subject to regulation but known to have harmful environmental and human health effects. Among these are fine particulates, toxic trace elements and polycyclic aromatic hydrocarbons (PAH), which will be addressed in the following sections.

b. Fine Particulates

The emission of fly ash from coal combustion involves the mobilization of suspended particulate matter (or particulates) ranging in size from greater than 30 microns in diameter to less than 1 micron into the stack gas. However, the removal efficiency of fly ash collection equipment such as the electrostatic precipator tends to decrease with decreasing particle size so that the smaller particulates are preferentially emitted. Small particulates are of concern because they are retained in the lungs. The range of particulate sizes that have the highest lung retention are from about 0.1 to 5 microns in diameter, with

---

*In late 1978, the EPA issued a proposed revised set of NSPS that would require FGD for nearly all coal burned, regardless of sulfur content and would limit NO_x emission to 0.26 kg/GJ (0.6 lb/10^6 Btu) and particulate emissions to 0.013 kg/GJ (0.03 lb/10^6 Btu).

peak retention occurring at around 1 to 2 microns. Particles larger than 5 microns are not retained to any significant degree, and therefore are of less concern as a health hazard.

Measurements of particle size distribution in fly ash from coal combustion have shown that the mass-weighted median diameter for particulates entering an electrostatic precipitator is around 20 microns, while for those exiting the median diameter is 1 to 5 microns. Furthermore, of the entering particulates, only 4 to 10% (by mass) are less than 5 microns in diameter, while about 50% of the exiting particulates are less than 5 microns in diameter.[6] Thus, although electrostatic precipitators may have removal efficiencies for total particulates in excess of 99%, the efficiency for particulates less than 5 microns in diameter is 90 to 95%. Applying those results to the emissions from the 800 MW coal-fired power plant, and adjusting them to the assumed collection efficiency for that plant, yields an emission rate of particulates less than 5 microns diameter of approximately 50 kg/hr.

c. Trace Elements

The emission of trace elements from a coal-fired power plant depends on the concentrations of those elements in the coal as well as on the various physical-chemical processes taking place during combustion and fly ash collection. Certain trace elements tend to be concentrated on fly ash relative to bottom ash, and are concentrated further on the fly ash exiting the electrostatic precipitator. Also, some of the more volatile elements are emitted from combustion as gases and escape the precipitator. Consequently, the emission rate of certain trace elements is higher than one would calculate based on a uniform distribution of trace elements in bottom ash, collected fly ash, and emitted fly ash.

The concentration of several trace elements in Wyoming subbituminous coal is shown in Table VI-6. Although many more trace elements are found in coal, those in Table VI-6 are listed because of their

known toxic effects. The concentrations of trace elements in coal varies widely, and the concentrations in Table VI-6 should be considered representative rather than definitive.

To estimate the rate at which the trace elements listed in Table IV-6 are emitted in the power plant stack gases, one must know the degree to which they are concentrated in the fly ash that escapes the electrostatic precipitator. Of several studies that have been made of the phenomenon, the one that was made under conditions most closely matching the conceptual power plant design of this study was of trace element distribution in a 350 MW power plant burning Wyoming subbituminous coal and using an electrostatic precipitator (99.1% efficiency) for fly ash emission control.[8] That plant's enhancement factors (concentration in emitted fly ash relative to concentration in coal ash) for the trace elements listed in Table VI-6 were as follows: Sb, 5.6; As, 0.071; Be, 2; Cd, 5; Pb, 11; Hg, 140; Se, 54; Zn, 3.7. We assumed that the enhancement factors apply to the electrostatic precipitator only. No further enhancement is assumed for the FGD system, which is assumed to remove 50% of the fly ash exiting the precipitator. In general, trace element emissions depend on the fly ash removal system employed (e.g., baghouses, Venturi scrubbers) as well as the specific properties of the coal and ash.

Table VI-6

CONCENTRATIONS OF SEVERAL TOXIC TRACE ELEMENTS IN POWDER RIVER BASIN COAL

Element	Concentration (ppm wt.)
Antimony (Sb)	0.67
Arsenic (As)	3.0
Beryllium (Be)	0.7
Cadmium (Cd)	2.1
Lead (Pb)	7.2
Mercury (Hg)	0.1
Selenium (Se)	0.73
Zinc (Zn)	33.0

Source: References 7 and 8.

We used the concentration factors plus the total rate of particulate emissions from the power plant to calculate the emission rate of toxic trace elements. The total rate of emission of those elements in the stack gas as well as in the solid waste stream (bottom ash plus collected fly ash) is shown in Table VI-7.

Another source of potential trace element pollution is leaching from the solid waste disposal site. The significance of this problem will depend on the permeability of the soil on site, the amount of annual precipitation, the chemical forms of the trace elements and their resulting solubilities, and the distance to the nearest aquifier. Studies on the leachability of trace elements from coal ash and scrubber sludge have indicated that, of the trace elements listed in Table VI-6, mercury and selenium are the most likely to pose problems.[9]

Regulations proposed under the Resource Conservation and Recovery Act of 1976 for the disposal of hazardous wastes may verylikely be applied to coal combustion wastes. In that case, strict disposal practices would be required.

Table VI-7

EMISSION OF TOXIC TRACE ELEMENTS FROM
AN 800 MW COAL-FIRED POWER PLANT

Element	Emission Rate (g/hr)	
	Solid Waste	Stack Gas
Sb	271	6.2
As	1,240	0.35
Be	287	2.3
Cd	852	17.0
Pb	2,850	130.0
Hg*	1	40.0
Se	282	20.0
Zn	13,450	200.0

*Hg is emitted primarily as a gas. The FGD system is assumed to have no effect.

d. Polycyclic Aromatic Hydrocarbons

The final minor emission of concern from coal combustion is of a class of compounds known as polycyclic aromatic hydrocarbons (PAH). This class includes both known (e.g. benzo(a)pyrene) and suspected carcinogens. The emission of PAH results from incomplete combustion and varies depending on burner type, amount of excess air used, and other process variables. Measurements of the emission of several types of PAH from a coal-fired power plant using a standard front-wall burner and equipped with an electrostatic precipitator have been made.[10] Those results, scaled to the 800 MW size assumed for this study, are shown in Table VI-8.

D. Coal Gasification Plant

A coal gasification plant has the potential for producing more pollution than a power plant that consumes an equivalent amount of coal. There are two major sources of additional pollution: dissolved and suspended solids in process condensates, and organic and sulfur emissions that result from clean up of the synthesis gas before methanation.

Table VI-8

EMISSIONS OF POLYCYCLIC AROMATIC HYDROCARBONS FROM AN 800-MW COAL-FIRED POWER PLANT

Compound	Emission Rate, g/hr
Fluoranthrene	0.61
Pyrene	1.4
Benzo(a)pyrene	0.14
Benzo(e)pyrene	0.18
Benzo(ghi)pyrene	0.053

Source: Reference 10

The production of SNG requires contact of the coal with steam and oxygen at high temperature and pressure. Some of the steam reacts with the coal, but an excess is required to establish favorable reaction conditions. Not all coal, steam, and oxygen reactions yield CH_4, CO and H_2. Tar, oil, light hydrocarbons, aromatics, polycyclic aromatics, cyanide, ammonia, carbonyl sulfide, and hydrogen sulfide are also produced. All those compounds are partially soluble in water. When the gases leaving the gasification reactor are cooled to remove oil and entrained ash, the water and soluble organics and inorganics condense. The soluble materials and the ash must be removed from the water before it can be reused or released to the environment.

The clean-up of the synthesis gas has the potential for releasing hydrocarbons and reduced sulfur compounds such as H_2S and COS to the air. The release of sulfur, if uncontrolled, would be the same as would occur from simply burning the coal, but the reduced sulfur compounds are more objectionable because they are both toxic and malodorous. The hydrocarbon emissions are caused both by losses of solvent in the synthesis gas clean-up step (usually Rectisol or Selexol), and by the hydrocarbon levels in the synthesis gas, which are higher than they would be in flue gas from coal combustion. Some of those hydrocarbons are removed by the gas clean-up solvent and released into process vent streams.

Table VI-9 is a detailed listing of the major sources of air, water, and solid pollution associated with SNG production. Figure VI-3 is a schematic diagram of an integrated system for limiting water pollution, primarily by eliminating discharge to surface waters, minimizing air pollution, and disposing of solid residuals in a form that could be placed in the mined-out area of the coal mine. Proper design choices for the system could limit water discharges to reuse applications and water in the solids stream.

Such a pollution control system contains many features common to the system proposed for the coal-fired power plant. In particular, the cooling tower is used to evaporate excess water and much of the water blowdown from boilers, and ash handling and FGD residuals are contained

Table VI-9

MAJOR SOURCES OF POLLUTION FOR A COAL GASIFICATION PLANT

Medium	Source	Emissions
Air	Boiler and heater stacks	SO_x NO_x CO Hydrocarbons Particulates (fly ash) Trace elements
	SNG Process train (including sulfur recovery plant)	SO_2 H_2S COS Hydrocarbons
	Coal handling and crushing	Coal dust
Solid		
	Gasifier	Bottom ash Char
	Boilers and heaters	Bottom ash
	Flue gas treatment	Fly ash FGD solids
	Sulfur recovery plant	Sulfur
	Coal storage	Coal fines Heavy metal hydroxides
	Wastewater treatment system	Biological solids Heavy metals High molecular weight organic compounds
Water		
	Cooling tower blowdown Water treatment blowdown Boiler blowdown Process condensates	Dissolved solids Suspended solids Heavy metals H_2S HCN Thiocyanate Organic carbon compounds Suspended solids
	Boiler ash handling	Suspended solids Dissolved solids Heavy metals
	FGD system	Dissolved solids Suspended solids
	Coal pile	Dissolved solids (heavy metals) Suspended solids Organic carbon compounds

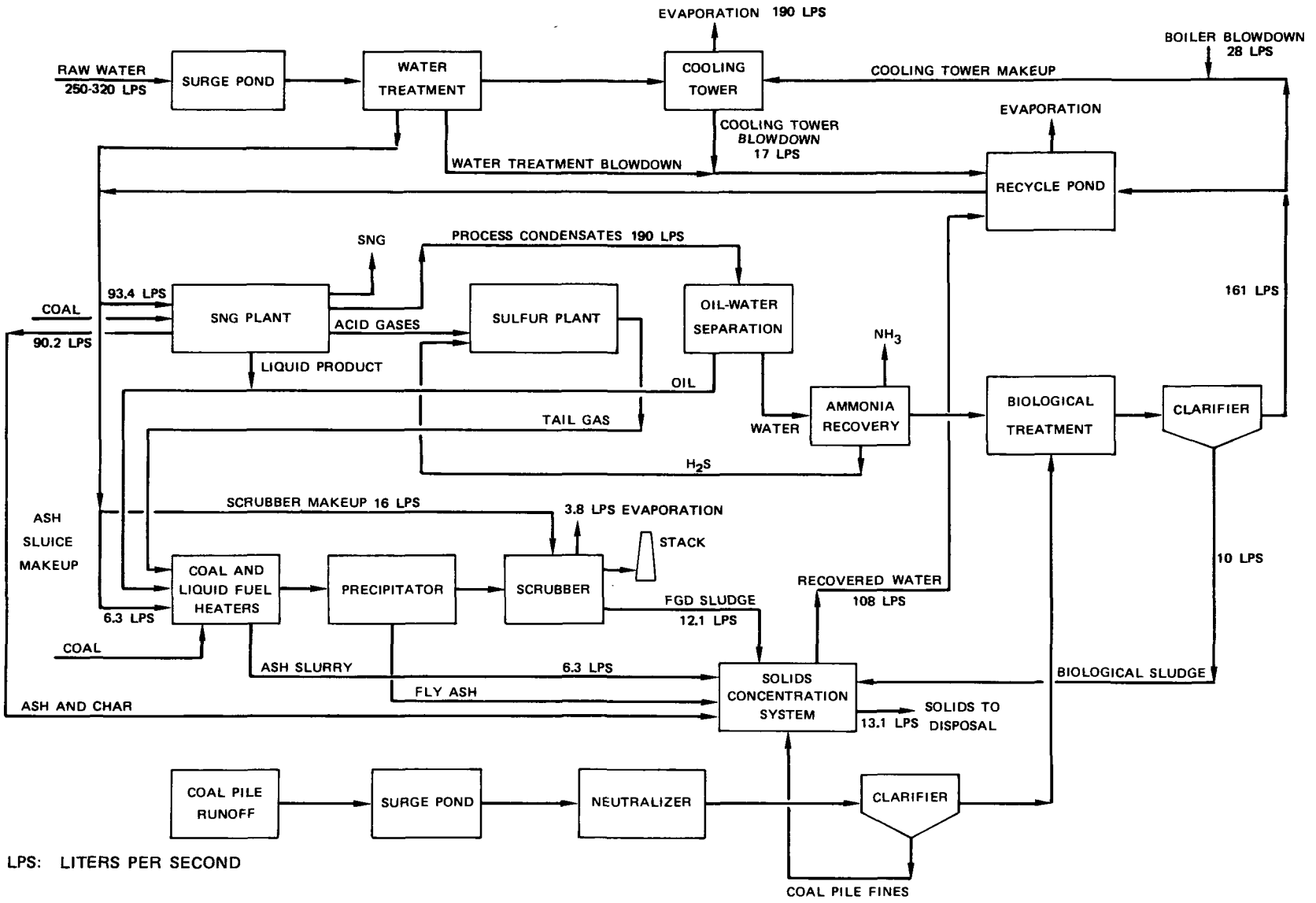

LPS: LITERS PER SECOND

FIGURE VI-3. INTEGRATED AIR, WATER, AND SOLIDS POLLUTION CONTROL SYSTEM FOR A HYGAS COAL GASIFICATION PLANT THAT PRODUCES 7.8 MILLION nm^3 OF SNG PER DAY

in the solids stream that is disposed in the coal mine. The coal gasification plant has a utility plant that burns coal and liquid hydrocarbons to generate power, steam, and process heat. The flue gases from those combustion operations are treated to remove particulates and sulfur in the same manner as for the power plant in Section VI-C. Coal pile runoff and particulate emissions from the coal pile and grinding and drying are handled in the same way as they were for the power plant.

The two major additions to the pollution control system are a sulfur recovery plant and its associated tail gas treatment system, which treats sulfur-containing gases produced by synthesis gas cleanup and by the process condensate treatment system.

1. Sulfur Recovery Plant

The raw synthesis gas produced by gasification contains reduced sulfur compounds, primarily H_2S, and an excess of CO_2 in addition to the required H_2 and CO. All sulfur compounds must be removed before the synthesis gas can be converted to methane. Numerous processes have been proposed to remove the CO_2 and H_2S, which together are called acid gases. The processes include scrubbing with molten carbonates, scrubbing with amine solutions such as diethanolamine (DEA), and scrubbing with organic solvents such as methanol. The process proposed for all commercial-sized gasification plants is the Rectisol process which uses refrigerated methanol. The Rectisol process makes use of the different solubilities of H_2S and CO_2 in methanol to separate the acid gases into three product streams (in addition to the purified synthesis gas) -- an H_2S-free stream which contains CO_2 and hydrocarbons, an H_2S-rich stream which contains most of the H_2S (10-15% by volume) as well as some CO_2 and methanol, and an H_2S-lean stream (1-2% by volume), that contains much of the CO_2 and some hydrocarbons. The process can be operated to concentrate more than half of the CO_2 in the stream that is free of H_2S.

Downstream treatment of those three streams to remove the sulfur involves a choice of two commercially proven processes, Claus and Stretford. The Claus process can remove 95% of the H_2S in a stream, along with much of the COS. However, it requires minimum input concentrations of 10-15% H_2S. The H_2S-rich stream produced by the Rectisol process could be treated by a Claus process, which removes some COS and most H_2S (about 90% at the low concentration in the H_2S-rich stream). The Stretford process is more versatile and could treat the H_2S-lean stream; however, it is difficult to operate, materials such as the cyanate and thiosulfate are formed by chemical reactions in the Stretford solution and require a purge and make-up to maintain the solution activity, and it will not remove COS. Neither process removes hydrocarbons. A treatment sequence to achieve low levels of sulfur emission as well as control of hydrocarbons would involve Claus treatment of the H_2S-rich stream (because that stream contains most of the COS). The Stretford process would be used to treat the H_2S-lean stream, followed by incineration of both tail gases. The H_2S-free stream would be vented to the atmosphere. Incineration destroys the hydrocarbons and converts reduced sulfur compounds such as H_2S and COS to SO_2. Such a treatment sequence would allow an SNG plant to meet the hydrocarbon and sulfur NSPS for gasification proposed by the EPA, but not more stringent standards such as those proposed by New Mexico. Best available technology, which would bring the plant into compliance with the most stringent regulations proposed, would involve removal of SO_2 from the incinerated tail gases. There are a number of tail gas treatment systems such as Scot (Shell Development Co.) and Beavon (Union Oil Co.), but a simpler procedure would be to use an SO_2 scrubber.

The pollution control system shown in Figure VI-3 achieves both incineration and SO_2 scrubbing of the sulfur plant tail gas by routing it to the utility plant. Incineration of the tail gas would require energy equivalent to several percent of the product SNG, so that incineration should not be practiced without heat recovery. Incineration can be achieved most easily by using the oil-fired process heaters or steam boilers as incinerators. The incinerated tail gas is then

routed with the flue gas through the utility plant SO_2 scrubber. The sulfur plant tail gas is small relative to the utility flue gases, so the impact on the design of the flue gas treatment system is small. The treatment sequence is expected to remove more than 98% of the sulfur in the acid gases (90% in the sulfur plant and 85% of the remainder in the SO_2 scrubber).

2. Process Condensate Treatment System

The process condensates come from three principal sources: quenching and scrubbing of the raw synthesis gas to remove oils and ash carryover; condensation after shifting; and cooling of the synthesis gas by the Rectisol process. After removal of the ash, the condensates contain hydrogen sulfide and ammonia, thiocyanates, phenols, aromatic and fatty acids, acid tars, oil, light hydrocarbons, heavy metals, and small amounts of suspended solids. The oil fractions can be separated and removed by skimming, which leaves behind parts per million quantities (solubility limit) of the various components, as well as some colloidal oil and tar. Many of those compounds are polycyclic aromatic hydrocarbons, and are considered carcinogenic.

In the Lurgi gasifiers that have been operated commercially, the condensates contain large amounts of phenols (approximately 5 kg/tonne of coal gasified), which are removed by extraction. The condensates from the Synthane demonstration process contain phenols and water-soluble acid tars that can also be removed by extraction. The Hygas reactor, however, produces less than half of the phenols that the Lurgi reactor does. As a result, some full-scale designs for Hygas omit the extraction step. The phenol concentration in the pooled condensate stream is only several hundred ppm, which makes it a suitable feed for a biological treatment system.

Besides phenol, the other principal components of some of the condensates are H_2S and ammonia, which can be readily removed by steam

stripping. Many plant designs call for separating the ammonia from the sulfide during stripping; the ammonia is sold as a by-product and the sulfide routed to the sulfur plant for recovery. The stripping operation also removes many of the volatile hydrocarbons from the condensates; some are recovered as a recycle oil, and many are burned when the sulfur plant tail gas is incinerated.

The condensate treatment system in Figure VI-3 includes a solids/water/oil-tar separation step, steam stripping to recover ammonia and H_2S and biological treatment. The treated water can be used for several kinds of recycle and reuse applications. The water is not clean enough to be used as process water, and could not be economically used for boiler make-up. It would, however, be suitable for cooling tower make-up or dust control on mine roads, coal piles, etc., and might even be useful for revegetation, although continued use as irrigation water is not recommended because of the probable presence of sulfate and chloride salts.

Because of the carcinogenic potential of both the heavy metals and polycyclic aromatics, as well as the potential for the release of volatile organics through this treatment sequence, Figure VI-4 shows the treatment sequence in more detail, where it is evident that:

- The sour water stripper removes most of the volatile organics.
- Flocculation and clarification prior to biological treatment removes many of the heavy metals, much of the colloidal tar and oil, and polycyclic aromatics, which are highly insoluble.
- Biological treatment removes phenol and most of the biologically degradable organic carbon. Organics with a high molecular weight, including polycyclic aromatics, are adsorbed onto the biological solids and removed from solution. Heavy metal levels are reduced to their solubility limit at pH 7 by adsorption of the metal hydroxide colloids on to the biological solids.

As a result, the final treated water is well oxidized and relatively free of heavy metals and organics with high molecular

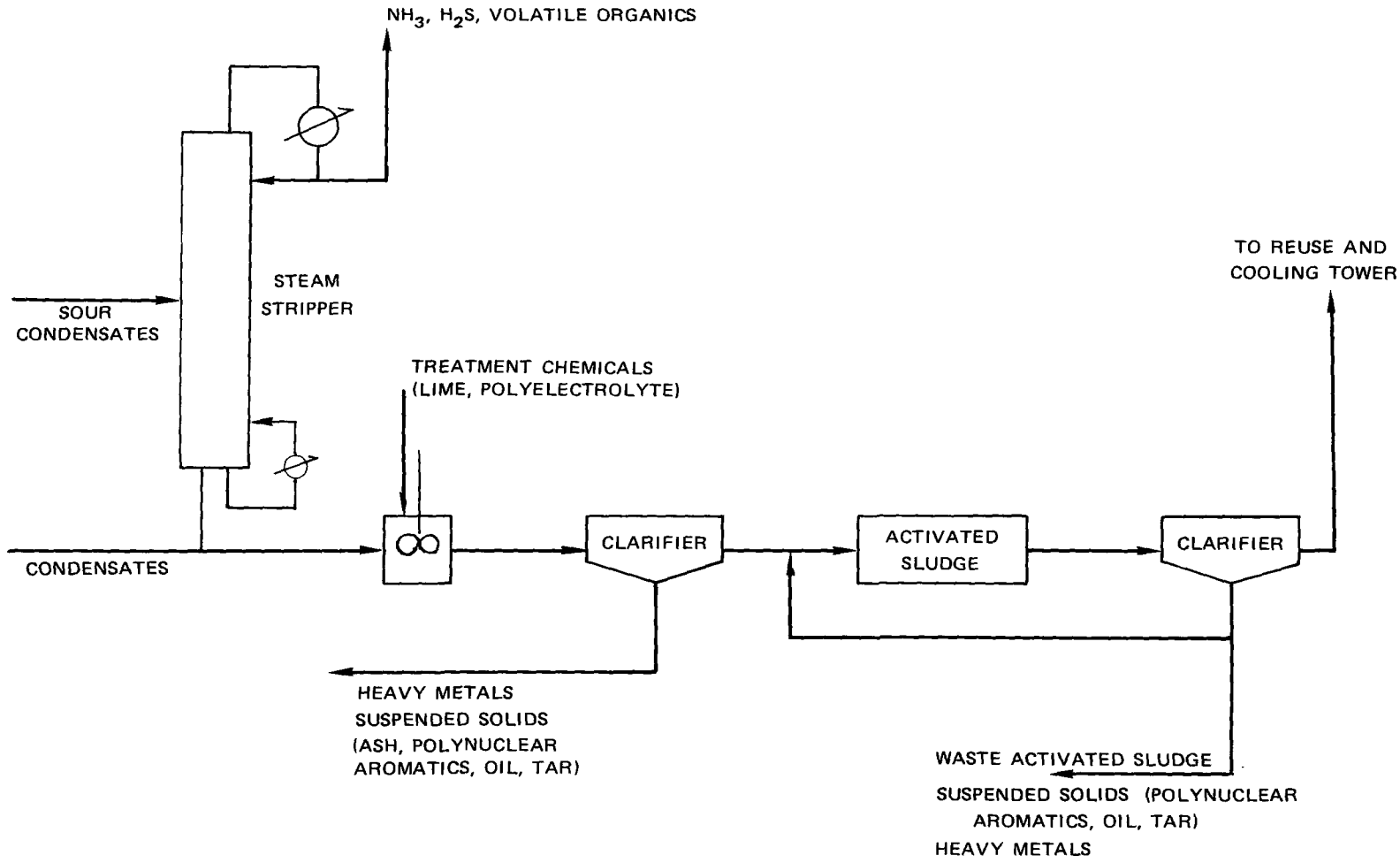

FIGURE VI-4. WASTE WATER TREATMENT PLANT FOR COAL GASIFICATION

weights. Release of those compounds to the environment during reuse or drift and evaporation losses from the cooling tower is small.

3. Solids Processing System

The solids processing system is similar to the design used for the coal-fired power plant. Dewatered calcium sulfate-calcium sulfite from the FGS system is mixed with dewatered ash from the gasifier, dewatered ash from the condensate treatment system, dewatered sludge from the biological treatment system, and dry fly ash to produce a solids stream containing approximately 40% water. The solids stream can be placed in the mine provided it has no contact with surface or ground waters. If the solids did contact water, they would be a source of heavy metal and organic carbon pollution.

4. Pollutant Emissions

The major pollutant emissions from the Hygas coal gasification plant, assuming the controls discussed in the previous section, are shown in Table VI-10. The emission of regulated pollutants (SO_2, NO_x, particulates) from the utility plant are all in compliance with Federal NSPS for coal- and oil-fired boilers. Federal standards for coal gasification do not exist, although standards have been proposed by EPA for sulfur and hydrocarbon emissions from the gasification train (excluding fuel combustion in the utility plant) for first generation Lurgi technology.[13] The emissions shown in Table IV-10 more than meet those standards by using sulfur plant tail gas incineration and scrubbing. The emission of methane/ethane hydrocarbons with the CO_2 vent stream is not affected by the proposed regulation because it applies only to non-methane, non-ethane hydrocarbons. No separate regulations have been proposed for COS, and the sum of COS and SO_2 from the tail gas does not exceed the proposed sulfur emission standard.

No emission of water pollutants is shown in Table VI-10 because all wastewater is treated and recycled for use within the plant, resulting in zero discharge of wastewater from the plant site.

Emissions of other pollutants not listed in Table VI-10 are discussed below.

a. Other Combustion-Related Emissions

The emissions of fine particulates, trace elements, and PAH from the combustion of coal in the utility plant are similar to those calculated for the 800 MW coal-fired power plant, because combustion conditions are similar and we have assumed identical control devices. The resulting emissions of those pollutants are shown in Table VI-11.

The other source of combustion emissions is the use of byproduct oil as boiler fuel. That oil resembles a light distillate fuel oil, and has a very high content of C_6+ aromatics. The amount of ash and trace elements contained in the oil are almost impossible to quantify, but are likely to be very small compared to the feed coal. We assume the oil has a sulfur content of 0.1%. Particulates emitted from oil combustion are mainly in the form of fine soot resulting from incomplete combustion. Such particulates are on the order of a few tenths to several microns in diameter. Thus, all particulate emissions from oil combustion are in the fine particulate category (less than 5 microns in diameter).

The emissions of PAH from various types of oil burners have been measured.[14] We assume that the results from a steam-atomized burner (the most commonly used type) apply to the combustion of the byproduct oil. The higher-than-normal content of aromatics in the oil may result in a higher content of PAH in the flue gases, but we cannot quantify the effect.

TABLE VI-10

MAJOR EMISSIONS FROM HYGAS COAL GASIFICATION PLANT
(7.8 MILLION nm^3 OF SNG PER DAY)

Source	Emissions Without Control Devices: Type	Emissions Without Control Devices: Rate (kg/hr)	Control Method: Device	Control Method: Efficiency (%)	Emissions Remaining With Best Control: Rate (kg/hr)
Utility plant					
Coal combustion	Particulates	3,150	Precipitator, FGD	99.5	16
	SO_2	820	FGD unit	85	120
	NO_x	--	Burner design	--	400
	Hydrocarbons	--	Burner design	--	10
	CO	--	Burner design	--	32
Fuel oil combustion	Particulates	45	FGD unit	50	23
	SO_2	43	FGD unit	85	6.4
	NO_x	--	Burner design	--	130
	Hydrocarbons	--	Burner design	--	25[a]
	CO	--	Burner design	--	17
Acid gas removal/ sulfur recovery					
Tail gas	Sulfur	3,550	Claus & Stretford Units	90	
			FGD	85	110(SO_2)
	Hydrocarbons	-- [b]	Incineration	--	-- [b]
CO_2 vent	COS	14[c]	None	--	14
	Hydrocarbons	6,800[d]	None	--	6,800
Coal pile	Coal dust	120[e]	None	--	120
Coal handling and crushing	Coal dust	270[f]	Baghouse	99	3
Solid waste disposal	Fly ash	3,100			3,100
	Boiler ash	790	Burial		790
	Gasifier ash	49,100	in		49,100
	FGD solids	2,200	Controlled		2,200
	Biological solid	1,800	Landfill or		1,800
	Interstitial wtr	47,300	Mine		47,300
	Total	104,300			104,300

[a]Assumes fuel oil combustion/tail gas incineration results in hydrocarbon emissions equal to 50 ppm of combined fuel oil and tail gas combustion exhaust stream.

[b]Included in hydrocarbon emissions from fuel oil combustion/tail gas incineration.

[c]Assuming 35 ppm in CO_2 vent gas.

[d]Primarily methane and ethane.

[e]From Reference 2 emissions for gravel and aggregate.

[f]From Reference 13.

The emissions of fine particulates and PAH from oil combustion are shown in Table VI-11, along with those from coal combustion. The total combustion-related emission of those pollutants from a coal gasification facility is also shown.

Table VI-11

COMBUSTION-RELATED EMISSIONS OF FINE PARTICULATES, TRACE ELEMENTS AND POLYCYCLIC AROMATIC HYDROCARBONS FROM THE HYGAS COAL GASIFICATION PLANT

Pollutant	Emissions, g/hr		
	Coal	Oil	Total
Fine particulates	8,300	22,700	31,000
Trace elements			
Sb	0.98	-	0.98
As	0.06	-	0.06
Be	0.36	-	0.36
Cd	2.7	-	2.7
Pd	21.0	-	21.0
Hg	6.3	-	6.3
Se	3.2	-	3.2
Zn	32.0	-	32.0
Polycyclic aromatic hydrocarbons			
Fluoranthrene	0.10	0.25	0.35
Pyrene	0.22	0.28	0.50
Benzo(a)pyrene	0.02	0.04	0.06
Benzo(e)pyrene	0.03	-	0.03
Benzo(ghi)pyrene	0.01	-	0.01
Benzo(a)anthracene	-	1.7	1.7
Phenanthrene	-	0.03	0.03

b. Other Potential Emissions

The integrated pollution control system illustrated in Figure VI-3 is designed to concentrate all liquid and solid waste effluent streams into a single solid waste stream which minimizes the handling and disposal problems associated with multiple waste streams, many of which contain toxic materials. Of particular concern are the wastewater streams that contain such contaminants as cyanides, toxic organics, and PAH. Although most carbon compounds of concern are likely to be removed in the biological treatment ponds, PAH are not as susceptible to biological degradation as other organics, and might pose a health hazard in the effluent discharge. Toxic trace elements are also of concern in effluent streams. Many of these are likely to be mobilized into the gas phase at the high temperatures found in the gasifier, and measurements of the trace element content of solid residues from Hygas coal gasification indicate that this is the case.[15] The fate of those mobilized elements is not known, although most of them, except for the most volatile, are likely to be removed in the various condensate streams downstream of the gasifier. In that case, they would ultimately end up in a single, concentrated solid waste stream. Some of the more volatile elements, such as mercury, might end up in the synthesis gas stream, in which case they could be condensed into the Rectisol cold methanol stream and be reemitted with the CO_2 vent gas or sulfur plant tail gas, or they could find their way into the product SNG stream. Such effects are nearly impossible to quantify until actual measurements are made on an operating plant. Fugitive emissions of toxic gases may also be a significant problem, but again, they are nearly impossible to quantify.

Overall, the most significant environmental control problem will be the disposal of the concentrated solid waste stream which will contain nearly all of the toxic and potentially carcinogenic chemicals. Because of the potential for leaching of those materials from the solid waste, its disposal must be carefully controlled. Burial in mined-out areas of the surface mines has been proposed as a solution, but only if

there are no nearby aquifiers that can be contaminated. Because of the occurrence of near-surface aquifers in many coal regions of the West, more stringent disposal requirements are likely to be imposed under the Resource Conservation and Recovery Act and other regulations. These could include the use of controlled disposal ponds lined with clay or other impermeable materials.

E. Coal Liquefaction Plant

A coal conversion plant that produces liquid hydrocarbons is similar in many respects to an SNG plant. Coal is contacted with hydrogen under conditions of high temperature and pressure to convert it to liquid and gaseous hydrocarbons. The coal char remaining from liquefaction is used to produce hydrogen by gasifying it with steam and oxygen in a separate reactor. Therefore, the major difference between a gasification and liquefaction plant is that during gasification the reactions of steam, oxygen, and coal to produce hydrogen and the reaction of hydrogen with coal to produce liquid and gaseous hydrocabons take place in one reactor, whereas in a liquefaction plant they take place in separate reactors and under different conditions.

Because the overall reactions are similar, the wastes produced are similar to those produced in an SNG plant. Table VI-12 summarizes the major pollutants produced by the various processing operations. The emission sources listed are similar to those for SNG except that H-Coal requires a coal drying operation as part of the coal preparation step.

1. Pollution Control System

The important pollution control systems for this plant complex are the sulfur plant, the flue gas treatment system, the wastewater treatment system, and the solids handling system.

Table VI-12

MAJOR SOURCES OF POLLUTION FOR A COAL LIQUEFACTION PLANT

Medium	Source	Emissions
Air	Boiler and heater stacks	SO_x
		NO_x
		CO
		Hydrocarbons
		Particulates (fly ash)
		Trace elements
	Coal handling and drying	Particulates
		SO_2
		NO_x
		Hydrocarbons
		CO
Solid	Boilers and heaters	Bottom ash
		Fly ash
		FGD solids
	Water treatment	Suspended solids
	Hydrogen plant	Ash and char
	Sulfur recovery plant	Sulfur
	Coal pile	Coal fines
		Heavy metal hydroxides
	Waste water treatment system	Biological solids
		Heavy metals
		High molecular weight organic compounds
Water	Cooling tower blowdown	Dissolved solids
	Water treatment blowdown	Suspended solids
	Boiler blowdown	Heavy metals
	Process condensates	H_2S
		HCN
		Ammonia
		Thiocyanate
		Organic carbon compounds
		Suspended solids
	Boiler and hydrogen plant ash handling	Suspended solids
		Dissolved solids
		Heavy metals
	FGD system	Dissolved solids
		Suspended solids
	Coal storage	Dissolved solids (heavy metals)
		Suspended solids
		Organic carbon compounds

The sulfur plant is much simpler than required for SNG production because the major gases requiring treatment to remove sulfur are produced in the H-Coal reactor where only coal, hydrogen, and hydrocarbons are present. The gas stream produced is not diluted with CO_2, and a simple amine scrubber can be used to produce a very concentrated H_2S stream. In addition, the conceptual design of the H-Coal plant uses a different strategy for cleanup of the synthesis gas produced by the gasifier than was used in the SNG plant design. In H-Coal, H_2S (and some CO_2) is removed by an amine scrubber, and the gas is then shifted to convert CO to CO_2 and steam to hydrogen. Most of the CO_2 is removed after shifting. In an SNG plant, on the other hand, the synthesis gas is shifted first, before any H_2S is removed; then both H_2S and CO_2 are removed in a single step using Rectisol or Selexol. As a result of the H-Coal strategy, the H_2S-rich stream (a combination of the H_2S streams from the two amine scrubbers) is over 30% H_2S, which is a suitable feed for a Claus plant, and there is no H_2S-lean stream requiring treatment in a Stretford plant. Tail gas treatment includes incineration and lime/limestone scrubbing to control hydrocarbon, H_2S, and COS emissions. Incineration is accomplished with heat recovery using fuel gas produced by the liquefaction reaction, and scrubbing is accomplished using the utility plant scrubbers. The flue gas treatment system is the same as was used for the SNG and power plant cases.

The wastewater treatment plant is similar to the one proposed for the SNG plant. Process condensates are skimmed to remove liquid hydrocarbons (tars and oils), settled to remove suspended ash and soot, and steam stripped to remove H_2S and ammonia. The ammonia is recovered as a product and the H_2S is sent to the sulfur plant. The water still contains thiocyanates, phenols, aromatic and fatty acids, heavy metals, and polycyclic aromatic compounds. The organic material is probably both qualitatively and quantitatively different from the organic material produced by a SNG plant because of processing differences, but very little data exist to confirm this. We have assumed that no soluble organic materials (phenol in particular) are present in amounts that can be economically recovered.

The wastewater treatment plant is designed to flocculate and remove suspended solids and heavy metals using lime and organic polymers, and to biologically oxidize the organic material. After the treatment sequence of stripping, flocculation, and biological oxidation, the process condensates, which are free of heavy metals, polycyclic aromatics, and volatile organic compounds, are suitable for cooling tower make-up or dust control in the mine or in coal preparation.

The solids handling system is the same as for SNG. The solids stream produced for disposal is approximately 40% water, making it easy to handle. Burial must be in a place suitable for hazardous materials, because the soluble materials in the solid stream could pollute both surface and ground waters.

Figure VI-5 shows the integrated water, air, and solid pollution control system. The water flows are approximate and show only the major water evaporation and water recycle loop. Evaporation losses in the recycle pond and in the ash quenching operations have been neglected. The cooling tower evaporates water at a rate of 132 liters/sec (2,100 gal/min), and the scrubber evaporates 7.6 liters/sec (121 gal/min). The only water discharge is 9.9 liters/sec (157 gal/min) carried away in the combined solids stream (FGD solids, fly ash, boiler bottom ash, hydrogen plant slag, and waste activated sludge from biological treatment). If this stream is buried in the mine under conditions where it contacts neither surface nor underground waters, the plant has zero discharge of water. (The water balance is not exact, but we constructed it using reasonable assumptions to demonstrate that zero discharge is possible for this type of plant.)

The neglected streams include approximately 25 liters/sec (400 gal/min) of boiler blowdown, which will be balanced by evaporation during quenching operations and evaporation from the recycle pond. Additional water inputs to the plant include approximately 76 liters/sec (1,200 gal/min) for dust control on roads and in the mine 95 liters/sec (1,500 gal/min) boiler feed water, and 19 liters/sec (300 gal/min) for

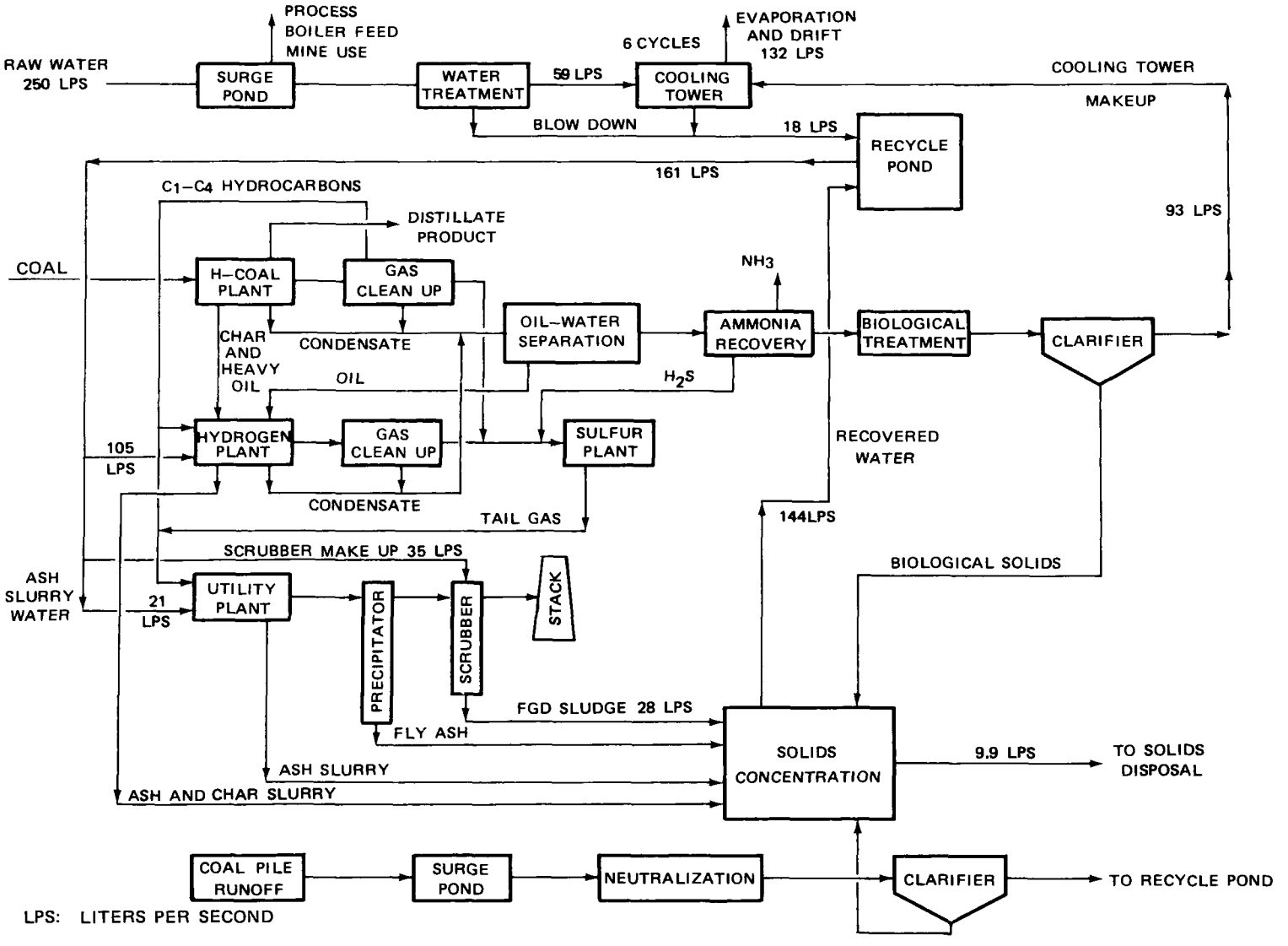

FIGURE VI-5. INTEGRATED POLLUTION CONTROL SYSTEM FOR AN H-COAL LIQUEFACTION PLANT THAT PRODUCES 7950 m^3 PER DAY OF FUEL

showers, washrooms, and miscellaneous process uses, resulting in a total water consumption of 250-320 liters/sec (4,000-5,000 gal/min).

2. Pollutant Emissions

The major pollutant emissions for an H-Coal liquefaction facility are summarized in Table VI-13. As in the case of the coal gasification plant, the control devices for coal and by-product gas combustion in the utility plant will meet or exceed current NSPS. There are currently no standards or proposed standards for coal liquefaction. However, the level of controls specified for sulfur recovery and subsequent tail gas treatment should more than meet any likely standards.

No water pollutant emissions are shown in Table VI-13 because the treatment system has been designed to achieve zero discharge.

a. Other Combustion-Related Emissions

The combustion of coal and by-product gas in the utility plant results in the emission of fine particulates, trace elements, and PAH. The emissions from coal combustion are analogous to those from the coal-fired power plant. For gas combustion, no significant quantities of trace elements should be emitted. However, fine particulates resulting from incomplete combustion and some PAH are emitted.[14]. The emissions of those pollutants from both coal and gas combustion, and the totals from the two sources, are shown in Table VI-14.

b. Other Potential Pollutants

As in the case of coal gasification, most of the effluent streams containing toxic waste products are combined and concentrated into a single solid waste stream that must be carefully disposed of.

TABLE VI-13

MAJOR EMISSIONS FROM H-COAL LIQUEFACTION
($7,950\ m^3$ OF DISTILLATE FUEL OIL PER DAY)

Source	Emissions Without Control Devices: Type	Emissions Without Control Devices: Rate (kg/hr)	Control Method: Device	Control Method: Efficiency (%)	Emissions Remaining With Best Control: Rate (kg/hr)
Utility plant Coal combustion	Particulates	7;690	Precipitator	99	39
	SO_2	2,000	FGD	85	300
	NO_x	990	Burner design	--	990
	Hydrocarbons	24	Burner design	--	24
	CO	80	Burner design	--	80
Fuel gas combustion	Particulates	7.3	FGD	50	3.6
	SO_2	--	--	--	--
	NO_x	210	Burner design	--	210
	Hydrocarbons	2.2[a]	Burner design	--	2.2
	CO	12	Burner design	--	12
Coal dryer	Coal dust	6,320	Multiple cyclones & venturi scrubber	99	63
Acid gas removal/ sulfur recovery	Sulfur	4,390	Claus Unit	95	
			FGD	85	66(SO_2)
	Hydrocarbons	-- [b]	Incineration	--	-- [b]
Coal pile	Coal dust	180[c]	None	--	180
Coal handling & crush	Coal dust	410[d]	Baghouse	99	4.1
Solid waste disposal	Fly ash	7,700			7,700
	Boiler ash	1,900	Burial		1,900
	FGD solids	5,200	in		5,200
	Hyd.plant slag	58,300	Controlled		58,300
	Biological Solid	1,800	Landfill		1,800
	Interstitial wtr	35,800	or Mine		35,800
	Total	110,700			110,700

[a]Tail gases are a minor component in flue gas. Hydrocarbon emission is the standard factor for gas-fired boiler.

[b]Included in emissions from fuel gas combustion/tail gas incineration.

[c]From Reference 2 emissions for gravel and aggregate.

[d]From Reference 13.

Although no quantitative measurements have taken place, the amount of higher molecular weight organics produced in coal liquefaction are likely to be greater than in coal gasification, because the process conditions for coal liquefaction are designed precisely for producing a wide range of liquid hydrocarbons, while coal gasification process conditions are designed to maximize the production of methane, carbon monoxide, and hydrogen. Many types of PAH are likely to be found in the coal liquefaction product, which contains a large fraction of aromatics. There is some concern over the release of those compounds during combustion in various end use applications. The effects have not been quantified, however.

Table VI-14

COMBUSTION-RELATED EMISSIONS OF FINE PARTICULATES, TRACE ELEMENTS AND POLYCYCLIC AROMATIC HYDROCARBONS FROM AN H-COAL LIQUEFACTION PLANT

	Emissions (g/hr)		
Pollutant	Coal	Gas	Total
Fine particulates	20,100	3,600	23,700
Trace elements			
Sb	2.5	-	2.5
As	0.14	-	0.14
Be	0.94	-	0.94
Cd	6.9	-	6.9
Pb	16.0	-	16.0
Hg	53.0	-	53.0
Se	8.1	-	8.1
Zn	81.0	-	81.0
Polycyclic aromatic hydrocarbons			
Fluoranthrene	0.25	0.26	0.51
Pyrene	0.57	0.35	0.92
Benzo(a)pyrene	0.06	0.02	0.08
Benzo(e)pyrene	0.07	0.04	0.11
Benzo(ghi)pyrene	0.02	-	0.02
Coronene	-	0.03	0.03
Phenanthrene	-	0.18	0.18

The effluent stream with the largest concentration of organics (and probably trace elements) is the sour process condensate from the H-Coal reactor. It is treated in an oil separation unit, and steam stripped for removal of ammonia and H_2S before being sent to the biological treatment ponds. Ultimately, the residue from that stream is combined with the solid waste stream for disposal and the treated water will be recycled to the cooling towers.

Other air emission sources around the plant include fugitive emissions from high pressure vessels and piping and emission of hydrocarbons (mostly methane and ethane) with the CO_2 vent streams from acid gas removal in the hydrogen plant. Such emissions have not been quantified, however.

F. Pipelines

The environmental factors associated with pipeline construction and operation are physiography, hydrology, vegetation, wildlife, and air quality. Within the context of each of these divisions, the various impacts of construction, operation, and maintenance are discussed below.

1. Physiography

The types of soil found within the various regions crossed by the pipeline routes are important because the pipelines are constructed below ground. Construction actions that create temporary or permanent soil alteration include access road construction, vegetation clearing, trenching, blasting, materials storage/stockpiling, equipment movement, and backfilling. The operation and maintenance activities that affect soil conditions are access road maintenance, regulation control, and facility repair. The environmental impacts of most concern are compaction and subsidence, slope stability, and surface erosion.

During the right-of-way construction processes, the vegetation is removed and the soil is laid bare. Potential revegetation of this stripped area is highly variable. Prior to regrowth, the right-of-way strip approximates a continuously fallow condition and is much more sensitive to erosion than the natural state. The area subject to damage is determined by the width of the construction right-of-way, which typically is 30 m (100 ft.).

Heavy equipment movement has an adverse effect on the soils by creating gullies and subsequent erosion. Where regional slope erosion has not been a problem in the past and where revegetation or land use has precluded erosion, no serious effects are apt to occur.

The stream and river bank erosion at river crossings depends on the nature of the river and the composition of the bed and bank materials. However, because problems of this nature generally have engineering solutions, mitigation is generally possible.

Carefully planned pipeline construction usually does not cause or add to existing slope stability problems. However, two general categories of possible slope stability hazards must be considered: (1) existing unstable slopes whose future stability or instability depends on specific soil structure and slope details; and (2) some steep slopes not involved in past sliding action may, nonetheless, be unstable and therefore potential slide areas.

However, soil slide masses exist and should be considered potentially troublesome ground during construction. Many old soil slides continue to move downhill intermittently or, in some cases, continuously, in a slow, glacier-like fashion. If the rock and soil composing the slide mass are relatively loose and fragmented, the potential for slide tends to increase.

Other problematical soil conditions are those soils with a high water table and those with low fertility. Both of these conditions pose

environmental problems if disturbed. The soils with high water tables have a high potential for adverse change in the physical and biological environment. Disturbance of very low fertility soils has adverse implications for the speed of revegetation.

2. Hydrology

The potential for creating environmentally adverse effects are high when pipelines are constructed across streams, rivers, and lakes. Pipeline construction, operation, and maintenance can have a detrimental effect on existing water resources, and thus on vegetation cover, wildlife habitat, and the recreation. Construction activities that can affect hydrologic resources are access roads, access canals, vegetation clearing, trenching and dewatering, blasting, equipment movement, dredging, structures, and waste disposal. Operation and maintenance activities that can impact hydrologic resources are access road maintenance, access canal maintenance, vegetation control, liquid release, and facility repair.

Areas of major environmental concern include lakes and rivers or stream crossings, surface water conditions, and groundwater. Crossings above the high water level are not aesthetic. In addition, the construction of a pipeline on fill and/or pier supports in a lake or river adversely affects the water quality by increasing water turbidity, thus reducing the value of the lake or river as a recreational resource. Another impact, not as severe, occurs when pipelines and access roads are constructed near lake or river shores.

Existing surface water conditions affect the pipe and its maintenance requirements. Excessive turbidity downstream reduces the penetration of light into the water and reduces the photosynthetic activity of submerged vegetation. Excessive sediment loads in streams having gravel or rubble-type bottoms are damaging to trout and salmon because the sediment fills the interstices of the gravel or stones on the streambed, thus eliminating spawning grounds.

Dewatering of trenches and other excavations is difficult where the water table is near the ground surface and aquifer permeability and porosity is high. Dewatering operations can cause significant effects on aquifer compaction (which may lead to ground subsidence), interference with water supplies, and changes in the water table affecting vegetation and wildlife habitat near the right-of-way.

3. Vegetation

The type of vegetation a pipeline right-of-way crosses is extremely important in its influence on wildlife habitat, economic resources, visual perception and land use. Removal or destruction of vegetation related to the constuction, operation, and maintenance phases is one of the most obvious environmental impacts, particularly because of the complex relationships between vegetative cover and the other factors.

Construction activities that lead to temporary or permanent destruction or alteration of vegetation are the creation of access roads, vegetation clearing, trenching, materials storage/stockpiling, equipment movement, backfilling, structures, and waste disposal. Operation and maintenance activities that affect the vegetative cover are access road maintenance, vegetation control, facility repair, and right-of-way abandonment. Specific impacts resulting from pipeline-related activities are dependent on the type of vegetation crossed by the pipeline (natural resource areas, wetlands, forestlands, and agricultural land).

Pipeline route configurations should avoid areas of designated unique natural resources valuable for observation and/or scientific research because of their relatively pristine quality. The mere physical presence of a cleared pipeline right-of-way has substantial detrimental impact on this quality.

Construction of pipelines in forested regions requires the complete removal of vegetation from the right-of-way. This action effects an

immediate and long-term change in the beauty of the forest; it also exposes bare soil to wind and water erosion with adverse impact on soil resources and water quality.

Rights-of-way through grasslands or brushlands with scattered trees (woodland) normally has minor impact when planned in accordance with existing tree patterns. However, in areas of denser tree cover, extensive clearing adversely affects the woodland habitat.

When pipelines are routed through cultivated land, pasture, and range land, the main impact is the permanent loss of crops from land required for compressor station structures and permanent access roads. Periodic maintenance or emergency repair by way of temporary paths across fields also results in crop losses. However, the impact on agricultural resources is usually low because the original soil fertility can be established after burial of the pipe and normal crop production can resume.

4. Wildlife

Adverse impacts to wildlife and wildlife habitat vary throughout any region because of varying habitat type and range and diverse methods of construction, operation, and maintenance. In general, disruption of the terrestrial wildlife by a project reaches its highest point at certain vulnerable locations along the route during the construction phase. In vast areas of single habitat type surrounding a pipeline right-of-way, the relative effect is low. In some locations, some reclamation may be required.

The presence of compressor stations and mainline valves along a right-of-way permanently eliminates the prior vegetation and wildlife from the site. Much of the land surface of these properties is covered with concrete, gravel, or asphalt and installations are typically enclosed with chain link fences. Compared to the volume of adjacent

habitat, this effect is comparatively minor, although the impacts are absolute and irreversible.

The impacts on terrestrial wildlife of operation of the compressor stations are not sufficiently known. However, compressor stations are noisy and in the interest of avoiding wildlife disturbance should be acoustically treated.

The temporary gross physical disturbance and siltation of aquatic habitat at river crossings is probably the most serious problem to prevent during construction. Also, during the testing phase of pipeline construction, large amounts of water may be discharged in a relatively short time into water courses, temporary holding ponds or onto nearby ground that drains into the water courses along a right-of-way. The timing and magnitude of these releases can affect aquatic populations.

Streamside slash and other debris that may drift into the water courses crossed by a pipeline right-of-way requires adequate disposal. Organic debris can block streams and prevent or curtail fish movements and migrations and cause disruption of spawning.

After construction, a pipeline, properly buried under several feet of sand, gravel, and varying depths of water, exerts no discernible effect on either the character of the refilled bottom or on water quality, quantity or rate of flow. Potential impacts on the water resources, similar to those from construction, would stem from repair of the pipeline.

5. Air Quality

The major impact on air quality by pipeline operations is the emissions from the compressor or pumping stations distributed over the 1,300 km (800 mi) length of the pipeline. The fuel consumption by these stations was discussed in Chapter V.

The emissions from the turbine-powered compressor stations on the natural gas pipeline are shown in Table VI-15 . For the pipeline in the system we assumed, a total of 11 compressor stations are spaced at intervals of approximately 110 km (67 mi).

The air pollutant emissions from the diesel-powered pumping stations on the liquid fuels pipeline are shown in Table VI-16. Ten such stations are spaced at intervals of approximately 130 km (80 mi) along the 1,300 km pipeline we assumed.

Because the emissions are so dispersed, they do not create a significant air pollution problem. However, when compressor or pumping stations are located near urbanized areas, the emissions add to the pollutant loading generated by automobiles, industry, and other sources.

G. Fuel Distribution

1. Tank Trucks

Dispersed 26-MW fuel-cell power plants will sometimes be constructed in residential areas. Naphtha-fueled power plants will probably be supplied by tank trucks. The trucks designed for such short hauls are normally straight, rigid-bodied trucks able to service a decentralized market.

Most tank trucks today are diesel-powered because less maintenance is required and because diesel fuel is less expensive than gasoline. Modern tank trucks have become progressively lighter and stronger because of aluminum alloys, stainless steel, and reinforced fiberglass which is now used in the construction of the tank compartments instead of carbon steel.

Table VI-15

AIR POLLUTANT EMISSIONS FROM A COMPRESSOR STATION ON AN 81 CM (32 IN.) NATURAL GAS PIPELINE

Pollutant	Emissions, kg/hr (lb/hr)	
NO_x	33.0	(72.0)
CO	13.0	(29.0)
Hydrocarbons*	2.5	(5.5)
SO_2	0.065	(0.14)

*Non-methane hydrocarbons represent 5 - 10% of the total.
Source: Reference 2.

Table VI-16

AIR POLLUTANT EMISSIONS FROM A PUMPING STATION ON A 51 CM (20 IN.) LIQUID FUELS PIPELINE

Pollutant	Emissions, kg/hr (lb/hr)	
NO_x	44.0	(98.0)
CO	9.6	(21.0)
Hydrocarbons	3.5	(7.8)
Particulates	3.2	(7.0)
SO_x	2.9	(6.5)
Aldehydes	0.67	(1.5)

Source: Reference 2.

Tank trucks are designed mainly for travel along highways and thoroughfares and not residential streets. When these trucks do utilize such streets their presence is very noticeable because of their size and noise levels. Tank trucks used to deliver fuel to fuel-cell facilities would create impacts such as air pollution, safety hazards, and the possibility of damage to the surface of the street due to the weight of the trucks.

Tank trucks are substantially larger than the average automobile. Because of their size they have aesthetic impact. The significance of the impact will depend on the time of day in which deliveries are made, the frequency of deliveries, and the appearance of the truck itself.

Trucks are a safety hazard mainly due to their size. They are more damaging when they collide with another vehicle or a person than the standard automobile which normally travels through the community.

The safety hazard these trucks pose in a community is dependent on the times of delivery and the makeup of the neighborhood -- whether there are children playing in the street, older people who are no longer very agile, or whether it is mainly a community of young and middle aged people who are generally working during the day and would for the most part be unaware of the tank trucks.

The most noticeable and well studied impacts of trucks is their noise level. The noise impact is the most significant environmental impact resulting from fuel distribution. To provide an idea of the contribution of each source to the overall noise created by a diesel truck, Table VI-17 presents a weighted sound level at 15 m (50 ft.) The noise levels increase with vehicle speed and also depend upon variables such as the road surface, axle loading, tread design, and wear condition. Change in any of the variables can result in variations in noise level of up to 20 dB at constant vehicle speed. Truck tires are generally noisier than automobile tires because of their size and other

design constraints. Engine-generated noise normally dominates at speeds below 45 mph. This noise radiates directly from the engine exhaust and intake openings and from vibrating engine casing. Other major sources of truck noise are turbulent aerodynamic flow over the body and the rattling of loose mechanical parts.

Diesel truck noise is considered a nuisance as well as disruptive; it is termed "intermittent single-event" noise. Generally, this type of noise interferes with speech and other activities for brief intervals. The impact this noise will have on different communities will depend on the residual noise level, and as can be seen in Table VI-18 there are differences in the noise levels found in even residential communities.

Table VI-17

DIESEL TRUCK NOISE SOURCES

Source	Weighted Sound Level at 15m, dB(A)
Engine	78
Exhaust	85
Intake	75
Fan	82
Tires	75 (less than 58 km/hr)
	95 (greater than 58 km/hr)
Total	88 (less than 58 km/hr)
	96 (greater than 58 km/hr)

Source: Reference 16.

Table VI-18

URBAN AND SUBURBAN DETACHED HOUSING RESIDENTIAL AREAS AND APPROXIMATE DAYTIME RESIDUAL NOISE LEVEL (L_{90})

Neighborhood Description	Typical Range dB(A)	Average dB(A)
Quiet suburban residential	36 to 40	38
Normal suburban residential	41 to 45	43
Urban residential	46 to 50	48
Noisy urban residential	51 to 55	53
Very noisy urban residentiaL	56 to 60	58

Source: Reference 17.

Finally, the effect of these tank trucks on the air quality of the community is important. Currently, about 54 percent (by weight) of all air pollution in the United States is emitted by mobile sources and between 50 and 75% of the total weight of three pollutants -- hydrocarbons, carbon monoxide, and nitrogen oxide -- come from transportation. Air pollution affects humans, animals, plants, materials, and visibility. The impacts from the air pollution emitted by automobiles has had significant detrimental impacts. Diesel trucks add pollutants to the air of any community through which they travel, but when compared to the already existing problem this impact can be considered insignificant as a pollutant source. Table VI-19 provides a summary of diesel truck emission.

2. Unit Train (Fuel Oil)

The impacts of the unit train supplying distillate fuel oil to a combined cycle power plant are generally similar to those of the coal unit train. However, due to the lower weight of a 100-tank car unit

train, its emissions would be correspondingly less. The air pollutant emissions for the coal unit train were shown in Table VI-3. The loaded coal train data should be multiplied by 0.52 to obtain the emissions from a tank car unit train carrying distillate fuel oil; the round trip averages should be multiplied by 0.63.

Table VI-19

AIR POLLUTANT EMISSIONS FROM
A DIESEL-POWERED TANK TRUCK

Pollutant	Emissions	
	g/km	lb/mi
CO*	18.0	(0.063)
Hydrocarbons*	2.9	(0.010)
NO_x *	11.0	(0.040)
SO_x **	1.7	(0.006)
Particulates	0.81	(0.003)
Aldehydes	0.2	(0.0006)

*EPA estimates for 1990 model year vehicles.

**Assumes fuel sulfur content of 0.2 %.

H. Combined Cycle Power Plant

Because the combined-cycle power plant burns low-sulfur distillate fuel, no stack gas emission controls are necessary. The most serious emisson problem is the large amount of NO_x produced in the high-temperature combustor. The various methods of controlling the formation of NO_x were discussed in Section IV-D. The H-Coal distillate fuel contains 0.23% bound organic nitrogen (see Section IV-C). Combustion tests have shown that approximately one-half of bound nitrogen in fuel is converted to NO_x in the combustor, resulting in an emission level of about 0.065 kg NO_x/GJ (0.15 lb $NO_x/10^6$ Btu) for H-coal distillate fuel. That means that fixation of nitrogen from the

feed air must yield no more than 0.065 kg NO_x/GJ (0.15 lb $NO_x/10^6$ Btu) to meet a possible NSPS of 0.13 kg NO_x/GJ (0.3 lb $NO_x/10^6$ Btu). The use of proper burner design, water injection, and staged combustion has been shown to control NO_x to low levels in conventional gas turbines operating at 1,000-1,100°C (1,850-2,000°F). Whether such low levels can be achieved in a 1,370°C (2,500°F) turbine is not known. However, for the purpose of analysis, we assume that through water injection and other control measures the NSPS for NO_x is met.

The emission of SO_2 was calculated on the basis of a sulfur content in the H-Coal distillate product of 0.11%. The emissions of other pollutants were calculated using emission factors for oil-fired turbines. The major emissions to the air from the 270-MW combined-cycle power plant are shown in Table VI-20.

Table VI-20

EMISSIONS FROM A 270-MW COMBINED-CYCLE POWER PLANT

Source	Type	Emissions (kg/hr)
Stack gases	particulates	48.0
	SO_2	91.0
	NO_x[a]	240.0
	Hydrocarbons[b]	23.0
	CO[b]	23.0
Cooling tower blowdown,	Suspended solids[c]	5.6
boiler blowdown,	Oil and grease[c]	2.8
and fuel preparation	Iron[c]	0.2
	Copper[c]	0.2
	Chlorine[c]	0.003

[a]Assumes that NSPS of 0.3 lb $NO_x/10^6$ Btu fuel is met.
[b]Source: Reference 18.
[c]Based on effluent limitation guidelines in Reference 5.

No solids handling facilities are required for the combined-cycle plant because no solid wastes are generated in its operation. The main source of wastewater is the cooling tower blowdown, which contains small amounts of dissolved solids and heavy metals. In addition, a small discharge of water from the fuel treatment section contains dissolved salts of sodium and potassium in addition to some suspended oils. All wastewater is assumed to receive appropriate treatment prior to discharge.

The calculation of toxic trace element and PAH emissions from the combined-cycle power plant is difficult because of a lack of knowledge of the trace element concentration in the H-Coal distillate fuel and the potential of this fuel to form PAH in the high-temperature combustor. However, we assume that the trace element content of H-Coal liquids will be at least an order of magnitude lower than in the feed coal. This assumption results from measurements of the trace element content of SRC and COED process liquid products relative to the feed coal from which they are derived.[19] Reduction in concentration varied with the particular trace element and the process. However, an overall reduction factor of about 10 represents a reasonable average. Using that factor, and the assumption that all trace elements contained in the fuel oil are emitted with the stack gases. The emissions of trace elements from the 270 MW combined-cycle power plant are shown in Table VI-21.

Table VI-21

EMISSIONS OF TOXIC TRACE ELEMENTS FROM
A 270-MW COMBINED-CYCLE POWER PLANT

Element	Emissions (g/hr)
Sb	3.0
As	13.5
Be	3.2
Cd	9.5
Pb	32.0
Hg	0.45
Se	3.3
Zn	150.0

The only reasonable assumption that we can make regarding the emissions of PAH from the combined-cycle plant is that they will be similar to those from conventional oil-fired boilers. Extensive testing of combustion products must be performed before it is known whether combustion of coal-derived fuels will result in substantially higher PAH emissions. Estimation of PAH emission based on analogy with conventional oil combustion is shown in Table VI-22.

I. 26-MW Fuel-Cell Power Plant (SNG)

Emissions from the System 2 power plant were estimated based on rated-load operation. Under normal conditions, only one process stream leaves the power plant (Stream 33). The composition of this stream is shown in Table VI-23.

Production of NO_x pollutants in the combustion zone of the reformer furnace was assessed using the equilibrium and kinetic model procedures described later in Section VI-M. The results, shown in Table VI-24 indicate negligible NO_x production.

Table VI-22

EMISSION OF PAH FROM A 270-MW COMBINED-CYCLE POWER PLANT

Compound	Emission (g/hr)
Pyrene	0.55
Fluoranthene	0.50
Phenanthrene	3.3
Benzo(a)pyrene	0.087
Benzo(a)anthracene	0.050

Table VI-23

COMPOSITION OF EFFLUENT PROCESS STREAM
FOR A NOMINAL 26-MW FUEL-CELL POWER PLANT

Component	Emission Rate at Rated Load (kg/hr)
CO_2	9,140
H_2O (vapor)	8,270
O_2	2,940
N_2	58,100
CO	Nil*
CH_4	Nil*
NO_x	See Table VI-24
Particulates	Nil
Waste heat to atmosphere	116 GJ/hr

*Based on equilibrium combustion calculations.

Table VI-24

PREDICTED REFORMER FURNACE NO_x PRODUCTION

Residence Time[a] (msec)	Predicted NO_x Levels[b] Mole Fraction	Equivalent gNO_x/hr
5	6.0×10^{-13}	4.66×10^{-5}
10	1.2×10^{-12}	9.32×10^{-5}
100	1.2×10^{-11}	9.32×10^{-4}

[a]Adiabatic flame temperature = 1,161°C (2,121°F)

[b]At rated load, assuming NO_x molecular wt = 30.

The power plant has little effect on the environment. The major effluents are water, CO_2, and thermal energy, which are dissipated directly into the atmosphere. The system is water-conservative, requiring no make-up water for its operation. Thus, it adds no thermal pollution to rivers, lakes, or streams.

Power plant operation does involve the generation and flow of hydrogen-rich mixtures. Leakage could result in explosions; however, proper component design and fabrication procedures minimize this potential hazard.

Other pollution aspects of the power plant are reviewed below.

1. Spent Fuel-Cell Stack Disposal

The molten carbonate fuel-cell stacks are assumed to have a nominal working life of 40,000 hours. Periodic replacement is required during the operating life of the power plant. Because molten carbonate cells do not use expensive noble metal catalysts, stack recovery is not required. Rather, suitable disposal procedures can be expected to be developed to handle the discarded stacks. Few problems should arise, even though replacement of all power plant stacks involves discarding about 87 tonnes (96 tons) of lithium aluminate tile plus mixed lithium/potassium carbonate electrolyte. Disposal of the remaining stack components, including sintered nickel electrodes and stainless steel structural members, should be straightforward.

2. Spent Catalyst Guard Bed Disposal

The power plant contains several catalyst and adsorbent beds that require periodic replacement. The resulting pollution burden is small. For example, the spent sulfur guard bed involves removal of about 0.018 kg (0.04 lb) of zinc sulfide per MWh of operation. This is

equivalent to 1,310 kg/yr (2,880 lb/yr), assuming 3,000 hours annual operating time at full load. Spent reforming catalyst (nickel) could be returned to the supplier for safe disposal.

3. Noise

Noise levels generated by the power plant have not been defined. The plant contains rotating machinery that will have characteristic noise signatures. Scaled-up phosphoric acid power plants are expected to generate 55 dBA at 30 m (100 ft).[20] Similar levels should apply to the molten carbonate power plant.

J. 26-MW Fuel-Cell Power Plant (Naphtha)

Emissions from the System 3 power plant, operating at rated load, were estimated, using the bases discussed in Section VI-I. As shown in Table VI-25 and VI-26, the power plant has little impact on the environment. Although the naphtha feed contains sulfur, no sulfur oxide emissions are shown in Table VI-25. The fuel conditioning section contains a hydrodesulfurization unit and zinc oxide guard bed to adsorb H_2S. Replacement of spent guard beds involves the removal of about 0.014 kg (0.03 lb) of zinc sulfide per MWh of operation. This is equivalent to 900 kg/yr (1,980 lb/yr), assuming 3,000 hours annual operating time at full load.

The target sulfur level in the naphtha feed to the reformer is 0.2 ppm sulfur. We assume that this sulfur, after conversion to H_2S in the reformer, is retained on the nickel reforming catalyst. There is also increasing evidence that small quantities of sulfur may be retained within the molten carbonate fuel cell itself.

Table VI-25

COMPOSITION OF EFFLUENT PROCESS
STREAM FOR A NOMINAL 26-MW FUEL-CELL POWER PLANT

Component	Emission Rate at Rated Load (kg/hr)
CO_2	13,100
H_2O (vapor)	6,040
O_2	3,250
N_2	65,100
CO	Nil*
CH_4	Nil*
NO_x	See Table VI-26
Particulates	Nil
Waste heat to atmosphere	111 GJ/hr

*Based on equilibrium combustion calculations.

Table VI-26

PREDICTED REFORMER FURNACE NO_X PRODUCTION

Residence Time[a] (msec)	Predicted NO_x Levels[b] Mole Fraction	Equivalent (gNO_x/hr)
5	4.8×10^{-12}	3.92×10^{-4}
10	9.6×10^{-12}	7.83×10^{-4}
100	9.6×10^{-11}	7.83×10^{-3}

[a]Adiabatic flame temperature = 1,225°C (2,236°F)
[b]At rated load, assuming NO_x molecular wt = 30.

Other environmental factors are similar to those of the SNG-fueled power plant, discussed in the previous section. The naphtha-fueled power plant is also water-conservative and does not generate water-borne thermal pollution. Spent fuel-cell stack disposal in this case involves discarding about 69 tonnes (79 tons) of mixed electrolyte plus ceramic tile. Environmentally acceptable means must be developed for disposal of spent catalysts, including:

- Hydrodesulfurization (Ni-Mo)
- Reforming (Ni)
- Shift conversion

Lastly, noise pollution characteristics for the naphtha-fueled power plant remain to be defined. However, they are expected to be similar to scaled-up phosphoric acid power plants, as discussed in the previous section.

K. Electricity Transmission and Distribution

Meeting the increasing demand for electric energy requires not only additions to the energy generating capacity, but also additions to the capacity to move the electric power from the location of the generating plant to the dispersed users of the electricity. Power transmission lines of increasing length and voltage capacity are becoming more important as new generating plants are located farther from the final energy users than older plants. New and planned transmission lines will interconnect electric systems in different areas to improve the reliability and level of service. Today's transmission lines carry power at higher voltages, on the average, than those existing a decade ago. The trend toward higher voltages is expected to continue as research extends the technical limits of transmission line capacity. However, research is required to solve some of the increased environmental impacts expected of the higher capacity lines.

1. Transmission Line Characteristics

a. Voltages

At present, transmission lines operate at voltages of between 115 and 800 kV. Lines operating at voltages below 115 kV are considered subtransmission and distribution lines. Future line voltages of 1,200 and 1,500 kV are the subject of current research and development.

b. Towers

The size and design of transmission lines towers are primarily dependent on the voltage of the line and number of circuits to be carried. The height of the towers and the minimum line sag determines the spacing between the towers. Thus, higher towers can be spaced farther apart and carry the same voltage.

c. Right-of-Way

All overhead transmission lines require a right-of-way relatively clear of vegetation such as tall trees, which could fall into the towers or lines, and other vegetation, which could hamper movements of the people who maintain the line. The width of the right-of-way is generally proportional to the voltage of the line, but many other factors such as number of circuits, topography, vegetation, surrounding land use, type of land purchase or lease, and land values also determine the width of the right-of-way. For example, a 345-kV transmission line sited in a flat agricultural area might require a 30 m (100 ft) right-of-way, while the same size line in a rugged, forested terrain might require a 76 m (250 ft) right-of-way. Table VI-27 shows average right-of-way widths for different voltage lines.

Table VI-27

AVERAGE REQUIREMENTS FOR RIGHTS-OF-WAY

Voltages (kV)	Right-of-Way Width, m (ft)
345	46 (150)
500	61 (200)
765	76 (250)
1,200	91 (300)

2. Transmission Line Impacts

a. Electrical Impacts

Impacts related to the electrical characteristics of transmission lines fall into two categories: impacts related to electric fields surrounding the lines and those related to corona discharge. Electric fields are known to induce voltages in objects under the lines, which can result in unpleasant or possibly hazardous (under rare conditions with children) electric shock. A few experts suggest that 60 Hz electromagnetic fields are hazardous to people and animals, although experts do not generally agree on what are the biological effects of fields produced by transmission lines.

Corona and electric fields at ground level both increase directly with increase in operating voltage of a transmission line. Existing transmission systems cause little or no concern over electrical impacts because operating voltages have been below 500 kV until very recently. However, high voltage transmission systems are now being designed at voltages up to 765 kV and research is being done on 1,200 and 1,500 kV-lines. Thus, controlling the impacts of corona and electric fields is increasingly important in designs of present and future transmission systems.

1) Corona and Related Impacts--Corona, or corona discharge, refers to a luminous discharge (due to ionization of the air surrounding a conductor) caused by the voltage gradient exceeding the breakdown voltage of air. The discharge yields heat, light, audible noise, electrical static, and vibration. Irregularities on the conductor surfaces such as water drops are many times more conducive to corona discharges than are clean, dry conductors. Thus, corona discharges predominantly occur during wet weather such as rain, heavy snow, or fog.

Audible noise (AN) is produced by corona discharges from a transmission line. Because of this association, AN during wet weather is much louder than during dry weather. In fact, dry weather levels, which may average 35 dB for a 765-kV line, are generally masked by background noise and therefore are not a cause for concern. During rain or heavy snow, a 765-kV line will produce a noise level of about 56 dB(A) measured 38 m (125 ft) from centerline (the approximate edge of the right-of-way). Because AN is roughly proportional to the operating voltage of the transmission line, a line operating at less than 765 kV will generally produce less than 56 dB(A) under identical conditions of rain or snow. Although 56 dB(A) is below the safety threshold for hearing damage (70 dB), it is high enough to interfere with sleep, mask speech, and cause general annoyance.

Sleep interference becomes a potential problem when bedroom noise levels reach 33-35 dB(A). Residences located at or very near the edge of the right-of-way might experience, during wet weather with windows partly open, indoor noise levels between 34 and 43 dB(A) and 23 dB(A) with windows closed. Of course, these noise levels depend on the type of building, its orientation to the transmission line, and the location of adjacent buildings that could block or reflect the noise. Generally, therefore, sleep interference might occur in residences near a right-of-way.

Speech interference, or speech masking, may become a problem at noise levels of around 55 dB(A). Because noise levels inside

buildings are about 10 to 30 dB lower than outdoor noise levels the same distance from the lines, indoor noise generally will not cause speech masking. However, out of doors, near the edge of a right-of-way, speech masking might be expected during wet weather.

Noise experts disagree on the nature of the annoyance: some say that annoyance is caused by speech or sleep interference; some say it is a psychological reaction to noise separate from the other effects. In either case, annoyance can be more dependent on the characteristics of the noise and the meaning the noise conveys to the person than on the actual noise level.

Like audible noise, radio and television interference are caused by corona discharges on transmission lines and are therefore a problem only in wet weather. The interference increases with higher voltage lines and decreases with greater distance from the lines.

Ionization of the air surrounding conductors during corona discharge creates free oxygen radicals (O^-) that combine with oxygen molecules (O_2) to produce ozone (O_3). Ozone production during wet weather is about 30 times the rate during fair weather. Calculations of the production of ozone from some proposed 765 kV lines in New York state indicated that under worst conditions (wet weather and slow wind moving parallel to a long straight stretch of lines for several hours), the lines would increase the ambient concentration of ozone by 5 to 9 parts per billion (ppb) measured directly under the lines. This increase in concentration would fall quickly as measurement points moved laterally away from the lines. The present federal air quality standard for ozone is 80 ppb not to be exceeded more than 1 hour per year. Concentrations of 50 ppb are necessary before even the most sensitive plants are damaged. Thus, ozone is not considered to be a serious impact of transmission line operation.

Electrical Fields and Related Impacts--An operating transmission line creates an electric field that is strongest at the surface of the

conductor, but decreases rapidly with increasing distance from the conductor. Electric fields can cause shocks, may adversely affect the operation of cardiac pacemakers, and are suspected by some people of having physiological and psychological effects on animals and humans.

When an ungrounded object such as a bus is parked under a transmission line operating at high voltage, the electric field induces a voltage on the object. A grounded person (e.g., one standing on dirt or in a puddle of water) touching the bus will create a path for current to flow to the ground and will discharge the induced voltage. The discharge will be felt as an electric shock similar to the electric shock one experiences by walking across a carpet and touching a doorknob on a dry day. The magnitude of the shock depends on the field strength around the ungrounded object, the size and grounding of the object, the strength of contact and grounding of the person, and the orientation of the object in the field. The 765-kV lines proposed for New York state were calculated to have the potential to be hazardous to a small, grounded child touching a large, ungrounded vehicle in worst case circumstances. The shock currents calculated for these lines were much higher (by a factor of about 100) than shock currents measured under experimental conditions. Therefore, electric shocks from transmission lines should be considered a remote but real hazard.

Certain types of pacemakers may be affected by exposure to electromagnetic fields of the magnitudes found under 765-kV transmission lines. Some pacemakers are designed to stand by while the heart is functioning normally and begin pacing the heart when they pick up abnormal electric signals from the heart. Because this type of pacemaker must be sensitive to the electrical characteristics of the heart, artificial electrical interference caused by the patient standing in a large electric field (from a transmission line, a microwave oven, or any of several other sources) may cause the pacemaker to switch into its active mode and begin giving signals to the heart. In that case, the heart would be getting two conflicting signals -- one natural and one from the pacemaker. Interference of this type, while not optimal for the

patient, does not appear to be a serious hazard. Although many cases of interference (none from transmission line operation) have been recorded, no cases of death or serious damage from this type of interference have been documented. Transmission lines operating at voltages less than 765 kV are not thought to cause pacemaker interference except in very unusual circumstances.

That electric fields produced by transmission lines constitute a direct health hazard to people and animals has not yet been proven to the satisfaction of the U.S. scientific community. Russian experiments with substation workers report subjective neurologic disorders such as headache, sluggishness, fatigue, and sleepiness. However, numerous experiments in the United States and other countries have failed to duplicate these results. As with the other effects related to the electrical characteristics of the lines, electric fields increase with higher voltage lines.

Table VI-28

60 Hz ELECTRIC AND MAGNETIC FIELDS

Location of Measurement	Electric Field (volts/meter)	Magnetic Field (gauss)
Center of kitchen	3	--
30 cm (12 in) from oven broiler	130	--
Private dwelling (away from appliances)	--	0.001-0.1
Close to electric can opener,electric shaver, or hair dryer	--	5 or greater
Maximum field under operating 765-kV lines	10,000	0.5
765-kV at 38 m (125 ft) (edge of right-of-way)	2,500	0.15
765-kV at 152 m (500 ft)	100	0.01

Exposure to electric and magnetic fields is a relatively common experience because all electric appliances create fields. Fields from appliances differ somewhat from those of transmission lines in both magnitude (see Table VI-28) and decreases of magnitude with distance from the source.

b. Physical Impacts

Apart from their electrical characteristics, transmission lines may affect an area simply by the physical presence of towers and rights-of-way. A transmission line may disrupt the visual quality of an area, or it may limit or affect the uses of the surrounding lands.

Visual Impacts--One of the most obvious effects of transmission lines is the effect on the visual character of the area. The severity of this effect can range from negligible in highly developed areas with many existing utility lines to significant in relatively undeveloped areas valued for their scenery. In flat terrain and in areas characterized by low growing vegetation, the towers constitute the major visual impact. Long, straight sections of transmission lines present a definite visual disruption. In mountainous terrain, especially heavily vegetated areas, the right-of-way is visually disrupting; the long strip of cleared land can be seen at greater distance than the towers. Although the specific tower height and right-of-way width vary under different circumstances, higher operating voltages require higher towers and wider rights-of-way. Although good tower design and careful siting can reduce the visual impact of transmission line corridors, more intense visual disruption is to be expected as operating voltages increase in the future.

Land Use Impact--Transmission lines can limit uses of the surrounding land, and prohibit most uses of the right-of-way corridor itself because of the necessity to prevent undue hazards or provide access for surveillance and maintenance of the lines. Homes and air-

ports are notable examples of land uses that are limited around transmission lines. In urban areas, the right-of-way may need to be fenced to prevent access to the towers (which could constitute an "attractive nuisance"). Like a fenced highway, a fenced utility corridor creates a barrier to movement. Because of the shock hazard, buses should not stop for passengers under or adjacent to the lines. Gasoline should not be pumped into tanks where the fields are strong enough to produce a spark between the pump nozzle and the vehicle.

The presence and operation of transmission lines may affect agriculture in and around the corridor in several ways. The towers and lines may present a physical barrier to row cropping and to aerial seeding, fertilizing, and spraying. Electrical fields from operating transmission lines can induce voltages on large agricultural vehicles, and cause shocks to farmers working with vehicles near the lines. Similarly, metal irrigation equipment, especially the high sprayer type, may be prohibited within a certain distance of the lines.

L. Gas Furnace

The only item of residential heating and cooling equipment that does not have negligible environmental impact is the gas furnace in System 1. The emission of air pollutants from a residential gas furnace with an output of 70 MJ/hr (66,000 Btu/hr) were calculated from standard emission factors. Those emissions are shown in Table VI-29.

M. 100-kW Fuel-Cell Power Plant

Emission characteristics of the 100-kW power plant were estimated, based on rated-load operation. Under normal operation, the only effluent stream leaving the power plant is the combined air exhaust and reformer furnace flue gas. The composition of this stream (after discharge from condenser E-5) is shown in Table VI-30. This stream leaves the system saturated with water vapor at 127°C. Consequently, fogging occurs on cold days.

Table VI-29

EMISSION OF AIR POLLUTANTS FROM A 70 MJ/HR RESIDENTIAL GAS FURNACE

Pollutant	Emissions (g/hr)
NO_x	4.0
SO_2	0.03
CO	1.0
Particulates	0.50
Hydrocarbons	0.40

Source: Reference 2

Table VI-30

COMPOSITION OF EFFLUENT STREAM FROM 100-kW FUEL-CELL POWER PLANT

Component	Emission Rate at Rated Load, kg/hr
CO_2	54.6
H_2O (vapor)	55.5
O_2	54.0
N_2	443.0
CO	Nil*
CH_4	Nil*
NO_x	See Table VI-28
Particulates	Nil

*Based on equilibrium combustion calculations

We have attempted to predict NO_x emissions, based on the nonoptimized system design. Production of NO_x is expected during operation of the reformer furnace burner. The method used was developed by H. Shaw and begins with the calculation of equilibrium NO mole fraction.[21] The NASA-Lewis Equilibrium Program was used for this purpose. The NO_x mole fraction in the furnace effluent was then calculated for residence times of 5, 10, and 100 msec, based on the equilibrium mole fractions of NO, OH, O_2, and N_2, at the adiabatic flame temperature and atmospheric pressure. As shown in Table VI-31, NO_x emissions were found to be linear functions of residence time and can thus be easily adjusted, if the residence time estimate is defined more precisely. The method of Shaw is based on the Zeldovich mechanism (including OH) with an empirical correction for "prompt NO_x." Because "prompt NO_x" would not be expected to contribute significantly at the stoichiometry and for the fuel composition used in this study, we neglected it. Also, no NO_x contribution from fuel-bound nitrogen would be expected because no nitrogen compounds were specified in the input fuel composition. The emission rate given in Table VI-31 was calculated assuming that NO rather than NO_2 is the pollutant.

Table VI-31

PREDICTED REFORMER FURNACE NO_x PRODUCTION

Residence Time,[a] (msec)	Predicted NO_x Levels[b] Mole Fraction	Equivalent (gNO_x/hr)
5	3.6×10^{-7}	831
10	7.2×10^{-7}	1660
100	7.2×10^{-6}	16,600

[a]Adiabtic flame temperature = 1642°C (2987°F.)

[b]At rated load, assuming NO_x molecular wt. = 30

As indicated earlier, the reformer furnace effluent temperature in the nonoptimized base-case design was excessive. In turn, that results in relatively high levels of predicted NO_x emissions, even for short residence times. Further study is required to develop a system integration scheme with lower furnace combustion temperature and lower NO_x emissions.

Although the environmental characteristics of fuel-cell power plants are expected to be very favorable, little effort has been directed toward defining actual emission rates from complete power plants. The only published data, reported by United Technology Corporation, and quoted frequently, were obtained in 1970. Those data, shown in Table VI-32, were probably measured using small natural gas-fired 12.5-kW fuel cells developed by UTC for the TARGET program.

The NO_x rates shown are about 100 times lower than those predicted for the base-case system. indicating that proper operation of the reformer furnace should not be a problem. New studies to measure the pollution characteristics of phosphoric acid fuel cell power plants are under way. The Department of Energy has included this technology in its recent Environmental Development Plan.[20]

Table VI-32

PUBLISHED POLLUTION CHARACTERISTICS OF EXPERIMENTAL PHOSPHORIC ACID FUEL CELLS

Emission Type	Emission Rate Range (kg/MWh)*
SO_2	0 - 0.00014
NO_2	0.063 - 0.11
Hydrocarbons	0.014 - 0.10
Particulates	0 - 0.000014

*Quoted by UTC (22), based on a study by York Research Corporation, Y-7306, April 1970. Fuel type was not specified.

Other pollution aspects of the 100 kW power plant are reviewed below.

1. Spent Fuel-Cell Stack Disposal

The nominal life of phosphoric acid fuel-cell stacks is assumed to be 40,000 hours. Thus, periodic stack replacement is required during the operating life of the power plant. For economic reasons, stack disposal involves recovery and recycle of expensive platinum electrocatalysts. This recovery step would take place at a central facility, probably at the fuel-cell assembly plant site, or at a catalyst supplier plant. The recovery process, as yet undefined, may result in pollutant emissions.

Dismantling of the stack in an environmentally acceptable manner will require procedures for disposal of the cell hardware (mostly carbon/graphite components), probably via incineration. The 100 kW power plant also contains about 15.3 kg of phosphoric acid electrolyte and 61 kg of silicon carbide matrix. Suitable disposal procedures for these potential pollutants must be developed.

2. Spent Catalyst Bed Disposal

The 100 kW power plant contains several catalyst beds that require periodic replacement. These include the zinc oxide guard chambers for odorant sulfur compound removal, the reformer reactor (nickel catalyst), and the shift conversion reactors (copper and zinc catalysts). Spent catalysts could be returned to the vendors for safe disposal.

3. Normal Power Plant Operation

The principal gaseous emissions from the power plant were discussed above. Other potential environmental impacts during normal power plant operations include:

- Possible phosphoric acid vapor release into the process air stream, which limits fuel-cell life. Suitable guard beds, probably containing iron adsorbents, used to prevent entry of corrosive acid vapors into the water recovery condenser systems, require periodic disposal.

- Similar constraints apply to the use of circulating silicon oil coolant, used to remove waste heat from the fuel cell. New total energy power plant designs have switched to water/steam or circulating air coolants.

- The 100 kW power plant was designed to be water-conservative. Thus, no impact on local water supplies is expected.

- Noise pollution from the power plant has not been defined. The plant contains rotating machinery equipment, such as fans, blowers and pumps, with characteristic noise signatures. Experimental data on prototype models are required to assess noise levels.

N. References--Chapter VI

1. PEDCo. Environmental Specialists, Inc., "Wyoming Air Quality Maintenance Area Analysis," U.S. Environmental Protection Agency, Region VIII (May 1976).

2. "Compilation of Air Pollutant Emission Factors," U.S. Environmental Protection Agency, AP-42 (February 1976).

3. A. J. Dvorak, et al., "The Environmental Effects of Using Coal for Generating Electricity," Nuclear Regulatory Commission Report NUREG-0252 (June 1977).

4. E. Goldman and P. J. Keller, "Water Reuse in the Electric Generating Industry," National Conference on Complete Water Reuse, 1973.

5. "Development Document for Proposed Effluent Limitations Guidelines and New Source Performance Standards for the Steam Electric Power Generating Point Source Category," U.S. Environmental Protection Agency, EPA 440/1-73/029 (1974).

6. G. D. Case, et al., "Health Effects and Related Standards for Fossil Fuel and Geothermal Power Plants," Lawrence Berkeley Laboratory Report No. LBL-5287 (January 1977).

7. P. Zubovic, "Geochemistry of Trace Elements in Coal," U.S. Geological Survey (1975).

8. Radian Corporation, "Coal-Fired Power Plant Trace Element Study," U.S. Environmental Protection Agency, Region VIII (September 1975).

9. W. F. Holland, et al., "The Environmental Effects of Trace Elements in the Pond Disposal of Ash and Flue Gas Desulfurization Sludge," Electric Power Research Institute (September 1975).

10. S. T. Cuffe and R. W. Gersite, "Emissions from Coal-Fired Power Plants: A Comprehensive Summary," U.S. Department of Health, Education and Welfare, Public Health Service (January 1970).

11. "Western Gasification Company Coal Gasification Project and Expansion of Navajo Mine by Utah International, Inc., New Mexico -- Final EIS," U.S. Department of the Interior, Bureau of Reclamation (January 1976).

12. Cameron Engineers, Inc., "Evaluation of Background Data Relating to New Source Performance Standards for Lurgi Gasification," U.S. Environmental Protection Agency Report EPA 600/7-77-057.

13. U.S. Environmental Protection Agency," Standards Support and Environmental Impact Statement: Recommended Standards of Performance for Coal Gasification Plants" (1976).

14. R. P. Hangebrauck, D. J. von Lehmden, and J. E. Meeker, "Emissions of Polynuclear Aromatic Hydrocarbons and Other Pollutants from Heat Generation and Incineration Processes," J. Air Pollution Control Assn., 14(7): 267-78 (1964).

15. A. Attari, "Fate of Trace Constituents of Coal During Gasification," U.S. Environmental Protection Agency Report EPA-650/2-73-004 (August 1973).

16. U.S. Government Interagency Commercial Vehicle Post-1980 Goals Study (1973).

17. Report of the Administrator of the U.S. Environmental Protection Agency to the President and Congress on Noise (February 1972).

18. D. T. Beecher, et al., "Energy Conversion Alternatives Study -- Combined Gas/Steam Turbine Plant Using Coal-Derived Liquid Fuel," NASA CR-134942 (November 1976).

19. C. E. Jahnig, "Evaluation of Pollution Control in Fossil Fuel Conversion Processes, Liquefaction: Section 2, SRC Process," U.S. Environmental Protection Agency Report EPA-650/2-74-009-4 (1975) and W. D. Shults, ed., "Preliminary Results: Chemical and Biological Examination of Coal-Derived Liquids," Oak Ridge National Laboratory Report ORNL/NSF/EATC-18 (1976).

20. U.S. Department of Energy, Environmental Development Plan, Conservation Research and Technology, FY 1977, DOE/EDP-0017 (March 1978).

21. H. Shaw, "The Effects of Water, Pressure, and Equivalence Ratio on Nitric Oxide Production in Gas Turbines," J. of Engineering for Power, pp. 240-246 (July 1974).

22. United Technologies Corp., "Venture Analysis Case Study for On-Site Fuel Cell Energy Systems," Vol. II, Final Report, p. A-11 (July 31, 1978).

VII. CAPITAL AND OPERATING COSTS OF SYSTEM COMPONENTS

This chapter describes the costs of constructing and operating the components of the five energy supply systems described in Chapter IV. The objective is to compare the economics of the five systems in terms of the cost of heating and cooling residences and the system's capital intensiveness. Sensitivities of the component costs to variations in the costs of systems components are also analyzed.

Because comparison of the systems is a major objective of the analysis, it is important to use consistent cost estimation procedures for the various system components, insofar as possible. Thus, we treated all system components as if they were operated by a regulated utility, with the following exceptions: coal mine, liquid fuel delivery, and residential heating and cooling equipment. This assumption, which allows for a uniform cost analysis, is reasonable because all major system components are associated with electrical generating plants and the fuel networks that supply them.

The bases of the regulated utility economics used in the cost analyses of the system components are as follows:

- All costs are in constant mid-1977 dollars.
- Plant sizes are set to take maximum reasonable advantage of economies of scale and are characteristic of a mature industry.
- Source of capital is 35% equity (at a 15% rate of return) and 65% debt (at 10% interest).
- Plant construction, start-up, and operating schedule is shown below. (The construction schedule would be shorter for fuel-cell power plants and combined-cycle power plants.):

Year	Depreciable Investment	Land	Working Capital	Expenses	Revenue
1	-5%	-100%	--	--	--
2	-20	--	--	--	--
3	-50	--	--	--	--
4	-25	--	--	--	--
5	--	--	-100%	-60%	+60%
6	--	--	--	-100	+100
Final	--	--	+100	-100	+100

- Project tax life is 20 years for coal conversion facilities, fuel-cell power plants and combined-cycle power plants, and 30 years for pipelines and coal-fired power plants. Straight line depreciation is assumed.

- Plant investment factors:

  - Start-up expenses, 5% of plant facilities investment (PFI)

  - Working capital

Feed to liquid plants	15 days
Feed to coal plants	30 days
Labor for plants	3 months
Other cash expenses	1 month

- Plant on-stream factors:

- Coal conversion facilities	90%
- Intermediate load electrical generating plants	35%
- Pipelines	95%

- Labor factors:

- Operating labor (OL)	$7.00/hour
- Supervision (S)	15% OL
- Maintenance labor (ML)	2% PFI
- Administrative & support labor	20% (OL+ML+S)
- Payroll burden, all labor	35%

- Maintenance supplies — 2% PFI

- Administrative expense — 2% PFI

- Property taxes and insurance — 2.5% PFI

- By-product credits will be assessed depending on plant location and potential by-product markets.

- Land cost is $25,000 per hectare or $10,000 per acre (includes basic site preparation)

- Income taxes include the 48% federal corporate income tax plus 4% state income tax for a total of 52%, applied against taxable income.

- Prices for energy supplied will be 20- or 30-year average values.

- When appropriate, various contingency factors are applied to the cost of an individual plant or facility depending on its commercial experience. However, no across-the-board contingency is applied.

- The utility rate base is the sum of depreciable investment (PFI + interest during construction + start-up costs), land, and working capital. Return on rate base (P) is defined as:

$$P = d(i) + (1-d)r,$$

where d = debt fraction,
i = interest rate on debt
$1-d$ = equity fraction
r = return on equity.

An SRI computer program was used to calculate the 20- or 30-year average cost of energy, based on the capital and operating factors presented above.

The exceptions to these cost bases in the calculation of capital and operating costs of system components will be addressed individually in the following sections.

A. Coal Mine

The capital and operating costs of a 4.5 million tonne (5 million ton) per year surface mine operating in the Powder River Basin were evaluated using a cost model developed at SRI. The model uses a simplified set of equations that relate mining costs to the

geological characteristics of the region (e.g., overburden and seam thickness), size of the mine, and type of mine (area, open pit, or contour). To calculate the mining costs, financial parameters must be specified. The parameters used in the cost analysis are as follows:

- Mine life -- 30 years
- Debt-to-equity ratio -- 50/50
- Interest rate on debt -- 10%
- Rate of return on equity -- 15% discounted cash flow (DCF)
- Straight line depreciation.

Because various items of mining equipment must be replaced after 5, 10, or 20 years, they are depreciated on a separate schedule. Their replacement costs are calculated as a deferred investment in the year of replacement. These costs are incorporated into a financial model which computes the coal mine revenue required to achieve the specified rate of return on equity. The resulting cost of producing coal is an average over the life of the mine. Using the mine characteristics discussed in Chapter IV, the resulting capital investment required is shown in Table VII-1.

The cost of producing coal from the mine is shown in Table VII-2. Production costs include labor, supplies, union welfare payments, general and administrative expense, and a reclamation fee mandated in the Surface Coal Mining and Reclamation Act of 1977. Capital-related charges include depreciation, depletion allowance, return on investment, and debt payment. In addition, a $1.10/tonne ($1.00/ton) royalty payment for federal coal lease is assumed, along with state severence taxes of 20% of the selling price (an approximate average of current Montana and Wyoming state severence taxes). The resulting selling price of the coal is $6.69/tonne ($6.08/ton).

Table VII-1

CAPITAL INVESTMENT REQUIRED FOR A 4.5 MILLION TONNE (5 MILLION TON) PER YEAR SURFACE COAL MINE IN THE POWDER RIVER BASIN

		Investment ($ Million)	Percent
Primary Equipment		10.6	28
Overburden drilling	0.43		
Overburden excavation	4.7		
Coal drilling	0.06		
Coal loading	1.09		
Coal hauling	3.7		
Spoil handling	0.22		
Topsoil handling	0.37		
Supporting Equipment		3.4	9
Total Equipment		14.0	37
Exploration		0.06	--
Land		0.20	1
Preproduction		13.2	35
Interest During Construction		2.7	7
Working Capital		7.9	20
Total Initial Investment		38.1	100
Deferred Capital Investment		17.5	

Table VII-2

OPERATING COSTS FOR A 4.5 MILLION TONNE
(5 MILLION TON) PER YEAR SURFACE COAL MINE
IN THE POWDER RIVER BASIN

		$ Million/year	$/tonne ($/ton)
Labor		2.2	0.48 (0.44)
Operating crews	0.68		
Hourly support	0.31		
Salaried labor	0.46		
Payroll burden	0.73		
Welfare		4.3	0.95 (0.86)
Supplies		2.5	0.55 (0.50)
G&A		1.6	0.35 (0.32)
Taxes and Insurance		0.26	0.05 (0.05)
Reclamation Fee		1.75	0.39 (0.35)
Miscellaneous		0.30	0.06 (0.06)
Capital Charges (debt payment, depreciation return on investment, and income taxes)		7.4	1.63 (1.48)
Royalties		5.0	1.10 (1.00)
Subtotal		25.3	5.57 (5.06)
Severence tax (20%)		5.1	1.12 (1.02)
Total		30.4	6.69 (6.08)

B. Unit Train

The cost of unit train service is currently a controversial topic because of the incipient competition from coal slurry pipelines. Although some current unit train prices may be more affected by competition than by cost, the cost of shipping coal will be calculated, using the financial parameters described at the beginning of the chapter. Two factors that are important to unit train cost are:

- Existence of track of adequate quality along desired route
- Other rail traffic that can share track costs.

Estimated investment costs for 80 km (50 mi) of new single track with siding and two unit trains are given in Table VII-3. Operating costs are shown in Table VII-4, and are based on the assumption that the 80 km of new track is used to transport 23 million tonnes (25 million tons) of coal per year, so that the unit train operation in question must bear only 5.6% of the cost of constructing and maintaining the track. The cost of shipping coal is $0.27 per GJ ($0.29 per million Btu), or 0.44 cents per tonne-km (0.64 cents per ton-mile).

The cost of shipping coal is sensitive to the amount of traffic sharing the 80 km of new track, as is evident in Figure VII-1. Coal shipping costs range from 0.42 cents per tonne-km (0.62 cents per ton-mile), assuming 45 million tonnes (50 million tons) per year of traffic, to 0.89 cents per tonne-km (1.3 cents per ton-mile) assuming that no other traffic uses the track.

C. Coal-Fired Power Plant

Table VII-5 gives a detailed estimate of the capital investment for a new 800-MW plant along with the percentage of the cost associated with the various items of equipment. The total capital investment is $674 million, or $843 per kW of installed capacity. Table VII-6 displays the operating costs and revenue required for such a plant.

Table VII-3

ESTIMATED INVESTMENT FOR 80 km (50 mi) OF NEW TRACK AND TWO 100-CAR UNIT TRAINS

Cost Component	Investment ($ Million)	Percent
Rolling stock (2 unit trains)		
8 locomotives, 3,000 hp each	2.4	23
200 aluminum-sided 91 tonne (100 ton) (net) hopper cars	8.2	77
Subtotal for Trains	10.6	100
Track construction		
Land acquisition cost	2.0	4
Grading and preparation	16.0	35
Structures and culverts	5.5	12
Roadway	4.5	10
Communication	2.0	4
Grade crossings	0.5	1
Ties	10.0	22
Rails	5.5	12
Subtotal for Track Construction	46.0	100
Interest during construction of track	4.9	
Working capital	0.2	
Organization and start-up expenses	2.4	
Total Capital Investment	64.1	

Table VII-4

OPERATING COST AND REVENUE REQUIRED FOR NEW UNIT TRAIN, 80 km (50 mi) NEW TRACK, AND 1,200 km (750 mi) EXISTING TRACK

Operating Cost	$ Million/Year	Cents/GJ[a] (Cents/10^6 Btu)
Raw materials		
Diesel fuel at $0.09/liter ($.35/gal)	0.9	4 (4)
Maintenance materials	0.7	3 (3)
Total Raw Materials	1.6	6 (6)
Labor (including payroll burden)		
Operating and supervision	1.0	4 (4)
Maintenance	1.5	6 (6)
Administrative and support	0.5	2 (2)
Total Labor	3.0	11 (12)
Fixed costs[b]		
General and administrative expenses	1.0	4 (4)
Property taxes and insurance	0.3	1 (1)
Plant depreciation	0.7	2 (2)
Total Fixed Costs	1.2	5 (5)
Total Operating Costs	5.8	22 (23)
Return on rate base and income tax	1.4	5 (5)
Total Revenue Required	7.2	27.5 (29)
Source of Revenue		
Delivered coal	7.2	27.5 (29)

[a]Assumes 80 km of new track is shared by 23 x 10^6 tonnes per year of coal traffic.

[b]Totals may not equal sum of numbers in column because of rounding errors.

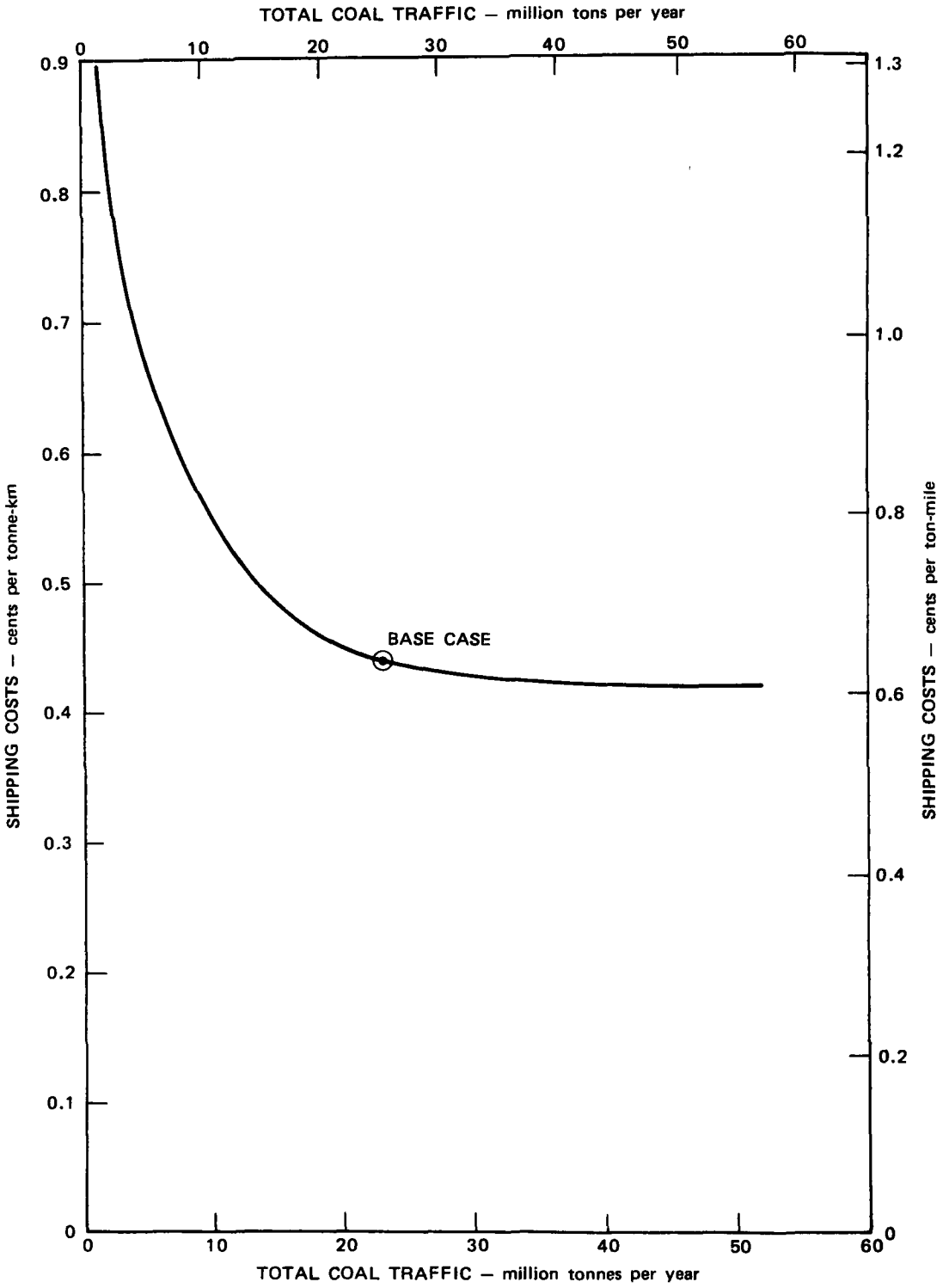

FIGURE VII-1. SENSITIVITY OF UNIT TRAIN COSTS TO VOLUME OF TRAFFIC ON NEW PORTION (80 km) OF TRACK

Table VII-5

CAPITAL INVESTMENT FOR 800-MW COAL-FIRED POWER PLANT WITH FGD

Plant Section	Investment ($ Million)	Percent
Steam generators	133	27
Turbine generators and associated equipment	86	18
Coal handling equipment	7	1
Stack	5	1
Other mechanical equipment, heating, etc.	12	2
Piping	49	10
Controls and instrumentation	12	2
Electrical equipment	12	2
Electrical bulk materials	38	8
Subtotal Power Facilities	354	71
Electrostatic precipitator and ash handing	66	14
FGD system	72	15
Subtotal	492	100
Engineering and home office service, including fees	54	
Total Plant Facilities Investment	546	
Land	5	
Interest during construction	90	
Organization and start-up expenses	27	
Working capital	6	
Total Capital Investment	674	

Table VII-6

OPERATING COSTS AND REVENUE REQUIREMENTS
FOR 800-MW COAL-FIRED POWER PLANT WITH FGD (35% LOAD FACTOR)

Operating Cost	$ Million/Year	Mills/kWh
Raw materials		
Coal at $12.30/tonne ($11.20/ton) delivered	16	6.5
Lime at $39/tonne ($35/ton)	1	0.4
Maintenance materials	4	1.6
Total Raw Materials	21	8.5
Sludge disposal at $10/tonne ($9/ton)	2	0.8
Labor		
Operating and supervision	2	0.8
Maintenance	4	1.6
Administrative, support, and burden	4	1.6
Total Labor	10	4.0
Fixed costs[a]		
Administrative expense	6	2.4
Property taxes and insurance	7	2.9
Depreciation	11	4.5
Total Fixed Costs	24	9.8
Total Annual Operating Costs	57	23.1
Return on rate base and income tax[a]	30	12.2
Revenue Required for Electricity at Busbar	87	35.3

[a]Assumes plant is 50% depreciated after 15 years of base-load operation, and is then reassigned to intermediate load service.

The cost of electricity shown here is based on current construction costs and a capacity factor (35%) typical of a cycling plant. In addition, the initial capital cost of the plant is assumed to be 50% depreciated after 15 years of baseload service before reassigning the plant to intermediate load service in the 1990s. The remaining investment value of the plant is then depreciated over 30 years of intermediate load service, and the yearly capital recovery factor is reduced by one-half to reflect the reduced rate base. Therefore, the capital recovery cost per unit of electricity will not change compared to that for a baseload plant, since the annual capital recovery charges and the load factor have both been reduced by a factor of two.

Figure VII-2 shows the sensitivity of the cost of electricity to the delivered cost of coal and the capital cost of the plant.

D. Coal Gasification Plant

Table VII-7 shows the investment cost for each section of the SNG manufacturing process for a plant making 7.8×10^6 nm^3 (275×10^6 scf) per day of SNG. Less than half of the required investment is for main process plants; the majority (58%) of the investment is for support facilities.

Operating costs and revenue required for the Hygas installation are shown on Table VII-8. With a regulated utility rate basis, SNG is estimated to be produced at a cost of $2.90 per GJ ($3.06 per million Btu). Only ammonia is assumed to have a by-product value. If a large western coal gasification industry were to develop, the remotely located by-product sulfur is not expected to have a large market. Figure VII-3 shows the SNG price sensitivity to changes in coal price and in the capital requirements of the process plants.

E. Coal Liquefaction Plant

Table VII-9 shows the details of the estimated capital investment cost for an H-Coal plant producing 7,950 m^3 per day (50,000 barrels

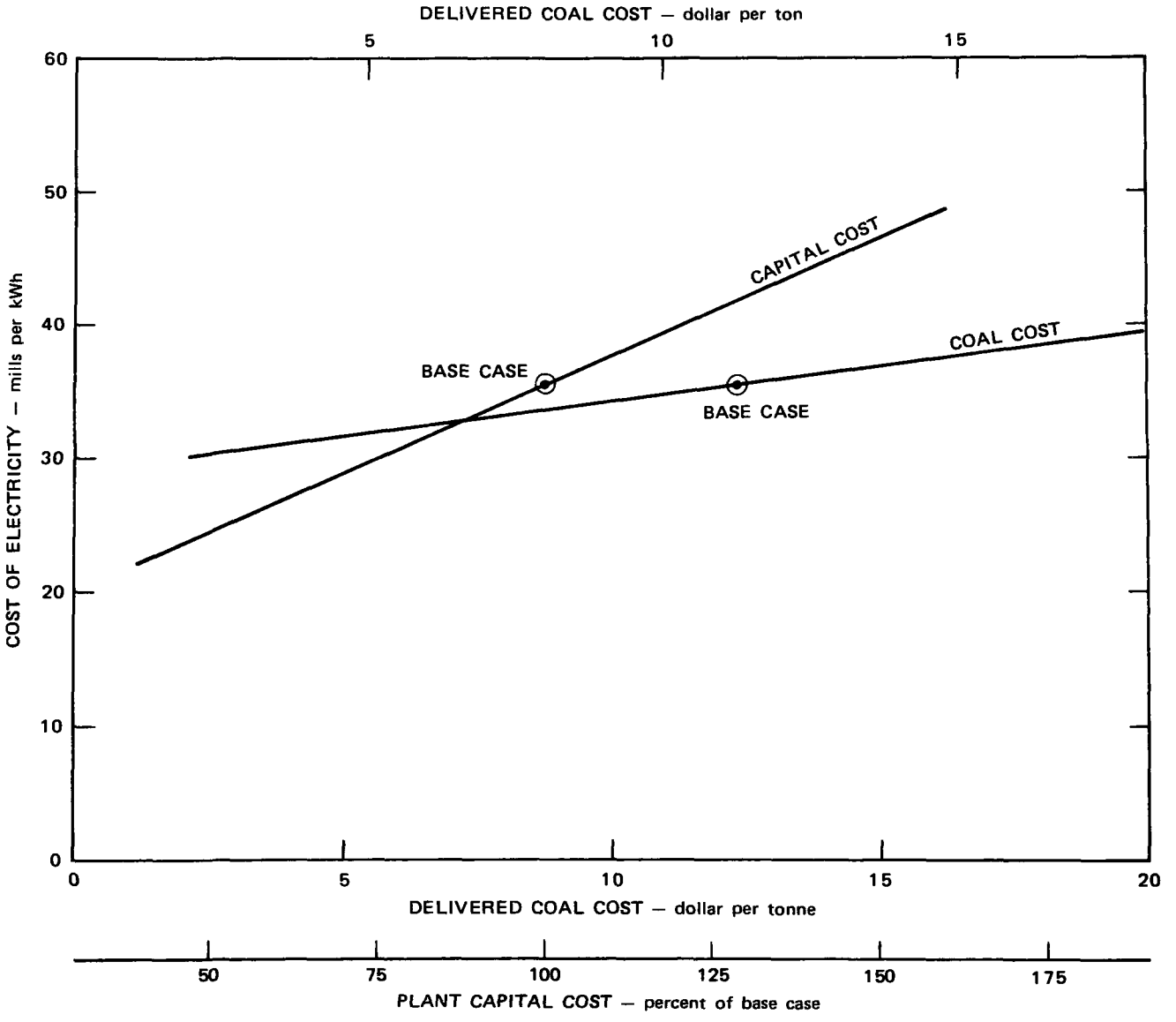

FIGURE VII-2. SENSITIVITY OF THE COST OF ELECTRICITY TO PLANT CAPITAL COST AND DELIVERED COAL COST

Table VII-7

INVESTMENT REQUIRED FOR A 7.8 x 10^6 nm^3 (275 x 10^6 scf) PER DAY SNG PLANT BASED ON THE HYGAS PROCESS

Plant Section	Investment ($ Million)	Percent
Coal storage & reclaiming	14	2
Coal grinding	18	2
Coal slurry pumping	27	3
Gasification	47	6
Raw gas quench	20	2
Shift	33	4
Acid gas scrubbing	113	14
Methanation	30	4
Water reclamation	61	8
Sulfur recovery	63	8
Solids disposal	9	1
SNG drying	1	-
Steam & utilities	143	18
Water systems	18	2
Oxygen plant	47	6
General facilities	71	9
Contractor fees	79	10
Initial catalyst and chemicals	9	1
Total Plant Facilities Investment	803	100
Land	2	
Interest during construction	132	
Paid-up royalties	2	
Working capital	13	
Start-up costs	40	
Total Capital Investment	992	

Table VII-8

OPERATING COSTS AND REVENUE REQUIREMENTS FOR A 7.8 x 10^6 nm^3 (275 x 10^6 scf) PER DAY SNG PLANT BASED ON THE HYGAS PROCESS

Operating Costs	$ Million/Year	Cents/GJ (Cents/10^6 Btu)
Raw materials		
Coal at $6.69/tonne ($6.08/ton)	38	44 (47)
Water	1	1 (1)
Catalyst and chemicals	4	5 (5)
Maintenance materials	16	19 (20)
Total Raw Materials	64	69 (73)
Labor (including payroll burden)		
Operating & supervision	3	4 (4)
Maintenance	16	18 (19)
Administrative and support	4	5 (5)
Total Labor	23	27 (28)
Fixed costs		
Administrative expense	16	19 (20)
Property tax & insurance	20	23 (24)
Depreciation	49	56 (59)
Total Fixed Costs	85	98 (103)
Total Annual Operating Cost	167	194 (204)
Return on rate base & income tax[a]	88	101 (107)
Total Revenue Required	255	295 (311)
Sources of Revenue		
SNG	256	290 (306)
By-product ammonia at $165/tonne ($150/ton)	4	5 (5)
	255	295 (311)

[a]20-year average values.

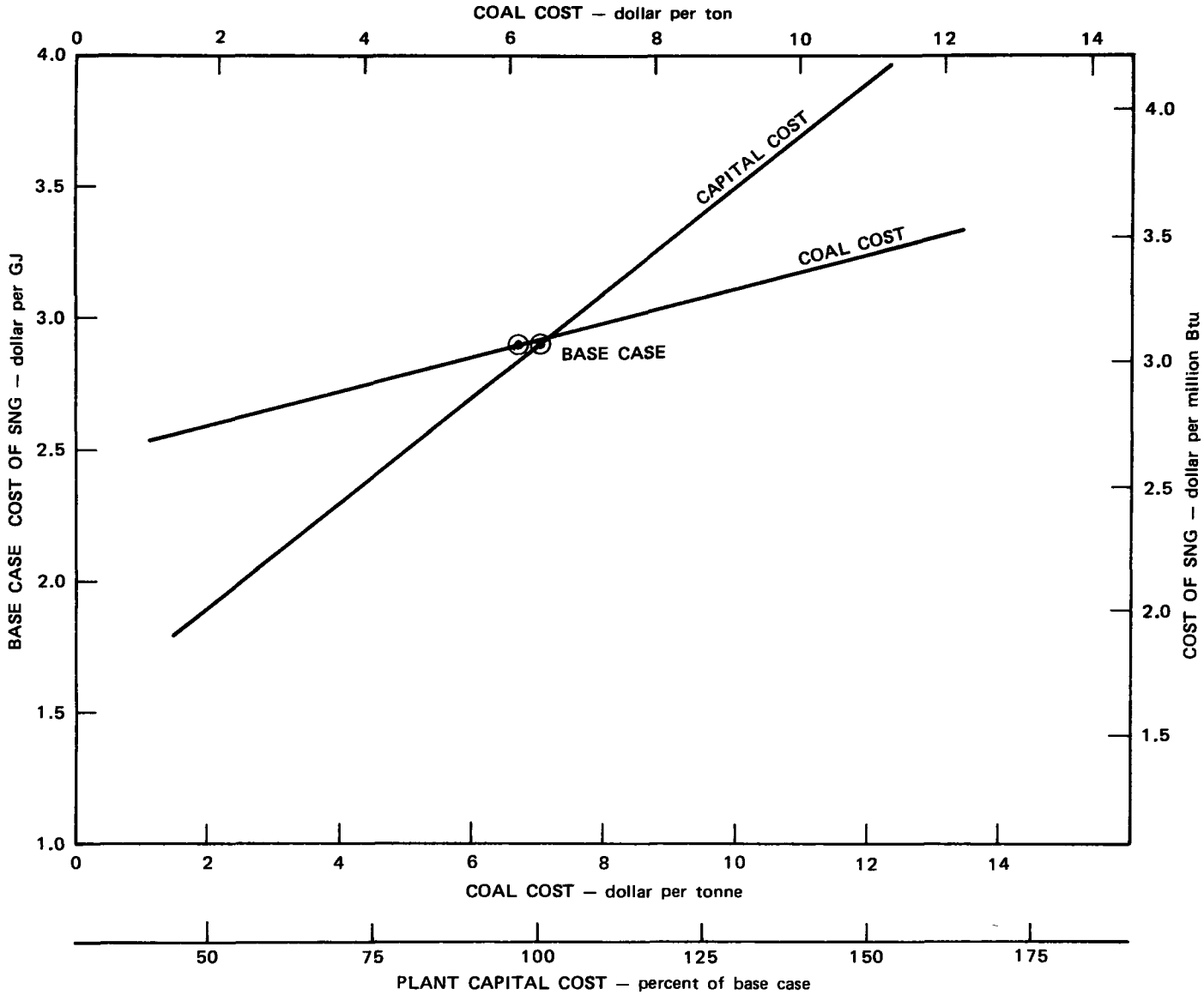

FIGURE VII-3. SENSITIVITY OF THE COST OF SNG TO PLANT CAPITAL COST AND COAL COST

Table VII-9

CAPITAL INVESTMENT FOR A 7,950 m^3 (50,000 bbl) PER DAY PLANT PRODUCING DISTILLATE FUEL OIL FROM COAL BY THE H-COAL PROCESS

Plant Section	Investment ($ Million)	Percent
Coal storage, handling, and preparation	45	5
Slurry preparation	17	2
Hydrogenation section	130	14
Product separation and fractionation	40	4
Steam reforming hydrogen	23	3
Partial oxidation hydrogen	170	19
Oxygen	50	5
Sulfur and ammonia recovery	85	9
Utilities and steam	180	20
General facilities	80	9
Contractor fees	90	10
Total Plant Facilities Investment	910	100
Land	2	
Interest during construction	149	
Paid-up royalties	2	
Working capital	16	
Start-up costs	46	
Total Capital Investment	1,125	

Table VII-10

CAPITAL INVESTMENT FOR A 7,630 m^3 (48,000 bbl) PER DAY PLANT PRODUCING NAPHTHA AND FUEL OIL FROM COAL BY THE H-COAL PROCESS

Plant Section	Investment ($ Million)	Percent
Coal storage, handling, and preparation	45	5
Slurry preparation	17	2
Hydrogenation section	130	13
Product separation and fractionation	40	4
Steam reforming hydrogen	23	2
Partial oxidation hydrogen[a]	180	19
Oxygen[a]	54	5
Sulfur and ammonia recovery[a]	87	9
Utilities[a]	190	20
General facilities[a]	84	9
Naphtha hydrotreater[a]	18	2
Contractor fees	95	10
Total Plant Facilities Investment	963	100
Land	2	
Interest during construction	158	
Paid-up royalties	2	
Working capital	17	
Start-up costs	48	
Total Capital Investment	1,190	

[a]Plant sections changed due to addition of naphtha hydrotreater.

per day) of distillate fuel oil. Table VII-10 gives the cost of the same plant with the additional facilities necessary to hydrotreat the naphtha portion of the product so that it is suitable for steam reforming. The remainder of the distillate product (200-495°C or 400-925°F) is assumed to be sold as fuel oil. The added cost of hydrotreating the naphtha includes the expanded oxygen plant, partial oxidation gasifier, sulfur and ammonia recovery, and utilities, as well as the cost of the hydrotreating plant. These new and expanded plant sections add $65 million, or about 5.8%, to the base liquefaction plant capital investment.

Tables VII-11 and VII-12 give the operating costs and revenue requirements for fuel oil production without and including the naphtha hydrotreating step. When producing only fuel oil the required revenue is $3.02 per GJ ($3.19 per million Btu). If the naphtha is to be hydrotreated for steam reforming, the non-naphtha distillate is assumed to be sold as a by-product at $2.84 per GJ ($3.00 per million Btu). The cost of hydrotreated naphtha is then $3.77 per GJ ($3.97 per million Btu).

Figure VII-4 shows the sensitivity of distillate fuel oil cost to the cost of feed coal and to the capital cost of the process plant. Figure VII-5 shows the sensitivity of hydrotreated naphtha to the cost of feed coal and to the credit allowed for by-product fuel oil.

F. Gas Pipeline

The estimated investment required for an 81-cm (32-in.) gas pipeline is shown in Table VII-13. Cost for physical equipment and installation is $480 million, and total capital investment including equipment, land, interest during construction, and working capital is $548 million. Investment costs vary widely depending on construction difficulty. The midwestern location for the pipeline in this study should allow relatively easy construction because the route should not pass through urban areas, mountainous areas, or very rocky soil. Table VII-14 gives the operating costs and revenue required for the SNG

Table VII-11

OPERATING COSTS AND REVENUE REQUIREMENTS FOR A 7,950 m^3 (50,000 bbl) PER DAY PLANT PRODUCING DISTILLATE FUEL OIL FROM COAL BY THE H-COAL PROCESS

Operating Costs	$ Million/Year	Cents/GJ (Cents/10^6 Btu)
Raw materials		
Coal at $6.69/tonne	49	50 (53)
Water	3	3 (3)
Catalyst and chemicals	10	10 (11)
Maintenance materials	18	18 (19)
Total Raw Materials	80	81 (86)
Labor (including payroll burden)		
Operating & supervision	5	5 (5)
Maintenance	18	19 (20)
Administrative and support	5	5 (5)
Total Labor	28	29 (30)
Fixed costs		
Administrative expense	18	19 (20)
Property tax and insurance	23	23 (24)
Depreciation	55	56 (59)
Total Fixed Costs	96	98 (103)
Total Annual Operating Cost	204	208 (219)
Return on rate base and income tax[a]	100	101 (107)
Total Revenue Required	304	309 (326)
Sources of Revenue		
Distillate fuel oil	298	302 (319)
By-product ammonia at $165/tonne	6	7 (7)
	304	309 (326)

[a]20-year average values.

Table VII-12

OPERATING COSTS AND REVENUE REQUIREMENTS FOR A 7,630 m^3 (48,000 bbl) PER DAY PLANT PRODUCING NAPHTHA AND FUEL OIL FROM COAL BY THE H-COAL PROCESS

Operating Costs	$ Million/Year	Cents/GJ (Cents/10^6 Btu)
Raw Materials		
Coal at $6.69/tonne	49	51 (54)
Water	3	3 (3)
Catalyst and chemicals	12	12 (13)
Maintenance materials	19	20 (21)
Total Raw Materials	83	86 (91)
Labor (including payroll burden)		
Operating & supervision	5	5 (5)
Maintenance	19	20 (21)
Administrative and support	5	5 (5)
Total Labor	29	30 (31)
Fixed Costs		
Administrative expense	19	20 (21)
Property tax and insurance	24	25 (27)
Depreciation	59	62 (65)
Total Fixed Costs	102	107 (113)
Total Annual Operating Cost	214	224 (237)
Return on rate base and income tax[a]	106	111 (117)
Total Revenue Required	320	335 (354)
Sources of Revenue		
Hydrotreated naphtha at $3.77/GJ ($3.97/10^6 Btu)	166	174 (184)
By-product fuel oil at $2.84 GJ ($3.00/10^6 Btu)	147	153 (162)
By-product ammonia at $165/tonne	7	8 (8)
	320	335 (354)

[a]20-year average values.

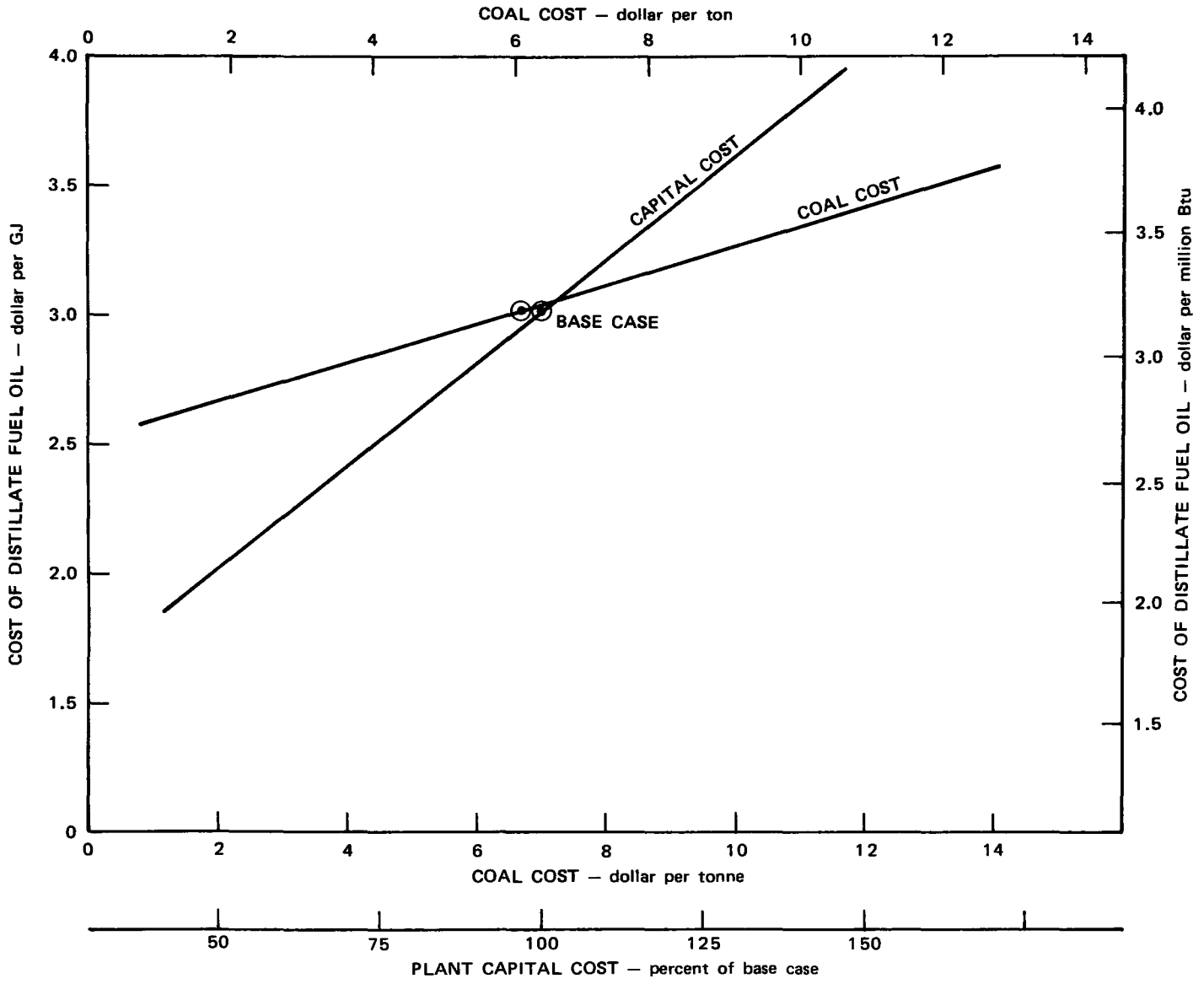

FIGURE VII-4. SENSITIVITY OF THE COST OF DISTILLATE FUEL OIL TO PLANT CAPITAL COST AND COAL COST

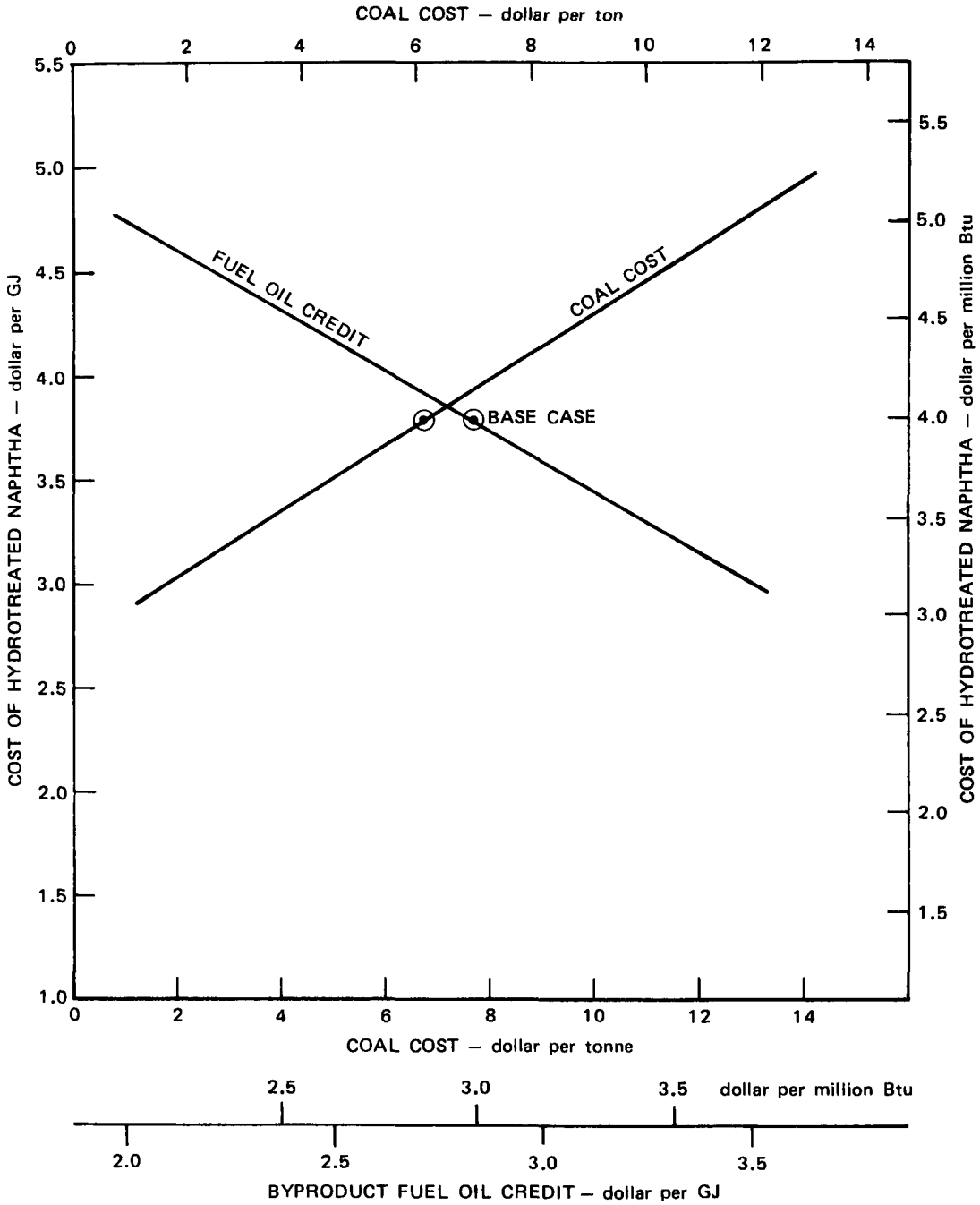

FIGURE VII-5. SENSITIVITY OF THE COST OF HYDROTREATED NAPHTHA TO PLANT CAPITAL COST AND BYPRODUCT FUEL OIL CREDIT

Table VII-13

CAPITAL INVESTMENT FOR A 81-cm (32-in.) DIAMETER GAS TRANSMISSION PIPELINE -- 1,300 km (800 mi)

Cost Component	Investment ($ Million)	Percent
Line pipe	151	32
Pipe coatings	9.9	2
Valves	7.4	2
River and road crossings	0.2	--
Cathodic protection	0.2	--
11 compressor stations	107	22
Miscellaneous	9.2	2
Communications and metering	3.5	1
Subtotal for Materials	296	62
Pipeline construction	116	24
Compressor station construction	27.2	6
Engineering design	37.3	8
Survey and mapping	2.5	1
Subtotal for Services	183	38
Total for Construction of Pipeline	480	100
Land (right of way) and damages	6.4	
Interest during construction	54.8	
Working capital	7.5	
Total Capital Investment	548	

Table VII-14

OPERATING COSTS AND REVENUE REQUIREMENTS FOR AN 81-cm (32-in.) DIAMETER GAS PIPELINE -- 1,300 km (800 mi)

Operating Costs	$ Million/Year	Cents/GJ[a] (Cents/10^6 Btu)
Raw materials		
SNG fuel at $2.90/GJ ($3.06/million Btu)	62	26 (27)
Maintenance materials	4	1 (1)
Total Raw Materials	66	27 (28)
Labor (including payroll burden)		
Operating and supervision	2	1 (1)
Maintenance	2	1 (1)
Administrative and support	1	1 --
Total Labor	5	2 (2)
Fixed costs		
Administrative expense	10	4 (4)
Property tax and insurance	12	5 (5)
Depreciation	17	7 (7)
Total Fixed Costs	39	16 (17)
Total Annual Operating Costs	110	45 (47)
Return on rate base and income tax	48	19 (20)
Total Revenue Required	158	64 (68)
Source of Revenue		
Delivered SNG	158	64 (68)

[a]Totals may not equal sum of numbers in column because of rounding errors.

pipeline. The $0.64 per GJ ($0.68 per million Btu) required revenue assumes:

- Utility financing.
- $2.90 per GJ ($3.06 per million Btu) price for SNG at the gasification plant.
- Thirty-year project and tax lives.

Figure VII-6 shows the sensitivity of required revenue to the parameters of SNG price and pipeline capital cost.

Figure VII-7 shows the sensitivity of gas transmission cost to economies of scale. The costs for the 81-cm (32-in.) diameter pipeline chosen as an example in this report could be significantly changed if a different diameter pipeline were used. Moreover, existing pipelines that are fully depreciated could offer transportation service at considerably reduced prices. As shown on Table VII-14, the cost of delivering SNG in a newly capitalized pipeline is $0.64 per GJ, but an older system with no capital charges or income tax would have a cost of $0.36 per GJ. If an existing system were also of larger diameter (say 122 cm), the delivered cost would drop to about $0.26 per GJ.

G. Liquids Pipeline

The 15,900 m^3 (200,000 barrel) per day liquid pipeline is smaller in diameter (51 cm) than the SNG pipeline (81 cm), so that the liquid pipeline is less expensive than the SNG line. In addition, the liquid pipeline uses pumping stations rather than more expensive compressor stations. Estimated investment costs for the liquid pipelines are shown in Table VII-15. Total capital investment is $309 million for a 1,300-km (800 mi) pipeline.

Table VII-16 shows the operating cost and revenue requirements for fuel oil pipeline shipments. A cost is included for diesel oil to fuel

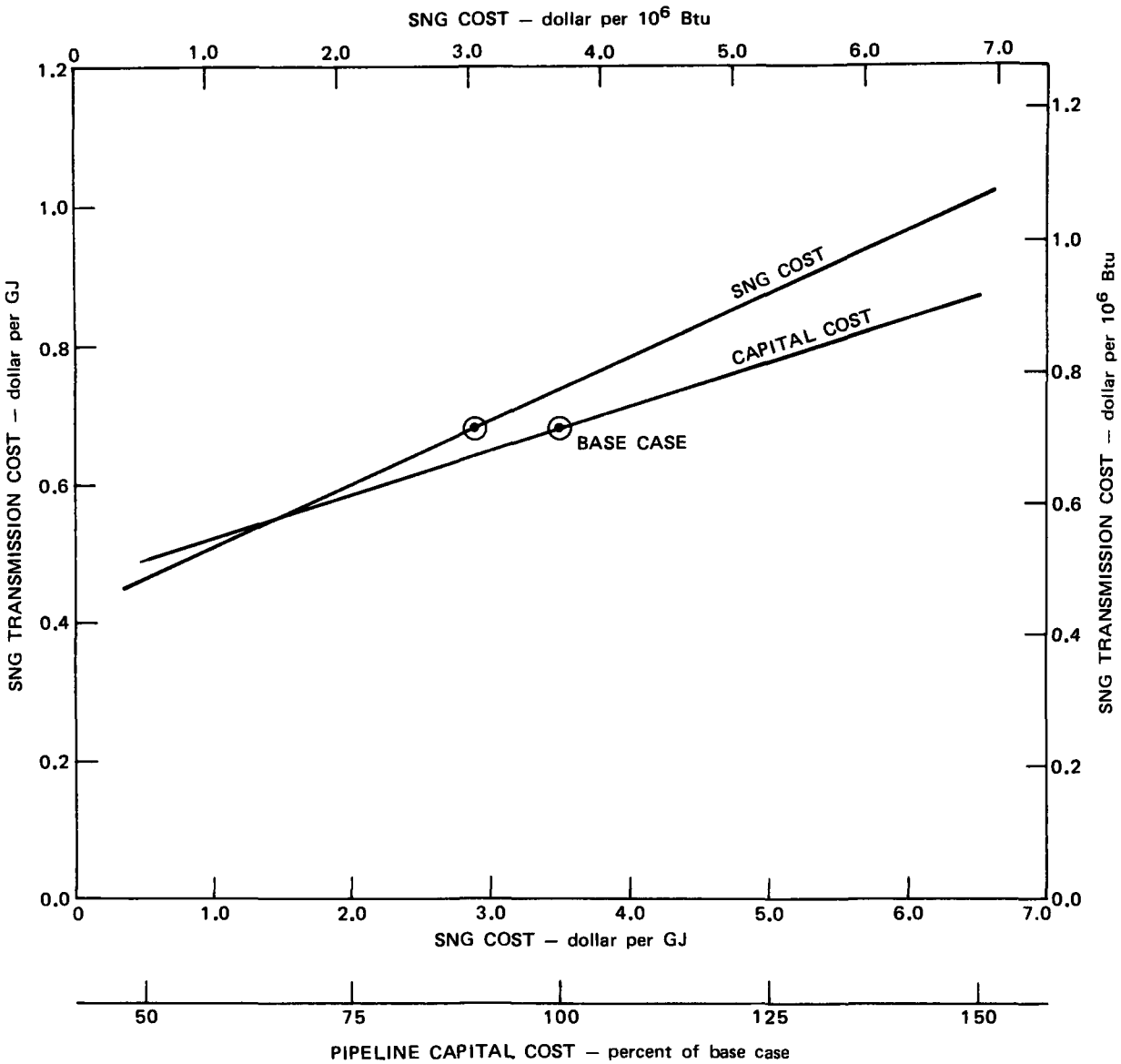

FIGURE VII-6. SENSITIVITY OF SNG TRANSMISSION COST TO PIPELINE CAPITAL COST AND SNG COST

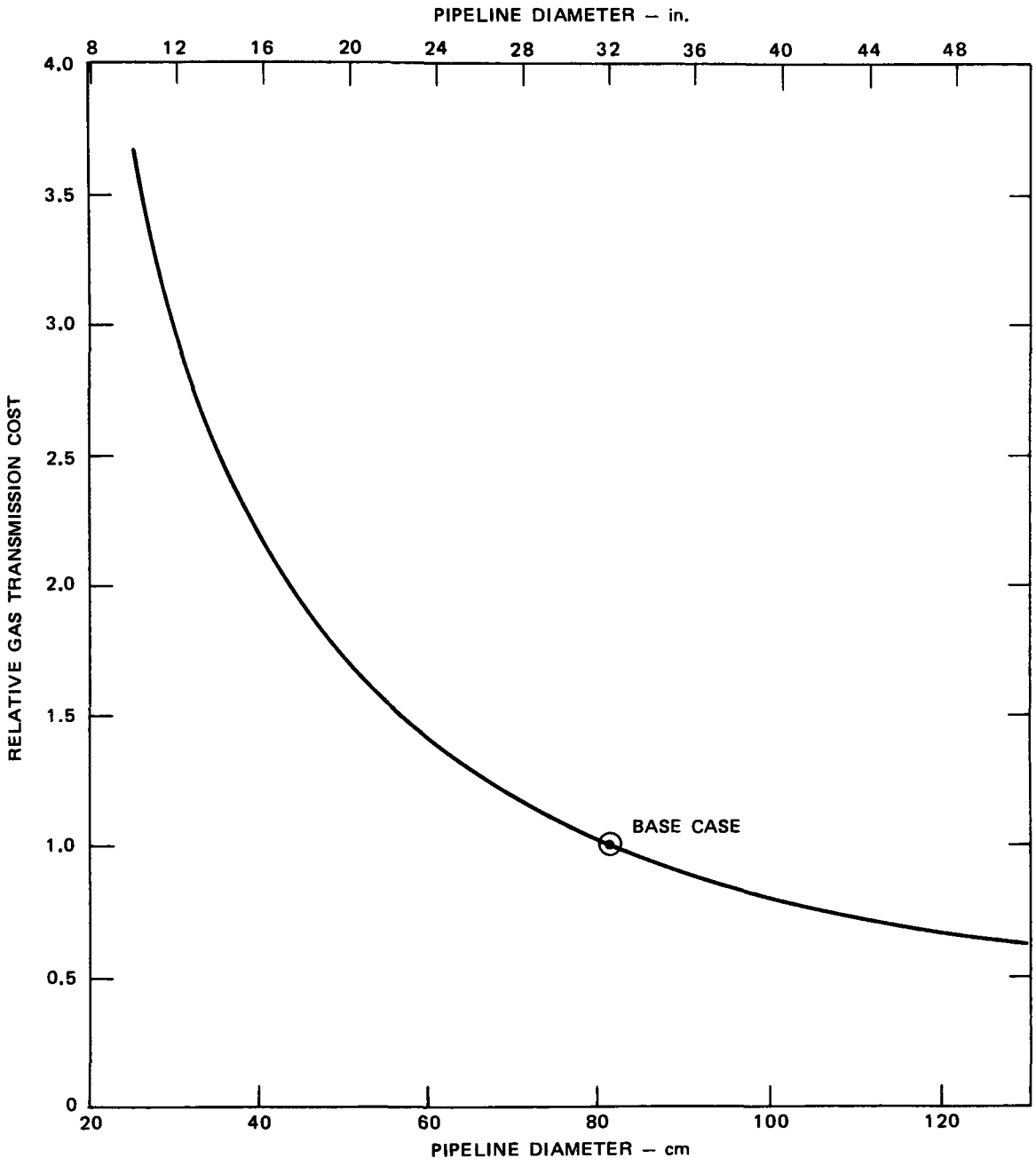

FIGURE VII-7. EFFECT OF PIPE DIAMETER ON SNG TRANSMISSION COSTS (1300 km Distance)

Table VII-15

CAPITAL INVESTMENT FOR A 51-cm (20-in.) DIAMETER
COAL LIQUIDS PIPELINE -- 1,300 km (800 mi)

Cost Component	Investment ($ Million)	Percent
Line pipe	80.4	33
Pipe coating	5.7	2
Valves	2.4	1
Cathodic protection	0.2	--
Miscellaneous	7.5	3
Communication and metering	5.4	2
Subtotal for Materials	102	41
Pipline construction	98.0	40
10 pump stations construction	22.4	9
Engineering	22.2	9
Survey and mapping	2.4	1
Subtotal for Services	145	59
Total for Construction of Pipeline	247	100
Land (right of way) and damages	4.0	
Interest during construction	25.3	
Working capital	33.1	
Total Capital Investment	309	

Table VII-16

OPERATING COSTS AND REVENUE REQUIREMENTS FOR A
51-cm (20-in.) DIAMETER LIQUIDS PIPELINE -- 1,300 km (800 mi)

Operating Costs	$ Million/Year	Cents/GJ (Cents/10^6 Btu)
Raw materials		
Diesel fuel for pumps	6.9	2 (2)
Maintenance materials	0.2	-- --
Total Raw Materials	7.1	2 (2)
Labor (including payroll burden)		
Operating and supervision	1.6	-- --
Maintenance	2.0	0.5 (0.5)
Administrative and support	0.7	-- --
Total Labor	4.3	1 (1)
Fixed costs		
Administrative expense	4.9	1 (1)
Property tax and insurance	6.2	1.5 (1.5)
Depreciation	9.1	2 (2)
Total Fixed Costs	20.2	5 (5)
Total Annual Operating Costs	31.6	8 (8)
Return on rate base and income tax	30.9	8 (8)
Total Revenue Required	62.5	15 (16)
Source of Revenue		
Fuel Oil	62.5	15 (16)

the pump drivers that must be purchased from a source external to the pipeline operation. The total cost of shipping coal-derived distillate fuel oil is $0.15 per GJ ($0.16 per million Btu).

When coal-derived naphtha and fuel oil are sent through the same pipeline, the shipping costs change slightly because of the difference in heating value between the two products. The cost of shipping naphtha is $0.16 per GJ ($0.17 per million Btu), while that of the fuel oil is $0.14 per GJ ($0.15 per million Btu).

As in the SNG pipeline case, a larger diameter liquid pipeline would lower the naphtha and fuel oil shipping cost on a heating value basis. Figure VII-8 shows the sensitivity of fuel oil shipment cost to the capital cost of the pipeline.

H. Liquid Fuel Distribution

Important factors that determine the cost of transporting distillate fuel by train are shipping distance, car size, number of cars per train, terrain, train speed, and loading and unloading times. Representative costs of transporting fuel by unit train are shown in Figure VII-9. These costs are based on 37,850-liter (10,000-gallon) tank cars, 100 cars per train, and 56 km-per-hour (35 mph) average train speed. Costs include standing time for loading and unloading and empty backhaul. The annual capital charges are assumed to be 20% of the investment. The resulting capital charges account for 15% of the shipping cost, with operating and maintenance costs making up the remaining 85%.

Costs of trucking naphtha are shown in Figure VII-10. A 34,000-liter (9,000-gallon) truck, operating at an average road speed of 64 km per hour (40 mi per hour), with a one-stop delivery and empty backhaul, is assumed. Capital charges account for 40% of the trucking cost based on a 30% annual charge rate, and operating and maintenance costs make up the remaining 60% of trucking costs. Trucks with smaller

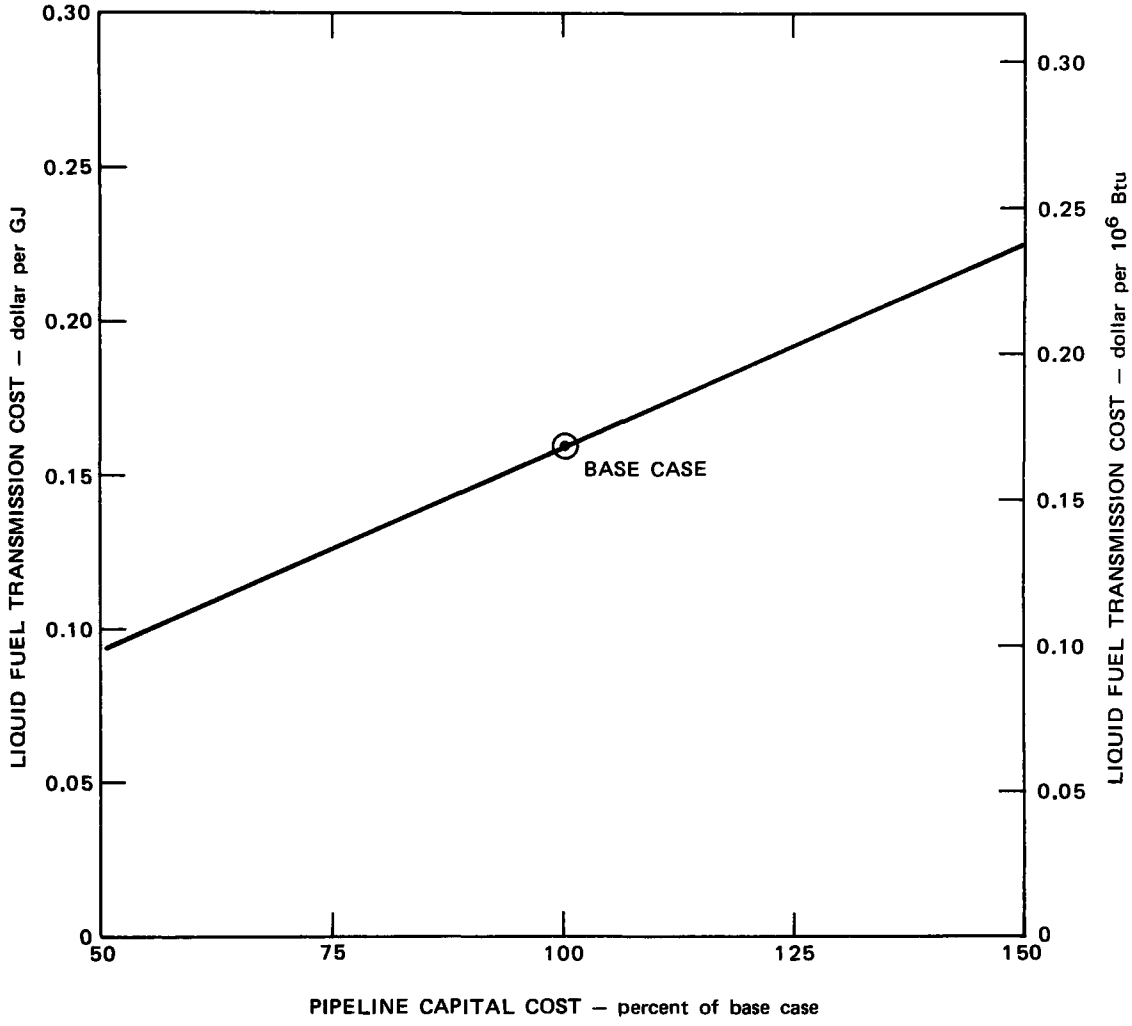

FIGURE VII-8. SENSITIVITY OF LIQUID FUEL TRANSMISSION COST TO PIPELINE CAPITAL COST

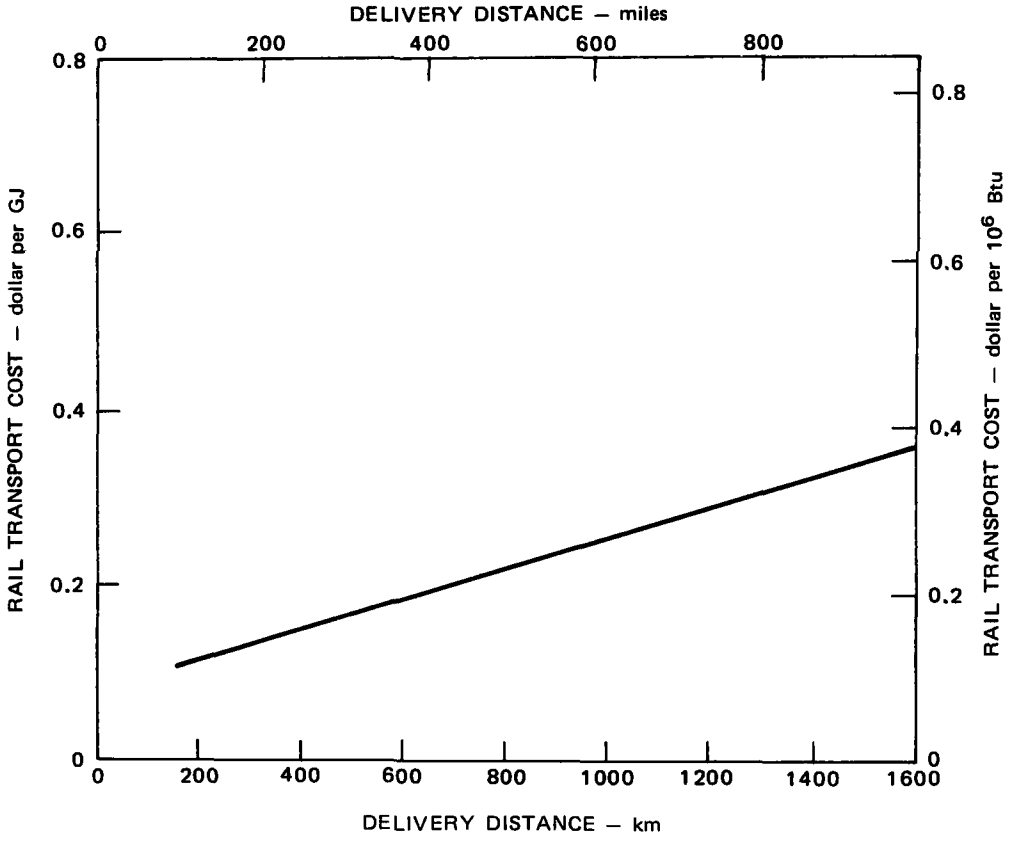

FIGURE VII-9. RAILROAD TANK CAR TRANSPORT COSTS (Fuel Oil)

capacity, lower operating speed, and making more deliveries will have higher trucking costs than those indicated in Figure VII-10.

To estimate the cost of distributing distillate fuel via train to a centralized combined-cycle power plant and of distributing naphtha to dispersed 26-MW fuel-cell power plants requires that assumptions be made about the relative distances of these facilities from the pipeline terminus. A reasonable assumption is that the pipeline terminates near any of the three cities under consideration -- Omaha, Des Moines, or Kansas City. Because fuel-cell power plants would be located near load centers, the distribution of naphtha by truck would involve relatively short distances. If an average distance of 40 km (25 mi) is assumed, the cost of distributing naphtha would be about $0.07 per GJ ($0.07 per million Btu). To this distribution cost must be added the cost of storing the naphtha at the bulk storage terminal prior to delivery. This cost has been estimated to be about $0.01 per GJ ($0.01 per million Btu).[1] Thus, the total storage and delivery cost of naphtha is about $0.08 per GJ ($0.08 per million Btu).

If the combined-cycle power plant is assumed to be centrally located with respect to the three cities, a distance from the bulk terminal to the plant of about 160 km (100 mi) would be reasonable. The total cost of shipping distillate fuel via railroad tank cars (including storage costs) would then be approximately $0.12 per GJ ($0.12 per million Btu).

Because of the low cost of shipping liquid fuels compared to their production costs, it is clear that large changes in the assumed shipping distances will not significantly affect the delivered cost of these fuels.

I. Gas Distribution

The costs of distributing natural gas from large interstate pipelines to individual customers vary widely around the country. A number

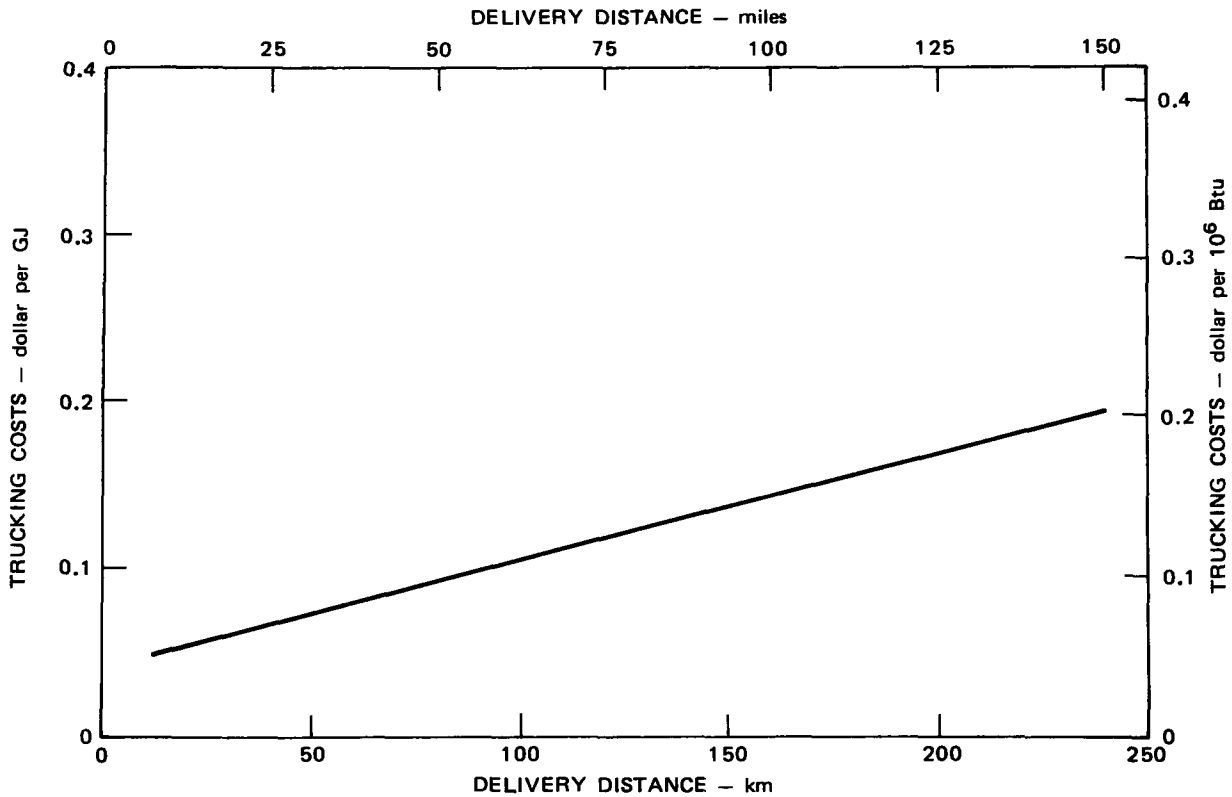

FIGURE VII-10. TANK TRUCK TRANSPORTATION COSTS (Naphtha)

of key variables, including density of the distribution network and age of equipment, are important in determining these costs. Because of the many possible variables, it is more appropriate to use actual costs of gas distribution rather than to attempt to derive such costs from estimates of capital and operating costs.

Historically, the cost of transmitting and distributing natural gas has been a large fraction of the total cost of gas paid by residential customers. From 1971 to 1975 the average wellhead price of natural gas increased from 0.643 to 1.57 cents per nm^3 (18.2 to 44.5 cents per 1,000 scf).[2] During the same period the average residential price increased from 4.06 to 6.11 cents per nm^3 ($1.15 to $1.73 per 1,000 scf).[2] The difference between the wellhead and selling price is the cost of gas transmission and distribution; it increased from 3.43 to 4.52 cents per nm^3 ($0.97 to $1.28 per 1,000 scf). Thus, gas transmission and distribution costs are large and have been increasing, although not nearly so rapidly as wellhead gas prices.

The cost of distributing gas, as opposed to the total cost of transmission and distribution, can be derived from data given in the American Gas Association publication, Gas Facts.[2] The distribution costs can be approximated as the difference between the price of gas paid by local gas utilities to pipeline companies (gas sold for resale) and the price by residential, commercial, or industrial customers. To determine costs specific to the region of interest, we used data from the West North Central states, which encompass Omaha, Des Moines, and Kansas City.

In 1975 the average price paid for natural gas by gas utilities was $0.66 per GJ ($0.70 per million Btu). The average prices paid by residential and commercial customers were $1.30 and $1.04 per GJ ($1.37 and $1.10 per million Btu), respectively. Therefore, the cost of distributing gas to residential and commercial customers may be estimated at $0.54 and $0.38 per GJ ($0.57 and $0.40 per million Btu). Assuming that distribution costs increased at about the same rate from 1975 to 1977 as

they did from 1971 to 1975 (about 7% per year), the 1977 cost of distributing natural gas in the West North Central states would be $0.62 per GJ ($0.65 per million Btu) for residential customers and $0.44 per GJ ($0.46 per million Btu) for commercial customers.

In subsequent cost calculations the cost of distributing natural gas to dispersed 26-MW fuel-cell power plants will be assumed to correspond most nearly to that of distributing gas to large commercial customers.

J. Combined-Cycle Power Plants

The capital investment required for a 270-MW combined-cycle power plant is shown in Table VII-17. The total capital cost of $86.1 million represents an investment of $319 per kW of installed capacity. This total includes the cost of fuel treatment for the coal derived distillate fuel oil and of advanced gas turbines.

The cost of generating electricity in intermediate load operation (35% capacity factor) is shown in Table VII-18, based on a delivered cost of H-Coal distillate of $3.29 per GJ ($3.47 per million Btu). The high cost of this fuel results in fuel-related costs of nearly half the cost of generating electricity. The total cost of electricity from the combined-cycle plant is 46.9 mills per kWh.

Figure VII-11 displays the sensitivity of the cost of electricity to the cost of distillate fuel and the plant capital investment.

K. 26-MW Fuel-Cell Power Plant (SNG)

Manufacturing costs for the molten carbonate fuel-cell power plant were estimated using the bases discussed below. These bases apply to both the System 2 and System 3 dispersed site power plants. The

Table VII-17

CAPITAL INVESTMENT FOR A 270-MW COMBINED-CYCLE POWER PLANT USING DISTILLATE FUEL FROM THE H-COAL PROCESS

Plant Section	Investment ($ Million)	Percent
Fuel preparation	2.4	3
Gas turbine-generator sets	20.0	27
Waste heat boilers	4.7	6
Steam turbine-generator set	15.0	20
Process mechanical equipment	5.9	8
Electrical equipment	6.5	9
Civil and structural	5.8	8
Piping and instrumentation	4.2	6
Engineering & home office services	6.8	9
Miscellaneous	3.1	4
Total Plant Facilities Investment	74.4	100
Land	0.3	
Interest during construction	6.0	
Organization and start-up expenses	3.9	
Working capital	1.5	
Total Capital Investment	86.1	

Table VII-18

OPERATING COSTS AND REVENUE REQUIREMENTS FOR A 270-MW COMBINED-CYCLE POWER PLANT USING DISTILLATE FUEL FROM COAL (35% LOAD FACTOR)

Operating Costs	$ Million/Year	Mills/kWh
Raw materials		
H-Coal distillate @ $3.29 per GJ ($3.47 per million Btu) delivered	19.6	24.2
Water	0.1	0.1
Maintenance materials	1.2	1.4
Labor		
Operating and supervision	0.6	0.7
Maintenance	1.7	2.1
Administrative and support	0.5	0.6
Fixed costs		
General administrative expenses	1.5	1.8
Property taxes and insurance	1.9	2.3
Depreciation	4.2	5.1
Return on rate base and income tax	7.5	9.1
Total Revenue Required	38.8	46.9
Source of Revenue		
Electric Power	38.8	46.9

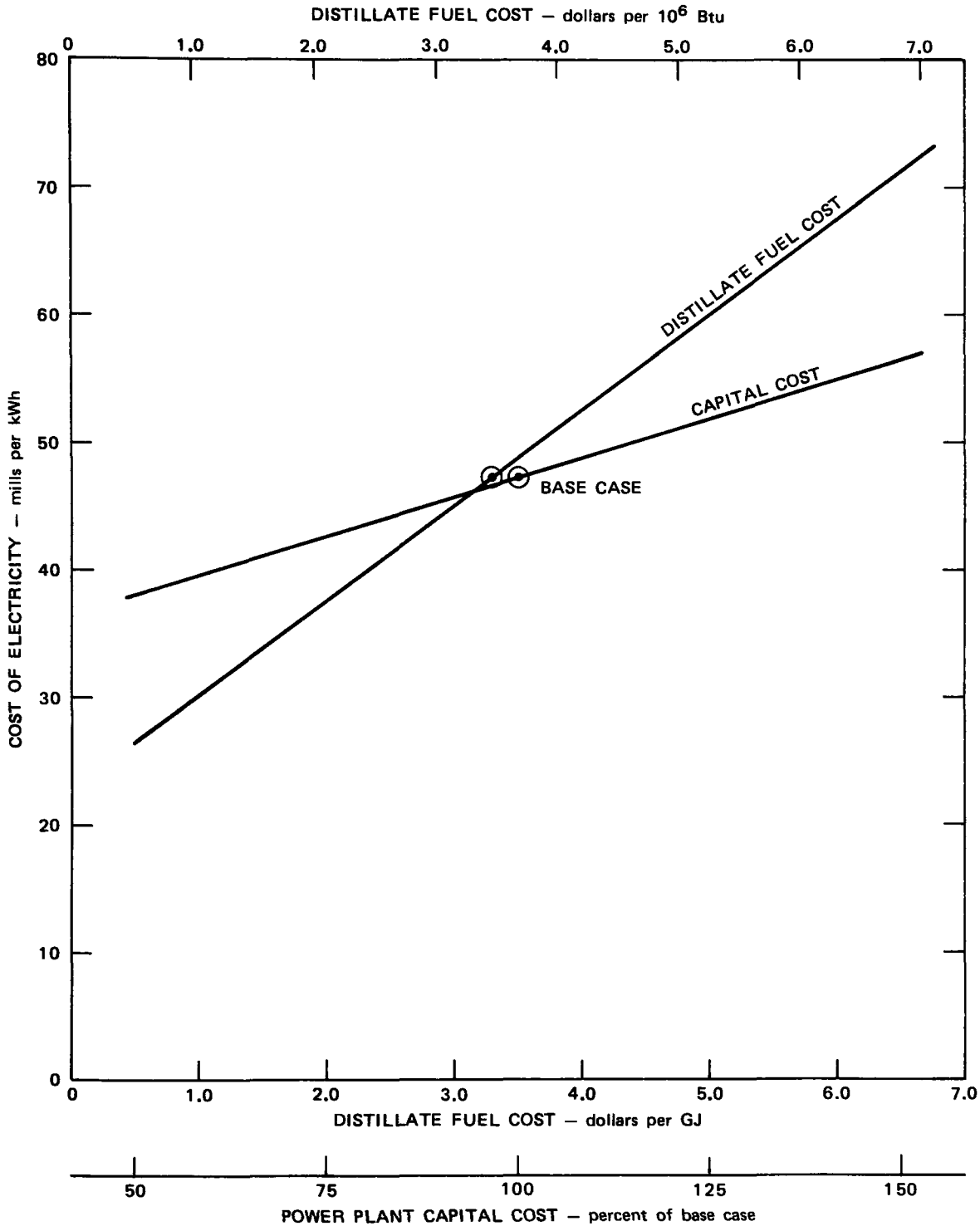

FIGURE VII-11. SENSITIVITY OF COST OF ELECTRICITY TO POWER PLANT CAPITAL COST AND DISTILLATE FUEL COST

following system components are included: fuel-cell trailer; reformer module; equipment module; condenser (E-7); and power conditioner. Those modular assemblies are designed to be transported to the plant site, installed on concrete pads, and interconnected with preassembled sections of piping and ductwork.

1. Fuel-Cell Trailer Cost

The shippable fuel-cell trailer, rated at 3.34 MW, contains eight stacks. Fabricated from structural steel, it is enclosed by corrugated steel panels. The stack cost estimates are based on the molten carbonate fuel-cell design described by UTC in the ECAS program.[3] Supplementary information was obtained from recent ERC reports.[4] The estimates were based on calculations of actual quantities of raw materials used to fabricate the components. Current cost of raw materials, in the form expected to be used, were obtained from vendor contacts. Fabrication costs were then determined by multiplying the material cost by a manufacturing cost factor, which was selected based on the production rate and the degree of automation envisioned for the manufacturing facility. The factors reflect manufacturing value added, including direct and supervisory labor plus other manufacturing burdens (e.g., maintenance and inventory costs).

The accuracy of this type of estimate mainly depends on the assumptions made concerning the design configuration, such as material thickness and the selection of the materials. The application of incorrect manufacturing cost factors presents a lesser risk because they tend to fall within a fairly predictable range for all manufacturing facilities operating at high production rates. It can safely be assumed that profitable businesses will employ the most advanced methods in order to remain competitive.

The fuel-cell stack components and vendor quotes for materials costs are listed in Table VII-19. The estimated cost of an individual

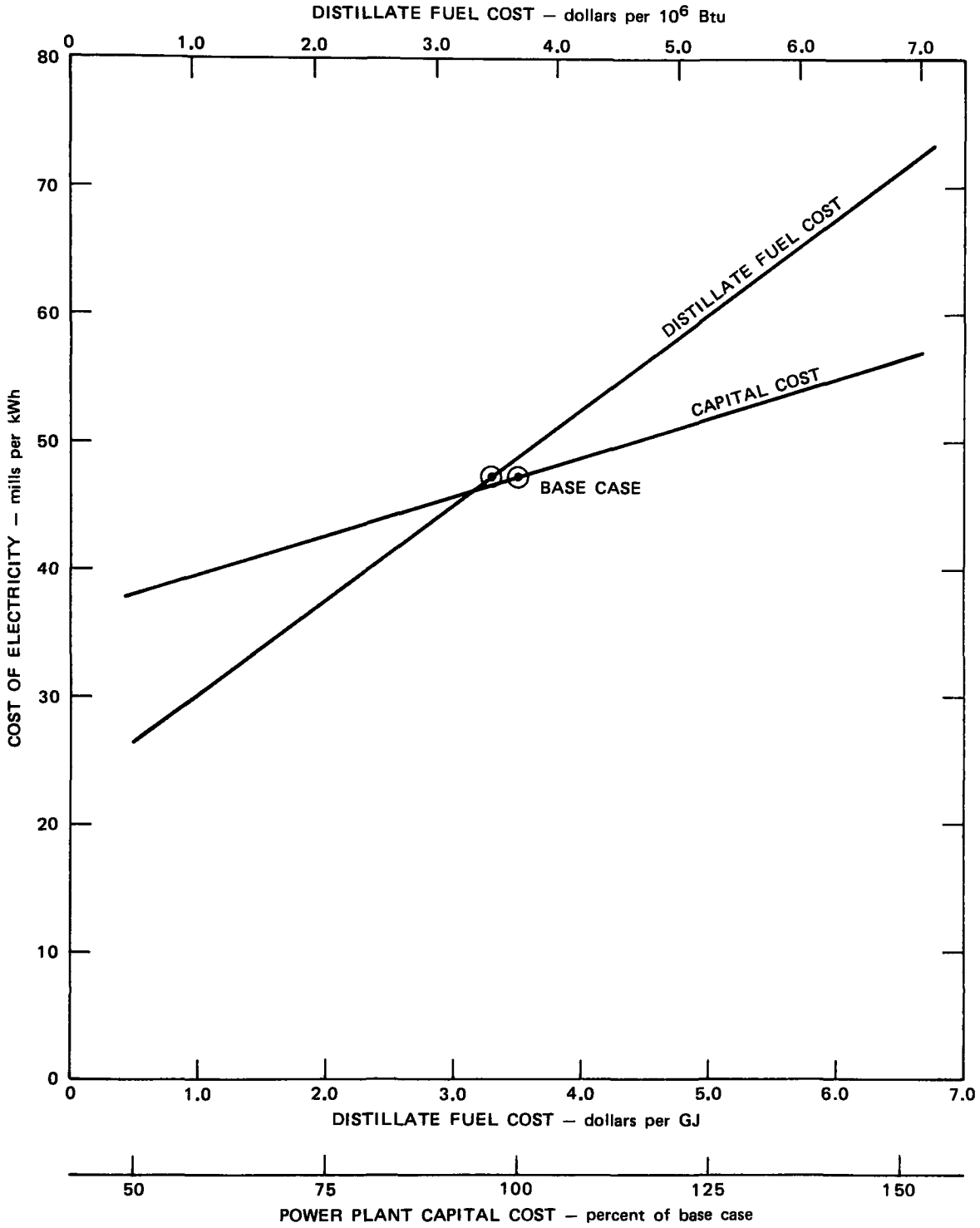

FIGURE VII-11. SENSITIVITY OF COST OF ELECTRICITY TO POWER PLANT CAPITAL COST AND DISTILLATE FUEL COST

following system components are included: fuel-cell trailer; reformer module; equipment module; condenser (E-7); and power conditioner. Those modular assemblies are designed to be transported to the plant site, installed on concrete pads, and interconnected with preassembled sections of piping and ductwork.

1. Fuel-Cell Trailer Cost

The shippable fuel-cell trailer, rated at 3.34 MW, contains eight stacks. Fabricated from structural steel, it is enclosed by corrugated steel panels. The stack cost estimates are based on the molten carbonate fuel-cell design described by UTC in the ECAS program.[3] Supplementary information was obtained from recent ERC reports.[4] The estimates were based on calculations of actual quantities of raw materials used to fabricate the components. Current cost of raw materials, in the form expected to be used, were obtained from vendor contacts. Fabrication costs were then determined by multiplying the material cost by a manufacturing cost factor, which was selected based on the production rate and the degree of automation envisioned for the manufacturing facility. The factors reflect manufacturing value added, including direct and supervisory labor plus other manufacturing burdens (e.g., maintenance and inventory costs).

The accuracy of this type of estimate mainly depends on the assumptions made concerning the design configuration, such as material thickness and the selection of the materials. The application of incorrect manufacturing cost factors presents a lesser risk because they tend to fall within a fairly predictable range for all manufacturing facilities operating at high production rates. It can safely be assumed that profitable businesses will employ the most advanced methods in order to remain competitive.

The fuel-cell stack components and vendor quotes for materials costs are listed in Table VII-19. The estimated cost of an individual

Table VII-19

FUEL-CELL STACK COMPONENTS

Component	Dimensions, cm (in)	Materials	Weight/cell, kg (lb)		Cost, $/kg ($/lb)		Source
Electrolyte tile	100.3 x 100.3 x 0.089 (39.5 x 39.5 x 0.035)	40% Li AlO_2 21% Li_2CO_3 39% K_2CO_3	0.89 0.92 0.86	(1.95) (2.03 (1.90)	6.16 1.94 0.51	(2.80) (0.88) (0.23)	Lithium Co. (America)
		Total Tile Weight:	2.62	(5.88)	2.88	(1.31)	(Average)
Anode	92.2 x 92.2 x 0.076 (36.3 x 36.3 x 0.030) (56% Porosity)	Ni Powder	2.51	(5.53)	5.94	(2.70)	International Nickel
Cathode	92.2 x 92.2 x 0.038 (36.3 x 36.3 x 0.015 (56% Porosity)	Ni Powder	1.26	(2.77)	5.94	(2.70)	International Nickel
Cathode collector	100.3 x 100.3 x 0.152 (39.5 x 36.3 x 0.060) Stock Thk = 0.010 (0.004)	304 SS	0.75	(1.64)	4.27	(1.94)	Rodney Metals
Anode collector	92.2 x 92.2 x 0.102 (36.3 x 36.3 x 0.040) Stock Thk = 0.010 (0.004)	304 SS	0.69	(1.51)	4.27	(1.94)	Rodney Metals
Cell separator	100.3 x 100.3 x 0.102 (39.5 x 39.5 x 0.040)	304 SS	1.14	(2.51)	4.27	(1.94)	Rodney Metals
		Total Cell Weight:	9.02	(19.84)			
Stack end plates	120.6 x 120.6 x 7.6 (47.5 x 47.5 x 3) Stock Thk = 0.952 (0.375)	430 SS	352 (775)/stack		1.78	(0.81)	U.S. Steel
Tie rods (16)	1.9 (0.75) Diam.	430 SS	81 (178)/stack		1.78	(0.81)	U.S. Steel
Springs (16)	--	302 SS	109 (240)/stack		2.16	(0.98)	U.S. Steel
		Total Stack Weight:	5,141 (11,311)				

fuel-cell trailer is $359,000, as shown in Table VII-20. The piping, wiring, enclosure, and assembly material cost was arbitrarily based on an assumed structure weight of 3,270 kg (7,200 lb), costed at $2.20/kg ($1/lb). The assigned cost factor of 3.0 reflects a less automated, more labor-intensive, manufacturing operation.

Table VII-20 shows that the costliest items are the fuel-cell components, which make up 87.5% of the total. To minimize labor costs, the most advanced production machinery would have to be used. The capital investment for this facility has not been estimated, but it would probably be quite high.

Table VII-20

FUEL-CELL TRAILER COST SUMMARY

Component[a]	Raw Material Cost, $1000	Mfg. Cost Factor	Mfg. Cost $1000	Total Cost[b] $1000	% Total Trailer Cost
Electrolyte tile	31.4	1.2	37.7	69.1	19.2
Anode	60.9	0.6	36.6	97.5	27.2
Cathode	30.5	0.6	18.3	48.8	13.6
Collectors	24.9	1.2	29.9	54.8	15.3
Separators	19.9	1.2	23.8	43.7	12.2
End plates	5.0	1.3	6.5	11.5	3.2
Tie rods	1.2	0.6	0.7	1.9	0.5
Springs	1.9	0.6	1.1	3.0	0.8
Miscellaneous[c]	7.2	3.0	21.6	28.8	8.0
Total	182.9		176.2	359.1	100

[a]Eight stacks/trailer.

[b]Total cost = raw material + manufacturing cost.

[c]Piping, wiring, enclosure, and assembly.

Considerable manufacturing development effort will be required for the electrolyte tile production facility. A major problem area will be tile cracking, unless a flexible tile configuration can be developed. Electrolyte tiles are currently manufactured in a noncontinuous process. Lithium aluminate powder is mixed with finely ground lithium and potassium carbonate. The mixture is then placed in a mold, compressed, and fired in a furnace. Ultimately, a completely automated production facility should be used, similar to those developed for electrode manufacture. At present, sintered nickel electrodes are manufactured commercially in a continuous 30-cm (12-in.) wide strip using a slurry method for applying the nickel powder to a nickel-plated steel substrate. Material cost at present is 50% of the total manufactured cost. The manufacturer hopes to increase this to 75% with improved methods.

Fabrication of collectors and separators will be fairly straightforward. The collectors can be formed in large stamping presses, which would require some handling of individual pieces. A continuous roll forming production line could be used, which could result in a cost factor lower than the assumed 1.2. The separator, however, is a more complex component and will always require more labor. It consists of an outer frame containing metal seal surfaces and fuel manifolding, welded to the cell separating sheet. This configuration will require handling of more than one part and seam welding to join the parts together.

The assumed thicknesses of the electrolyte tile (0.089 cm), collectors (0.010 cm), and separators (0.010 cm) are reasonably optimistic projections, based on the current status of molten carbonate fuel-cell design. The latter are fabricated from 304 stainless steel. If corrosion of the stainless steel parts requires that they be replaced by nickel, their material cost will almost double. Using nickel should not affect the manufacturing cost, however, and would only increase the total cost by 14%.

A comparatively small portion of the total cost (12.5%) is for the stack hardware, structures, and enclosure. The production rates of these items are too low to justify highly sophisticated and automated machinery -- thus a higher manufacturing cost factor was used.

Developing the manufacturing technology for fabricating most components should not be difficult. The exception to this may be the manufacture of the electrolyte tile. A more flexible electrolyte structure is needed and perhaps can be developed.

2. Reformer Module Cost

The cost of the reformer module was calculated from Exxon data on cylindrical-type reformer furnaces. The total material and labor costs were determined for the fabrication of a single unit. A direct labor rate of $9/hr was assumed and a factory overhead rate of 200% was used. A learning factor of 0.9 was then applied to the labor cost to determine the average cost per unit for 400 modules. Eighty percent of the cost of the reformer is for the reactor and heat exchanger tubing and manifolding. Stainless steel is required throughout because of the high operating temperature. The total cost of the reformer is $504,000, of which 43% is the cost of the heat exchangers (E-1 through E-4).

3. Equipment Module Cost

The equipment module cost was determined by calculating the total F.O.B. cost of heat exchangers, blowers, electric motor drivers, and other components based on Exxon cost data and discussion with vendors. The cost breakdown is shown in Table VII-21. The use of canal-type recuperators for exchangers E-5 and E-6 resulted in substantial cost reduction.

Table VII-21

EQUIPMENT MODULE COST BREAKDOWN

Item	Cost, $1000
Exchanger E-5	9.6
E-6	58.2
ZnO guard bed	3.0
Knockout drum	1.5
Blower B-1	12.3
B-3	44.9
B-4	20.6
B-5	21.0
P-1	2.5
Module fabrication	55.0
Total Equipment Module Cost	228.6

4. Condenser Cost

The condenser section, exchanger E-7, consists of two bays of air-fin heat exchangers, 3.4 x 9.2 m (11 x 30 ft). Each bay has two fans. The cost of these units ($15,000 per bay) was determined from Exxon cost data. Each bay would be shipped to the power plant site and erected on concrete piers.

5. Power Conditioning Costs

Projected costs of power conditioning equipment have been reported by Westinghouse.[5] They vary from $50 to $70/kW, depending on the input DC voltage. An average cost of $60/kW was assumed for this study.

6. Total Power Plant

Total installed costs were estimated for the base case System 2 power plant. Total manufactured costs were calculated by summing the costs for each system component. Installation-related costs were then estimated. Here, site preparation costs include grading and installation of access roadways, but not the cost of land. No cost allowance was made for buildings and similar facilities, because the system is assumed to operate unattended.

Other indirect costs were estimated as 40% of total manufactured cost and 25% of total installation costs. These indirect costs reflect general and administrative expense, taxes and insurance, interest on investment, sales and marketing expense, return on investment, and contingencies, if any. Architect and engineering charges are not explicitly detailed. Also, escalation and interest charges during construction were not included. Site preparation and installation time for the modular power plant is assumed to be short.

A breakdown of the estimated power plant cost is given in Table VII-22. Total installed cost for the base-case system is $12,530,000, equivalent to $522/kW of net output (24.0 MW). This value is higher than expected, but substantial investment cost reduction is possible.

The ultimate optimization of any power plant is a complex trade-off between investment charges and fuel charges, reflecting constraints placed on the system. The power plant here has been constrained to meet a heat rate of 7,910 kJ/kWh (7,500 Btu/kWh) and to be water-conservative. If those constraints were relaxed, investment costs and the cost of delivered energy could be reduced.

For example, in many locations, the amount of water necessary for reforming is readily available from local supplies and total water conservation would not be necessary. Water requirements are about

Table VII-22

NOMINAL 26-MW FUEL-CELL POWER PLANT COST ESTIMATE

Item	No. in System	Unit Cost, $1000	Total Cost, $1000
Fuel-cell trailer	8	359.1	2,873
Reformer/heat exchanger package	4	504	2,016
Equipment module	4	228.6	914
Condenser (E-7)	4	60	240
Power conditioner and switchgear	4	402	1,608
Electrical wiring, controls and instrumentation	--	--	534
Total Manufactured Cost			8,185
Site preparation	--	--	481
Freight and insurance	--	--	82
Mechanical structures, foundations and piping	--	--	294
Total Installation Costs			857
Other indirect costs + profit[a]			3,488
Total Power Plant Installed Cost			12,530

[a]Taken as 40% of total manufactured cost + 25% of total installation costs.

0.57 liter/kWh (0.15 gal/kWh). In the tricity study region, 1 kWh is worth 30-50 mills. Water consumption would only add 0.07 mills/kWh, a negligible amount. As a result, E-2, the knockout drum, blower B-2, and the water recycle pump could be eliminated, and the size of E-5 could be decreased. Fuel cell performance and the heat exchange characteristics of exchanger E-5 would also be affected; thus, although it is not clear exactly what the final cost of electricity will be, the investment cost can be lowered.

As explained earlier, slightly higher heat rates are also cost-effective. For example, the base-case design voltage was chosen as 0.8 V per cell. A decrease to 0.787 V per cell increases the current density and reduces the number of fuel-cell modules by 19%. Furthermore, because more waste heat is available, the temperature-driving forces in the reformer and heat exchangers E-1, E-2, E-3, and E-4 are larger, so less heat transfer surface would be required. That would noticeably reduce investment cost. The resulting increase in heat rate would increase the fuel cost by only 1.6%.

The combined effect of relaxing the constraints will clearly lower the optimum cost of electricity, primarily by lowering the investment cost. However, the exact calculation of that optimum would require substantial additional effort, requiring analysis of several cases.

Molten carbonate fuel-cell technology is at an early stage of development, but performance improvements and cost reductions can be projected for most system components. These expected reductions will result from current and future R&D programs and system optimization studies. The impact of these potential improvements was assessed by assuming the following:

- Improved fuel-cell designs, resulting in a 50% increase in current density, hence power density, at the design cell voltage.
- A 15% reduction in the quantity of materials used in stack construction.

- Cost reductions for specific components, including:
  - Reformer/heat exchanger package 25%
  - Equipment module 15%
  - Condenser (E-7) 10%
  - Power conditioner 20%
  - Electrical wiring, etc. 15%
- A 15% reduction across-the-board in installation-related costs.

Simultaneous achievement of all cost reduction projections would lower the installed cost of the System 2 power plant by 27% from $522/kW to $380/kW. The optimistic projection is listed in Table VII-23, along with the additional capital requirements for a completely installed and operating plant.

Operating and maintenance (O&M) costs for operating the power plant must also be estimated. Firm bases for such estimates are not available. Periodic stack replacement costs could range from 0.2 to 0.4 cent/kWh, excluding replacement labor costs. This estimate assumes 40,000 hr operating life at full-rated load (24.0 MW). Fuel conversion catalyst replacement costs should be low. Equipment maintenance and replacement costs should also be low, reflecting, say, a 20-year expected life. Thus, total O&M costs could be taken as 0.5 cents/kWh. Finally, local ordinances may require attended operation of fuel-cell power plants.

The cost of producing electricity from the nominal 26-MW fuel-cell power plant is shown in Table VII-24. The delivered cost of SNG is based on the production, pipeline, and distribution costs presented in previous sections. Capital-related charges are based on the optimistic power plant costs given in Table VII-23. The O&M cost is that discussed in the preceding paragraph.

Table VII-23

OPTIMISTIC COST PROJECTION FOR NOMINAL 26-MW FUEL-CELL POWER PLANT

Item	Total Cost, $1000
Fuel-cell trailer	1,628
Reformer/heat exchanger package	1,512
Equipment module	777
Condenser (E-7)	216
Power conditioner	1,286
Electrical wiring, controls, and instrumentation	454
Total Manufactured Cost	5,873
Site preparation	409
Freight and insurance	59
Mechanical structures, foundations, and piping	250
Total Installation Costs	718
Other indirect costs + profit	2,529
Total Power Plant Installed Cost	9,120
Land	20
Interest during construction	460
Working capital	240
Start-up costs	90
Total Capital Investment	9,930

Table VII-24

OPERATING COSTS AND REVENUE REQUIREMENTS
FOR A NOMINAL 26-MW FUEL-CELL POWER PLANT

Operating Costs	$Million/Year	Mills/kWh
SNG fuel at $3.98/GJ ($4.20 per million Btu)	2.22	30.2
Operation and maintenance	0.37	5.0
Administrative expense	0.18	2.4
Property taxes and insurance	0.23	3.1
Depreciation	0.48	6.5
Total Annual Operating Costs	3.48	47.2
Return on rate base and income tax	0.87	11.8
Total Revenue Required	4.35	59.0
Sources of Revenue		
Electric power	4.35	59.0

Figure VII-12 shows the sensitivity of the cost of electricity to changes in fuel costs and power plant capital costs. Use of the capital costs estimated in Table VII-22 would increase the cost of electricity to 69.4 mills/kWh.

L. 26-MW Fuel-Cell Power Plant (Naphtha)

Investment cost estimates for the System 3 power plant were made based on the detailed evaluation of System 2 component costs. Adjustments were made to reflect differences in size and performance. A breakdown of the reformer package cost is given in Table VII-25.

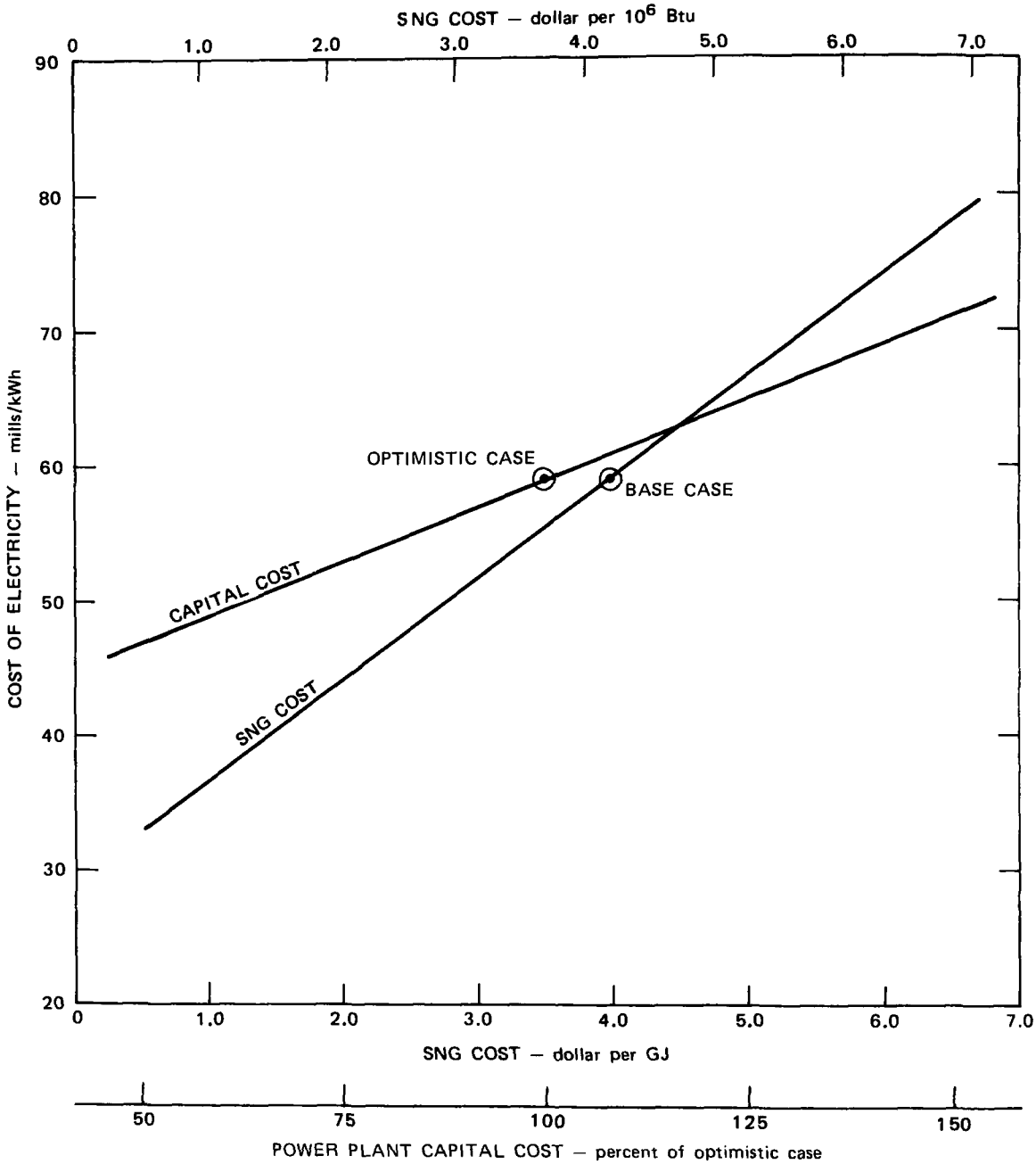

FIGURE VII-12. SENSITIVITY OF THE COST OF ELECTRICITY TO POWER PLANT CAPITAL COST AND SNG COST

Table VII-25

COST BREAKDOWN OF NAPHTHA REFORMER PACKAGE

Cost Item	Total Manufactured Cost, $1000
Reformer tubes	135.0
Exchanger tubes	
E-1	73.0
E-2	81.7
E-3	51.9
E-4	120.5
Tube manifolds	190.8
Catalyst	19.3
Burner	22.4
Structures	116.2
Total	806.2

The cost of the reformer package is high compared with reformer cost estimates reported in the literature because it contains heat exchangers E-1 to E-4, which make up 57% of the total cost. The reformer portion alone would cost about $35/kW for either System 2 or 3.

A summary of component costs for the equipment module is shown in Table VII-26. The reduction in the size of heat exchanger E-6 accounts for the lower cost of the equipment module, compared with System 2. The cost for both systems was reduced by replacing the shell and tube heat exchangers E-5 and E-6 by canal type units, which cost around $161/m^2$ ($15/ft^2$) compared to $592/m^2$ ($55/ft^2$) for the shell and tube configuration.

A breakdown of the estimated plant cost is given in Table VII-27 (see Section VII-K for costing approach). Total installed cost for the non-optimized base-case System 3 power plant is $13,740,000, equivalent to $537/kW of net output (25.6 MW). This bottom-line cost is about the

Table VII-26

EQUIPMENT MODULE COST BREAKDOWN

Component	Total Manufactured Cost, $1000
Exchanger	
E-5	14.0
E-6	46.5
Blowers:	
B-1	13.3
B-3	47.0
B-4	21.0
B-5	23.0
B-6	0.5
Shift reactor	2.0
Hydrodesulfurizer	2.0
ZnO bed	2.5
Pump: P-1	2.8
Knockout	1.7
Module fabrication	53.4
Total	229.7

Table VII-27

NOMINAL 26-MW FUEL-CELL POWER PLANT COST ESTIMATE

Item	No. in System	Unit Cost, $1000	Total Cost, $1000
Fuel-cell trailer	8	284	2,296
Reformer/heat exchanger package	4	806	3,225
Condenser (E-7)	4	75	300
Equipment module	4	230	920
Power conditioner and switchgear	4	75	1,710
Electrical wiring, controls and instrumentation	--	--	560
Total Manufactured Cost			9,011
Site preparation	--	--	505
Freight and insurance	--	--	90
Mechanical structures, foundations, and piping	--	--	308
Total Installation Costs			903
Other indirect costs + profit[a]			3,830
Total Power Plant Installed Cost			13,740

[a]Taken as 40% of total manufactured cost + 25% of total installation costs.

same as that estimated for the System 2 power plant. The reformer package cost for the naphtha system is higher. However, this is counter-balanced by a much lower fuel-cell trailer cost, resulting from the selection of a lower design voltage that yields higher power density:

- System 2 (SNG): 0.8 V/cell @ 120 mA/cm^2 = 96.0 mW/cm^2
- System 3 (Naphtha): 0.78 V/cell @ 165 mA/cm^2 = 128.7 mW/cm^2

As before, opportunities exist for major cost reduction in the System 3 power plant. The impact of future improvements in cell design and performance and systems concepts was assessed, using the projected cost reduction factors presented in Section VII-K. Here, it was assumed that improved cell design would result in an increase in power density of 40%, rather than 50%. The power density estimated for System 3 already reflects improvements due to the selection of a more favorable design point.

Simultaneous achievement of all cost reduction projections would lower the installed cost of the System 3 power plant by 25%, from $537/kW to $404/kW. The optimistic projection is shown in Table VII-28.

As with System 2, plant O&M costs are assumed to be about 0.5 ¢/kWh, based on a target stack life of 40,000 hr and routine catalyst bed replacement.

The cost of producing electricity from the power plant is shown in Table VII-29, based on the optimistic capital cost estimate and a load factor of 35%. The cost of delivered naphtha includes production, pipeline, and truck delivery costs.

Figure VII-13 shows the sensitivity of the cost of electricity to fuel costs and capital costs. If the capital cost estimate given in Table VII-27 is used, the cost of electricity increases to 69.9 mills/kWh.

Table VII-28

OPTIMISTIC COST PROJECTION FOR NOMINAL 26-MW FUEL-CELL POWER PLANT

Item	Total Cost, $1000
Fuel-cell trailer	1,394
Reformer/heat exchanger package	2,419
Equipment module	782
Condenser (E-7)	270
Power conditioner	1,368
Electrical wiring, controls, and instrumentation	476
Total Manufactured Cost	6,709
Site preparation	432
Freight and insurance	67
Mechanical structures, foundations, and piping	262
Total Installation Costs	761
Other indirect costs + profit	2,874
Total Power Plant Installed Cost	10,340
Land	20
Interest during construction	520
Working capital	140
Start-up costs	100
Total Capital Investment	11,120

Table VII-29

OPERATING COSTS AND REVENUE REQUIREMENTS
FOR A NOMINAL 26-MW FUEL-CELL POWER PLANT

Operating Costs	$1,000/Year	Mills/kWh
Naphtha fuel at $4.01/GJ ($4.23 per million Btu)	2.33	29.7
Operation and maintenance	0.39	5.0
Administrative expense	0.21	2.7
Property taxes and insurance	0.26	3.3
Depreciation	0.55	7.0
Total Annual Operating Costs	3.74	47.7
Return on rate base and income tax	0.98	12.5
Total Revenue Required	4.72	60.1
Sources of Revenue		
Electric power	4.72	60.1

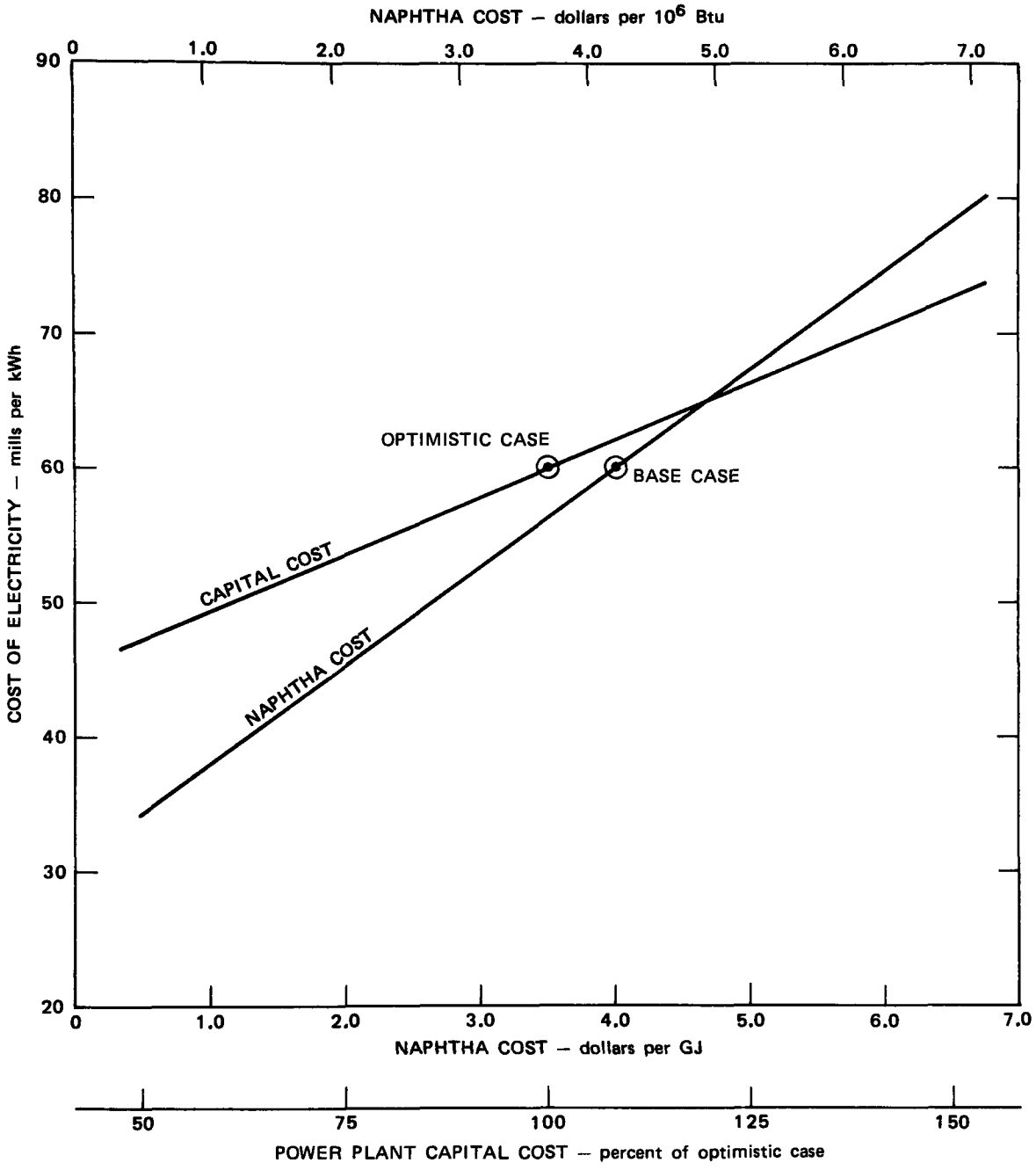

FIGURE VII-13. SENSITIVITY OF THE COST OF ELECTRICITY TO POWER PLANT COST AND NAPHTHA COST

M. Electricity Transmission and Distribution

As in the case of gas distribution, the cost of transmitting and distributing electricity varies widely, and it is extremely difficult to construct such costs for a particular situation. However, average costs of transmission and distribution (T&D) can be computed from numerous statistics. Using these statistics we calculated T&D costs for two cases. The first represents a typical utility situation in which electricity is generated in central power stations, transmitted via high voltage power lines to substations, from which it is distributed to individual residences. The second case represents the situation in which electricity is generated in dispersed fuel-cell power plants that are connected at the substation level, thus eliminating a substantial part of the transmission cost (interties to the rest of the grid are still required for reliability, however). Distribution is the same as in the first case.

The T&D cost is paid by residential customers in two components. The first is a fixed monthly charge that represents fixed costs to the utility that are not related to the amount of electricity used -- metering, power poles, billing, and so on. The second is more or less proportional to the amount of electricity used. These components can be estimated by examining statistics of the Federal Power Commission[6] (FPC) and the Edison Electric Institute[7] (EEI). According to EEI statistics the average residential cost of T&D in 1975 was 15.7 mills per kWh. In the same year, the average residential use of electricity was 681 kWh per month. Therefore, the average monthly T&D charge was $10.67.

The average fixed charges for residential customers may be determined from data on average monthly residential bills compiled by the FPC.[6] Using the average of data for January 1, 1975 and applying least squares analysis to nationwide average electric bills as a function of the electricity used, the following formula may be derived:

$$C = \$3.59 + \$0.0286\ E \qquad (1)$$

where C is the monthly charge for electricity and E is the amount of electricity used in kWh. (Analysis of data for utilities in Kansas City, Omaha, and Des Moines yields a result not significantly different from the above formula.) Thus, the average monthly fixed charge of $3.59 accounts for about one-third of residential T&D costs. The remaining portion that is included in the term proportional to the amount of electricity used may be calculated as follows:

Since the total average month T&D charge is $10.67, the following equation must be satisfied:

$$\$10.67 = \$3.59 + 681\ y \qquad (2)$$

where y is the portion of the electrical rate that represents T&D charges. Solving this equation yields y = $0.0104/kWh. Thus, the national average charge for T&D in 1975 can be represented as:

$$C_{T\&D} = \$3.59 + \$0.0104\ E \qquad (3)$$

Using FPC statistics for monthly electrical bills on January 1, 1977 to update Equation 1, we arrive at the following formula:

$$C = \$3.57 + \$0.0345\ E \qquad (4)$$

Thus, while the fixed portion of residential electricity charges remained essentially unchanged between 1975 and 1977, the variable portion increased by 21%. To determine the 1977 equivalent of Equation 3, one must know the proportion of the increase in the variable charge rate due to generation cost increases and that due to T&D cost increases. According to EEI, fuel costs alone accounted for 40% of the increase in the average cost of all electricity in 1975, and 50% in 1976. EEI figures also show that the average cost of electricity was 2.70 cents/kWh in 1975 and 3.22 cents/kWh in 1977. Using an average

percentage increase due to increased fuel costs of 45%, the net increase due to fuel costs alone was 0.45 (3.22 - 2.70) = 0.23 cents/kWh. Thus, of the increase in variable charge rate for residential electricity of (3.45 - 2.86) = 0.59 cents/kWh, 0.23 cents can be attributed to fuel cost increases. The remaining 0.36 cents must be accounted for by other generation and T&D cost increases.

The most straightforward way of allocating cost increases is to scale them according to the ratio of the T&D and generation (minus fuel costs) components of the variable electricity charge rate in 1975. The T&D component was previously determined to be 1.04 cents/kWh. The generation component is then (2.86 - 1.04) = 1.82 cents/kWh. In 1975, fuel costs accounted for 0.93 cents/kWh of the cost of electricity, on the average. Therefore, nonfuel generation costs were (1.82 - 0.93) = 0.89 cents/kWh. Allocating the nonfuel 1975-1977 cost increase of 0.36 cents/kWh to variable T&D and nonfuel generation in the ratio of 1.04/0.89 results in a variable T&D cost increase of 0.19 cents/kWh and a nonfuel generation cost increase of 0.17 cents/kWh. Thus, the cost equation for monthly residential T&D charges for 1977 is:

$$C_{T\ \&\ D} = \$3.57 + \$0.0123\ E \qquad (5)$$

The average monthly electricity use per residential customer in 1977 was 729 kWh,[7] so that the average T&D cost was increased 9.5% over 1975: $C_{T\&D}$ = (3.57 + 0.0123 x 729)/729 = 1.72 cents/kWh.

Equation 5 represents the average cost of T&D for the typical utility situation (Case 1) discussed at the beginning of this section. To calculate the costs appropriate to a distribution of electricity from dispersed fuel-cell power plants, Equation 5 must be broken into components of transmission and distribution, and estimates of transmission cost savings applied to the transmission component.

Bottaro and Baughman[8] have estimated the average national breakdown of residential T&D costs per kWh as follows:

Transmission:	32.2%
Distribution:	50.5
General:	17.3.

The "general" category applies to office and overhead expenses that cannot be allocated specifically to transmission or distribution. Applying these percentages to the average residential T&D cost of 1.72 cents/kWh in 1977 results in the following charges:

Transmission:	0.55 cents/kWh
Distribution:	0.87
General:	0.30.

By convention, we have allocated the fixed portion of the monthly charge rate in Equation 5 to distribution. This part amounts to $3.77/729 = 0.49 cents/kWh on the average. The remaining 0.38 cents/kWh distribution charge must then be included in the variable portion of Equation 5, as must the transmission and general charge components.

The savings in transmission charges resulting from employing dispersed fuel-cell power plants may be obtained from the work of Wood et al.[9] They estimated that the total capital cost of transmission installed between 1975 and 1985 would be $166/kW of new generating capacity, including $26/kW for transmission substations and $40/kW for subtransmission. They also estimated that for every kW of fuel-cell capacity that replaces a kW of central station capacity, $29-36/kW of transmission costs could be saved if the fuel-cell power plants were connected on the low voltage side of transmission-supplied substations (appropriate for 26-MW fuel-cell power plants). Using the convention of Bottaro and Baughman,[8] subtransmission lines are included in the distribution system. Therefore, of a total of $126/kW investment for transmission, $29-36/kW or 23-29% of transmission capital costs can be saved by employing dispersed fuel cells.

According to Bottaro and Baughman's statistics, 0.51 cent/kWh of average transmission costs are equipment related. Thus, if about 25% of these costs can be saved, the resulting savings is 0.13 cent/kWh. Thus, the T&D cost equation appropriate for dispersed fuel-cell power plants is Equation 5 with 0.13 cents/kWh subtracted from the variable portion of the rate, or

$$C_{T\&D} = \$3.57 + \$0.0110\ E. \qquad (6)$$

The above calculations have used national average data on T&D costs rather than data for the West North Central states. However, examination of Bottaro and Baughman's results broken down on a regional basis indicates that the figures for the West North Central states are very close to the national average.

N. 100-kW Fuel-Cell Power Plant

Cost estimates were prepared for the 100-kW power plant based on the equipment specifications discussed in Section IV-E. Costs were estimated by determining the actual quantities of raw materials used to fabricate the components. Current costs of these materials in the form expected to be used were obtained from vendor contacts. Quotes were based on large quantity purchases. Fabrication costs were determined by multiplying the raw material cost by a manufacturing-cost factor, which was selected according to the production rates involved and the degree of automation envisioned for the manufacuring facility. The production rate for cells was assumed to be sufficient to justify the development and utilization of continuous fabrication processes for the cell component parts.

The cost breakdown for fuel-cell stacks is given in Table VII-30. Total stack cost for the 100-kW power plant is estimated at $20,000. Catalyst cost is a major factor, based on the initial acquisition cost of platinum.

Table VII-30

FUEL-CELL STACK COSTS
(Production Rate = 1,000 Systems/Year)

Component/Configuration	Raw Material Cost, $1,000	Mfg. Cost Factor	Mfg. Cost, $1,000	Total Cost, $1,000
Catalyst - Platinum Total loading/cell - 0.001 g/cm^2 (0.002 lb/ft^2)	9.3	0.05	0.47	9.77
Electrode support layers Graphite fiber paper - 0.024 g/cm^2 (0.05 lb/ft^2)	2.5	0.6	1.5	4.0
Electrolyte matrix Silicon carbide fiber - 0.039 g/cm^2 (0.08 lb/ft^2)	1.07	0.6	0.64	1.71
Bipolar plate - carbon/ phenolic resin - 0.44 g/cm^2 (0.9 lb/ft^2)	0.62	1.5	0.93	1.55
Cooling cartridge - carbon plate with copper tube grid	0.54	1.5	0.82	1.36
Stack hardware - end plates, manifolding, tie rods	0.71	1.4	0.99	1.70
Total	14.74		5.35	20.09[a]

[a]Total for 100-kW power plant (4 stacks).

The cost of the catalyst is obviously dependent on the base price of platinum, which fluctuates. The price of $6/g, used for this study, includes a processing charge of $0.39/g over a base material price of $5.61/g. At least 80% of this material cost could be reclaimed when the cell stacks are replaced.

Graphite fiber paper is the major cost component in the electrode support substrate. According to one vendor contact (Stackpole Carbon Co.), today's price of $88/kg ($40/lb) inludes a processing charge of $18 to 22/kg ($8 to 10/lb), for a total market of 1.1 million kg (0.5 million lb) per year. A future price of $62 to 66/kg ($28 to 30/lb) could be expected if the market increased to 9 to 11 million kg (4 to 5 million lb) per year. Other applications, such as graphite-filled automobile body panels, are expected to help achieve this forecast market.

Low-cost methods are presently being developed for producing silicon carbide fibers for the electrolyte matrix. Ultimately, the cost of these fibers is expected to approach $13.20/kg ($6/lb), but this is an optimistic projection. This study assumes a cost of $17.60/kg ($8/lb) for silicon carbide.

The bipolar plates are produced by a compression molding process using a mixture of graphite and phenolic powders. This relatively high cost procedure results in a rather high manufacturing cost, even though the raw material cost is low -- $0.90/kg ($0.41/lb).

The total stack cost is reasonable and not overly optimistic. The estimated cost is somewhat higher than reported by ERC, primarily because of the following reasons:

- Selection of a lower cell performance characteristic and design point, yielding a power density of 727 W/m^2 (67.6 W/ft^2). This increased the required cell area by 33%.
- Use of a higher current value for platinum catalyst cost.

- Incorporation of cooling grids costing $6.60 each, as part of the circulating coolant system for heat recovery from the stack.

Clearly, improvements in catalyst utilization and projected cell performance are prime areas for cost reduction.

The final cost estimate for the 100-kW power plant is shown in Table VII-31. The estimate is based on large quantity purchases of raw materials. Major components such as fuel-cell stacks, reformers, and heat exchangers could be manufactured in separate facilities or purchased. All components are assembled into a single unit at an assembly plant at an assumed production rate of 1000 units/yr. This facility would include areas for fabrication and welding of steel structures, and a small assembly line. System piping and wiring could be fabricated.

The total manufacturing cost is estimated to be $46,610, which is equivalent to $466/kW output at rated power. The projected FOB selling price is $65,254 or $652/kW, assuming a mark-up of 40% for other indirect expenses and profit.

The nonoptimized base-case design study used conservative estimates of fuel-cell performance. The impact of future optimization and performance improvement programs on system cost was assessed. The optimistic projection would be consistent with the later stages of the assumed 1980-2000 time frame established for this study. Cost reductions might be needed if systems are to meet the 40,000-hr life goal. Major improvements can be projected in the area of fuel-cell stack design, construction, and performance including:

- A reduction in platinum catalyst loading to 0.75 mg/cm^2 (0.0015 lb/ft^2), together with a doubling of current density (at 0.65 cell voltage) to 224 mA/cm^2 (208 amp/ft^2). In effect, only two stacks would be required for the 100-kW power plant.

- A 15% reduction in the quantity of materials used in stack construction.

Table VII-31

COST SUMMARY FOR 100-kW POWER PLANT

Unit	Cost ($)
Fuel-cell stacks	20,000
Reformer	3,800
Heat exchangers	
E-1A	400
E-1B	120
E-2A	150
E-2B	200
E-3	80
E-4	1,500
E-5	5,700
E-6	400
E-7	300
E-8	600
Blower B-1	1,600
Pumps	
P-1	240
P-2	400
H.T. shift	300
Cat. G-3A	600
L.T. shift	200
Cat. G-66A	1,120
Inverter	6,000
Instrumentation	400
Enclosure	800
Piping, wiring, miscellaneous	500
Assembly & test	1,200
Total Manufacturing Cost	46,610
Other indirect costs + profit (40%)	18,644
F.O.B. selling price	65,254
Freight and insurance	650
Installation	2,500
Total Installed Cost	68,400

- A 15% reduction across-the-board in the manufactured cost of the reformer, shift converters, heat exchangers and miscellaneous cost items (e.g., instrumentation).

- A 20% cost reduction for the DC/AC inverter and associated power conditioning equipment.

Simultaneous achievement of all cost reduction projections would lower the FOB price of the 100-kW power plant by 34%, from $652 to $430/kW. Additional savings could be expected if platinum catalyst recovery and recycle is carried out. The optimistic projection is listed in Table VII-32.

Table VII-32

OPTIMISTIC COST PROJECTION OF ADVANCED 100-kW POWER PLANT

Unit	Cost ($)
Fuel-cell stacks (2)	8,050
Reformer	3,230
Heat exchangers	8,032
Blower	1,600
Pumps	640
Shift converters	1,887
Inverter	4,800
Miscellaneous[a]	2,465
Total Manufacturing Cost	30,704
Other indirect costs + profit (40%)	12,282
FOB selling price	42,986
Freight and insurance	430
Installation	2,500
Total Installed Cost	45,900

[a]Instrumentation, enclosure, piping, wiring, assembly, and testing.

This study has focused on costs associated with manufacturing a single 100-kW power plant product line. If market surveys show that larger power plants are required, some further cost reduction might occur, based on capacity factor scale-up relationships, e.g., the 0.6 factor rule. Alternatively, added multiples of 100-kW units might be installed. This approach would probably be most cost-effective, after system reliability and redundancy factors are analyzed.

O&M costs for operating the 100 kW power plant also must be estimated, but firm bases for such estimates are not available. Periodic stack replacement material costs could range from 0.2 to 0.5 ¢/kWh, assuming 40,000-hr operations at full rated level (100 kW). Fuel conversion catalyst replacement costs should be low. Equipment maintenance and replacement costs should also be low, reflecting, say, a 15-year expected life. Finally, local ordinances may require attended operation of total energy power plants.

The cost of producing electricity and heat from the 100-kW power plant depends strongly on the particular application in which it is used. Table IV-33 illustrates a particular case in which the load factor for electricity production is 35%, and 75% of the recovered heat can be utilized, with an assigned value of $2.84/GJ ($3.00 per million Btu). The actual costs for the application in System 5 must be determined from a calculation of annual heat and electricity use. That calculation is carried out is Chapter VIII. Figure VII-14 shows the sensitivity of the cost of electricity to load factor and hot water credit.

O. Hot Water Distribution System

The cost of the system for delivering 82°C (180° F) hot water from the 100-kW fuel-cell power plant to 20 townhouses represents a substantial portion of the total energy supply cost for the housing complex. Table VII-34 shows a breakdown of those costs, which have been estimated

Table VII-33

OPERATING COSTS AND REVENUE REQUIREMENTS FOR A 100-kW FUEL-CELL POWER PLANT WITH HEAT RECOVERY
(35% Load Factor; 75% of Recovered Heat Utilized)

Operating Costs	$1,000/Year	Mills/kWh
SNG fuel at $4.16/GJ ($4.39 per million Btu)	14.4	46.9
Operation and maintenance	1.5	5.0
Administrative expense	0.9	3.0
Property taxes and insurance	1.1	3.7
Depreciation	2.3	7.5
Total Annual Operating Costs	20.2	65.8
Return on rate base and income tax	4.0	13.0
Total Revenue Required	24.2	78.8
Sources of Revenue		
Recovered heat at $2.84/GJ	2.7	8.7
Electric power at 70.1 mills/kWh	21.5	70.1
Total	24.2	78.8

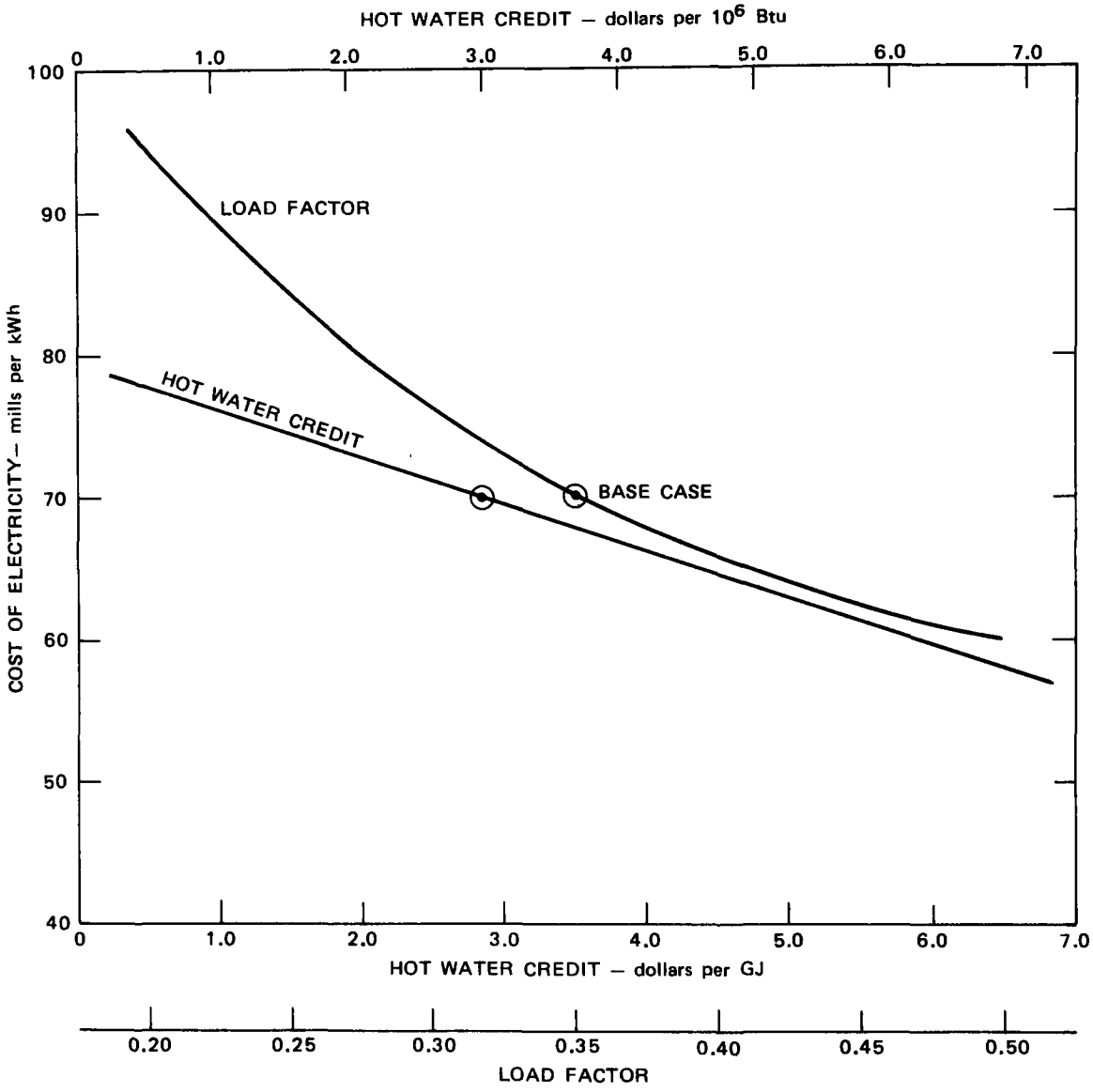

FIGURE VII-14. SENSITIVITY OF THE COST OF ELECTRICITY TO LOAD FACTOR AND HOT WATER CREDIT

Table VII-34

CAPITAL INVESTMENT REQUIRED FOR A SYSTEM THAT DELIVERS 82°C (180°F) HOT WATER TO TWENTY TOWNHOUSES

Cost Component	Investment ($1,000)	Percent
Materials		
5-cm diameter pipe (46m)	0.25	--
3-cm diameter pipe (850m)	2.9	5
2-cm diameter pipe (610m)	1.2	2
Pipe fittings	14.5	24
Pipe insulation (1510m)	4.4	7
Pumps (2)	4.5	8
Compression tank	0.42	1
Hot water coils - space heating (20)	4.5	8
Hot water coils - DHW (20)	3.0	5
Total Materials	35.7	60
Labor	8.6	15
Other (permits, trenching, etc.)	2.5	4
Subtotal Direct Costs	46.8	79
Overhead (15% of direct costs)	7.0	12
Profit (10% of direct costs & overhead)	5.4	9
Total Capital Investment	59.2	100

using standard construction cost estimation procedures. The size of the piping, fittings and valves was based on a maximum hot water flow rate of 1.40 liter/sec (22.1 gal/min) from the fuel-cell heat recovery system. Included in the cost of the system are the costs of the heating coils that transfer heat from the hot water stream to the DHW tank and to the space heating air in each residence. The single most costly expense category is pipe fittings. This includes the valves that control the flow of hot water from the fuel cell to the residences and back, and all elbows, connectors, and so on. Total cost of the heat delivery system, $59,200, is higher than that of the fuel-cell power plant, and amounts to nearly $3,000 per residence.

The annual ownership cost of this system is assumed to be borne by the owners of the townhouses, and is shared equally among the 20 residences. Financing is assumed to be included in home mortgages of the individual owners. Financing terms are as follows: 20% down payment, with the remaining 80% financed over 30 years at 10% interest. The annual cost of such a loan (principal repayment plus interest) is given by the following formula:

$$C = P\, i \frac{(1 + i)^n}{(1 + i)^n - 1}$$

where C is the annual cost, P is the principal, i is the interest rate, and n is the term of the loan in years. For a principal $P = 0.80 \times \$2,960 = \$2,368$, and the loan terms given above, the homeowner's annual cost is $251. To obtain the average annual cost, the down payment of $592 is averaged over the 30-year term of the loan, or $20 per year. The average annual cost, per residence, of the heat delivery system is therefore $271.

P. Gas Furnace and Air Conditioner

The costs of the gas furnace and air conditioner that supply heating and cooling to the residences described in Section IV-A are based on

published estimates of the costs of the specific models discussed.[10] Included are estimates of the cost of duct work for delivering the heated or cooled air to the various rooms of the residence and venting for the exhaust gases from the furnace.

The total installed cost of the gas furnace/air conditioning system is shown in Table VII-35. The equipment costs are based on the wholesale price typically paid by a building contractor. The total cost includes labor for installing the equipment plus the contractor's overhead and profit.

The annual homeowner's cost of owning this equipment, based on the considerations discussed in the previous sections, amounts to $195. In addition, Westinghouse[10] has estimated the annual average maintenance cost of the equipment to be $99 per year, based on statistics compiled by gas and electric utilities. Therefore, the total yearly cost of owning and maintaining this heating and air conditioning system is $294.

Table VII-35

CAPITAL COST FOR A RESIDENTIAL HEATING AND COOLING SYSTEM -- GAS FURNACE AND AIR CONDITIONER

Cost Component	Investment, $	Percent
Equipment		
Gas furnace (70 MJ/hr)	225	11
Air conditioner (32 MJ/hr)	498	23
Duct work	704	33
Subtotal Equipment	1,427	67
Labor	257	12
Subtotal Labor & Equipment	1,684	79
Overhead (15% labor & equipment)	253	12
Profit (10% labor, equipment & overhead)	194	9
Total Capital Investment	2,131	100

Q. Heat Pumps

The costs of the advanced heat pumps described in Sections IV-B and IV-E were estimated by Westinghouse using a heat pump model that costed each component individually, then added the cost of all components to obtain the total.[10] The total installed costs of the two heat pumps are shown in Table VII-36. As before, the equipment costs are based on those paid by a building contractor.

Annual average ownership costs for the heating and cooling systems are $231 for the 26.0-MJ/hr (24,600-Btu/hr) system and $194 for the 19.3-MJ/hr (18,300-Btu/hr) system. Based on heat pump statistics gathered by electric utilities, Westinghouse estimates the yearly average maintenance cost to be $120 for either heat pump. Thus, the total annual maintenance and ownership costs are $351 and $314 for the 26.0-MJ/hr and 19.3-MJ/hr systems, respectively.

Table VII-36

CAPITAL COSTS FOR RESIDENTIAL HEATING AND COOLING SYSTEMS -- HEAT PUMPS

Cost Component	26 MJ/hr Heat Pump		19.3 MJ/hr Heat Pump	
	Investment, $	Percent	Investment, $	Percent
Equipment				
Heat pump	1138	45	844	40
Duct work	621	25	598	28
Subtotal Equipment	1759	70	1442	68
Labor	237	9	237	11
Subtotal Equipment & Labor	1996	79	1679	79
Overhead (15% of labor & equipment)	299	12	252	12
Profit (10% of labor, equipment & overhead)	230	9	193	9
Total Investment	2525	100	2124	100

R. References--Chapter VII

1. R. P. Stickles, et al., "Assessment of Fuels for Power Generation by Electric Utility Fuel Cells," Electric Power Research Institute Report 318 (October 1975).

2. American Gas Association, "Gas Facts, 1975" (1976).

3. J. M. King, Jr., "Energy Conversion Alternatives Study - United Technologies Phase II Final Report," NASA CR 134955, FCR-0237 (October 19, 1976).

4. S. Abens, et al., "High Temperature Molten Carbonate Fuel-Cells," Fourth Quarter Technical Progress Report E-3-4 (March 1977) and Fifth Quarter Technical Progress Report E-3-5 (July 1977).

5. P. Wood, "AD/DC Power Conditioning and Control for Advanced Conversion and Storage Technology," EPRI 390-1-1 (August 1975).

6. Federal Power Commission, "Monthly Electric Utility Bills" (January 1, 1976 and January 1, 1977).

7. Electrical World, various issues.

8. M. L. Baughman and D. J. Bottaro, "Electric Power Transmission and Distribution Systems Costs and Their Allocation," IEEE Transactions on Power Apparatus and Systems, p. 782 (May-June 1976).

9. W. Wood, M. P. Bhavaraju, and P. Yatcko, "Economic Assessment of the Utilization of Fuel Cells in Electric Utility Systems," Electric Power Research Institute Report EM-336 (November 1976).

10. H. S. Kirschbaum and S. E. Veyo, "An Investigation of Methods to Improve Heat Pump Performance and Reliability in a Northern Climate," Electric Power Research Institute Report EM-319 (January 1977).

VIII. THERMAL AND ELECTRICAL LOAD CALCULATIONS

To complete the analysis of the five systems, the energy use characteristics of the residences described in Chapter IV must be known. Those residences are the ultimate users of the energy supplied by the other system components. The determination of their annual energy consumption will allow the costs, energy use, and environmental impacts of the systems to be appropriately scaled for comparison.

As discussed in Chapter III, our study focuses on the heating and cooling components of residential energy use. That emphasis is reasonable, because approximately 60% of residential energy use in the United States is for heating and cooling. Also, because the energy demand for heating and cooling varies widely with the time of day, those portions of the residential energy load tend to contribute substantially to the utility's "intermediate load" electricity demand, which is the type of load that the electricity generating components of the systems are designed to meet.

In addition to the heating and cooling demand, the demand created by other loads in the residences — lights and appliances -- must be known for two reasons. First, the cost per kWh of electricity to the customer will depend on the total monthly electricity use. Second, in System 5, the amount of heat supplied by the fuel-cell power plant, and thus the amount of heat required of the heat pumps, will depend on the total electrical load of the residences.

The electrical loads we used for lights and appliances are statistical averages. The heating and cooling loads, however, and their resultant electricity demand, have been determined on the basis of the following information: (1) the daily temperature variations in the

Omaha-Des Moines-Kansas City region during a typical year; (2) the thermal response of the residences to those variations; and (3) the performance of the heating and cooling equipment as a function of temperature and the thermal demands of the residence. In the following sections, the use of those pieces of information to calculate final residential energy demand is described.

A. Light and Appliance Loads

The electrical loads generated by lights and appliances in a residence are a function of the number and types of appliances, the number of occupants, their living pattern, and so on. Although those factors vary substantially from one household to the next, the quantities of interest to utilities, as well as to this study, are the average loads determined by the characteristics of multiple households. Such statistical information is readily available.

The average light and appliance loads will be characterized for the three types of residences described in Chapter IV. The first, which will be called Residence 1, is supplied by System 1. It uses both gas and electricity. In addition to a gas furnace, it is assumed to have a gas range and water heater. All other appliances are electric, and include an air conditioner, clothes washer and dryer, refrigerator/freezer, television, dishwasher, and other small appliances such as a toaster and food mixer.

The second type of residence, called Residence 2, is supplied by Systems 2, 3, and 4. Residence 2 is all-electric, and in addition to having a 26.0-MJ/hr (24,600-Btu/hr) heat pump for heating and cooling, it employs an electric water heater and range. The use of lights and other appliances is the same as for Residence 1.

Residence 3, which is supplied by System 5, is similar to Residence 2 except that it employs a smaller heat pump (19.3 MJ/hr or 18,300 Btu/hr)

and its domestic hot water (DHW) is supplied entirely by heat recovered from the fuel-cell power plant; therefore, no electric water heating is required.

The components of electricity consumption, by lights and appliances as well as monthly totals, for the three types of residences are shown in Table VIII-1, as determined from national statistics.[1,2] Those figures do not include air conditioner or heat pump loads -- they will be determined in following sections.

To determine the ability of the System 5 fuel-cell power plant to respond to the electrical and thermal loads of the townhouses, one must know the variations in the light and appliance loads of Residence 3 with the time of day. Those load variations have been previously estimated,[3] and are shown in Figure VIII-1. The loads shown are the average hourly loads per residence. The actual load profile for an individual residence would look considerably different, having many abrupt changes in load as various appliances were turned on and off.

The load profile in Figure VIII-1 is seen to be at a minimum of 0.27 kW in the late night and early morning hours when only the refrigerator and perhaps one or two small lights are using power. Peak demands of 2.83 and 2.46 kW occur during the hours of 9-10 a.m.

Table VIII-1

MONTHLY LIGHT AND APPLIANCE ELECTRICAL LOADS FOR THREE TYPES OF RESIDENCES

	Electricity Use (kWh/Month)		
	Residence 1	Residence 2	Residence 3
Source			
Lights	145	145	145
Water heater	--	380	--
Range	--	100	100
Other appliances	490	490	490
Total	635	1,115	735

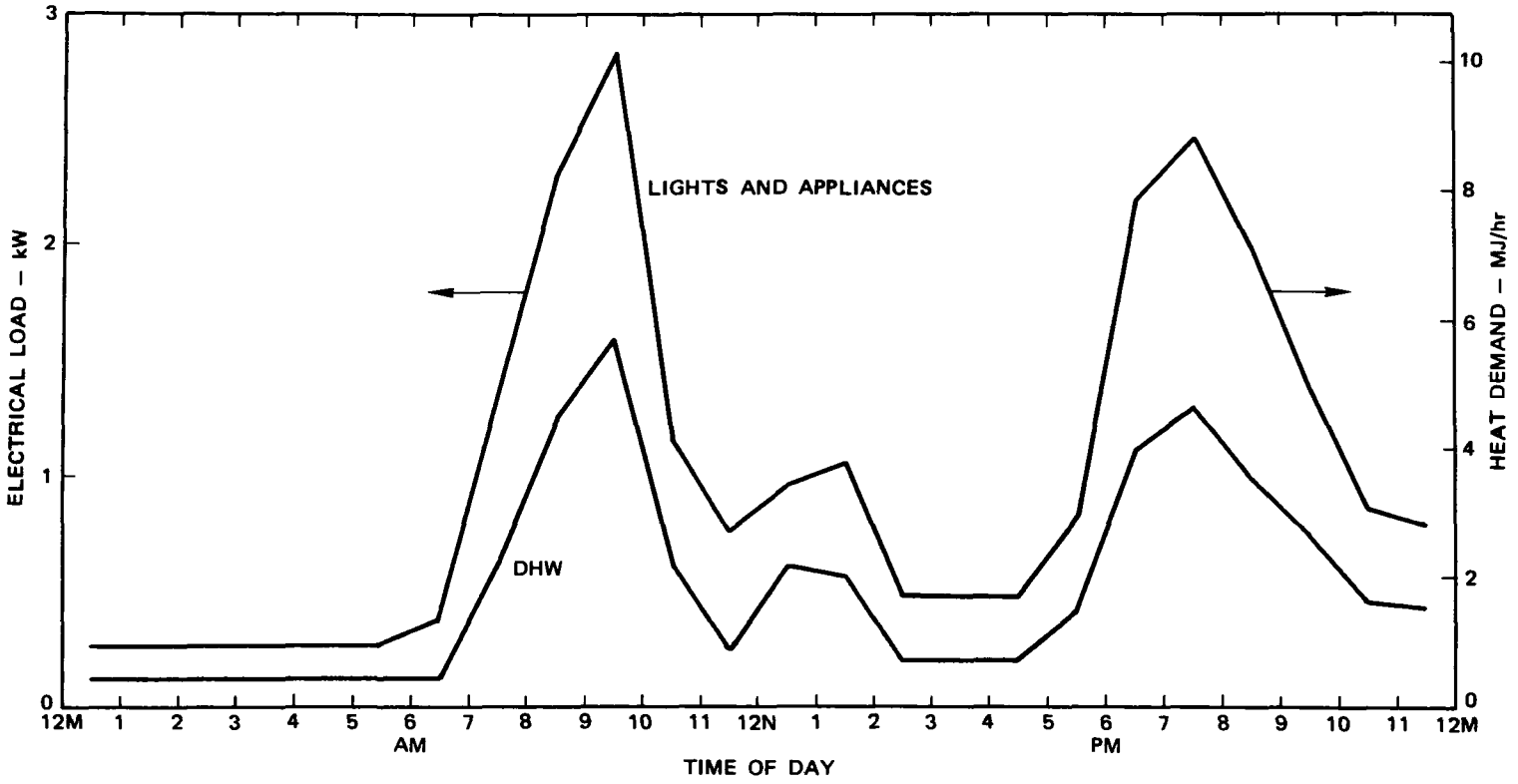

FIGURE VIII-1. VARIATION IN HOURLY AVERAGE LIGHT AND APPLIANCE LOADS AND DHW DEMAND WITH TIME OF DAY – RESIDENCE 3

and 7-8 p.m., respectively, when the bulk of domestic activities are taking place.

Also shown in Figure VIII-1 is the DHW demand profile, which will also be required in the supply/demand calculations for System 5.

B. Daily Temperature Variations

Data on temperature variations for most cities can be obtained from the Environmental Data Service of the National Oceanic and Atmospheric Administration. Temperatures are reported every 3 hours, every day of the year. In addition, daily and monthly averages are reported, as well as daily extremes, along with various statistical temperature data. To determine typical seasonal heating and cooling requirements, one must examine temperatures averaged over many years. Table VIII-2 shows the normal monthly average temperatures for the period 1941-1970 for Des Moines, Omaha, and Kansas City.

Table VIII-2

NORMAL MONTHLY AVERAGE TEMPERATURES, °C (°F)

Month	Kansas City		Omaha		Des Moines	
January	-2.3	(27.8)	-5.2	(22.6)	-7.0	(19.4)
February	0.6	(33.1)	-2.2	(28.0)	-4.3	(24.2)
March	5.1	(41.2)	2.8	(37.1)	1.1	(33.9)
April	12.8	(55.0)	11.3	(52.3)	9.7	(49.5)
May	18.3	(65.0)	17.2	(63.0)	16.1	(60.9)
June	23.3	(73.9)	22.3	(72.2)	21.4	(70.5)
July	26.0	(78.8)	25.1	(77.2)	23.9	(75.1)
August	25.2	(77.4)	24.2	(75.6)	22.9	(73.3)
September	20.4	(68.8)	19.1	(66.3)	17.9	(64.3)
October	14.8	(58.6)	13.3	(55.9)	12.4	(54.3)
November	6.4	(43.6)	4.4	(40.0)	3.2	(37.8)
December	1.7	(32.3)	-2.2	(28.0)	-3.9	(25.0)

Temperatures for Omaha are a reasonable average of temperatures for the three cities. Therefore, in all further calculations, only temperature data for Omaha was used. Monthly temper- ature data for Omaha for the 10 years including 1966, 1968, and 1970-77 were analyzed to find particular months that were most representative of normal monthly conditions[4] (statistics for 1967 and 1969 were not available). Both monthly average temperatures and monthly heating (or cooling) degree-days were compared to obtain the best match. Occasionally, when two months were very similar, other data such as monthly minimum and maximum temperatures were compared. The results of the matching procedure are shown in Table VIII-3, in which the normal monthly temperatures and heating (or cooling) degree-days for Omaha are compared with the average temperatures and degree-days for the actual months chosen as the best match. Those months are indicated by the year in which they occur.

Table VIII-3

COMPARISON OF NORMAL MONTHLY CONDITIONS WITH
ACTUAL MONTHLY CONDITIONS OF MONTHS CHOSEN AS "BEST MATCH"

	Normal Conditions		Actual Conditions		
Month	Average Temperature (°C)	Heating (Cooling) Degree-Days (°C)	Year	Average Temperature (°C)	Heating (Cooling) Degree-Days (°C)
January	-5.2	730	1975	-5.3	728
February	-2.2	576	1968	-2.6	603
March	2.8	481	1971	2.9	474
April	11.3	217	1974	11.4	211
May	17.2	(48)	1972	16.9	(41)
June	22.3	(131)	1975	22.5	(134)
July	25.1	(210)	1970	25.2	(214)
August	24.2	(186)	1970	24.6	(210)
September	19.1	(61)	1977	19.7	(58)
October	13.3	167	1974	12.9	167
November	4.4	417	1966	4.5	412
December	-2.2	637	1966	-2.1	629

Table VIII-3 shows that the conditions of the actual months chosen very closely match the normal temperature condition. Those months are assumed to constitute a "typical" year for Omaha, and the daily temperature variations were used to calculate heating and cooling loads.

C. Thermal Response of the Residences

Daily temperature data can be used to calculate heating and cooling loads if the thermal characteristics of the residences are known. A method for calculating those loads has been developed by Westinghouse[5] (its report may be referred to for details of the derivation of the method.) Basically, the thermal response of the residence is calculated by using an electric circuit analog to derive the appropriate response functions. The difference between external and internal temperatures is analogous to voltage, heat flow is analogous to current, and thermal conductivity and heat capacity are analogous to electrical conductivity (the reciprocal of resistance) and capacitance, respectively.

The result of that analysis for heating loads is given in Equations 1-3, as follows:

$$Q_L(t) = Q_{avg} + \Delta Q_L(t) \tag{1}$$

$$Q_L(t) = G_1 \ \Delta T_a(t) + G_1(\alpha_2 - \alpha_1) \int_0^t \Delta T_a(t')dt' + C \tag{2}$$

$$C = \frac{-G_1}{24} \int_0^{24} \Delta T_a(t)dt \frac{-G_1}{24} (\alpha_2 - \alpha_1) \int_0^{24} dt \int_0^t \Delta T_a(t')dt' \tag{3}$$

$$\frac{-C_2 \ (T_{avg1} - T_{avg2})}{48}$$

In Equation 1, $Q_L(t)$ is the heating load in kJ/hr (or Btu/hr) as a function of the time of day, t (in hours); Q_{avg} is the daily average heating load calculated using the average daily temperature and the heat

loss equation discussed in Chapter IV, and ΔQ_L (t) is the variable portion of the heating load to be calculated by Equations 2 and 3. In Equation 2, G_1, α_1, and α_2 are thermal parameters of the residence, ΔT_a is the difference between the temperature at t and the daily average temperature, and C is a constant of integration to be calculated by Equation 3. In Equation 3, C_2 is another thermal parameter of the residence, T_{avg2} is the daily average temperature of the day for which the heating load is being calculated, and T_{avg1} is the average temperature of the previous day.

It can be seen from Equations 1-3 that calculating the daily average heating load by integrating over the 24-hour period will result in exactly Q_{avg}, modified slightly by the addition of the third term in Equation 3. That term represents the long-term thermal storage capacity of the residence. It will also average to zero, however, if the calculation is carried out over a successive period of days -- say, for a month. Thus, for calculating monthly and seasonal heating loads, it is clear that the use of Q_{avg} is sufficient to provide the needed information to an acceptable level of accuracy. Recall that for Residences 1 and 2, Q_{avg} is given by:

$$Q_{avg} = 39{,}900 - 360\ T_{avg}\ \text{kJ/hr} \tag{4}$$

or

$$(Q_{avg} = 37{,}800 - 610\ T_{avg}\ \text{Btu/hr}),$$

where T_{avg} is the average daily temperature in ^{o}C or ^{o}F. For Residence 3, the heating load is:

$$Q_{avg} = 23{,}800 - 230\ T_{avg}\ \text{kJ/hr} \tag{5}$$

or

$$(Q_{avg} = 22{,}600 - 390\ T_{avg}\ \text{Btu/hr}).$$

Because of the complicated relationship between heating load, electrical load, and electrical and heating supply for the Residence 3 case, one must consider whether daily average calculations can effectively repre-

sent the averaged effect of hourly load variations. This question is discussed in the following section.

The calculation of cooling loads is considerably more complicated than the calculation of heating loads; not only does temperature vary throughout the day, but so does solar heat input (insolation) and latent heat infiltration (the latent heat content of humid outside air entering the house). However, several simplifying assumptions can make the task easier. First, most of the cooling load is registered during summer afternoons. Therefore, figures for average summer afternoon insolation and relative humidity provide reasonable estimates of solar heating and latent heat infiltration.

Second, the daily average cooling load can be estimated in a way similar to that for the heating load. Instead of the average daily temperature, however, the average temperature is used for the hours during which cooling is required. The parameters that contribute to the cooling loads for Residences 1, 2, and 3 are shown in Table VIII-4. The heat input from people and appliances is similar to that used to calculate heating loads. The heat input from latent heat infiltration was calculated using a technique given in the ASHRAE handbook,[6] and is based on an average moisture content of 0.0131 kg H_2O per kg of air for exterior air (average summer afternoon conditions for Omaha), 0.0117 kg H_2O per kg of air for interior air (corresponding to 26°C wet bulb interior temperatures). The figures for sensible heat input (via heat transfer through the walls and infiltration of warm air) and solar heat input were derived in the Westinghouse report[5].

Using the parameters listed in Table VIII-4 to calculate the cooling load as a function of exterior temperature results in the following equation for Residences 1 and 2:

$$Q^c_{avg} = 380\ T_{avg} - 43{,}800\ \text{kJ/hr} \qquad (6)$$

or

$$(Q^c_{avg} = 650\ T_{avg} - 41{,}600\ \text{Btu/hr})$$

with T_{avg} expressed in °C or °F, as appropriate.

To calculate the design cooling loads discussed in Chapter IV, the moisture content corresponding to the 97.5% temperatures for Omaha (34°C or 93°F dry bulb and 26°C or 78°F wet bulb) was used -- 0.0175 kg H_2O per kg of air. Use of that quantity yields latent heat infiltration of 5,700 kJ/hr (5,400 Btu/hr) for Residences 1 and 2 and 2,850 kJ/hr (2,700 Btu/hr) for Residence 3.

The seasonal heating and cooling loads may now be calculated for Residences 1, 2, and 3 by using the equations developed in this section and the temperature data for a "typical" year for Omaha. The heating season is assumed to extend from October 1 through April 30, and the cooling season from May 1 through September 30. The seasons overlap somewhat (i.e., some heating is required in May and September, and some cooling is required in April and October), but it is small and may be ignored.

Calculation of heating loads is straightforward. The daily average temperature is used to calculate the daily average heat load for each day in which the average temperature is below 17°C (62°F) for Residences 1 and 2, and below 14°C (58°F) for Residence 3. Those are the temperatures at which the internal heat sources (people, lights, and appliances) are sufficient to maintain the interior temperature at 21°C (70°F); above those temperatures the heating load is zero. The daily average heating loads are then multiplied by 24 and summed over the number of days in the month to obtain the total monthly heating loads.

Table VIII-4

COMPONENTS OF THE COOLING LOAD -- OMAHA SUMMER AFTERNOON CONDITIONS

Component	Residences 1 and 2	Residence 3
Heat input from people, lights, & appliances	4,960 kJ/hr (4,700 Btu/hr)	4,960 kJ/hr (4,700 Btu/hr)
Solar heat input	3,380 kJ/hr (3,200 Btu/hr)	840 kJ/hr (800 Btu/hr)
Latent heat infiltration	1,390 kJ/hr (1,310 Btu/hr)	700 kJ/hr (660 Btu/hr)
Sensible heat input	380 kJ/hr-°C (200 Btu/hr-°F)	240 kJ/hr-°C (125 Btu/hr-°F)

The calculation of cooling loads is slightly more complicated. Only those portions of the day during which the external temperature exceeds 26°C (78°F) are used in the calculation. The recorded tri-hourly temperatures[4] are examined to determine the number of hours during which the temperature exceeded 26°C. The average temperature during those hours is used to calculate the average cooling load using Equations 6 and 7. The cooling load is then multiplied by the number of hours during which the temperatures exceeded 26°C to obtain the total daily cooling load. The daily cooling loads are then summed to obtain the cooling loads for each month.

The calculated results for heating and cooling loads are shown in Table VIII-5. The heating load for either type of residence far exceeds the cooling load. Thus, the use of heat pumps that are optimized for heating performance (as described in Chapter IV) is fully justified.

Table VIII-5

SUMMARY OF HEATING AND COOLING LOADS BY MONTH

Month	Residences 1 and 2		Residence 3	
	Heating Load, GJ (Million Btu)			
October	3.52	(3.34)	1.32	(1.25)
November	10.1	(9.62)	5.22	(4.95)
December	16.1	(15.3)	9.00	(8.53)
January	19.0	(18.0)	12.6	(11.9)
February	15.5	(14.7)	8.67	(8.22)
March	11.8	(11.2)	6.28	(5.95)
April	4.80	(4.55)	2.00	(1.90)
Total	80.9	(76.7)	45.0	(42.7)
	Cooling Load, GJ (Million Btu)			
May	1.03	(0.98)	0.69	(0.65)
June	2.91	(2.76)	1.92	(1.82)
July	5.17	(4.90)	3.40	(3.22)
August	4.48	(4.25)	2.95	(2.80)
September	0.73	(0.69)	0.49	(0.46)
Total	14.3	(13.6)	9.44	(8.95)

D. Energy Consumption for Heating and Cooling

The final step in the sequence outlined at the beginning of the chapter is to calculate the response of the heating and cooling equipment to the heating and cooling loads derived in previous sections, and ultimately to calculate the energy consumed by that equipment. For Residences 1 and 2, the calculations are relatively straightforward. The energy consumed by the gas furnace is simply equal to the heating load divided by the thermal efficiency of the furnace, which is 0.60 (see Chapter V). For the heat pump operating in the heating mode, the heating load is compared to the heat output of the heat pump at a given temperature. If the heating capacity of the heat pump exceeds the heating load, the heat pump will be operating only part of the time. The fraction of the time the heat pump is on is called the duty factor. The average electricity demand by the heat pump (in kW) is equal to its electricity demand at the temperature in question multiplied by the duty factor.

When the heating load exceeds the capacity of the heat pump, supplemental electric resistance heating must be used to make up the difference. The heat pump operates continuously and consumes power at its rated capacity at the temperature in question. The resistance heaters will consume power at an average rate that will equal the difference between the heating load and the heat supply of the heat pump. The total power demand is the power demand of the heat pump plus the average power demand of the resistance heaters.

Calculation of power demand for the heat pump operating in the cooling mode and the air conditioner is similar, except that when the cooling load exceeds the cooling capacity, the duty factor is 1.0 and the air conditioner or heat pump power demand is equal to its rated demand at the temperature in question. That is a consequence of there being no "supplemental cooling capacity." In practice, that means that at temperatures above the balance point of the cooling device, the interior temperature of the residence cannot be maintained at the "set" temperature, but will actually be somewhat higher.

In principle, the calculations described above should be carried out for every hour of the heating and cooling seasons to determine the total electricity consumption. However, because the heat pump and air conditioner are reasonably close to being linear in their electricity demand as a function of temperature, the use of daily average temperatures closely approximates actual energy use.

The heat pump and air conditioner average power demands were used in conjunction with the daily average temperature data for Omaha's "typical" year to compute the monthly electricity use for each type of residence.

Table VII-6 shows the monthly electricity use for heating and cooling and the total seasonal electricity use, including light and appliance use of 635 kWh/month for Residence 1, and 1,115 kWh/month for Residence 2.

Table VIII-6

ELECTRICITY CONSUMPTION FOR HEATING AND COOLING (kWh)

	Residence 1			Residence 2		
Month	Heating	L&A[a]	Total	Heating	L&A	Total
October	27	635	662	292	1,115	1,407
November	79	635	714	1,025	1,115	2,140
December	125	635	760	2,293	1,115	3,408
January	148	635	783	2,968	1,115	4,083
February	121	635	756	2,108	1,115	3,223
March	92	635	727	1,307	1,115	2,422
April	37	635	672	413	1,115	1,528
Seasonal Total	629	4,445	5,074	10,406	7,805	18,211
Month	Cooling	L&A	Total	Cooling	L&A	Total
May	137	635	772	107	1,115	1,222
June	384	635	1,019	307	1,115	1,422
July	690	635	1,325	552	1,115	1,667
August	594	635	1,229	471	1,115	1,586
September	96	635	731	73	1,115	1,188
Seasonal Total	1,901	3,175	5,076	1,510	5,575	7,085
Annual Total	2,530	7,620	10,150	11,916	13,380	25,296

[a]L&A = light and appliances.

For Residence 1, the electricity used for heating is only that consumed by the gas furnace's electric fan motor. The total consumption of natural gas (or SNG) by the furnace is 135 GJ (128 million Btu) over the entire heating season.

The calculation of heating energy use is a more difficult task for Residence 3 than for Residences 1 and 2 because of the strong functional relationship between temperature, heating load, and electrical load. To explore that relationship, we calculated the variations in those parameters over a 24-hr day. We considered two major independent variables -- the exterior temperature, and the light and appliance electrical load. The variations in temperature are taken from the temperature data for the Omaha "typical year", and the light and appliance loads are shown in Figure VIII-1. The DHW demand shown in that figure was an important input to our calculation.

To calculate the heating load that must be met by a combination of the heat pump and fuel-cell recovered heat, Equations 1, 2, and 3 were used with the appropriate thermal constants for Residence 3. We integrated those equations numerically, so that heat loads could be calculated over a 24-hr period.

In addition to the temperature, heat load, DHW load, and light and appliance electrical load, the inputs required for the program are the functions that relate heat pump input and output to temperature, fuel-cell heat recovered to electrical load, and heat transfer efficiency to heat pump output and fuel-cell heat recovered. The first three are obtained from data presented in Chapters IV and V, and the fourth is obtained from the manufacturer's literature on the Trane WC-18 heating coil (see Section V-P). The four functions were represented by algebraic expressions that were fitted to numerical data.

With all the above inputs formulated, we calculated hourly average electrical loads, heat pump duty factors, and the amount of recovered fuel-cell heat delivered to the space heating system. The operation of the program is described in Appendix C.

The amount of recovered fuel-cell heat available when only lights and appliances are operating are illustrated along with the DHW demand in Figure VIII-2. The figure shows that there will always be sufficient recovered fuel-cell heat to supply all DHW needs for the residences in System 5, even when the only electrical load is the basic light and appliance load. Additional heat recovered from the fuel-cell power plant beyond that required to meet DHW demand will be used to satisfy the space heating load. When there is no space heating load, the extra heat is discharged to the atmosphere.

As an example of the performance of the 100-kW fuel-cell power plant and associated equipment in meeting the electrical and thermal loads of 20 townhouse residences, as well as of the computational program discussed previously, the coldest day of the "typical" year for Omaha was chosen. The highest electrical demand of the heating season occurs on that day, so that the capability of the 100-kW fuel-cell power plant to meet that demand for 20 residences must be determined. The actual temperature data were for January 12, 1975. On that day the temperature ranged from -23°C (-9°F) to -13°C (8°F) with an average temperature of -17°C (1.5°F). Figure VIII-3 shows the variation in temperature with time of day along with the hourly average heating loads for Residence 3 calculated using Equations 1, 2, and 3. The heating load closely follows the temperature, with the peak load of 24.8 MJ/hr (23,490 Btu/hr) occurring at 6-7 a.m. That heating load must be met by a combination of recovered fuel-cell heat, heat pump output, and electric resistance heat.

The program that calculates the performance of the energy supply system for the townhouses was run using the temperature data and heating loads shown in Figure VIII-3. The results are illustrated in Figures VIII-3 and VIII-4. Figure VIII-3 shows the portion of the heating load per residence that is met by heat recovered from the fuel-cell power plant. Over the 24-hr period, that amount is 234 MJ (221,600 Btu), or 42% of the total heating load of 558 MJ (529,100 Btu); in addition, the fuel-cell power plant supplies 44.9 MJ (42,500 Btu) of DHW demand.

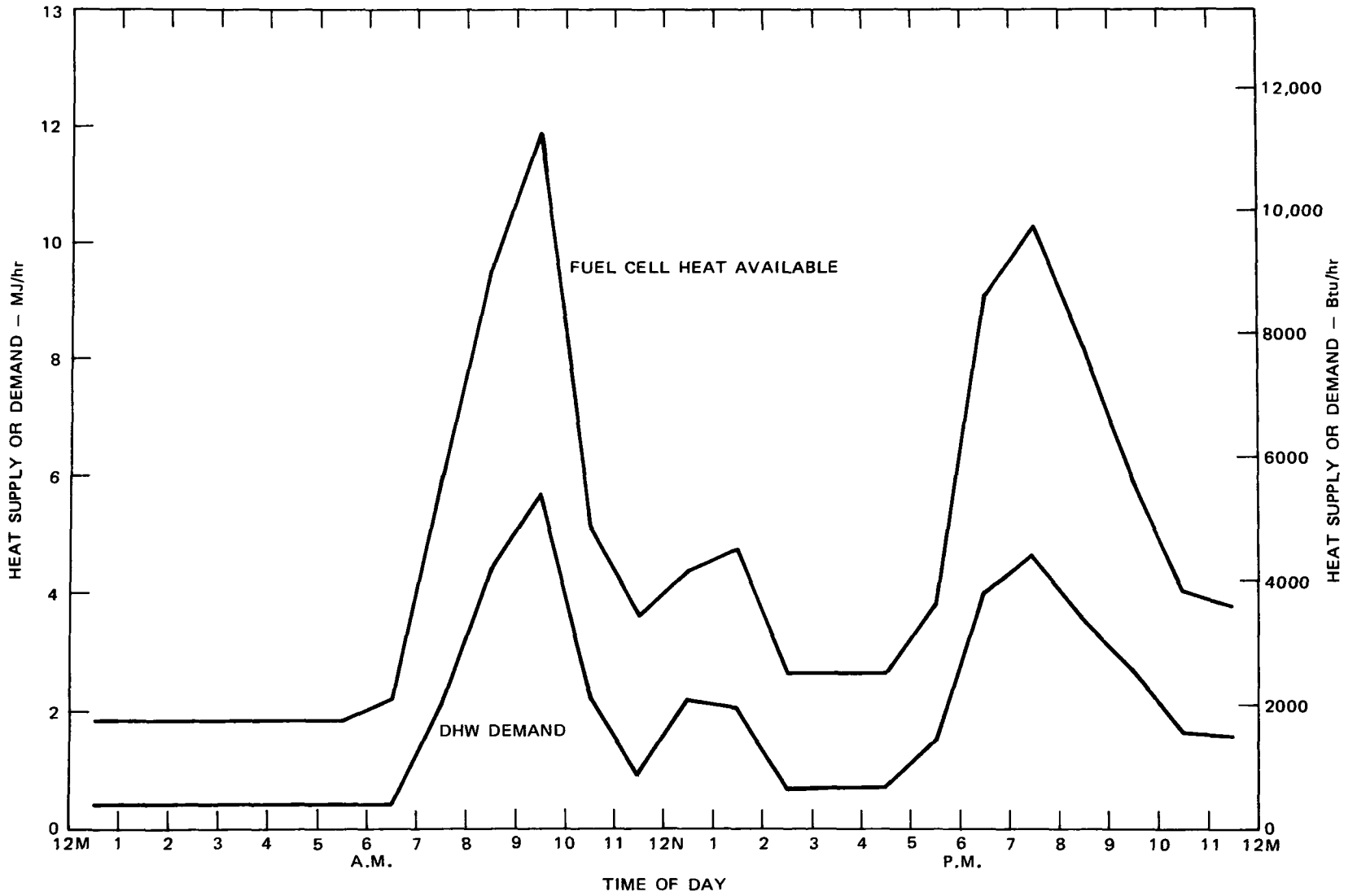

FIGURE VIII-2. DHW DEMAND RELATIVE TO FUEL CELL HEAT AVAILABLE FROM OPERATION OF LIGHTS AND APPLIANCES

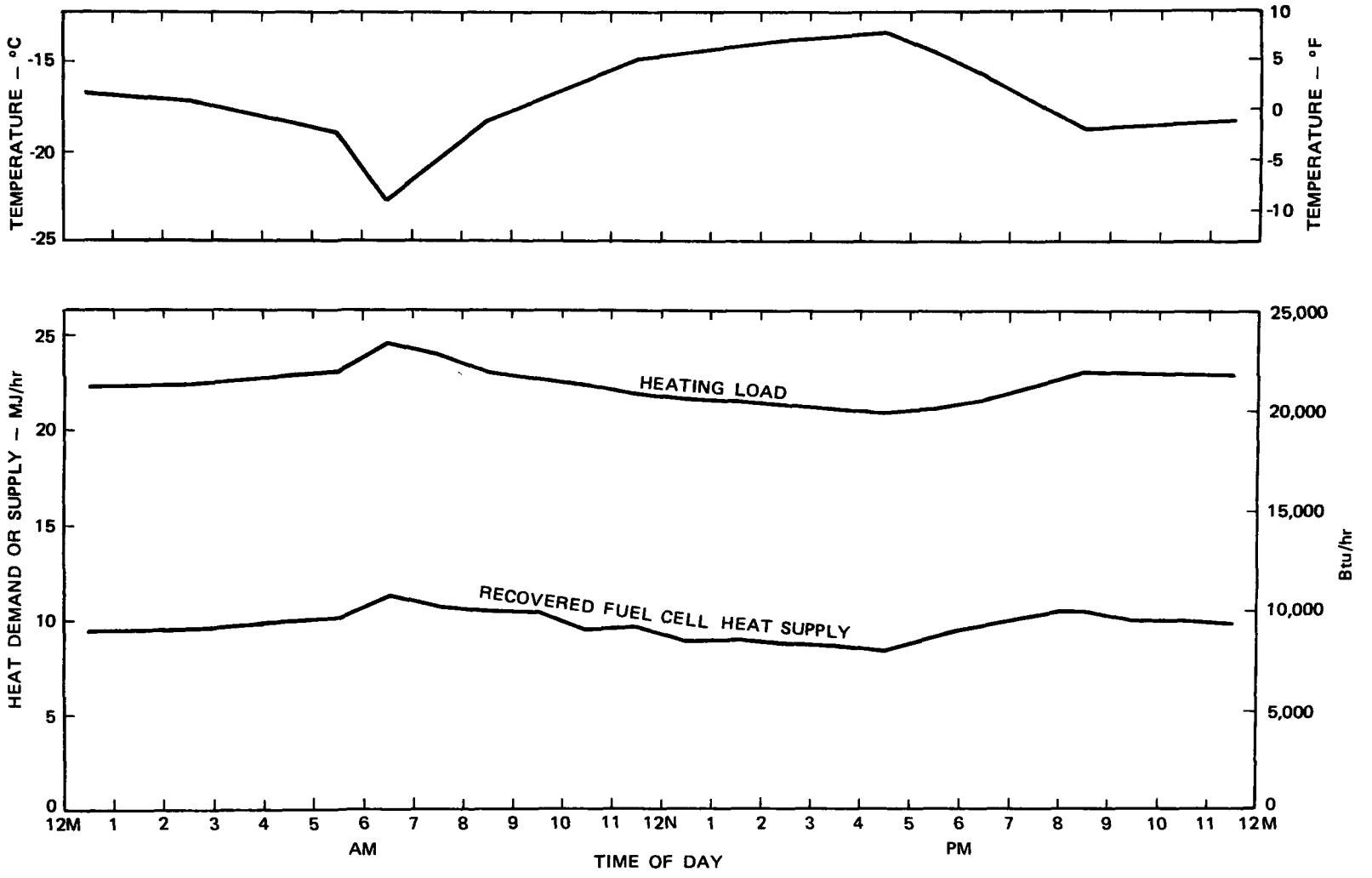

FIGURE VIII-3. HOURLY AVERAGE TEMPERATURE, HEATING LOAD, AND SUPPLY OF RECOVERED FUEL CELL HEAT FOR RESIDENCE 3 ON THE COLDEST DAY OF THE YEAR

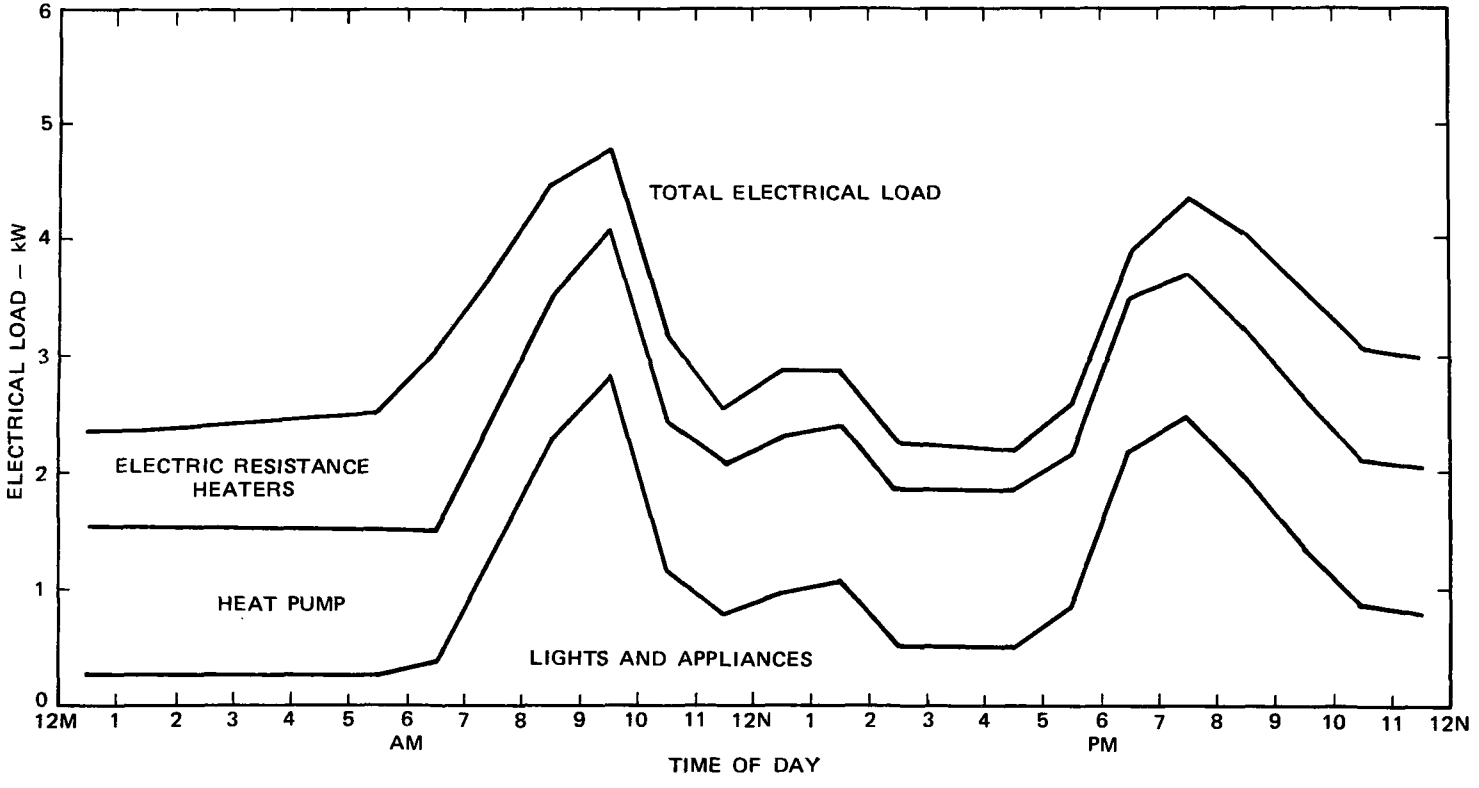

FIGURE VIII-4. HOURLY AVERAGE ELECTRICAL LOADS FOR RESIDENCE 3 ON THE COLDEST DAY OF THE YEAR

Figure VIII-4 shows the hourly average electrical load per residence, categorized according to lights and appliances, heat pump, and electrical resistance heat. The figure clearly shows that the average electrical load does not exceed the 5 kW per residence capacity of the fuel-cell power plant. However, peak concident electrical demand could exceed the 5 kW capacity during high demand periods, because the loads in Figure VIII-4 are hourly averages rather than actual instantaneous loads.

To determine whether the calculation discussed above would be required for each day of the heating season to arrive at accurate monthly and seasonal electricity consumption for System 5, the daily averages of the heating and electrical loads presented above were compared to those derived from daily average temperature, heating load, light and appliance load, and DHW demand. Average light and appliance load and DHW demand of 1.01 kW and 1,870 kJ/hr (1,770 Btu/hr), respectively, along with the average temperature of -17°C (1.5°F) and space heating load of 23.2 MJ/hr (22,000 Btu/hr), were used to calculate the following daily average parameters:

- Average electrical load: 3.20 kW
- Recovered fuel-cell heat delivered to the space heating system: 9,810 kJ/hr (9,300 Btu/hr).

The corresponding parameters derived by averaging the hourly values calculated previously are 3.04 kW and 9,740 kJ/hr (9,230 Btu/hr). These results, as well as others obtained from daily temperature data for less severe temperature conditions, indicate that the use of daily average values in the calculation of average electrical loads and recovered fuel-cell heat supply yield acceptable agreement (generally within 5%) with values calculated from 24-hour data. Therefore, the daily average method was used to calculate monthly and seasonal electricity consumption and fuel-cell heat utilization for the townhouse residences.

Figure VIII-5 shows the heating system electrical load (heat pump plus electric resistance heaters) and recovered fuel-cell heat delivered

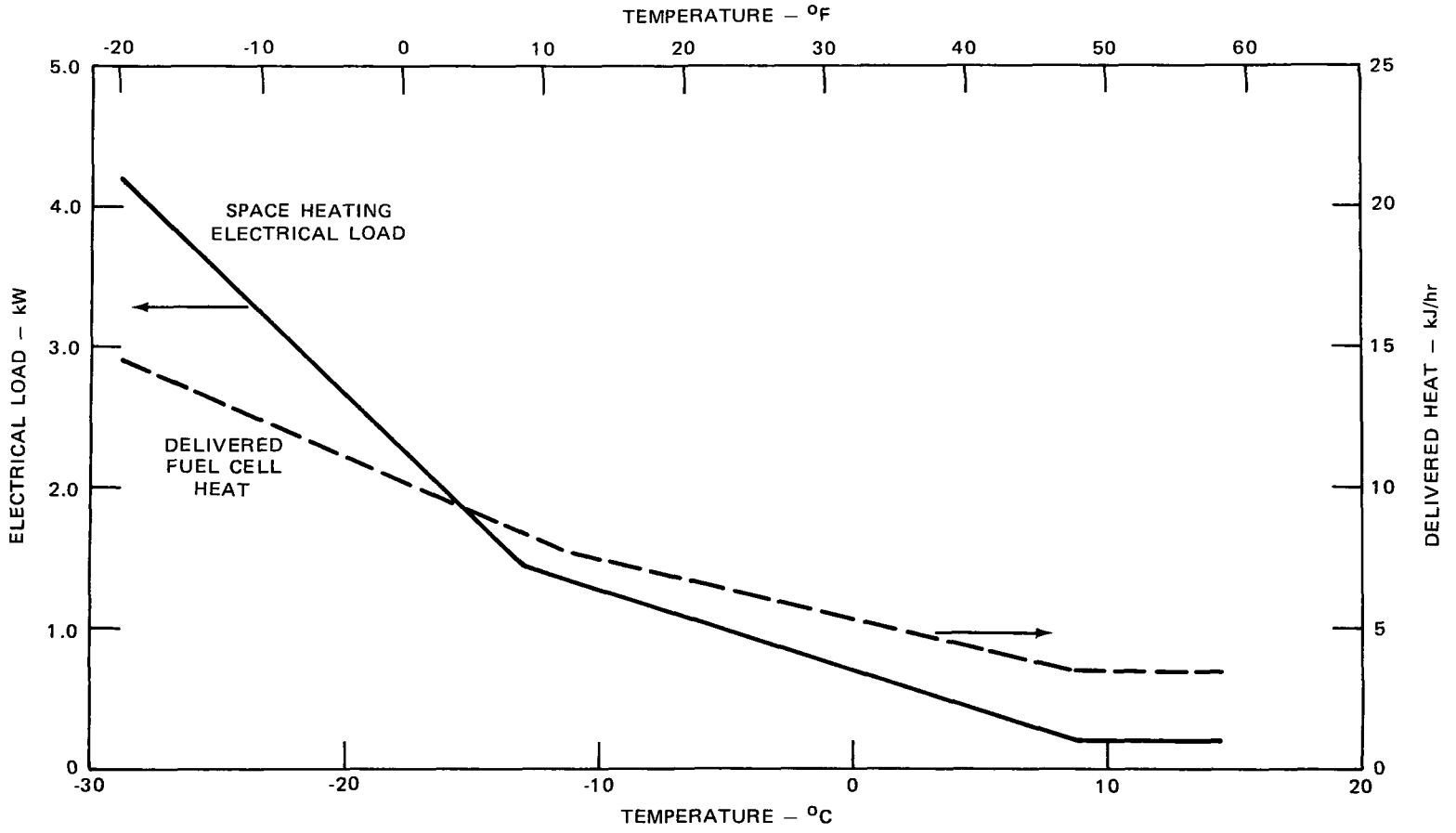

FIGURE VIII-5. VARIATIONS IN AVERAGE SPACE HEATING ELECTRICAL LOAD AND DELIVERED FUEL CELL HEAT WITH EXTERNAL TEMPERATURE

to the heating system as a function of external temperature. They are based on an average light and appliance load of 1.01 kW and a DHW load of 1,870 kJ/hr (1,770 Btu/hr). The electrical load curve shows a leveling in slope at about 9°C (48°F). That is the point at which recovered fuel-cell heat is sufficient to supply the heating load of the residences. Above that point the only electricity requirement is the 0.21 kW consumed by the heat pump fan motor, which must be on whenever space heat is required. Both curves are remarkably linear considering the complicated functional relationship between the various system parameters.

To calculate cooling season energy requirements, the same method was employed as for Residences 1 and 2, because recovered fuel-cell heat does not enter into the calculation. To check the peak cooling demand against the capacity of the 100-kW power plant, temperatures for the hottest day of the "typical" year (represented by July 1, 1970) were used to calculate hourly electrical loads. The results of that calculation are shown in Figure VIII-6. Again, the peak of the average hourly demand of lights and appliances plus heat pump operating in the cooling mode does not exceed the 5 kW per residence capacity of the fuel-cell power plant.

Using the methods discussed above, the monthly and seasonal heating, cooling, and total electrical consumption for Residence 3 were calculated, along with the amount of recovered fuel-cell heat utilized to meet the heating load. The results of those calculations are shown in Table VIII-7. Total use of recovered fuel-cell heat for space heating is 22.7 GJ (21.5 million Btu) for the heating season. In Section VIII-B the seasonal heating load for Residence 3 was given as 45.0 GJ (42.7 million Btu). Therefore, recovered fuel-cell heat supplies 50% of the total space heating requirement in addition to the total yearly DHW requirement of 16.3 GJ (15.5 million Btu).

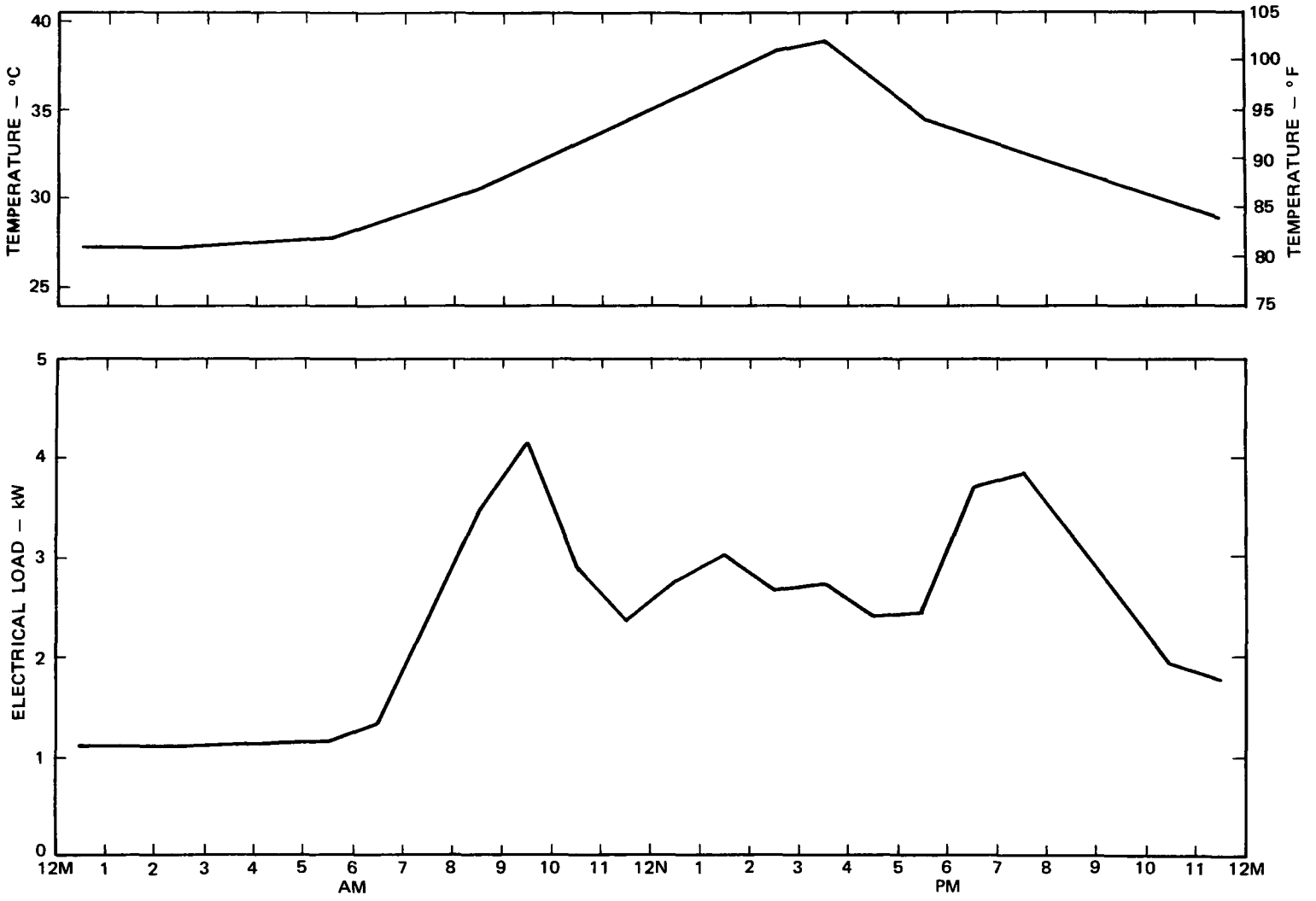

FIGURE VIII-6. HOURLY AVERAGE TEMPERATURE AND ELECTRICAL LOAD FOR RESIDENCE 3 ON THE HOTTEST DAY OF THE YEAR

The annual electricity consumption for Residence 3 is 12,790 kWh. The annual load factor of 0.292 for a 100-kW power plant supplying 20 townhouses is obtained by dividing 20 times 12,790 kWh by the electrical capacity of the fuel-cell power plant (100 kW x 8,760 hr = 876,000 kWh). This is somewhat lower than the 0.35 load factor assumed for other types of power plants in this study. However, it is a reasonable value for a power plant that is expected to meet all the electrical requirements of a limited number of residences, ranging from minimum to peak loads.

Table VIII - 7

RESIDENCE 3 ELECTRICITY CONSUMPTION AND FUEL-CELL HEAT UTILIZATION

	Utilization of Recovered Fuel-Cell Heat (GJ)			Electricity Consumption (kWh)		
Month	DHW[a]	Space Heating	Total	Heating	L&A[b]	Total
October	1.36	1.10	2.46	98	735	833
November	1.36	3.12	4.48	342	735	1,077
December	1.36	4.43	5.79	598	735	1,333
January	1.36	4.98	6.34	756	735	1,491
February	1.36	4.06	5.42	620	735	1,355
March	1.36	3.46	4.82	415	735	1,150
April	1.36	1.51	2.87	118	735	853
Seasonal Total	9.52	22.7	32.2	2,947	5,145	8,092
May	1.36	--	1.36	69	735	804
June	1.36	--	1.36	201	735	936
July	1.36	--	1.36	375	735	1,110
August	1.36	--	1.36	324	735	1,059
September	1.36	--	1.36	51	735	786
Seasonal Total	6.80	--	6.80	1,020	3,675	4,695
Annual Total	16.30	22.7	39.0	3,967	8,820	12,787

[a]DHW = domestic hot water.

[b]L&A = light and appliances.

E. References--Chapter VIII

1. Gordian Associates, Inc., "Evaluation of the Air-to-Air Heat Pump for Residential Space Conditioning," Federal Energy Administration Report FEA/D-76/340 (April 1976).

2. Stanford Research Institute, "Patterns of Energy Consumption in the United States," Office of Science and Technology (January 1972).

3. Hittman Associates, Inc., "Residential Energy Consumption - Single Family Housing," Department of Housing and Urban Development Report HUD-HAI-2 (September 1975).

4. U.S. Department of Commerce, National Oceanic and Atmospheric Administration, Environmental Data Service, "Local Climatological Data -- Omaha, Nebraska."

5. H. S. Kirschbaum and S. E. Veyo, "An Investigation of Methods to Improve Heat Pump Performance in a Northern Climate," Electric Power Research Institute Report EM-319 (January 1977).

6. American Society of Heating, Refrigerating, and Air Conditioning Engineers, Handbook of Fundamentals (New York 1972).

IX. COMPARATIVE ANALYSIS

Because the cost, efficiency, and environmental parameters for the various system components have been determined, the overall performance of each of the five systems can now be analyzed and compared. The subsequent analysis in this chapter compares the relative merits of the systems rather than measuring them against some absolute standard of performance. However, to establish a benchmark against which the other systems can be compared, System 1 is considered to be closest to the current energy supply situation; other systems are assessed as having advantages or disadvantages compared to System 1.

All costs, energy consumption, and environmental impacts are expressed in terms of the total heating and cooling supplied to the residences. The unit of measure is 1 GJ (0.948 million Btu) of heating and cooling. A summary of the overall advantages and disadvantages of the systems is presented in Chapter X.

A. Energy Efficiency

The overall energy efficiencies of each of the five systems are determined by the thermal efficiency factors presented in Chapter V. For several system components, however, efficiencies were calculated as a function of percent of rated load (fuel-cell power plants, combined cycle power plants) or as a function of exterior temperature (heat pumps, air conditioners). Therefore, seasonal or annual average efficiencies are used to evaluate overall system performance. Annual or seasonal consumption of electricity required to meet the annual heating and cooling loads (or cooling load alone) can be used to determine the average coefficient of performance (COP)for the heat pumps and air

conditioner. From the heating and cooling loads and electricity consumption calculated in Chapter VIII, the annual average COPs are as follows:

- Residence 1: air conditioner; COP = 2.09
- Residence 2: heat pump; COP = 2.22
- Residence 3: heat pump; COP = 2.22.

For the 26-MW fuel-cell power plants and the combined cycle power plant, we assume the annual average load factor to be 0.35. However, the variation in load that results in this average cannot be readily determined. For example, the power plant could be operating at full load 35% of the year and be shut off for the remaining 65%. An infinite number of variations in load could average to 35%. However, because the plants are intended for intermediate cycling duty, they will operate at less than the rated load for a substantial period of time. Moreover, they will probably be shut down for a number of hours each day during nonpeak hours. Therefore, the average load factor during operation will be somewhere between 0.35 and 1.0. Based on the heat rates and load factors given in Chapter V, we have chosen the following nominal average heat rates:

- 26-MW fuel-cell power plant (SNG) - 7,600 kJ/kWh (7,200 Btu/kWh)
- 26 MW fuel-cell power plant (naphtha) - 7,400 kJ/kWh (7,000 Btu/kWh)
- Combined-cycle power plant - 7,200 kJ/kWh (6,800 Btu/kWh).

Because the 100-kW fuel-cell power plant is designed to meet all electricity requirements of the townhouse complex, it has a fairly low load factor -- 0.292 -- as determined in Chapter VIII. Because the power plant must operate continuously, and therefore have many hours of operation during low load periods, that load factor probably represents a true average load factor for the power plant. From the variation in electricity and heat generation efficiencies with load factor presented

in Chapter V, the average efficiencies can be determined. The average efficiency is 0.30 for electricity conversion, and 0.36 for heat generation, assuming an average load factor of 0.292.

Using the average energy efficiency factors presented above, the overall system efficiencies for heating and cooling residences were determined (see Figures IX-1 through IX-5). The figures are drawn so that the energy supplied from one component to the next is shown beside the line connecting the components. Any external energy requirement is shown beside the system component that requires it, with a small arrow indicating input to that component. The efficiency of each component is shown within the box that represents the component.

The representation of System 5 in Figure IX-5 is slightly different than the others. It shows 25.7 GJ of heat supplied to the space heat delivery system from the 100-kW fuel-cell power plant. Only part of that heat (12.8 GJ) is coproduced with the generation of electricity to supply the heat pump. The remainder (12.9 GJ) is coproduced with the generation of electricity for lights and appliances. However, the figure shows only the fuel supply to the power plant needed to produce power for the heat pump. That is because electricity is required for lights and appliances even with no heat demand, and, after DHW demand is met, the excess heat generated by the power plant would be rejected to the atmosphere if there were no heating load. Because a heating load does exist, however, heat that would have been wasted is used effectively to reduce the electricity required by the heat pump. Therefore, the energy efficiency for heating and cooling is based on the incremental electricity consumption by the heat pump assuming that the light and appliance as well as the DHW loads constitute the base system demand.

To clarify the energy supply and demand picture for System 5, Figure IX-6 shows the annual flows of energy per residence, including light and appliance and DHW demand.

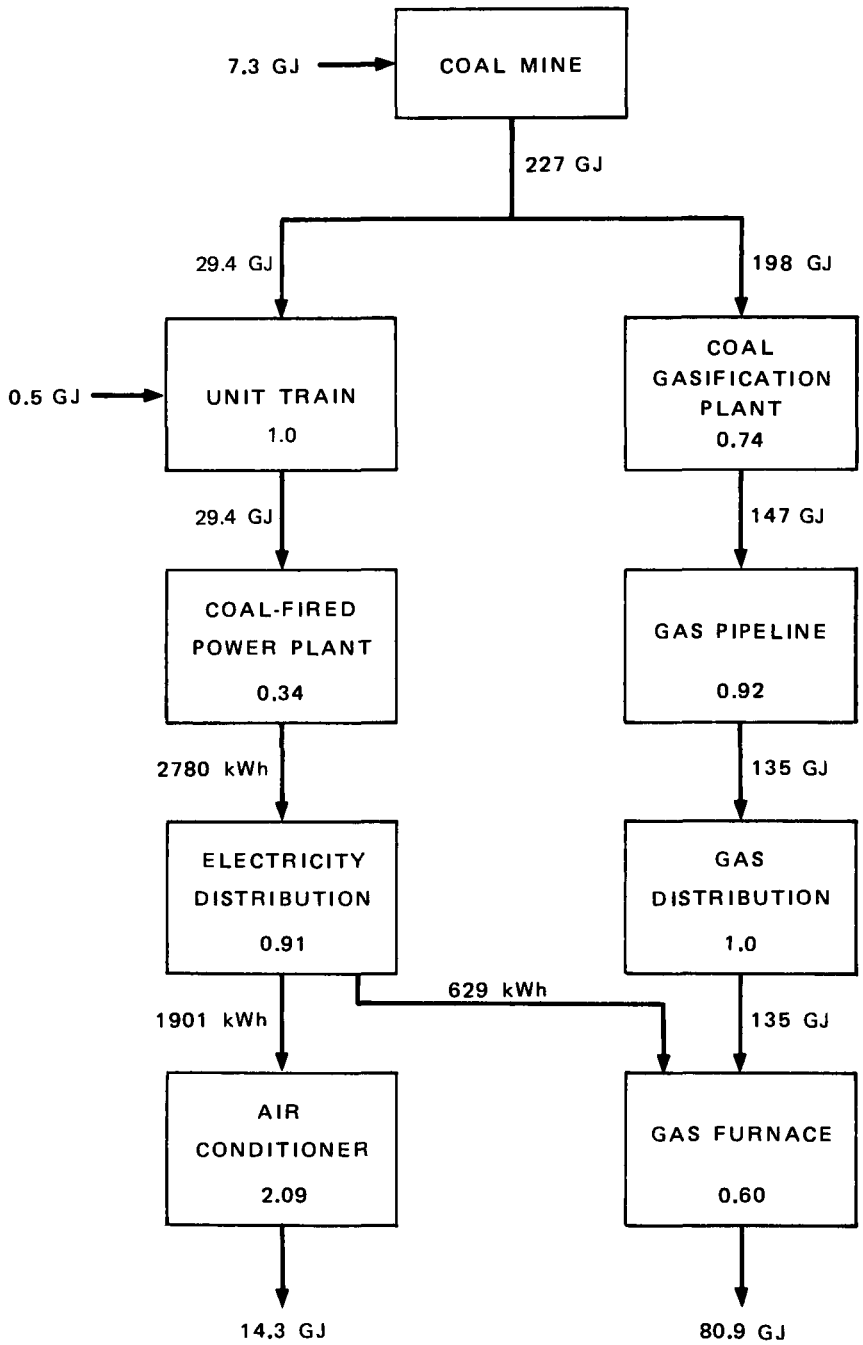

$$\text{ENERGY EFFICIENCY} = \frac{14.3 + 80.9}{227 + 7.3 + 0.5} = 0.41$$

FIGURE IX-1. ANNUAL ENERGY FLOWS AND ENERGY EFFICIENCY FOR SYSTEM 1

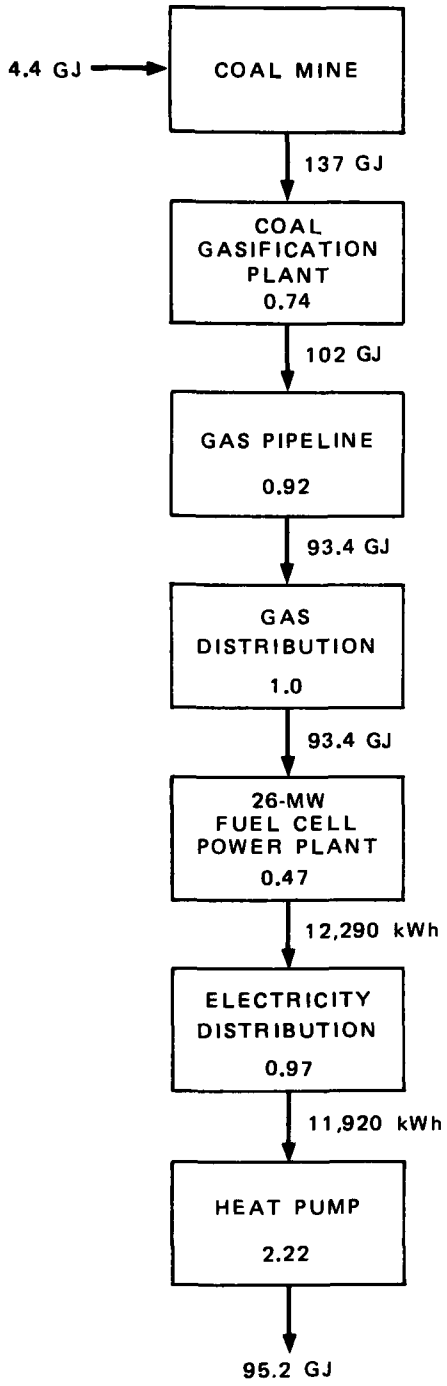

$$\text{ENERGY EFFICIENCY} \quad \frac{95.2}{137 + 4.4} = 0.67$$

FIGURE IX-2. ANNUAL ENERGY FLOWS AND ENERGY EFFICIENCY FOR SYSTEM 2

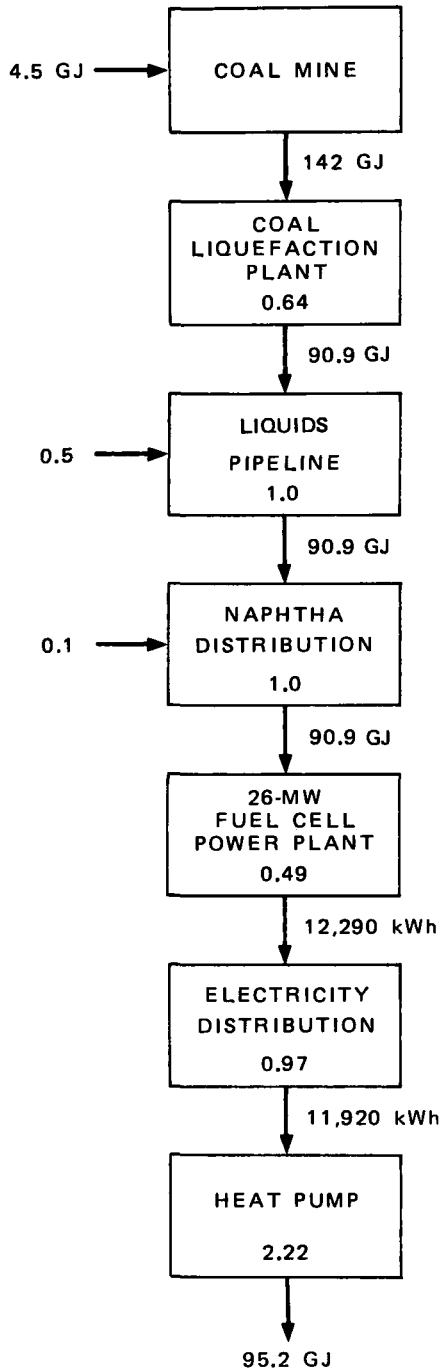

$$\text{ENERGY EFFICIENCY} = \frac{95.2}{142 + 4.5 + 0.5 + 0.1} = 0.65$$

FIGURE IX-3. ANNUAL ENERGY FLOWS AND ENERGY EFFICIENCY FOR SYSTEM 3

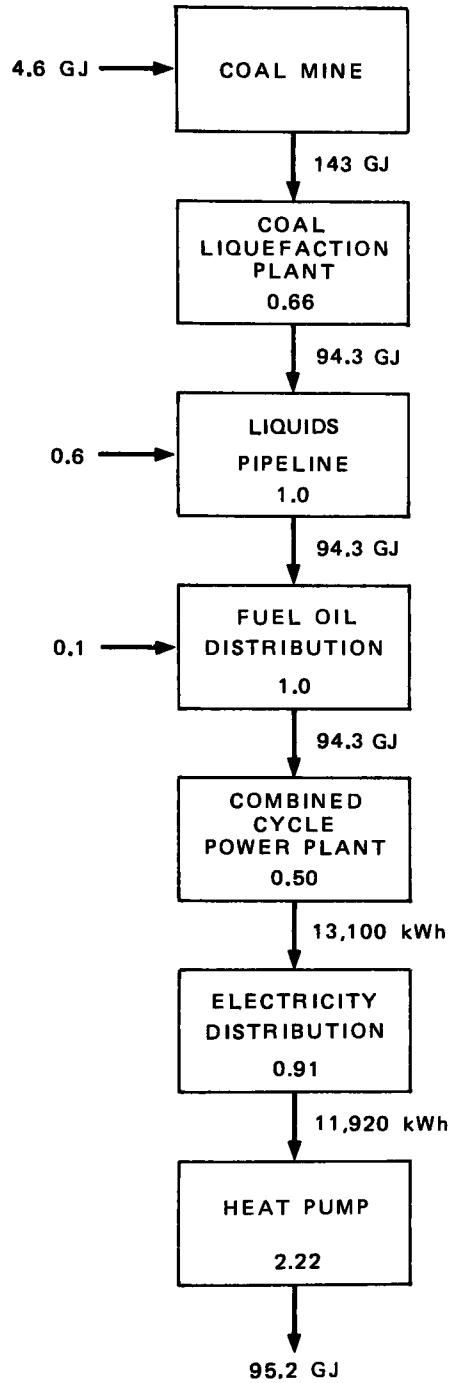

$$\text{ENERGY EFFICIENCY} = \frac{95.2}{143 + 4.6 + 0.6 + 0.1} \quad 0.64$$

FIGURE IX-4. ANNUAL ENERGY FLOWS AND ENERGY EFFICIENCY FOR SYSTEM 4

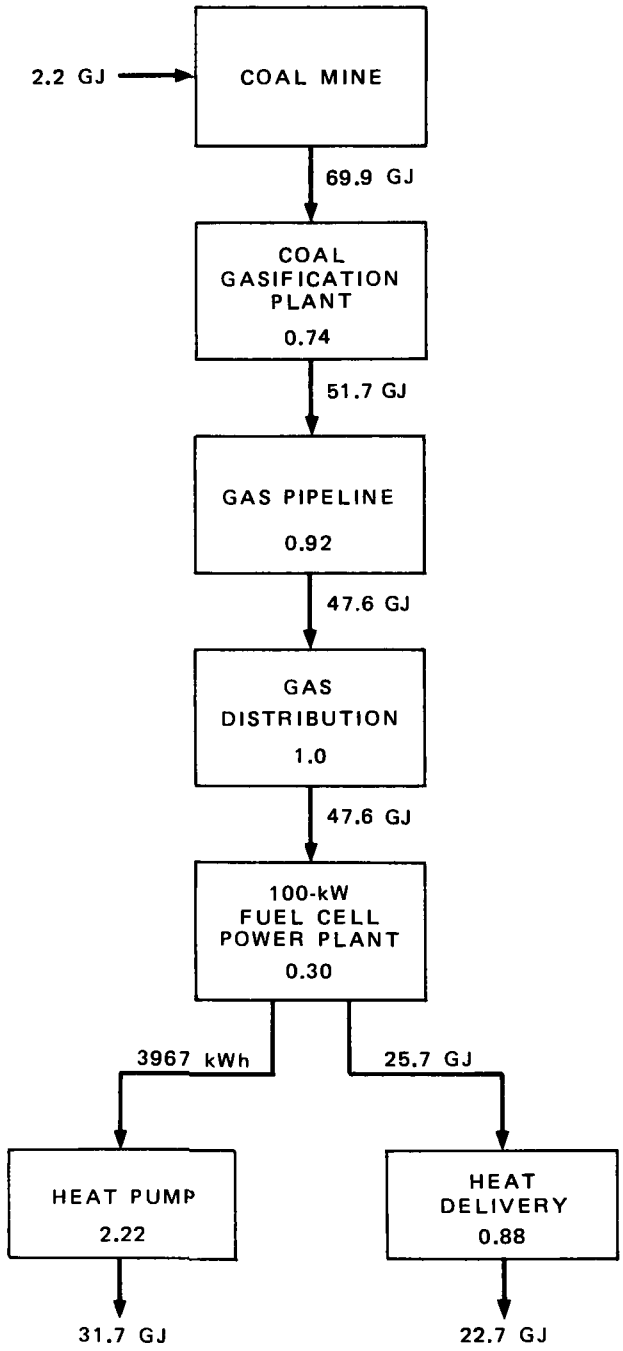

$$\text{ENERGY EFFICIENCY} = \frac{31.7 + 22.7}{69.9 + 2.2} = 0.75$$

FIGURE IX-5. ANNUAL ENERGY FLOWS AND ENERGY EFFICIENCY FOR SYSTEM 5

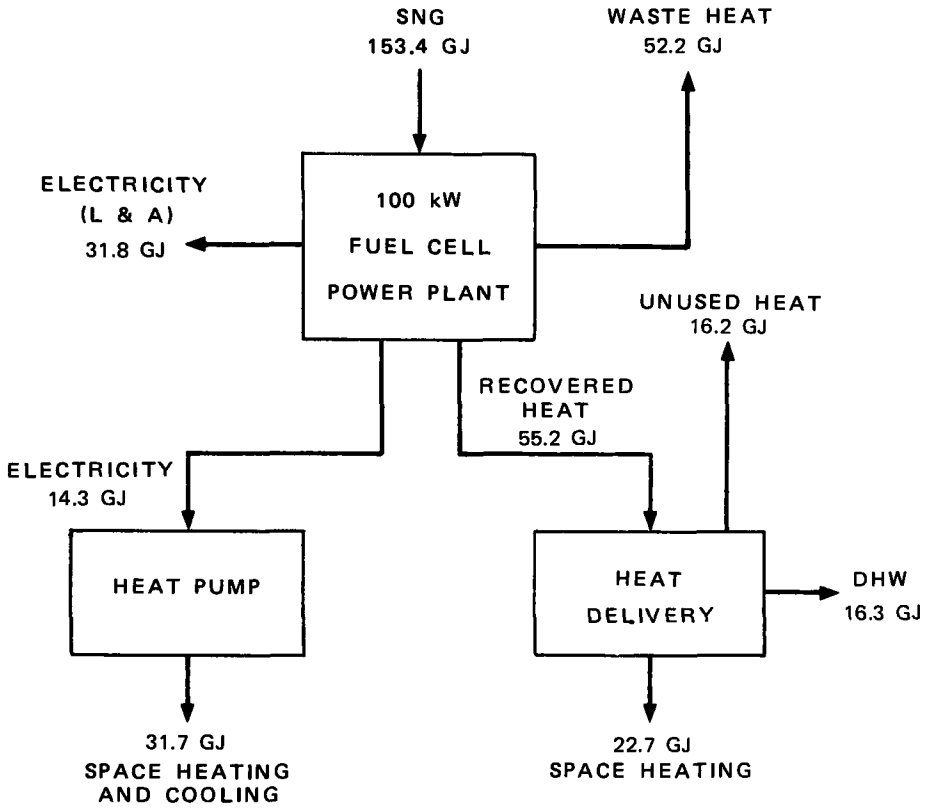

FIGURE IX-6. TOTAL ANNUAL ENERGY FLOWS (PER RESIDENCE) FOR FUEL CELL POWER PLANT SUPPLYING TOWNHOUSES

Based on heating and cooling only, System 5 has the highest overall energy efficiency -- 0.75. System 1 has the lowest efficiency at 0.41. Systems 2, 3, and 4 are comparable, although System 2 has a slight advantage at 0.67.

Overall, Systems 2 through 5 are considerably more efficient (greater than 50%) than System 1, primarily because of the high efficiencies of the advanced electricity generating technologies and the use of heat pumps rather than the gas furnace. The advantages in recovering fuel-cell heat in System 5 are clearly demonstrated, although they are not dramatic; the efficiency is just 12% greater than System 2, the next most efficient system. Even though heat is recovered from the 100-kW phosphoric acid fuel cell, the electricity generating efficiency of the 26-MW molten carbonate fuel cell is 50% higher. This high efficiency, combined with an efficient heat pump to generate space heating, considerably reduces the advantage of recovering heat from a low electrical efficiency phosphoric acid fuel cell. Optimizing of the relative amounts of heat and electricity generated by the 100-kW fuel cell (determined by the actual heat and electrical loads it is expected to meet) would result in higher system efficiency. However, such an optimization was beyond the scope of this study.

B. Economics

1. Cost of Heating and Cooling

The cost of providing heating and cooling to the residences can be readily calculated using cost factors developed in Chapter VII and the energy consumption estimates derived in Chapter VIII. The figure of merit to be used in comparing the five systems is the cost of providing 1 GJ of heating and cooling, which is derived by dividing the annual cost of providing heating and cooling by the total annual heating and cooling load. The annual cost of heating and cooling is the sum of the fixed annualized cost of heating and cooling equipment plus the cost of gas and/or electricity consumed by the equipment.

The costs derived by this method represent the true incremental cost to the consumer of obtaining heating and cooling from each of the five systems. These costs would never appear on the gas or electric bill of a customer as shown here, of course, because new sources of gas or electricity supply are integrated into the supply system, and the customer sees only the average cost of supplying gas or electricity from all sources in the system.

The costs of the various system components derived in Chapter VII may be used directly as shown, except that the cost of electricity transmission and distribution must be derived using Equations VII-(5) and VII-(6), and the cost of electricity from the 100-kW fuel-cell power plant is somewhat different than that shown in Table VIII-34 because of differing load factors and because recovered heat is not explicitly credited.

The costs of electricity transmission and distribution for each of the residences are based on the total electricity consumption shown in Chapter VIII and calculated using Equations VII-(5) and VII-(6). Those costs are as follows:

- Residence 1 - 16.5 mills/kWh (System 1)
- Residence 2 - 12.7 mill/kWh (Systems 2 and 3)
- Residence 3 - 14.0 mills/kWh (System 4).

The annual average costs of heating and cooling for each of the five systems are shown in Tables IX-1 through IX-5. The cost shown next to each system component is the cumulative cost of energy supplied by the component. The heating and cooling cost calculation is summarized at the bottom of each table.

Not surprisingly, System 1 has the lowest cost of heating and cooling because it employs the most conventional technology and has the fewest energy conversion steps. Furthermore, even though it is the least efficient system, the cost of the coal that the system uses is so

low ($0.33/GJ) that the effect of low efficiency on the final cost of heating and cooling is not significant. (The cost of coal contributes only $0.79 to the total heating and cooling cost of $10.10/GJ).

Table IX-1

COST OF HEATING AND COOLING FOR SYSTEM 1

Coal Mine	$0.33/GJ
Unit train	$0.61/GJ
Coal-fired power plant	$9.81/GJ (35.3 mills/kWh)
Electricity transmission and distribution	$15.40/GJ (55.3 mills/kWh)
Coal gasification plant	$2.90/GJ
Gas pipeline	$3.54/GJ
Gas distribution	$4.16/GJ
Air Conditioner/gas furnace	$294/yr

$$\text{Cost of heating and cooling} = \frac{\$294 + 1{,}901\ \text{kWh}/(\$0.0553/\text{kWh}) + 135\ \text{GJ}\ (\$4.16/\text{GJ})}{95.2\ \text{GJ}}$$

$$= \$10.1/\text{GJ}$$

Table IX-2

COST OF HEATING AND COOLING FOR SYSTEM 2

Coal mine	$0.33/GJ
Coal gasification plant	$2.90/GJ
Gas pipeline	$3.54/GJ
Gas distribution	$3.98/GJ
26-MW fuel-cell power plant	$16.40/GJ (59.0 mills/kWh)
Electricity distribution	$20.40/GJ (73.5 mills/kWh)
Heat pump	$351/yr

$$\text{Cost of Heating and Cooling} = \frac{\$351 + 11{,}920\ \text{kWh}\ (\$0.0735/\text{kWh})}{95.2\ \text{GJ}}$$

$$= \$12.90/\text{GJ}$$

Table IX-3

COST OF HEATING AND COOLING FOR SYSTEM 3

Coal mine	$0.33/GJ
Coal liquefaction plant	$3.77/GJ
Liquids pipeline	$3.93/GJ
Naphtha distribution	$4.01/GJ
26-MW fuel-cell power plant	$16.70/GJ (60.1 mills/kWh)
Electricity distribution	$20.80/GJ (74.7 mills/kWh)
Heat pump	$351/yr

$$\text{Cost of Heating and Cooling} = \frac{\$351 + 11{,}920 \text{ kWh } (\$0.0747/\text{kWh})}{95.2 \text{ GJ}}$$

$$= \$13.00/\text{GJ}$$

Table IX-4

COST OF HEATING AND COOLING FOR SYSTEM 4

Coal mine	$0.33/GJ
Coal liquefaction plant	$3.02/GJ
Liquids pipeline	$3.17/GJ
Fuel oil distribution	$3.29/GJ
Combined-cycle power plant	$13.00/GJ (46.9 mills/kWh)
Electricity transmission and distribution	$18.20/GJ (65.5 mills/kWh)
Heat Pump	$351/yr

$$\text{Cost of Heating and Cooling} = \frac{\$351 + 11{,}920 \text{ kWh } (\$0.0655/\text{kWh})}{95.2 \text{ GJ}}$$

$$= \$11.90/\text{GJ}$$

Table IX-5

COST OF HEATING AND COOLING FOR SYSTEM 5

Coal mine	$0.33/GJ
Coal gasification plant	$2.90/GJ
Gas pipeline	$3.54/GJ
Gas distribution	$4.16/GJ
100-kW fuel-cell power plant	$24.2/GJ (87.1 mills/kWh)
Heat pump	$314/yr
Heat delivery system	$271/yr

$$\text{Cost of Heating and Cooling*} = \frac{\$314 + \$271 + 3{,}970 \text{ kWh } (\$0.0871/\text{kWh})}{70.7 \text{ GJ}}$$

$$= \$13.20/\text{GJ}$$

* Includes DHW

The heating and cooling costs of Systems 2 and 3 are comparable primarily because the cost of delivered fuels for the power plants are nearly identical. Although coal-derived naphtha is much more expensive to produce than SNG, the transport and distribution costs of SNG are much higher than for naphtha.

The heating and cooling cost for System 4 is about 8% lower than for Systems 2 and 3, primarily because of the lower fuel and capital costs for the combined-cycle power plant. That difference is partly offset by higher T&D costs and transmission losses, but not enough to raise the final heating and cooling cost to the level of those of the fuel-cell systems.

The cost of heating and cooling for System 5 also includes the costs of supplying DHW because the heat recovery and delivery systems are designed to provide both space heating and hot water, and their costs cannot be readily separated. On this basis, the cost of heating and cooling for System 5 are marginally higher than for Systems 2 and 3, although that result is, of course, sensitive to the nature of loads supplied by the fuel-cell power plant.

To determine the effects of load variations on the cost of heating and cooling, those costs were determined for heating loads both higher and lower than the Residence 3 loads derived in Chapter VIII. The cooling load was allowed to vary with the heating load in a linear fashion, and all other variables were held constant, including DHW load, light and appliances loads, and power plant electrical load factor. Holding the electrical load factor means, in effect, that the number of residences supplied by the power plant will vary inversely with the heating load. The annualized cost of the heat pump was allowed to vary with the heating load while the cost of the heat delivery system, per residence, was held constant. Finally, the quantity of heat supplied by the fuel cell per kWh, along with the heat pump performance characteristics, were assumed to be the same as in the Residence 3 base case.

The results of the sensitivity calculations are shown in Figure IX-7. The cost of heating and cooling is displayed as a function of both the annual heating load and the ratio of heating load to light and appliance load. The light and appliance load constitutes the base electrical demand, which determines how much of the heat is available for space heating and DHW.

Figure IX-7 clearly shows the effect of increasing heating load on the system economics. In particular, a heating load equal to that of Residence 2 (80.9 GJ per year) results in a heating and cooling cost of $11.50/GJ, which is less than Systems 2, 3, or 4. Overall, the cost of heating and cooling varies from +17% to -14% of the base case over a range of 0.5 to 2.0 times the base case heating load.

One difficulty in comparing the heating and cooling costs of System 5 with those of the other systems is that the fuel-cell power plant in System 5 supplies all electricity for the residences. In Systems 1 though 4, the light and appliances loads are presumed to be supplied by grid electricity (and some gas in System 1), which costs about $0.04/kWh in 1977 prices, while the light and appliance loads in System 5 are supplied by expensive electricity from the fuel-cell power

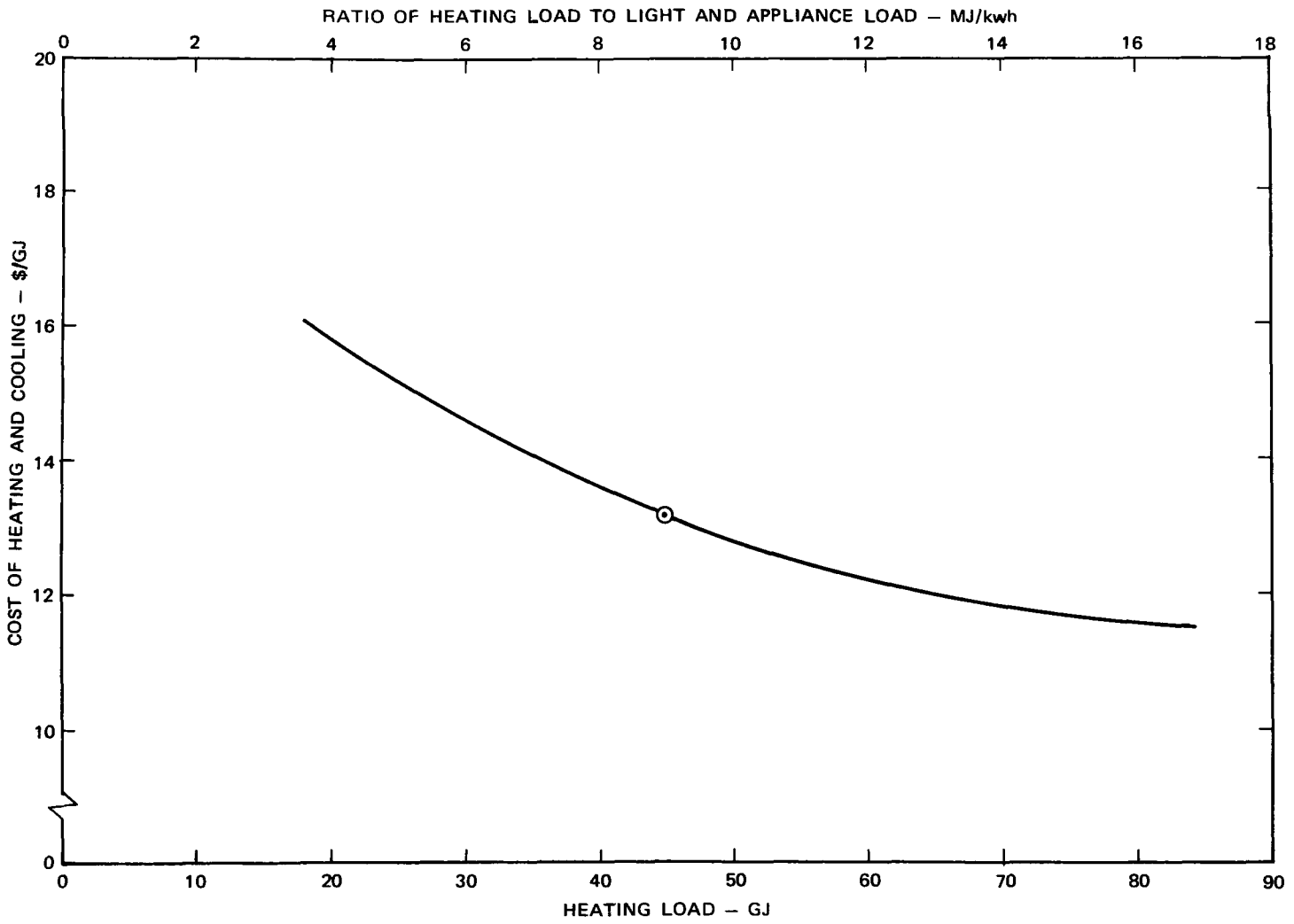

FIGURE IX-7. VARIATION IN THE COST OF HEATING AND COOLING WITH HEATING LOAD – SYSTEM 5

plant. To provide a more uniform comparison of System 5 with the other systems, the total annual energy costs of Residence 3 were determined, as supplied by Systems 1 through 5.

To calculate the total annual energy costs for Systems 2 through 4 supplying Residence 3, the light and appliance load for Residence 3 was increased from 8,820 to 13,350 kWh per year to account for DHW demand, and the heat pump load was increased from 3,967 to 6,967 kWh per year to account for the fact that recovered fuel-cell heat would not be available. For System 1, the light and appliance load of Residence 3 was reduced by 1,200 kWh per year because of the absence of the electric range. Gas consumption by appliances included 32.9 GJ per year for DHW and 11.1 GJ for the gas range. Furthermore, the figures for consumption of gas and electricity for heating and cooling were adjusted to account for the lower loads of Residence 3 relative to Residence 1.

The average grid price of electricity for Systems 1 through 4 was determined from total electrical loads and Equations VII-(4), (5), and (6). The average gas price for supplying DHW and range loads for System 1 was assumed to be the 1977 average of about $2.00/GJ. The annualized cost of heating and cooling equipment was reduced to account for the lower heating and cooling loads of Residence 3.

With the assumptions discussed above, the following total annual energy supply costs for Residence 3 as supplied by Systems 1 through 5 were calculated:

- System 1 cost = $250 + 75 GJ ($4.16/GJ)
  + 44 GJ ($2.00/GJ) + 1,605 kWh (0.0553/kWh)
  + 7,620 kWh ($0.0391/kWh)
  = <u>$1,040</u>

- System 2 cost = $314 + 13,348 kWh ($0.0366/kWh)
  + 6967 kWh ($0.0739/kWh)
  = <u>$1,320</u>

- System 3 cost = \$314 + 13,348 kWh (\$0.0366/kWh)
  + 6,967 kWh (0.0751/kWh)
  = \$1,330

- System 4 cost = \$314 + 13,348 kWh (\$0.0366/kWh)
  + 6,967 kWh (\$0.0661/kWh)
  = \$1,270

- System 5 cost = \$314 + \$271 + 12,787 kWh (\$0.0871/kWh)
  = \$1,700

System 5 is not economical in terms of supplying the total energy requirements of Residence 3 compared with other systems. The high cost of System 5 is partly caused by the low power plant load factor, partly by the high cost of the heat delivery system, and partly by the use of the fuel-cell power plant to supply electricity to the residences at all times, even when the heat demand is very low.

The optimum arrangement for System 5 would be to use grid electricity during periods of low heat demand and to use electricity from the fuel-cell power plant when the heat demand is high. The appropriate mix would have to be determined through an optimization procedure that is beyond the scope of this study.

Moreover, the 100-kW power plant in System 5 cannot be expected to meet any conceivable load by itself, even if it is designed to meet the largest average load in a typical year. Excursions above the power plant rated load could readily occur on cold winter days. Also, during extreme temperature periods, the total load could be well in excess of design capacity. The only feasible solutions are for the residences to be connected to the utility grid as a backup in high demand periods, or to have a load management system in which noncritical appliances (such as clothes dryers) would be automatically shut off during high demand periods. In the former case, the residences would have to pay a utility hook-up charge of about \$3.57 per month (according to Equation VII-(4)) even when no power was consumed, which would add about \$0.19/GJ to the cost of heating and cooling or \$42.80 per year to the total annual residential energy cost. An additional cost would also be incurred for a load management system, although such a cost was not determined in this study.

2. Capital Intensiveness

Another measure of the relative economic attractiveness of the five systems is the amount of capital required to install the various system components. Because capital may be considered a scarce resource, the capital intensiveness of the systems will measure the relative ease of initially establishing the systems, which is independent of the life-cycle system cost that was calculated in the previous section.

The unit appropriate for measuring the capital intensiveness of Systems 1-5 is the capital required to provide 1 GJ of heating and cooling per year, which may be calculated by using the component energy flows displayed in Figures IX-1 through IX-5, along with the capital intensiveness for each system component. However, the calculation of component capital intensiveness is complicated somewhat; two figures may be derived: (1) the amount of capital investment required per unit of peak energy output, and (2) the capital required per unit of average energy output. For the systems under consideration in this study, the capital investment per unit of average energy output will be used, because, by and large, the systems components are not sized to meet peak system demands and are effectively decoupled from one another. For example, the output from the coal gasification plant is fairly constant in time, while the output of the fuel-cell power plant that it supplies fluctuates daily and even hourly. The inherent storage capacity of the natural gas transport and distribution system, plus the varying demands of other users of SNG, effectively eliminate such demand fluctuations in the coal gasification plant output, and peak demands have relative little effect on the plant's capacity. That argument is not strictly true for each system component — for example, the 100-kW fuel-cell power plant is sized to meet the peak electricity demand of the townhouse in an average year. However, because the argument is generally applicable, the average energy outputs will be used for all systems components for consistency.

The resulting figures for capital intensiveness of the system components are shown in Table IX-6. Those figures are based on the total capital investments presented in Chapter VII and the yearly energy output of the system components. In some cases, capital investments were not explicitly given in Chapter VII, and the capital intensiveness was estimated using the data at hand. For example, the capital intensiveness of gas distribution was estimated by assuming that 90% of gas distribution charges are capital-related (the same proportion as for the gas pipeline) and by using a capital recovery factor of 18% per year (typical for utility economics). The figure for the coal-fired power plant represents one-half of the initial investment because the plant is assumed to be 50% depreciated when it is assigned to intermediate-load duty.

Table IX-6

CAPITAL INTENSIVENESS OF THE SYSTEM COMPONENTS

Component	Capital Intensiveness
Coal mine	$0.41 per GJ/yr
Unit train	$0.53 per GJ/yr
Coal-fired power plant	$1,210 per kW (avg.)
Coal gasification plant	$11.40 per GJ/yr
Coal liquefaction plant (fuel oil)	$11.40 per GJ/yr
Coal liquefaction plant (naphtha)	$12.60 per GJ/yr
Gas pipeline	$ 2.20 per GJ/yr
Liquids pipeline	$ 0.74 per GJ/yr
Liquid fuel distribution (fuel oil)	$ 0.09 per GJ/yr
Liquid fuel distribution (naphtha)	$ 0.11 per GJ/yr
Gas distribution	
Residential	$3.10 per GJ/yr
Commercial	$2.20 per GJ/yr
Combined-cycle power plant	$911 per kW (avg.)
26-MW fuel-cell power plant (SNG)	$1,180 per kW (avg.)
26-MW fuel-cell power plant (naphtha)	$1,240 per kW (avg.)
Electricity transmission and distribution	
Central power plant	$550 per kW (avg.)
Dispersed power plant	$490 per kW (avg.)
100-kW fuel-cell power plant	$1,570 per kW (avg.)
Gas furnace	$11.00 per GJ/yr
Air conditioner	$86.60 per GJ/yr
26-MJ/hr heat pump	$26.50 per GJ/yr
Residence 3 heating and cooling system	$71.90 per GJ/yr

The figures for capital intensiveness presented in Table IX-6 were combined with the energy flows shown in Figures IX-1 through IX-5 to obtain the total capital intensiveness per GJ/yr of heating and cooling for each of the five systems (see Tables IX-7 through IX-11). The trends are similar to those displayed in the cost of heating and cooling calculations shown in Tables IX-1 through IX-5. The capital intensiveness of System 1 is the lowest of the five, as expected. Systems 2 through 4 are comparable, with System 4 having about a 10% advantage over system 2. The capital intensiveness of System 5 is much higher than that of any other system, primarily because of the high investment required for the heat delivery system. If heating and cooling equipment, the cost of which is borne by the consumer rather than the utilities, is excluded from the calculations, System 5 has the lowest capital intensiveness of any system. Therefore, System 5 would be very attractive to the utilities because of the initial investment

Table IX-7

CAPITAL INTENSIVENESS FOR SYSTEM 1
($ per GJ/yr of Heating and Cooling)

Coal mine	$0.98
Unit train	0.17
Coal-fired power plant	4.02
Electricity transmission and distribution	1.67
Air conditioner	13.00
Coal gasification plant	17.60
Gas pipeline	3.15
Gas distribution	4.40
Gas furnace	9.35
Total	$54.34

Table IX-8

CAPITAL INTENSIVENESS FOR SYSTEM 2
($ per GJ/yr of Heating and Cooling)

Coal mine	$ 0.59
Coal gasification plant	12.10
Gas pipeline	2.18
Gas distribution	2.16
26-MW fuel-cell power plant	17.30
Electricity transmission and distribution	7.04
Heat pump	26.50
Total	$67.87

Table IX-9

CAPITAL INTENSIVENESS FOR SYSTEM 3
($ per GJ/yr of Heating and Cooling)

Coal mine	$ 0.61
Coal liquefaction plant	12.00
Liquids pipeline	0.71
Naphtha distribution	0.10
26-MW fuel-cell power plant	18.20
Electricity transmission and distribution	7.04
Heat pump	26.50
Total	$65.10

Table IX-10

CAPITAL INTENSIVENESS FOR SYSTEM 4
($ per GJ/yr of Heating and Cooling)

Coal mine	$ 0.62
Coal liquefaction plant	11.30
Liquids pipeline	0.73
Fuel oil distribution	0.09
Combined-cycle power plant	14.30
Electricity transmission and distribution	7.87
Heat pump	26.50
Total	$61.40

Table IX-11

CAPITAL INTENSIVENESS FOR SYSTEM 5
($ per GJ/yr of Heating and Cooling)

Coal mine	0.41
Coal gasification plant	8.33
Gas pipeline	1.49
Gas distribution	2.09
100-kW fuel-cell power plant	10.10
Heat pump/heat delivery	71.90
Total	94.30*

*Includes DHW for this system only.

required. However, the consumer would be discouraged from participating in such an arrangement because of the large initial equipment cost.

C. Environmental Impact

The environmental aspects of the system components were analyzed in Chapter VI. Those analyses can be used to develop enviromental impact profiles of the five systems. Qualitative judgments play an important role in comparing the systems because an absolute quantitative ranking of the systems is generally not possible, nor would it necessarily be desirable.

1. Pollutant Emissions

The emissions of air and water pollutants and solid wastes developed in Chapter VI for system components were used to calculate the total emissions for the five systems. So that the systems could be compared on an equivalent basis, the emissions were normalized on the basis of pollutants emitted per GJ of heating and cooling. These quantities are shown in Tables IX-12 through IX-16. Because the unit of reference is 1 GJ of heating and cooling, the amount of energy issuing from each component is generally greater or less than that amount, depending on the various component efficiencies, and is shown in parentheses below the name of each system component.

A dash in any column means that none (or an insignificant amount) of that pollutant is produced. The entries in each pollutant emission column have not been added to obtain total emissions per GJ of heating and cooling, primarily, because emissions from the various system components take place in different geographical regions and the resulting pollutant burden to the environment must be examined in each location. Also, point sources (e.g., coal gasification plant) occur over a relatively small geographical area, while other emissions are spread over a large area (e.g., unit trains). The resulting pollutant burdens to the environment are considerably different depending on the nature of the source.

Table IX-12

POLLUTANT EMISSIONS ASSOCIATED WITH SYSTEM 1

(g Per GJ of Heating and Cooling)

	Coal Mine (2.38)*	Unit Train (0.30)*	Power Plant (0.102)*	Electricity T&D (0.093)*	Air Conditioner (0.15)*	Coal Gasification Plant (1.54)*	Gas Pipeline (1.42)*	Gas Distribution (1.42)*	Gas Furnace (0.85)*
Air Pollutants									
SO_2	0.38	0.80	28	--	--	33	0.033	--	0.36
NO_x	6.4	5.0	91	--	--	75	17	--	49
Part.**	0.21/19	0.36/_	1.8/4.2	--	--	4.3/18	0.85/_	--	6.1/_
HC	0.36	1.3	2.2	--	--	4.9	1.4	--	4.9
CO	1.1	1.8	7.3	--	--	6.3	6.8	--	12
PAH	1.8×10^{-5}	2.2×10^{-5}	8.4×10^{-5}	--	--	3.8×10^{-4}	5.4×10^{-5}	--	6.2×10^{-4}
Sb	--	--	2.2×10^{-4}	--	--	1.4×10^{-4}	--	--	--
As	--	--	1.2×10^{-5}	--	--	8.4×10^{-6}	--	--	--
Be	--	--	8.1×10^{-5}	--	--	5.0×10^{-5}	--	--	--
Cd	--	--	6.0×10^{-4}	--	--	3.8×10^{-4}	--	--	--
Pb	--	--	4.6×10^{-3}	--	--	2.9×10^{-3}	--	--	--
Hg	--	--	1.4×10^{-3}	--	--	8.8×10^{-4}	--	--	--
Se	--	--	7.1×10^{-4}	--	--	4.5×10^{-4}	--	--	--
Zn	--	--	7.1×10^{-3}	--	--	4.5×10^{-3}	--	--	--
Water Pollutants									
Suspended Solid	0.76	--	0.71	--	--	--	--	--	--
Oil and Grease	--	--	0.35	--	--	--	--	--	--
Iron	0.013	--	0.024	--	--	--	--	--	--
Manganese	0.0026	--	--	--	--	--	--	--	--
Copper	--	--	0.024	--	--	--	--	--	--
Chlorine	--	--	4.6×10^{-4}	--	--	--	--	--	--
Solid Waste	--	--	1,900	--	--	13,000	--	--	--

*GJ supplied by the system component per GJ of heating and cooling.

**Fine particulates/coarse particulates.

Table IX-13

POLLUTANT EMISSIONS ASSOCIATED WITH SYSTEM 2

(g Per GJ of Heating and Cooling)

	Coal Mine (1.44)*	Coal Gasification Plant (1.06)*	Gas Pipeline (0.980)*	Gas Distribution (0.980)*	Fuel-Cell Power Plant (0.464)*	Electricity Distribution (0.450)*	Heat Pump (1.0)*
Air Pollutants							
SO_2	0.23	23	0.022	--	--	--	--
NO_x	3.9	52	12	--	5.3×10^{-7}	--	--
Part.**	0.13/11	3.0/12	0.59/_	--	--	--	--
HC	0.22	3.4	0.97	--	--	--	--
CO	0.67	4.3	4.7	--	--	--	--
PAH	1.1×10^{-5}	2.6×10^{-4}	3.7×10^{-5}	--	--	--	--
Sb	--	9.6×10^{-5}	--	--	--	--	--
As	--	5.8×10^{-6}	--	--	--	--	--
Be	--	3.4×10^{-5}	--	--	--	--	--
Cd	--	2.6×10^{-4}	--	--	--	--	--
Pb	--	2.0×10^{-3}	--	--	--	--	--
Hg	--	6.1×10^{-4}	--	--	--	--	--
Se	--	3.1×10^{-4}	--	--	--	--	--
Zn	--	3.1×10^{-3}	--	--	--	--	--
Water Pollutants							
Suspended Solid	0.46	--	--	--	--	--	--
Iron	0.0076	--	--	--	--	--	--
Manganese	0.0016	--	--	--	--	--	--
Solid Waste	--	8,900	--	--	--	--	--

*GJ supplied by the system component per GJ of heating and cooling.

**Fine particulates/coarse particulates

Table IX-14

POLLUTANT EMISSIONS ASSOCIATED WITH SYSTEM 3

(g per GJ of Heating and Cooling)

	Coal Mine (1.49)*	Coal Liquefaction Plant (0.954)*	Liquids Pipeline (0.954)*	Naphtha Distribution (0.954)*	Fuel-Cell Power Plant (0.464)*	Electricity Distribution (0.450)*	Heat Pump (1.0)*
Air Pollutants							
SO_2	0.24	29	0.55	0.11	--	--	--
NO_x	4.0	95	8.4	0.71	1.1×10^{-5}	--	--
Part.**	0.13/12	1.9/21	0.61/_	0.052/_	--	--	--
HC	0.23	2.1	0.67	0.19	--	--	--
CO	0.69	7.3	1.8	1.2	--	--	--
PAH	1.1×10^{-5}	1.5×10^{-4}	2.8×10^{-5}	6.1×10^{-6}	--	--	--
Sb	--	2.0×10^{-4}	--	--	--	--	--
As	--	1.1×10^{-5}	--	--	--	--	--
Be	--	7.5×10^{-5}	--	--	--	--	--
Cd	--	5.5×10^{-4}	--	--	--	--	--
Pb	--	4.2×10^{-3}	--	--	--	--	--
Hg	--	1.3×10^{-3}	--	--	--	--	--
Se	--	6.4×10^{-4}	--	--	--	--	--
Zn	--	6.4×10^{-3}	--	--	--	--	--
Water Pollutants							
Suspended Solid	0.48	--	--	--	--	--	--
Iron	0.0079	--	--	--	--	--	--
Manganese	0.0016	--	--	--	--	--	--
Solid Waste	--	8,800	--	--	--	--	--

*GJ supplied by the system component per GJ of heating and cooling.

**Fine particulates/coarse particulates.

Table IX-15

POLLUTANT EMISSIONS ASSOCIATED WITH SYSTEM 4

(g per GJ of Heating and Cooling)

	Coal Mine (1.50)*	Coal Liquefaction Plant (0.990)*	Liquids Pipeline (0.990)*	Fuel Oil Distribution (0.990)*	Combined-Cycle Power Plant (0.495)*	Electricity T & D (0.450)*	Heat Pump (1.0)*
Air Pollutants							
SO_2	0.24	29	0.57	0.32	46	--	--
NO_x	4.0	95	8.7	2.1	122	--	--
Part.**	0.13/12	1.9/21	0.63/_	0.15/_	24/_	--	--
HC	0.23	2.1	0.70	0.55	12	--	--
CO	0.69	7.3	1.9	0.76	12	--	--
PAH	1.1×10^{-5}	1.5×10^{-4}	2.9×10^{-5}	4.9×10^{-6}	2.3×10^{-3}	--	--
Sb	--	2.0×10^{-4}	--	--	1.5×10^{-3}	--	--
As	--	1.1×10^{-5}	--	--	6.9×10^{-3}	--	--
Be	--	7.5×10^{-5}	--	--	1.6×10^{-3}	--	--
Cd	--	5.5×10^{-4}	--	--	4.8×10^{-3}	--	--
Pb	--	4.2×10^{-3}	--	--	0.016	--	--
Hg	--	1.3×10^{-3}	--	--	2.3×10^{-4}	--	--
Se	--	6.4×10^{-4}	--	--	1.7×10^{-3}	--	--
Zn	--	6.4×10^{-3}	--	--	0.076	--	--
Water Pollutants							
Suspended Solid	0.48	--	--	--	2.9	--	--
Oil and Grease	--	--	--	--	1.4	--	--
Iron	0.0080	--	--	--	0.10	--	--
Manganese	0.0017	--	--	--	--	--	--
Copper	--	--	--	--	0.10	--	--
Chlorine	--	--	--	--	1.5×10^{-3}	--	--
Solid Waste	--	8,800	--	--	--	--	--

*GJ supplied by the system component per GJ of heating and cooling.

**Fine particulates/coarse particulates

Table IX-16

POLLUTANT EMISSIONS ASSOCIATED WITH SYSTEM 5

(g per GJ of Heating and Cooling)

	Coal Mine (1.28)*	Coal Gasification *Plant* (0.951)*	Gas *Pipeline* (0.875)*	Gas *Distribution* (0.875)*	Fuel-Cell *Power Plant* (0.978)*	Heat Pump and *Heat Recovery* (1.0)*
Air Pollutants						
SO_2	0.20	20	0.02	--	--	--
NO_x	3.4	46	10	--	6.3	--
Part.**	0.11/10	2.7/11	0.52/_	--	--	--
HC	0.19	3.0	0.86	--	4.2	--
CO	0.59	3.9	4.2	--	--	--
PAH	9.7×10^{-6}	2.3×10^{-4}	3.3×10^{-5}	--	--	--
Sb	--	8.6×10^{-5}	--	--	--	--
As	--	5.2×10^{-6}	--	--	--	--
Be	--	3.1×10^{-5}	--	--	--	--
Cd	--	2.3×10^{-4}	--	--	--	--
Pb	--	1.8×10^{-3}	--	--	--	--
Hg	--	5.4×10^{-4}	--	--	--	--
Se	--	2.8×10^{-4}	--	--	--	--
Zn	--	2.8×10^{-3}	--	--	--	--
Water Pollutants						
Suspended Solid	0.41	--	--	--	--	--
Iron	0.0068	--	--	--	--	--
Manganese	0.0014	--	--	--	--	--
Solid Waste	--	8,000	--	--	--	--

*GJ supplied by the system component per GJ of heating and cooling.

**Fine particulates/coarse particulates.

To account for such factors, the pollutant emissions from the systems components were classified into three categories -- (1) those emitted in the mine or near-mine region, (2) those emitted during transport to the end-use region, and (3) those emitted in the end-use region. The resulting assignment of system components to each category is shown below:

- Category 1 - coal mine, coal gasification plant, coal liquefaction plant
- Category 2 - unit train, gas pipeline, liquids pipeline
- Category 3 - coal-fired power plant, combined-cycle power plant, fuel-cell power plants, liquid fuel delivery, gas furnace

Although the emission of pollutants in each category can be considered separately, an overall emission parameter for each pollutant for an entire system is desirable. Such parameters can be formulated if appropriate weighting factors can be assigned for pollutant emissions in each category. Weighting factors should be chosen on the basis of the likely effects of pollutant emissions on human health and the environment in each category.

First, because the emissions from Category 2 are dispersed, they should be weighted relatively less than the emissions from Categories 1 or 3. The gas and liquids pipelines have 10 or 11 separate emission sources spaced at about 80 km (50 mi), whereas the unit train emissions are continuous. Because emissions from different pipeline pumping stations are unlikely to interact, the total emissions can be assigned a weighting factor of about 1/10. This factor will also be applied to the unit train emissions to equalize all components in Category 2.

The relative weighting of Categories 1 and 3 is complex and difficult. On one hand, Category 3 emissions could be weighted higher because (1) the Omaha-Kansas City-Des Moines region is much more highly populated than the Powder River Basin, and therefore the human exposure to a given pollutant release will be greater, (2) additional pollutant emissions will exacerbate an existing urban pollution problem, and (3)

the highly productive agricultural environment of the region could be adversely affected, whereas the Powder River Basin has low agricultural productivity. On the other hand, Category 1 emissions could be weighted higher because (1) the Powder River Basin is a near-pristine environment that should be protected from significantly increased pollutant levels, (2) the growth in energy production in the region will substantially increase the population that will be exposed to pollutants, and (3) such growth will result in pollutant levels and control problems now facing more urbanized areas.

Because of these considerations, there is no clear-cut choice for weighting Category 1 emissions with respect to Category 3 emissions. Furthermore, no quantitative method can be used to assign weighting factors with any degree of confidence. Therefore, we decided to weight the two categories equally. That choice does not mean that the impacts of pollutant emissions in the two regions will be the same. Rather, it acknowledges that the differences in impacts are not resolvable within the scope of this study.

The weighted pollutant emissions that result from application of the weighting factors discussed above are shown in Table IX-17.* Those emissions can be used to compare the overall environmental impact of the five systems. However, to fully account for the relative effects of the various pollutants emitted from the systems components, some standard that serves as a measure of those effects must be used. Such standards, and their use in arriving at relative system rankings, are discussed below.

a. Air Pollutants

Although ambient air quality standards have been set for SO_2, NO_x, CO, hydrocarbons and particulates, those for PAH and trace

---

*The weighted emissions are equal to (Category 1 emissions plus one-tenth of Category 2 emissions plus Category 3 emissions) divided by 2.1.

Table IX-17

GEOGRAPHICALLY WEIGHTED POLLUTANT EMISSIONS FOR THE FIVE SYSTEMS

(g per GJ of Heating and Cooling)

	System 1	System 2	System 3	System 4	System 5
Air Pollutants					
SO_2	29.4	11.1	14.0	36.0	9.6
NO_x	106	27.2	47.9	107	27.0
Part.*	6.9/19.6	1.5/11.0	1.0/15.7	12.5/15.7	1.4/10.0
HC	6.0	1.8	1.2	7.1	3.6
CO	13.1	2.6	4.5	10.0	2.3
PAH	5.3×10^{-4}	1.3×10^{-4}	8.1×10^{-5}	1.2×10^{-3}	1.2×10^{-4}
Sb	1.7×10^{-5}	4.6×10^{-5}	9.5×10^{-5}	8.1×10^{-4}	4.1×10^{-5}
As	9.7×10^{-6}	2.8×10^{-6}	5.2×10^{-6}	3.3×10^{-3}	2.5×10^{-6}
Be	6.2×10^{-5}	1.6×10^{-5}	3.6×10^{-5}	8.0×10^{-4}	1.5×10^{-5}
Cd	4.7×10^{-4}	1.2×10^{-4}	2.6×10^{-4}	2.7×10^{-3}	1.1×10^{-4}
Pb	3.6×10^{-3}	9.5×10^{-4}	2.0×10^{-3}	9.6×10^{-3}	8.6×10^{-4}
Hg	1.1×10^{-3}	2.9×10^{-4}	6.2×10^{-4}	7.3×10^{-4}	2.6×10^{-4}
Se	5.5×10^{-4}	1.5×10^{-4}	3.0×10^{-4}	1.1×10^{-3}	1.3×10^{-4}
Zn	5.5×10^{-3}	1.5×10^{-3}	3.0×10^{-3}	3.9×10^{-2}	1.3×10^{-3}
Water Pollutants					
Suspended Solid	0.70	0.22	0.23	1.6	0.20
Oil and Grease	0.17	--	--	0.67	--
Iron	0.018	0.0036	0.0038	0.051	0.0032
Manganese	1.2×10^{-3}	7.6×10^{-5}	7.6×10^{-4}	8.1×10^{-4}	6.7×10^{-4}
Copper	0.011	--	--	0.048	--
Chlorine	2.2×10^{-4}	--	--	7.1×10^{04}	--
Solid Waste	7,100	4,200	4,200	4,200	3,800

*Fine particulates/coarse particulates.

elements still need to be determined. Fortunately, occupational exposure standards have been developed by the Occupational Safety and Health Administration (OSHA) and have been recommended by the American Conference of Governmental Industrial Hygienists (ACGIH) and the National Institute for Occupational Safety and Health (NIOSH) for nearly all pollutants of interest (see Table IX-18). The standards are designed to protect workers who are continuously exposed for 8 hours per day, 40 hours per week. The allowable concentrations for occupational exposure tend to be somewhat higher than those that are designed to protect the general public. While these standards do not provide a direct measure of the environmental impacts of pollutants, they do provide a basis for assessing the relative effects of pollutants on human health.

Table IX-18

OCCUPATIONAL EXPOSURE STANDARDS FOR TOXIC POLLUTANTS
TIME-WEIGHTED AVERAGES (mg/m^3)

Pollutant	ACGIH Recommendation	OSHA Standard	NIOSH Recommendation
SO_2	13	13	5
NO_2	9	-	-
Particulates	-	2.4-10 (coal dust)*	-
Hydrocarbons	-	400 (naphtha)	350 (alkanes)
CO	55	55	39
PAH	-	-	-
Sb	0.5	0.5	-
As	0.5	0.5	-
Be	0.002	0.002	0.002
Cd	0.05	0.1	0.04
Pb	0.15	0.2	0.15
Hg	0.05	-	0.05
Se	0.2	0.2	-
Zn	5.0	5.0	5.0

*Respirable fraction.

Unfortunately, no occupational standards for PAH or any compound included in this category currently exist. However, several of those compounds are well known carcinogens and, in particular, exposures to benzo(a)pyrene (BaP) has been correlated with excess lung cancers in coke-oven workers and those in similar occupations.[1] Such correlations indicate that significant effects begin to occur at levels between 0.00001 and 0.001 mg/m^3. Given that BaP is only one of a number of PAH compounds that may be contributing to lung cancer, and that total PAH emissions are of interest here, a standard of 0.001 mg/m^3 for total PAH provides very roughly the same level of protection as those standards listed in Table IX-18.

The standards shown in Table IX-18 will be used to define the relative hazards of the pollutants listed. No attempt will be made to attain an absolute measure of the impacts of the various system components, and indeed, the standards were not designed to be used in such a fashion.

Using the standards shown, weighting factors representing the relative hazards of the various pollutants were developed (see Table IX-19). The factors are simply the inverse of the occupational exposure standards, but because of the roughness of the measure of relative hazard, the factors are given to only one significant figure. There are no standards for particulates as such, just for respirable coal dust. However, using this analog for a particulate standard is reasonable when deriving a weighting factor. Having the same weighting factor for SO_2, NO_2, and particulates is also reasonable, especially considering that the National Ambient Air Quality Standards for those pollutants are about the same, that is, annual average values of 80, 100, and 75 mg/m^3 for SO_2, NO_2, and particulates, respectively.

The weighting factors shown in Table IX-19 were multiplied by the geographically weighted air pollutant emissions in Table IX-17 and divided by the sum of the weighting factors to arrive at a hazard-weighted air pollutant emission factor for each of the five systems (see Table IX-20). They clearly indicate that Systems 2 and 5

Table IX-19

WEIGHTING FACTORS FOR THE RELATIVE HAZARDS OF AIR POLLUTANTS

Pollutant	Weighting Factor
PAH	1,000
Be	500
Hg	20
Cd	20
Pb	6
Se	5
Sb	2
As	2
Zn	0.2
SO_2	0.1
NO_2	0.1
Particulates	0.1
CO	0.02
Hydrocarbons	0.003

Table IX-20

HAZARD-WEIGHTED AIR POLLUTANT EMISSION FACTORS FOR THE FIVE SYSTEMS

System 1	0.0097
System 2	0.0027
System 3	0.0042
System 4	0.013
System 5	0.0026

have the least air pollution impact; Systems 1 and 4 have the highest and System 3 lies in between.

b. Water Pollutants

The emission of water pollutants by the five systems occurs from only two sources -- the coal mine and power plant wastewater discharge. Neither of these is a major source of toxic water pollutants, and the pollutants that are emitted must meet EPA effluent guidelines. To achieve a simple ranking of the systems, it is not necessary to derive weighting factors as was done for air pollutants because the relative ranking of the systems is the same for each pollutant listed in Table IX-17. Examination of Table IX-17 indicates that System 4 has the highest water pollution impact, System 1 has the next highest, Systems 2 and 3 are comparable, and System 5 has the lowest.

c. Solid Waste

With the exception of System 1, the only sources of solid waste in the five systems are the coal gasification and liquefaction plants. Even in System 1, only 13% of the solid waste originates from the coal-fired power plant. The remainder is from coal gasification. It would be extremely difficult to assess the relative hazard of the two types of waste. Both contain coal ash and char, FGD solids, and sludge from the biological oxidation ponds. If the wastes are properly disposed of, they present little environmental hazard. The main source of concern is the possibility of toxic materials leaching from the waste piles into aquifers, as discussed in Chapter VI. Again, the different types of waste cannot be distinguished in terms of their potential for leaching. The method of disposal and the properties of the disposal site will probably have more bearing on the likelihood of leaching than the composition of the waste.

Thus, no weighting factors were applied to the quantities of solid waste produced by the systems. Therefore, according to Table IX-17, System 1 clearly has the largest solid-waste impact, System 5 has the least, and Systems 2, 3, and 4 are identical, with a somewhat higher impact than System 5.

2. Land Use, Noise, and Aesthetics

Several other environmental factors should be considered when comparing the five systems. For purposes of analysis, those factors are categorized as land use, noise, and aesthetics.

a. Land Use

To assess the effect on land use, the amount of land occupied or disturbed by the systems to produce the energy required for heating and cooling residences was calculated. An appropriate measure of land use is the area occupied or disturbed multiplied by the length of time it is effectively removed from other purposes such as agriculture, housing, recreation, or wildlife support and plant habitat. For facilities such as coal conversion plants, it is the area occupied multiplied by the lifetime of the facility. For activities such as coal mining, it is the area disturbed multiplied by the length of time from mining to final reclamation. To compare the five systems, all such measures are normalized to the energy output of the facility or activity and ultimately to the heating and cooling supplied to residences, with the impact factor measured in m^2-year/GJ.

Systems components that have significant effects on land occupancy or disturbance are shown in Table IX-21. The scaling factors are based on estimates of the land occupied by energy conversion facilities, land disturbance, and right-of-way quantities presented in Chapter VI, and on the following assumptions: (1) Four years are

required for complete reclamation of land disturbed by coal mining; (2) land disruption from pipeline construction persists for 2 years; (3) the land disruption from electricity transmission is based on a figure of 0.5 km (0.3 mi) of new transmission lines required per megawatt of added generating capacity in Missouri, Nebraska, and Iowa,[2] and on a right-of-way of 30 m (100 ft). The right-of-way is assumed to be disturbed for 2 years, while the land occupied by the towers (50 m^2 per tower with towers spaced every 0.3 km)[3] is disturbed for the lifetime of the line.

The right-of-way factor shown in Table IX-21 is appropriate for central generating facilities. For dispersed fuel-cell power plants, it should be multiplied by 0.75 to reflect the reduced transmission requirements discussed in Section VII-M.

Using the factors presented in Table IX-21 and the energy efficiency quantities shown in Figures IX-1 through IX-5, the land use per GJ of heating and cooling can be calculated for the five systems (see Table IX-22).

Table IX-21

LAND USE FACTORS FOR SYSTEM COMPONENTS

Component	Land Use, (m^2-yr/GJ)
Coal mine	0.018
Unit train	0.0053
Coal-fired power plant	0.12
Coal gasification plant	0.023
Coal liquefaction plant	0.021
Gas pipeline	0.011
Liquids pipeline	0.0062
Combined-cycle power plant	0.045
26-MW fuel-cell power plant	0.0081
Electricity transmission	0.057

Table IX-22

TOTAL LAND USE FOR THE FIVE SYSTEMS
(m^2-year/GJ of Heating and Cooling)

System 1	0.11
System 2	0.084
System 3	0.076
System 4	0.10
System 5	0.055

Systems 1 and 4 require the greatest land use, followed by Systems 2, 3, and 5, with System 5 needing only one-half the land of Systems 1 and 4. We have made no judgments as to the relative value of land in the regions encompassed by the five systems. Such complex considerations are beyond the scope of this study. In practice, the actual siting of the components of energy sytstems, and therefore the nature of the land that is disturbed, will result from trade-offs among economic, environmental, and social factors that will be very site-specific.

b. Noise

The noise characteristics of the system components as they affect the general public were identified in Chapter VI. Although many components are very noisy, not all of them need be heard by the public. Large centralized facilities such as coal mines and coal conversion plants are generally located sufficiently far from residential, commercial, and recreational areas so that significant noise levels are not disturbing. On the other hand, equipment such as locomotives and fuel delivery trucks pass near or through populated areas, and thus expose large numbers of people to high noise levels.

The main sources of obtrusive noise and their average noise levels are summarized in Table IX-23. An urban residential

background noise level of 48 dBA is considered average (see Table VI-17). Against such a background, transmission lines and fuel-cell power plants are relatively modest sources of additional noise. In quiet suburban residential areas with background noise levels of 38 dBA, their noise levels would be much more noticeable and could result in some speech masking and sleep disturbance. The noise emitted from trains and tank trucks, however, would obviously be the most objectionable, because it is many times higher than background levels, even in the noisiest urban areas. However, transmission-line and fuel-cell power plant noise is more or less continuous, but that from trains and trucks is intermittent.

The most useful way to compare the noise impact of the five systems is to determine the number of major noise sources contained in each system. Thus, System 5 has the lowest impact because it has only one low-level noise source (the 100-kW fuel-cell power plant). System 2 has two low-level noise sources (transmission line and fuel-cell power plant) and therefore has the next highest impact. Systems 1 and 4 both have one high-level and one low-level noise source. Finally, System 3, with one high-level and two low-level noise sources, has the greatest impact, although it is only marginally greater than Systems 1 and 4.

Table IX-23

SOURCES OF INVOLUNTARY EXPOSURE TO HIGH NOISE LEVELS

Source	Noise Level (dBA)
Transmission lines	55
Fuel-cell power plants	55
Unit trains	90-100
Tank trucks	88

c. Aesthetics

Evaluation of the aesthetic impacts of the five systems, even on a relative basis, is difficult because of the many value judgments involved and the lack of quantitative bases of comparison. Furthermore, the systems and their components are so similar that, with few exceptions, broad aesthetic differences among the systems are not readily discernible.

One noticeable aesthetic impact, however, is the visible plume caused by the emission of coarse particulates from the operation of some system components. (See Tables IX-12 through IX-16.) Although such emissions have relatively little health impact, they degrade visibility near the sites of system components that emit coarse particulates. Such degradation constitutes a major aesthetic impact.

The relative impact of coarse particulate emissions from each system can be evaluated by consulting Table IX-17, which presents the geographically weighted emissions of air pollutants from each system. According to that table, System 5 has the lowest impact, with emissions lower by a factor of two than System 1, which has the highest impact. System 2 has slightly higher emissions than System 5, and the emissions of Systems 3 and 4 are equal, both being about midway between Systems 1 and 5.

Another significant aesthetic impact of the five systems is caused by electrical transmission lines, which are perhaps the most extensive and noticeable aspect of the entire electrical energy system, including its associated fuel cycle. The use of dispersed power plants in Systems 2, 3, and 5 significantly reduces this impact. In principle, System 5 can avoid the use of transmission lines entirely, but in practice the residences may have to be connected to the electrical grid to ensure reliability; such a connection implies the use of some transmission facilities.

The use of dispersed 26-MW power plants does not eliminate electrical transmission entirely because interties with the rest of the utility system are needed. As discussed in Chapter VII, however, the requirement for transmission facilities can be reduced on the order of 25% compared to centralized generating facilities as represented by Systems 1 and 5.

Finally, siting dispersed fuel-cell power plants in urban/residential areas has aesthetic implications. Such plants will be a departure from the usual mix of homes, apartment buildings, commercial buildings, shopping complexes, schools, parks, and so on. However, the plants will be fairly unobtrusive, consisting of clusters of rectangular structures about 3 m (10 ft) in height. The use of proper landscaping and site design should mitigate any unattractive features.

D. System Performance

All the systems analyzed in this study are based on advanced coal conversion and/or electricity generation technologies that have yet to be proven in commercial-scale operation. The cost, efficiency, and environmental analyses of the systems are based on the assumption that the performance goals set by the developers of the technologies would be achieved in practice, and that they would be capable of performing as specified in the applications set forth in Chapter IV. The implication of those assumptions is that the systems would be less efficient, more costly, and more environmentally intrusive than our analyses have shown if those performance goals were not met.

In addition to those obvious effects, the desirability of implementing the systems will be strongly affected by considerations of reliability, lifetime, and performance characteristics of the major components. Thus, it is reasonable to ask what effect such considerations will have on the relative attractiveness of each of the five systems, and to what extent uncertainties about those characteristics will affect the implementation of the systems.

In examining those aspects of the systems, we need address only those components that represent truly new technologies. Other components, such as pipelines, transmission lines, and coal mines, have well known characteristics, and their performance parameters have been established by many years of use. Therefore, little additional light can be shed on their contribution to the overall effectiveness of the systems.

All the systems contain either an advanced coal gasification or coal liquefaction facility (Hygas and H-Coal) which utilize second-generation technologies with attractive characteristics that could be commercially available in the 1990s. Extensive programs, funded by the Department of Energy and private groups, are now under way to prove those technologies at the pilot and demonstration plant stages, and to address the engineering and design problems that must be solved before commercial development is possible.

The Hygas process has an advantage because a pilot plant based on this process has been operating since 1971, while the H-Coal pilot plant is only now being constructed. Many successful tests have been run on the Hygas pilot plant, although several problems remain to be solved, including introduction of the high-pressure coal slurry into the reaction vessel, maintaining proper reaction conditions in the three-stage gasifier, and corrosion of vessel materials. In addition, the construction and operation of the large, high-pressure reactors envisioned for a commercial plant have never been carried out.

The H-Coal process faces similar problems of high-pressure slurry operation and materials corrosion. In addition, the lifetime of the hydrogenation catalyst may be limited and, if so, catalyst regeneration techniques must be developed. Also, a reliable process for separating the liquid products from unreacted char and ash has yet to be demonstrated.

Although the Hygas and H-Coal processes were chosen for analysis in Chapter IV, the implementation of the systems does not depend on the successful development of those particular processes. Other technology choices could provide the needed coal conversion. The Lurgi gasification process, for example, is a commercially available technology that could provide pipeline gas for residences and fuel-cell power plants. In fact, that technology has been chosen for use in commercial coal gasification plants proposed by several pipeline companies.

The SRC II process, for which a pilot plant is operating in Ft. Lewis, Washington, is designed to produce low sulfur fuel oil along with a naphtha by-product. Additional hydrotreating of those products could probably be used to produce suitable turbine fuel or reformable fuel-cell fuel, respectively.

Thus, other coal conversion technologies would enable the implementation of Systems 1 through 5, although at higher costs, lower efficiencies, and possibly greater environmental impact than indicated in Chapters V, VI, and VII. Overall, coal gasification is more likely than coal liquefaction to be implemented on a commercial scale in the time frame considered in this study, primarily because of the more advanced state of coal gasification technology, the widespread demand for the product, and the high cost of alternative sources (e.g., imported LNG). Thus, Systems 1, 2, and 5, which are based on coal gasification, are favored over Systems 3 and 4.

The electricity generation technologies are the other key components of the systems. Of the four types of technologies analyzed, coal-fired power plants clearly have advantages because of their ease of implementation, reliability, and operational experience. However, compared to combined-cycle power plants and fuel-cell power plants, they have slow startup and shutdown and are not very suitable for quick-response, load-following applications. Generally, gas turbines used as spinning reserves must provide that capability.

Gas turbine/steam turbine combined-cycle power plants are by now a well-established component of the utility power generation base. Gas turbines are among the more reliable electricity-generating devices, and the heat recovery systems and steam turbines that constitute the remainder of the power plant are highly reliable and use well known technology. Advances in combined-cycle power plant performance depend on developments in gas turbine technology. To achieve the operating temperatures and concommitant efficiencies discussed in Chapter IV will require gas turbines that use ceramic vanes and blades in the expander that can withstand the thermal shock associated with cycling at high temperatures. Because gas turbines are continuously undergoing development for aircraft and industrial applications, as well as for power plant use, it seems likely that higher temperature operation can be achieved.

The use of coal-derived liquids in gas turbines is under investigation by the Department of Energy. Although no actual tests have been carried out, some coal liquids may be suitable turbine fuels, although additional processing may be required in some cases to increase the hydrogen-to-carbon ratio and reduce viscosity.

Because fuel cells are a new technology in power plant applications, they are at a disadvantage compared to coal-fired power plants and combined-cycle power plants. Once implemented, however, they offer a number of operational advantages, as discussed in Chapter II (e.g., ease of load-following, low maintenance). If the demonstration of first-generation fuel-cell power plants in utility applications proves successful, and if stack lifetime goals are achieved, then the operational basis for implementing fuel cells will have been established. There would remain, of course, the accomplishment of a successful marketing and commercialization strategy, the consideration of which is beyond the scope of this study.

If first-generation (phosphoric acid) fuel cells can be successfully marketed, then the advantages inherent in second-generation (molten carbonate) cells should lead to even more widespread utilization. As discussed in Chapter II, the main technological problems to be overcome are the stability of the stack materials under cycling conditions at high temperatures, seal corrosion, and electrode sintering. These problems are being addressed by ongoing programs sponsored by the Department of Energy and private groups.

The use of fuel cells in on-site power generation applications, as envisioned in System 5, is attractive in many respects, but has certain operational disadvantages, including the need for load management to avoid having to oversize the power plant to meet all conceivable loads, and the requirement for reasonably good matching between electrical and thermal loads. The implementation of such systems depends largely on consumer aceptance of the concept, as well as on finding conditions under which they will be economical.

A final key component in the energy systems is the advanced heat pump described in Chapter IV. Although heat pumps have been commercially available for many years, only recently have they achieved a level of reliability that will make them widely acceptable in residential heating and cooling applications. With wider markets, the R&D required to achieve the advances described in Chapter IV should be readily justifiable to companies that manufacture heat pumps. The technological requirements are relatively simple. The successful development and marketing of advanced heat pumps will make electrically based residential energy systems considerably more attractive compared to gas-based systems than they are now.

In summary, System 1 has the fewest technological barriers to overcome, is the most likely to be implemented, and can provide the needed energy requirements in a satisfactory and reliable manner. Systems 2 and 4 are approximately comparable in their difficulties of implementation, which center on the fuel cell and coal liquefaction

components, respectively. Once implemented, System 2 will have an advantage because of the operational benefits of the fuel-cell power plant. System 5 must rank somewhat lower than System 2 because of the operational disadvantages of the on-site power plant, as discussed previously. Finally, System 3 appears to have the greatest relative difficulty of implementation because it contains both coal liquefaction and fuel-cell components. Assuming this system were implemented, its operational advantages would be similar to those of System 2. However, those advantages would probably not outweigh the difficulties of implementation.

From the preceding discussion, the ranking of the systems based on their performance characteristics are as follows, from highest to lowest: Systems 1, 2, 4, 5, and 3.

E. References--Chapter IX

1. National Academy of Sciences, "Particulate Polycyclic Organic Matter," (Washington D.C., 1972).

2. Electrical World, various issues.

3. General Electric Company, "Transmission LIne Reference Book -- 345 kV and Above," Electric Power Research Institute.

X. SUMMARY AND CONCLUSIONS

The comparative analyses carried out in Chapter IX enable the relative advantages and disadvantages of the five systems to be determined. A tabulation of ordinal rankings of the five systems in each category examined in Chapter IX is shown in Table X-1. In the table, a ranking of 1 indicates the most desirable system (i.e., the lowest cost, highest efficiency, lowest environmental impact), a ranking of 2 the next most desirable, and so on. Using Table X-1 as a guide, the relative advantages and disadvantages of each system are summarized below.

A. Summary of Advantages and Disadvantages

1. System 1 (Coal-Fired Power Plant; SNG)

System 1 has the lowest heating and cooling costs, as well as the lowest capital cost of any of the five systems. In addition, this system is most likely to meet the required performance standards, provide residential energy reliably, and be widely adopted by utilities, primarily because it employs the fewest number of new or advanced technologies.

On the other hand, System 1 is the least energy-efficient of the five systems, requiring 83% more energy resources to provide the same amount of heating and cooling than the most efficient system. In addition, it has the largest environmental impact of any system, ranking lowest in four out of six categories, including the important categories of air pollution and solid waste.

Table X-1

SYSTEM RANKINGS IN VARIOUS CATEGORIES

	System 1	System 2	System 3	System 4	System 5
Economics					
Operating Cost	1	3	4	2	5
Capital	1	4	3	2	5
Efficiency	5	2	3	4	1
Environment					
Air	5	2	3	4	1
Water	4	2*	2*	5	1
Solid Waste	5	2*	2*	2*	1
Noise	3*	2	5	3*	1
Land Use	5	3	2	4	1
Aesthetics	5	2	3	4	1
System Performance	1	2	4	3	5

*Rankings are essentially equal. Differences are too small to be resolved.

2. System 2 (26 MW Fuel Cell - SNG)

Although System 2 ranks about midway in its cost of heating and cooling, it requires almost the highest initial capital investment. Its overall system performance is second only to System 1, and it is also second highest in energy efficiency. It also ranks highly in nearly all environmental categories except land use.

3. System 3 (26 MW Fuel Cell-Naphtha)

Because of its similarity to System 2, System 3 ranks closely with that system, although its rankings are somewhat lower in most categories. It is somewhat less costly to install than System 2, but somewhat more costly to operate. The most noticeable difference between the two systems is that System 3 ranks considerably lower in the noise and system performance categories.

4. System 4 (Combined Cycle Power Plant)

System 4 has advantageous capital and operating costs compared with most other systems, and ranks midway with respect to system performance criteria and solid waste generation. However, it ranks next to last in terms of energy efficiency, and has low ranking in four of six environmental categories.

5. System 5 (100-kW Fuel Cell with Heat Recovery)

The rankings for this system present the most interesting picture of the five systems, because its rankings occur only in the extreme categories, 1 or 5. It ranks highest in all noneconomic categories except system performance, in which it ranks last. It also ranks last in both capital and operating cost, but as shown in Chapter IX, the operating costs are sensitive to the electrical and thermal loads that the system is required to meet.

B. Conclusions

Although we cannot categorically state which system is "best" or "worst" overall, several important implications result from our system analyses, especially in regard to the desirability of the implementation of energy systems based on fuel cells. However, those implications are applicable only to coal-based, intermediate-load electricity generation for residential energy use as covered in this report and should not be considered necessarily applicable to other types of systems such as those based on different fuel sources or different end uses.

First, economics is not a driving force for implementing the three fuel-cell systems (Systems 2, 3, and 5). Even under optimistic assumptions about the cost of fuel cells, those systems are not competitive with the alternatives. When only the cost of heating and cooling is considered, System 5 could be competitive with the next least costly system (System 4) under the appropriate conditions (high thermal-to-electrical demand ratio), but the cost of supplying all residential energy requirements is still very high compared to the other systems, and substantial optimization procedures would have to be carried out to determine the most economical applications.

Fuel-cell systems are more energy-efficient than the alternatives, partly because of the high efficiency of fuel cells and their potential for heat recovery, and partly because of reduced transmission losses resulting from dispersed siting. Thus, energy resources -- in this case, coal -- are conserved. Although coal is not as limited a resource as petroleum and natural gas, its conservation is clearly beneficial because it minimizes social and political pressures resulting from increased coal mining in the West, and it extends the lifetime of the most accessible, lowest cost coal reserves. High system efficiencies could convey economic benefits as well, but only at coal prices considerably higher than those currently in effect for western surface mining. For example, System 5 would have a lower cost of heating and cooling than System 1 only if the price of coal were at

least ten times higher than that derived in Chapter VII ($0.33/GJ or $6.69/tonne).

In addition, the three fuel-cell systems have less environmental impact, primarily because of the low emission rates of the fuel-cell power plants, which particularly benefit areas where pollutant loadings already approach or exceed those allowable by law. Recent environmental legislation, such as the Clean Air Act Amendments of 1977, clearly favors the siting of power generation facilities with the lowest possible pollutant emission rates in nonattainment and "prevention of significant deterioration" areas. In areas removed from power plant operation, such as coal resources areas where conversion plants are located, lower pollutant outputs per unit of energy ultimately consumed will also be beneficial. When pollutant loadings begin to exceed statutory limits in those areas, new conversion facilities will have to be located elsewhere, entailing greater costs for coal shipment, construction of additional rail lines, and so on.

Furthermore, other environmental attributes, such as lower land-use impact of fuel-cell systems, generally mean that the siting of power plants and related facilities (e.g., transmission lines) is easier than for alternative systems.

A full quantitative assessment of the environmental benefits of fuel-cell systems was not possible in this study, and indeed, such benefits are very site-specific. They depend heavily on such factors as the local pollutant loadings at the time of implementation, local land-use characteristics, and the availability of suitable sites for solid-waste disposal.

Finally, the fuel-cell systems considered here have a range of system performance characteristics depending on fuel type and application. If fuel-cell demonstration programs and early commercial use show that fuel cells will perform as projected in terms of load-following, reliability, and stack lifetime, then implementation of

fuel-cell systems will be greatly enhanced. However, new energy technologies are often justifiably met with some distrust and skepticism, especially by utilities, who must be concerned with the reliability and performance of the electric power system and who may not be willing to take even small risks when older, more familiar technologies are available.

Ultimately, the utilization of fuel-cell power plants in various energy systems will be driven not by economic considerations, but primarily by environmental and operational ones. Those utilities constrained by environmental, siting, and other noneconomic factors should find fuel-cell systems attractive alternatives to other methods of power generation.

As is the case for most promising, but yet unproven, energy technologies, the support of the federal government will be important to the ultimate success of fuel cells as a commercially viable concept. DOE, EPA, NASA, and other federal agencies have provided considerable funding for fuel-cell development. This financial support, which has increased substantially in recent years, will help to ensure the technical success of fuel-cell R&D programs. However, to ensure success in the marketplace, additional steps will have to be taken relatively early in the commercialization process, to assure that momentum is not lost and that companies manufacturing fuel cells have a market for their first, more costly units. As production increases, and costs decline, conventional market forces should result in wider market penetration.

Steps that the government could take to assist in early commercialization, subsequent to successful demonstration of first generation fuel cells, include:

- Purchase of fuel-cell power plants for use in government installations such as military bases.
- Additional investment tax credits and/or loan guarantees for utilities that purchase fuel cells.

- Incentives for the use of on-site fuel-cell power plants with heat recovery in federally-funded housing projects.

- Legislative initiatives to ensure that innovative electrical generation technologies such as fuel cells will be allowed to use natural gas and petroleum fuels until the time when synthetic fuels become available.

Prior to implementation of these actions, extensive cost/benefit analyses should be undertaken to ensure that the benefits that accrue from the implementation of fuel cells (fuel savings, environmental and operational) are justified in terms of the public and private expenditures required to achieve them.

In the coming years, all new power sources will be subject to intense scrutiny by the government, by environmental groups, and by the general public. They will be required to meet strict environmental standards, yet provide electric power efficiently, reliably, and at an acceptable cost. It appears that energy systems based on fuel cells will be among the most likely to meet those requirements.

Appendix A

ENTHALPIES BASED ON THE GIRDLER CATALYSTS DATA HANDBOOK

The enthalpies given in Sections IV-B and IV-C of this report are based on information tabulated in Girdler Catalysts, Physical and Thermodynamic Properties of Elements and Compounds, published by the Girdler Company, Louisville, Kentucky. This book is a standard reference for process and reactor engineering.

The Girdler data use a reference state of zero for the enthalpy of the elements at a temperature of absolute zero. This standard state is different from that found in many other references, such as Perry's Chemical Engineer's Handbook, but it is extremely useful. The tabulations allow rapid enthalpy calculations and intermediate temperatures are easily interpolated. Enthalpy balances on reactants and products give the heat of reaction directly. Furthermore, because having a process stream below the standard state is impossible, many confusing sign changes are avoided. It is important, however, that all enthalpies in a given calculation are based on the standard state.

1. Naphtha Enthalpy Calculations

The enthalpy of the coal-derived naphtha feed for System 3 was converted to the Girdler Catalysts basis after assuming the following enthalpic properties:

$\Delta H_{C_{Na}}$ = Heat of Combustion = 46.8 MJ/kg (20,100 Btu/lb)

$\Delta H_{V_{Na}}$ = Heat of Vaporization = 326 kJ/kg (140 Btu/lb)

$C_{P_{Na}}$ = Heat Capacity (gas) = 1.65 kJ/kg-°C (0.395 Btu/lb-°F) @ 16°C (60°F)

Note that the heat capacity was varied with temperature proportional to the heat capacity of toluene, as given in Girdler Catalysts. The enthalpy of the naphtha at the standard state is given by:

$$\Delta H_{C_{Na}} = \sum_i n_i \Delta H_{i_{products}} - \sum_i n_i \Delta H_{i_{reactants}}$$

where n_i is the number of moles of products or reactants, and ΔH_i is the enthalpy of products or reactants.

Based on 100g of naphtha: g atom C = 7.11
g atom H = 14.60
g atom O = negligible

The reaction equation is thus:

$$C_{7.11}H_{14.60} + 14.41\ O_2 \longrightarrow 7.11\ CO_2 + 7.30\ H_2O.$$

Below is a tabulation summarizing the naphtha enthalpy calculations:

Enthalpy	n_i (g mole)	ΔH_i (kJ/g mole)	$n_i \Delta H_i^o$ (kJ)
$\Delta H^o_{H_2O}$	7.30	-229.0	-1670
$\Delta H^o_{CO_2}$	7.11	-384.0	-2730
$\Delta H^o_{O_2}$	14.41	8.4	121
$\Delta H_{V_{H_2O}}$	7.30	-442.0	-3230
$\Delta H_{C_{Na}}$	100.00 g	-46.8 kJ/g	-4680
ΔH^o_{Na}	ΔH^o_{Na} (liq., 16°C) = -1.77 kJ/g		-177 kJ/100g

In the tabulation above, ΔH_i is the total enthalpy of the stream or component i, and ΔH_{V_i} is the heat of vaporization of component i.

Enthalpies of naphtha as a vapor at 16°C were calculated as follows:

$$\Delta H^{o}_{Na}\ (\text{gas},\ 16^{o}C) = \Delta H^{o}_{Na}\ (\text{liq.}\ 16^{o}C) + \Delta H_{V_{Na}}$$

$$= -1.77 + 0.33 = -1.44\ \text{kJ/g}$$

Enthalpies of naphtha as a vapor at other temperatures were calculated as follows:

$$\Delta H^{o}_{Na}\ (\text{gas},\ 38^{o}C) = \Delta H^{o}_{Na}\ (\text{gas},\ 16^{o}C) + (38^{o}C - 16^{o}C) \times C_{P_{Na}}\ (16^{o})$$

$$= -1.44 + (22)\ (0.00165) = -1.40\ \text{kJ/g}$$

Enthalpies at other temperatures were calculated by numerical integration, using appropriate heat capacities.

2. <u>SR-52 Enthalpy Program</u>

A simple matrix program was written on a programmable hand calculator to facilitate the rapid calculation of stream enthalpies. The program calculates enthalpies at intermediate temperatures by a straight line interpolation. The program requires that stream flow rates, Girdler Catalysts enthalpies and the temperature of the stream be entered into the calculator before each calculation, because the storage capacity of the SR-52 is limited. The basic equation of the program is:

$$\Delta H^{o}_{stream} = \begin{pmatrix} n_o \\ \dot{n}_i \\ \dot{n}_n \end{pmatrix} \left(\Delta H^{o}_{1}(T) \ . \ . \ . \ H^{o}_{n}\Delta(T) \right)$$

where n_i is expressed in g mole/hr, and $H^{o}_{i}(T)$ is expressed in kJ/g mole.

Appendix B

MOLTEN CARBONATE FUEL-CELL PERFORMANCE

A study of molten carbonate fuel-cell performance was undertaken to determine what factors contribute to cell power output. This study developed a calculational model that can reproduce published data on molten carbonate fuel-cell performance.

1. Cell Performance

The survey of the literature[1-5] indicated that at moderate current densities (i.e., well removed from diffusion limits), cell performance can be approximated by the equilibrium cell voltage between the anode and cathode streams minus a term proportional to the current density. This term is mostly internal resistance of the cell, although at low current densitites, varous electrode and electrolyte polarizations also can appear to be linear with current density. A study of this model shows that:

- Cell voltage increases slightly with increased total pressures.
- Cell voltage is decreased by the presence of diluents.
- As the gas moves along the anode or cathode, the reactants are consumed and the gas is less reactive, so that at constant cell voltage the current density decreases down the length of the cell.
- Increasing the electrolyte thickness decreases cell voltage by increasing the internal resistance.
- H_2 is the most active anode reactant. However, CO is continuously shifted by H_2O to form more H_2 so that a mole of CO is virtually equivalent to a mole of H_2 in the anode.

- o CH_4 is inert in the anode at these temperatures.
- o At the cathode, CO_2 has a more dramatic effect on the voltage than oxygen because the voltage is proportional to $\ln (CO_2)$ and $\ln (O_2)^{1/2}$. Therefore, both excess O_2 and CO_2 are necessary for good cathode performance.

The features of the model described above were computerized on a programmable hand calculator. This program can predict the voltage and current density of a molten carbonate fuel cell with varying anode and cathode feeds, pressures, fuel utilizations, and cell resistances.

After the local activity of an electrode was reduced to a single resistance parameter, it was still necessary to do extensive calculation to determine the performance of a total cell. The anode is required to run at high conversion levels of the total CO and H_2 in the feed gas, so that the equilibrium potential varies considerably with distance down the length of the cell. Therefore, the calculation procedure described in greater detail in Section 2 of this appendix was developed. It consists of the following steps:

(1) The feed gas was equilibriated with respect to the water gas shift reaction: $CO + H_2O \rightleftharpoons H_2 + CO_2$

(2) The equilibrium voltage relative to all components at unit activity was calculated:

$$\Delta E = (RT/2F)\ln\left[(CO_2)(H_2O)/(H_2)\right].$$

(3) The local current density was calculated from the cell polarization minus the local polarization via $i = (\eta-\Delta E)/(R_{int} + R_{ext})$. R_{int} was set at 0.95 ohm-cm^2 for present technology and R_{ext} at 0.3 ohm-cm^2 for a total of 1.25 ohm-cm^2.

(4) Using this current density, the distance required to convert a quantity of hydrogen equal to 10% of the total H_2 and CO remaining was calculated.

(5) Also computed was the change in pressures and flow rates due to the production of steam and CO_2 via the electrochemical reaction: $H_2 + CO_3^{=} \longrightarrow H_2O + CO_2 + 2e$. The program then recycled to Step (1).

The calculation was repeated for 2, 6, 12, and 18 cycles to obtain 19, 47, 72, and 85% conversion of the gases. The average current density was calculated from the cumulative current densities and distances. The computations were repeated at various polarizations to obtain performance curves.

These detailed calculations were not repeated at the cathode because cathode gases are run to only 50% conversion. A good correlation could be obtained with the data reported by Ackerman[1] on methane reformate at 50% air conversion, using the mean of the cathode polarizations at the inlet and outlet of the cell. Because the cathode polarizations are given by $E = (RT/2F)\ell n\left[(CO_2).(O_2)^{\frac{1}{2}}\right]$, the mean polarization is the log mean gas pressure combination. At very low current densities and low anode conversions, the model breaks down slightly, but at higher conversions, and current densities between 50 and 200 mA/cm^2, the results seem to be useful and reliable.

2. <u>High Conversion Performance of Molten Carbonate Fuel Cell</u>

The first step in the calculation is the determination of the extent of the water-gas shift reaction:

$$CO + H_2O \rightleftharpoons H_2 + CO_2$$

or, abbreviated:

$$A + B \rightleftharpoons C + D.$$

If N is the loss in pressure of the CO or H_2O due to the shift, then

$$\frac{(C + N)\ (D + N)}{(A - N)\ (B - N)} = K, \text{ the equilibrium constant}$$

K was taken at 1.85 in this work, although more careful interpolation shows that at 650°C (1,202°F) a value of 1.92 would be more appropriate:

$$N = \frac{Y - \sqrt{Y^2 - 4(K-1)(KAB-CD)}}{2(K-1)}$$

where $Y = K(A+B) + C+D$.

N was then subtracted from the pressures for CO and H_2O and added to those of H_2 and CO_2 to obtain the equilibriated pressures.

Next the equilibrium "polarization" of the anode was calculated.

$$\eta = \frac{RT}{2F} \ \ell n \left[\frac{(CO_2)(H_2O)}{(H_2)} \right]$$

The local current density was calculated via

$$U = (\eta_o - \eta)/R$$

Here η_o is the constant applied polarization and R is the combined internal and external resistance.

The distance increment, ΔX, was not fixed at the start but was calculated so as to consume a charge ΔQ equal to 10% of the remaining combustibles, H_2 and CO.

$$\Delta Q = \frac{V_g \ [(CO_2)+(H_2)]}{10P_{TOT}}$$

V_g is the gas flow rate expressed as mA/cm where all gas molecules are taken as containing 2 electrons per mole.

The starting gas flow rate can be chosen arbitrarily because the cell length will vary accordingly and the calculated current density will not change. However, for convenience, the inlet gas flow rate was taken as $100 \cdot P_{TOT}/[(CO) + (H_2)]$. Then ΔQ reads directly as percent conversion.

$$\Delta X = \Delta Q/U$$

ΔX and ΔQ are summed cumulatively into storage registers to give the total cell length and total conversion, respectively. The average current density at any point is given by $\Sigma\Delta Q/\Delta X$.

After each increment of hydrogen conversion the various gas pressures must be adjusted because of the consumption of hydrogen and the formation of steam and CO_2, and the increase in total gas flow rate, all due to the reaction:

$$H_2 + CO_3^{=} \longrightarrow H_2O + CO_2 + 2e^-$$

Thus, first (H_2) is decremented by $\Delta Q \cdot P_{TOT}/V_g$ while (H_2O) and (CO_2) are incremented by the same quantity. Then V_g is adjusted via $V'_g = V_g + \Delta Q$ and all gas pressures are reduced by the factor V_g/V'_g.

Finally, all gas pressures are fed back into the water-gas shift subroutine and the whole process is repeated.

The process is halted after 2, 6, 12, and 18 cycles to give 19, 47, 72, and 85% conversion. At each point the corresponding average current densities and gas compositions may be obtained. The whole process may be repeated with other values of η_o. The cell voltage corresponding to a value of η_o is given by

$$E \text{ cell (mV)} = 1015 + \eta_c - \eta_o$$

Here, 1,015 mV is the theoretical cell potential at 650°C (1,202°F) and 101 kPa (1 atm) pressure of all reactant gases.

η_c is the mean cathode potential calculated from the average of $(RT/2F)\ln\left[(CO_2).(O_2)^{\frac{1}{2}}\right]$ at the cathode inlet and outlet.

3. References--Appendix B

1. J. P. Ackerman, "Molten Carbonate Fuel Cell Systems - Status and Potential," Paper No. 391, National Electrochemical Society, 151st Meeting, Philadelphia, PA, May 8-13, 1977.

2. J. M. King, "Energy Conversion Alternatives Study - United Technologies Phase II Final Report," NASA CR-134955 (October 1976).

3. H. Selman, et al., Abstract No. 393, Electrochemical Society, 151st National Meeting, Philadelphia, PA, May 8-13, 1977.

4. Institute of Gas Technology, "Fuel Cell Research on Second-Generation Molten Carbonate Systems," Project 8984, Quarterly Status Report (Jan. 1 - March 31, 1977).

5. H. A. Liebhafsky and E. C. Cairns, Fuel Cells and Fuel Batteries, Chapter 12 (Wiley, New York, 1968).

Appendix C

ENERGY SUPPLY/DEMAND PROGRAM FOR RESIDENCES SUPPLIED BY THE 100-kW FUEL-CELL POWER PLANT

A Texas Instruments SR-59 calculator was programmed to calculate hourly average energy parameters associated with the use of a 100-kW fuel-cell power plant to supply electricity and heat to townhouse residences. The basic features of that system were described in Chapter IV. For each residence, the program calculates the hourly average electrical load, heat pump duty factor, and recovered fuel-cell heat delivered to the space heating system.

The inputs to the program are the hourly average external temperature, heating load, hot water load, and light and appliance electrical load. Fuel-cell power plant, heat pump, and heat exchanger performance parameters are stored internally.

The operation of the program is illustrated by the flow chart shown in Figure C-1. The variables shown in the flow chart are defined below (all parameters represent hourly averages).

T:	External temperature, ^{o}F or ^{o}C.
Q:	Space heating load, Btu/hr or kJ/hr.
HW:	Domestic hot water (DHW) load, Btu/hr or kJ/hr.
E:	Light and appliance electrical load, kW.
E':	Total electrical load, kW.
HF(E or E'):	Fuel-cell heat recovered as a function of electrical load, Btu/hr or kJ/hr.

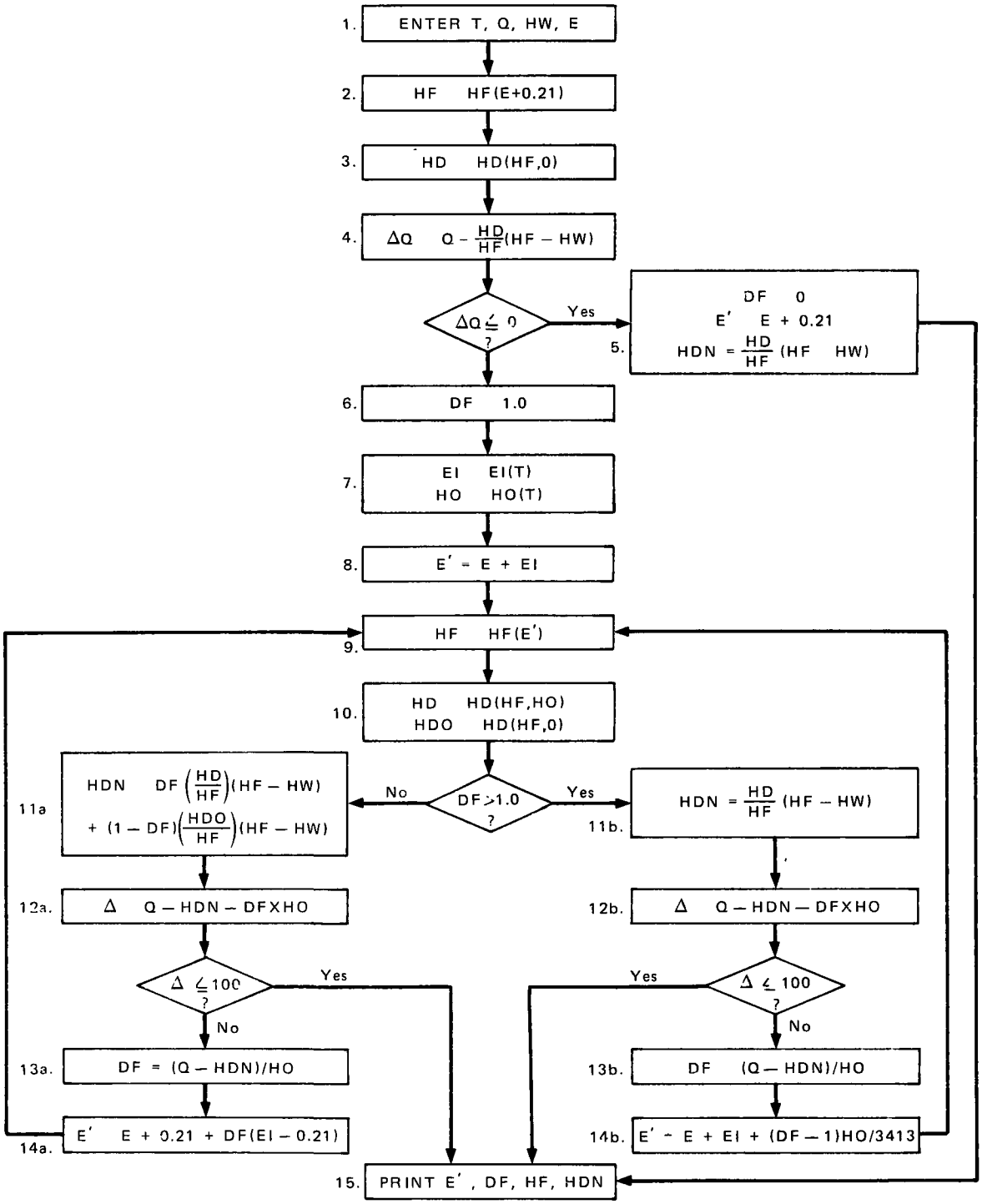

FIGURE C-1. PROGRAM FOR ENERGY SUPPLY/DEMAND CALCULATIONS

EI(T):	Heat pump electrical load as a function of temperature, kW.
HO(T):	Heat pump output as a function of temperature, Btu/hr or kJ/hr.
HD(HF, HO):	Heat delivered to space heating system through heat exchanger as a function of recovered fuel-cell heat and heat pump output, Btu/hr or kJ/hr.
HDN:	Net recovered fuel-cell heat delivered to space heating system, after DHW demand is satisfied, Btu/hr or kJ/hr.
DF:	Heat pump duty factor -- ratio of net space heating demand to heat pump output.

The operation of the program, as displayed in Figure C-1, begins with the specification of the key input variables in Step 1. Steps 2-4 then determine whether recovered fuel-cell heat is sufficient to meet both DHW and space heating loads without operation of the heat pump. If so, the program ends and values of the output parameters are printed (the value of E is increased by 0.21 kW, which is the fan power requirement in the space heating system). If not, the remaining variables are initialized in Steps 6-8.

The iterative part of the program begins in Step 9. The program proceeds through either one of two independent branches, depending on whether DF is greater or less than 1. Physically, the heat pump duty factor can never exceed 1.0. However, for purposes of the program it is allowed to do so, simply indicating that the net space heating load exceeds the capacity of the heat pump and that electric resistance heating must be added. The program ceases to iterate when the heat supply (net recovered fuel-cell heat plus heat pump heat plus electric resistance heat, if required) equals the heat demand, Q. This balance

is considered to have been achieved when the difference between supply and demand is less than 100 kJ/hr. If the heat supply and demand do not balance, a new duty factor and electrical load (E') are calculated and the program iterates again.

TECHNICAL REPORT DATA
(Please read Instructions on the reverse before completing)

1. REPORT NO. EPA-600/7-79-105b	2.	3. RECIPIENT'S ACCESSION NO.
4. TITLE AND SUBTITLE Comparative Assessment of Residential Energy Supply Systems That Use Fuel Cells (Technical Report)		5. REPORT DATE April 1979
		6. PERFORMING ORGANIZATION CODE
7. AUTHOR(S) R. V. Steele, D. C. Bomberger, K. M. Clark, R. F. Goldstein, R. L. Hays, M. E. Gray, G. Ciprios*, R. J. Bellows*, H. H. Horowitz, and C. W. Snyder*		8. PERFORMING ORGANIZATION REPORT NO.
9. PERFORMING ORGANIZATION NAME AND ADDRESS SRI International 333 Ravenswood Avenue Menlo Park, California 94025		10. PROGRAM ELEMENT NO. EHB534
		11. CONTRACT/GRANT NO. 68-02-2180
12. SPONSORING AGENCY NAME AND ADDRESS EPA, Office of Research and Development Industrial Environmental Research Laboratory Research Triangle Park, NC 27711		13. TYPE OF REPORT AND PERIOD COVERED Final; 9/76 - 1/79
		14. SPONSORING AGENCY CODE EPA/600/13

15. SUPPLEMENTARY NOTES IERL-RTP project officer is Gary L. Johnson, MD-63, 919/541-2745. (*) Coauthors are Exxon personnel.

16. ABSTRACT The report gives results of a comparison of residential energy supply systems using fuel cells. Twelve energy systems, able to provide residential heating and cooling using technologies projected to be available toward the end of this century, were designed conceptually. Only a few systems used fuel cells. All systems used Western coal as the primary energy source, and all residences were assumed to have identical heating and cooling demands typical of the mid-continent U.S. After screening, five systems were analyzed in detail. The entire energy cycle, from coal mine to end use, was examined for costs, efficiency, environmental impact, and applicability. The five energy systems are: (1) a coal-fired power plant supplying electricity and a coal gasification plant supplying SNG; (2) a 26-MW fuel-cell power plant fueled by coal-derived SNG supplying electricity; (3) a 26-MW fuel-cell power plant fueled by coal-derived naphtha supplying electricity; (4) a combined-cycle power plant fueled by coal-derived fuel oil supplying electricity; and (5) a 100-kW fuel-cell power plant fueled by coal-derived SNG, sited in a housing complex, supplying electricity to heat pumps, with heat recovered from the fuel cell supplying supplemental space heating and hot water. Results indicate that the fuel cell systems are most costly, most efficient, and have least environmental impact.

17. KEY WORDS AND DOCUMENT ANALYSIS

a. DESCRIPTORS		b. IDENTIFIERS/OPEN ENDED TERMS	c. COSATI Field/Group	
Pollution	Assessments	Pollution Control	13B	14B
Fuel Cells	Coal Gasification	Stationary Sources	10B	13H
Energy Conversion	Coal	Substitute Natural Gas		21D
Techniques	Naphthas		10A	07C
Residential Buildings	Fuel Oil		13M	
Heating	Natural Gas		13A	
Cooling Systems	Heat Pumps			

18. DISTRIBUTION STATEMENT Unlimited	19. SECURITY CLASS (This Report) Unclassified	21. NO. OF PAGES 482
	20. SECURITY CLASS (This page) Unclassified	22. PRICE

EPA Form 2220-1 (9-73)